

# Visible light mediated activation of vinyl halides

**Dissertation**

**Zur Erlangung des Doktorgrades der Naturwissenschaften**

Dr. rer. nat.

**der Fakultät für Chemie und Pharmazie**

**der Universität Regensburg**



vorgelegt von

**Thomas Föll**

aus Niederaichbach

**Regensburg 2019**

Diese Arbeit wurde angeleitet von: Prof. Dr. Oliver Reiser

Promotionsgesuch eingereicht am: 30.01.2019

Promotionskolloquium am: 27.02.2019

Prüfungsausschuss: Vorsitz: Prof. Dr. Hubert Motschmann

1. Gutachter: Prof. Dr. Oliver Reiser
2. Gutachter: Prof. Dr. Julia Rehbein
3. Gutachter: Prof. Dr. Robert Wolf

Der experimentelle Teil der vorliegenden Arbeit wurde in der Zeit von November 2015 bis Oktober 2018 unter der Leitung von Prof. Dr. Oliver Reiser am Lehrstuhl für Organische Chemie der Universität Regensburg angefertigt.

Herrn Prof. Dr. Oliver Reiser möchte ich herzlich für die Aufnahme in seinen Arbeitskreis, die Themenstellung, sowie für die anregenden Diskussionen und seine stete Unterstützung während der Durchführung dieser Arbeit danken.





*Meiner Familie*

*„Real success is finding your lifework in the work that you love”*

-David McCullough

# Table of contents

<b>A Introduction .....</b>	<b>1</b>
1 Generation and reactivity of vinyl radicals .....	1
2 Photophysical background of photocatalysts .....	8
3 Reactions of vinyl radicals promoted by visible light .....	11
<b>B Visible light mediated activation of vinyl halides.....</b>	<b>30</b>
1 Introduction .....	30
2 Preliminary studies with vinyl bromides .....	32
2.1 Cleavable redox auxiliary as activating group .....	32
2.2 Controlling the reduction potential.....	39
2.3 Utilizing the reductive quenching cycle .....	44
2.4 Formation of the vinyl radical <i>in situ</i> by a multicomponent cascade process .....	50
2.5 Conclusion.....	57
3 Visible light mediated activation of $\alpha$ -chloro cinnamates.....	58
3.1 Literature background .....	58
3.2 Optimization of the reaction conditions .....	61
3.3 Substrate scope.....	64
3.4 Up-scaling of the photochemical transformation and enantioselective synthesis of $\alpha$ -alkylidene- $\gamma$ -aryl- $\gamma$ -butyrolactone ( <b>238</b> ) .....	70
3.5 Unraveling the halogen paradox - Mechanistic discussions, computational details and control experiments .....	76
3.6 Conclusion.....	84
4 Visible light mediated activation of $\alpha$ -chloro cinnamitriles .....	85
4.1 Optimization of the reaction conditions .....	85
4.2 Substrate scope.....	88
4.3 Proposed reaction mechanism .....	92
4.4 Conclusion and outlook.....	93
<b>C Summary .....</b>	<b>94</b>
<b>D Zusammenfassung .....</b>	<b>97</b>
<b>E Experimental part.....</b>	<b>100</b>
1 General information .....	100
2 Preliminary studies with vinyl bromides .....	101
3 Synthesis of $\alpha$ -halo cinnamates ( <b>228a</b> – <b>228u</b> ) .....	109
4 Synthesis of enol acetates ( <b>152a</b> – <b>152m</b> ).....	123
5 Photochemical functionalization of $\alpha$ -chloro cinnamates ( <b>229aa</b> – <b>229ra</b> ).....	130
6 Photochemical reaction setup for big scale synthesis of <b>229aa</b> .....	153

7 Enantioselective synthesis of $\alpha$ -alkylidene- $\gamma$ -aryl- $\gamma$ -butyrolactone ( <b>238</b> ).....	154
8 Synthesis of $\alpha$ -chloro cinnamitriles ( <b>248a – 248h</b> ).....	156
9 Photochemical functionalization of $\alpha$ -chloro cinnamitriles ( <b>249aa – 249ga</b> ).....	161
<b>F References</b> .....	<b>175</b>
<b>G Appendix</b> .....	<b>183</b>
1 Reduction potentials of $\alpha$ -halo cinnamates .....	183
2 NMR spectra of new compounds .....	184
3 Chiral HPLC chromatograms .....	298
4 X-ray crystallography data .....	300
5 Curriculum Vitae .....	307
<b>H Acknowledgement</b> .....	<b>309</b>
<b>I Declaration</b> .....	<b>311</b>

## Abbreviations

Å	angstrom	cm <sup>-1</sup>	wavenumbers
A	ampere	conv	conversion
abs	absolute	CT	charge transfer
Ac	acetyl	CV	cyclic voltammetry
AcOH	acetic acid	Cy	cyclohexyl
AIBN	azobisisobutyronitrile		
anhyd	anhydrous	δ	chemical shift (ppm) downfield from TMS
aq	aqueous	ΔT	heat
Ar	aryl	d	days; doublet (spectral)
atm	atmosphere	dap	2,9-bis( <i>p</i> -anisyl)-1,10-phenanthroline
ATRA	atom transfer radical addition	DCC	<i>N,N'</i> -dicyclohexylcarbodiimide
		DCE	1,2-dichloroethane
BDE	bond dissociation energy	DCM	dichloromethane
Bn	benzyl (PhCH <sub>2</sub> )	decomp.	decomposition
Boc	<i>tert</i> -butoxycarbonyl	dF(CF <sub>3</sub> )ppy	2-(2,4-difluorophenyl)-5-(trifluoromethyl)pyridine
bpy	2,2'-bipyridine, 2,2'-bipyridyl	DIPEA	<i>N,N</i> -diisopropylethylamine
br	broad (spectral peak)	DMDC	dimethyl dicarbonate
Bu	butyl	DMN	1,5-dimethoxynaphthalene
BuLi	butyl lithium	DMAP	4-( <i>N,N</i> -dimethylamino)pyridine
Bz	benzoyl (PhCO)	DME	1,2-dimethoxyethane
		DMF	<i>N,N</i> -dimethylformamide
°C	degrees Celsius	DMSO	dimethylsulfoxide
C	catalyst	<i>dr</i>	diastereomeric ratio
CBS	Corey-Bakshi-Shibata	dtbbpy	4,4'- <i>diter</i> tbutyl-2,2'-bipyridine
<sup>13</sup> C-NMR	carbon NMR		
Cbz	carboxybenzyl	E <sub>1/2</sub> <sup>o</sup>	standard reduction potential
CFL	compact fluorescent lamp	ed.	edition
<i>cf.</i>	confer	Ed.	editor(s)
CI	chemical ionization		
cm	centimeter		

EDA	electron-donor-acceptor	J	Joule
EDG	electron donating group	<i>J</i>	coupling constant (in NMR analysis)
<i>ee</i>	enantiomeric excess		
<i>e.g.</i>	<i>exempli gratia</i> , for example	k	kilo
equiv	equivalent(s)	K	Kelvin
ESI	electrospray ionization	kcal	kilocalorie
Et	ethyl		
<i>et al.</i>	and others (co-authors)	L	liter; ligand
EWG	electron withdrawing group	LAH	lithium aluminum hydride
		LDA	lithium diisopropylamide
F	Faraday	LED	light emitting diode
FPW	Freeze-Pump-Thaw	$\lambda_{\max}$	max UV-vis wavelength
		LUMO	lowest unoccupied molecular orbital
g	gram(s); gaseous		
		$\mu$	micro
h	hour(s)	m	meter; milli; multiplet (spectral)
HAT	hydrogen atom transfer	M	molar (moles per liter)
<sup>1</sup> H-NMR	proton NMR	M <sup>+</sup>	parent molecular ion (in MS)
HOMO	highest occupied molecular orbital	max	maximum
HPLC	high-performance liquid chromatography	MCR	multicomponent reaction
HRMS	high-resolution mass spectrometry	Me	methyl
HSAB	hard soft acid base	MeCN	acetonitrile
h $\nu$	light	MHz	megahertz
Hz	Hertz	min	minute(s); minimum
		mL	milliliter
		MLCT	metal to ligand charge transfer
<sup>i</sup> Bu	<i>iso</i> -butyl	mm	millimeter
<i>i.e.</i>	that is	mM	millimolar
IET	intramolecular electron transfer	mmHg	millimeter of mercury
IR	infrared	mmol	millimole(s)
ISC	intersystem crossing	mol	mole(s)

mp	melting point	Ref	reference
MS	mass spectrometry; molecular sieves	R <sub>f</sub>	retention factor (in chromatography)
Ms	mesyl (methanesulfonyl)	rt	room temperature
<i>m/z</i>	mass to charge ratio (in MS)		
		s	seconds; singlet (spectral)
NBS	<i>N</i> -bromosuccinimide	sat.	saturated
nm	nanometer	SCE	saturated calomel electrode
NMR	nuclear magnetic resonance	sept	septet (spectral)
ns	nanosecond(s)	SET	single electron transfer
Nu	nucleophile	sext	sextet (spectral)
OXONE <sup>®</sup>	potassium peroxymonosulfate	t	triplet (spectral)
		T	temperature
PCET	proton-coupled electron transfer	TBAB	tetra- <i>n</i> -butylammonium bromide
PCM	polarizable continuum model	TBHP	<i>tert</i> -butyl hydroperoxide
PET	photoinduced electron transfer	TBS	<i>tert</i> -butyldimethylsilyl ether
pH	proton log units	<sup>t</sup> Bu	<i>tert</i> -butyl
Ph	phenyl	TEMPO	2,2,6,6-tetramethylpiperidine 1-oxyl
PMB	4-methoxybenzyl ether	TES	Triethylsilyl ether
ppm	part(s) per million	Tf	trifluoromethanesulfonyl (triflyl)
ppy	2-phenylpyridine	TFA	trifluoroacetic acid
<sup>i</sup> Pr	<i>iso</i> -propyl	TFAA	trifluoroacetic anhydride
PTSA	<i>p</i> -toluenesulfonic acid	Tfoc	2,2,2-trifluoroethoxy carbonyl
		THF	tetrahydrofuran
q	quartet (spectral)	TLC	thin-layer chromatography
quin	quintet (spectral)	TMS	trimethylsilyl, tetramethylsilane, thermomorphic solvent system
		<i>t</i> <sub>R</sub>	retention time (in chromatography)
R	arbitrary moiety	Ts	<i>p</i> -toluenesulfonyl (tosyl)
rac.	racemic	TS	transition state
red	reduction		
redox	reduction-oxidation	UV	ultraviolet (light)

UV-Vis ultraviolet-visible absorption  
spectroscopy

vis visible

vol volume

vs versus

X arbitrary reagent 1; halogen

Y arbitrary reagent 2

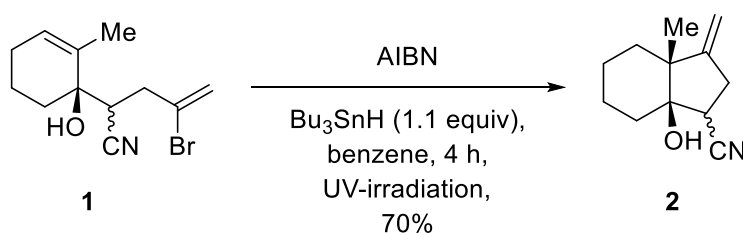


## A Introduction

### 1 Generation and reactivity of vinyl radicals

It has been slightly more than 100 years since the pioneering work of Gomberg who discovered the first organic free radical upon treatment of triphenylmethyl chloride with elemental zinc.<sup>[1]</sup> A century later, free radicals have become an integral part of modern organic chemistry and are nowadays widely employed. In this regard, remarkable advances have been achieved in the field of different reaction types including chain reactions, defunctionalization chemistry, complex intramolecular cyclizations, radical translocations, or exceptional rearrangements.<sup>[2-7]</sup>

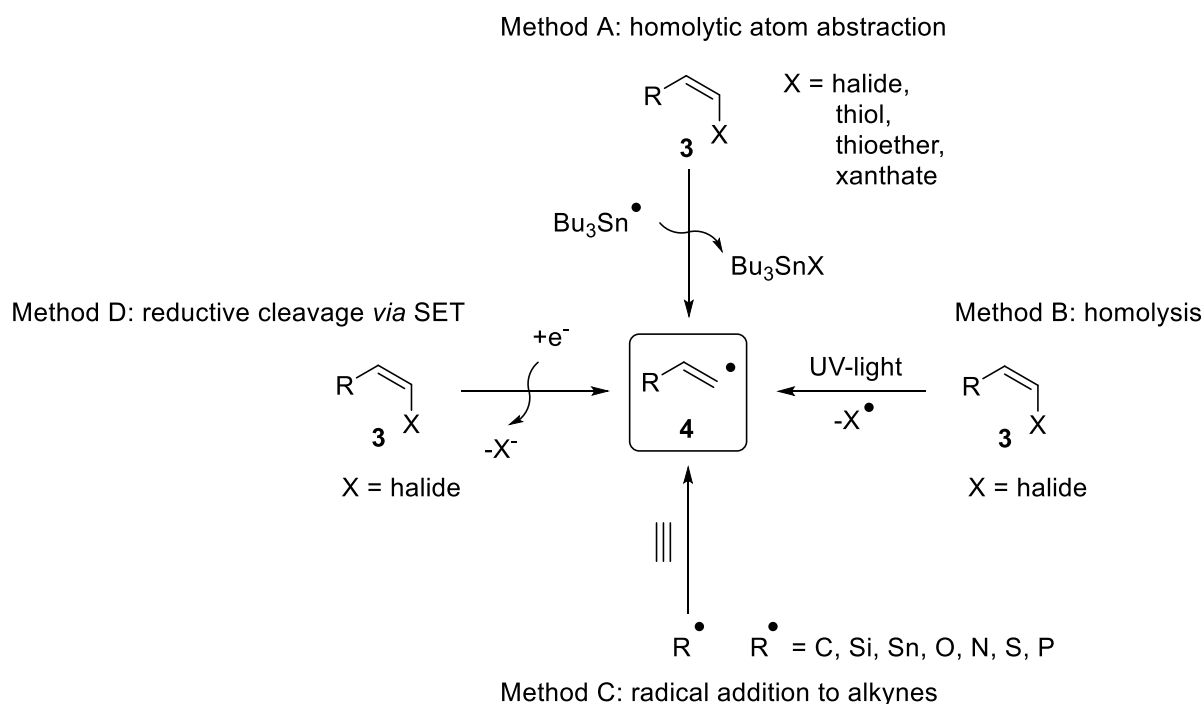
With the discovery of trialkyltin hydrides as radical precursors in the 1960s,<sup>[8,9]</sup> numerous applications and different kinds of radicals were reported. However, these transformations were predominantly based on alkyl radicals and comparatively less attention was dedicated to vinyl radicals.<sup>[10-12]</sup> Being considered too reactive and uncontrollable, only a handful reports described vinyl radicals as intermediates. It took until the 1980s when pioneering work by Curran and Stork turned their attention towards vinyl radicals as intermediates for radical transformations (Scheme 1).<sup>[13-16]</sup>



**Scheme 1.** An early example of a reaction proceeding *via* a vinyl radical intermediate by Stork in 1982.<sup>[13]</sup>

In principle, there are different ways to initiate radical transformations and therefore to access vinyl radical intermediates (Scheme 2). Without doubt, one of the most dominant methods to trigger radical transformations is the utilization of tin related compounds. Usually, the combination of Bu<sub>3</sub>SnH or bulkier Ph<sub>3</sub>SnH together with radical starters such as AIBN represent excellent radical precursors. Upon thermal or photoinitiated decomposition of

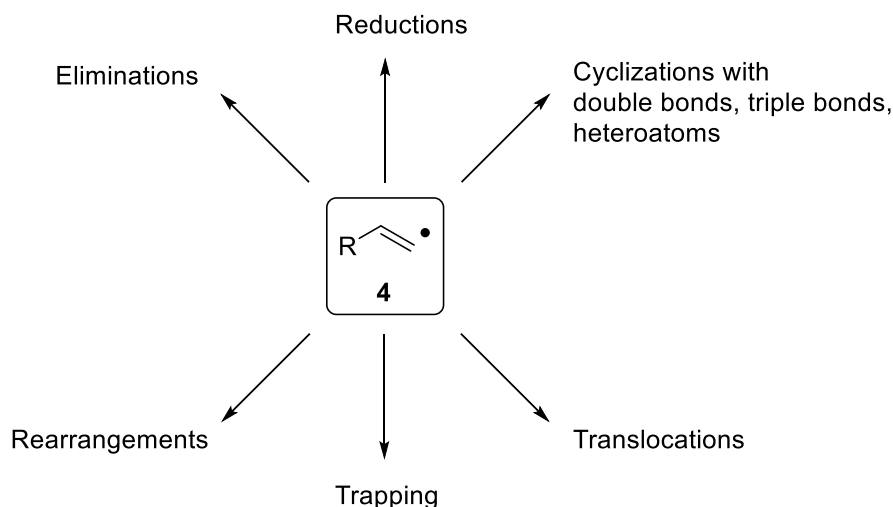
AIBN, the corresponding *isobutyronitrile* radical readily abstracts the hydrogen atom from the organotin compound due to the relatively weak Sn-H bond (78 kcal/mol).<sup>[17]</sup> The corresponding trialkyl stannane radical  $R_3Sn^\bullet$  is able to homolytically abstract a halogen atom from the substrate giving rise to a carbon-centered radical. Besides halogen atoms, other activation groups rely on thiols, thioethers, or xanthates as they readily react with  $R_3Sn^\bullet$  forming strong Sn-S bonds.<sup>[6]</sup> This methodology has been widely exploited to directly access a vinyl radical intermediate from any vinyl-X substrate (Scheme 2, Method A).<sup>[6,10-12]</sup>



**Scheme 2.** Different approaches to access a vinyl radical intermediate.

As an alternative approach, vinyl radicals can be generated by direct homolysis of vinyl halides using very energetic UV-light (Scheme 2, Method B).<sup>[18,19]</sup> Furthermore, vinyl radicals commonly occur as intermediates upon addition of various radical sources to triple bonds. In this regard, carbon-centered, tin-centered, sulfur-centered, or other heteroatom-centered radicals are widely employed (Scheme 2, Method C).<sup>[5-7]</sup> Lastly, vinyl radicals can be produced *via* single electron reduction. Again, vinyl halides serve as vinyl radical precursors but this time, the vinyl radical is released upon reductive cleavage of the C-halogen bond. This principle has first been realized electrochemically,<sup>[20]</sup> and more recently *via* photoredox catalysis (Scheme 2, Method D).<sup>[21-25]</sup>

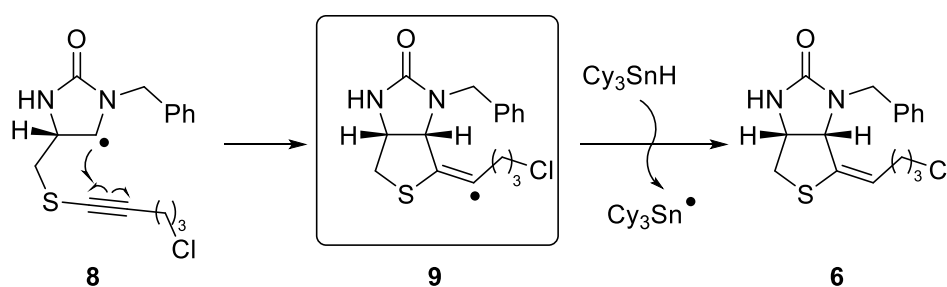
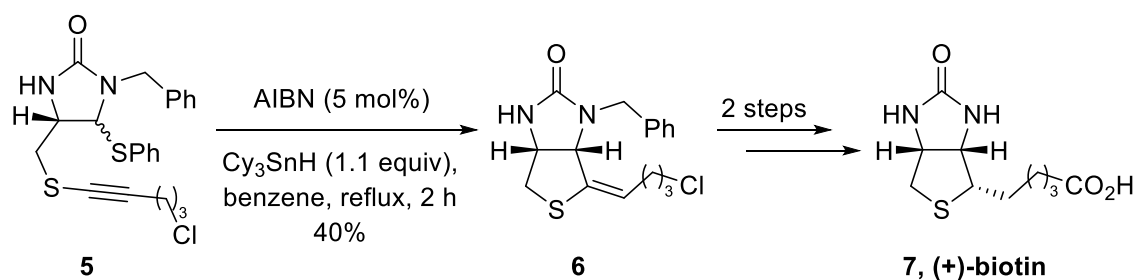
Among all these different options to access vinyl radicals, a broad range of reactivities have been reported. An overview is given in the following Scheme 3.



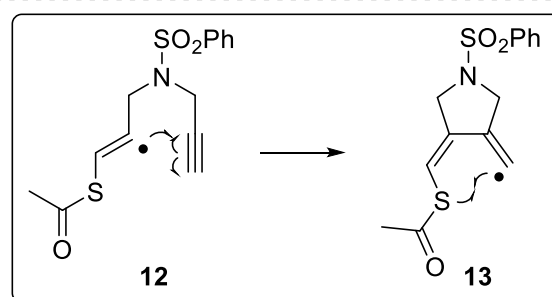
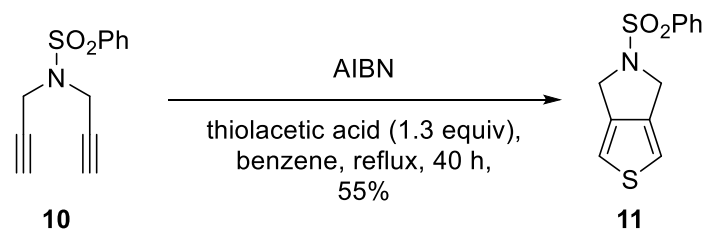
**Scheme 3.** General reactivity of vinyl radical intermediates.

In the simplest way, the vinyl radical is immediately quenched by hydrogen abstraction stemming from either  $R_3SnH$  or the solvent which is often utilized in defunctionalizations of vinyl halides or quenching of vinyl radical intermediates, *e.g.* after addition to triple bonds.<sup>[26-30]</sup> Corey *et al.* have proven that this principle can be exploited in the enantioselective total synthesis of (+)-biotin (**7**) (Scheme 4).<sup>[26]</sup> The key step included homolytic desulfurylation of thioether **5** with  $Cy_3SnH$  and AIBN. The resulting  $\alpha$ -amino radical **8** readily undergoes 5-*exo*-dig ring closure to vinyl radical **9** which is rapidly quenched to **6**.

Radical cyclization reactions are commonly used to construct complex ring systems. Besides simple reductions, vinyl radicals readily cyclize with double bonds,<sup>[13,31-33]</sup> triple bonds,<sup>[34,35]</sup> or with heteroatoms.<sup>[36]</sup> In this regard, an early example was provided by Padwa *et al.* in a tandem cyclization to construct thiophene **11** in moderate yields (Scheme 5).<sup>[35]</sup> The reaction sequence is initiated by radical addition of a thioacetyl radical onto the triple bond of **10**, resulting in a vinyl radical intermediate **12** which undergoes 5-*exo*-dig ring closure. The corresponding second vinyl radical **13** finally cyclizes at the sulfur position giving rise to thiophene **11**.



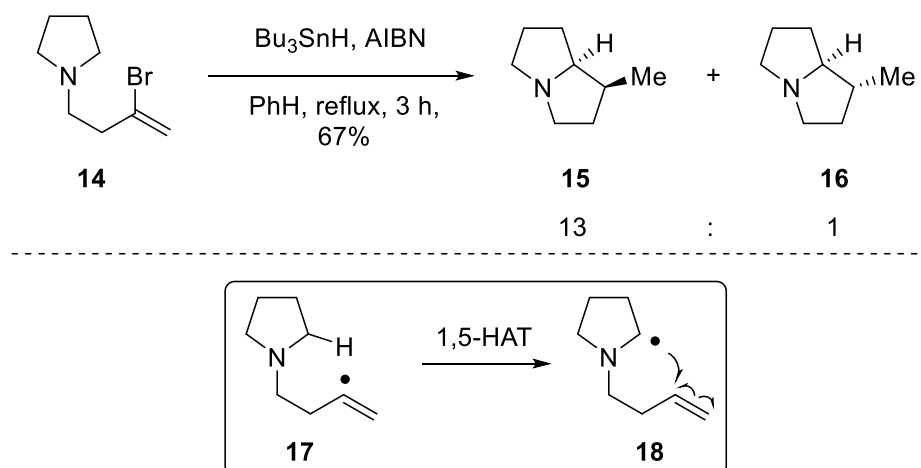
**Scheme 4.** Radical quenching of the vinyl radical as key step in the synthesis of (+)-biotin.<sup>[26]</sup>  
Cy = cyclohexyl.



**Scheme 5.** Tandem radical cyclization by Padwa *et al.*<sup>[35]</sup>

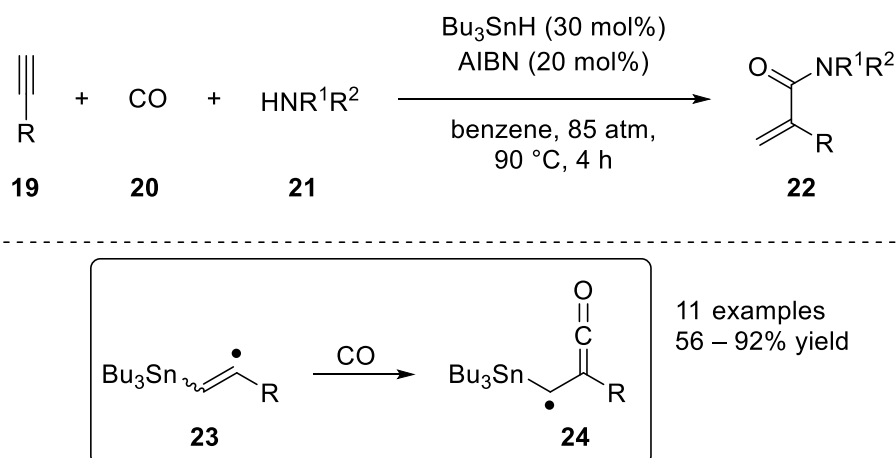
Radical translocations emerged as a powerful tool in organic chemistry.<sup>[37]</sup> Often being considered as a side reaction, such rearrangements proved to be surprisingly predictable and controllable. The most commonly translocations involve a 1,5-,<sup>[14,16,38-42]</sup> or 1,6-HAT<sup>[43-45]</sup> (HAT = hydrogen atom transfer). The group of Pillai successfully demonstrated that vinyl

radicals efficiently undergo 1,5-HAT and such translocations can be applied for the synthesis of ( $\pm$ )-heliotridane **15** (Scheme 6).<sup>[46]</sup> The vinyl radical **17** is generated upon homolytic bromide abstraction from  $\text{Bu}_3\text{Sn}^\bullet$  which undergoes 1,5-HAT to  $\alpha$ -amino radical **18**. Subsequent 5-*exo*-trig cyclization and quenching of the primary radical gives rise to the final product.



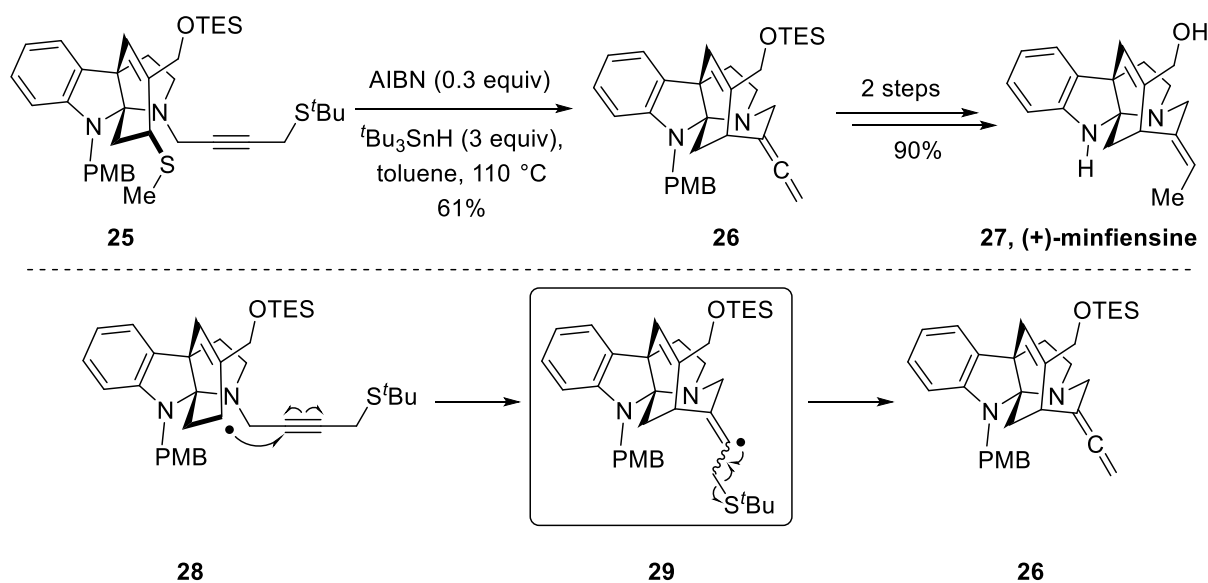
**Scheme 6.** Radical translocation of vinyl radical **17** as key step in the synthesis of ( $\pm$ )-heliotridane (**15**).<sup>[46]</sup>

The group of Ryu successfully achieved alkyne carbonylation with radicals (Scheme 7).<sup>[47]</sup> In this report, a vinyl radical is produced by addition of tributyl stannane radical  $\text{Bu}_3\text{Sn}^\bullet$  to alkyne **19**. The corresponding vinyl radical **23** undergoes carbonylation to generate a  $\alpha$ -ketenyl radical **24**. Addition of amine **21** and subsequent 1,4-H shift affords the final product **22** in moderate to excellent yields.



**Scheme 7.** Trapping of the vinyl radical **23** with carbon monoxide.<sup>[47]</sup>

In 2009, MacMillan and co-workers reported an enantioselective total synthesis of (+)-minfiensine (**27**) in nine steps with an overall yield of 21%. This synthetic route featured a cascade organocatalytic sequence to construct the central tetracyclic pyrroloindoline core **25** (not depicted), followed by a 6-*exo*-dig radical cyclization with  $t\text{Bu}_3\text{SnH}$  and AIBN to give the final piperidinyll scaffold **26** (Scheme 8).<sup>[48]</sup>



**Scheme 8.** Enantioselective total synthesis of (+)-minfiensine by MacMillan in 2009.<sup>[48]</sup>  
TES = Triethylsilyl ether; PMB = 4-Methoxybenzyl ether.

Although the combination of trialkyltin hydrides and AIBN has been well-established to initiate radical transformations, the presented work commonly suffered from decisive drawbacks. Stoichiometric amounts or even an excess of highly toxic organotin compounds were required. Combined with harsh activation conditions such as high temperatures or hazardous UV-light, considerable concerns were raised about the necessity of these ecologically questionable conditions.<sup>[49]</sup> As soon as the toxic properties associated with organotin compounds became public, it has become a global interest to search for more sustainable alternatives. Reaction procedures using only catalytic amounts of  $\text{Bu}_3\text{SnH}$  should reduce tin-contaminated waste,<sup>[50]</sup> tin-recycling systems were developed to relieve the environment,<sup>[51]</sup> or organotin hydride substituents were introduced.<sup>[49,52]</sup> However, it would be much more desirable to completely switch to more benign activation methods.

Herein, visible light mediated photoredox catalysis represents an elegant solution. Although first pioneering work was already described by the groups of Kellogg,<sup>[53,54]</sup> Deronizer,<sup>[55]</sup>

Okada,<sup>[56]</sup> and others<sup>[57-59]</sup> in the late 1970s, only little attention was given to this process. However, 30 years later, this activation methodology attracted full attention. Yoon's success on the [2+2] cycloaddition of enones,<sup>[60]</sup> MacMillan's work on asymmetric alkylation of aldehydes,<sup>[61]</sup> and Stephenson's protocol for hydrodehalogenation were considered to be groundbreaking.<sup>[62]</sup>

The following two sections will first briefly introduce the underlying physical processes in a common photoredox catalyzed reaction and subsequently summarize major contributions in this area referring to the generation and functionalization of vinyl radicals with visible light.

## 2 Photophysical background of photocatalysts

The principle behind visible light driven processes is the employment of photocatalysts which are capable of absorbing photons in this specific region of the electromagnetic spectrum. This is essential since most organic molecules are not able to interact with visible light.<sup>[63]</sup> These common molecules can only be excited by highly unfavorable UV-light.<sup>[23]</sup> However, this is usually undesired because chemical transformations might suffer from selectivity problems or decomposition of substrates. Additionally, reactions associated with very energetic UV-light are afflicted with safety hazards, and require cost-intensive light sources as well as glassware.<sup>[64]</sup> However, these issues can be ingeniously circumvented by photoredox catalysis. Instead of harmful UV-light, photocatalysts can be employed which can transfer single electrons (SET = single electron transfer) upon excitation with mild and benign visible light.<sup>[23]</sup> Herein, established photocatalysts are typically based on transition metal complexes<sup>[65,66]</sup> or organic dyes.<sup>[67-69]</sup> Despite the cost-efficiency of organic chromophores, problems can arise from high catalyst loadings and instability or degradation under certain reaction conditions.<sup>[69]</sup> Therefore, transition metal complexes are generally considered to be superior. In this regard, the most powerful complexes are based on ruthenium and iridium complexes with polypyridyl ligands (Figure 1).<sup>[22,65,70-72]</sup> However, photochemical transformations driven by copper have also found great applications due to its unique behavior compared to the latter.<sup>[73-78]</sup>



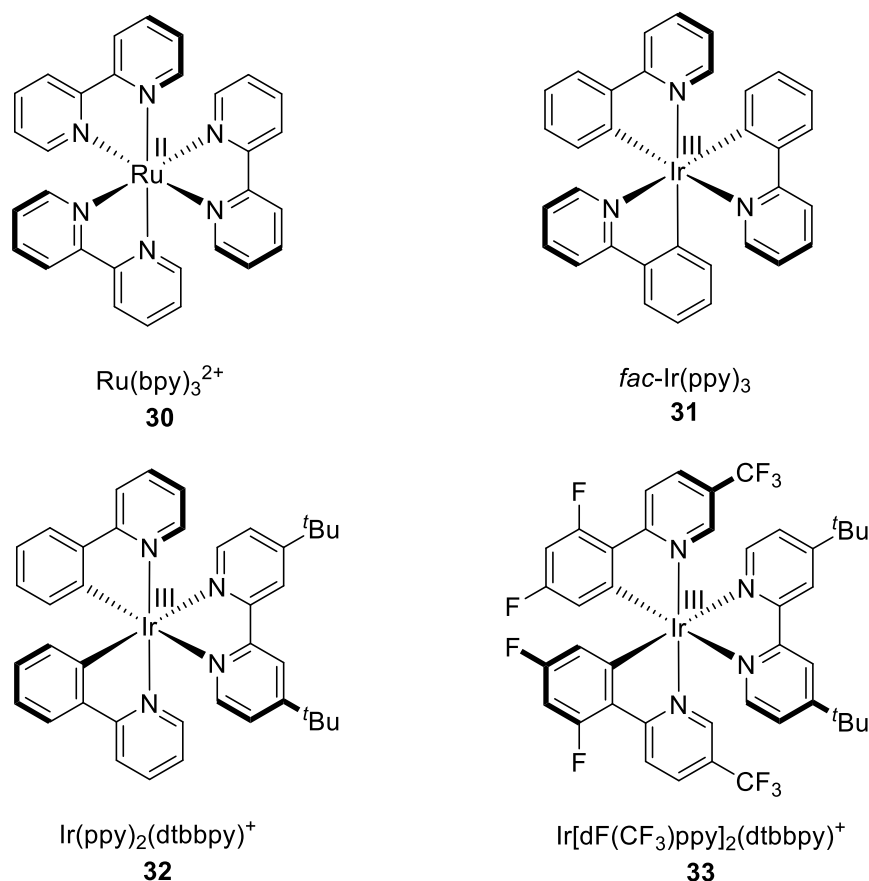
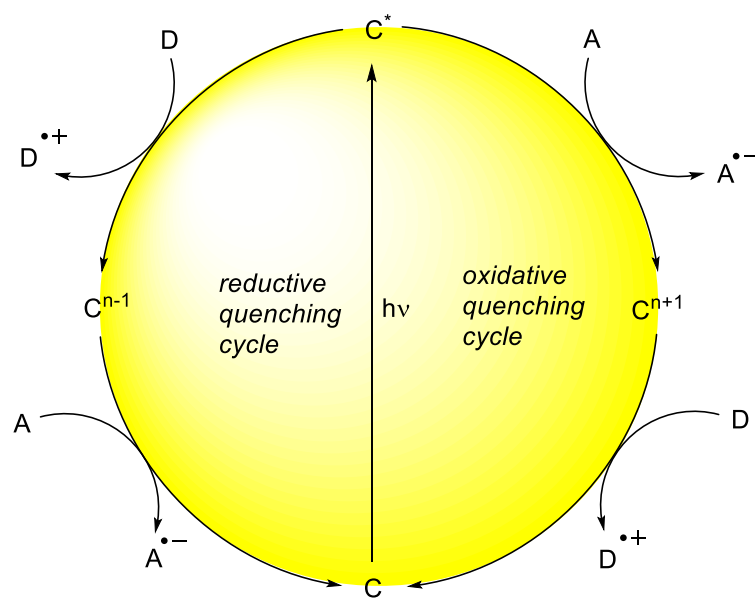


**Figure 1.** Selected example of commonly employed transition metal photocatalysts.

To understand the following visible light mediated transformations and to get familiar with the commonly used terminology, it is inevitable to concisely introduce the photophysical processes behind these reactions. Such photocatalysts as depicted in Figure 1 exhibit strong absorption bands in the visible region of the light spectrum. Upon irradiation with a specific wavelength from simple LEDs, fluorescent light bulbs or Xe lamps, the photocatalyst **C** gains energy and reaches a long-lived excited state **C**<sup>\*</sup> (Scheme 9).<sup>[72]</sup> In this particular state, the photocatalyst is a powerful reducing as well as oxidizing agent. Therefore, the photocatalyst can either donate one single electron to the substrate **A** which oxidizes the catalyst (oxidative quenching cycle) or accept one electron from the substrate **D** which reduces the catalyst (reductive quenching cycle). As a result, this gives highly reactive intermediates **A**<sup>•-</sup> or **D**<sup>•+</sup> and simultaneously an oxidized (**C**<sup>n+1</sup>) or reduced (**C**<sup>n-1</sup>) species of the catalyst (n = oxidation state of the catalyst). To regenerate the catalyst, the opposed process needs to take place in order to regain its ground state **C**. Ideally, **D** and **A** can be assigned to the same molecule which makes this process highly efficient and economically valuable as no chemical waste is

produced. However, reactions for which only one substrate is of interest, so-called sacrificial electron donors or acceptors can be utilized. This helps to close the catalytic cycle or to access more redox active species of the catalyst. For example, tertiary amines are very prevalent reagents to serve as reductants due to the availability and low cost.<sup>[79]</sup> However, caution is required as these oxidized amines are excellent radical hydrogen donors (HAT = hydrogen atom transfer), meaning they can easily quench radical intermediates which often results in undesired by-products.<sup>[79]</sup> As sacrificial electron acceptor,<sup>[79]</sup> methyl viologen can be employed.<sup>[80,81]</sup> The reaction pathway taking place depends on each individual reaction and can often be tailored by careful refinement of the conditions. For example, each photocatalyst in each electrochemical half reaction exhibit unique redox properties. As a rule of thumb, it is generally valid that the reduced catalyst  $C^{n-1}$  is a stronger reductant and similarly the oxidized catalyst  $C^{n+1}$  a better oxidant compared to the excited state of the catalyst  $C^*$ . This principle is often exploited when challenging substrate with high redox potentials are employed.<sup>[82,83]</sup>



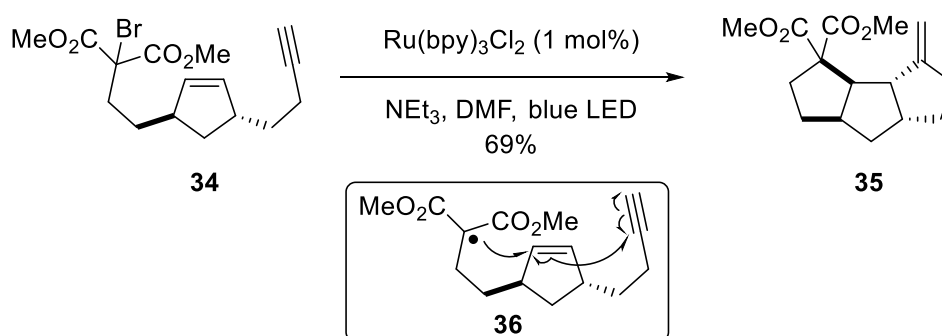
**Scheme 9.** General overview of a photoredox catalytic process.

This compact summary of a visible light mediated process should help to understand the following chemical transformations. The photophysical background of common photocatalysts has been well studied and fully characterized in the past,<sup>[73,84-91]</sup> and these processes along with photophysical properties of the catalysts have already been discussed and tabulated multiple times much more in detail in related articles.<sup>[23,66,70,72,92]</sup>

### 3 Reactions of vinyl radicals promoted by visible light

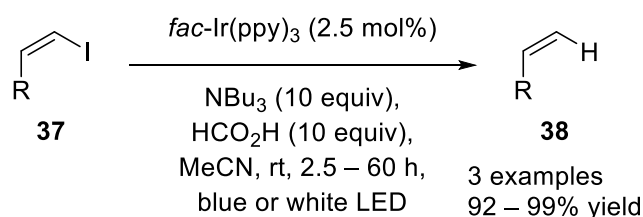
With the revival of visible light photoredox catalysis by the group of Yoon, MacMillan and Stephenson, not much time went by until first reactions involving vinyl radicals as intermediates were reported. The following part should summarize major contributions in this area which have been achieved up to this date.

In 2010, Stephenson and co-workers discovered a method for the single electron reduction of bromomalonate **34** with visible light.<sup>[93]</sup> Upon irradiation, the reductively quenched catalyst transfers one single electron to **34**. The resulting radical first reacts intramolecularly with cyclopentene, followed by a 5-*exo*-dig ring closure. Subsequently, the resulting vinyl radical intermediate is quenched *via* hydrogen atom transfer (HAT) by previously oxidized  $\text{NEt}_3$  (Scheme 10).



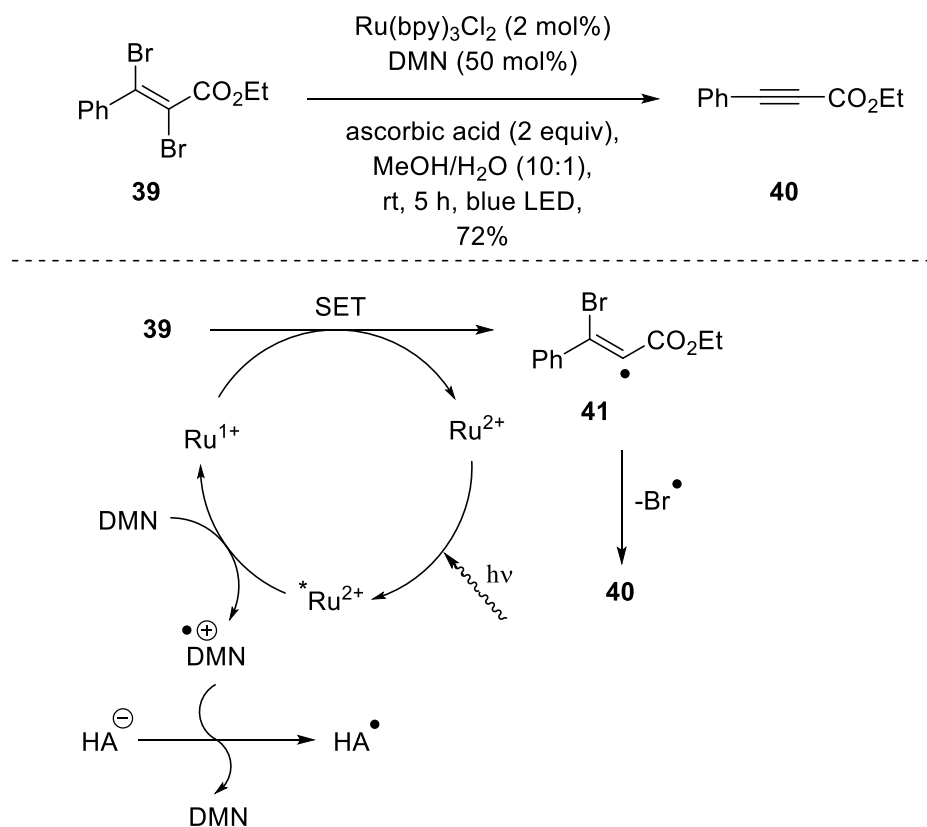
**Scheme 10.** Tin-free radical cyclization initiated by visible light photoredox catalysis.<sup>[93]</sup>

Later, they were able to further expand the scope for dehalogenations to unactivated vinyl halides as depicted in Scheme 11. Utilizing the reductive quenching cycle of *fac*- $\text{Ir}(\text{ppy})_3$ , several vinyl iodides **37** were subjected to optimized photochemical conditions yielding hydrodehalogenated products **38** in excellent yields.<sup>[94]</sup>



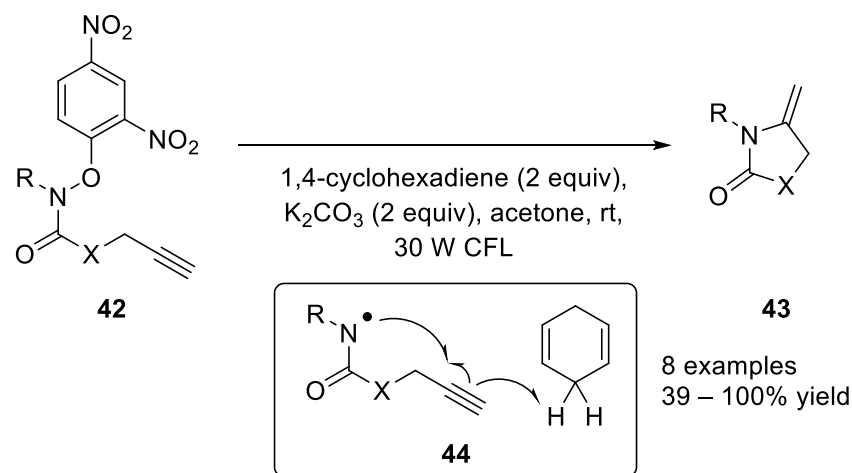
**Scheme 11.** Tin-free radical dehalogenation of unactivated vinyl iodides **37**.<sup>[94]</sup>

Reiser and co-workers investigated the combination of 1,5-dimethoxynaphthalene (DMN) and ascorbic acid for the reductive debromination with visible light (Scheme 12).<sup>[95]</sup> Herein, the vinyl radical is directly formed upon activation of vinyl bromide **39**. The resulting vinyl radical **41** undergoes fast halide elimination to give **40**.



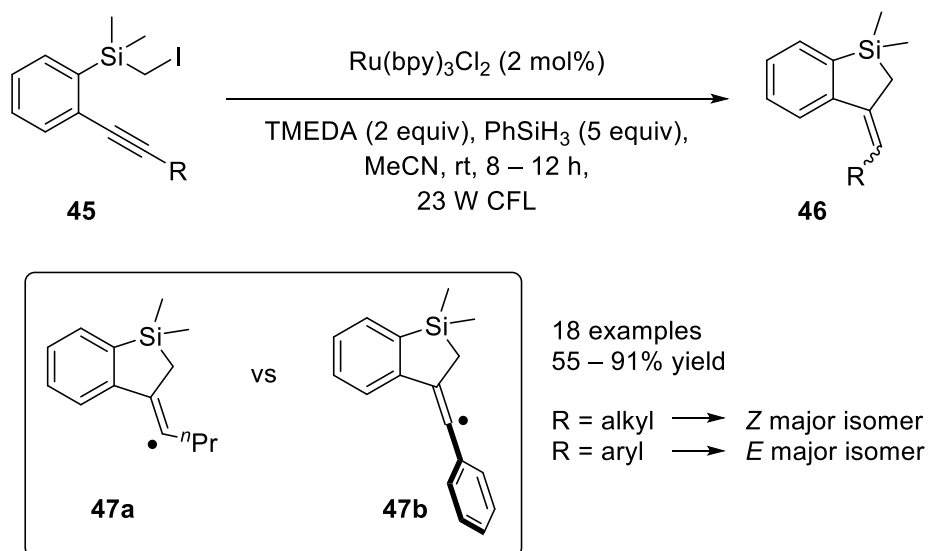
**Scheme 12.** Photocatalytic reductive debromination of *vic*-dibromoalkene **39**.<sup>[95]</sup> HA<sup>-</sup> = Ascorbate ion.

Nitrogen-centered radicals were generated from electron-poor aryloxyamides **42** using visible light from a compact fluorescent lamp by the group of Leonori (Scheme 13).<sup>[96]</sup> These amidyl radicals readily undergo intramolecular 5-*exo*-dig ring closure which gives rise to a vinyl radical. Hydrogen abstraction from 1,4-cyclohexadiene gave the final product in moderate to high yields. However, during their studies the authors noticed that the reaction also worked in the absence of a photocatalyst which made a mechanistical proposal for the initial N-O fragmentation difficult.



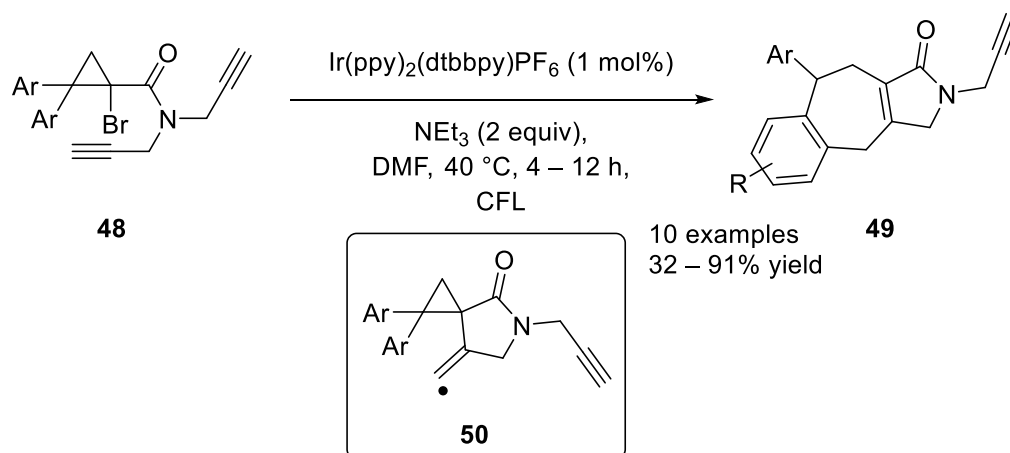
**Scheme 13.** Visible light promoted 5-*exo*-dig cyclization of amidyl radicals.<sup>[96]</sup>

Furthermore, Song *et al.* have proven that substituents of terminal alkynes can have a beneficial effect on the diastereoselectivity (Scheme 14).<sup>[97]</sup> Herein, they showed that alkyl substituents adjacent to the vinyl radical gave predominantly the *Z*-isomers while aryl groups resulted in *E*-isomers, respectively. The authors assumed that H-abstraction from  $\text{PhSiH}_3$  might be one of the key factors and concluded that the configuration of the vinyl radical defined the stereoselective outcome.



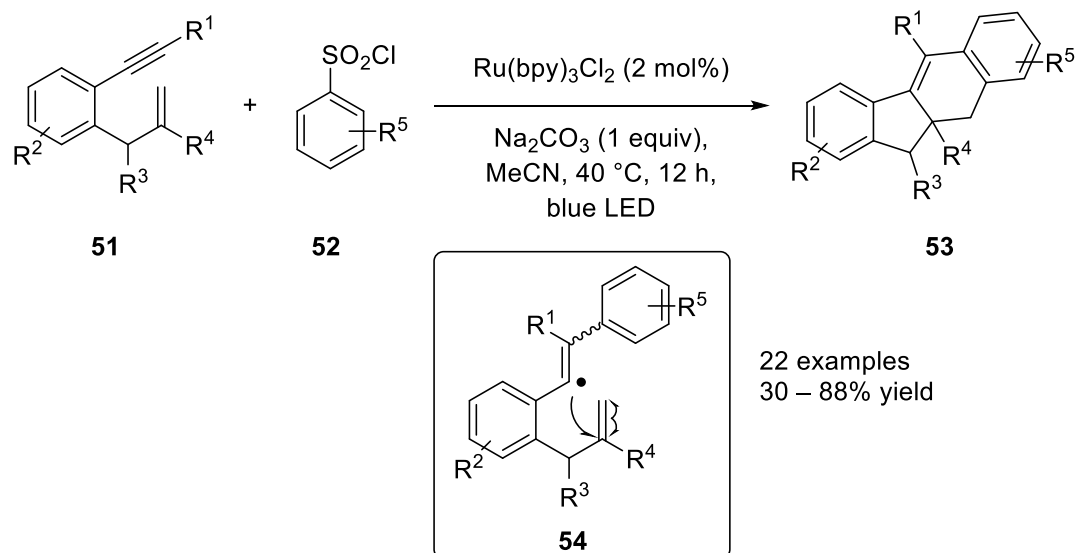
**Scheme 14.** Visible light mediated synthesis of benzosilolines.<sup>[97]</sup>

Stephenson *et al.* demonstrated that bromocyclopropanes could undergo a radical cyclization cascade after visible light promoted single electron reduction (Scheme 15).<sup>[98]</sup> The vinyl radical **50** is formed after 5-*exo*-dig cyclization of the cyclopropyl radical and the alkyne. However, the full reaction mechanism to product **49** was unclear as several potential mechanistic pathways were proposed to construct the seven-membered ring **49**.



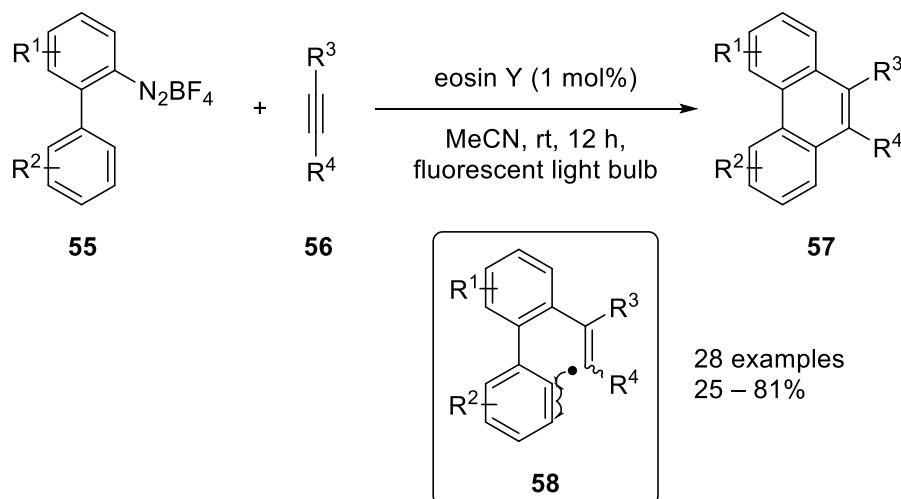
**Scheme 15.** Visible light mediated tandem cyclization of bromocyclopropanes **48**.<sup>[98]</sup>

Li and co-workers disclosed a tandem cyclization of 1,6-enynes with arylsulfonyl chlorides by using visible light photoredox catalysis (Scheme 16).<sup>[99]</sup> This protocol tolerates a great variety of substitution patterns. The vinyl radical intermediate is formed after addition of the aryl radical to the alkyne **51** which subsequently undergoes a tandem cyclization to construct the polycyclic ring system **53** which is a ubiquitous motif and can be found in many natural products, biomolecules, and optoelectronic materials.



**Scheme 16.** Tandem cyclization of 1,6-enynes with aryl sulfonyl chlorides.<sup>[99]</sup>

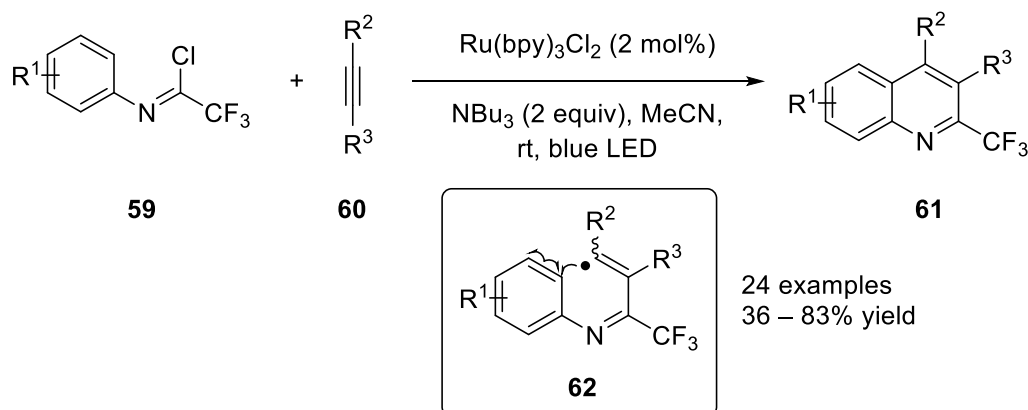
A novel [4+2] benzannulation protocol was developed by the group of Zhou (Scheme 17).<sup>[100]</sup> Here, aryl radicals are generated from aryl diazonium salts **55** which can readily react with alkynes **56**, resulting in a vinyl radical intermediate **58** which can further cyclize with the ring system. Oxidation to the cation regenerates the photocatalyst and re-aromatization gives product **57**.



**Scheme 17.** Visible light mediated synthesis of phenanthrenes **57**.<sup>[100]</sup>

Zhou *et al.* have proven that trifluoroacetimidoyl chlorides **59** serve as an excellent source for trifluoroacetimidoyl radicals under visible light photoredox conditions (Scheme 18).<sup>[101]</sup>

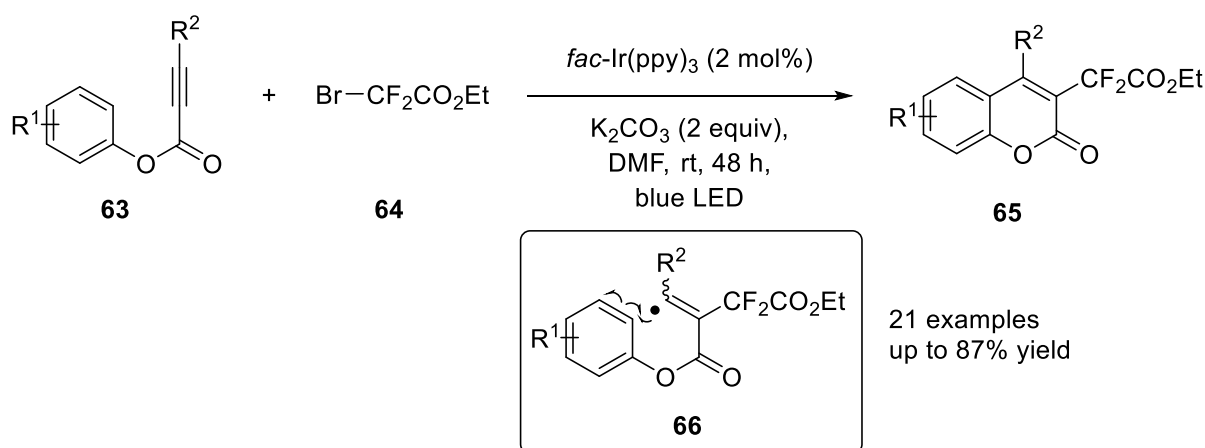
Utilizing the reductive quenching cycle, the photocatalyst  $\text{Ru}(\text{bpy})_3\text{Cl}_2$  is able to cleave the C-Cl bond of **59**. Radical addition to the alkyne affords a vinyl radical intermediate **62** which subsequently cyclizes with the aromatic ring to form 2-trifluoromethyl quinoline **61**.



**Scheme 18.** Visible light induced radical cyclization of trifluoroacetimidoyl chlorides.<sup>[101]</sup>

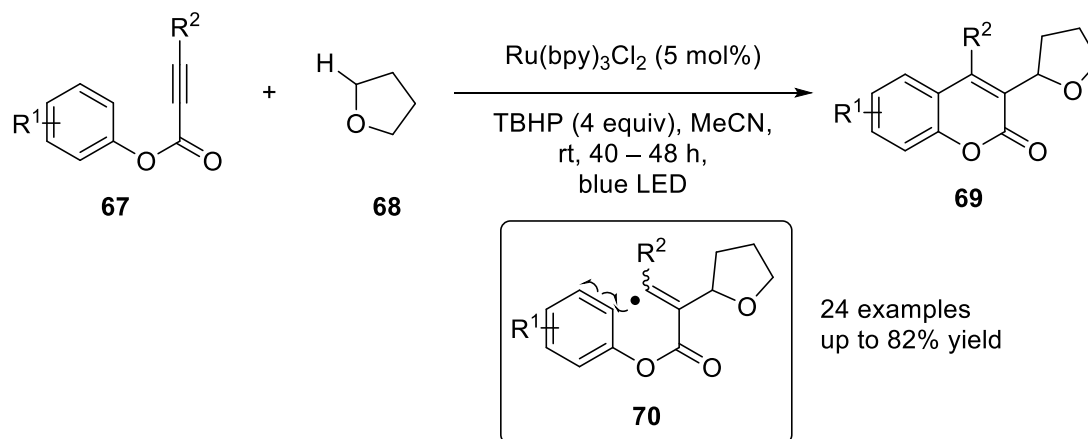
Recently, Ji *et al.* described a mild and efficient method for the synthesis of 3-difluoroacetylated coumarins *via* visible light (Scheme 19).<sup>[102]</sup> Herein, a  $\cdot\text{CF}_2\text{CO}_2\text{Et}$  radical was formed from **64** by oxidative quenching of the excited photocatalyst *fac*- $\text{Ir}(\text{ppy})_3$ . Radical addition to the triple bond affords a vinyl radical which undergoes intramolecular radical cyclization to construct difluorosubstituted coumarins. The proposed mechanism was supported by TEMPO trapping of the  $\cdot\text{CF}_2\text{CO}_2\text{Et}$  radical. However, the scope of the reaction was limited to  $\text{Br-CF}_2\text{CO}_2\text{Et}$  as the authors failed to transfer this protocol to  $\text{Br-CHF}_2\text{CO}_2\text{Et}$  or  $\text{Br-CF}_2\text{PO}(\text{OEt})_2$ . Later, the substrate scope was further extended to construct indenones under very similar reaction conditions by Rastogi and co-workers.<sup>[103]</sup>





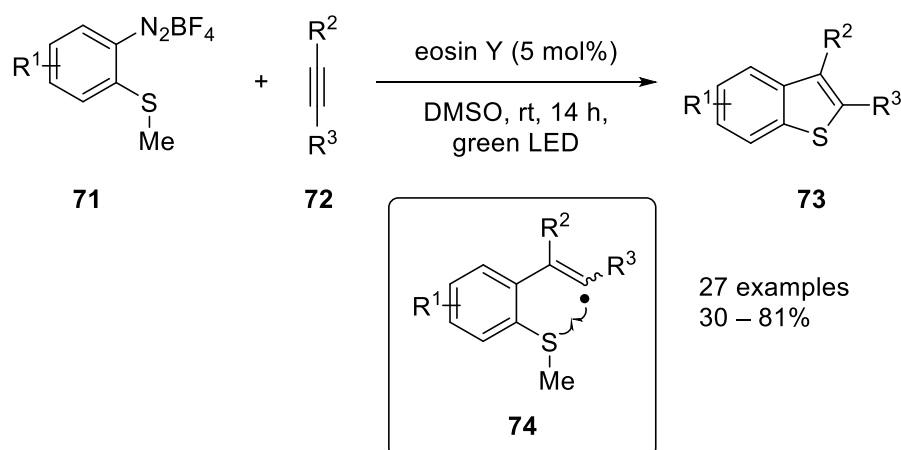
**Scheme 19.** Visible light mediated radical aryldifluoroacetylation of alkynes.<sup>[102]</sup>

A very similar reaction was developed by She and co-workers in 2016 (Scheme 20).<sup>[104]</sup> In this report, THF served as source for  $\alpha$ -oxo radicals *via* hydrogen abstraction from *tert*-butoxyl radicals which were formed upon single electron reduction of *tert*-butoxyl radicals (TBHP). Apart from that, the reaction mechanism is congruent with the previously discussed transformation.



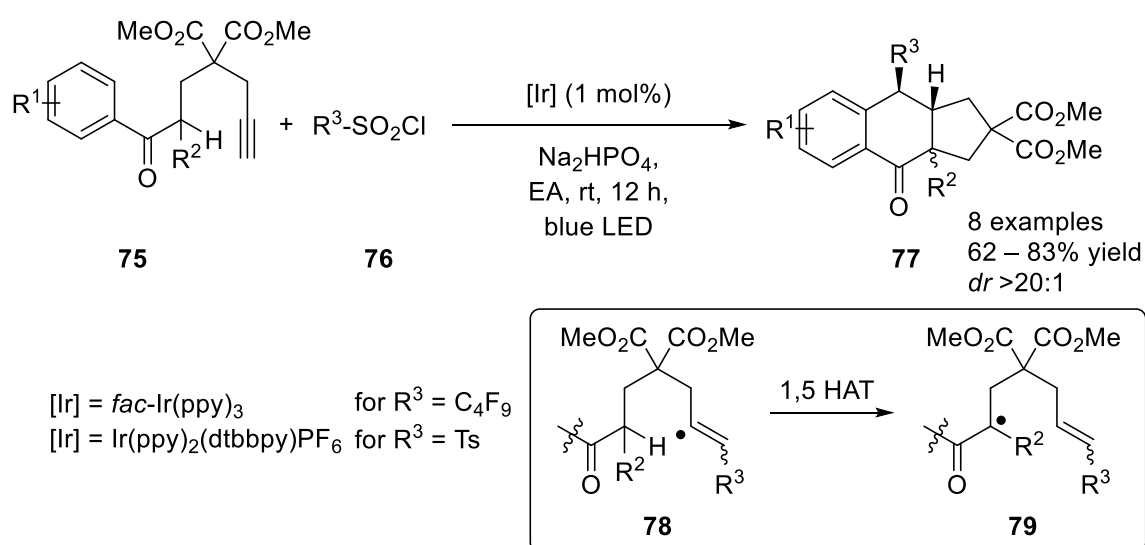
**Scheme 20.** Visible light promoted synthesis of substituted coumarins **69**.<sup>[104]</sup>

König *et al.* utilized aryl diazonium salts **71** as precursors for aryl radicals under metal-free conditions with eosin Y as photocatalyst (Scheme 21).<sup>[105]</sup> This aryl radical readily reacts with an excess of alkyne **72** resulting in a vinyl radical intermediate **74** which is capable of cyclizing at the sulfur position. The proposed mechanism is supported by successful TEMPO trapping of both the aryl radical and the vinyl radical intermediate.



**Scheme 21.** Visible light photocatalytic synthesis of benzothiophenes **73**.<sup>[105]</sup>

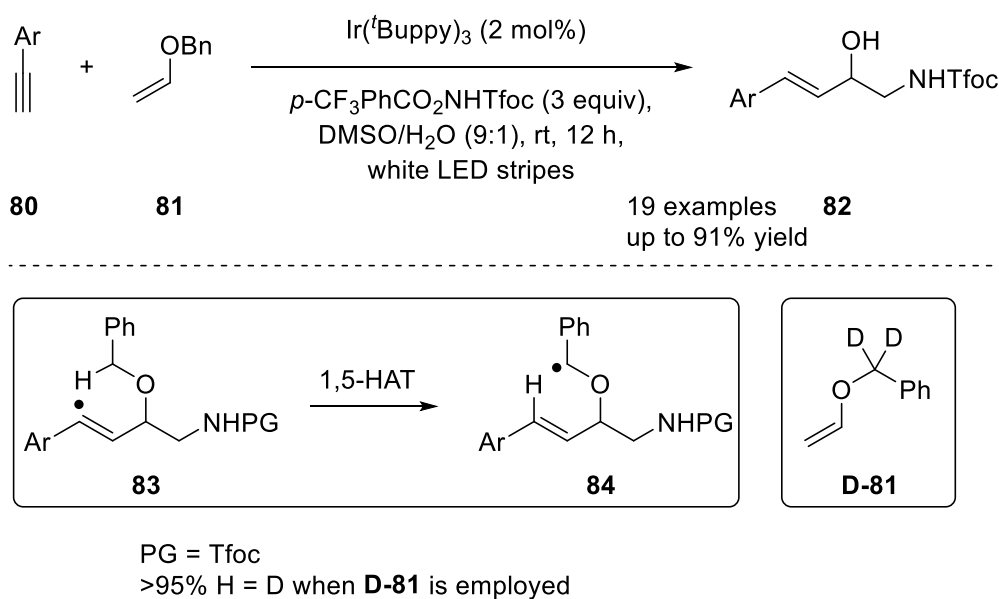
Recently, the group of Liu developed a stereoselective radical cyclization cascade of sulfonyl chlorides **76** with terminal alkynes **75** (Scheme 22).<sup>[106]</sup> The key elementary step in this transformation includes a 1,5-hydrogen transfer of the vinyl radical intermediate **78** which is followed by a stereoselective 5-*exo*-trig cyclization.



**Scheme 22.** Stereoselective radical cyclization cascade.<sup>[106]</sup>

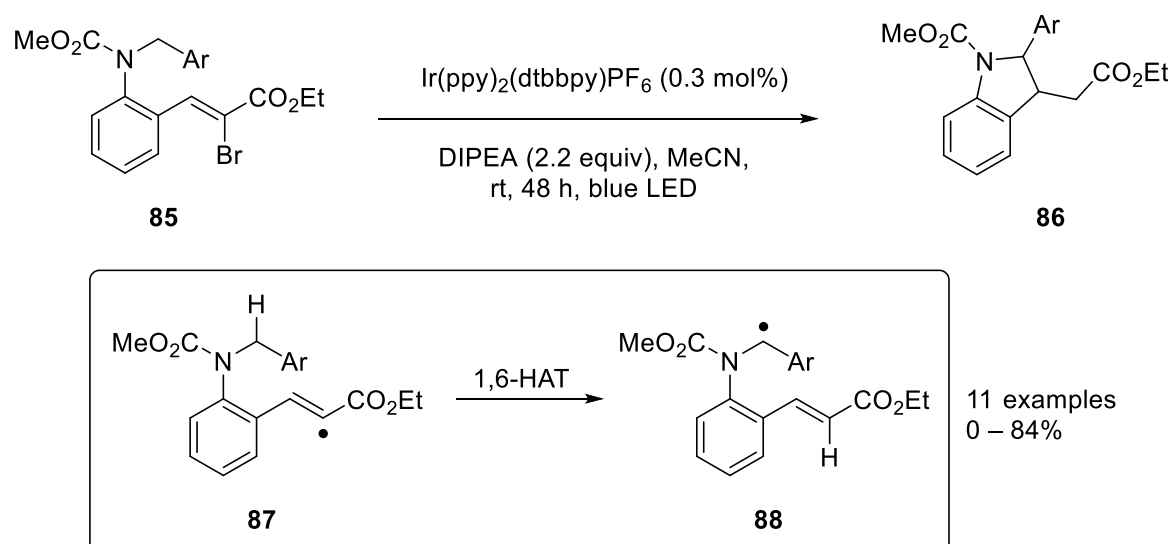
A novel synthesis of  $\beta$ -amino alcohol derivatives **82** was achieved by the group of Yu (Scheme 23).<sup>[107]</sup> Reductive cleavage of *p*-CF<sub>3</sub>PhCO<sub>2</sub>NHTfoc by the excited photocatalyst produces a nitrogen-centered radical ( $\dot{\text{N}}\text{HTfoc}$ ). This electrophilic N-radical adds to the electron rich double bond of **81**. Subsequently, the electron rich radical intermediate reacts

with comparably electron poor alkyne **80** to produce a vinyl radical intermediate **83**. The key step of this synthesis is a 1,5-HAT of this vinyl radical which gives rise to a  $\alpha$ -oxo radical **84**. This radical is oxidized to the cation, therefore regenerating the photocatalyst and generating the final product upon nucleophilic substitution with H<sub>2</sub>O forming benzaldehyde as stoichiometric by-product. The 1,5-HAT as key step is supported by deuterated benzyl vinyl ether **D-81** which gives rise to >95% deuteration of the vinyl proton in the final product.



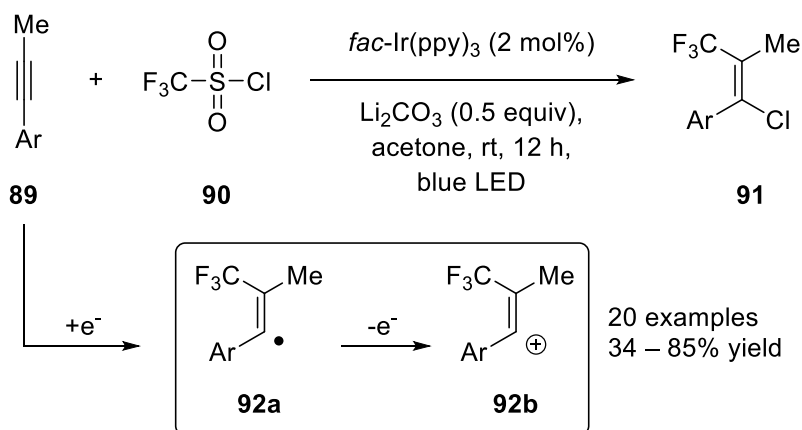
**Scheme 23.** Photoredox induced radical relay toward functionalized  $\beta$ -amino alcohol derivatives.<sup>[107]</sup>  
Tfoc = 2,2,2-trifluoroethoxy carbonyl.

A tandem cyclization of vinyl radicals to access indolines was investigated by Reiser and co-workers (Scheme 24).<sup>[108]</sup> The authors propose single electron transfer to cleave the C-Br bond in **85** by reductively quenched iridium photocatalyst Ir(ppy)<sub>2</sub>(dtbbpy)PF<sub>6</sub>. The resulting vinyl radical **87** readily undergoes 1,6-HAT which affords  $\alpha$ -amino radical **88**. Cyclization with the double bond and quenching of the alkyl radical by previously oxidized amine produces the final product **86** and closes the catalytic cycle.



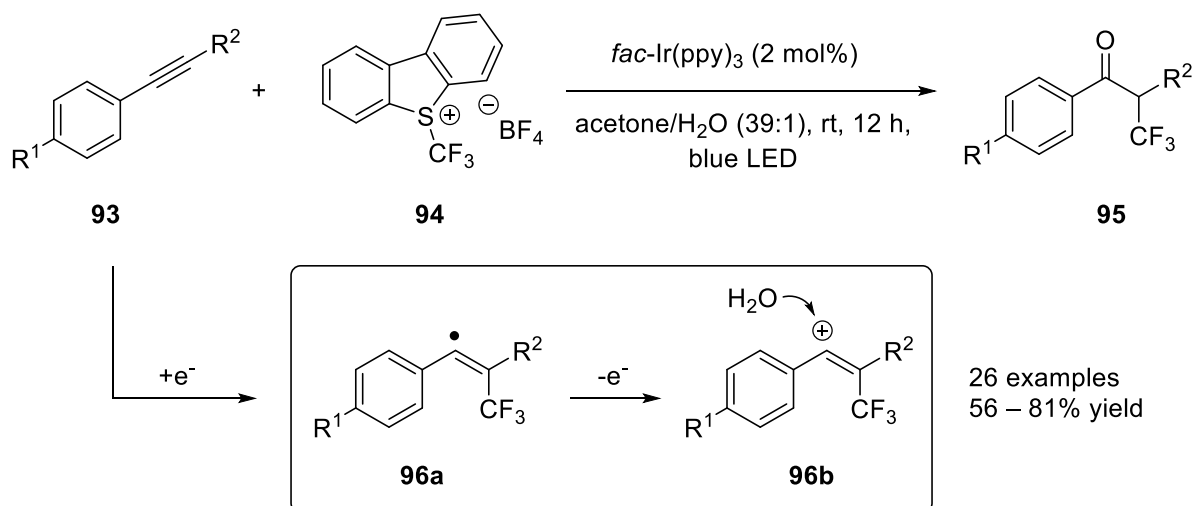
**Scheme 24.** Hydrogen atom transfer as key step to approach indolines promoted by visible light.<sup>[108]</sup>

Very recently, Han and *et al.* disclosed a stereoselective chlorotrifluoromethylation of alkynes using visible light (Scheme 25).<sup>[109]</sup> Utilizing the oxidative quenching cycle of excited photocatalyst *fac*-Ir(ppy)<sub>3</sub> leads to decomposition of commercially available triflyl chloride (**90**). The resulting electron poor trifluoromethyl radical adds to alkyne **89** which gives a vinyl radical intermediate. To close the catalytic cycle, the authors propose oxidation of the vinyl radical to the corresponding cation which is trapped by previously formed Cl<sup>-</sup>. This transformation produced tetrasubstituted alkenes **91** which could further be utilized in Suzuki-coupling reactions. The stereoselectivity is assumed by the stabilization effect of the aromatic ring adjacent to the vinyl radical. This established protocol could also be extended to sulfonyl chlorides as coupling partners which led to chlorosulfonylated products.<sup>[110]</sup>



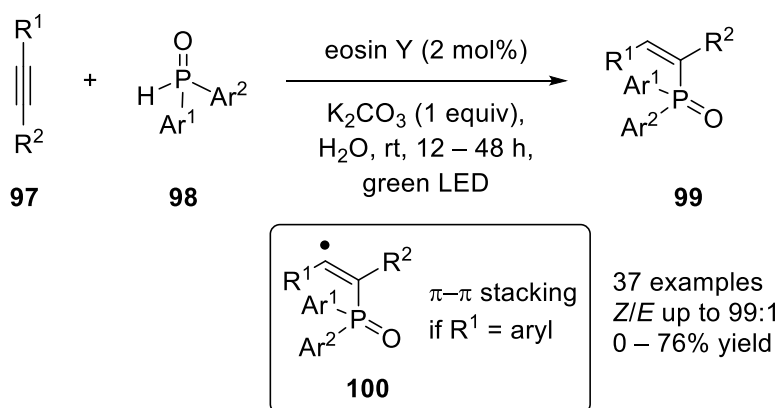
**Scheme 25.** Stereoselective chlorotrifluoromethylation of alkynes by visible light photoredox catalysis.<sup>[109]</sup>

Later, the same group published a similar protocol to access different  $\alpha$ -trifluoromethyl ketones in moderate to high yields (Scheme 26).<sup>[111]</sup> This time, Umemoto's reagent (**94**) was utilized as CF<sub>3</sub> radical precursor. Upon radical addition of the CF<sub>3</sub> radical to the triple bond, the authors again propose the oxidation of the vinyl radical to the cation which is subsequently trapped by H<sub>2</sub>O. The final product is formed after deprotonation and keto-enol tautomerism. The mechanistical proposal is supported by D<sub>2</sub>O and H<sub>2</sub><sup>18</sup>O labeling control experiments. Both the deuterated proton as well as the <sup>18</sup>O isotope were found to be highly enriched in the final product **95**.



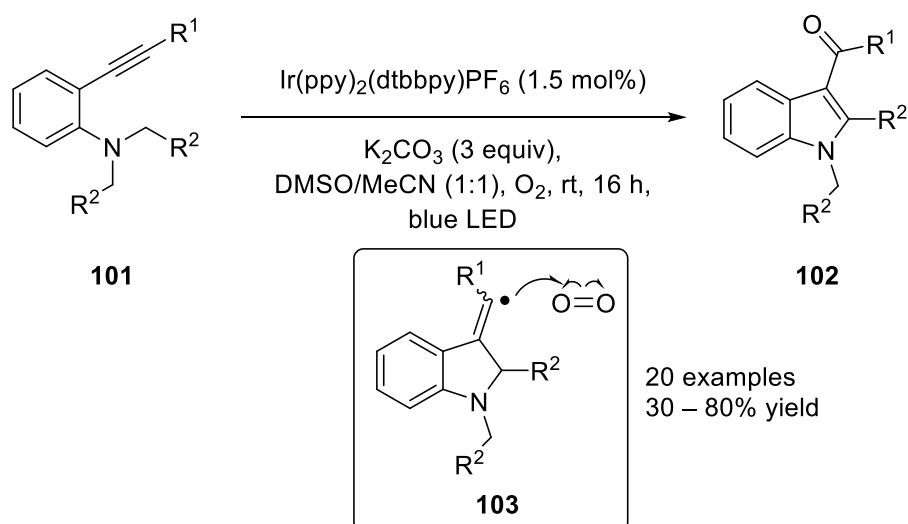
**Scheme 26.** Multicomponent oxidative trifluoromethylation of alkynes *via* photoredox catalysis.<sup>[111]</sup>

Using visible light and eosin Y as organic dye, Lei *et al.* reported a *Z*-selective radical addition of diaryl phosphine oxides **98** to alkynes **97** in H<sub>2</sub>O (Scheme 27).<sup>[112]</sup> Reductive quenching of excited photocatalyst gives rise to a phosphinoyl radical after proton-coupled electron transfer (PCET). Subsequently, the radical adds to the triple bond of the alkyne resulting in a vinyl radical intermediate. The authors propose reduction of this vinyl radical to the corresponding anion by the organic dye which closes the catalytic cycle. Protonation of the anion gives the final product. The high selectivity is presumed to be due to the strong  $\pi$ - $\pi$  stacking interactions of both the aromatic ring of the phenyl acetylene as well as the aromatic substituents at the phosphorus atom. The mechanistical proposal is supported by isotope-labeling studies with D<sub>2</sub>O.



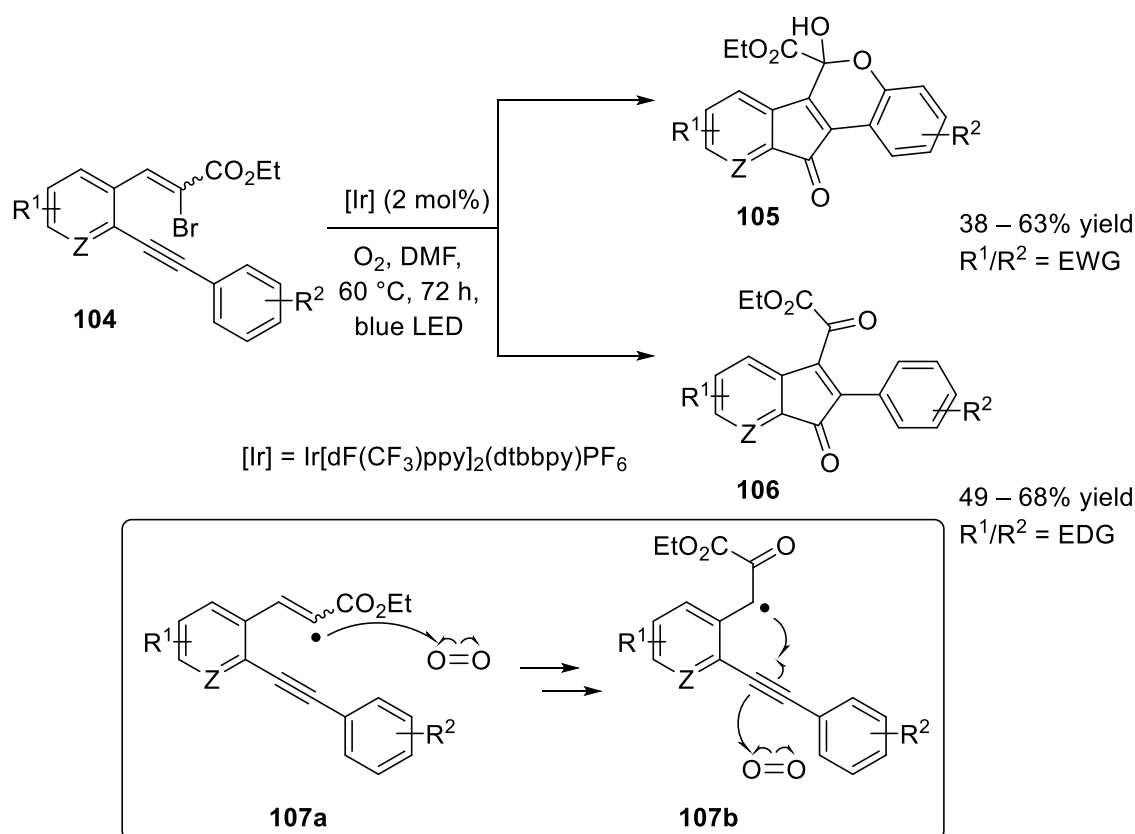
**Scheme 27.** *Z*-selective addition of diaryl phosphine oxides to alkynes under visible light photoredox conditions.<sup>[112]</sup>

A novel synthesis of 3-acylindoles **102** was achieved by Zhou and co-workers (Scheme 28).<sup>[113]</sup> The nitrogen atom of substrate **101** can easily be oxidized to the radical cation by the excited photocatalyst which makes the  $\alpha$ -amino C-H bond in the molecule significantly acidic. As a result, **101** readily loses a proton to give the  $\alpha$ -amino radical.<sup>[79]</sup> After 5-*exo*-dig cyclization, the corresponding vinyl radical **103** is trapped by molecular oxygen, eventually leading to **102** after regeneration of the catalyst, together with H<sub>2</sub>O as the only stoichiometric by-product. However, the authors could not completely rule out the possibility that oxygen sources other than O<sub>2</sub> might be responsible for the carbonyl functionality in the end.



**Scheme 28.** Visible light mediated synthesis of 3-acylindoles **102**.<sup>[113]</sup>

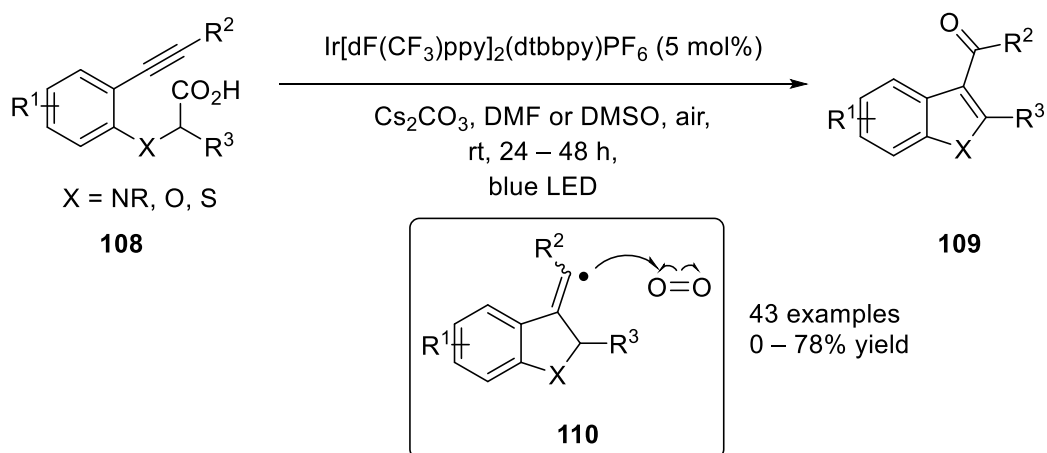
Recently, Reiser and co-workers contrived a novel visible light promoted activation of  $\alpha$ -bromo cinnamates by energy transfer mechanism (Scheme 29).<sup>[114]</sup> Due to the long excited-state lifetime ( $\tau = 2300$  ns),<sup>[70]</sup>  $\text{Ir}[\text{dF}(\text{CF}_3)\text{ppy}]_2(\text{dtbbpy})\text{PF}_6$  is able to transfer the energy to extended  $\pi$ -systems such as  $\alpha$ -bromo cinnamate derivatives **104**. This results in homolytic cleavage of the C-Br bond. Subsequently, the vinyl radical intermediate is trapped by molecular oxygen which eventually leads to a  $\alpha$ -keto radical. This radical undergoes 5-*endo*-dig cyclization resulting in another vinyl radical intermediate which is, again, trapped by  $\text{O}_2$ . It is notable that molecules bearing electron withdrawing substituents in the starting material undergo  $6\pi$ -electrocyclization which give rise to dihydroindeno[1,2-*c*]chromenes **105**, whereas electron donating groups result in indenones **106**. The reaction mechanism is supported by several control experiments including different  $^{18}\text{O}_2$  labeling experiments which revealed that molecular oxygen is, indeed, incorporated two times in the reaction process.



**Scheme 29.** Visible light promoted synthesis of dihydroindeno[1,2-*c*]chromenes **105** and indenones **106**.<sup>[114]</sup>

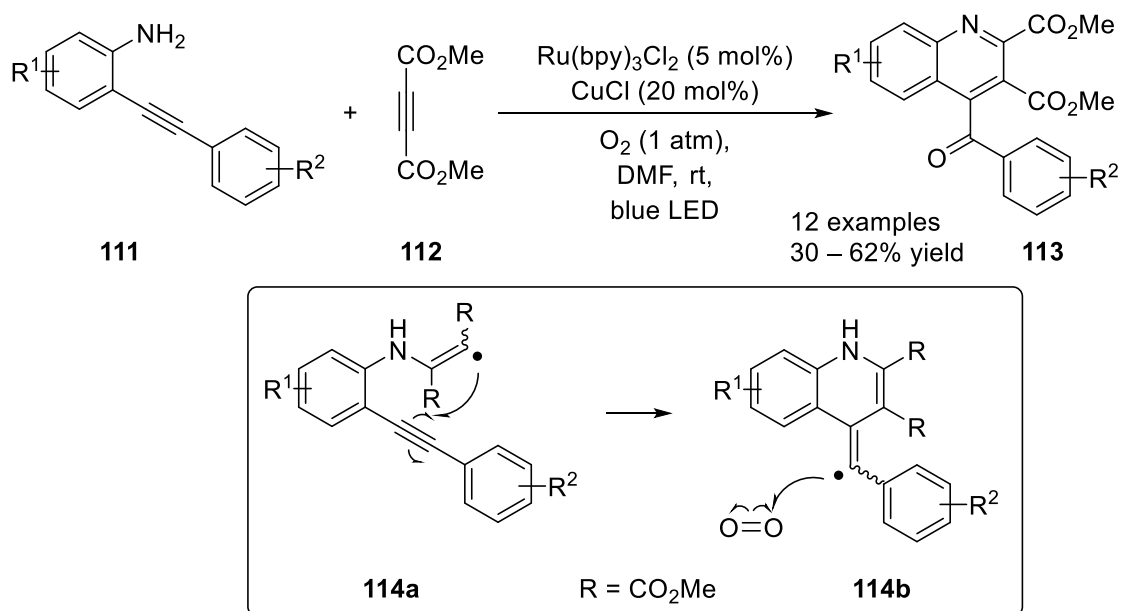
An efficient strategy to access 3-acyl indoles, benzofurans, or benzothiophenes was developed by Xia *et al.* (Scheme 30).<sup>[115]</sup> Upon visible light and base induced decarboxylation of **108**, the radical rapidly undergoes 5-*exo*-dig cyclization, resulting in a vinyl radical intermediate which is trapped by molecular oxygen. Protonation and elimination of  $H_2O$  give rise to carbonylated heterocycles **109**. The scope of the reaction is large, however the transformation suffers from high catalyst loadings.  $^{18}O_2$  labeled control experiments revealed that the oxygen atom of the carbonyl group is indeed derived from  $O_2$ .





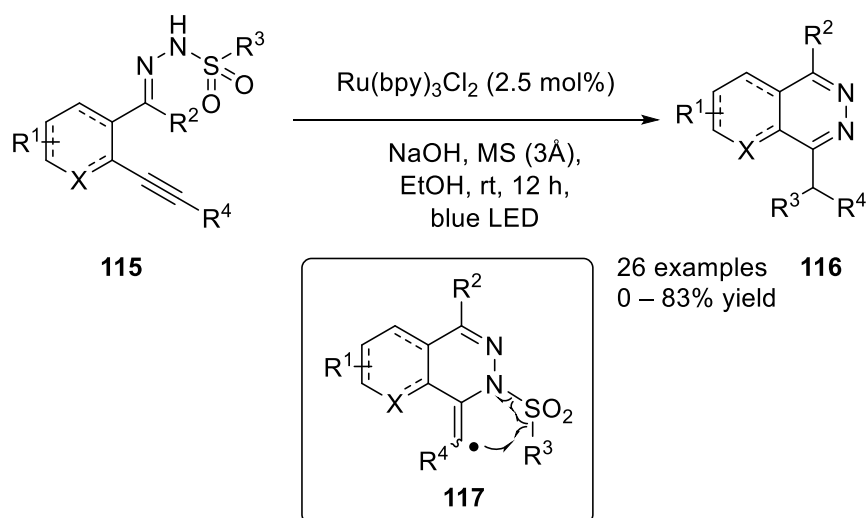
**Scheme 30.** Visible light promoted synthesis of carbonylated heteroaromatic compounds.<sup>[115]</sup>

A dual transition metal-visible light photoredox catalyzed synthesis of quinoline derivatives was reported by Xia and co-workers (Scheme 31).<sup>[116]</sup> Therein, a nitrogen-centered radical is proposed after deprotonation and single electron oxidation of **111** which subsequently adds to alkyne **112**. The resulting vinyl radical intermediate **114a** undergoes 6-*exo*-dig cyclization which gives rise to another vinyl radical **114b**. This intermediate reacts with molecular oxygen resulting in a copper-oxygen species which eventually leads to the final product **113**.



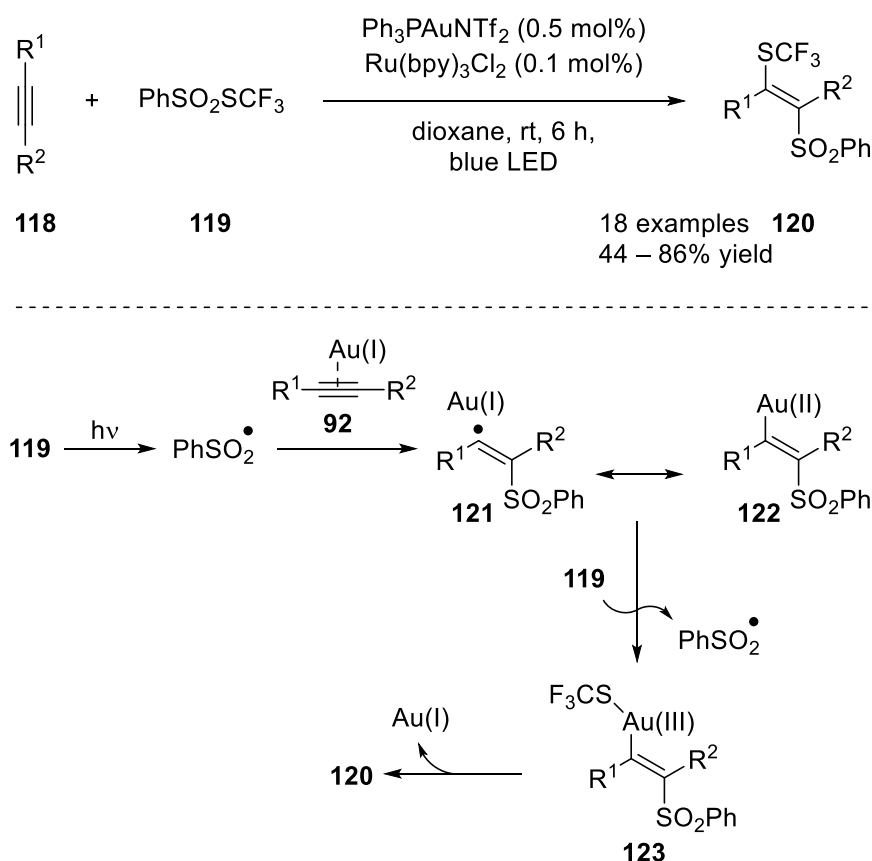
**Scheme 31.** Visible light promoted synthesis of quinoline derivatives.<sup>[116]</sup>

A visible light mediated radical hydroamination reaction followed by a radical Smiles rearrangement was achieved by Belmont and *et al.* (Scheme 32).<sup>[117]</sup> Upon deprotonation with NaOH, hydrazone **115** can easily be oxidized by the excited photocatalyst Ru(bpy)<sub>3</sub>Cl<sub>2</sub>, resulting in a N-centered radical. This radical rapidly undergoes 6-*exo*-dig cyclization to afford vinyl radical key intermediate **117** which spontaneously rearranges and releases SO<sub>2</sub>. Single electron reduction regenerates the photocatalyst and product **116** is formed after protonation.



**Scheme 32.** Visible light mediated radical Smiles rearrangement. The rearrangement of key vinyl radical intermediate **117** and SO<sub>2</sub> extrusion is depicted in the box.<sup>[117]</sup>

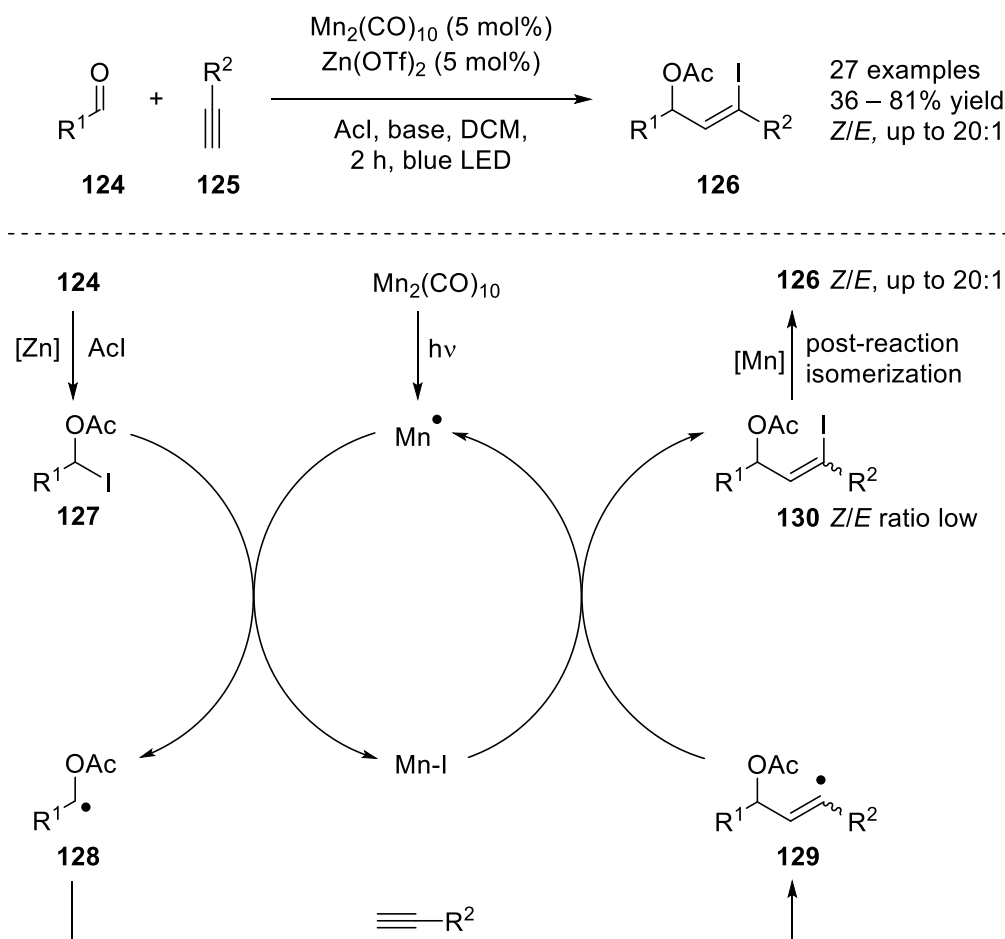
Xu and co-workers demonstrated that the combination of gold and photoredox catalysis can be an efficient approach to thio-functionalized vinylsulfones **120** *via* atom transfer radical addition (ATRA) of PhSO<sub>2</sub>SCF<sub>3</sub> (**119**) to alkynes with excellent stereo- and regiocontrol (Scheme 33).<sup>[118]</sup> The gold catalyst Ph<sub>3</sub>PAuNTf<sub>2</sub> served as a π acid to activate the alkyne and is crucial for the high *E/Z* selective outcome. The authors propose a phenylsulfonyl radical (PhSO<sub>2</sub>•) upon irradiation which adds to the gold-activated alkyne. The resulting vinyl radical **121** might interact with the gold catalyst forming an Au(II) intermediate **122**. This transition state favors the *E* configuration of the intermediate which explains the high diastereoselective outcome of this transformation. The final product **120** can be formed *via* reductive elimination of the Au(III) intermediate **123**.



**Scheme 33.** Atom transfer radical addition of **119** to alkyne.<sup>[118]</sup>

Very recently, a net redox-neutral generation and reaction of ketyl radicals was developed by Nagib and co-workers (Scheme 34).<sup>[119]</sup> In this transformation,  $\alpha$ -acetoxy iodides **127** were synthesized *in situ* by treating the corresponding aldehydes **124** with catalytic amounts of  $\text{Zn}(\text{OTf})_2$ . This significantly lowered the reduction potential, making the single electron reduction much more accessible. These  $\alpha$ -acetoxy iodides were coupled in ATRA reactions with alkynes which gave rise to synthetically versatile *Z*-vinyl halides **126** in up to 20:1 diastereomeric ratio. However, this reaction differs from the classic photoredox transformations as no photons are used for the turnover of one catalytic cycle. Instead, visible light is used to access the active species of the catalyst. Upon irradiation, the precatalyst dimer  $\text{Mn}_2(\text{CO})_{10}$  is homolytically cleaved to  $\cdot\text{Mn}(\text{CO})_5 (= \text{Mn}\cdot)$ . This catalytically active species is able to abstract  $\text{I}\cdot$  from  $\alpha$ -acetoxy iodides **127** to produce a ketyl radical intermediate **128** and a Mn-I species. The ketyl radical readily reacts with alkyne **125** giving rise to a vinyl radical intermediate **129**. This recombines with Mn-I to provide the final product **126** and closes the catalytic cycle. Regarding the high diastereomeric ratio in the product, the authors propose a

post-reaction product isomerization mechanism. They supported this theory by conducting a control experiment of a 1:1 *E/Z* mixture of the product which readily epimerized in the presence of the active Mn-catalyst.



**Scheme 34.** Manganese catalyzed net redox-neutral generation and functionalization of ketyl radicals with visible light.  $\text{Mn}^\bullet = \text{Mn}(\text{CO})_5$ .<sup>[119]</sup>

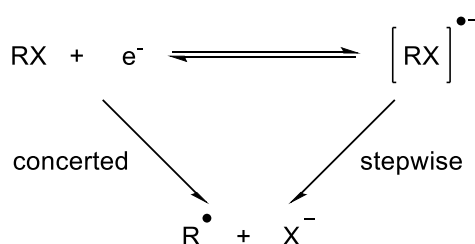
Visible light photoredox catalysis proves to be a future-oriented tool and many notable reactions were reported over the last years.<sup>[21-25,69,76,120,121]</sup> Many of these powerful transformations were previously in the need of toxic chemicals like  $\text{SnBu}_3\text{H}$  or required harsh reaction conditions such as dangerous UV-light or highly elevated temperatures. Herein, visible light represents an elegant solution to circumvent these issues as benign and mild activation method. However, nearly all of these great examples on visible light mediated generation and functionalization of vinyl radical intermediates focused on intramolecular transformations. In sharp contrast, intermolecular reactions attracted much less attention and only few reports can be contemporary found in the literature. From a synthetic point of view,

this would be much more desirable as it would dramatically increase the potential to unlock novel and unprecedented bond formations. Therefore, the main part of this thesis deals completely with the comparably underexplored intermolecular functionalization of vinyl radicals.

## B Visible light mediated activation of vinyl halides

### 1 Introduction

Selective activation of C(sp<sup>2</sup>)-halogen bonds represents one key aspect of modern organic synthesis. In this regard, palladium-catalyzed cross-coupling reactions proved to be a milestone for constructing novel C-C bonds and have been well studied over the past 50 years.<sup>[122-126]</sup> As an alternative approach, C(sp<sup>2</sup>)-halogen bonds can be activated by single electron reduction. First realized *via* electrochemical methods in the 1970s,<sup>[127]</sup> this principle, however, remained comparably underexplored. Upon uptake of one single electron, the C-X (X = halogen atom) bond of the substrate is decisively weakened.<sup>[128]</sup> As a consequence, the corresponding radical anion (C-X<sup>•-</sup>) readily undergoes fragmentation into a carbon-centered radical (C<sup>•</sup>) and a halide anion (X<sup>-</sup>) (Scheme 35).<sup>[128,129]</sup> Conversely, analogous dissociation into the carbanion (C<sup>-</sup>) and the halide radical (X<sup>•</sup>) is rather unlikely due to electronic reasons.<sup>[130]</sup>



**Scheme 35.** Reductive cleavage of C-X bonds. R = C<sub>aryl</sub> or C<sub>vinyl</sub>; X = halogen atom.

In the past, various kinetic studies and calculations regarding the bond fragmentation have been performed. It has been shown that cleavage of the C-X bond can either follow a concerted or a stepwise mechanism.<sup>[128,129,131,132]</sup> While for aliphatic compounds a concerted mechanism is proposed after uptake of one electron,<sup>[133,134]</sup> both pathways might be possible for aromatic C-X bonds.<sup>[128,135]</sup> Therefore, compounds having relatively large bond dissociation energies (BDE) of the C-X bond like chloro- or bromobenzene are considered to follow a stepwise mechanism whereas a concerted mechanism is proposed in the case of iodobenzene.<sup>[129,136,137]</sup>

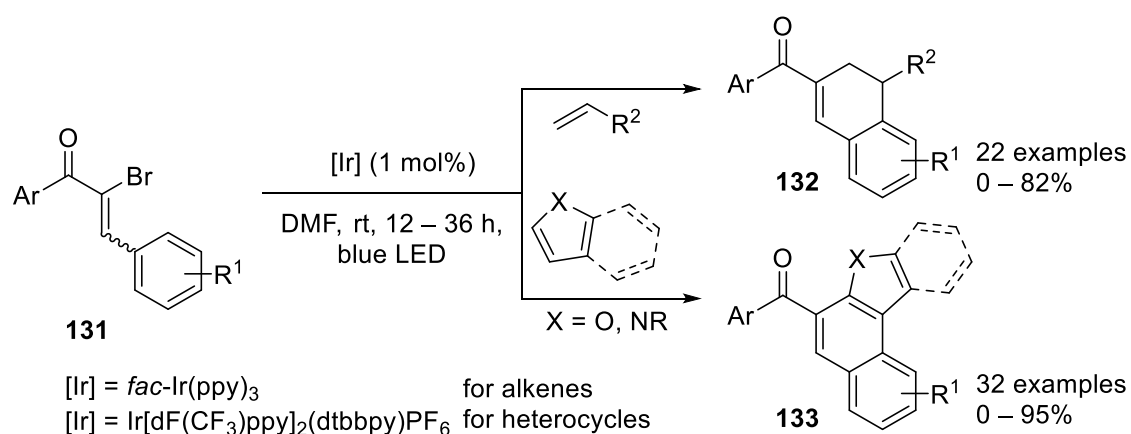
Each compound is defined by its standard reduction potential  $E_{1/2}^{\circ}$  which describes an electrochemical half reaction and represents the tendency of a compound to undergo single electron reduction or oxidation. According to this, strongly shifted negative values imply that such substrates are hard to reduce and require an increased electrical potential and *vice versa*.<sup>[70]</sup> The standard reduction potential of a compound can easily be obtained by cyclic voltammetry (CV) and is generally measured in volts at standard conditions. In this thesis all values are referred to the saturated calomel electrode (SCE). However, limitations for such transformations are often observed for molecules bearing low lying  $\pi^*$ -orbitals like  $\text{NO}_2$ -substituted compounds.<sup>[83,138,139]</sup> Such molecules regularly exhibit similar reduction potentials regardless of their complete structure. This is mainly due to the fact that nitro functional groups are excellent electron acceptors.<sup>[130,140]</sup> As a result, this can dramatically disturb the bond fragmentation because cleavage can only occur when the accepted electron is actually located in the  $\sigma^*$ -orbital of the C-X bond.<sup>[132,141]</sup>

In the recent years, electrochemistry emerged as a valuable tool in organic chemistry.<sup>[20,142]</sup> In this regard, even challenging C-X bond fragmentations were accessible by applying high currents. Still, electrochemical processes suffer from one crucial drawback as these redox reactions can either be oxidative or reductive, but not both at the same time.<sup>[24]</sup> This limitation can be elegantly overcome by visible light mediated photoredox catalysis. The combination of reductive cleavage to access free radicals, followed by subsequent oxidation of radical intermediates is a commonly utilized principle in photoredox catalysis which enabled the formation of spectacular and unprecedented new bonds.<sup>[21,63,76]</sup>

## 2 Preliminary studies with vinyl bromides

### 2.1 Cleavable redox auxiliary as activating group

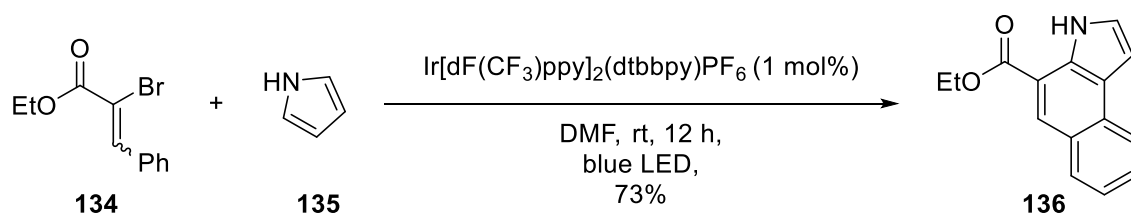
Although it has already been shown that vinyl radicals are versatile intermediates in organic chemistry (*vide supra*), the direct formation of such radicals by activation of C(sp<sup>2</sup>)-X bonds with visible light, however, attracted much less attention and only few examples were reported in the literature.<sup>[94,95,114,138,139]</sup> In 2014, Reiser and co-workers successfully introduced  $\alpha$ -bromo chalcones **131** as useful vinyl radical precursors (Scheme 36).<sup>[138,139]</sup> Upon irradiation with visible light, the C-Br bond of **131** could be cleaved after injection of one single electron by the excited iridium photocatalyst. After Br<sup>-</sup> extrusion, the vinyl radical was readily coupled with a large number of alkenes or various heterocycles which gave rise to substituted 3,4-dihydronaphthalenes **132** or complex polycyclic compounds **133**.



**Scheme 36.** Visible light mediated activation of  $\alpha$ -bromo chalcones **131**.<sup>[138,139]</sup>

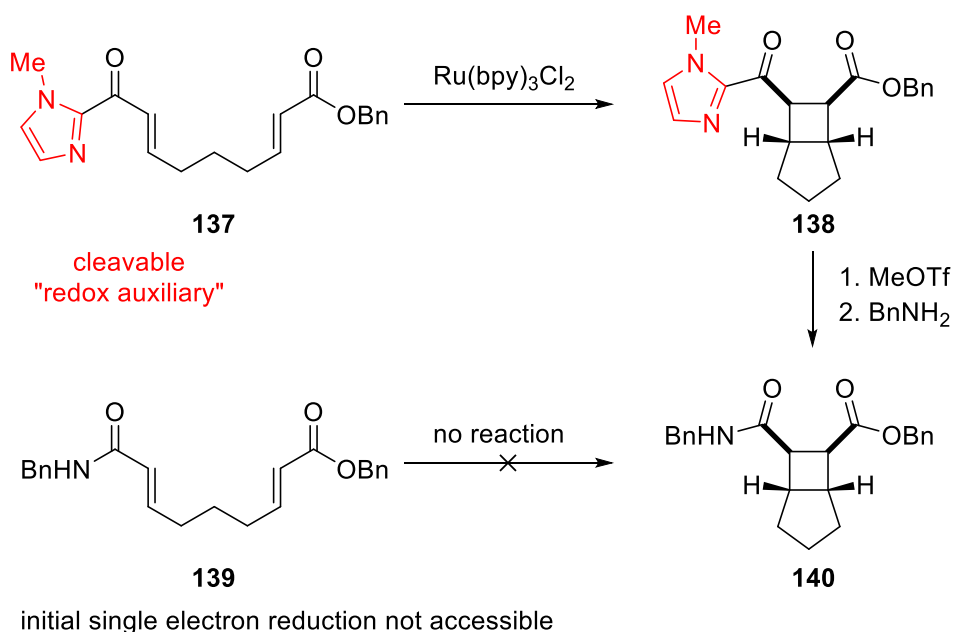
Even though the scope of the reaction was large, this transformation suffered from a severe drawback. The reaction was strongly limited to the extended  $\pi$ -system of the chalcone scaffold. In fact, the authors disclosed only one example for which the developed protocol was successfully transferred to a decreased  $\pi$ -system such as  $\alpha$ -bromo ethyl cinnamate (**134**) (Scheme 37). Yet, from a synthetic point of view, this would be highly desirable. In sharp contrast to the aromatic ring of the chalcone, the ester functionality allows further transformation into chemically useful compounds.





**Scheme 37.** Successful coupling of  $\alpha$ -bromo ethyl cinnamate (**134**) with pyrrole (**135**).<sup>[138]</sup>

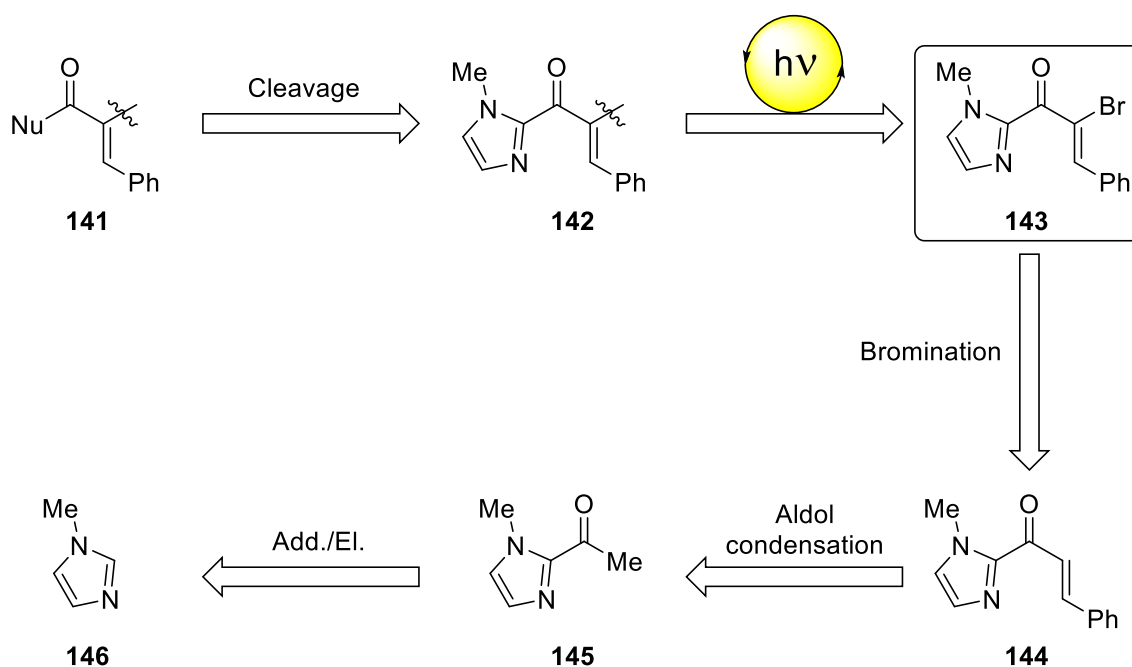
In 2012, Yoon and co-workers demonstrated that  $\alpha,\beta$ -unsaturated 2-imidazolyl ketones **137** readily underwent [2+2] cycloaddition with a variety of Michael acceptors (Scheme 38).<sup>[143]</sup> These cyclobutane adducts could be easily converted into carboxamides, esters, thioesters, and acids by subsequent cleavage of the imidazolyl core. Most importantly, these products were not accessible *via* the direct visible light mediated cycloaddition of the  $\alpha,\beta$ -unsaturated carbonyl compounds. The authors found that the involvement of an aryl enone turned out to be a strict requirement for the successful photoreaction. However, by installing an imidazolyl “redox auxiliary” they were capable of miming the aromatic property of the aryl enone and concluded that the imidazolyl group temporarily modulates the reduction potential.



**Scheme 38.** Overcoming the limitation for the [2+2] cycloaddition of enones.<sup>[143]</sup>

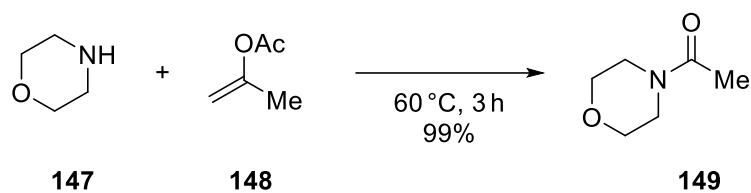
The key step in both syntheses consisted of an initial single electron reduction of the model substrate by the excited photocatalyst. Therefore, it seemed feasible that the previously

discussed limitation of the chalcones might also be elegantly overcome by following this principle. A retrosynthetic plan to key  $\alpha$ -bromo chalcone derivative **143** as photochemical precursor was easily designed and is depicted in Scheme 39. Acetylation of commercially available *N*-methylimidazole (**146**) should give ketone **145** which can undergo an aldol condensation with benzaldehyde to produce imidazolyl-substituted chalcone derivative **144**. The final  $\alpha$ -bromo chalcone derivative **143** as vinyl radical precursor should be achieved *via* selective bromination. Subsequent photochemical coupling and cleavage of the auxiliary should overcome previously mentioned aryl limitation and give access to a broad variety of novel carbonyl functional groups which might be valuable building blocks for future transformations.



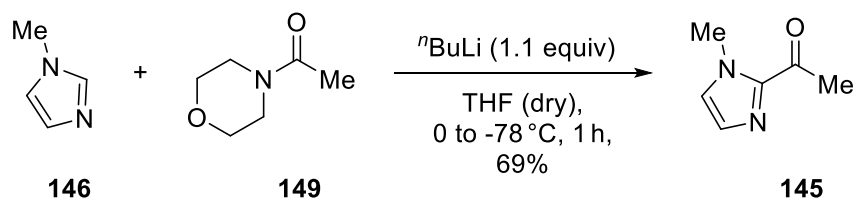
**Scheme 39.** Retrosynthetic route to  $\alpha$ -bromo chalcone derivative **143** as photochemical precursor.

Based on the literature, *N*-acetylated morpholine (**149**) seemed to be the most promising reagent for the acylation of *N*-methylimidazole (**146**) which could be quantitatively obtained by stirring morpholine (**147**) in isopropenyl acetate (**148**) at elevated temperatures (Scheme 40).<sup>[144]</sup>



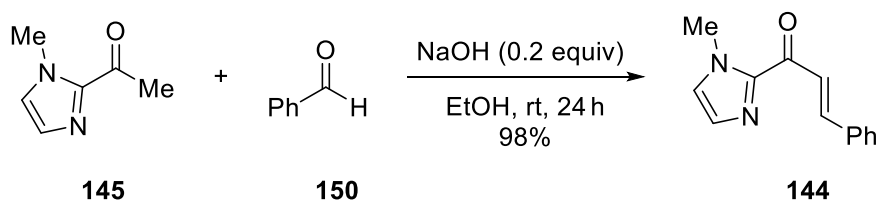
**Scheme 40.** Acetylation of morpholine (**147**).

Acetylation of *N*-methylimidazole (**146**) was carried out by treating **146** with  $n$ BuLi at low temperatures. The corresponding anion was subsequently trapped by previously synthesized acyl imidazole **149** to give ketone **145** in high yields (Scheme 41).<sup>[145,146]</sup>



**Scheme 41.** Preparation of imidazolyl ketone **145**.

The desired chalcone derivative **144** was quantitatively prepared in a Claisen-Schmidt condensation of **145** with benzaldehyde (**150**) (Scheme 42).<sup>[145,146]</sup>

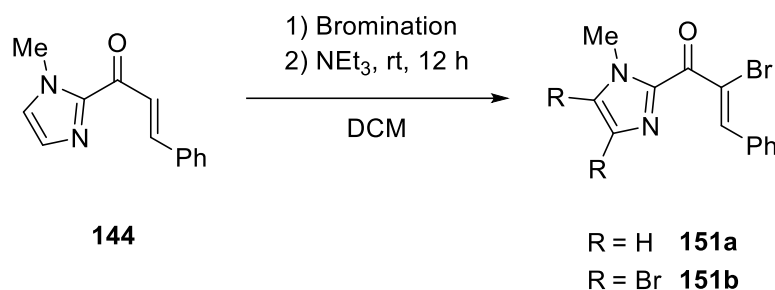


**Scheme 42.** Claisen-Schmidt condensation to **144**.

Selective  $\alpha$ -bromination of **144** was carried out under previously established conditions for chalcones.<sup>[138]</sup> Therefore, Br<sub>2</sub> was prepared *in situ* by oxidation of HBr with OXONE<sup>®</sup> (= potassium peroxymonosulfate), followed by selective bromide elimination with NEt<sub>3</sub> to vinyl bromide **151**. Unfortunately, bromination of the aromatic ring also occurred which undeniably led to a complex reaction mixture (Table 1, entry 1). As bromination of

imidazole is well known,<sup>[147]</sup> a short screening was conducted in order to increase the selectivity (Table 1).

**Table 1.** Bromination of chalcone derivative **144**.<sup>a</sup>

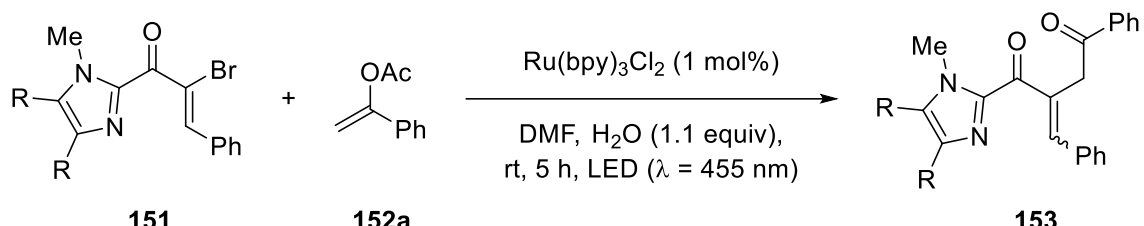


Entry	Bromination agent	Yield (%) <sup>c</sup>
		<b>151a</b> / <b>151b</b>
1 <sup>b</sup>	HBr, <i>OXONE</i> <sup>®</sup>	complex mixture
2 <sup>c</sup>	Br <sub>2</sub>	44 / -
3 <sup>d</sup>	HBr, <i>OXONE</i> <sup>®</sup>	- / 74

<sup>a</sup>Reactions were performed on a 2 mmol scale in DCM. NEt<sub>3</sub> (5 equiv) was added after full bromination was observed. <sup>b</sup>HBr (2 equiv), *OXONE*<sup>®</sup> (1.2 equiv), rt, 3 d. <sup>c</sup>Br<sub>2</sub> (1.2 equiv), 0 °C, 1 h. <sup>d</sup>HBr (4 equiv), *OXONE*<sup>®</sup> (2.4 equiv), rt, 3 d. <sup>e</sup>Isolated yields.

Direct addition of Br<sub>2</sub> at lower temperature was found to successfully suppress the undesired bromination of the imidazole ring and **151a** was isolated in moderate yields (entry 2). Still, formation of by-products diminished the yield. In addition, it was decided to take fully brominated product **151b** into account since the imidazole scaffold should be cleaved in the course of the subsequent transformations anyhow and, in principle, should not disturb the photochemical coupling. Gratifyingly, using an excess of HBr and *OXONE*<sup>®</sup> resulted in desired product **151b** in high yields (entry 3).

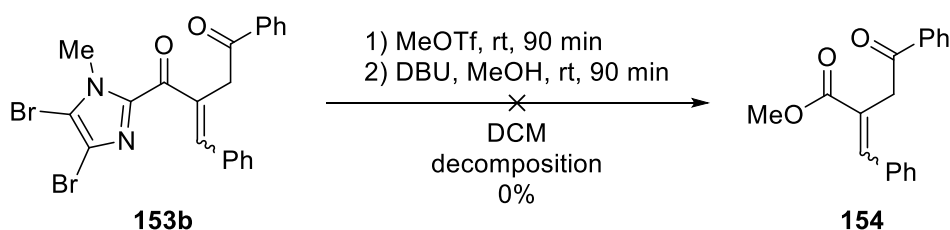
With both products in hand, vinyl bromides **151a** and **151b** were subjected to photochemical test reactions. Preliminary studies were carried out using electron rich enol acetate **152a**, a classic trapping reagent in photochemical couplings (Table 2).<sup>[148,149]</sup>

**Table 2.** Preliminary studies of newly synthesized  $\alpha$ -bromo chalcone derivatives.<sup>a</sup>


Entry	Substrate	Product	Yield (%) <sup>b</sup>
1	R = H <b>151a</b>	R = H <b>153a</b>	-
2	R = Br <b>151b</b>	R = Br <b>153b</b>	45

<sup>a</sup>Reactions were performed on a 0.5 mmol scale with **151** (1 equiv), **152a** (5 equiv), H<sub>2</sub>O (1.1 equiv), Ru(bpy)<sub>3</sub>Cl<sub>2</sub> (1 mol%) in 2 mL DMF. <sup>b</sup>Combined isolated yields of separated *E* and *Z* isomer. *E/Z* ratio of approximately 1:1.

As enol acetates have already been proven to serve as reliable trapping reagents for  $\alpha$ -bromo chalcones in the past, the photochemical coupling seemed to be promising.<sup>[150]</sup> Unfortunately, no product was formed when substrate **151a** was subjected to previously optimized reaction conditions (entry 1).<sup>[151]</sup> In contrast, the fully brominated substrate **151b** was successfully coupled with enol acetate **152a** as the expected 1,4-dicarbonyl compound **153b** was isolated in moderate yields (entry 2). Before any further optimization was attempted, it was a priori checked if photocoupled product **153b** can in general be converted to ester **154**. Methylation should transform the imidazolyl scaffold in a good leaving group which could then be replaced by nucleophiles. However, no product was formed when the previously developed protocol from Yoon and co-workers was applied. Instead, complete decomposition of the starting material took place (Scheme 43).<sup>[143]</sup>

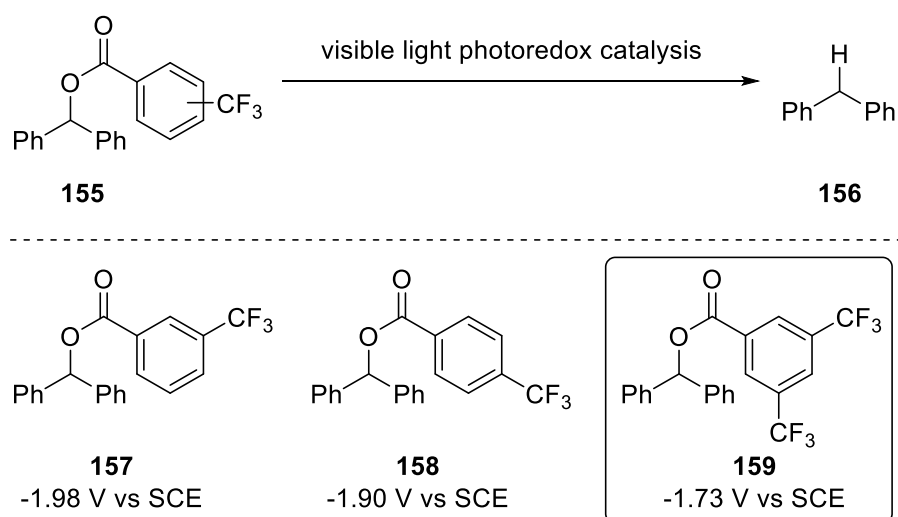
**Scheme 43.** Failed cleavage of the imidazolyl redox auxiliary.<sup>[143]</sup>

In summary, the visible light mediated activation of  $\alpha$ -bromo chalcone derivatives **151a** and **151b** was examined. As previous investigations were prone to be strictly limited to the

aromatic moiety of chalcones, it was attempted to bypass these tedious requirements with the help of a cleavable redox auxiliary. In this regard, a broader substrate scope should be accessible by cleaving the auxiliary after the successful photoreaction as the group of Yoon has already demonstrated.<sup>[143]</sup> Although the synthesis to chalcone derivative **144** was easily achieved, the bromination step appeared to be sensitive towards side reactions. Nevertheless, non-brominated and fully brominated products **151a** and **151b** were isolated and subjected to previously optimized photoconditions. Surprisingly, only the fully brominated substrate **151b** could be successfully coupled, albeit only in moderate yields. Unfortunately, substitution of the 2-imidazolyl auxiliary failed. Due the sluggish bromination step, combined with the disappointing photoreaction and the unsuccessful cleavage of the auxiliary, this project was stopped at this time. Even if the cleavage of fully brominated substrate **153b** would have worked, the bad atom economy in **153b** makes this process highly inefficient and environmentally unsustainable.

## 2.2 Controlling the reduction potential

A central part in visible light mediated photoredox catalysis is defined by the standard reduction potential  $E_{1/2}^\circ$ . Each photocatalyst exhibits its own unique reduction potential in each stage of the photochemical cycle and thereby often points out the limitation of a photochemical transformation.<sup>[70]</sup> As a consequence, the photocatalyst must exhibit a more negative reduction potential to successfully enable single electron transfer to the substrate. While this issue can easily be solved by applying higher currents in electrochemistry, photochemical transformations are in that regard often confined. In the past, these electrochemical limitations could be circumvented by *in situ* transformations into more reactive intermediates,<sup>[152]</sup> or by converting electrochemically inert functional groups into redox active substrates facilitating single electron reduction.<sup>[153,154]</sup> In order to shift the electrochemical potential to a region which is more accessible for the photocatalyst, thereby making single electron reduction more likely, it is often helpful to introduce electron withdrawing groups.<sup>[70]</sup> This principle has already been exploited in photoredox chemistry with visible light and is exemplarily outlined by previous work on photochemical deoxygenation of alcohols by the group of Reiser (Scheme 44).<sup>[154]</sup> Here, the authors demonstrated that activated benzoates **159** readily underwent single electron reduction. In sharp contrast to unactivated benzoates, the reduction potential could be considerably manipulated by trifluoromethylations.



**Scheme 44.** Benzoates as activation group for photochemical deoxygenation with visible light. Influence of the trifluoromethyl substitution on the reduction potential.<sup>[154]</sup>

In the previous chapter it has been mentioned that  $\alpha$ -bromo chalcone (**131**) could be readily photochemically activated and successfully coupled with a great variety of substrates while structurally related  $\alpha$ -bromo ethyl cinnamate (**134**) turned out to be surprisingly inert. Indeed, cyclic voltammetry measurements quickly revealed that **134** is by far more difficult to reduce. Compared to  $\alpha$ -bromo chalcone (**131**) with a reduction potential of -0.88 V vs SCE,<sup>[138]</sup>  $\alpha$ -bromo ethyl cinnamate (**134**) exhibits a significantly more challenging reduction potential of -1.54 V vs SCE (Table 3). Therefore, in the oxidative quenching cycle, only the precious iridium-based photocatalyst *fac*-Ir(ppy)<sub>3</sub> ( $E_{M^+/M^*}^\circ = -1.73$  V vs SCE) should be able to reduce **134** which explains the previously observed sluggish reactivity (*cf.* Chapter 3).

**Table 3.** Comparison of the reduction potential of **131** and **134** along with the reduction potentials of commonly employed photocatalysts.<sup>a</sup>

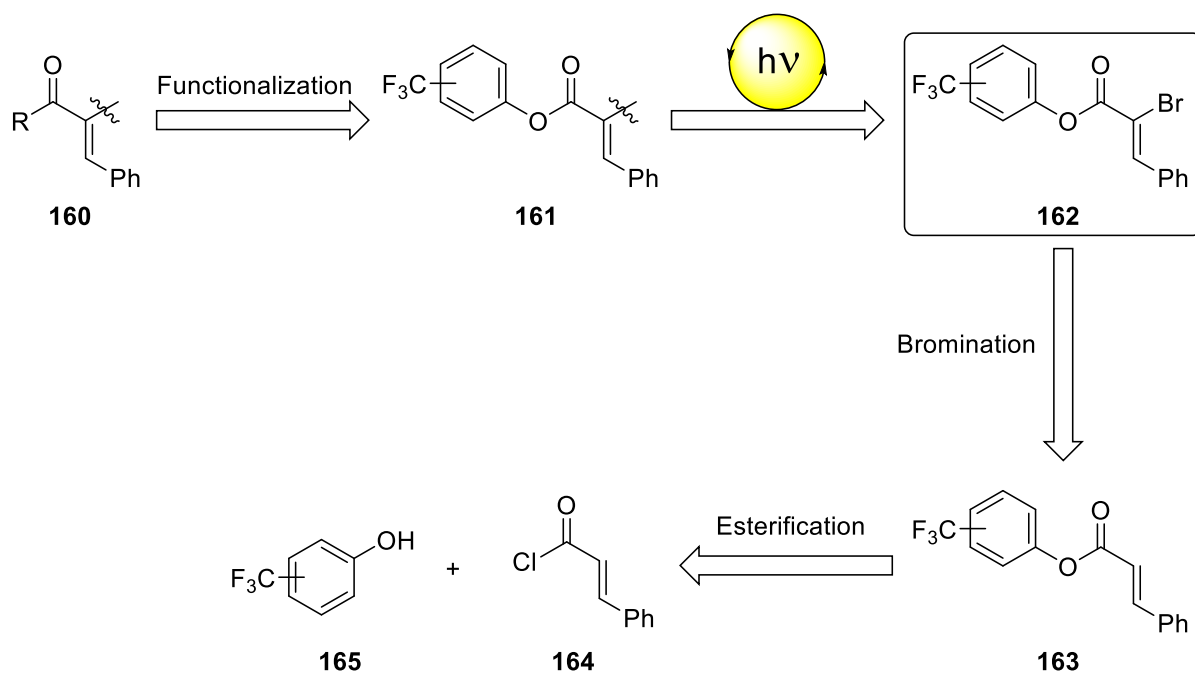


Entry	Photocatalyst	$E_{M^+/M^*}^\circ$	$E_{M/M^-}^\circ$
1	Ru(bpy) <sub>3</sub> Cl <sub>2</sub>	-0.81 V	-1.33 V
2	Ir[dF(CF <sub>3</sub> )ppy] <sub>2</sub> (dtbbpy)PF <sub>6</sub>	-0.89 V	-1.37 V
3	Ir(ppy) <sub>2</sub> (dtbbpy)PF <sub>6</sub>	-0.96 V	-1.51 V
4 <sup>b</sup>	Cu(dap) <sub>2</sub> Cl	-1.43 V	-
5 <sup>c</sup>	<i>fac</i> -Ir(ppy) <sub>3</sub>	-1.73 V	-2.19 V

<sup>a</sup> $E_{M^+/M^*}^\circ$  = oxidative quenching cycle;  $E_{M/M^-}^\circ$  = reductive quenching cycle. All potentials are given in V vs the saturated calomel electrode (SCE).<sup>[70]</sup> Measurements were performed in MeCN at rt unless otherwise noted. <sup>b</sup>Determined in DCM. <sup>c</sup>Determined in EtOH / MeOH, 1:1.

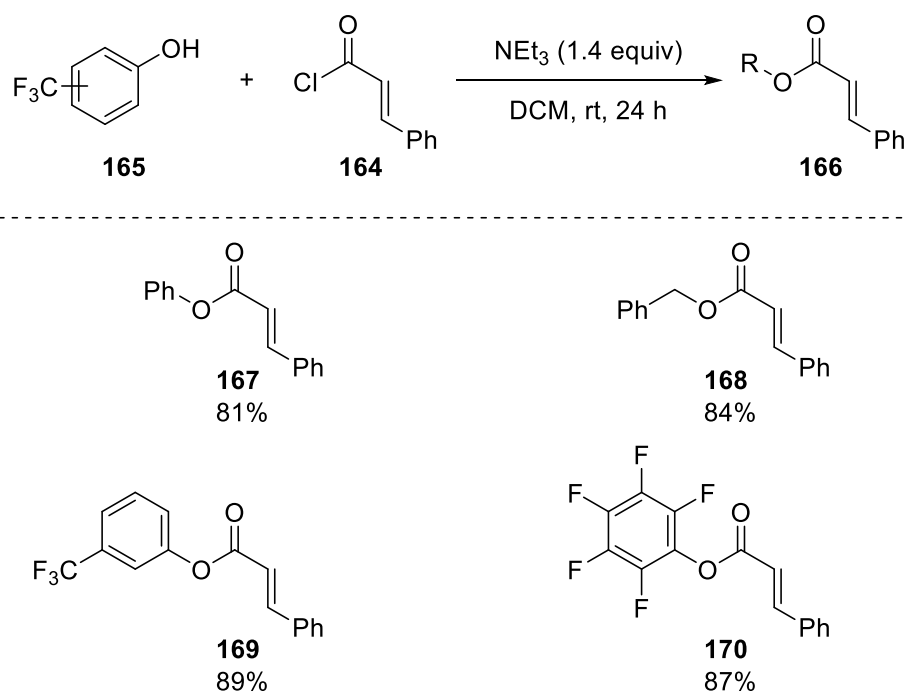
However, in terms of sustainability it would be much more desirable to use a more abundant metal like ruthenium as central part of the catalyst. Therefore, based on previous investigations regarding the reduction potential of fluorinated benzoates, a similar trend was envisioned with trifluoromethylated phenyl cinnamates **162**. These should be easily accessible by esterification of commercially available cinnamoyl chloride (**164**) with phenols **165**. Bromination should be carried out similarly to the previously described procedure and transesterification or ester saponification should help to overcome present substrate limitation after ensued photochemical coupling (Scheme 45).



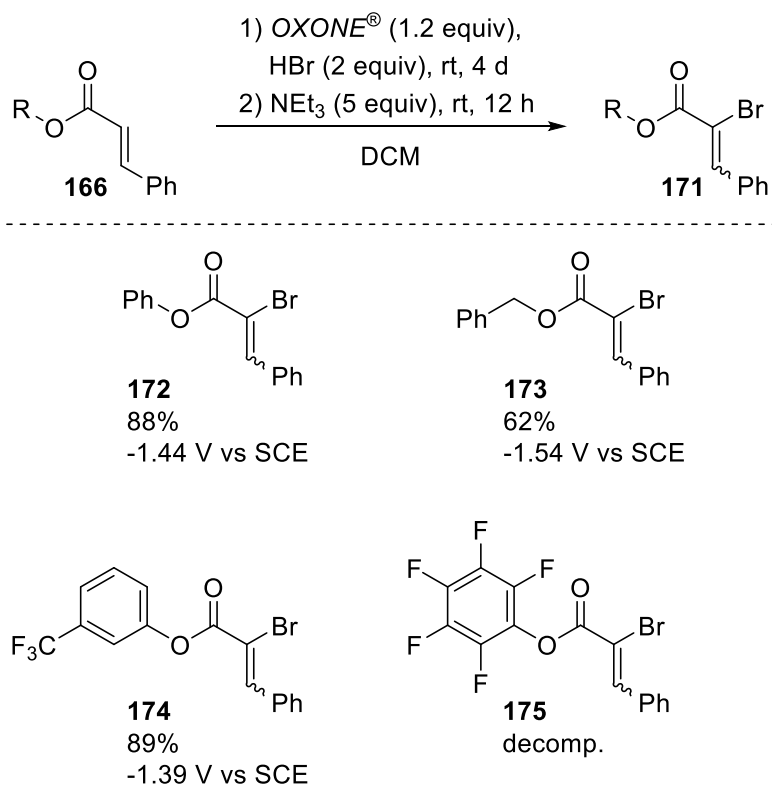


**Scheme 45.** Retrosynthetic route to fluorinated  $\alpha$ -bromo phenyl cinnamates **162**.

Utilizing a standard protocol for esterifications of cinnamoyl chloride with phenols,<sup>[155]</sup> a variety of substituted phenyl cinnamates **166** were obtained in excellent yields (Scheme 46). In addition, phenyl cinnamate (**167**) and benzyl cinnamate (**168**) were also synthesized and should serve as reference value to  $\alpha$ -bromo ethyl cinnamate (**134**). Subsequent bromination and elimination gave desired  $\alpha$ -brominated products in high yields except for perfluorinated phenyl cinnamate (**175**) which decomposed under such conditions (Scheme 47).



**Scheme 46.** Synthesis of fluorinated phenyl cinnamates.

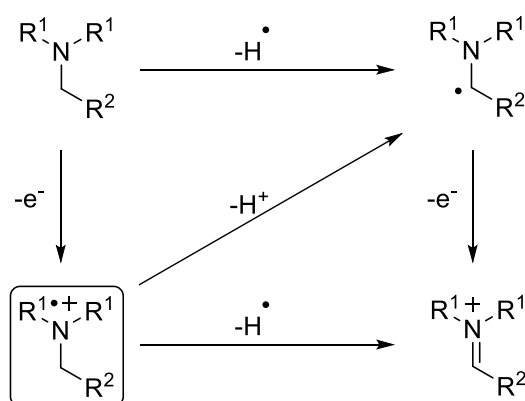


**Scheme 47.** Synthesis of  $\alpha$ -bromo phenyl cinnamates along with their measured reduction potential. Products obtained as *E/Z* mixtures. For details see Experimental part.

However, cyclic voltammetry measurements of these newly synthesized substrates revealed that the desired substitution effect was non-existent. Unfortunately, trifluorosubstituted substrate (**174**) exhibited nearly the same reduction potential as non-substituted phenyl cinnamate (**172**) and a negligible outcome compared to  $\alpha$ -bromo ethyl cinnamate (**134**). This was unexpected because in the case of the benzoates, the 3-substituted trifluoromethylated substrates perceptibly differed from the non-substituted.<sup>[154]</sup> Unfortunately, the introduction of additional trifluoromethyl substituents seemed to be disproportionately cost-intensive and required hazardous starting materials.<sup>[156]</sup> Therefore, further evaluation of trifluoromethylated phenyl cinnamates was omitted.

### 2.3 Utilizing the reductive quenching cycle

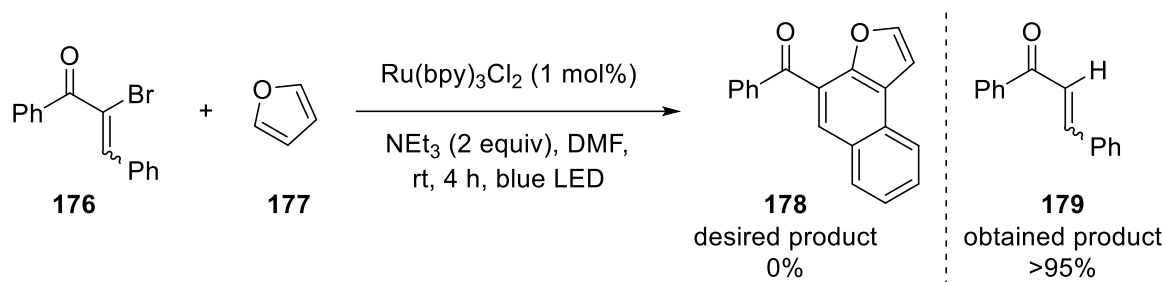
In principal, a photoreaction can follow two different reaction pathways. The excited state of the photocatalyst can be oxidatively or reductively quenched, often depending on the specific reaction conditions. In this regard, additives might help to drive the reaction into one direction and therefore to get control over the mechanism. So far, the preceding reactions were performed in the oxidative quenching cycle and did not require any additives. Both cycles are in general limited by their unique reduction potentials. In fact, much stronger reducing capabilities of the photocatalysts can be reached by utilizing the reductive quenching cycle.<sup>[70]</sup> This pathway can easily be accessed by adding substrates which are readily oxidized. In this regard, reliable reductants are typically based on low-priced trialkylamines.<sup>[92]</sup> While reactions performed in the reductive quenching cycle generally proceed considerably faster,<sup>[82]</sup> problems can hereby arise with the oxidized amines. Single electron oxidation of trialkylamines results in substantial acidification of the C-H bond adjacent to the nitrogen atom which considerably weakens the bond strength.<sup>[157,158]</sup> As a result, these oxidized amines ( $R_3N^{+\bullet}$ ) are extraordinary hydrogen donors (Scheme 48).<sup>[79]</sup> This can often be desired, *e.g.* in the case of defunctionalizations,<sup>[62,94]</sup> but on the contrary this can also dramatically disturb the mechanism and lead to undesired by-products.<sup>[159,160]</sup> In order to suppress the formation of by-products it might help to employ aromatic amines lacking any  $\alpha$ -C-H bonds like  $NPh_3$  or derivatives thereof.<sup>[79,159]</sup>



**Scheme 48.** Simplified model of trialkylamines in photoredox catalysis.<sup>[79]</sup>

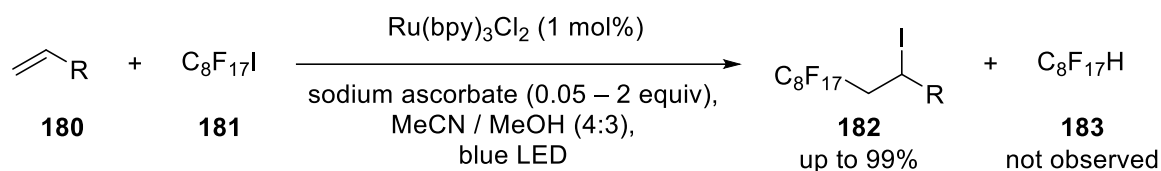
As all attempts to broaden the substrate scope by manipulating the aryl enone system failed so far (*vide supra*), direct functionalization of  $\alpha$ -bromo ethyl cinnamate (**134**) was reconsidered.

Utilizing the reductive quenching cycle, different iridium-based photocatalysts should generally be able to successfully inject one electron into **134**. However, previous investigations on chalcones **176** have already shown that simple trialkylamines like  $\text{NEt}_3$  exclusively formed unprofitable hydrodehalogenated product **179** instead of desired polycyclic compound **178** (Scheme 49).<sup>[138]</sup>



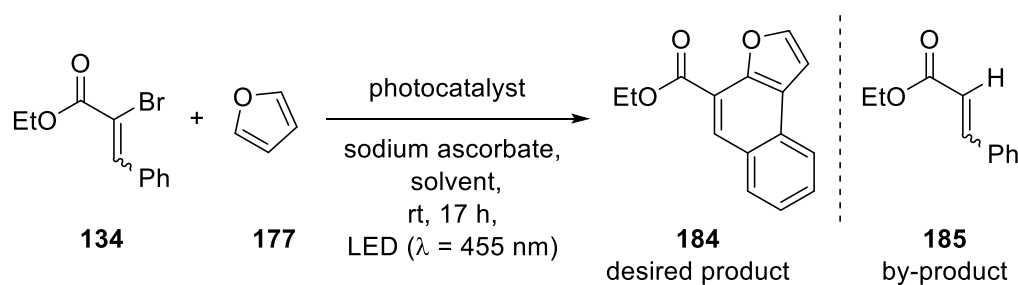
**Scheme 49.** Visible light mediated coupling of  $\alpha$ -bromo chalcone (**176**) with furan (**177**).<sup>[138]</sup>

In 2012, Stephenson and co-workers successfully suppressed undesired hydrodehalogenated product **183** by utilizing inexpensive sodium ascorbate as sacrificial electron donor. In this regard, the authors developed a protocol which completely eliminated unpreferred hydrodehalogenated side-product by using substoichiometric amounts of reductant (Scheme 50).<sup>[82]</sup>



**Scheme 50.** Sodium ascorbate as reductive quencher in photoredox catalysis.<sup>[82]</sup>

Inspired by these results, it was hypothesized that these findings could also be utilized for the functionalization of  $\alpha$ -bromo ethyl cinnamate (**134**) in the reductive cycle. For a reasonable comparison, furan (**177**) was chosen as trapping reagent as it has already been successfully employed in the coupling with  $\alpha$ -bromo chalcones in the reductive quenching cycle (Table 4).<sup>[138]</sup>

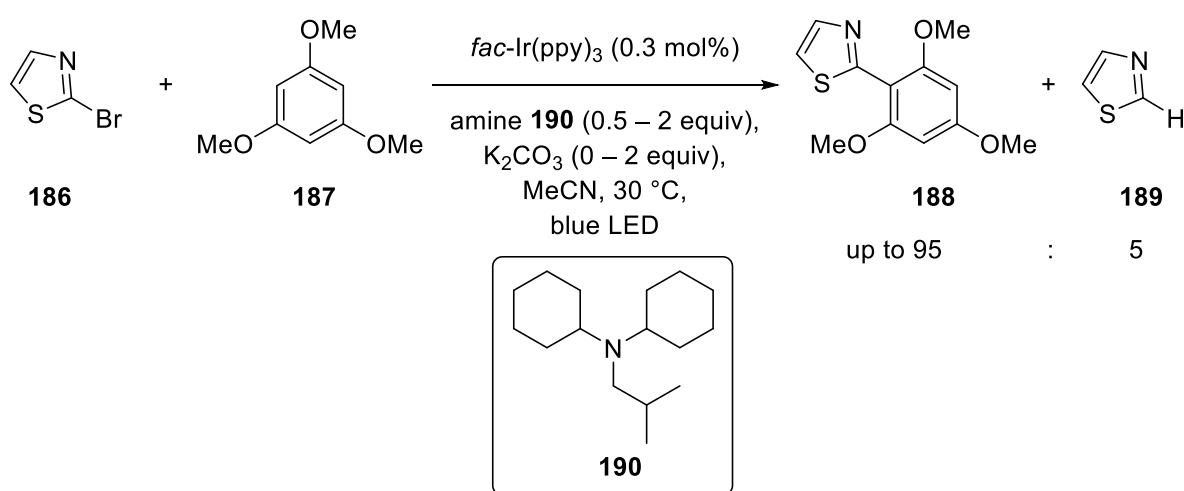
**Table 4.** Visible light mediated coupling of  $\alpha$ -bromo ethyl cinnamate (**134**) and furan (**177**) with sodium ascorbate as reductive quencher.<sup>a</sup>

Entry	Catalyst (1 mol%)	Sodium ascorbate (equiv)	Solvent	Yield (%) <sup>b</sup> of <b>184</b>
1	<i>fac</i> -Ir(ppy) <sub>3</sub>	1.5	MeCN / MeOH	-
2	Ir(ppy) <sub>2</sub> (dtbbpy)PF <sub>6</sub>	2.0	MeCN / MeOH	traces
3 <sup>c</sup>	Ir(ppy) <sub>2</sub> (dtbbpy)PF <sub>6</sub>	1.0	MeCN / MeOH	traces
4 <sup>d</sup>	Ir(ppy) <sub>2</sub> (dtbbpy)PF <sub>6</sub>	0.35	MeCN / MeOH	traces

<sup>a</sup>Reactions were performed with **134** (0.5 mmol), **177** (2.5 mmol), photocatalyst (1 mol%) in MeCN (1.4 mL) and MeOH (1.0 mL). <sup>b</sup>Isolated yields after column chromatography. <sup>c</sup>No full conversion was observed. <sup>d</sup>Only 50% conversion was observed.

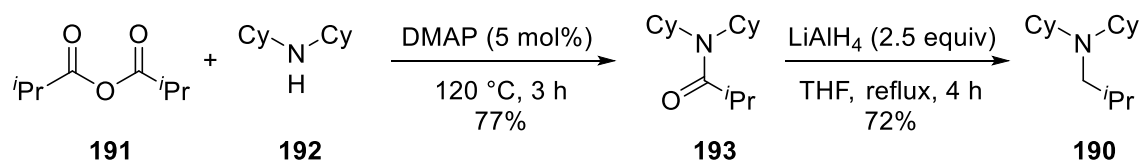
Preliminary studies were carried out with either *fac*-Ir(ppy)<sub>3</sub> or Ir(ppy)<sub>2</sub>(dtbbpy)PF<sub>6</sub> since these two catalysts exhibit the highest reducing power in the reductive quenching cycle. Both photocatalysts should be in the range of  $\alpha$ -bromo ethyl cinnamate (**134**) with a measured reduction potential of -1.54 V vs SCE. Surprisingly, strongly reducing *fac*-Ir(ppy)<sub>3</sub> ( $E_{M/M}^{\circ} = -2.19$  V vs SCE)<sup>[70]</sup> was found to be completely inactive (entry 1). Turning to less reducing Ir(ppy)<sub>2</sub>(dtbbpy)PF<sub>6</sub> ( $E_{M/M}^{\circ} = -1.51$  V vs SCE)<sup>[70]</sup> resulted in full conversion of starting material with two equivalents of sodium ascorbate (entry 2). Unfortunately, only traces of product were found and only hydrodehalogenated product was obtained. As sodium ascorbate seemed to be the obvious hydrogen source,<sup>[95,161]</sup> the amount of the sacrificial electron donor was next lowered (entry 3 or 4). As a result, this suppressed the formation of reduced product but resulted in incomplete consumption of the starting material. Therefore, no rise of desired product was obtained. Although the reductively quenched Ir(ppy)<sub>2</sub>(dtbbpy)PF<sub>6</sub> was indeed capable of activating  $\alpha$ -bromo ethyl cinnamate (**134**), the nature of the vinyl radical seemed to be too reactive.<sup>[3,7]</sup> Even an excess of electron rich trapping reagent did not outcompete undesired hydrogen atom transfer (HAT) by the oxidized sodium ascorbate.

As sodium ascorbate was found to be unsuitable as reductive quencher, alternative reagents were needed. Recently, Weaver and co-workers were confronted with a similar problem during their studies on the functionalization of 2-azoyl radicals.<sup>[162,163]</sup> While working on the photo-induced activation of 2-bromo thiazoles (**186**), the authors also struggled with undesired hydrogen atom abstraction by the reductive quencher which inevitably resulted in unprofitable defunctionalization to thiazole (**189**). However, they were able to overcome this issue by exploiting the bad solubility of nonpolar amines like **190** in MeCN.<sup>[163]</sup> By this means, it was possible to keep the active amine concentration low minimizing the formation of defunctionalized by-product **189** (Scheme 51).



**Scheme 51.** Photocatalytic generation of 2-azoyl radicals with unconventional amines as single electron reductants.<sup>[163]</sup>

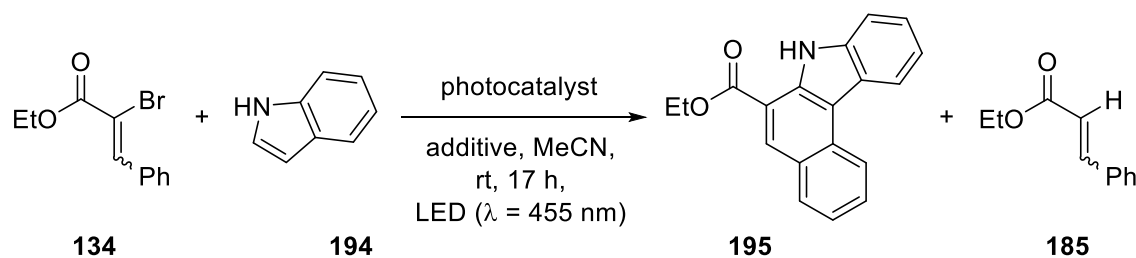
Different unpolar trialkylamines were screened and best results were obtained with bulky *N*-cyclohexyl-*N*-isobutylcyclohexanamine (**190**) which exhibits a solubility of only 0.01 M in MeCN at ambient temperature, more than a hundredfold less than DIPEA for example (1.3 M in MeCN).<sup>[163]</sup> Due to the structural relation of aryl radicals to vinyl radicals, it was speculated that undesired hydrodefunctionalization could also be suppressed under such conditions. *N*-cyclohexyl-*N*-isobutylcyclohexanamine (**190**) was quickly synthesized by literature known reduction of amide **193** with LiAlH<sub>4</sub> (Scheme 52).<sup>[164]</sup>



**Scheme 52.** Synthesis of *N*-cyclohexyl-*N*-isobutylcyclohexanamine (**190**).<sup>[164]</sup> Cy = cyclohexyl.

With bulky amine **190** in hand, different tertiary amines were tested as potential additives (Table 5). Indole (**194**) was chosen as model substrate this time. First test reactions were carried out with Ir(ppy)<sub>2</sub>(dtbbpy)PF<sub>6</sub> since this photocatalyst exhibited the highest activity so far. Unfortunately, when the reaction was performed with commercially available NBu<sub>3</sub>, only decomposition of starting material was observed (entry 1). Gratifyingly, <sup>*i*</sup>BuN(Cy)<sub>2</sub> (**190**) as potential reductant promoted the reaction as 19% of polycyclic compound **195** was isolated (entry 2). However, hydrodebrominated product **185** still turned out to be the major product in this reaction even though <sup>*i*</sup>BuN(Cy)<sub>2</sub> was not completely dissolved in MeCN. Reducing the amount of sacrificial electron donor and adding K<sub>2</sub>CO<sub>3</sub> as non-redox active co-base did not give better results (entry 3). In order to push the yield more into the direction of desired coupling product, the amount of indole was increased (entry 4). As expected, higher yields of **195** were obtained, while simultaneously the amount of by-product **185** was decreased. Lastly, different photocatalysts were screened (entry 5 – 6). It turned out that all catalysts were nearly equally active but none of them gave better yields than 25% of the corresponding product.



**Table 5.** Photomediated coupling between  $\alpha$ -bromo ethyl cinnamate (**134**) and indole (**194**).<sup>a</sup>

Entry	Catalyst	Indole (equiv)	Electron donor (equiv)	Yield (%) <sup>b</sup>
				<b>195</b> / <b>185</b>
1	Ir(ppy) <sub>2</sub> (dtbbpy)PF <sub>6</sub>	(2.0)	NBu <sub>3</sub> (2.0)	-
2	Ir(ppy) <sub>2</sub> (dtbbpy)PF <sub>6</sub>	(2.0)	<sup>t</sup> BuN(Cy) <sub>2</sub> (2.0)	19 / 42
3 <sup>c</sup>	Ir(ppy) <sub>2</sub> (dtbbpy)PF <sub>6</sub>	(2.0)	<sup>t</sup> BuN(Cy) <sub>2</sub> (0.5)	16 / 32
4	Ir(ppy) <sub>2</sub> (dtbbpy)PF <sub>6</sub>	(5.0)	<sup>t</sup> BuN(Cy) <sub>2</sub> (2.0)	24 / 6
5	Ir[dF(CF <sub>3</sub> )ppy] <sub>2</sub> (dtbbpy)PF <sub>6</sub>	(5.0)	<sup>t</sup> BuN(Cy) <sub>2</sub> (2.0)	25 / 13
6	Ru(bpy) <sub>3</sub> Cl <sub>2</sub>	(5.0)	<sup>t</sup> BuN(Cy) <sub>2</sub> (2.0)	24 / 26

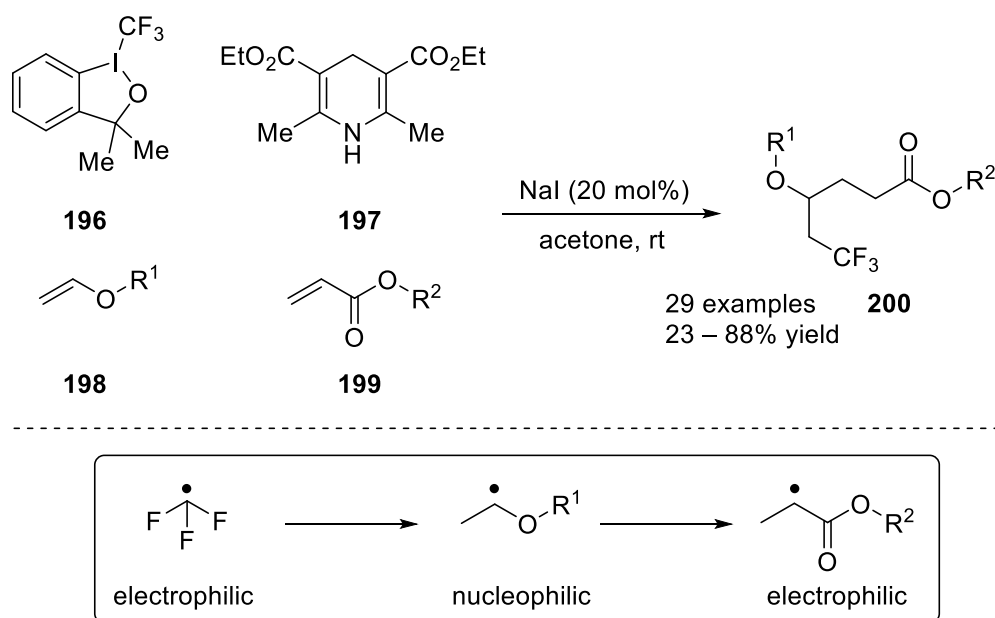
<sup>a</sup>Reactions were performed on a 0.5 or 0.3 mmol scale with 1 mol% photocatalyst in 2.5 mL solvent.

<sup>b</sup>Yields were determined by <sup>1</sup>H-NMR analysis using 1,3,5-trimethoxybenzene as internal standard. Both isomers of undesired hydrodehalogenated products **185** were formed. <sup>c</sup>K<sub>2</sub>CO<sub>3</sub> (2.0 equiv) was added as additional base.

In conclusion, the observed conversion of starting material was rather low in all cases. Additionally, undesired reduced product **185** was either predominantly formed or at least to a significant extent. This could be slightly suppressed by increasing the amount of trapping reagent. However, further increase of the equivalents of indole would not have been feasible, as isolation problems would become problematic. As ethyl cinnamate (**185**) is industrially produced by esterification of cheap cinnamic acid, this defunctionalization is completely unprofitable.

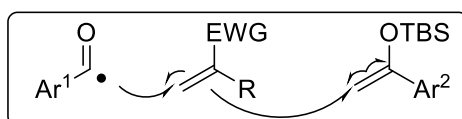
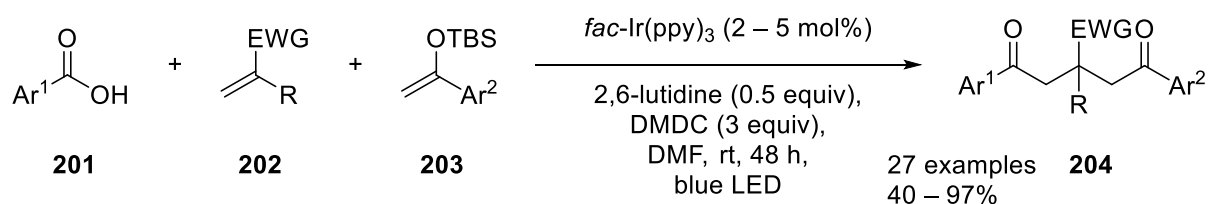
## 2.4 Formation of the vinyl radical *in situ* by a multicomponent cascade process

Multicomponent reactions (MCRs) represent a powerful tool in organic chemistry to quickly access complex structures from simple starting materials by forming multiple bonds at one time.<sup>[165-170]</sup> A MCR is usually defined as an one-pot reaction with at least three different components which incorporates large fragments of all starting materials in the final framework of the product. As a consequence, this can quickly result in a huge database of different derivatives due to possible functionalization at diverse locations in the molecule. However, the most prevalent MCRs are based on ionic reactions, whereas radical processes are rather scarce.<sup>[171]</sup> Problems can obviously arise by competing cross-reactions of the radicals which lead to tedious side-products, therefore diminishing the yield. However, this can be bypassed *via* radical polar effects or by careful adjustment of the stoichiometry or the conditions.<sup>[172,173]</sup> This has been very recently exploited by Chu and co-workers in a four-component radical trifluoromethylation cascade reaction. Therein, an electrophilic CF<sub>3</sub>-radical was first created from Togni's reagent (**196**) and Hantzsch ester (**197**) by an electron-donor-acceptor complex (EDA) which was first coupled with an electron-rich alkene **198** and subsequently with an electron-deficient olefin **199** (Scheme 53).<sup>[174]</sup>



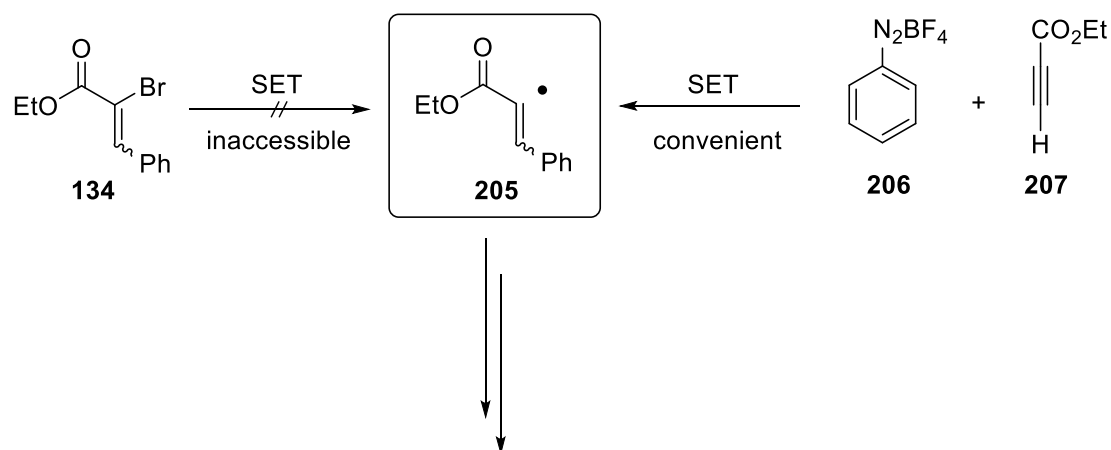
**Scheme 53.** Multicomponent radical cascade by Chu *et al.* Radical cross-reactivity was successfully suppressed *via* radical polar effect.<sup>[174]</sup>

Although some mixed ionic / radical multicomponent processes mediated by visible light can be found,<sup>[175-178]</sup> pure multicomponent radical reactions are rather scarce. Very recently, Wallentin and co-workers disclosed a photoredox three-component reaction (Scheme 54).<sup>[179]</sup> Again, selectivity prevailed by a radical polar effect. Based on the oxidative quenching cycle of *fac*-Ir(ppy)<sub>3</sub>, acyl radicals were generated from anhydrides which were formed *in situ* from carboxylic acids **201** and dimethyl carbonate (DMDC). These electron-rich acyl radicals readily react with electron-deficient double bonds **202** which can further couple with electron-rich silyl enol ethers **203**.



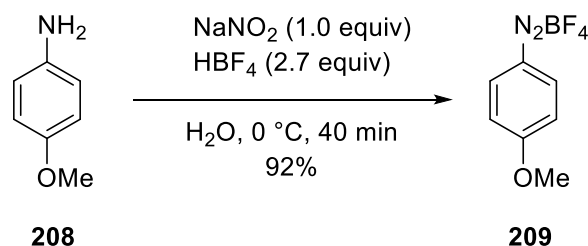
**Scheme 54.** Visible light mediated redox-neutral three-component reaction.<sup>[179]</sup>

As the direct activation of the C-Br bond of **134** through a photoinduced electron transfer (PET) was found to be unsuitable to access vinyl radical key intermediate **205**, it was next hypothesized if such a reactive intermediate could be created *in situ* from other readily accessible radical precursors (Scheme 55). In principle, vinyl radicals can be formed by the addition of carbon-centered radicals to alkynes.<sup>[3,5,7]</sup> In order to access a similar intermediate, an aryl radical should be coupled with ethyl propiolate (**207**). In this regard, aryl diazonium salts have already been proven to be suitable aryl radical precursors in photoredox catalysis due to their relatively high reduction potentials.<sup>[105,148,177,180-183]</sup>



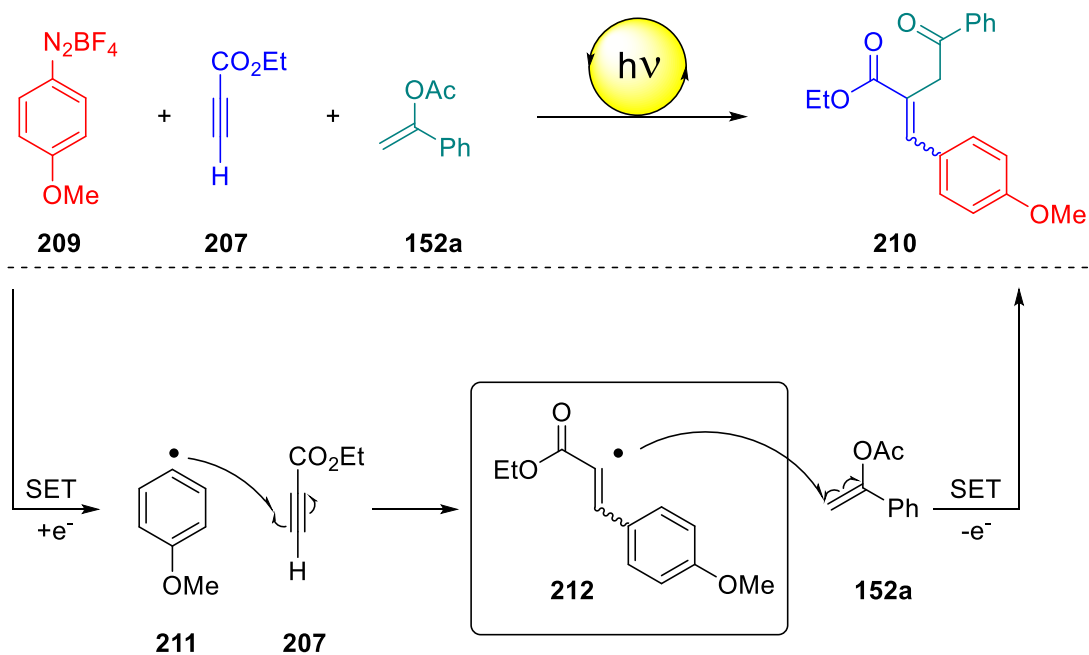
**Scheme 55.** Planned synthetic design to access vinyl radical key intermediate *in situ*.

Ethyl propiolate (**207**) was commercially available and aryl diazonium tetrafluoroborates **206** can easily be obtained by treating the corresponding aniline with  $\text{NaNO}_2$  in the presence of  $\text{HBF}_4$ .<sup>[148]</sup> In order to increase the radical polar effect, electron-rich aryl diazonium salt **209** was chosen as model substrate (Scheme 56).



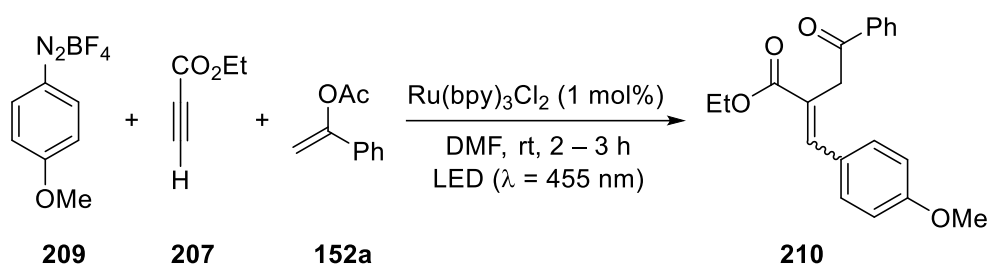
**Scheme 56.** Synthesis of aryl diazonium salt **209**.<sup>[148]</sup>

Again, previously synthesized enol acetate (**152a**) should serve as trapping reagent (*cf.* Chapter 2.1). Selectivity should be preserved by radical polar effect. Therefore, electron-rich aryl radical **211** should readily add to electron-deficient ethyl propiolate (**207**) to give relatively electron-poor vinyl radical key intermediate **212** which can further be coupled with electron-rich enol acetate **152a** (Scheme 57). However, selectivity problems can easily occur through side-reactions. In this regard, the photoinduced direct coupling between aryl diazonium salts and enol acetates have already been described in the literature,<sup>[148]</sup> as well as HAT to quench either the aryl radical intermediate,<sup>[182]</sup> or the vinyl radical intermediate.<sup>[138]</sup>



**Scheme 57.** Planned photocatalytic three-component cascade reaction.

With all starting materials in hand, first test reactions were performed with  $\text{Ru}(\text{bpy})_3\text{Cl}_2$ , because this photocatalyst has already proven to be active for the coupling of vinyl radicals with enol acetates (*cf.* Chapter 2.1).<sup>[150,151]</sup> Also DMF seemed to be the most suitable solvent as visible light induced photoredox reactions with aryl diazonium salts,<sup>[148,182,184,185]</sup> as well as previous reports on vinyl radicals were conducted in this polar solvent (Table 6).<sup>[138,139]</sup>

**Table 6.** Visible light promoted three-component reaction.<sup>a</sup>

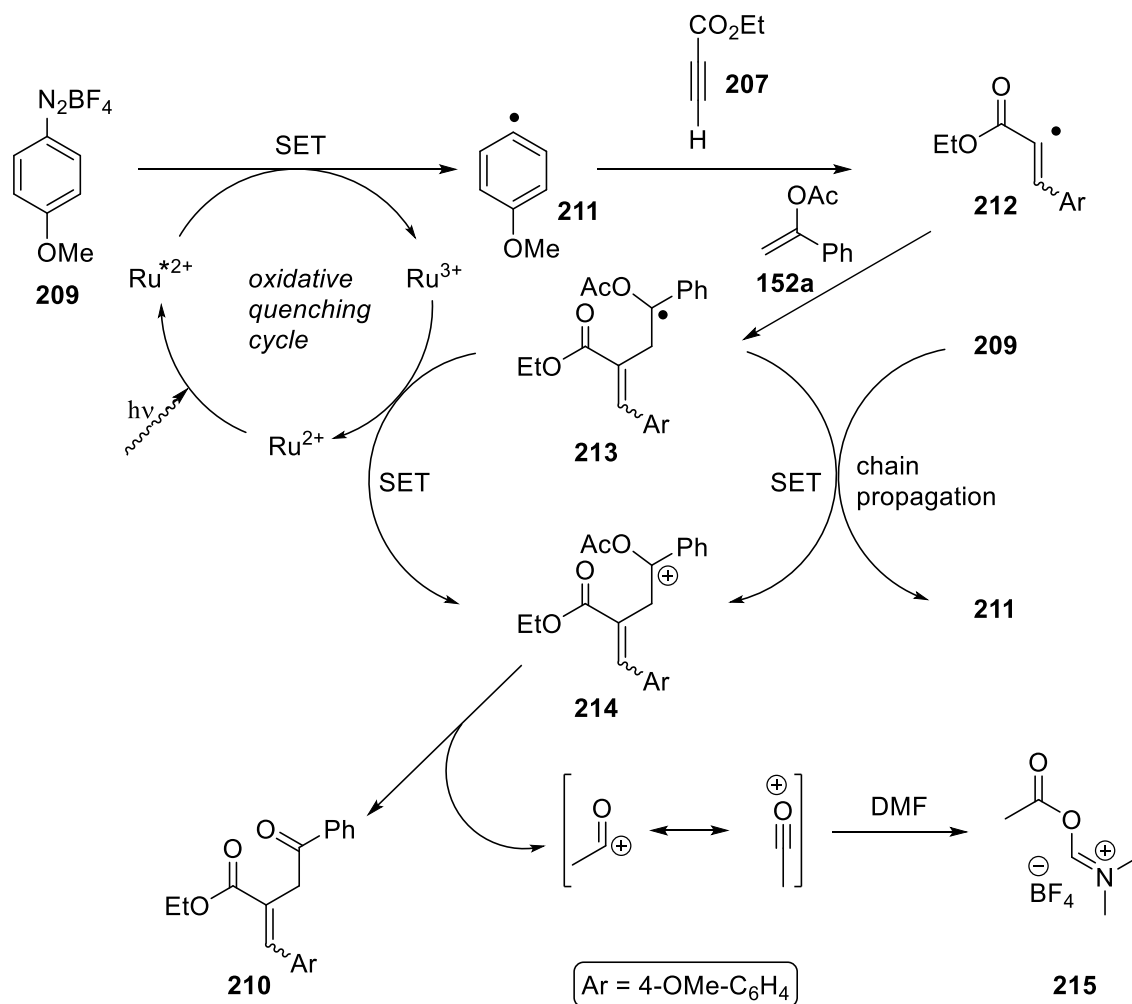
Entry	Aryl diazonium salt <b>209</b> (equiv)	Ethyl propiolate <b>207</b> (equiv)	Enol acetate <b>152a</b> (equiv)	DMF (mol/L)	Yield (%) <sup>b</sup>
1	1.0	2.0	1.2	0.2	- <sup>c</sup>
2	1.0	6.0	1.2	0.2	19
3	2.0	6.0	1.0	0.2	22
4	2.0	6.0	1.0	0.5	27
5	2.0	6.0	1.0	0.16	- <sup>c</sup>

<sup>a</sup>Reactions were performed on a 0.5 or 0.3 mmol scale with 1 mol% photocatalyst in DMF. <sup>b</sup>Combined isolated yields of separated *E* and *Z* isomer after purification *via* column chromatography. <sup>c</sup>Complex reaction mixture was obtained.

However, first reaction with only two equivalents of alkyne **207** only resulted in a complex mixture between potential desired product **210** and several literature known by-products (Table 6, entry 1).<sup>[138,148,182]</sup> In order to minimize cross-reactivity and push the selectivity more to product **210**, the amount of ethyl propiolate (**207**) was investigated next. Indeed, an excess of six equivalents of **207** gave the desired coupling product in 19% yield (entry 2). But still, significant amounts of cross-reactions prevented higher yields of **210**. Slightly higher yields were obtained by using an excess of diazonium salts which made the enol acetate the stoichiometric limiting compound (entry 3). A higher concentration reduced the amount of by-products, but nonetheless only 27% yield of desired product could be isolated (entry 4). As expected, when the reaction mixture was more diluted, only traces of product were obtained and side reactions were favored (entry 5).

Scheme 58 depicts a plausible reaction mechanism based on recent literature reports.<sup>[148,149]</sup> The catalytic cycle is initiated by photoexcitation of  $\text{Ru}(\text{bpy})_3\text{Cl}_2$  with visible light. The excited catalyst is oxidatively quenched by aryl diazonium salt **209** providing aryl radical **211**. This electron-rich radical can couple with electron-deficient alkyne **207** generating vinyl radical intermediate **212**. Subsequently, this electron-poor radical can be trapped by

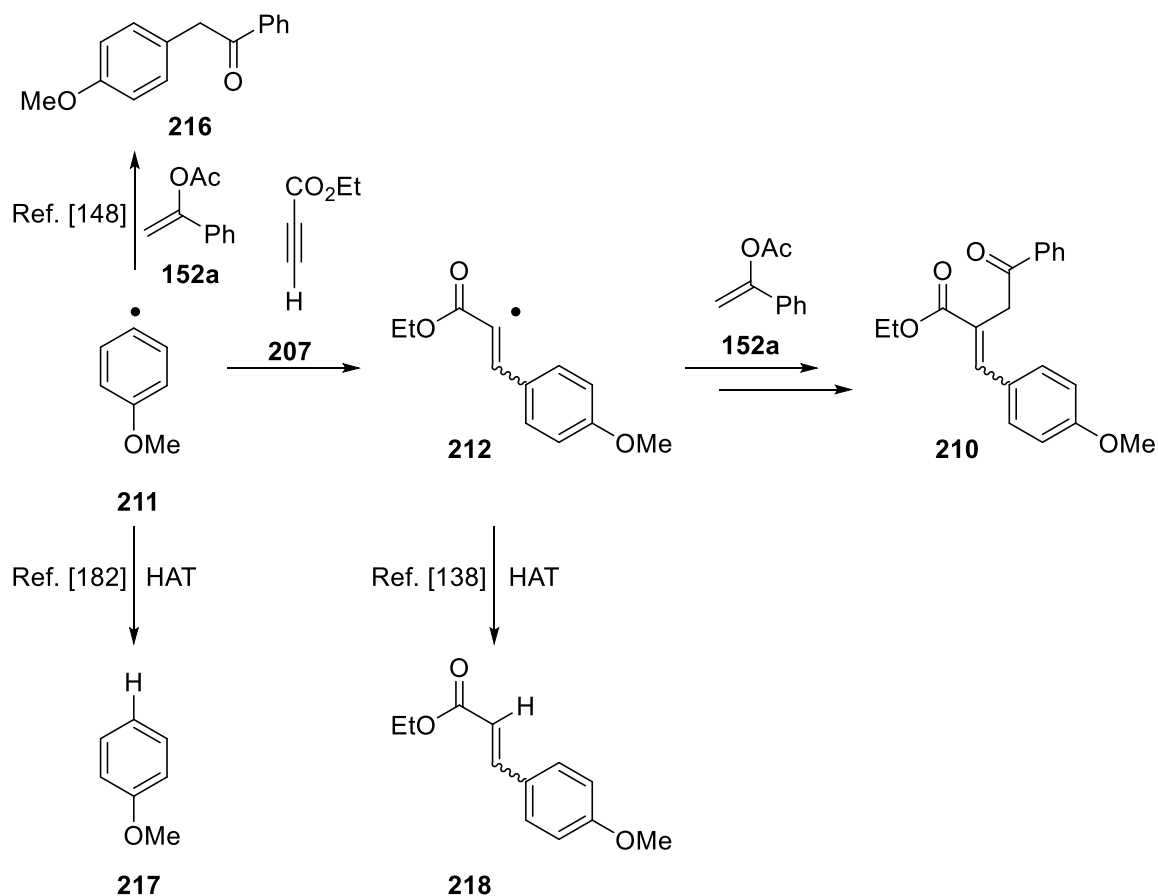
electron-rich enol acetate **152a**. Radical **213** is oxidized to the cation **214** via another SET either by the photocatalyst which closes the catalytic cycle or by initiating a radical chain process. Product **210** is formed after release of an acyl cation which can be trapped by DMF for example.



**Scheme 58.** Plausible reaction mechanism to form product **210**.

Unfortunately, only small amounts actually followed this pathway as only 27% of desired product was isolated at best. Indeed, the proposed reaction mechanism is prone towards several side reactions (Scheme 59). At first, the concentration of alkyne **207** needs to be high enough to lead the reaction towards vinyl radical intermediate **212** instead of literature known coupling with enol acetate **152a**.<sup>[148]</sup> However, simultaneously the concentration of enol acetate **152a** also needs to be high for an efficient trapping of the vinyl radical intermediate **212** in order to suppress HAT to ethyl cinnamate **218**.<sup>[138]</sup> Additionally, a slight excess of aryl

diazonium salt is recommended as defunctionalization to anisole (**217**) will always be present to some extent.<sup>[182]</sup> Unfortunately, this leads to a dilemma. While one side-reaction can be efficiently suppressed, it favors another but does not necessarily increase the yield of desired product.



**Scheme 59.** Potential side reactions which can occur during the reaction. Horizontal arrows lead to the desired product, whereas vertical arrows lead to literature known by-products.

In principle, higher yields are possible by further enhancing the radical polar effect. Therefore, more electron donating or electron withdrawing substituents might be installed to suppress undesired cross-reactions. However, this would make this transformation highly dependent on electronic effects, therefore dramatically decreasing the scope and thus limiting its synthetic value. Therefore, further screening to optimize this reaction was omitted.



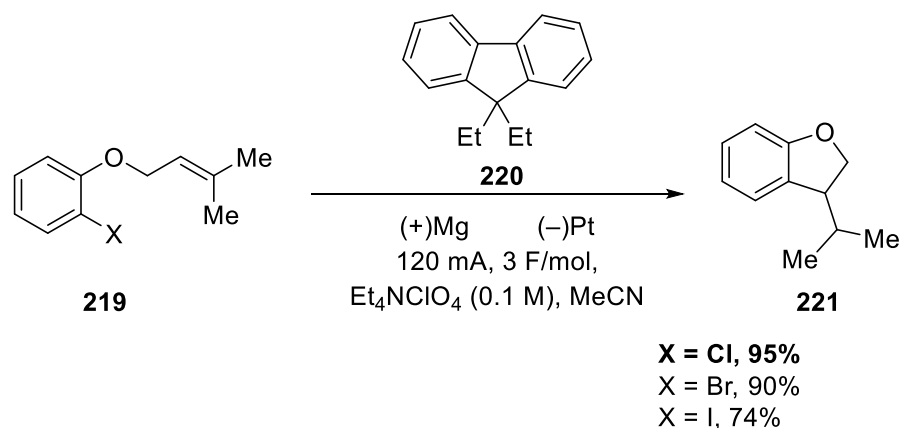
## 2.5 Conclusion

In summary, a great variety of attempts were tested in order to bypass previous limitations in photoredox chemistry. Based on previous investigations, it was found that the aryl enone system seemed to be a strict requirement for the photochemical activation of  $\alpha$ -bromo chalcones with visible light.<sup>[138,139]</sup> It has been tried to mimic the aromatic nature of chalcones with the help of an aromatic redox auxiliary. Thus, a 2-imidazolyl substituted  $\alpha$ -bromo chalcone derivative was synthesized. Supported by the literature, this auxiliary should be easily cleavable after the photoreaction. However, it turned out that the synthetic route towards desired chalcone derivative was not straightforward. Additionally, the yield in the photochemical step was disappointingly low and subsequent substitution of the 2-imidazolyl core failed. In another attempt several phenyl cinnamates were examined. It was tried to shift the reduction potentials into higher regions which would make them more accessible for established photocatalysts in the oxidative quenching cycle. In this way, several phenyl cinnamates bearing electron withdrawing groups were synthesized. However, it was found that these substitutions exhibited nearly no effect on the reduction potentials compared to simple ethyl cinnamate. As the oxidative quenching cycle seemed to be ineffective, the reductive quenching cycle was investigated next. Here, activation of  $\alpha$ -bromo ethyl cinnamate was achieved but coupling of the vinyl radical failed. Instead, only hydrodebrominated product was obtained, an omnipresent obstacle associated with the reductive quenching cycle. At last, it was tried to access the vinyl radical *in situ*. Thus an aryl radical should first add to an alkyne forming the vinyl radical intermediate. This intermediate should further be trapped with enol acetates giving highly desirable 1,4-dicarbonyl compounds. Indeed, the product was formed and could be isolated but unfortunately, this multicomponent reaction was prone to numerous side reactions. This cross-reactivity could not be bypassed which strongly diminished the yield of desired product.

### 3 Visible light mediated activation of $\alpha$ -chloro cinnamates<sup>1</sup>

#### 3.1 Literature background

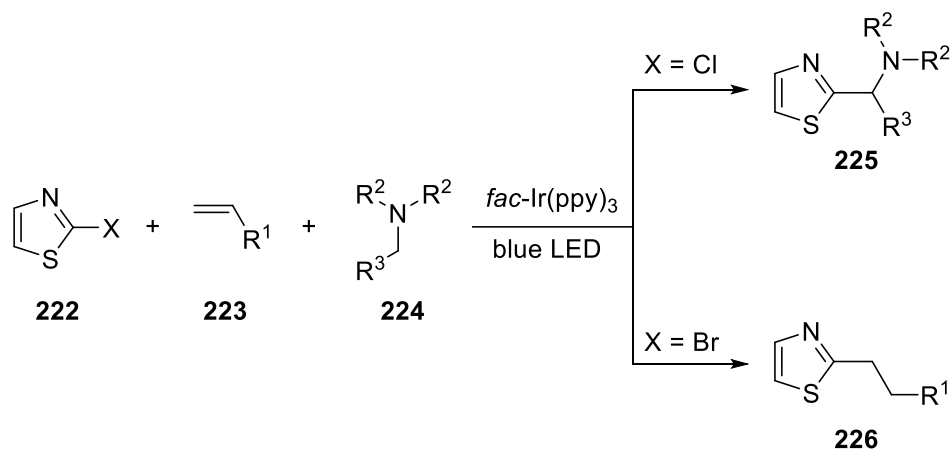
Selective activation of C(sp<sup>2</sup>)-chloride bonds using transition metal catalysis is still highly in demand. In sharp contrast to its heavier analogues, chloro-substituted substrates generally exhibit attractive starting materials since they are readily available at a lower cost and also in terms of sustainability superior and therefore significantly preferred. On the contrary, activation of C(sp<sup>2</sup>)-chloride bonds is often considered challenging due to their noticeable higher bond dissociation energy.<sup>[186]</sup> Therefore, activation of C(sp<sup>2</sup>)-chlorides frequently requires special designed catalysts or harsh reaction conditions.<sup>[187]</sup> In principle, reactivity strictly correlates with the bond dissociation energies of C-halogen bonds,<sup>[188,189]</sup> however, some inconsistencies regarding the activation *via* electrochemical methods can be found in the literature. In 2012, Suga and co-workers reported the electro-reductive cyclization of aryl halides **219** promoted by 9,9-diethylfluorene (**220**) as mediator (Scheme 60).<sup>[190]</sup> Despite having the most negative reduction potential, the chloro-substituted compound exhibited the highest reactivity compared to its aryl bromide or iodide derivative. This is unusual because the expected result should be the other way round. Unfortunately, the authors could not give a plausible explanation regarding this exceptional trend.



**Scheme 60.** Electro-reductive cyclization of aryl halides promoted by fluorene derivatives.<sup>[190]</sup>

<sup>1</sup> This chapter is partially based on T. Föll, J. Rehbein, O. Reiser, *Org. Lett.* **2018**, *20*, 5794-5798. Appropriate copyrights have been obtained where necessary.

Although it is clearly known that the bond dissociation energies of the  $C(sp^2)-X$  follows the order  $F > Cl > Br > I$ ,<sup>[186]</sup> the dissociation and fragmentation rate of  $C(sp^2)-X^{\bullet-}$  attracted considerable attention in the past.<sup>[128,129,131-133]</sup> It has been suggested that the bond dissociation energy in the ground state is negligible because the carbon-halogen bond loses the majority of the bond strength after addition of one electron.<sup>[130]</sup> The group of Zhang estimated the bond dissociation energies of benzyl chloride and benzyl bromide in the radical anion species ( $RX^{\bullet-}$ ). Therein, they concluded that the C-Cl bond is exergonic (-6.5 kcal/mol) towards cleavage to the benzyl radical and the chloride anion whereas the C-Br bond in the corresponding benzyl bromide was found to be endoenergetic (2.5 kcal/mol).<sup>[130]</sup> This means that fragmentation would unexpectedly be more favored in the case of the chloride. However, later the group of Daasbjerg performed similar calculations for the same substrates.<sup>[191]</sup> In this study, the author found that these values should be substantially more negative for both substrates. In fact, both substrates should be unstable whereas dissociation in case of the bromide should be even slightly more favored (-50 kcal/mol for  $RCI^{\bullet-}$  and -56 kcal/mol for  $RBr^{\bullet-}$ ). However, this would suggest that despite the huge difference in the ground state, the bond dissociation energies of both substrates suddenly converge to a similar value after activation, thereby making the previous difference in energy negligible. As a consequence, both substrates should immediately undergo fragmentation after injection of one single electron. Besides these theoretical studies, there are also additional experimental discrepancies in visible light photoredox catalysis. Weaver and co-workers demonstrated that 2-halo azoles **222** exhibited complete different reactivity based on the attached halogen atom. Therein, they reported that 2-chloro azoles readily underwent C-H functionalization with amines whereas under similar conditions 2-bromo azoles were preferably coupled with alkenes even in the presence of amines (Scheme 61).<sup>[162,192]</sup> The authors concluded that the fragmentation rate of the radical anion is responsible for the different reactivity.<sup>[162]</sup>

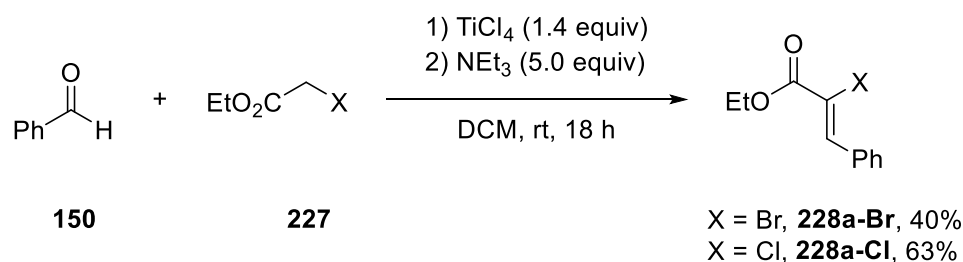


**Scheme 61.** Different reactivity of 2-halo azoles.<sup>[162,163,192]</sup>

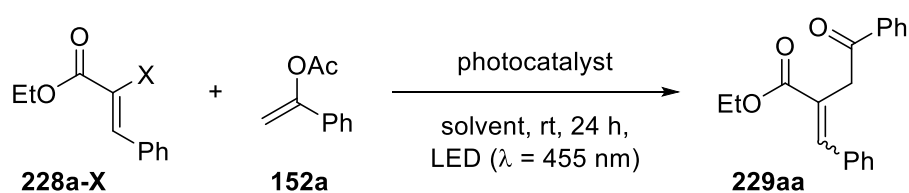
Furthermore, it has been proposed that photochemically generated Br<sup>-</sup> could easily be oxidized to Br<sup>•</sup> in the presence of Ru(bpy)<sub>3</sub>Cl<sub>2</sub>.<sup>[193-195]</sup> This has been exploited to form Br<sub>2</sub> *in situ*. However, this mechanistic proposal remains questionable because such transformations were only investigated with CBr<sub>4</sub> as Br<sup>-</sup> source and in the past it has already been demonstrated that fragmentation of polyhalomethanes also works in the absence of any photocatalyst.<sup>[196]</sup>

### 3.2 Optimization of the reaction conditions

In the past, vinyl bromides bearing an extended  $\pi$ -system such as  $\alpha$ -bromo chalcones **131** were found to be excellent vinyl radical precursors under typical photocatalytic conditions with visible light (*vide supra*). However, all attempts to transfer such transformations to more reduced  $\pi$ -systems such as  $\alpha$ -bromo ethyl cinnamate (**228a-Br**) gave only mediocre results at best so far. This decrease of the conjugated  $\pi$ -system is also reflected in the observed difference for the measured reduction potentials. Indeed, the gap between both substrates is tremendous ( $E_{\text{RX/RX}}^{\circ} = -0.88$  V vs SCE for  $\alpha$ -bromo chalcone;  $E_{\text{RX/RX}}^{\circ} = -1.54$  V vs SCE for **228a-Br**), thereby substantially hampering the initial single electron transfer. Nonetheless, **228a-Br** should be amenable for highly reducing *fac*-Ir(ppy)<sub>3</sub> ( $E_{\text{M}^+/\text{M}^{\bullet}}^{\circ} = -1.73$  V vs SCE). As utilizing the reductive quenching cycle in order to reach more negative reduction potentials was found to be unproductive, the oxidative quenching cycle with abovementioned photocatalyst was re-investigated. Additionally, considering the aforementioned literature aspects regarding the fragmentation of C(sp<sup>2</sup>)-halogen bonds *via* single electron reduction, photochemical activation of vinyl chlorides also seemed theoretically feasible. Therefore,  $\alpha$ -chloro ethyl cinnamate (**228a-Cl**) was incorporated in the primary screening experiments. Gratifyingly, both substrates are amenable in one step. Applying the general procedure developed by Jothi *et al.*, **228a-Br** and **228a-Cl** were both obtained in reasonable yields as diastereomerically pure *Z* isomer (Scheme 62).<sup>[197]</sup>



**Scheme 62.** Titanium mediated synthesis of  $\alpha$ -halo cinnamates **228a-Br** and **228a-Cl**.

**Table 7.** Catalyst screening and reaction optimization.<sup>a</sup>

Entry	Photocatalyst	$E_{\text{M}^+/\text{M}^{\bullet}}^{\circ}$ (V vs SCE)	X	Solvent	Yield (%) <sup>b</sup>
1	<i>fac</i> -Ir(ppy) <sub>3</sub>	-1.73	Br	DMF	16
2	<i>fac</i> -Ir(ppy) <sub>3</sub>		Br	MeCN	8
3	<i>fac</i> -Ir(ppy) <sub>3</sub>		Cl	DMF	43
4	<i>fac</i> -Ir(ppy) <sub>3</sub>		Cl	MeCN	58
5 <sup>c</sup>	<i>fac</i> -Ir(ppy) <sub>3</sub>		Cl	MeCN	98
6 <sup>d</sup>	<i>fac</i> -Ir(ppy) <sub>3</sub>		Cl	MeCN	15
7	Ir(ppy) <sub>2</sub> (dtbbpy)PF <sub>6</sub>	-0.96	Cl	MeCN	-
8	Ir[dF(CF <sub>3</sub> )ppy] <sub>2</sub> (dtbbpy)PF <sub>6</sub>	-0.89	Cl	MeCN	-
9	Ru(bpy) <sub>3</sub> Cl <sub>2</sub>	-0.81	Cl	MeCN	-
10 <sup>e</sup>	Cu(dap) <sub>2</sub> Cl	-1.43	Cl	MeCN	-
11 <sup>f</sup>	-		Cl	MeCN	-
12 <sup>g</sup>	<i>fac</i> -Ir(ppy) <sub>3</sub>		Cl	MeCN	-

<sup>a</sup>Standard reaction conditions: **228a-X** (0.5 mmol), **152a** (2.5 mmol), photocatalyst (1 mol%), solvent (c = 0.1 M), N<sub>2</sub> atmosphere, rt, 24 h, blue LED ( $\lambda = 455 \text{ nm}$ ). <sup>b</sup>Isolated yields after purification *via* column chromatography. *E/Z* ratio of approximately 1:1 in all cases. <sup>c</sup>2mol% catalyst. <sup>d</sup>Under O<sub>2</sub> atmosphere. <sup>e</sup>Green LED ( $\lambda = 530 \text{ nm}$ ) was used. <sup>f</sup>No photocatalyst. <sup>g</sup>No light.

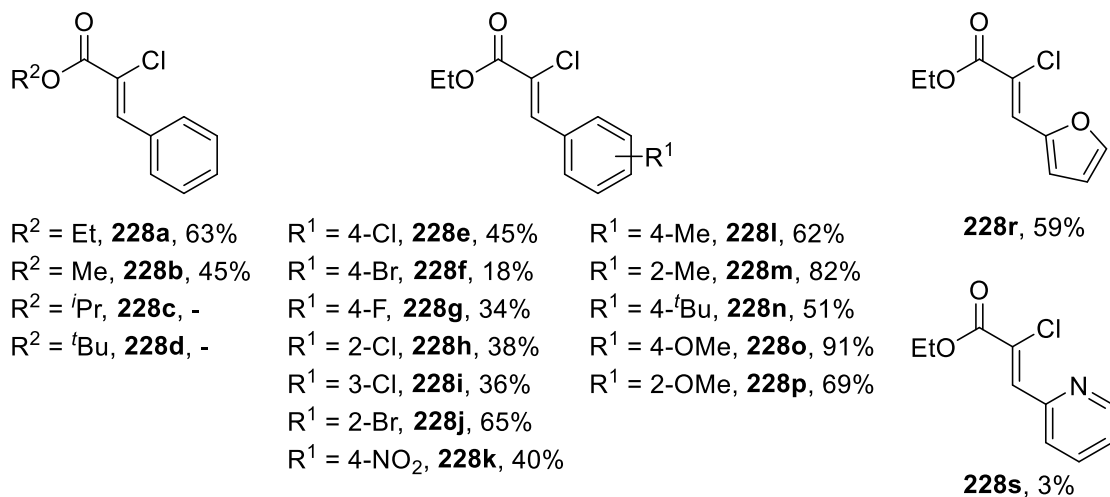
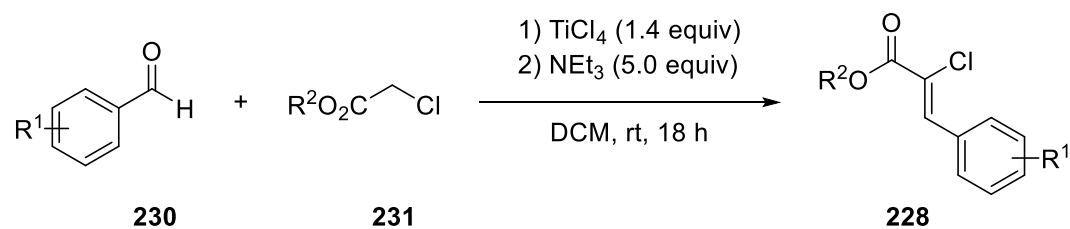
With both vinyl halides in hand, first test reactions were carried out using *fac*-Ir(ppy)<sub>3</sub> as photocatalyst (Table 7). Again, enol acetate **152a** should serve as coupling partner. Despite a reduction potential of -1.54 V vs SCE in MeCN and thereby clearly in the range of the photocatalyst, **228a-Br** was found to be unsuitable and gave only traces of the desired compound in this transformation (entry 1 and 2). Subjection of **228a-Cl**, which reduction potential was priorly determined to be -1.64 V vs SCE in MeCN, to similar reaction conditions surprisingly gave desired 1,4-dicarbonyl compound **229aa** in much higher yields. Both DMF and MeCN were found to be suitable solvents and gave rise to **229aa** in moderate yields (entry 3 and 4). Since MeCN slightly outperformed noxious DMF concerning the yield, further optimizations were performed in more benign MeCN. Full consumption of starting material and an extraordinary clean conversion towards **229aa** was obtained after increasing

the catalyst loading to 2 mol% (entry 5). However, an inert atmosphere seemed to be a strict requirement in this transformation as strongly diminished yields were obtained under O<sub>2</sub> atmosphere (entry 6). Among other established photocatalysts, *fac*-Ir(ppy)<sub>3</sub> was identified as the solely active catalyst which is in line with their more positive reduction potential (entry 7 – 10). Finally, control experiments proved a photocatalytically driven process as no conversion was observed in the absence of either photocatalyst or light (entry 11 and 12).

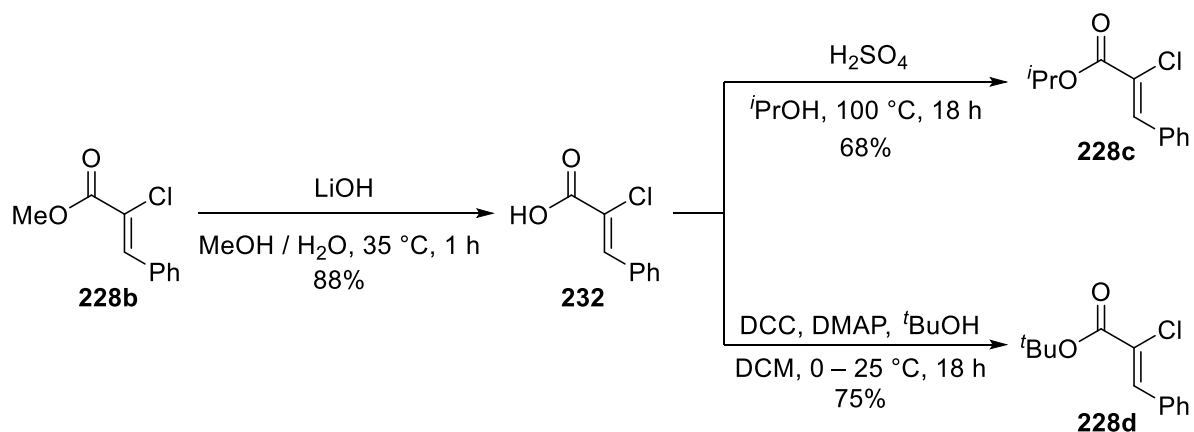
### 3.3 Substrate scope

It has been shown that *fac*-Ir(ppy)<sub>3</sub> is indeed an efficient photocatalyst for the single electron reduction of  $\alpha$ -chloro ethyl cinnamate (**228a-Cl**) in MeCN. Furthermore, after chloride extrusion the resulting vinyl radical intermediate could be readily coupled. Using benign visible light as sole energy source, it was found that enol acetate **152a** is an excellent trapping reagent which gave rise to **229aa** in marvelous yields. As activation of C(sp<sup>2</sup>)-chlorides is generally highly demanded and the presented reaction produced synthetically useful 1,4-dicarbonyl compounds, it was decided to further investigate this transformation. Therefore, a large set of both  $\alpha$ -chloro cinnamates **228** and enol acetates **152** as trapping reagents was synthesized. Gratifyingly, most  $\alpha$ -chloro cinnamates were accessible by applying previously described reaction sequence for **228a-Br** and **228a-Cl**.<sup>[197]</sup> Therefore, a large set of substrates with various electron donating or withdrawing groups attached on the aromatic ring was synthesized from the corresponding readily available benzaldehydes **230** (Scheme 63). Concerning heterocyclic derivatives, electron rich 2-furyl-substituted and electron poor 2-pyridyl derivative were taken into account. Unfortunately, the reaction failed for the synthesis of sterically demanding esters **228c** and **228d**. However, these substrates were easily accessed after saponification of the methyl ester **228b** to the carboxylic acid **232** and subsequent re-esterification (Scheme 64). Further potential limitations should be pointed out by the non-existent or disconnected  $\pi$ -systems of the substrates **228t** and **228u**. A chlorination elimination sequence was tried for **228t** whereas **228u** was obtained in an Fe(0) mediated protocol developed by Mioskowski *et al.* (Scheme 65 and 66).<sup>[198,199]</sup>

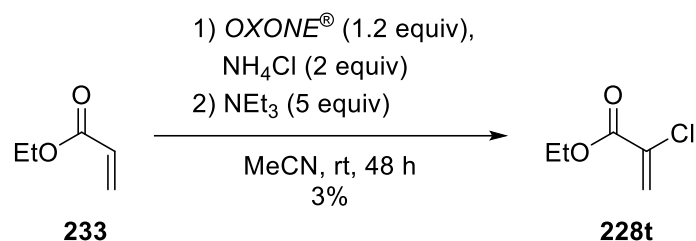




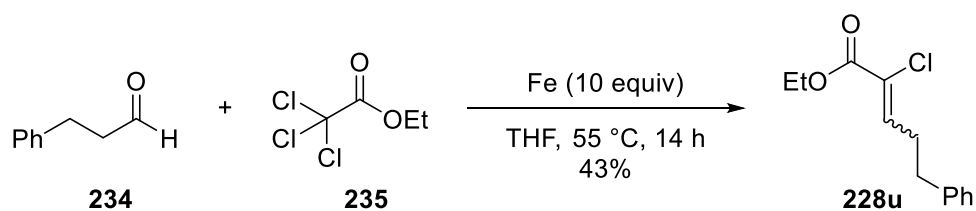
**Scheme 63.** Synthesis of  $\alpha$ -chloro cinnamates *via* titanium mediated olefination.<sup>[197]</sup>



**Scheme 64.** Saponification of methyl ester **228b** and subsequent esterification to **228c** and **228d**.

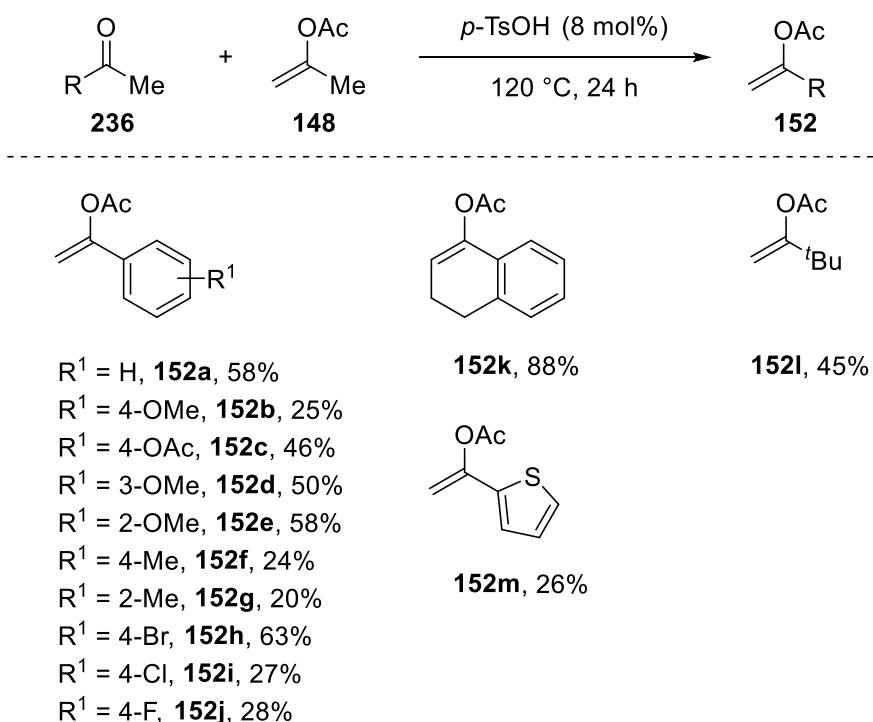


**Scheme 65.** Synthesis of **228t** by applying a protocol by Nama *et al.*<sup>[199]</sup>



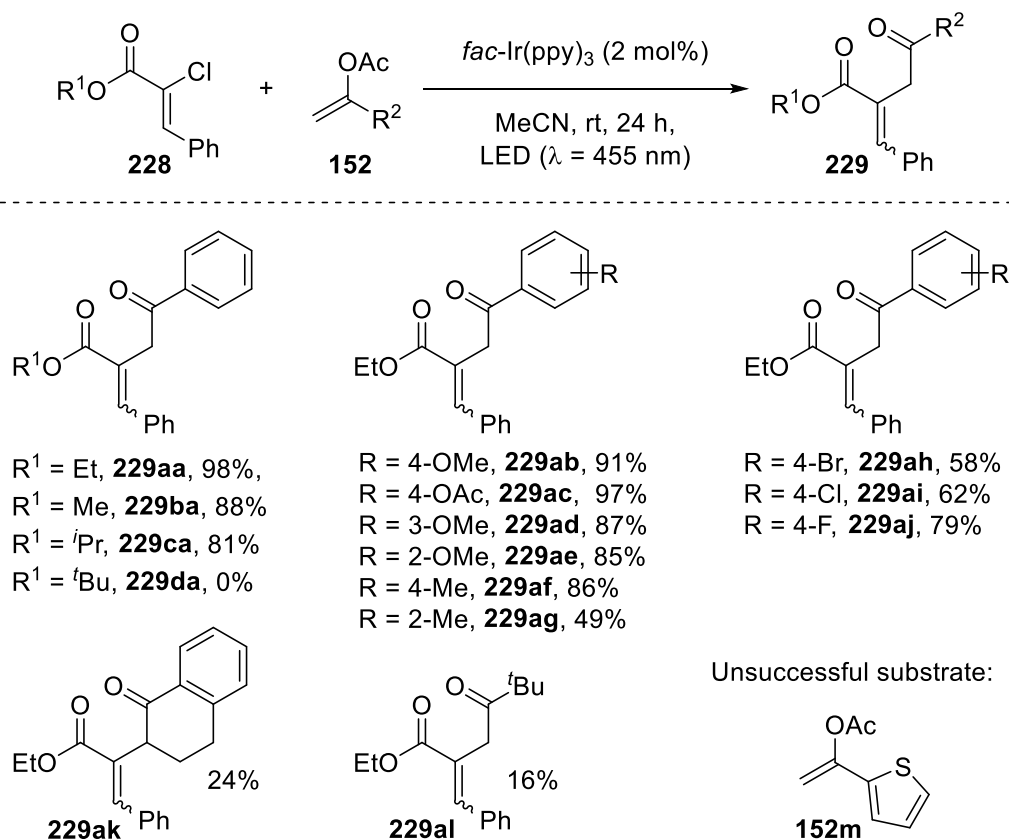
**Scheme 66.** Synthesis of **228u** by applying a protocol by Mioskowski *et al.*<sup>[198]</sup>

An overview of the successfully prepared enol acetates **152** is depicted in Scheme 67. Such compounds can be obtained in an acid catalyzed reaction between isopropenyl acetate (**148**) and the corresponding ketone **236**.<sup>[200]</sup> Again, focus was laid on several electron withdrawing or electron donating groups at different positions at the aromatic ring. Also sterically demanding derivative **152k**, aliphatic compound **152i** and heterocyclic **152m** should reveal limitations of the planned photocatalytic coupling with  $\alpha$ -chloro cinnamates.



**Scheme 67.** Preparation of enol acetates **152**.<sup>[200]</sup>

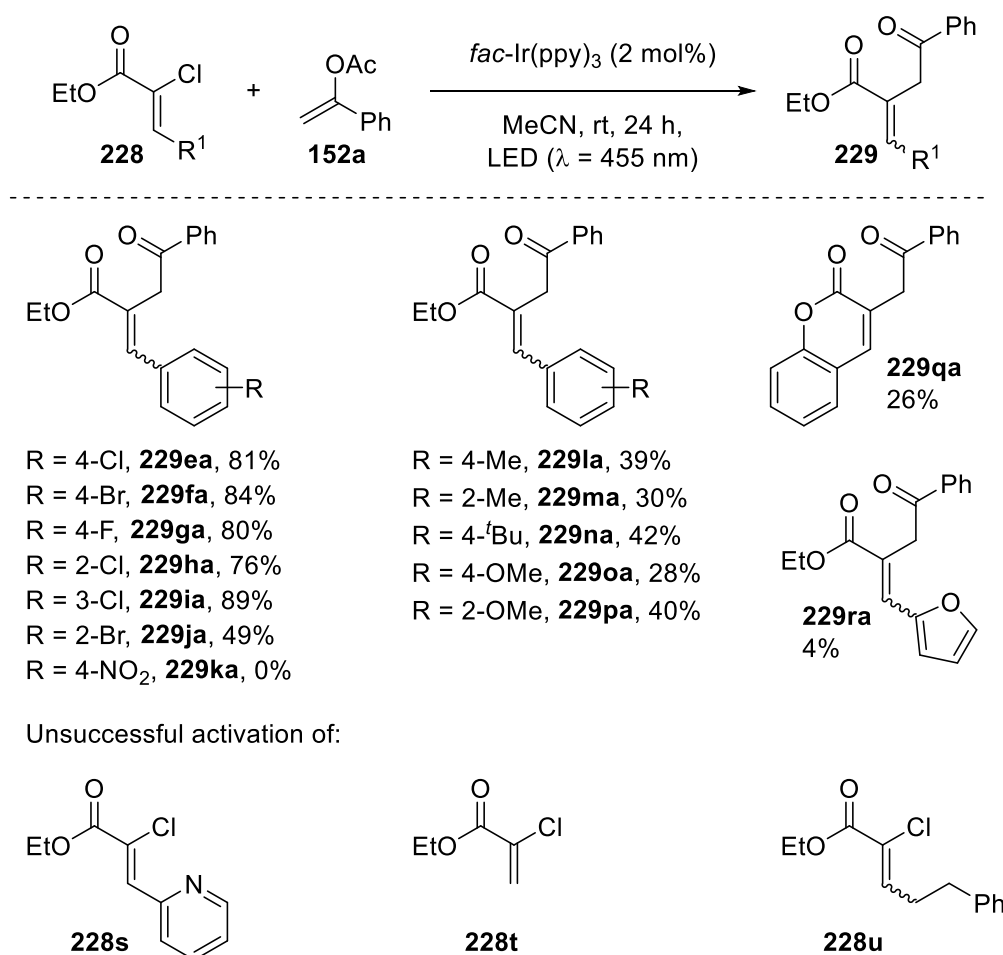
Having synthesized a great variety of  $\alpha$ -chloro cinnamates and enol acetates, both substrates were subjected to previously optimized reaction conditions (Table 7, entry 5). Gratifyingly, ester substitution was well tolerated except for sterically bulky <sup>t</sup>Bu-ester **229da** (Scheme 68, **229aa** – **229ca**). Focusing back on originally prepared ethyl ester **228a-Cl**, several enol acetates were investigated next. As expected, a large number of electron rich enol acetates could be readily coupled reflecting the electrophilic nature of the vinyl radical (**229ab** – **229af**). Additionally, high yields usually prevailed at ortho- or para-substituted compounds. Moreover, weak electron acceptors still gave the desired 1,4-dicarbonyl compound in appreciable yields (**229ah** – **229aj**). Notably, no cross-reactivity was observed with attached halogen substituents in the aromatic moiety of the enol acetates. However, the transformation was found to be sensitive towards sterically more demanding trapping reagents (**229ak**). Unfortunately, aliphatic enol acetates gave the desired product only in strongly diminished yields (**229al**) and heterocyclic enol acetate **152m** was not tolerated at all due to known cross-reaction of radical intermediates to such scaffolds.<sup>[138,180]</sup> In all cases, an *E/Z* distribution of nearly 1:1 was observed which might be attributed to the low rotation barrier of vinyl radicals.<sup>[201,202]</sup> However, control experiments<sup>[201,202]</sup> proved that both starting material **228** and product **229** undergo isomerization under these photoconditions.



**Scheme 68.** Scope of enol acetates **152** in the coupling with  $\alpha$ -chloro cinnamates **228**. Standard reaction conditions: **228** (0.5 mmol), **152** (2.5 mmol),  $fac$ -Ir(ppy)<sub>3</sub> (2 mol%) in 5 mL of MeCN. Combined isolated yields of separated *E* and *Z* isomer after purification *via* column chromatography. *E/Z* ratio of approximately 1:1 in all cases, for details see Experimental part.

Next, previously synthesized  $\alpha$ -chloro cinnamates were subjected to optimized reaction conditions (Scheme 69). As electron acceptors generally shift the reduction potential to more positive values, thereby making single electron reduction by excited photocatalyst more feasible, high yields were expected in the case of electron withdrawing substituents.<sup>[70,83,130,191]</sup> In accordance with this prediction, photocatalytic activation of electron deficient  $\alpha$ -chloro cinnamates proceeded smoothly and gave rise to high yields of products (**229ea** – **229ja**). As aryl halides generally exhibit significantly more negative reduction potentials compared to vinyl halides and are therefore not even rudimentally in the range for  $fac$ -Ir(ppy)<sub>3</sub>,<sup>[83,128,129,183]</sup> chemoselectivity prevailed with both chloride (**229ea**, **229ha**, **229ia**) and bromide (**229fa**, **229ja**) atoms attached on the aromatic ring of the cinnamates. As previously observed, nitro groups (**229ka**) were not tolerated at all,<sup>[138,139]</sup> presumably due to efficient quenching of excited states by this functional group.<sup>[83,130,191]</sup> Moving to electron donating groups, restrictions of this photocatalytic transformation were

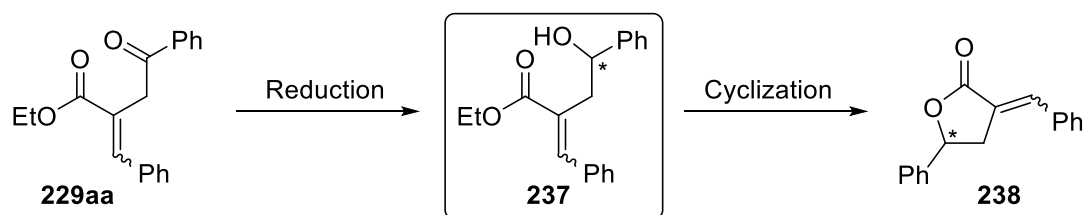
found for both weak and strong donors (**229la** – **229pa**) because such substituents hamper the initial single electron transfer by lowering the reduction potential.<sup>[130]</sup> Therefore, only strongly diminished yields in the range between 30 – 40% were obtained. Again, heterocyclic compounds were not tolerated at all due to cross-reactions of the vinyl radical occurring at the aromatic ring (**229ra**, **228s**). As expected, a conjugated  $\pi$ -system is a strict requirement for this transformation as can be seen from the unsuccessful activation of **228t** and **228u**.



**Scheme 69.** Scope of  $\alpha$ -chloro cinnamates **228**. Standard reaction conditions: **228** (0.5 mmol), **152a** (2.5 mmol),  $fac\text{-Ir(ppy)}_3$  (2 mol%) in 5 mL of MeCN. Combined isolated yields of separated *E* and *Z* isomer after purification *via* column chromatography. *E/Z* ratio of approximately 1:1 to 2:1 in all cases, for details see Experimental part.

### 3.4 Up-scaling of the photochemical transformation and enantioselective synthesis of $\alpha$ -alkylidene- $\gamma$ -aryl- $\gamma$ -butyrolactone (**238**)

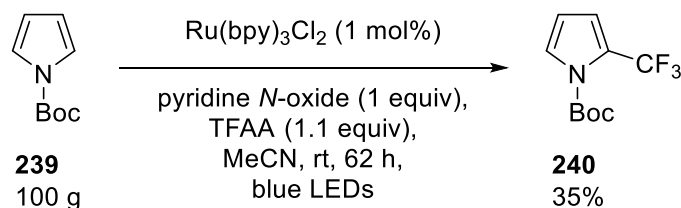
In the previous chapter the visible light mediated activation of vinyl chlorides was introduced. It has been shown that this process was well tolerated for a great variety of functional groups attached on both substrates. Most notably, this transformation gave rise to synthetically attractive 1,4-dicarbonyl compounds.<sup>[203,204]</sup> Such building blocks are generally highly demanded as they can easily be converted into furans, pyrroles, or other heterocycles.<sup>[205-209]</sup> However, such lucrative motifs are often tedious to access by conventional methods.<sup>[210]</sup> This newly developed process represents an excellent alternative using harmless reagents and gentle conditions. As related compounds of **229aa** have already been utilized for the construction of furans<sup>[211]</sup> or pyrroles,<sup>[209]</sup> a stereoselective approach to  $\alpha$ -alkylidene- $\gamma$ -butyrolactone was envisioned as application. Such scaffolds recently attracted much attention as biologically active compounds including anti-inflammatory, phytotoxic, or cytotoxic properties.<sup>[212-217]</sup> The key step towards the desired compound should be a chemo- and stereoselective reduction of the ketone moiety. The resulting chiral alcohol should easily cyclize under acidic conditions which gives rise to the  $\gamma$ -butyrolactone ring (Scheme 70). As both isomers of the 1,4-dicarbonyl compound were perfectly separable *via* column chromatography, this synthetic route should provide diastereomerically pure (*E*)-**238** and (*Z*)-**238**.



**Scheme 70.** Synthetic route towards desired  $\alpha$ -alkylidene- $\gamma$ -aryl- $\gamma$ -butyrolactone **238**. Either pure (*E*)-**229aa** or (*Z*)-**229aa** should provide diastereomerically pure (*E*)-lactone or (*Z*)-lactone.

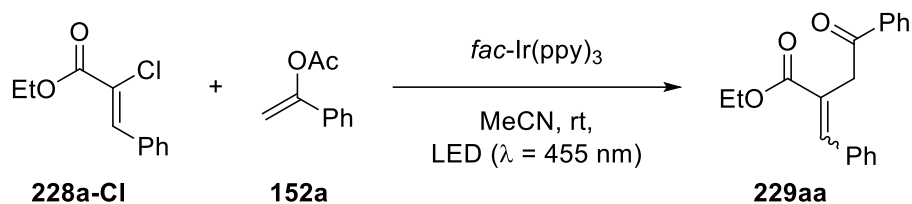
In order to perform a decent screening for the next steps, a substantial quantity of compound **229aa** needed to be synthesized first. So far, the photochemical transformation to **229aa** was only performed on a 0.5 mmol scale which is barely sufficient for one test reaction. Unfortunately, scaling a photoinduced process up to larger amounts is not trivial in sharp contrast to classic reactions.<sup>[218]</sup> Photoreactions are generally limited by Lambert-Beer's law

which describes the attenuation of light through the medium. In other words, a bigger reaction medium inevitably results in prolonged reaction times because light is no longer capable of penetrating the entire reaction medium. For visible light mediated processes this has already been successfully circumvented in 2012 by the invention of continuous-flow setups which are characterized by high surface-area-to-volume ratios,<sup>[219-221]</sup> enabling photoreactions on scales up to 1 kg.<sup>[222-224]</sup> However, Stephenson and co-workers also demonstrated that batch setups are also suitable for multi-gram scales (Scheme 71).<sup>[225]</sup>



**Scheme 71.** Scalable trifluoromethylation of *N*-Boc-pyrrole in a batch setup. TFAA = trifluoroacetic anhydride.<sup>[225]</sup>

A batch setup which has originally been employed for UV-light reactions was considered for the preliminary scale up experiment (see Experimental part for details). Similar to the previously utilized small batch system, irradiation should take place from the inside of the reaction medium. However, instead of a glass rod which was attached to one single LED, the irradiation apparatus now consisted of a hollow glass cylinder filled with a metal block. 30 high power LEDs ( $\lambda = 455$  nm) were wrapped around this metal block which was further connected to an internal water cooling system to maintain ambient temperature. The combined shaft could now be immersed in the previously prepared reaction mixture. A 20 mmol scale seemed most promising to preferably maintain previously optimized conditions as the complete apparatus was limited to 200 mL. Gratifyingly, utilizing this reaction setup gave rise to **229aa** in 61% yield. Most notably, the catalyst loading could be significantly reduced to 0.5 mol% compared to the original 2 mol%. Furthermore, no isolation problems occurred as MeCN was easily evaporated and the excess of enol acetate **152a** was distilled off. Subsequently, the residue was purified by column chromatography to separate both isomers of the product. This first test reaction was not further optimized as it already gave both (*E*)-**229aa** and (*Z*)-**229aa** in nearly 2 grams, respectively and thus sufficient material for some test reactions. A comparison of both reaction setups is depicted in Scheme 72.



40-fold increase →

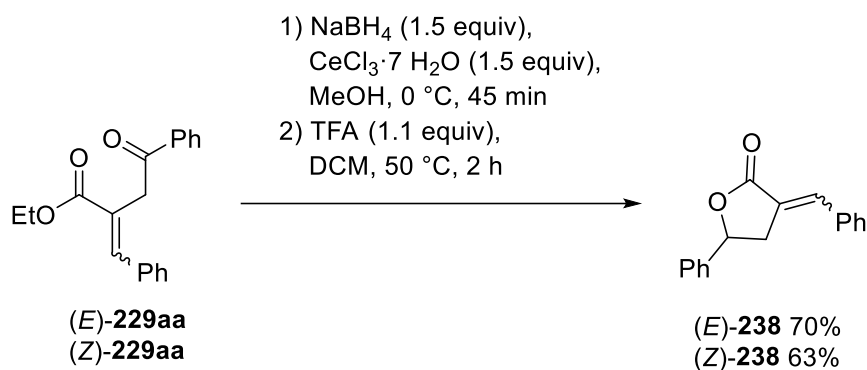


- |   |   |   |
|---|---|---|
| • 1 LED (24 h run time)                 | ↔ | • 30 LEDs (48 h run time)                           |
| • high catalyst loading (2 mol%)        | ↔ | • low catalyst loading (0.5 mol%)                   |
| • time-consuming degassing via FPT      | ↔ | • simplified degassing via N <sub>2</sub> -sparging |
| • 0.5 mmol (105 mg) substrate           | ↔ | • 20 mmol (4.2 g) substrate                         |
| • small amount of product (145 mg, 98%) | ↔ | • high amount of product (3.6 g, 61%)               |

**Scheme 72.** Comparison of small and big reaction setup. FPT = Freeze-Pump-Thaw.

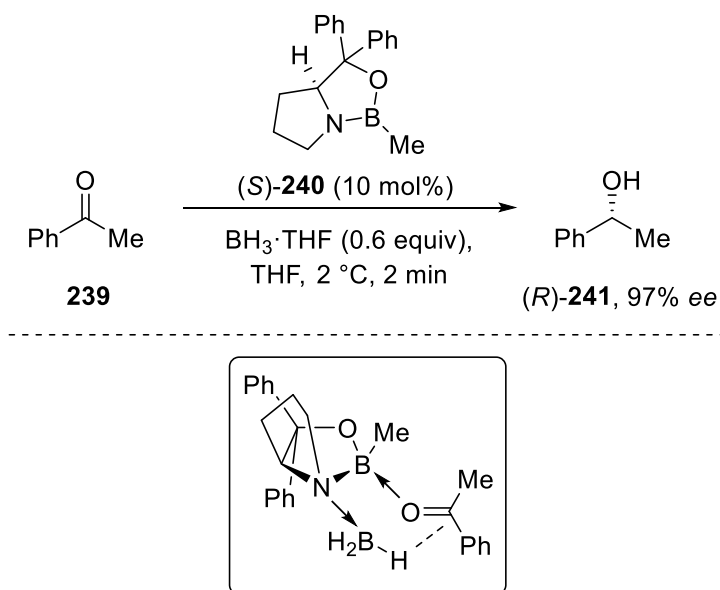
With substantial amounts of pure (*E*)-**229aa** and (*Z*)-**229aa** in hand, first test reactions could be carried out. However, before an enantioselective approach towards the desired  $\gamma$ -butyrolactone **238**, a racemic version needed to be synthesized. In this regard, a Luche reduction was considered in order to increase chemoselectivity and minimize side reactions.<sup>[226]</sup> Therefore, the combination of NaBH<sub>4</sub> and CeCl<sub>3</sub> should help to selectively reduce the ketone group in the presence of the  $\alpha,\beta$ -unsaturated ester in the molecule. Consistent with the HSAB concept, compound **229aa** underwent clean 1,2-reduction of the ketone using a slight excess of NaBH<sub>4</sub> and CeCl<sub>3</sub>. Acidification finally gave lactone ring closure to pure (*E*)-**238** and (*Z*)-**238** as racemates, respectively (Scheme 73).<sup>[227]</sup>





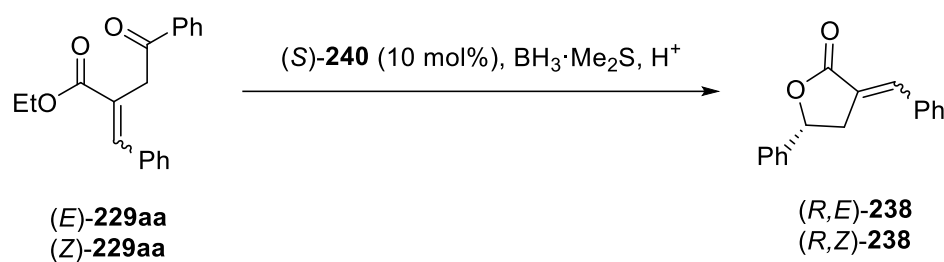
**Scheme 73.** Luche reduction and lactone ring closure to racemic (*E*)-238 and (*Z*)-238.<sup>[226,227]</sup>

In principle, NaBH<sub>4</sub> or related hydride sources represent reliable reagents for the reduction of carbonyls. Activation of the carbonyl group by lanthanide salts may further help to increase chemoselectivity and thus to overcome side reactions.<sup>[228]</sup> Unfortunately, the lack of any chiral information generally prevents these reagents from being suitable for the asymmetric reduction of prochiral compounds. Thus specially designed Lewis acid complexes were required in order to achieve stereocontrol.<sup>[229]</sup> In the past, there have been numerous attempts to force chirality using the combination of NaBH<sub>4</sub> or LiAlH<sub>4</sub> with chiral amino alcohols,<sup>[230,231]</sup> carboxylic acids,<sup>[232,233]</sup> or other additives.<sup>[234,235]</sup> However, these approaches often suffered from sparse substrate scopes or high amounts of chiral additives. An elegant solution was introduced by Corey, Bakshi, and Shibata in the late 1980s. Based on empirical studies of Itsuno and co-workers a few years earlier,<sup>[236,237]</sup> they developed a highly efficient oxazaborolidine mediated catalytic system for the stereoselective reduction of ketones with BH<sub>3</sub>.<sup>[238,239]</sup> Thus outstanding and especially predictable enantiomeric purity of products was achieved. The role of the catalyst was divided into activation of the comparatively inert BH<sub>3</sub> as hydride donor source while simultaneously efficiently shielding one site for the binding of the ketonic substrate to the catalyst (Scheme 74).<sup>[240]</sup> Oxazaborolidine catalyst (*S*)-240 (CBS catalyst) as depicted in Scheme 69 can easily be prepared in a few steps starting from commercially available and cheap (*S*)-proline.<sup>[241]</sup> This outstanding stereocontrol for the catalytic enantioselective reduction of ketones attracted significant attention in the past and led to remarkable advances ever since.<sup>[240,242]</sup>



**Scheme 74.** Proposed transition state for the enantioselective reduction of acetophenone (**239**) as model substrate.<sup>[239,240]</sup>

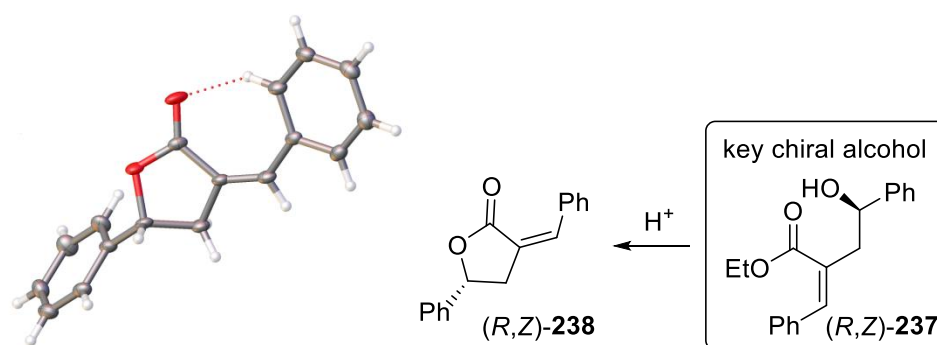
Having successfully synthesized racemic (*E*)-**238** and (*Z*)-**238**  $\gamma$ -butyrolactones, the next step was to perform the reduction of ketone **229aa** enantioselectively. In this regard, the aforementioned CBS reduction seemed to be most suitable. Lactonization should be carried out under the same conditions as already achieved for the racemic alcohols. First test reactions and optimizations were performed with oxazaborolidine catalyst (*S*)-**240** and BH<sub>3</sub>·Me<sub>2</sub>S as hydride source (Table 8). Based on the transition state and the predictive model for the CBS reductions, this reaction should preferably form (*R*)- $\gamma$ -butyrolactones in the end. When (*E*)-**229aa** was subjected to similar reaction conditions as for the Luche reduction, comparable regioselectivity was observed. Unfortunately, the starting material was poorly consumed and only approximately 25% reacted (entry 1). Prolonging the reaction time from 1 h to 4 h gave desired (*E*)-**238** lactone in 62% after acidification (entry 2). However, the compound exhibited a relatively poor enantiomeric excess (*ee*) of only 70%. In order to increase the stereoselectivity and therefore push the *ee*, the reaction temperature was lowered from 0 °C to -15 °C (entry 3). Gratifyingly, this increased the *ee* to 79% but the reaction proceeded significantly slower and needed 23 h for completion. When (*Z*)-**229aa** was subjected to these conditions though, the desired  $\alpha$ -alkylidene- $\gamma$ -aryl- $\gamma$ -butyrolactone was obtained in 70% yield in highly enantiomeric enriched form (entry 4).

**Table 8.** Optimization of the stereoselective synthesis of  $\alpha$ -alkylidene- $\gamma$ -aryl- $\gamma$ -butyrolactone **238**.<sup>a</sup>

Entry	Substrate	Conditions ( $\Delta T$ , t)	Product	Yield (%) <sup>b</sup>	<i>ee</i> (%) <sup>c</sup>
1	$(E)\text{-229aa}$	0 °C, 1 h	$(R,E)\text{-238}$	n.d.	-
2	$(E)\text{-229aa}$	0 °C, 4 h	$(R,E)\text{-238}$	62	70
3	$(E)\text{-229aa}$	-15 °C, 23 h	$(R,E)\text{-238}$	52	79
4	$(Z)\text{-229aa}$	-15 °C, 23 h	$(R,Z)\text{-238}$	70	89

<sup>a</sup>Standard reaction conditions:  $(E)\text{-229aa}$  or  $(Z)\text{-229aa}$  (1.0 equiv),  $(S)\text{-240}$  (0.1 equiv),  $\text{BH}_3\cdot\text{Me}_2\text{S}$  (1.3 equiv) in toluene under  $\text{N}_2$  atmosphere. <sup>b</sup>Isolated yields after purification *via* column chromatography. <sup>c</sup>*ee* determined *via* chiral HPLC. n.d. = not determined.

The absolute stereochemistry of  $(R,Z)\text{-238}$  was confirmed by X-ray crystallography (Scheme 75) and is perfectly in line with the previously discussed model for CBS reductions and also in agreement with structurally related, but much more simplified ketones such as acetophenone or the corresponding  $\beta$ - or  $\gamma$ -keto esters.<sup>[239]</sup>

**Scheme 75.** X-ray crystallography of  $(R,Z)\text{-238}$  and obtained key chiral alcohol in the CBS reduction.

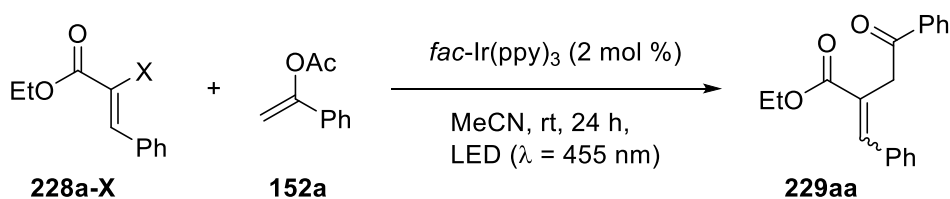
### 3.5 Unraveling the halogen paradox - Mechanistic discussions, computational details and control experiments<sup>2</sup>

The trend in reactivity for the aforementioned visible light mediated transformation is puzzling. It has been shown that activation of  $\alpha$ -chloro cinnamate **228a-Cl** under described photocatalytic conditions proceeded smoothly whereas  $\alpha$ -bromo cinnamate **228a-Br** seemed to be comparably persistent and surprisingly inert. This exceptional trend is unusual as the ease for the single electron transfer is expected to be the other way round.<sup>[128,129,132]</sup> Nevertheless, some discrepancies are reported in the literature regarding bond fragmentation of C-halogen bonds. It has been suggested that upon injection of one single electron to benzyl halides, the bond dissociation should be preferred for the chlorides in sharp contrast to the bromides (-6.5 kcal/mol for  $\text{RCl}^{\bullet-}$  and +2.5 kcal/mol for  $\text{RBr}^{\bullet-}$ ; R = benzyl).<sup>[130]</sup> However, another group later performed similar calculations regarding the bond dissociation energies for the same substrates and came to a different conclusion. Herein, the dissociation of the benzyl bromide radical anion should be slightly more favored, but nevertheless both radical anions were estimated to be much more negative and suddenly converge to a strongly shifted negative value (-50 kcal/mol for  $\text{RCl}^{\bullet-}$  and -56 kcal/mol for  $\text{RBr}^{\bullet-}$ ; R = benzyl).<sup>[191]</sup> This would suggest that the difference in energies becomes negligible and both intermediates should therefore exist completely dissociated.

In order to unravel the current halogen paradox, the visible light mediated activation of vinyl halides was further investigated. Therefore, all four vinyl halides were subjected to previously optimized reaction conditions (Table 9).

---

<sup>2</sup> Special thanks to Prof. Dr. Julia Rehbein (University of Regensburg) who performed the computational studies and contributed a lot to the final results.

**Table 9.** Comparison of  $\alpha$ -halo cinnamates **228a-X**.<sup>a</sup>

Entry	X	BDE vinyl-X (kcal/mol) <sup>[186]</sup>	$E_{\text{RX/RX}^{\bullet-}}^{\circ}$ (V) <sup>b</sup>	Conversion / Yield (%) <sup>c</sup>
1	F	123.7	-1.93	0 / 0
2	Cl	91.7	-1.64	100 / 98
3	Br	79.4	-1.54	23 / 23
4	I	61.9	n.d.	-

<sup>a</sup>Reactions were performed using optimized reaction conditions (*cf.* Chapter 3.2). <sup>b</sup>Reduction potentials were measured in MeCN vs SCE. <sup>c</sup>Conversion and yield were determined by <sup>1</sup>H-NMR analysis using 1,3,5-trimethoxybenzene as internal standard.

In agreement with the measured reduction potential (-1.93 V vs SCE) and the tabulated bond dissociation energies for the C-F bond (123.7 kcal/mol), initial electron transfer from excited  $fac\text{-Ir(ppy)}_3$  (-1.73 V vs SCE) to freshly prepared **228a-F** was prohibited and could not take place (entry 1). Unfortunately, **228a-I** could not be accessed in pure form due to rapid decomposition under ambient conditions. Therefore, it was not possible to obtain reliable experimental data for the photochemical conversion of **228a-I** for which bond fragmentation should have been most facile (entry 4). Focusing on **228a-Cl** and **228a-Br** (entry 2 and 3), the difference for the measured reduction potential was surprisingly rather marginal ( $\Delta E_{\text{RX/RX}^{\bullet-}}^{\circ} = 0.1$  V vs SCE). Nevertheless, single electron reduction of **228a-Br** should be slightly more favored. Even though the difference of the bond dissociation energies is huge in the ground state, the aforementioned discussions suggest that this might change after single electron reduction of **228a-Cl** and **228a-Br**.<sup>[130,191]</sup> Still, subsection of **228a-Cl** to previously optimized reaction conditions gave product **229aa** in significantly higher yields compared to **228a-Br**.

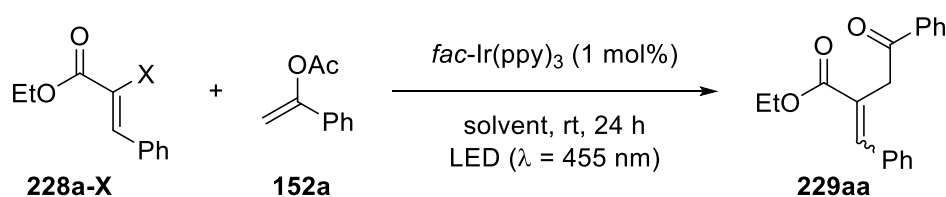
In order to get more insight, a cooperation with the group of Prof. Dr. Julia Rehbein from the University of Regensburg was started. Thus computational studies regarding the driving forces of the two elemental steps were performed which should help to solve the present problem (Table 10).

**Table 10.** Computed Enthalpies and Gibbs Free Energies for the two elemental steps.<sup>a</sup>

X	Gas phase		PCM (MeCN)	
	$\Delta H$ (kcal/mol)	$\Delta G$ (kcal/mol)	$\Delta H$ (kcal/mol)	$\Delta G$ (kcal/mol)
Step 1: Formation of the radical anion <b>228b-X</b> <sup>•-</sup>				
Br	-25.2	-26.2	-66.0	-68.1
Cl	-24.4	-25.1	-66.6	-65.4
Step 2: Dissociation into <b>242</b> and X <sup>-</sup>				
Br	13.3	4.5	-8.9	-18.5
Cl	21.8	12.4	-4.5	-15.4

<sup>a</sup>Calculations were performed by Prof. Dr. Julia Rehbein. Full computational details are not depicted in the Experimental part of this thesis but are downloadable free of charge from the Supporting Information of Ref. [243]. PCM = polarizable continuum model.

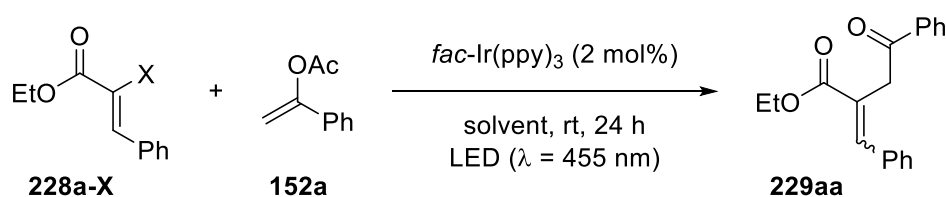
As can be seen from Table 10, the formation of the radical anion **228b-X**<sup>•-</sup> (Step 1) is favorable for both **228b-Cl** and **228b-Br** in the gas phase. However, dissociation into the carbon-centered radical **242** and the halide anion X<sup>-</sup> (Step 2) is unfavored in both cases which presumably corresponds to the lack of stabilizing structures with evolving or fully established charges in the gas phase. However, mimicking the dielectric effects by using a polarizable continuum model (PCM) of the solvent MeCN, which was used in the photochemical transformation, both elemental steps suddenly become exergonic. Nevertheless, fragmentation of the C-Br bond in **228b-Br**<sup>•-</sup> should be slightly more favored compared to **228b-Cl**<sup>•-</sup>. But yet, the free energies surprisingly become more convergent in MeCN ( $\Delta\Delta G = 3$  kcal/mol) whereas the gap between both substrates was huge in the gas phase and therefore dissociation in the case of the bromide clearly preferred. Interestingly, by computing reaction enthalpies for other solvents like benzene, DCM, or DMF revealed MeCN being presumably the most suitable solvent. This could be quickly confirmed by including other solvents in the original screening (Table 11).

**Table 11.** Comparison of **228a-Cl** and **228a-Br** in different solvents.<sup>a</sup>

Entry	Solvent	Yield (%) <sup>b</sup>	
		Br	Cl
1	benzene	-	-
2	chloroform	-	-
3	DMSO	14	18
4	DMF	16	43
5	MeCN	8	58
6	MeCN / H <sub>2</sub> O <sup>c</sup>	10	31

<sup>a</sup>Standard reaction conditions: **228a-X** (0.3 mmol), **152** (1.5 mmol), photocatalyst (1 mol%), solvent (c = 0.2 M), N<sub>2</sub> atmosphere, rt, 24 h, blue LED ( $\lambda = 455$  nm). <sup>b</sup>Yields were determined by <sup>1</sup>H-NMR analysis using 1,3,5-trimethoxybenzene as internal standard. <sup>c</sup>2 equiv H<sub>2</sub>O.

Going back to original 1 mol% catalyst loading, unipolar solvents were found to be completely unsuitable for this transformation which is in agreement with the computational results (entry 1 and 2). While there is no noticeable difference for DMSO as solvent (entry 3), a dramatic change was suddenly observed for DMF and MeCN though (entry 4 and 5). Again, MeCN was superior to other solvents which has also been suggested by the calculations but concerning the reactivity, **228a-Cl** seemed to be much more reactive compared to **228a-Br**. However, these experimental results are inconsistent with the theoretical results. In fact, the computational results suggest **228a-Br** being the more reactive substrate. Another control experiment finally confirmed this. Conducting an experiment under optimized reaction conditions in which **228a-Br** and **228a-Cl** were employed in a 1:1 ratio indeed identified **228a-Br** as the more reactive substrate. While the overall conversion of starting material and therefore the overall yield of **229aa** were now low, analysis of the crude reaction mixture surprisingly revealed an approximately threefold higher conversion for **228a-Br** (Table 12, entry 1 – 3). Notably, the overall conversion was somewhere between pure **228a-Br** or **228a-Cl**.

**Table 12.** Direct comparison of **228a-Cl** and **228a-Br** as well as equimolar amounts of both.<sup>a</sup>

Entry	X	Conversion (%) <sup>b</sup>	Yield (%) <sup>b</sup>
1	Cl	100	98
2	Br	23	23
3 <sup>c</sup>	Cl / Br, 1:1	38 <sup>d</sup>	30

<sup>a</sup>Reactions were performed using **228a-X** (0.5 mmol), **152a** (2.5 mmol), *fac*-Ir(ppy)<sub>3</sub> (2 mol%) in 5 mL MeCN (= optimized reaction conditions; *cf.* Chapter 3.2). <sup>b</sup>Conversion and yield were determined by <sup>1</sup>H-NMR analysis using 1,3,5-trimethoxybenzene as internal standard. <sup>c</sup>**228a-Cl** (0.25 mmol), **228a-Br** (0.25 mmol), **152a** (2.5 mmol), *fac*-Ir(ppy)<sub>3</sub> (2 mol% based on the total amount of 0.5 mmol **228a-X**) in 5 mL MeCN. <sup>d</sup>38% consisting of 58% conversion of **228a-Br** and 18% of **228a-Cl**, respectively.

Finally in line with the computed data, **228a-Br** was detected as the more reactive compound. In fact, **228a-Br** reacted approximately 3 times faster in contrast to competing **228a-Cl**. However, the yield was now surprisingly low and suspiciously similar to pure **228a-Br** as radical precursor (Table 12, entry 2 and 3). Therefore, it seemed most likely that the low yield was referred to **228a-Br**. The only difference between **228a-Br** and **228a-Cl** is the initial extrusion of the halide anion which will form acetyl bromide (AcBr) and acetyl chloride (AcCl) as stoichiometric by-product in the course of the reaction.<sup>[149]</sup> Indeed, the formation of both AcBr and AcCl was verified by <sup>1</sup>H-NMR analysis of the crude reaction mixture (Figure 2 and 3).



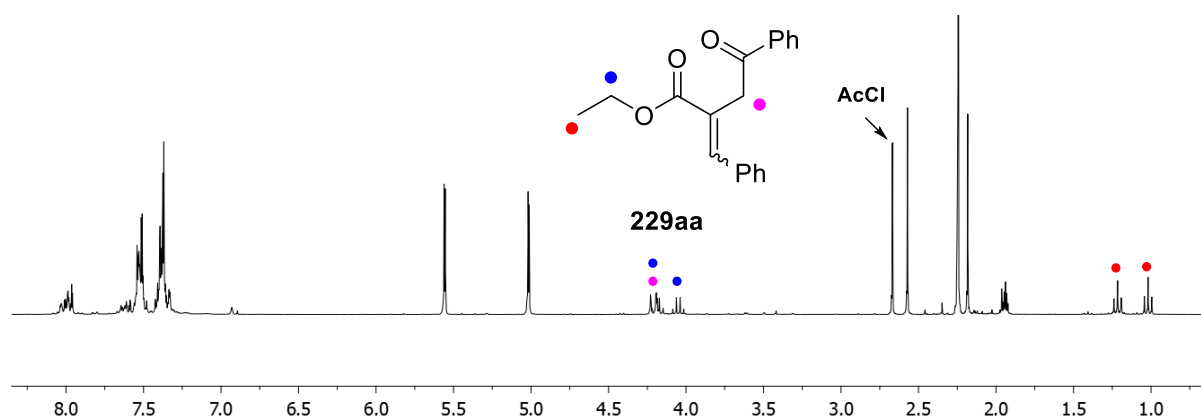


**Figure 2.** Crude reaction of **228a-Cl** in  $\text{CD}_3\text{CN}$ .

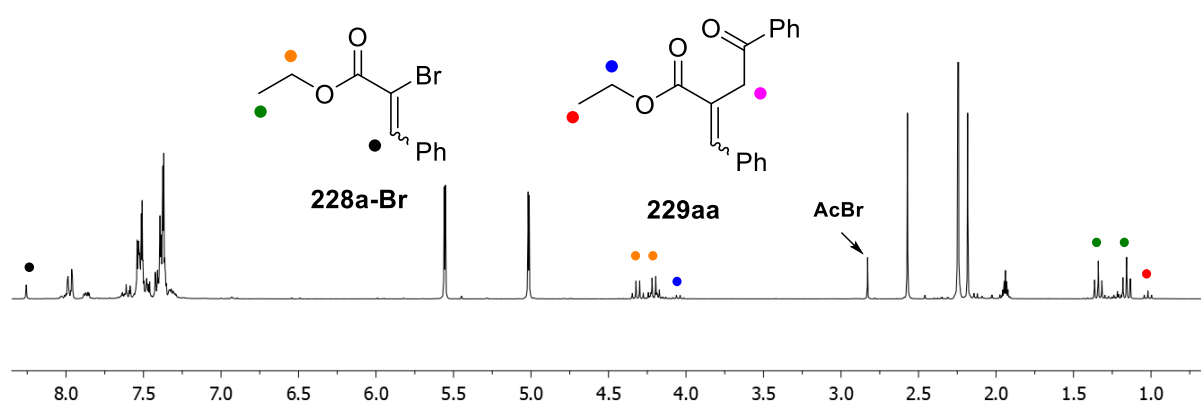


**Figure 3.** Crude reaction of **228a-Br** in  $\text{CD}_3\text{CN}$ .

Finally, when 0.5 equivalents of AcBr (reflecting a 50% conversion of a given reaction) were added to the optimized reaction with **228a-Cl**, only 22% of product **229aa** were now formed instead of the otherwise obtained 98%. This strongly indicates AcBr being a slow but nonetheless efficient catalyst poison. Indeed, stirring photocatalyst *fac*-Ir(ppy)<sub>3</sub> in the presence of AcBr led to full decomposition after irradiation for 24 h in MeCN which can clearly be seen in the succeeding depicted Figures 4 and 5. Studies by König *et al.*<sup>[244]</sup> and Stephenson and co-workers<sup>[245]</sup> have already demonstrated the susceptibility of *fac*-Ir(ppy)<sub>3</sub> towards degradation.

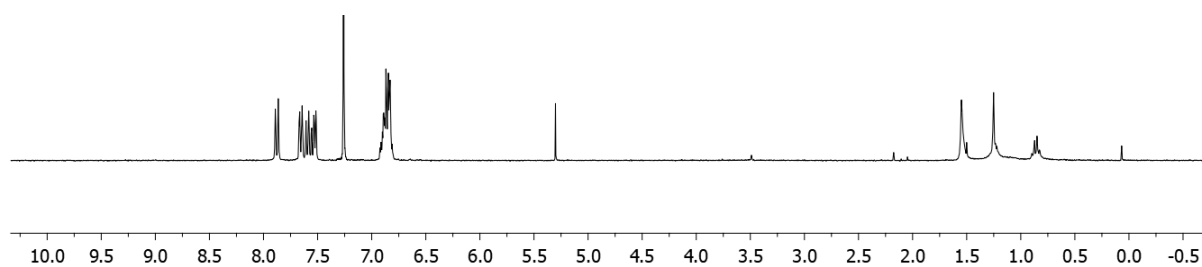


**Figure 4.**  $^1\text{H-NMR}$  of *fac*-Ir(ppy) $_3$  in  $\text{CDCl}_3$ .

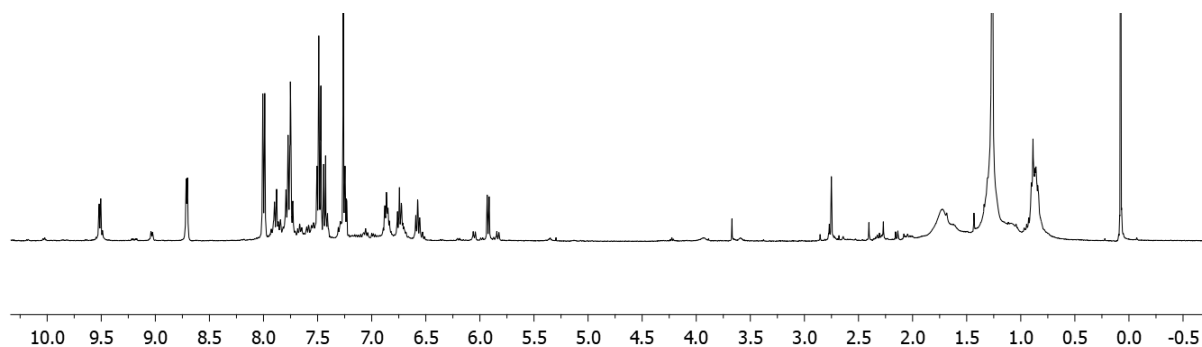
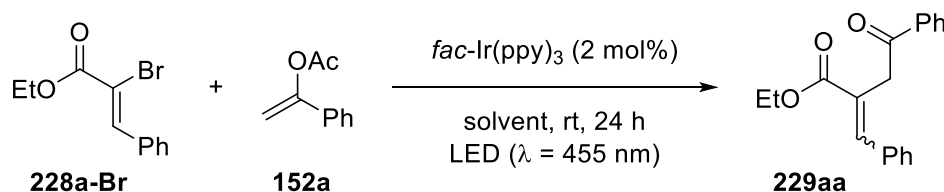


**Figure 5.**  $^1\text{H-NMR}$  of *fac*-Ir(ppy) $_3$  after irradiation for 24 h in the presence of AcBr.

Unfortunately, fast quenching of poisonous AcBr *via* additives to the reaction of **228a-Br** failed so far (Table 13). Thus neither the addition of stoichiometric amounts nor an excess of  $\text{H}_2\text{O}$  helped to improve the yield (entry 1 and 2). Furthermore, the addition of redox-neutral inorganic bases also did not exhibit a beneficial effect compared to the blank reaction with **228a-Br** (entry 3 and 4).

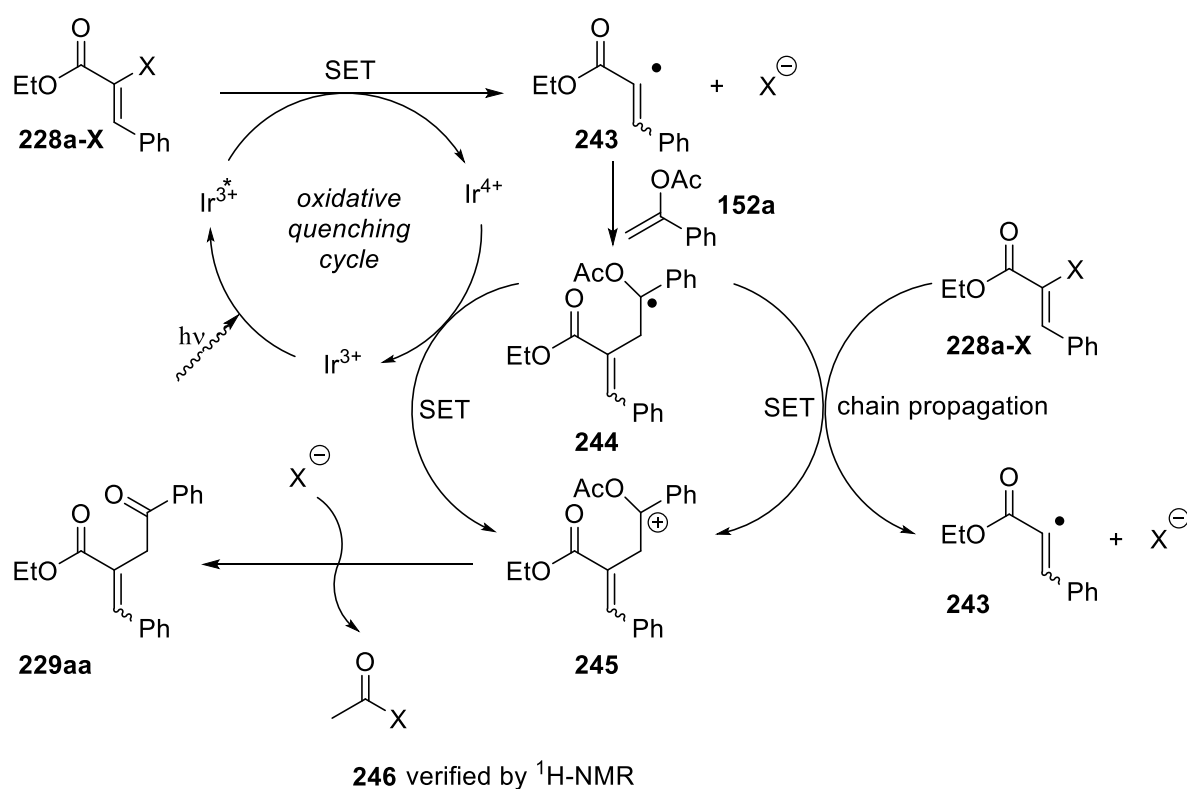
**Table 13.** Control experiments of **228a-Br** in the presence of various additives.<sup>a</sup>



Entry	Catalyst	Additive (2 equiv)	Solvent	Yield (%) <sup>b</sup>
1	<i>fac</i> -Ir(ppy) $_3$	$\text{H}_2\text{O}$	MeCN	31
2	<i>fac</i> -Ir(ppy) $_3$	-	MeCN	12
3	<i>fac</i> -Ir(ppy) $_3$	$\text{K}_2\text{HPO}_4$	MeCN / $\text{H}_2\text{O}$ , 4:1	20
4	<i>fac</i> -Ir(ppy) $_3$	$\text{Na}_2\text{CO}_3$	MeCN	27

<sup>a</sup>Reactions were performed using optimized reaction conditions for **228a-Cl**. <sup>b</sup>Yields were determined by  $^1\text{H-NMR}$  analysis using 1,3,5-trimethoxybenzene as internal standard.

With previously discussed results in mind and in accordance with precedent literature reports for similar transformations,<sup>[138,139,148,149]</sup> an absolutely plausible reaction mechanism is proposed in the following (Scheme 76). The photocatalytic cycle is initiated by the absorption of visible light ( $\lambda = 455 \text{ nm}$ ) by *fac*-Ir(ppy)<sub>3</sub>. The excited photocatalyst is now an excellent reductant ( $E_{M^+/M^*}^\circ = -1.73 \text{ V vs SCE}$ ) and therefore capable of reducing both **228a-Cl** ( $E_{RX/RX^\cdot}^\circ = -1.64 \text{ V vs SCE}$ ) and **228a-Br** ( $E_{RX/RX^\cdot}^\circ = -1.54 \text{ V vs SCE}$ ). After halide extrusion, the corresponding electrophilic vinyl radical intermediate **243** readily couples with electron rich enol acetate **152a** giving rise to radical intermediate **244**. Single electron oxidation forms cationic species **245** by either the photocatalyst which regenerates the catalyst or by initiating a chain mechanism. Formation of AcBr or AcCl finally produces the product.



**Scheme 76.** Proposed reaction mechanism.

### 3.6 Conclusion

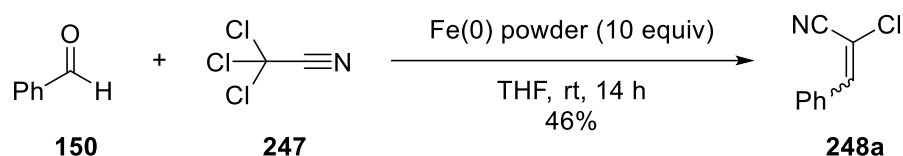
In summary, a photoinduced activation of  $\alpha$ -chloro cinnamates mediated by visible light was achieved. Based on the oxidative quenching cycle of highly reducing *fac*-Ir(ppy)<sub>3</sub>, vinyl radicals were readily generated *via* single electron reduction and efficiently coupled with enol acetates giving rise to a broad range of synthetically valuable 1,4-dicarbonyl compounds. Even though vinyl bromides should be superior in terms of single electron reduction and bond dissociation, calculations revealed that differences become more convergent in polar solvents like MeCN. In fact, it has been shown that vinyl bromides were unsuitable in this transformation, presumably due to efficient deactivation of the photocatalyst by acetyl bromide which was formed as stoichiometric by-product in the course of the reaction. Furthermore, the reaction could be run on a multi-gram scale and the products were found to be excellent building blocks for the synthesis of enantioenriched  $\alpha$ -alkylidene- $\gamma$ -aryl- $\gamma$ -butyrolactones.

## 4 Visible light mediated activation of $\alpha$ -chloro cinnamitriles

### 4.1 Optimization of the reaction conditions

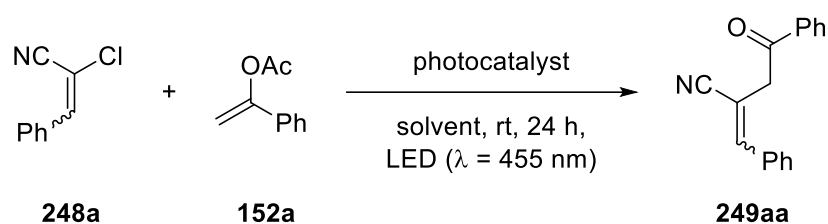
Cinnamitriles represent an important class of compounds.<sup>[246,247]</sup> They can easily be prepared from cinnamamides, cinnamaldoximes, or primary alcohols.<sup>[248-253]</sup> In principle, nitriles are very attractive synthons as they can easily be converted into to a broad range of different functional groups including esters,<sup>[254]</sup> carboxylic acids,<sup>[255]</sup> aldehydes,<sup>[256,257]</sup> ketones,<sup>[258]</sup> or amines.<sup>[259,260]</sup>

In the previous chapter the successful photochemical activation of vinyl chlorides from  $\alpha$ -chloro ethyl cinnamates was described. This newly developed method should now be further extended to other functional groups in order to broaden the substrate scope. It has already been demonstrated that numerous variations were tolerated at the aromatic moiety of both the cinnamates and the enol acetates. However, the ester functional group was only tested in respect to simple ester exchanges. So far, previous investigations on the photochemical activation of vinyl halides completely relied on carbonyl groups adjacent to the radical source (*vide supra*). As electron withdrawing properties seemed to be a strict requirement to promote the desired single electron transfer, a functional group with similar electronic properties was needed. In this regard, the cyano group seemed to perfectly match the desired demands. Therefore, light mediated activation of  $\alpha$ -chloro cinnamitriles was envisioned. Additionally, in terms of the high versatility of nitriles as building blocks for other functional groups, subsequent manipulations should give rise to a wide range of novel derivatives. Unfortunately, the previously synthetic route is not suitable to access the desired  $\alpha$ -chloro cinnamitrile. However, Mioskowski *et al.* reported a lucrative synthesis of  $\alpha$ -halo- $\alpha,\beta$ -unsaturated compounds from readily available benzaldehydes and activated polyhalides.<sup>[198]</sup> Fortunately, the desired nitrile is also amenable among other electron withdrawing groups. Thus, desired  $\alpha$ -chloro cinnamitrile (**248a**) was quickly prepared in moderate yields as a diastereomeric mixture (Scheme 77). Interestingly, (*E*)-**248a** was obtained as major isomer which is in accordance to literature data.<sup>[198,261]</sup> However, diastereomeric purity of the starting material seemed to be negligible as previous photocatalytic investigations with cinnamates have already been demonstrated.



**Scheme 77.** Preparation of  $\alpha$ -chloro cinnamionitrile (**248a**).<sup>[198]</sup> Product **248a** obtained as *E/Z* mixture. For details see Experimental part.

With sufficient amounts of vinyl chloride **248a** in hand, first test reactions were carried out (Table 14). Again, previously reliable enol acetates should serve as coupling partners. Unfortunately, applying optimized reaction conditions for the visible light mediated functionalization of  $\alpha$ -chloro cinnamates gave the desired product only in a disappointing yield of 31%, even with 2 mol% photocatalyst (entry 1). Focusing on 1 mol% catalyst, different photocatalysts in various solvents were screened (entry 2 – 19). Surprisingly, highly reducing *fac*-Ir(ppy)<sub>3</sub> which was found to be the only active catalyst for the functionalization of  $\alpha$ -chloro cinnamates was barely active and gave mediocre yields at best (entry 2 – 6). Switching to Ru(bpy)<sub>3</sub>Cl<sub>2</sub> or Ir[dF(CF<sub>3</sub>)ppy]<sub>2</sub>(dtbbpy)PF<sub>6</sub>, both catalysts were not capable of promoting this transformation (entry 7 – 11). However, Ir(ppy)<sub>2</sub>(dtbbpy)PF<sub>6</sub> seemed to be suitable for the activation of  $\alpha$ -chloro cinnamionitriles (entry 12 – 15). Again, polar solvents such as DMF or MeCN were superior compared to nonpolar solvents. Turning to DMF and MeCN, further screening revealed that higher concentrations gave slightly better yields (entry 16 and 17). Unfortunately, adding redox-neutral inorganic bases like K<sub>2</sub>HPO<sub>4</sub> or K<sub>2</sub>CO<sub>3</sub> did not help to increase the yield (entry 18 and 19). Again, 2 mol% of photocatalyst was required for complete consumption of the starting material (entry 20). Interestingly, elaborately dried DMF could be replaced by commercially available DMF in which desired product was obtained in 66% yield (entry 21). Finally, standard control experiments proved a visible light driven process (entry 22 and 23).

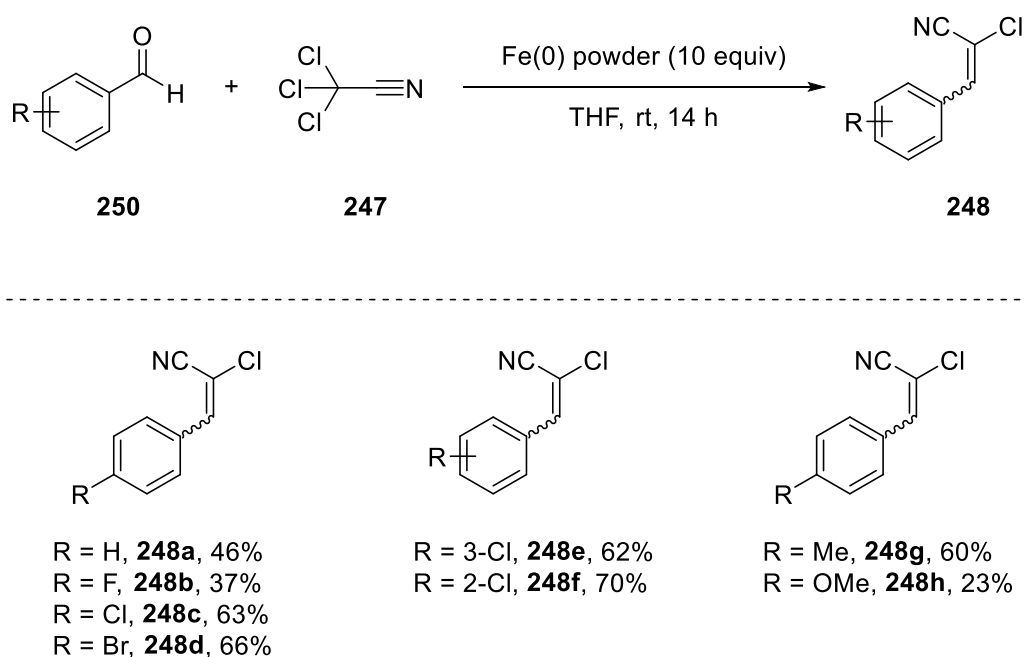
**Table 14.** Catalyst screening and reaction optimization.<sup>a</sup>

Entry	Photocatalyst	Additive (2 equiv)	Solvent	Yield (%) <sup>b</sup>
1 <sup>c</sup>	<i>fac</i> -Ir(ppy) <sub>3</sub>	-	MeCN	31
2	<i>fac</i> -Ir(ppy) <sub>3</sub>	-	DCM	9
3	<i>fac</i> -Ir(ppy) <sub>3</sub>	-	DMSO	5
4	<i>fac</i> -Ir(ppy) <sub>3</sub>	-	DMF	13
5	<i>fac</i> -Ir(ppy) <sub>3</sub>	-	MeCN	16
6	<i>fac</i> -Ir(ppy) <sub>3</sub>	-	THF	3
7	Ru(bpy) <sub>3</sub> Cl <sub>2</sub>	-	DMF	traces
8	Ru(bpy) <sub>3</sub> Cl <sub>2</sub>	-	MeCN	-
9	Ir[dF(CF <sub>3</sub> )ppy] <sub>2</sub> (dtbbpy)PF <sub>6</sub>	-	DCM	-
10	Ir[dF(CF <sub>3</sub> )ppy] <sub>2</sub> (dtbbpy)PF <sub>6</sub>	-	DMF	-
11	Ir[dF(CF <sub>3</sub> )ppy] <sub>2</sub> (dtbbpy)PF <sub>6</sub>	-	MeCN	-
12	Ir(ppy) <sub>2</sub> (dtbbpy)PF <sub>6</sub>	-	DCM	12
13	Ir(ppy) <sub>2</sub> (dtbbpy)PF <sub>6</sub>	-	DMSO	-
14	Ir(ppy) <sub>2</sub> (dtbbpy)PF <sub>6</sub>	-	DMF	27
15	Ir(ppy) <sub>2</sub> (dtbbpy)PF <sub>6</sub>	-	MeCN	27
16 <sup>d</sup>	Ir(ppy) <sub>2</sub> (dtbbpy)PF <sub>6</sub>	-	DMF	38
17 <sup>d</sup>	Ir(ppy) <sub>2</sub> (dtbbpy)PF <sub>6</sub>	-	MeCN	21
18 <sup>d</sup>	Ir(ppy) <sub>2</sub> (dtbbpy)PF <sub>6</sub>	K <sub>2</sub> HPO <sub>4</sub>	DMF	-
19 <sup>d</sup>	Ir(ppy) <sub>2</sub> (dtbbpy)PF <sub>6</sub>	K <sub>2</sub> CO <sub>3</sub>	DMF	-
20 <sup>d,e</sup>	Ir(ppy) <sub>2</sub> (dtbbpy)PF <sub>6</sub>	-	DMF	60
<b>21<sup>d,e</sup></b>	<b>Ir(ppy)<sub>2</sub>(dtbbpy)PF<sub>6</sub></b>	-	<b>DMF<sub>aq</sub></b>	<b>66</b>
22 <sup>d,e,f</sup>	-	-	DMF <sub>aq</sub>	-
23 <sup>d,e,g</sup>	Ir(ppy) <sub>2</sub> (dtbbpy)PF <sub>6</sub>	-	DMF <sub>aq</sub>	-

<sup>a</sup>Standard reaction conditions: **248a** (1 equiv), **152a** (5 equiv), photocatalyst (1 mol%), solvent (c = 0.1 M), N<sub>2</sub> atmosphere, rt, 24 h, blue LED (λ = 455 nm). <sup>b</sup>Isolated yields after purification *via* column chromatography or *via* <sup>1</sup>H-NMR analysis using 1,3,5-trimethoxybenzene as internal standard. *E/Z* ratio of approximately 2:1. <sup>c</sup>Optimized reaction conditions for the activation α-chloro cinnamates. <sup>d</sup>Solvent (c = 0.2 M). <sup>e</sup>2mol% catalyst. <sup>f</sup>No photocatalyst. <sup>g</sup>No light.

## 4.2 Substrate scope

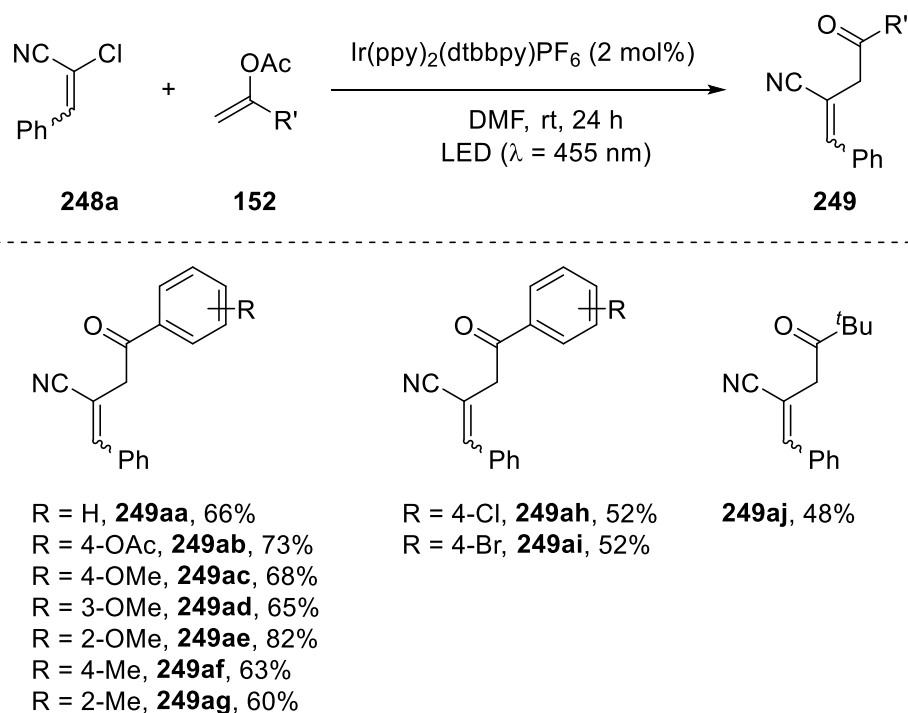
Having identified Ir(ppy)<sub>2</sub>(dtbbpy)PF<sub>6</sub> as optimal catalyst and DMF as most suitable medium, different derivatives should be subjected to such conditions. Fortunately, sufficient amounts of various enol acetates were still in stock. However, a variety of  $\alpha$ -chloro cinnamionitriles needed to be prepared first. Utilizing previously described procedure provided quick access to different derivatives (Scheme 78).



**Scheme 78.** Synthesis of a variety of  $\alpha$ -chloro cinnamionitriles by applying a protocol by Mioskowski *et al.*<sup>[198]</sup> Products obtained as *E/Z* mixtures. For details see Experimental part.

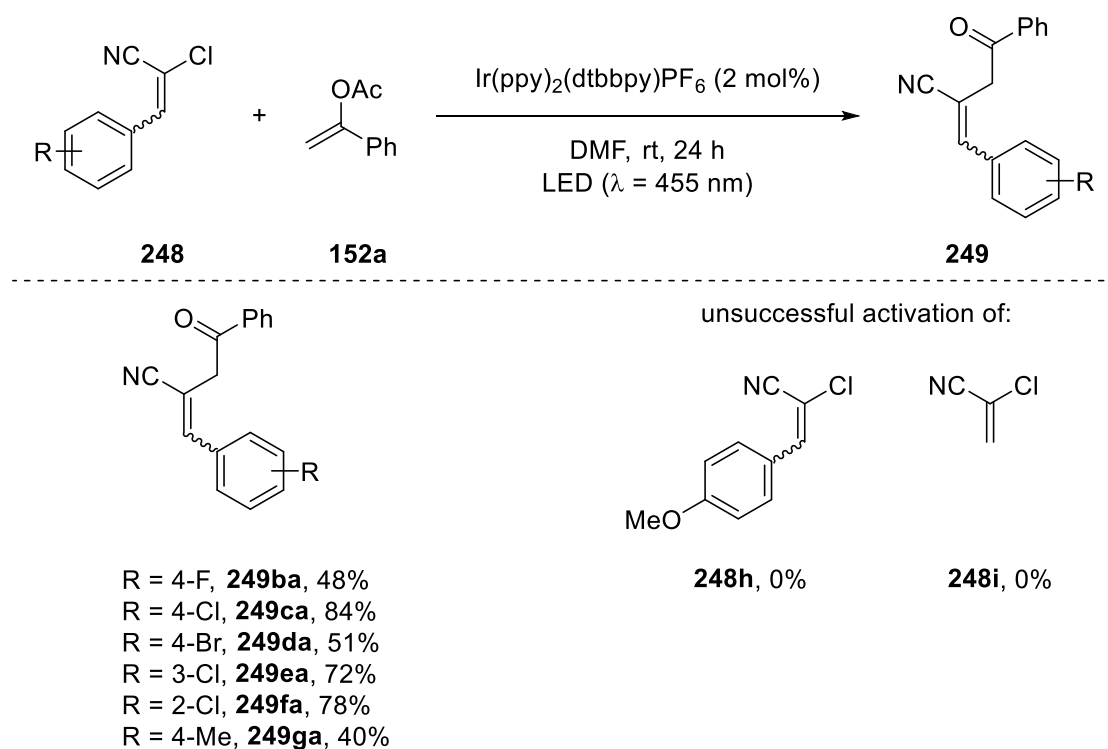
Utilizing previously optimized reaction conditions (Table 14, entry 21), various enol acetates were subjected to this newly developed transformation (Scheme 79). Similar to  $\alpha$ -chloro cinnamates, electron-rich enol acetates (**249aa** – **249ag**) could be readily coupled, reflecting again the electrophilic nature of the vinyl radical intermediate. In this regard, significantly higher yields up to 82% were achieved using strong electron donating substituents attached on the aromatic ring. Notably, ortho- (**249ae**, **249ag**) and meta- substitutions (**249ad**) were well tolerated. Switching to weak electron withdrawing groups, marginal lower but still moderate yields were obtained (**249ah**, **249ai**). Gratifyingly, aliphatic enol acetate gave product **249aj** in similar high yields compared to the aromatic coupling partners.





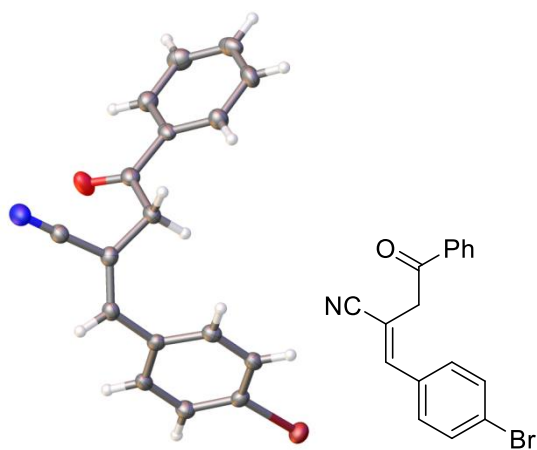
**Scheme 79.** Scope of enol acetates **152** in the coupling with  $\alpha$ -chloro cinnamionitrile **248a**. Standard reaction conditions: **248a** (0.5 mmol), **152** (2.5 mmol),  $\text{Ir}(\text{ppy})_2(\text{dtbbpy})\text{PF}_6$  (2 mol%) in 2.5 mL  $\text{DMF}_{\text{aq}}$ . Combined isolated yields of separated *E* and *Z* isomer after purification *via* column chromatography. *E/Z* ratio of approximately 2:1 in most cases, for details see Experimental part.

Next, the substrate scope of the previously prepared  $\alpha$ -chloro cinnamionitriles was investigated (Scheme 80). As expected, electron-deficient cinnamionitriles were well tolerated (**249ba** – **249fa**). In fact, even higher yields up to 84% were achieved compared to **248a** which was employed in the original screening. This transformation did not suffer from ortho- (**249fa**) or meta-substitution patterns (**249ea**). Concerning other  $\text{C}(\text{sp}^2)$ -halides (**249ba** – **249fa**), chemoselectivity completely prevailed. However, this reaction was revealed to be susceptible to even weak donors (**249ga**). Therefore, limitations were found for strong donating groups (**248h**) and also commercially available 2-chloroacrylonitrile (**248i**) could not be employed in this reaction.



**Scheme 80.** Scope of  $\alpha$ -chloro cinnamoyl nitriles. Standard reaction conditions: **248** (0.5 mmol), **152a** (2.5 mmol),  $\text{Ir(ppy)}_2(\text{dtbbpy})\text{PF}_6$  (2 mol%) in 2.5 mL  $\text{DMF}_{\text{aq}}$ . Combined isolated yields of separated *E* and *Z* isomer after purification *via* column chromatography. *E/Z* ratio of approximately 2:1 in most cases, for details see Experimental part.

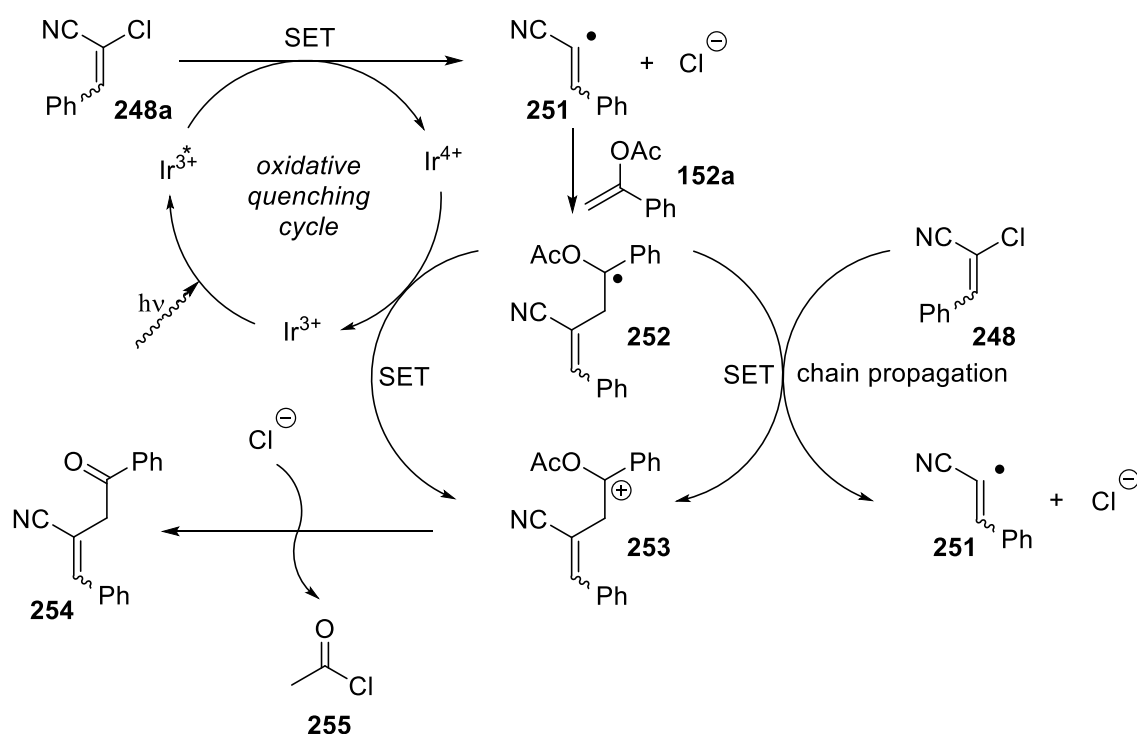
Compared to  $\alpha$ -chloro cinnamates (*cf.* Chapter 3), the activation of  $\alpha$ -chloro cinnamoyl nitriles was unfortunately slightly more sluggish. Overall, the isolated yields were comparatively lower and the functional group tolerance more vulnerable. However, the reaction was found to be more diastereoselective. While for the cinnamates an *E/Z* ratio of approximately 1:1 was observed in the products in most cases, a higher *E*-selective outcome of approximately 2:1 was observed for the cinnamoyl nitriles (see Experimental part for details). This means that the double bond is indeed isomerizing during the reaction under described photocatalytic conditions which could be unambiguously verified by X-ray crystallography for the major isomer of **249da** (Scheme 81).



**Scheme 81.** X-ray crystallography of the major isomer of **249da**.

### 4.3 Proposed reaction mechanism

A plausible reaction mechanism can be proposed based on precedent literature reports and is similar to the mechanism already proposed for the cinnamates.<sup>[138,139,148,149]</sup> Single electron transfer from previously excited iridium catalyst to the  $\alpha$ -chloro cinnamitrile **248a** leads to C-Cl bond dissociation and the vinyl radical key intermediate **251**. This electron-deficient radical can readily couple with electron rich enol acetate **152a** which provides radical intermediate **252**. This radical intermediate can be oxidized to the cation **253** by the photocatalyst which closes the catalytic cycle or by initiating a radical chain process. Subsequent acyl extrusion gives rise to acetyl chloride as stoichiometric by-product and provides product **254** (Scheme 82).



**Scheme 82.** Proposed reaction mechanism for the visible light mediated coupling of  $\alpha$ -chloro cinnamitriles and enol acetates.

#### 4.4 Conclusion and outlook

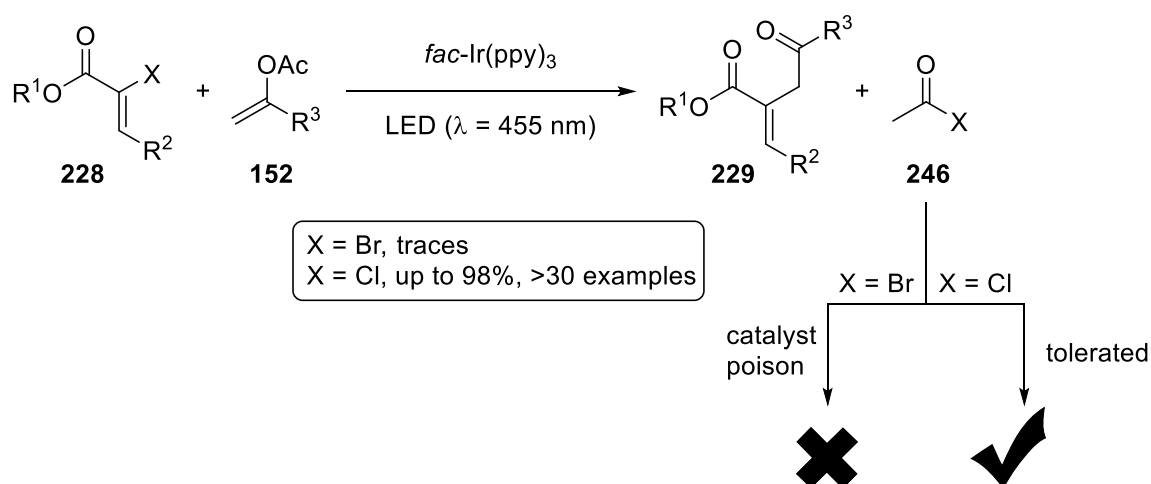
In summary, the newly developed protocol for the activation of vinyl chlorides was successfully extended to  $\alpha$ -chloro cinnamitriles. Thus photocatalytic activation of  $\alpha$ -chloro cinnamitriles was achieved. Whereas previous investigations in this group completely relied on carbonyls adjacent to the vinyl radical (*vide supra*), photochemical coupling was successfully extended to nitriles for the first time. In this regard,  $\alpha$ -chloro cinnamitriles could be readily prepared and subsequently efficiently coupled with numerous enol acetates under mild reaction conditions and visible light as sole energy source. A great variety of enol acetates were found to be excellent coupling partners but limitations were quickly revealed for cinnamitriles. Nevertheless, further conversion of the nitrile into other functional groups should provide access to a wide range of new derivatives in the future.

## C Summary

This thesis starts with a brief introduction to vinyl radicals in organic chemistry. Beginning with early examples such as the combination of  $\text{SnBu}_3\text{H}$  and AIBN in the 1980s, it later focuses on the generation of such intermediates through more benign visible light. After a short introduction to photoredox catalysis, it summarizes major contributions in this field from 2010 until the very recent date.

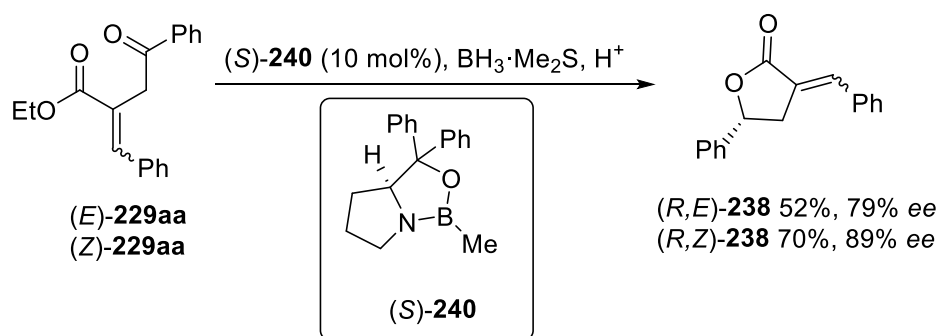
The main part of this thesis deals with the activation of vinyl bromides and chlorides *via* visible light photoredox catalysis. The initial situation is based on previous investigations on  $\alpha$ -bromo chalcones. Although these substrates readily undergo single electron reduction, this principle of activation could barely be transferred to less extended  $\pi$ -systems such as  $\alpha$ -bromo cinnamates. The chapter “Preliminary studies with vinyl bromides” illustrates that the inert reactivity of  $\alpha$ -bromo cinnamates is predominantly based on the more negative reduction potential. Several efforts to overcome this previously observed limitation are described. Unfortunately, all of these attempts were found to be unproductive and gave only mediocre results at best.

The two subsequent chapters cover research results with vinyl chlorides as radical precursors. The chapter “Visible light mediated activation of  $\alpha$ -chloro cinnamates” starts with a brief comparison of both vinyl halides and reveals that the chloro derivative surprisingly outcompetes the vinyl bromide in the visible light mediated coupling with enol acetates (Scheme 83).



**Scheme 83.** Visible light mediated coupling of  $\alpha$ -halo cinnamates **228** and enol acetates **152**.

The investigation of the reaction and its conditions demonstrates that  $\alpha$ -chloro cinnamates represent excellent radical precursors and these substrates can be readily coupled with enol acetates in high yields. Subsequent studies regarding the substrate scope reveal the limitations of the described reaction. This coupling proves to be suitable for photochemical up-scaling and the corresponding products can be readily converted to biologically active  $\gamma$ -butyrolactones. These substrates are first accessed as racemates in a Luche reduction and subsequently enantioenriched in a CBS reduction (Scheme 84).

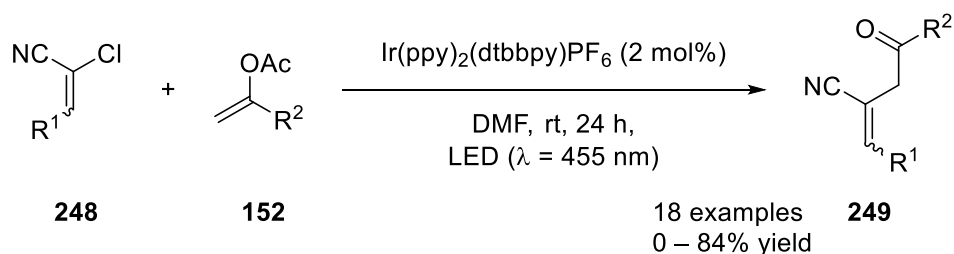


**Scheme 84.** Synthesis of enantioenriched  $\gamma$ -butyrolactones **238**.

This chapter later focuses on solving this current halogen paradox. Numerous control experiments and theoretical calculations reveal that the major difference between both substrates does not rely on the initial bond fragmentation but is rather based on efficient catalyst deactivation in the case of the vinyl bromide. It provides evidence that, in direct

comparison to the chloride, the vinyl bromide is consumed faster but nevertheless gives rise to lower yields due to poor conversion of the starting material. In the end, acetyl bromide which is formed as stoichiometric by-product in the described reaction is convicted as gradual but efficient catalyst poison for the photocatalyst *fac*-Ir(ppy)<sub>3</sub>.

The last chapter deals with the expansion of this newly gained results to the functionalization of  $\alpha$ -chloro cinnamitriles. After intense catalyst screening, Ir(ppy)<sub>2</sub>(dtbbpy)PF<sub>6</sub> is identified as the most active catalyst. Evaluation of the substrate scope demonstrates that the cinnamitriles are slightly inferior to the cinnamates regarding both the yield and the functional group tolerance but further functionalization of the nitrile group might give access to a broad range of new derivatives (Scheme 85).



**Scheme 85.** Visible light mediated coupling of  $\alpha$ -chloro cinnamitriles **248** with enol acetates **152**.

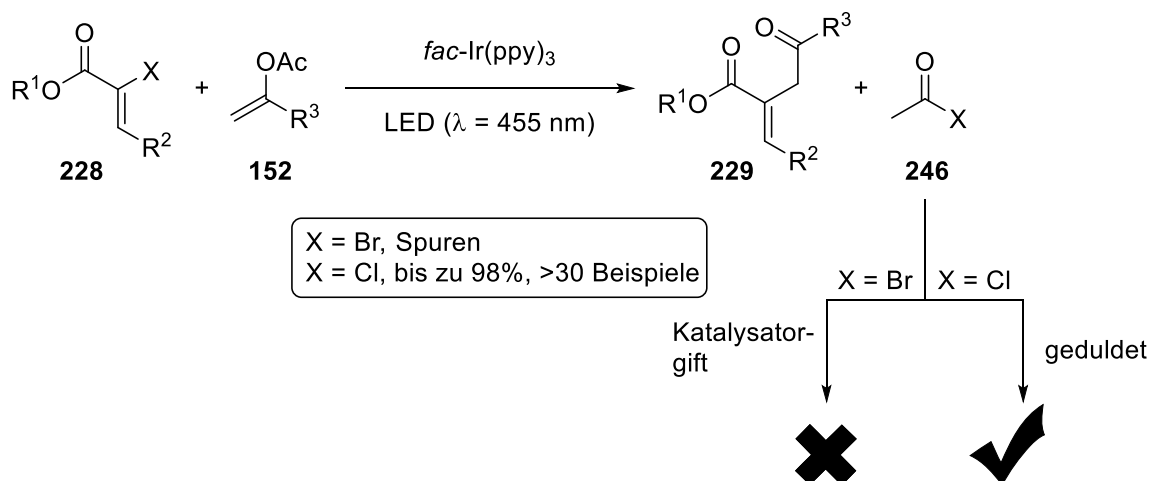


## D Zusammenfassung

Diese Arbeit beginnt mit einer kurzen Einführung in die Chemie der Vinylradikale. Der Fokus wird hierbei nach anfänglichen Beispielen mit  $\text{SnBu}_3\text{H}$  und AIBN auf die Erzeugung derartiger Intermediate mit Hilfe von sichtbarem Licht gelegt. Nach einer kurzen Einführung in die Photoredoxkatalyse wird ein Großteil der chemischen Umwandlungen auf diesem Gebiet zusammengefasst.

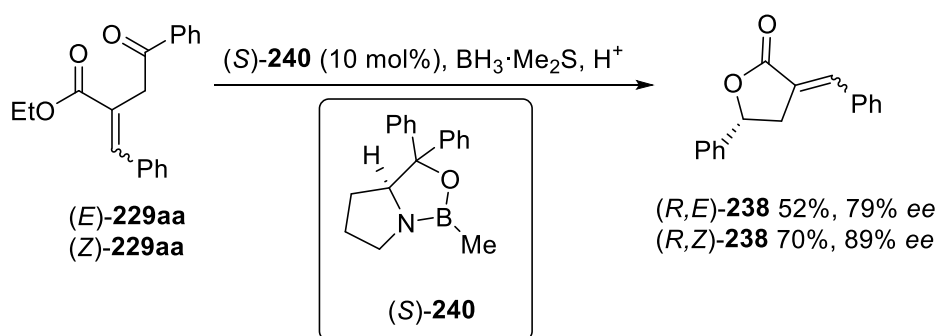
Der Hauptteil dieser Arbeit umfasst die Aktivierung von Vinylbromiden und -chloriden mit sichtbarem Licht. Dabei dienen jeweils vorangehende Studien mit  $\alpha$ -Bromochalkonen als Ausgangspunkt. Obwohl diese Substrate leicht Einzelelektronenreduktionen eingehen, konnte dieses Aktivierungsprinzip bislang kaum auf weniger ausgeprägte  $\pi$ -Systeme wie  $\alpha$ -Bromozimtsäureester übertragen werden. Das Kapitel „Preliminary studies with vinyl bromides“ verdeutlicht, dass das reaktionsträgere Verhalten der  $\alpha$ -Bromozimtsäureester maßgeblich dem erheblich negativeren Reduktionspotential zu Grunde liegt. Im Folgenden wird in unterschiedlichen Anläufen versucht, diese Hürde zu überwinden. Jedoch haben sich diese als eher unproduktiv und nicht zielführend erwiesen, da entsprechende Kopplungsprodukte nur in niedrigen Ausbeuten erhalten werden konnten.

Die zwei nachfolgenden Kapitel beschreiben die Forschungsergebnisse mit Vinylchloriden als Radikalvorstufen. Das Kapitel „Visible light mediated activation of  $\alpha$ -chloro cinnamates“ beginnt mit einem knappen Vergleich beider Halogenide und verdeutlicht, dass das Chlorderivat überraschenderweise eine höhere Aktivität bei der Kopplung mit Enolacetaten aufweist (Schema 1).



**Schema 1.** Kopplung von  $\alpha$ -Halozimtsäureester **228** mit Enolacetaten **152** mit Hilfe von sichtbarem Licht.

Die Untersuchung der Reaktion und ihrer Bedingungen zeigt, dass  $\alpha$ -Chlorozimtsäureester hervorragende Vinylradikalvorstufen darstellen und diese effizient mit Enolacetaten gekoppelt werden können. Im Folgenden wird die Substratbreite dieser neuen Aktivierungsmethode erkundet und deren Grenzen aufgezeigt. Im Anschluss wird die Umwandlung derartiger Produktbausteine in biologisch aktive  $\gamma$ -Butyrolactone beschrieben. Diese werden zunächst mit Hilfe einer Luche Reduktion in racemischer und später durch eine CBS Reduktion auch in enantiomerenangereicherten Form isoliert (Schema 2).

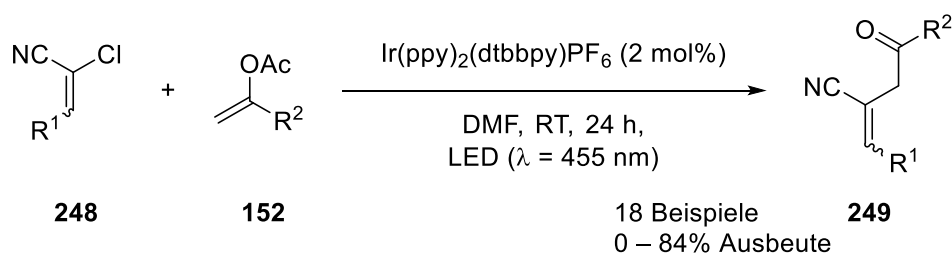


**Schema 2.** Darstellung von enantiomerenangereicherte  $\gamma$ -Butyrolactone **238**.

Zum Schluss widmet sich das Kapitel verstärkt dem Enträtseln des gegenwärtigen Halogenparadoxons. Zahlreiche Kontrollexperimente und begleitende theoretische Berechnungen deuten darauf hin, dass die unterschiedliche Aktivität beider Substrate weniger

auf die ursprüngliche Bindungsspaltung beruht, sondern vielmehr einer effizienten Katalysatordeaktivierung durch das im Falle des Vinylbromids gebildeten Acetylbromids zu Grunde liegt. Es wird bewiesen, dass im direkten Vergleich das Bromderivat zwar schneller abreagiert, aber dennoch geringere Ausbeuten aufgrund des schlechteren Umsatzes liefert. Somit wird letztlich aufgezeigt, dass Acetylbromid ein schleichendes Katalysatorgift für den Photokatalysator *fac*-Ir(ppy)<sub>3</sub> darstellt.

Das letzte Kapitel verdeutlicht, dass die kürzlich gewonnen Ergebnisse auf analoge Zimtsäurenitrile ausgeweitet werden können. Nach Optimierung der Reaktionsbedingungen wird sowohl die Substratbreite erkundet als auch deren Limitierung aufgezeigt. Diese Evaluierung offenbart, dass die entsprechenden Nitrile den Estern in puncto erhaltener Ausbeute und Verträglichkeit gegenüber funktionellen Gruppen unterlegen sind. Allerdings weisen die Produkte eine höhere Diastereoselektivität auf.



**Schema 3.** Kopplung von  $\alpha$ -Chlorzimtsäurenitrile **248** mit Enolacetaten **152** mit Hilfe von sichtbarem Licht.

## E Experimental part

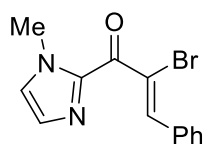
### 1 General information

All chemicals were used as received or purified according to Purification of Common Laboratory Chemicals.<sup>[262]</sup> Glassware was dried in an oven at 110 °C or flame dried and cooled under a dry atmosphere prior to use. All reactions were performed using Schlenk techniques. The blue light irradiation in batch processes was performed using a CREE XLamp XP-E D5-15 LED ( $\lambda = 450\text{-}465$  nm). Analytical thin layer chromatography was performed on Merck TLC aluminium sheets silica gel 60 F 254. Reactions were monitored by TLC and visualized by a short wave UV lamp and stained with a solution of potassium permanganate or vanillin. Column flash chromatography was performed using Merck flash silica gel 60 (0.040-0.063 mm). The melting points were measured on an OptiMelt MPA 100 (uncorrected). IR spectroscopy measurements were performed on an Agilent Gary 630 FTIR spectrometer equipped with a Diamond Single Reflection Accessory. Optical Rotation was measured in a Perkin Elmer Polarimeter or an ElmerAnton Paar MCP500 at 589 nm wavelength (sodium-*d*-line) in the specific solvent. X-ray measurements were performed by the crystallographic department of the University of Regensburg on Agilent Technologies SuperNova, Agilent Technologies Gemini R Ultra or Stoe IPDSI. Analytical HPLC was carried out on a Varian 920-LC with DAD. Chiralpak AS-H, Phenomenex Lux Cellulose-1 and 2 served as chiral stationary phase, and mixtures of *n*-heptane and *i*-PrOH were used for elution. NMR spectra were recorded on Bruker Avance 300 and Bruker Avance 400 spectrometers. Chemical shifts for <sup>1</sup>H-NMR were reported as  $\delta$ , parts per million, relative to the signal of CDCl<sub>3</sub> at 7.26 ppm. Chemical shifts for <sup>13</sup>C-NMR were reported as  $\delta$ , parts per million, relative to the center line signal of the CDCl<sub>3</sub> triplet at 77 ppm. Coupling constants *J* are given in Hertz (Hz). The following notations indicate the multiplicity of the signals: s = singlet, brs = broad singlet, d = doublet, t = triplet, q = quartet, quint = quintet, sept = septet, and m = multiplet. Mass spectra were recorded at the Central Analytical Laboratory at the Department of Chemistry of the University of Regensburg on a Varian MAT 311A, Finnigan MAT 95, Thermoquest Finnigan TSQ 7000 or Agilent Technologies 6540 UHD Accurate-Mass Q-TOF LC/MS. The yields reported are referred to the isolated compounds unless otherwise stated.

## 2 Preliminary studies with vinyl bromides

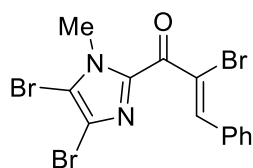
1-morpholinoethan-1-one (**149**),<sup>[144]</sup> 1-(1-methyl-1*H*-imidazol-2-yl)ethan-1-one (**145**),<sup>[145]</sup> (*E*)-1-(1-methyl-1*H*-imidazol-2-yl)-3-phenylprop-2-en-1-one (**144**),<sup>[145]</sup> ethyl 2-bromo-3-phenylacrylate (**134**),<sup>[138]</sup> *N*-cyclohexyl-*N*-isobutylcyclohexanamine (**190**),<sup>[164]</sup> and 4-methoxybenzenediazonium tetrafluoroborate (**209**)<sup>[148]</sup> were prepared according to literature and are in agreement with literature reference.<sup>[138,144,145,148,164,197]</sup>

### (*Z*)-2-bromo-1-(1-methyl-1*H*-imidazol-2-yl)-3-phenylprop-2-en-1-one (**151a**)



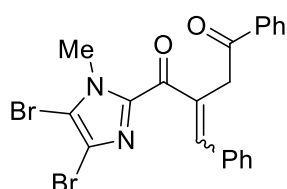
To a cooled solution of (*E*)-1-(1-methyl-1*H*-imidazol-2-yl)-3-phenylprop-2-en-1-one (**144**, 424 mg, 2.00 mmol, 1.00 equiv) in DCM (5 mL) was slowly added Br<sub>2</sub> (120 μL, 2.40 mmol, 1.20 equiv) at 0 °C. After stirring for 1 h at room temperature, NEt<sub>3</sub> (1.40 mL, 10.0 mmol, 5.00 equiv) was slowly added at 0 °C. After stirring for additional 24 h at room temperature, the reaction was diluted with DCM (15 mL) and washed with H<sub>2</sub>O (3 x 15 mL). The combined organic layers were dried over Na<sub>2</sub>SO<sub>4</sub>, the solvent was removed *in vacuo* and the residue was purified by column chromatography on SiO<sub>2</sub> (hexanes / EA, 6:1) to obtain (*Z*)-2-bromo-1-(1-methyl-1*H*-imidazol-2-yl)-3-phenylprop-2-en-1-one as yellow oil (257 mg, 882 μmol, 44%).

**R<sub>f</sub>** (hexanes / EA, 6:1) = 0.08; **IR** (neat): 3019, 1640, 1595, 1446, 1386, 1241, 1092, 920, 846, 771 cm<sup>-1</sup>; **<sup>1</sup>H-NMR** (400 MHz, CDCl<sub>3</sub>): δ 9.05 (s, 1H), 7.94 – 7.91 (m, 2H), 7.47 – 7.41 (m, 3H), 7.21 (d, *J* = 0.8 Hz, 1H), 7.11 (s, 1H), 4.02 (s, 3H); **<sup>13</sup>C-NMR** (101 MHz, CDCl<sub>3</sub>): δ 178.18, 146.95, 141.31, 134.39, 130.67, 130.34, 129.16, 128.33, 127.13, 122.80, 36.61; **HRMS** (APCI) *m/z* calculated for C<sub>13</sub>H<sub>12</sub>BrN<sub>2</sub>O ([M+H]<sup>+</sup>) 291.0128, found 291.0131.

**(Z)-2-bromo-1-(4,5-dibromo-1-methyl-1H-imidazol-2-yl)-3-phenylprop-2-en-1-one (151b)**

A 25 mL flask equipped with a magnetic stir bar was charged with (*E*)-1-(1-methyl-1*H*-imidazol-2-yl)-3-phenylprop-2-en-1-one (**144**, 424 mg, 2.00 mmol, 1.00 equiv), *OXONE*<sup>®</sup> (3.07 g, 5.00 mmol, 2.50 equiv) and DCM (10 mL). Subsequently, HBr (47%, 924  $\mu$ L, 8.00 mmol, 4.00 equiv) was added in one portion resulting in a dark red colored solution. After stirring for 3 d at room temperature, NEt<sub>3</sub> (2.80 mL, 20.0 mmol, 10.0 equiv) was carefully added. The reaction mixture was stirred for additional 12 h and subsequently transferred to a separating funnel and extracted with H<sub>2</sub>O (2 x 90 mL) and brine (90 mL). The combined organic layers were dried over Na<sub>2</sub>SO<sub>4</sub>, the solvent was removed *in vacuo* and the residue was purified by column chromatography on SiO<sub>2</sub> (hexanes / EA, 6:1) to obtain (*Z*)-2-bromo-1-(4,5-dibromo-1-methyl-1*H*-imidazol-2-yl)-3-phenylprop-2-en-1-one as yellow oil (699 mg, 1.56 mmol, 78%).

**R<sub>f</sub>** (hexanes / EA, 6:1) = 0.30; **IR** (neat): 3052, 2959, 2922, 1651, 1595, 1442, 1405, 1349, 1207, 1069, 976, 849, 790 cm<sup>-1</sup>; **<sup>1</sup>H-NMR** (300 MHz, CDCl<sub>3</sub>):  $\delta$  8.82 (s, 1H), 7.94 – 7.90 (m, 2H), 7.48 – 7.44 (m, 3H), 4.01 (s, 3H); **<sup>13</sup>C-NMR** (101 MHz, CDCl<sub>3</sub>):  $\delta$  176.89, 147.33, 141.59, 134.12, 130.81, 130.70, 128.43, 128.11, 121.77, 117.91, 113.74, 36.14; **HRMS** (ESI) *m/z* calculated for C<sub>13</sub>H<sub>10</sub>Br<sub>3</sub>N<sub>2</sub>O ([M+H]<sup>+</sup>) 446.8338, found 446.8337.

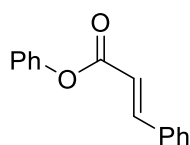
**2-benzylidene-1-(4,5-dibromo-1-methyl-1H-imidazol-2-yl)-4-phenylbutane-1,4-dione (153b)**

A flame dried Schlenk tube equipped with a magnetic stir bar was charged with (*Z*)-2-bromo-1-(4,5-dibromo-1-methyl-1*H*-imidazol-2-yl)-3-phenylprop-2-en-1-one (**151b**, 225 mg, 500  $\mu$ mol, 1.00 equiv), 1-phenylvinyl acetate (405 mg, 2.50 mmol, 5.00 equiv) and

Ru(bpy)<sub>3</sub>Cl<sub>2</sub> (3.70 mg, 5.00 μmol, 1.0 mol%). The flask was sealed with a plastic screw-cap, evacuated and backfilled with N<sub>2</sub> (3x). Dry DMF (2 mL) and H<sub>2</sub>O (10.0 μL, 0.55 mmol, 1.10 equiv) were added and the reaction was magnetically stirred for roughly 5 min under N<sub>2</sub> atmosphere until a homogeneous solution was observed. The resulting mixture was degassed by freeze-pump-thaw (3 cycles) and the plastic screw-cap was replaced by another plastic screw-cap with a Teflon sealed inlet for a glass rod. A high power LED (λ = 455 nm) was attached to the top of the glass rod, which then could act as an optical fiber. After irradiation for 3 h the LED was removed, the mixture was diluted with H<sub>2</sub>O (20 mL) and washed with EA (3 x 20 mL). The combined organic layers were dried over Na<sub>2</sub>SO<sub>4</sub>, the solvent was removed *in vacuo* and the residue was purified by column chromatography on SiO<sub>2</sub> (hexanes / EA, 10:1 to 5:1) to obtain (*E*)-**153b** (52.6 mg, 107 μmol, 22%) and (*Z*)-**153b** (31.9 mg, 65.3 μmol, 23%) as yellow oils as separated *E* and *Z* isomers. *E/Z* = 62:38.

**R<sub>f</sub>** (hexanes / EA, 6:1) = 0.20 (*E* Isomer), 0.13 (*Z* Isomer); **IR** (neat): 3060, 2955, 2922, 1684, 1625, 1408, 1326, 1215, 1002, 954, 928, 745, 685 cm<sup>-1</sup>; **<sup>1</sup>H-NMR** (300 MHz, CDCl<sub>3</sub>, *E* Isomer): δ 8.40 (s, 1H), 8.02 – 7.97 (m, 2H), 7.62 – 7.55 (m, 1H), 7.51 – 7.44 (m, 2H), 7.39 – 7.33 (m, 5H), 4.44 (s, 2H), 3.95 (s, 3H); **<sup>13</sup>C-NMR** (75 MHz, CDCl<sub>3</sub>, *E* Isomer): δ 197.44, 183.31, 146.88, 143.34, 136.58, 135.46, 134.13, 133.31, 129.14, 129.04, 128.68, 128.61, 128.32, 117.21, 112.34, 38.67, 35.78; **<sup>1</sup>H-NMR** (300 MHz, CDCl<sub>3</sub>, *Z* Isomer): δ 8.01 – 7.96 (m, 2H), 7.61 – 7.55 (m, 1H), 7.51 – 7.44 (m, 2H), 7.21 – 7.12 (m, 5H), 7.07 (s, 1H), 4.45 (d, *J* = 1.3 Hz, 2H), 3.94 (s, 3H); **<sup>13</sup>C-NMR** (75 MHz, CDCl<sub>3</sub>, *Z* Isomer): δ 196.97, 186.16, 146.89, 143.47, 139.21, 136.15, 136.07, 134.19, 133.47, 128.71, 128.56, 128.36, 128.06, 127.97, 117.64, 111.99, 46.63, 35.17; **HRMS** (ESI) *m/z* calculated for C<sub>21</sub>H<sub>17</sub>Br<sub>2</sub>N<sub>2</sub>O<sub>2</sub> ([M+H]<sup>+</sup>) 486.9651, found 486.9652.

### (*E*)-phenyl cinnamate (167)

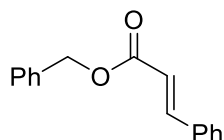


A 250 mL flask equipped with a magnetic stir bar and a dropping funnel was charged with phenol (3.76 g, 40.0 mmol, 1.00 equiv), NEt<sub>3</sub> (7.76 mL, 56.0 mmol, 1.40 equiv) and DCM (80 mL). Cinnamoyl chloride (6.66 g, 40.0 mmol, 1.00 equiv) diluted with DCM (80 mL),

was slowly added *via* dropping funnel. After stirring overnight, the mixture was transferred to a separating funnel and washed with  $\text{KHSO}_4$  (1.0 M, 160 mL) and  $\text{H}_2\text{O}$  (160 mL). The combined organic layers were dried over  $\text{Na}_2\text{SO}_4$ , the solvent was removed *in vacuo* and the residue was recrystallized in EtOH (10 mL) to obtain (*E*)-phenyl cinnamate as white powder (7.31 g, 32.6 mmol, 81%).

$^1\text{H-NMR}$  (300 MHz,  $\text{CDCl}_3$ ):  $\delta$  7.89 (d,  $J = 16.0$  Hz, 1H), 7.63 – 7.58 (m, 2H), 7.46 – 7.39 (m, 5H), 7.30 – 7.23 (m, 1H), 7.21 – 7.16 (m, 2H), 6.65 (d,  $J = 16.0$  Hz, 1H);  $^{13}\text{C-NMR}$  (75 MHz,  $\text{CDCl}_3$ ):  $\delta$  165.45, 150.82, 146.61, 134.19, 130.74, 129.48, 129.03, 128.34, 125.83, 121.67, 117.33.

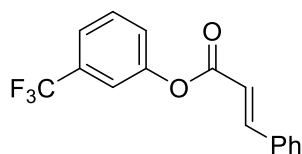
### (*E*)-benzyl cinnamate (168)



A 250 mL flask equipped with a magnetic stir bar and a dropping funnel was charged with benzyl alcohol (4.33 g, 40.0 mmol, 1.00 equiv),  $\text{NEt}_3$  (7.76 mL, 56.0 mmol, 1.40 equiv) and DCM (80 mL). Cinnamoyl chloride (6.66 g, 40.0 mmol, 1.00 equiv) diluted with DCM (80 mL), was slowly added *via* dropping funnel. After stirring overnight, the mixture was transferred to a separating funnel and washed with  $\text{KHSO}_4$  (1.0 M, 160 mL) and  $\text{H}_2\text{O}$  (160 mL). The combined organic layers were dried over  $\text{Na}_2\text{SO}_4$ , the solvent was removed *in vacuo* and the residue was purified by column chromatography on  $\text{SiO}_2$  (hexanes / EA, 12:1 to 10:1) to obtain (*E*)-benzyl cinnamate as colorless oil (7.96 g, 33.4 mmol, 84%).

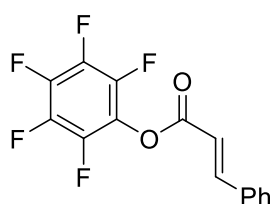
$R_f$  (hexanes / EA, 10:1 = 0.34;  $^1\text{H-NMR}$  (300 MHz,  $\text{CDCl}_3$ ):  $\delta$  7.74 (d,  $J = 16.0$  Hz, 1H), 7.56 – 7.50 (m, 2H), 7.46 – 7.34 (m, 8H), 6.50 (d,  $J = 16.0$  Hz, 1H), 5.26 (s, 2H);  $^{13}\text{C-NMR}$  (101 MHz,  $\text{CDCl}_3$ ):  $\delta$  166.83, 145.22, 136.10, 134.40, 130.39, 128.93, 128.64, 128.32, 128.30, 128.15, 117.92, 66.40.



**(E)-3-(trifluoromethyl)phenyl cinnamate (169)**

A 250 mL flask equipped with a magnetic stir bar and a dropping funnel was charged with (3-(trifluoromethyl)phenyl)methanol (3.24 g, 20.0 mmol, 1.00 equiv),  $\text{NEt}_3$  (3.88 mL, 28.0 mmol, 1.40 equiv) and DCM (40 mL). Cinnamoyl chloride (3.33 g, 20.0 mmol, 1.00 equiv) diluted with DCM (40 mL), was slowly added *via* dropping funnel. After stirring overnight, the mixture was transferred to a separating funnel and washed with  $\text{KHSO}_4$  (1.0 M, 80 mL) and  $\text{H}_2\text{O}$  (80 mL). The combined organic layers were dried over  $\text{Na}_2\text{SO}_4$ , the solvent was removed *in vacuo* and the residue was recrystallized in EtOH (5 mL) to obtain (E)-3-(trifluoromethyl)phenyl cinnamate as white powder (5.20 g, 17.8 mmol, 89%).

$^1\text{H-NMR}$  (400 MHz,  $\text{CDCl}_3$ ):  $\delta$  7.91 (d,  $J = 16.0$  Hz, 1H), 7.63 – 7.58 (m, 2H), 7.57 – 7.51 (m, 2H), 7.49 – 7.42 (m, 4H), 7.42 – 7.37 (m, 1H), 6.64 (d,  $J = 16.0$  Hz, 1H);  $^{13}\text{C-NMR}$  (101 MHz,  $\text{CDCl}_3$ ):  $\delta$  164.95, 150.92, 147.42, 134.00, 132.00 (q,  $J = 32.9$  Hz), 131.00, 130.02, 129.09, 128.43, 125.32, 122.61 (q,  $J = 3.8$  Hz), 119.02 (q,  $J = 3.9$  Hz), 116.65;  $^{19}\text{F-NMR}$  (376 MHz,  $\text{CDCl}_3$ ):  $\delta$  -63.14.

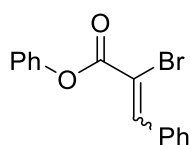
**(E)-perfluorophenyl cinnamate (170)**

A 250 mL flask equipped with a magnetic stir bar and a dropping funnel was charged with 2,3,4,5,6-pentafluorophenol (3.96 g, 21.5 mmol, 1.00 equiv),  $\text{NEt}_3$  (4.17 mL, 30.1 mmol, 1.40 equiv) and DCM (40 mL). Cinnamoyl chloride (3.58 g, 21.5 mmol, 1.00 equiv) diluted with DCM (40 mL), was slowly added *via* dropping funnel. After stirring overnight, the mixture was transferred to a separating funnel and washed with  $\text{KHSO}_4$  (1.0 M, 80 mL) and  $\text{H}_2\text{O}$  (80 mL). The combined organic layers were dried over  $\text{Na}_2\text{SO}_4$ , the solvent was removed

*in vacuo* and the residue was recrystallized in EtOH (5 mL) to obtain (*E*)-perfluorophenyl cinnamate as white powder (5.89 g, 18.8 mmol, 87%).

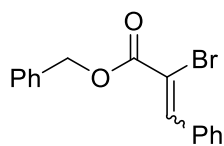
**<sup>1</sup>H-NMR** (300 MHz, CDCl<sub>3</sub>): δ 7.96 (d, *J* = 16.0 Hz, 1H), 7.64 – 7.58 (m, 2H), 7.49 – 7.42 (m, 3H), 6.66 (d, *J* = 16.0 Hz, 1H); **<sup>13</sup>C-NMR** (75 MHz, CDCl<sub>3</sub>): δ 162.67, 149.50, 133.54, 131.51, 129.15, 128.65, 114.19; **<sup>19</sup>F-NMR** (282 MHz, CDCl<sub>3</sub>): δ -152.99 (m, 2H), -158.69 (t, *J* = 21.7 Hz, 1H), -162.91 (m, 2H).

### phenyl 2-bromo-3-phenylacrylate (**172**)



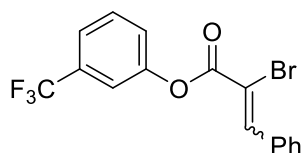
A 250 mL flask equipped with a magnetic stir bar was charged with (*E*)-phenyl 3-phenylacrylate (**167**, 4.04 g, 18.0 mmol, 1.00 equiv), *OXONE*<sup>®</sup> (13.3 g, 21.6 mmol, 1.20 equiv) and DCM (90 mL). Subsequently, HBr (47%, 4.16 mL, 36.0 mmol, 2.00 equiv) was added in one portion resulting in a dark red colored solution. After stirring for 4 d at room temperature, NEt<sub>3</sub> (12.5 mL, 90.0 mmol, 5.00 equiv) was carefully added. The reaction mixture was stirred for additional 12 h and subsequently transferred to a separating funnel and extracted with H<sub>2</sub>O (2 x 90 mL) and brine (90 mL). The combined organic layers were dried over Na<sub>2</sub>SO<sub>4</sub>, the solvent was removed *in vacuo* and the residue was purified by column chromatography on SiO<sub>2</sub> (hexanes / EA, 10:1) to obtain phenyl 2-bromo-3-phenylacrylate as a mixture of *E/Z* = 45:55 as yellow oil (4.78 g, 15.8 mmol, 88%).

**R<sub>f</sub>** (hexanes / EA, 10:1) = 0.32; **IR** (neat): 3060, 3026, 1738, 1591, 1490, 1446, 1341, 1241, 1170, 1026, 961, 849, 752, 685 cm<sup>-1</sup>; **<sup>1</sup>H-NMR** (300 MHz, CDCl<sub>3</sub>, *E* Isomer): δ 7.54 (s, 1H), 7.49 – 7.20 (m, 8H), 7.04 – 7.01 (m, 2H); **<sup>1</sup>H-NMR** (300 MHz, CDCl<sub>3</sub>, *Z* Isomer): δ 8.45 (s, 1H), 7.96 – 7.93 (m, 2H), 7.49 – 7.20 (m, 8H); **<sup>13</sup>C-NMR** (75 MHz, CDCl<sub>3</sub>, both Isomers): δ 162.79, 162.10, 151.04, 150.29, 142.56, 141.20, 134.77, 133.55, 130.66, 130.56, 129.60, 129.52, 129.28, 128.62, 128.57, 128.36, 126.34, 126.26, 121.46, 121.05, 112.03, 110.74; **HRMS** (CI) *m/z* calculated for C<sub>15</sub>H<sub>12</sub>O<sub>2</sub>Br ([*M*+*H*]<sup>+</sup>) 303.0015, found 303.0010.

**benzyl 2-bromo-3-phenylacrylate (173)**

A 250 mL flask equipped with a magnetic stir bar was charged with (*E*)-benzyl 3-phenylacrylate (**168**, 4.29 g, 18.0 mmol, 1.00 equiv), *OXONE*<sup>®</sup> (13.3 g, 21.6 mmol, 1.20 equiv) and DCM (90 mL). Subsequently, HBr (47%, 4.16 mL, 36.0 mmol, 2.00 equiv) was added in one portion resulting in a dark red colored solution. After stirring for 4 d at room temperature, NEt<sub>3</sub> (12.5 mL, 90.0 mmol, 5.00 equiv) was carefully added. The reaction mixture was stirred for additional 12 h and subsequently transferred to a separating funnel and extracted with H<sub>2</sub>O (2 x 90 mL) and brine (90 mL). The combined organic layers were dried over Na<sub>2</sub>SO<sub>4</sub>, the solvent was removed *in vacuo* and the residue was purified by column chromatography on SiO<sub>2</sub> (hexanes / EA, 10:1) to obtain benzyl 2-bromo-3-phenylacrylate as a mixture of *E/Z* = 42:58 as yellow oil (3.56 g, 11.2 mmol, 62%).

**R<sub>f</sub>** (hexanes / EA, 10:1) = 0.30; **IR** (neat): 3063, 3030, 2955, 2885, 1710, 1610, 1490, 1446, 1375, 1226, 1192, 1077, 1013, 928, 764, 689 cm<sup>-1</sup>; **<sup>1</sup>H-NMR** (400 MHz, CDCl<sub>3</sub>, *E* isomer): δ 7.38 – 7.36 (m, 2H), 7.32 – 7.30 (m, 3H), 7.30 – 7.27 (m, 1H), 7.24 (s, 1H), 7.22 – 7.18 (m, 4H), 5.19 (s, 2H); **<sup>1</sup>H-NMR** (400 MHz, CDCl<sub>3</sub>, *Z* isomer): δ 8.25 (s, 1H), 7.86 – 7.84 (m, 2H), 7.46 – 7.41 (m, 7H), 7.39 – 7.38 (m, 1H), 5.34 (s, 2H); **<sup>13</sup>C-NMR** (101 MHz, CDCl<sub>3</sub>, both isomers): δ 164.24, 163.27, 141.33, 140.03, 135.43, 134.77, 134.61, 134.49, 133.71, 130.36, 130.31, 128.88, 128.69, 128.56, 128.50, 128.45, 128.28, 128.12, 112.80, 111.32, 68.35, 67.98; **HRMS** (EI) *m/z* calculated for C<sub>16</sub>H<sub>13</sub>O<sub>2</sub>Br ([M]<sup>+</sup>) 316.0093, found 316.0090.

**3-(trifluoromethyl)phenyl 2-bromo-3-phenylacrylate (174)**

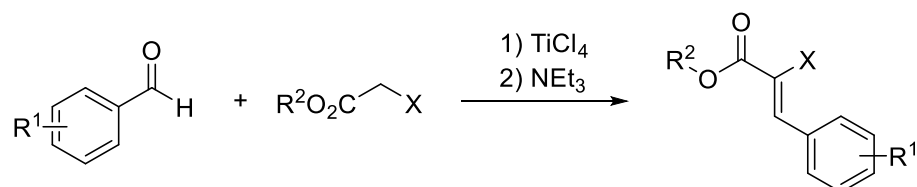
A 250 mL flask equipped with a magnetic stir bar was charged with (*E*)-3-(trifluoromethyl)phenyl 3-phenylacrylate (**169**, 5.14 g, 17.6 mmol, 1.00 equiv), *OXONE*<sup>®</sup> (13.0 g, 21.1 mmol, 1.20 equiv) and DCM (90 mL). Subsequently, HBr (47%, 4.06 mL,

35.2 mmol, 2.00 equiv) was added in one portion resulting in a dark red colored solution. After stirring for 4 d at room temperature,  $\text{NEt}_3$  (12.2 mL, 87.9 mmol, 5.00 equiv) was carefully added. The reaction mixture was stirred for additional 12 h and subsequently transferred to a separating funnel and extracted with  $\text{H}_2\text{O}$  (2 x 90 mL) and brine (90 mL). The combined organic layers were dried over  $\text{Na}_2\text{SO}_4$ , the solvent was removed *in vacuo* and the residue was purified by column chromatography on  $\text{SiO}_2$  (hexanes / EA, 10:1) to obtain 3-(trifluoromethyl)phenyl 2-bromo-3-phenylacrylate as a mixture of *E/Z* = 41:59 as yellow oil (5.81 g, 15.7 mmol, 89%).

**R<sub>f</sub>** (hexanes / EA, 10:1) = 0.38; **IR** (neat): 3071, 3030, 1736, 1606, 1490, 1449, 1326, 1237, 1162, 1121, 1066, 969, 928, 890, 797, 760, 693  $\text{cm}^{-1}$ ; **<sup>1</sup>H-NMR** (300 MHz,  $\text{CDCl}_3$ , *E* isomer):  $\delta$  7.61 (s, 1H), 7.46 – 7.39 (m, 7H), 7.24 – 7.21 (m, 2H); **<sup>1</sup>H-NMR** (300 MHz,  $\text{CDCl}_3$ , *Z* isomer):  $\delta$  8.46 (s, 1H), 7.96 – 7.93 (m, 2H), 7.58 – 7.56 (m, 2H), 7.51 – 7.47 (m, 5H); **<sup>13</sup>C-NMR** (75 MHz,  $\text{CDCl}_3$ , both isomers):  $\delta$  162.25, 161.74, 151.03, 150.28, 143.26, 142.42, 134.77, 133.34, 132.35, 131.92, 130.91, 130.64, 130.19, 130.10, 129.47, 128.67, 128.63, 128.30, 125.15, 125.13, 124.72, 123.13 (t, *J* = 3.7 Hz), 118.90 (d, *J* = 3.7 Hz), 118.44, 118.39, 118.34, 111.19, 110.20; **<sup>19</sup>F-NMR** (282 MHz,  $\text{CDCl}_3$ , both isomers):  $\delta$  -63.14, -63.23; **HRMS** (ESI) *m/z* calculated for  $\text{C}_{16}\text{H}_{10}\text{BrF}_3\text{NaO}_2$  ( $[\text{M}+\text{Na}]^+$ ) 392.9708, found 392.9709.

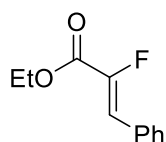
### 3 Synthesis of $\alpha$ -halo cinnamates (228a – 228u)

**General procedure (GP-A) for the synthesis of (Z)- $\alpha$ -halo cinnamates via titanium mediated olefination**<sup>[197]</sup>



A flame dried two-neck-flask equipped with a magnetic stir bar and a dropping funnel was charged with aromatic aldehyde (10.0 mmol, 1.00 equiv),  $\alpha$ -halo acetate (13.0 mmol, 1.30 equiv) and dry DCM (15 mL) under nitrogen atmosphere. Subsequently, TiCl<sub>4</sub> (14.0 mmol, 1.40 equiv) diluted with dry DCM (14 mL) was added dropwise over a period of 10 min. After stirring for additional 30 min at room temperature, NEt<sub>3</sub> (6.93 mL, 50.0 mmol, 5.00 equiv) was cautiously added in drops within 10 min. The resulting brown mixture was then stirred overnight. Upon completion of the reaction, the mixture was diluted with DCM (20 mL) and washed with HCl<sub>aq</sub> (1.0 M, 15 mL), H<sub>2</sub>O (15 mL) and brine (15 mL). The combined organic layers were dried over Na<sub>2</sub>SO<sub>4</sub>, the solvent was removed *in vacuo* and the residue was purified by column chromatography on SiO<sub>2</sub> (hexanes / EA, 15:1) to obtain the pure product.

#### ethyl (Z)-2-fluoro-3-phenylacrylate (228a-F)

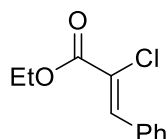


Following general procedure **GP-A** using benzaldehyde (1.01 mL, 10.0 mmol, 1.00 equiv), ethyl fluoroacetate (1.25 mL, 13.0 mmol, 1.30 equiv), TiCl<sub>4</sub> (1.54 mL, 14.0 mmol, 1.40 equiv), NEt<sub>3</sub> (6.93 mL, 50.0 mmol, 5.00 equiv) gave ethyl (Z)-2-fluoro-3-phenylacrylate (1.04 g, 5.36 mmol, 54%) as yellowish oil after purification on SiO<sub>2</sub> (hexanes / EA, 15:1).

**R<sub>f</sub>** (hexanes / EA, 10:1) = 0.42; **<sup>1</sup>H-NMR** (400 MHz, CDCl<sub>3</sub>):  $\delta$  7.66 – 7.64 (m, 2H), 7.43 – 7.35 (m, 3H), 6.92 (d,  $J$  = 35.3 Hz, 1H), 4.36 (q,  $J$  = 7.1 Hz, 2H), 1.39 (t,  $J$  = 7.1 Hz, 3H);

$^{13}\text{C-NMR}$  (101 MHz,  $\text{CDCl}_3$ ):  $\delta$  161.48 (d,  $J = 34.2$  Hz), 147.06 (d,  $J = 267.6$  Hz), 131.19 (d,  $J = 4.4$  Hz), 130.33 (d,  $J = 8.2$  Hz), 129.72 (d,  $J = 2.7$  Hz), 128.84, 117.53, 117.49, 61.93, 14.26;  $^{19}\text{F-NMR}$  (376 MHz,  $\text{CDCl}_3$ ):  $\delta$  -125.82.

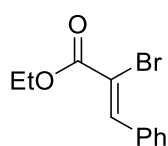
**ethyl (Z)-2-chloro-3-phenylacrylate (228a-Cl)**



Following general procedure **GP-A** using benzaldehyde (1.01 mL, 10.0 mmol, 1.00 equiv), ethyl chloroacetate (1.40 mL, 13.0 mmol, 1.30 equiv),  $\text{TiCl}_4$  (1.53 mL, 14.0 mmol, 1.40 equiv),  $\text{NEt}_3$  (6.93 mL, 50.0 mmol, 5.00 equiv) gave ethyl (Z)-2-chloro-3-phenylacrylate (1.33 g, 6.31 mmol, 63%) as colorless oil after purification on  $\text{SiO}_2$  (hexanes / EA, 15:1).

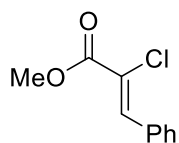
$R_f$  (hexanes / EA, 10:1) = 0.50;  $^1\text{H-NMR}$  (300 MHz,  $\text{CDCl}_3$ ):  $\delta$  7.91 (s, 1H), 7.87 – 7.82 (m, 2H), 7.47 – 7.40 (m, 3H), 4.36 (q,  $J = 7.1$  Hz, 2H), 1.39 (t,  $J = 7.1$  Hz, 3H);  $^{13}\text{C-NMR}$  (75 MHz,  $\text{CDCl}_3$ ):  $\delta$  163.45, 136.92, 132.98, 130.66, 130.20, 128.56, 122.23, 62.62, 14.26.

**ethyl (Z)-2-bromo-3-phenylacrylate (228a-Br)**



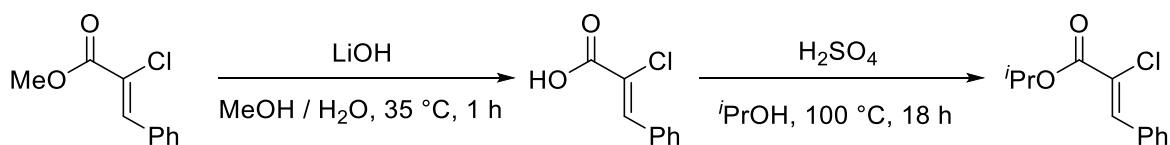
Following general procedure **GP-A** using benzaldehyde (1.01 mL, 10.0 mmol, 1.00 equiv), ethyl bromoacetate (1.45 mL, 13.0 mmol, 1.30 equiv),  $\text{TiCl}_4$  (1.53 mL, 14.0 mmol, 1.40 equiv),  $\text{NEt}_3$  (6.93 mL, 50.0 mmol, 5.00 equiv) gave ethyl (Z)-2-bromo-3-phenylacrylate (1.19 g, 4.66 mmol, 40%) as colorless oil after purification on  $\text{SiO}_2$  (hexanes / EA, 15:1).

$R_f$  (hexanes / EA, 10:1) = 0.50;  $^1\text{H-NMR}$  (300 MHz,  $\text{CDCl}_3$ ):  $\delta$  8.22 (s, 1H), 7.87 – 7.84 (m, 2H), 7.44 – 7.42 (m, 3H), 4.36 (q,  $J = 7.1$  Hz, 2H), 1.39 (t,  $J = 7.1$  Hz, 3H);  $^{13}\text{C-NMR}$  (75 MHz,  $\text{CDCl}_3$ ):  $\delta$  163.38, 140.80, 133.77, 130.21, 128.91, 128.44, 113.19, 62.83, 14.26.

**methyl (Z)-2-chloro-3-phenylacrylate (228b)**

Following general procedure **GP-A** using benzaldehyde (4.04 mL, 40.0 mmol, 1.00 equiv), ethyl chloroacetate (4.55 mL, 52.0 mmol, 1.30 equiv),  $\text{TiCl}_4$  (6.14 mL, 56.0 mmol, 1.40 equiv),  $\text{NEt}_3$  (27.7 mL, 200 mmol, 5.00 equiv) gave methyl (Z)-2-chloro-3-phenylacrylate (3.50 g, 17.8 mmol, 45%) as slightly yellow oil after purification on  $\text{SiO}_2$  (hexanes / EA, 15:1).

$R_f$  (hexanes / EA, 10:1) = 0.37;  $^1\text{H-NMR}$  (400 MHz,  $\text{CDCl}_3$ ):  $\delta$  7.92 (s, 1H), 7.86 – 7.83 (m, 2H), 7.47 – 7.41 (m, 3H), 3.91 (s, 3H);  $^{13}\text{C-NMR}$  (101 MHz,  $\text{CDCl}_3$ ):  $\delta$  163.97, 137.28, 132.93, 130.70, 130.29, 128.59, 121.82, 53.41.

**iso-propyl (Z)-2-chloro-3-phenylacrylate (228c)**

Preparation *via* **GP-A** failed. The title compound was thus synthesized by esterification of the free carboxylic acid.

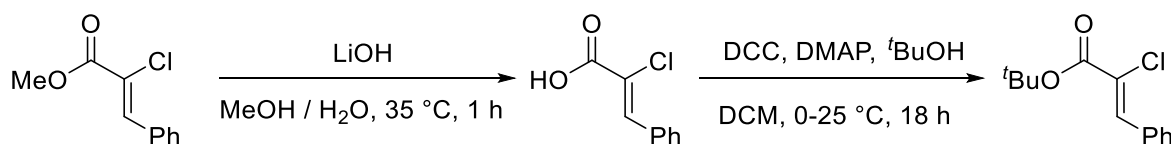
Methyl (Z)-2-chloro-3-phenylacrylate (**228b**, 1.00 g, 5.09 mmol, 1.00 equiv) and LiOH (244 mg, 10.2 mmol, 2.00 equiv) was dissolved in a mixture of MeOH (5 mL) and  $\text{H}_2\text{O}$  (1 mL). The reaction mixture was heated to 35 °C for 1 h. Subsequently, methanol was evaporated and the mixture was diluted with  $\text{H}_2\text{O}$  (20 mL) and washed with DCM (2 x 20 mL). The aqueous phase was acidified and washed with EA (3 x 20 mL). The combined organic layers were dried over  $\text{Na}_2\text{SO}_4$ , the solvent was removed *in vacuo* and (Z)-2-chloro-3-phenylacrylic acid (816 mg, 4.47 mmol, 88%) could be used without further purification.

**<sup>1</sup>H-NMR** (300 MHz, CDCl<sub>3</sub>): δ 10.14 (s, 1H), 8.06 (s, 1H), 7.94 – 7.87 (m, 2H), 7.49 – 7.43 (m, 3H); **<sup>13</sup>C-NMR** (75 MHz, CDCl<sub>3</sub>): δ 168.69, 139.50, 132.58, 131.02, 130.86, 128.69, 120.89.

A 100 mL flask was charged with (*Z*)-2-chloro-3-phenylacrylic acid (704 mg, 3.86 mmol, 1.00 equiv), <sup>i</sup>PrOH (25.0 mL, 325 mmol, 84.0 equiv) and conc. H<sub>2</sub>SO<sub>4</sub> (200 μL, 3.75 mmol, 0.97 equiv). The reaction was heated to 100 °C and stirred overnight. The mixture was allowed to cool to room temperature, quenched with sat. NaHCO<sub>3</sub> (15 mL) and washed with DCM (3 x 25 mL). The combined organic layers were dried over Na<sub>2</sub>SO<sub>4</sub>, the solvent was removed *in vacuo* and the residue was purified by column chromatography on SiO<sub>2</sub> (hexanes / EA, 15:1) to obtain pure *iso*-propyl (*Z*)-2-chloro-3-phenylacrylate as colorless oil (592 mg, 2.63 mmol, 68%).

**R<sub>f</sub>** (hexanes / EA, 6:1) = 0.48; **IR** (neat): 3060, 3030, 2981, 2937, 1714, 1617, 1490, 1446, 1375, 1263, 1200, 1103, 1021, 916, 861, 831, 767, 689 cm<sup>-1</sup>; **<sup>1</sup>H-NMR** (300 MHz, CDCl<sub>3</sub>): δ 7.88 (s, 1H), 7.87 – 7.82 (m, 2H), 7.45 – 7.40 (m, 3H), 5.18 (sept, *J* = 6.3 Hz, 1H), 1.37 (d, *J* = 6.3 Hz, 6H); **<sup>13</sup>C-NMR** (75 MHz, CDCl<sub>3</sub>): δ 162.90, 136.59, 133.06, 130.62, 130.10, 128.53, 122.72, 70.43, 21.83; **HRMS** (ESI) *m/z* calculated for C<sub>12</sub>H<sub>14</sub>ClO<sub>2</sub> ([*M*+*H*]<sup>+</sup>) 225.0677, found 225.0677.

#### *tert*-butyl (*Z*)-2-chloro-3-phenylacrylate (**228d**)



Preparation *via* **GP-A** failed. The title compound was thus synthesized by esterification of the free carboxylic acid.

Methyl (*Z*)-2-chloro-3-phenylacrylate (**228b**, 1.00 g, 5.09 mmol, 1.00 equiv) and LiOH (244 mg, 10.2 mmol, 2.00 equiv) was dissolved in a mixture of MeOH (5 mL) and H<sub>2</sub>O (1 mL). The reaction mixture was heated to 35 °C for 1 h. Subsequently, methanol was evaporated and the mixture was diluted with H<sub>2</sub>O (20 mL) and washed with DCM (2 x 20 mL). The aqueous phase was acidified and washed with EA (3 x 20 mL). The combined organic layers were dried over Na<sub>2</sub>SO<sub>4</sub>, the solvent was removed *in vacuo* and (*Z*)-2-chloro-3-phenylacrylic acid (816 mg, 4.47 mmol, 88%) could be used without further purification.

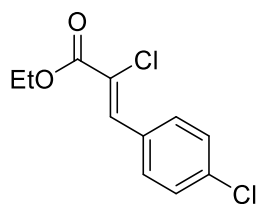


**<sup>1</sup>H-NMR** (300 MHz, CDCl<sub>3</sub>): δ 10.14 (s, 1H), 8.06 (s, 1H), 7.94 – 7.87 (m, 2H), 7.49 – 7.43 (m, 3H); **<sup>13</sup>C-NMR** (75 MHz, CDCl<sub>3</sub>): δ 168.69, 139.50, 132.58, 131.02, 130.86, 128.69, 120.89.

(Z)-2-chloro-3-phenylacrylic acid (465 mg, 2.55 mmol, 1.00 equiv), 4-DMAP (31.1 mg, 255 μmol, 0.10 equiv), and <sup>t</sup>BuOH (189 mg, 2.55 mmol, 1.00 equiv) was dissolved in DCM (10 mL). Subsequently, DCC (578 mg, 2.80 mmol, 1.10 equiv) was added at 0 °C. The reaction was stirred for additional 5 min at 0 °C. After stirring overnight at room temperature the reaction mixture was filtered, diluted with DCM (40 mL) and washed with HCl (0.5 M, 2 x 20 mL) and sat. NaHCO<sub>3</sub> (20 mL). The combined organic layers were dried over Na<sub>2</sub>SO<sub>4</sub>, the solvent was removed *in vacuo* and the residue was purified by column chromatography on SiO<sub>2</sub> (hexanes / EA, 8:1) to obtain pure *tert*-butyl (Z)-2-chloro-3-phenylacrylate as yellow oil (453 mg, 1.90 mmol, 75%).

**R<sub>f</sub>** (hexanes / EA, 6:1) = 0.55; **IR** (neat): 3056, 2981, 2933, 1710, 1617, 1490, 1446, 1394, 1367, 1282, 1252, 1203, 1151, 1077, 1043, 1013, 924, 842, 767, 609 cm<sup>-1</sup>; **<sup>1</sup>H-NMR** (400 MHz, CDCl<sub>3</sub>): δ 7.83 – 7.80 (m, 3H), 7.45 – 7.39 (m, 3H), 1.58 (s, 9H); **<sup>13</sup>C-NMR** (101 MHz, CDCl<sub>3</sub>): δ 162.27, 135.94, 133.22, 130.53, 129.92, 128.49, 123.76, 82.98, 28.03; **HRMS** (EI) *m/z* calculated for C<sub>13</sub>H<sub>15</sub>ClO<sub>2</sub> ([M]<sup>+</sup>) 238.0751, found 238.0754.

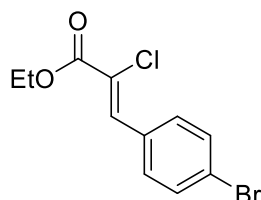
#### ethyl (Z)-2-chloro-3-(4-chlorophenyl)acrylate (228e)



Following general procedure **GP-A** using 4-chlorobenzaldehyde (1.41 g, 10.0 mmol, 1.00 equiv), ethyl chloroacetate (1.39 mL, 13.0 mmol, 1.30 equiv), TiCl<sub>4</sub> (1.54 mL, 14.0 mmol, 1.40 equiv), NEt<sub>3</sub> (2.77 mL, 20.0 mmol, 2.00 equiv) gave ethyl (Z)-2-chloro-3-(4-chlorophenyl)acrylate (1.10 g, 4.49 mmol, 45%) as colorless oil after purification on SiO<sub>2</sub> (hexanes / EA, 15:1).

**R<sub>f</sub>** (hexanes / EA, 10:1) = 0.40; **<sup>1</sup>H-NMR** (300 MHz, CDCl<sub>3</sub>): δ 7.85 (s, 1H), 7.82 – 7.76 (m, 2H), 7.43 – 7.38 (m, 2H), 4.35 (q, *J* = 7.1 Hz, 2H), 1.39 (t, *J* = 7.1 Hz, 3H); **<sup>13</sup>C-NMR** (75 MHz, CDCl<sub>3</sub>): δ 163.20, 136.12, 135.55, 131.86, 131.40, 128.87, 122.80, 62.74, 14.24.

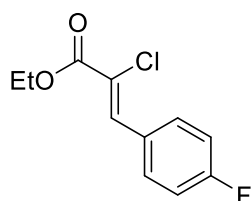
**ethyl (Z)-3-(4-bromophenyl)-2-chloroacrylate (228f)**



Following general procedure **GP-A** using 4-bromobenzaldehyde (1.85 g, 10.0 mmol, 1.00 equiv), ethyl chloroacetate (1.39 mL, 13.0 mmol, 1.30 equiv), TiCl<sub>4</sub> (1.54 mL, 14.0 mmol, 1.40 equiv), NEt<sub>3</sub> (2.77 mL, 20.0 mmol, 2.00 equiv) gave ethyl (Z)-3-(4-bromophenyl)-2-chloroacrylate (511 mg, 1.76 mmol, 18%) as colorless oil after purification on SiO<sub>2</sub> (hexanes / EA, 15:1).

**R<sub>f</sub>** (hexanes / EA, 10:1) = 0.40; **<sup>1</sup>H-NMR** (300 MHz, CDCl<sub>3</sub>): δ 7.83 (s, 1H), 7.74 – 7.69 (m, 2H), 7.58 – 7.53 (m, 2H), 4.35 (q, *J* = 7.1 Hz, 2H), 1.39 (t, *J* = 7.1 Hz, 3H); **<sup>13</sup>C-NMR** (75 MHz, CDCl<sub>3</sub>): δ 163.19, 135.62, 132.02, 131.84, 124.55, 122.94, 62.75, 14.24.

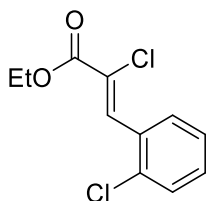
**ethyl (Z)-2-chloro-3-(4-fluorophenyl)acrylate (228g)**



Following general procedure **GP-A** using 4-fluorobenzaldehyde (1.05 mL, 10.0 mmol, 1.00 equiv), ethyl chloroacetate (1.39 mL, 13.0 mmol, 1.30 equiv), TiCl<sub>4</sub> (1.54 mL, 14.0 mmol, 1.40 equiv), NEt<sub>3</sub> (6.93 mL, 50.0 mmol, 5.00 equiv) gave ethyl (Z)-2-chloro-3-(4-fluorophenyl)acrylate (765 mg, 3.35 mmol, 34%) as colorless oil after purification on SiO<sub>2</sub> (hexanes / EA, 15:1).

$R_f$  (hexanes / EA, 10:1) = 0.40;  $^1\text{H-NMR}$  (400 MHz,  $\text{CDCl}_3$ ):  $\delta$  7.88 – 7.84 (m, 3H), 7.15 – 7.09 (m, 2H), 4.35 (q,  $J = 7.1$  Hz, 2H), 1.39 (t,  $J = 7.1$  Hz, 3H);  $^{13}\text{C-NMR}$  (101 MHz,  $\text{CDCl}_3$ ):  $\delta$  164.72, 163.34, 162.21, 135.63, 132.83, 132.75, 129.22, 129.18, 121.93, 121.91, 115.86, 115.65, 62.65, 14.24;  $^{19}\text{F-NMR}$  (376 MHz,  $\text{CDCl}_3$ ):  $\delta$  -109.28.

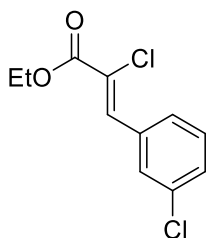
**ethyl (Z)-2-chloro-3-(2-chlorophenyl)acrylate (228h)**



Following general procedure **GP-A** using 2-chlorobenzaldehyde (1.12 mL, 10.0 mmol, 1.00 equiv), ethyl chloroacetate (1.39 mL, 13.0 mmol, 1.30 equiv),  $\text{TiCl}_4$  (1.54 mL, 14.0 mmol, 1.40 equiv),  $\text{NEt}_3$  (6.93 mL, 50.0 mmol, 5.00 equiv) gave ethyl (Z)-2-chloro-3-(2-chlorophenyl)acrylate (931 mg, 3.80 mmol, 38%) as colorless oil after purification on  $\text{SiO}_2$  (hexanes / EA, 15:1).

$R_f$  (hexanes / EA, 10:1) = 0.49;  $^1\text{H-NMR}$  (400 MHz,  $\text{CDCl}_3$ ):  $\delta$  8.15 (s, 1H), 7.98 – 7.93 (m, 1H), 7.47 – 7.43 (m, 1H), 7.36 – 7.31 (m, 2H), 4.38 (q,  $J = 7.1$  Hz, 2H), 1.40 (t,  $J = 7.1$  Hz, 3H);  $^{13}\text{C-NMR}$  (101 MHz,  $\text{CDCl}_3$ ):  $\delta$  162.92, 134.78, 133.85, 131.54, 130.78, 130.70, 129.67, 126.56, 125.01, 62.80, 14.22.

**ethyl (Z)-2-chloro-3-(3-chlorophenyl)acrylate (228i)**

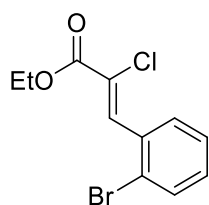


Following general procedure **GP-A** using 3-chlorobenzaldehyde (1.12 mL, 10.0 mmol, 1.00 equiv), ethyl chloroacetate (1.39 mL, 13.0 mmol, 1.30 equiv),  $\text{TiCl}_4$  (1.54 mL, 14.0 mmol, 1.40 equiv),  $\text{NEt}_3$  (6.93 mL, 50.0 mmol, 5.00 equiv) gave ethyl (Z)-2-chloro-3-(3-

chlorophenyl)acrylate (887 mg, 3.62 mmol, 36%) as yellowish oil after purification on SiO<sub>2</sub> (hexanes / EA, 15:1).

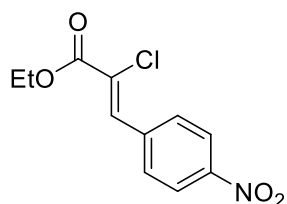
**R<sub>f</sub>** (hexanes / EA, 10:1) = 0.35; **IR** (neat): 3063, 2981, 1718, 1617, 1565, 1476, 1412, 1367, 1241, 1196, 1095, 1039, 998, 902, 861, 782, 682 cm<sup>-1</sup>; **<sup>1</sup>H-NMR** (300 MHz, CDCl<sub>3</sub>): δ 7.87 – 7.82 (m, 2H), 7.71 – 7.66 (m, 1H), 7.39 – 7.35 (m, 2H), 4.36 (q, *J* = 7.1 Hz, 2H), 1.39 (t, *J* = 7.1 Hz, 3H); **<sup>13</sup>C-NMR** (75 MHz, CDCl<sub>3</sub>): δ 163.05, 135.37, 134.65, 134.53, 130.21, 130.10, 129.78, 128.73, 123.66, 62.80, 14.22; **HRMS** (EI) *m/z* calculated for C<sub>11</sub>H<sub>10</sub>Cl<sub>2</sub>O<sub>2</sub> ([M]<sup>+</sup>) 244.0052, found 244.0050.

#### ethyl (Z)-3-(2-bromophenyl)-2-chloroacrylate (228j)



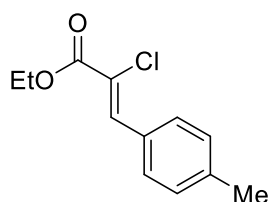
Following general procedure **GP-A** using 2-bromobenzaldehyde (1.16 mL, 10.0 mmol, 1.00 equiv), ethyl chloroacetate (1.39 mL, 13.0 mmol, 1.30 equiv), TiCl<sub>4</sub> (1.54 mL, 14.0 mmol, 1.40 equiv), NEt<sub>3</sub> (6.93 mL, 50.0 mmol, 5.00 equiv) gave ethyl (Z)-3-(2-bromophenyl)-2-chloroacrylate (1.87 g, 6.64 mmol, 65%) as colorless oil after purification on SiO<sub>2</sub> (hexanes / EA, 15:1).

**R<sub>f</sub>** (hexanes / EA, 10:1) = 0.41; **IR** (neat): 3056, 2981, 2907, 1722, 1621, 1584, 1464, 1435, 1367, 1237, 1200, 1118, 1039, 998, 849, 760, 719 cm<sup>-1</sup>; **<sup>1</sup>H-NMR** (300 MHz, CDCl<sub>3</sub>): δ 8.09 (s, 1H), 7.89 (dd, *J* = 7.8, 1.6 Hz, 1H), 7.64 (dd, *J* = 8.0, 1.2 Hz, 1H), 7.38 (td, *J* = 7.5, 1.0 Hz, 1H), 7.25 (td, *J* = 7.7, 1.6 Hz, 1H), 4.38 (q, *J* = 7.1 Hz, 2H), 1.40 (t, *J* = 7.1 Hz, 3H); **<sup>13</sup>C-NMR** (75 MHz, CDCl<sub>3</sub>): δ 162.88, 136.32, 133.38, 132.87, 130.89, 130.87, 127.14, 124.91, 124.88, 62.80, 14.22; **HRMS** (EI) *m/z* calculated for C<sub>11</sub>H<sub>10</sub>O<sub>2</sub>ClBr ([M]<sup>+</sup>) 287.9547, found 287.9551.

**ethyl (Z)-2-chloro-3-(4-nitrophenyl)acrylate (228k)**

Following general procedure **GP-A** using 4-nitrobenzaldehyde (1.51 g, 10.0 mmol, 1.00 equiv), ethyl chloroacetate (1.39 mL, 13.0 mmol, 1.30 equiv),  $\text{TiCl}_4$  (1.54 mL, 14.0 mmol, 1.40 equiv),  $\text{NEt}_3$  (6.93 mL, 50.0 mmol, 5.00 equiv) gave ethyl (Z)-2-chloro-3-(4-nitrophenyl)acrylate (1.02 g, 3.99 mmol, 40%) as orange solid after purification on  $\text{SiO}_2$  (hexanes / EA, 15:1).

$R_f$  (hexanes / EA, 10:1) = 0.18; **IR** (neat): 3127, 3093, 3026, 2944, 2903, 2851, 1710, 1617, 1509, 1345, 1263, 1200, 1110, 1032, 924, 853, 760, 682  $\text{cm}^{-1}$ ;  **$^1\text{H-NMR}$**  (300 MHz,  $\text{CDCl}_3$ ):  $\delta$  8.31 – 8.25 (m, 2H), 7.99 – 7.93 (m, 3H), 4.38 (q,  $J = 7.1$  Hz, 2H), 1.40 (t,  $J = 7.1$  Hz, 3H);  **$^{13}\text{C-NMR}$**  (75 MHz,  $\text{CDCl}_3$ ):  $\delta$  162.60, 147.99, 139.11, 134.27, 131.12, 126.11, 123.70, 63.12, 14.20; **HRMS** (EI)  $m/z$  calculated for  $\text{C}_{11}\text{H}_{10}\text{NO}_4\text{Cl}$  ( $[\text{M}]^+$ ) 255.0293, found 255.0295.

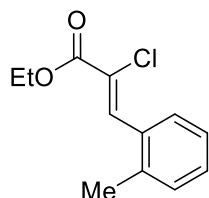
**ethyl (Z)-2-chloro-3-(*p*-tolyl)acrylate (228l)**

Following general procedure **GP-A** using 4-methylbenzaldehyde (1.18 mL, 10.0 mmol, 1.00 equiv), ethyl chloroacetate (1.39 mL, 13.0 mmol, 1.30 equiv),  $\text{TiCl}_4$  (1.54 mL, 14.0 mmol, 1.40 equiv),  $\text{NEt}_3$  (6.93 mL, 50.0 mmol, 5.00 equiv) gave ethyl (Z)-2-chloro-3-(*p*-tolyl)acrylate (1.40 g, 6.23 mmol, 62%) as yellow oil after purification on  $\text{SiO}_2$  (hexanes / EA, 15:1).

$R_f$  (hexanes / EA, 10:1) = 0.44;  **$^1\text{H-NMR}$**  (400 MHz,  $\text{CDCl}_3$ ):  $\delta$  7.88 (s, 1H), 7.76 (d,  $J = 8.2$  Hz, 2H), 7.24 (d,  $J = 8.1$  Hz, 2H), 4.35 (q,  $J = 7.1$  Hz, 2H), 2.39 (s, 3H), 1.39 (t,  $J = 7.1$  Hz,

3H);  $^{13}\text{C-NMR}$  (101 MHz,  $\text{CDCl}_3$ ):  $\delta$  163.60, 140.75, 136.92, 130.76, 130.24, 129.31, 121.23, 62.50, 21.56, 14.27.

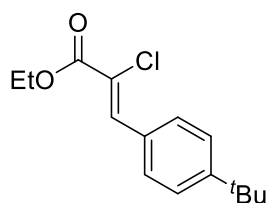
**ethyl (Z)-2-chloro-3-(*o*-tolyl)acrylate (228m)**



Following general procedure **GP-A** using 2-methylbenzaldehyde (1.16 mL, 10.0 mmol, 1.00 equiv), ethyl chloroacetate (1.39 mL, 13.0 mmol, 1.30 equiv),  $\text{TiCl}_4$  (1.54 mL, 14.0 mmol, 1.40 equiv),  $\text{NEt}_3$  (6.93 mL, 50.0 mmol, 5.00 equiv) gave ethyl (Z)-2-chloro-3-(*o*-tolyl)acrylate (1.83 g, 8.14 mmol, 82%) as colorless oil after purification on  $\text{SiO}_2$  (hexanes / EA, 15:1).

$R_f$  (hexanes / EA, 10:1) = 0.47; **IR** (neat): 3063, 2981, 1718, 1617, 1483, 1367, 1237, 1039, 1095, 998, 883, 863, 805, 764, 663  $\text{cm}^{-1}$ ;  $^1\text{H-NMR}$  (300 MHz,  $\text{CDCl}_3$ ):  $\delta$  8.05 (s, 1H), 7.79 – 7.73 (m, 1H), 7.31 – 7.22 (m, 3H), 4.37 (q,  $J = 7.1$  Hz, 2H), 2.35 (s, 3H), 1.40 (t,  $J = 7.1$  Hz, 3H);  $^{13}\text{C-NMR}$  (75 MHz,  $\text{CDCl}_3$ ):  $\delta$  163.28, 137.54, 136.15, 132.27, 130.23, 129.55, 129.02, 125.69, 123.89, 62.61, 20.01, 14.24; **HRMS** (EI)  $m/z$  calculated for  $\text{C}_{12}\text{H}_{13}\text{O}_2\text{Cl}$  ( $[\text{M}]^+$ ) 224.0599, found 224.0598.

**ethyl (Z)-3-(4-(*tert*-butyl)phenyl)-2-chloroacrylate (228n)**

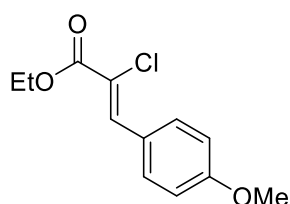


Following general procedure **GP-A** using 4-(*tert*-butyl)benzaldehyde (900  $\mu\text{L}$ , 5.38 mmol, 1.00 equiv), ethyl chloroacetate (745  $\mu\text{L}$ , 7.00 mmol, 1.30 equiv),  $\text{TiCl}_4$  (831  $\mu\text{L}$ , 14.0 mmol, 1.40 equiv),  $\text{NEt}_3$  (3.73 mL, 27.0 mmol, 5.00 equiv) gave ethyl (Z)-3-(4-(*tert*-butyl)phenyl)-2-

chloroacrylate (735 mg, 2.76 mmol, 51%) as yellow oil after purification on SiO<sub>2</sub> (hexanes / EA, 15:1).

**R<sub>f</sub>** (hexanes / EA, 10:1) = 0.42; **<sup>1</sup>H-NMR** (300 MHz, CDCl<sub>3</sub>): δ 7.89 (s, 1H), 7.84 – 7.79 (m, 2H), 7.48 – 7.43 (m, 2H), 4.35 (q, *J* = 7.1 Hz, 2H), 1.39 (t, *J* = 7.1 Hz, 3H), 1.34 (s, 9H); **<sup>13</sup>C-NMR** (101 MHz, CDCl<sub>3</sub>): δ 163.62, 153.80, 136.80, 130.65, 130.22, 125.56, 121.33, 62.51, 34.96, 31.14, 14.27.

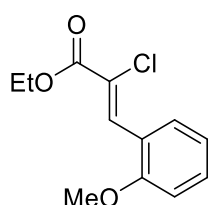
**ethyl (Z)-2-chloro-3-(4-methoxyphenyl)acrylate (228o)**



Following general procedure **GP-A** using 4-methoxybenzaldehyde (1.22 mL, 10.0 mmol, 1.00 equiv), ethyl chloroacetate (1.39 mL, 13.0 mmol, 1.30 equiv), TiCl<sub>4</sub> (1.54 mL, 14.0 mmol, 1.40 equiv), NEt<sub>3</sub> (2.77 mL, 20.0 mmol, 2.00 equiv) gave ethyl (Z)-2-chloro-3-(4-methoxyphenyl)acrylate (2.19 g, 9.10 mmol, 91%) as colorless oil after purification on SiO<sub>2</sub> (hexanes / EA, 15:1).

**R<sub>f</sub>** (hexanes / EA, 10:1) = 0.30; **<sup>1</sup>H-NMR** (300 MHz, CDCl<sub>3</sub>): δ 7.90 – 7.84 (m, 3H), 6.97 – 6.92 (m, 2H), 4.34 (q, *J* = 7.1 Hz, 2H), 3.86 (s, 3H), 1.38 (t, *J* = 7.1 Hz, 3H); **<sup>13</sup>C-NMR** (75 MHz, CDCl<sub>3</sub>): δ 163.77, 161.10, 136.51, 132.72, 125.65, 119.64, 114.01, 62.43, 55.40, 14.29.

**ethyl (Z)-2-chloro-3-(2-methoxyphenyl)acrylate (228p)**

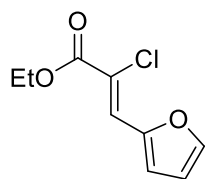


Following general procedure **GP-A** using 2-methoxybenzaldehyde (1.20 mL, 10.0 mmol, 1.00 equiv), ethyl chloroacetate (1.39 mL, 13.0 mmol, 1.30 equiv), TiCl<sub>4</sub> (1.54 mL,

14.0 mmol, 1.40 equiv),  $\text{NEt}_3$  (6.93 mL, 50.0 mmol, 5.00 equiv) gave ethyl (*Z*)-2-chloro-3-(2-methoxyphenyl)acrylate (1.66 g, 6.90 mmol, 69%) as yellowish oil after purification on  $\text{SiO}_2$  (hexanes / EA, 15:1).

$R_f$  (hexanes / EA, 10:1) = 0.30; **IR** (neat): 3056, 2981, 2940, 2840, 1714, 1599, 1483, 1394, 1367, 1233, 1192, 1110, 1025, 883, 849, 797, 752, 674  $\text{cm}^{-1}$ ;  **$^1\text{H-NMR}$**  (300 MHz,  $\text{CDCl}_3$ ):  $\delta$  8.24 (s, 1H), 8.08 (dd,  $J = 7.8, 1.5$  Hz, 1H), 7.42 – 7.35 (m, 1H), 7.04 – 6.99 (m, 1H), 6.94 – 6.91 (d,  $J = 8.3$  Hz, 1H), 4.36 (q,  $J = 7.1$  Hz, 2H), 3.88 (s, 3H), 1.39 (t,  $J = 7.1$  Hz, 3H);  **$^{13}\text{C-NMR}$**  (75 MHz,  $\text{CDCl}_3$ ):  $\delta$  163.57, 157.96, 132.09, 131.49, 130.17, 122.48, 122.01, 120.22, 110.53, 62.46, 55.62, 14.27; **HRMS** (EI)  $m/z$  calculated for  $\text{C}_{12}\text{H}_{13}\text{O}_3\text{Cl}$  ( $[\text{M}]^+$ ) 240.0547, found 240.0553.

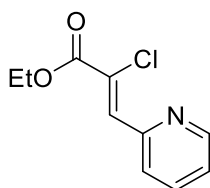
#### ethyl (*Z*)-2-chloro-3-(furan-2-yl)acrylate (228r)



Following general procedure **GP-A** using furan-2-carbaldehyde (828  $\mu\text{L}$ , 10.0 mmol, 1.00 equiv), ethyl chloroacetate (1.39 mL, 13.0 mmol, 1.30 equiv),  $\text{TiCl}_4$  (1.54 mL, 14.0 mmol, 1.40 equiv),  $\text{NEt}_3$  (6.93 mL, 50.0 mmol, 5.00 equiv) gave ethyl (*Z*)-2-chloro-3-(furan-2-yl)acrylate (1.18 g, 5.88 mmol, 59%) as yellow solid after purification on  $\text{SiO}_2$  (hexanes / EA, 15:1).

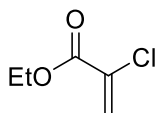
$R_f$  (hexanes / EA, 10:1) = 0.44;  **$^1\text{H-NMR}$**  (300 MHz,  $\text{CDCl}_3$ ):  $\delta$  7.83 (s, 1H), 7.58 (dd,  $J = 1.7, 0.6$  Hz, 1H), 7.28 (d,  $J = 3.6$  Hz, 1H), 6.57 (ddd,  $J = 3.6, 1.7, 0.6$  Hz, 1H), 4.33 (q,  $J = 7.1$  Hz, 2H), 1.36 (t,  $J = 7.1$  Hz, 3H);  **$^{13}\text{C-NMR}$**  (75 MHz,  $\text{CDCl}_3$ ):  $\delta$  163.05, 149.31, 144.84, 125.42, 119.18, 116.83, 112.72, 62.49, 14.24.



**ethyl (Z)-2-chloro-3-(pyridin-2-yl)acrylate (228s)**

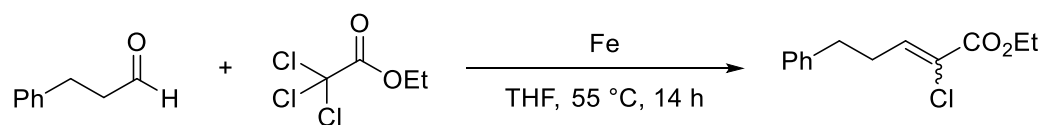
Following general procedure **GP-A** using picolinaldehyde (948  $\mu\text{L}$ , 10.0 mmol, 1.00 equiv), ethyl chloroacetate (1.39 mL, 13.0 mmol, 1.30 equiv),  $\text{TiCl}_4$  (1.54 mL, 14.0 mmol, 1.40 equiv),  $\text{NEt}_3$  (6.93 mL, 50.0 mmol, 5.00 equiv) gave ethyl (Z)-2-chloro-3-(pyridin-2-yl)acrylate (50.0 mg, 236  $\mu\text{mol}$ , 3%) as dark brown oil after purification on  $\text{SiO}_2$  (hexanes / EA, 15:1).

$R_f$  (hexanes / EA, 10:1) = 0.10;  $^1\text{H-NMR}$  (300 MHz,  $\text{CDCl}_3$ ):  $\delta$  8.54 – 8.50 (m, 1H), 7.66 (td,  $J = 7.7, 1.8$  Hz, 1H), 7.24 – 7.17 (m, 2H), 6.95 (s, 1H), 4.32 (q,  $J = 7.1$  Hz, 2H), 1.29 (t,  $J = 7.1$  Hz, 3H);  $^{13}\text{C-NMR}$  (75 MHz,  $\text{CDCl}_3$ ):  $\delta$  164.53, 151.90, 149.20, 136.61, 131.15, 123.47, 123.08, 62.18, 13.84.

**ethyl 2-chloroacrylate (228t)**

A 500 mL flask equipped with a magnetic stir bar was charged with ethyl acrylate (5.44 mL, 50.0 mmol, 1.00 equiv), *OXONE*<sup>®</sup> (36.9 g, 60.0 mmol, 1.20 equiv),  $\text{NH}_4\text{Cl}$  (5.88 g, 110 mmol, 2.20 equiv) and MeCN (250 mL). The reaction mixture was stirred for 24 h at room temperature before  $\text{NEt}_3$  (34.7 mL, 250 mmol, 5.00 equiv) was cautiously added. After stirring for additional 24 h, MeCN was evaporated and the residue was dissolved in DCM (250 mL) and washed with  $\text{H}_2\text{O}$  (250 mL) and brine (250 mL). The pure product (202 mg, 1.50 mmol, 3%) was obtained by distillation under reduced pressure as colorless liquid (55  $^\circ\text{C}$  / 25 mbar).

$^1\text{H-NMR}$  (300 MHz,  $\text{CDCl}_3$ ):  $\delta$  6.52 (d,  $J = 1.4$  Hz, 1H), 6.00 (d,  $J = 1.4$  Hz, 1H), 4.29 (q,  $J = 7.1$  Hz, 2H), 1.34 (t,  $J = 7.1$  Hz, 3H);  $^{13}\text{C-NMR}$  (75 MHz,  $\text{CDCl}_3$ ):  $\delta$  161.98, 131.68, 125.59, 62.60, 14.11.

**ethyl 2-chloro-5-phenylpent-2-enoate (228u)**

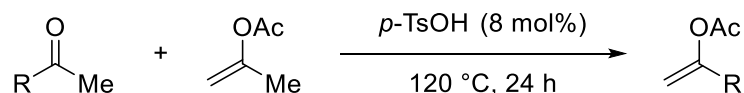
Preparation *via* **GP-A** failed. The title compound was thus synthesized in a Fe(0)-mediated synthesis.<sup>[198]</sup>

A flame dried 250 mL two-neck-flask equipped with a magnetic stir bar and a reflux condenser was charged with 3-phenylpropanal (1.33 mL, 10.0 mmol, 1.00 equiv), ethyl 2,2,2-trichloroacetate (1.51 mL, 11.0 mmol, 1.10 equiv) and Fe powder (5.58 g, 100 mmol, 10.0 equiv) and dry THF (100 mL) under nitrogen atmosphere. The reaction mixture was heated to 55 °C for 14 h. Upon completion, the reaction was filtered at room temperature, and the crude product was purified by column chromatography on SiO<sub>2</sub> (hexanes / EA, 15:1) to obtain ethyl 2-chloro-5-phenylpent-2-enoate as a mixture of *E/Z* = 15:85 as colorless oil (1.02 g, 4.27 mmol, 43%).

**R<sub>f</sub>** (hexanes / EA, 10:1) = 0.40; **<sup>1</sup>H-NMR** (300 MHz, CDCl<sub>3</sub>, *Z* Isomer): δ 7.34 – 7.27 (m, 2H), 7.25 – 7.18 (m, 3H), 7.10 (t, *J* = 7.1 Hz, 1H), 4.27 (q, *J* = 7.1 Hz, 2H), 2.84 – 2.78 (m, 2H), 2.72 – 2.64 (m, 2H), 1.33 (t, *J* = 7.1 Hz, 3H); **<sup>1</sup>H-NMR** (300 MHz, CDCl<sub>3</sub>, *E* Isomer): δ 7.34 – 7.27 (m, 2H), 7.25 – 7.18 (m, 3H), 6.47 (t, *J* = 7.1 Hz, 1H), 4.27 (q, *J* = 7.1 Hz, 2H), 2.93 – 2.85 (m, 2H), 2.84 – 2.78 (m, 2H), 1.34 (t, *J* = 7.1 Hz, 3H); **<sup>13</sup>C-NMR** (75 MHz, CDCl<sub>3</sub>, *Z* Isomer): δ 162.46, 143.59, 141.08, 140.56, 128.57, 128.32, 126.33, 125.32, 62.24, 33.70, 31.07, 14.18.

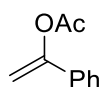
## 4 Synthesis of enol acetates (152a – 152m)

### General procedure (GP-B) for the synthesis of enol acetates<sup>[200]</sup>



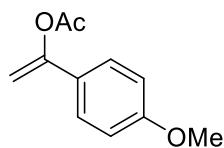
A 100 mL flask equipped with a magnetic stir bar, a reflux condenser and a drying tube was charged with ketone (50.0 mmol, 1.00 equiv), isopropenyl acetate (250 mmol, 5.00 equiv) and *p*-TsOH·H<sub>2</sub>O (4.00 mmol, 0.08 equiv). The reaction mixture was heated to 120 °C. After 24 h the reaction mixture was allowed to cool to room temperature and the remaining isopropenyl acetate was subsequently evaporated under reduced pressure. The residue was redissolved in Et<sub>2</sub>O (100 mL) and the resulting solution was washed with H<sub>2</sub>O (3 x 50 mL) and dried over Na<sub>2</sub>SO<sub>4</sub>. The solvent was evaporated *in vacuo* to give a dark red oil. The pure product was obtained by distillation under reduced pressure or by purification on SiO<sub>2</sub> (DCM / hexanes).

### 1-phenylvinyl acetate (152a)



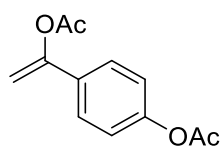
Following general procedure **GP-B** using acetophenone (5.83 mL, 50.0 mmol, 1.00 equiv), isopropenyl acetate (27.2 mL, 250 mmol, 5.00 equiv) and *p*-TsOH·H<sub>2</sub>O (761 mg, 4.00 mmol, 0.08 equiv) gave 1-phenylvinyl acetate (4.70 g, 29.0 mmol, 58%) as colorless oil after distillation under reduced pressure (88 °C / 5.6 mbar).

<sup>1</sup>H-NMR (300 MHz, CDCl<sub>3</sub>): δ 7.48 – 7.46 (m, 2H), 7.38 – 7.32 (m, 3H), 5.48 (d, *J* = 2.2 Hz, 1H), 5.03 (d, *J* = 2.1 Hz, 1H), 2.28 (s, 3H); <sup>13</sup>C-NMR (75 MHz, CDCl<sub>3</sub>): δ 169.08, 152.97, 134.28, 128.97, 128.54, 124.89, 102.15, 20.99.

**1-(4-methoxyphenyl)vinyl acetate (152b)**

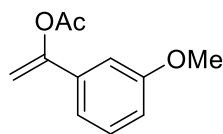
Following general procedure **GP-B** using 1-(4-methoxyphenyl)ethan-1-one (7.51 g, 50.0 mmol, 1.00 equiv), isopropenyl acetate (27.2 mL, 250 mmol, 5.00 equiv) and *p*-TsOH·H<sub>2</sub>O (761 mg, 4.00 mmol, 0.08 equiv) gave 1-(4-methoxyphenyl)vinyl acetate (2.34 g, 12.2 mmol, 25%) as white solid after distillation under reduced pressure (97 °C / 0.9 mbar).

**<sup>1</sup>H-NMR** (300 MHz, CDCl<sub>3</sub>): δ 7.44 – 7.37 (m, 2H), 6.90 – 6.84 (m, 2H), 5.36 (d, *J* = 2.2 Hz, 1H), 4.92 (d, *J* = 2.2 Hz, 1H), 3.81 (s, 3H), 2.27 (s, 3H); **<sup>13</sup>C-NMR** (75 MHz, CDCl<sub>3</sub>): δ 169.21, 160.18, 152.73, 126.84, 126.30, 113.92, 100.30, 55.33, 21.03.

**1-(4-acetoxyphenyl)vinyl acetate (152c)**

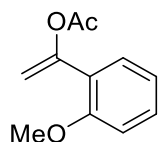
Following general procedure **GP-B** using 1-(4-hydroxyphenyl)ethan-1-one (2.72 g, 20.0 mmol, 1.00 equiv), isopropenyl acetate (13.1 mL, 120 mmol, 6.00 equiv) and *p*-TsOH·H<sub>2</sub>O (304 mg, 1.60 mmol, 0.08 equiv) gave 1-(4-acetoxyphenyl)vinyl acetate (2.01 g, 9.13 mmol, 46%) as white solid after purification on SiO<sub>2</sub> (DCM / hexanes, 1:1).

**R<sub>f</sub>** (hexanes / EA, 6:1) = 0.28; **IR** (neat): 3049, 2926, 2855, 1755, 1643, 1602, 1505, 1367, 1267, 1189, 1088, 1043, 1013, 961, 909, 887, 849, 812 cm<sup>-1</sup>; **<sup>1</sup>H-NMR** (300 MHz, CDCl<sub>3</sub>): δ 7.50 – 7.45 (m, 2H), 7.11 – 7.06 (m, 2H), 5.45 (d, *J* = 2.3 Hz, 1H), 5.03 (d, *J* = 2.3 Hz, 1H), 2.30 (s, 3H), 2.28 (s, 3H); **<sup>13</sup>C-NMR** (75 MHz, CDCl<sub>3</sub>): δ 169.27, 169.02, 152.14, 151.10, 132.06, 126.14, 121.72, 102.43, 21.17, 21.02; **HRMS** (EI) *m/z* calculated for C<sub>12</sub>H<sub>12</sub>O<sub>4</sub> ([M]<sup>+</sup>) 220.0730, found 220.0735.

**1-(3-methoxyphenyl)vinyl acetate (152d)**

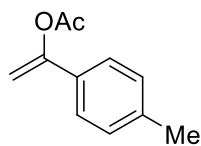
Following general procedure **GP-B** using 1-(3-methoxyphenyl)ethan-1-one (7.51 g, 50.0 mmol, 1.00 equiv), isopropenyl acetate (27.2 mL, 250 mmol, 5.00 equiv) and *p*-TsOH·H<sub>2</sub>O (761 mg, 4.00 mmol, 0.08 equiv) gave 1-(3-methoxyphenyl)vinyl acetate (4.77 g, 24.8 mmol, 50%) as colorless oil after distillation under reduced pressure (110 °C / 2.5 mbar).

**<sup>1</sup>H-NMR** (400 MHz, CDCl<sub>3</sub>): δ 7.27 (t, *J* = 8.0 Hz, 1H), 7.07 (d, *J* = 7.8 Hz, 1H), 7.00 – 6.99 (m, 1H), 6.88 (dd, *J* = 8.2, 2.3 Hz, 1H), 5.47 (d, *J* = 2.1 Hz, 1H), 5.03 (d, *J* = 2.0 Hz, 1H), 3.82 (s, 3H), 2.28 (s, 3H); **<sup>13</sup>C-NMR** (101 MHz, CDCl<sub>3</sub>): δ 169.08, 159.72, 152.77, 135.76, 129.63, 117.45, 114.29, 110.85, 102.48, 55.31, 21.00.

**1-(2-methoxyphenyl)vinyl acetate (152e)**

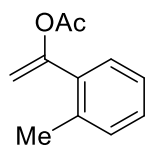
Following general procedure **GP-B** using 1-(2-methoxyphenyl)ethan-1-one (7.51 g, 50.0 mmol, 1.00 equiv), isopropenyl acetate (27.2 mL, 250 mmol, 5.00 equiv) and *p*-TsOH·H<sub>2</sub>O (761 mg, 4.00 mmol, 0.08 equiv) gave 1-(2-methoxyphenyl)vinyl acetate (5.60 g, 29.1 mmol, 58%) as colorless oil after purification on SiO<sub>2</sub> (DCM / hexanes, 1:1).

**R<sub>f</sub>** (DCM) = 0.54; **IR** (neat): 3004, 2940, 2840, 1755, 1636, 1599, 1490, 1461, 1435, 1367, 1282, 1244, 1192, 1125, 1073, 1017, 961, 887, 812, 752, 704 cm<sup>-1</sup>; **<sup>1</sup>H-NMR** (400 MHz, CDCl<sub>3</sub>): δ 7.35 (dd, *J* = 7.6, 1.7 Hz, 1H), 7.32 – 7.27 (m, 1H), 6.96 – 6.91 (m, 2H), 5.59 (d, *J* = 1.3 Hz, 1H), 5.15 (d, *J* = 1.3 Hz, 1H), 3.87 (s, 3H), 2.21 (s, 3H); **<sup>13</sup>C-NMR** (101 MHz, CDCl<sub>3</sub>): δ 169.08, 157.04, 150.27, 129.98, 128.46, 123.44, 120.47, 111.28, 106.59, 55.58, 21.01; **HRMS** (EI) *m/z* calculated for C<sub>11</sub>H<sub>12</sub>O<sub>3</sub> ([M]<sup>+</sup>) 192.0781, found 192.0785.

**1-(*p*-tolyl)vinyl acetate (152f)**

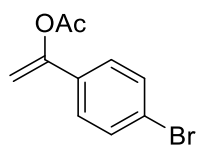
Following general procedure **GP-B** using 1-(*p*-tolyl)ethan-1-one (6.71 g, 50.0 mmol, 1.00 equiv), isopropenyl acetate (27.2 mL, 250 mmol, 5.00 equiv) and *p*-TsOH·H<sub>2</sub>O (761 mg, 4.00 mmol, 0.08 equiv) gave 1-(*p*-tolyl)vinyl acetate (2.08 g, 11.8 mmol, 24%) as white solid after distillation under reduced pressure (83 °C / 1.6 mbar).

<sup>1</sup>H-NMR (300 MHz, CDCl<sub>3</sub>): δ 7.37 – 7.34 (m, 2H), 7.17 – 7.14 (m, 2H), 5.43 (d, *J* = 2.1 Hz, 1H), 4.97 (d, *J* = 2.1 Hz, 1H), 2.35 (s, 3H), 2.28 (s, 3H); <sup>13</sup>C-NMR (75 MHz, CDCl<sub>3</sub>): δ 169.18, 153.03, 139.00, 131.43, 129.25, 124.79, 101.26, 21.26, 21.03.

**1-(*o*-tolyl)vinyl acetate (152g)**

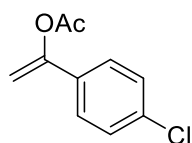
Following general procedure **GP-B** using 1-(*o*-tolyl)ethan-1-one (4.63 g, 34.5 mmol, 1.00 equiv), isopropenyl acetate (18.8 mL, 173 mmol, 5.00 equiv) and *p*-TsOH·H<sub>2</sub>O (525 mg, 2.76 mmol, 0.08 equiv) gave 1-(*o*-tolyl)vinyl acetate (1.20 g, 6.81 mmol, 20%) as colorless oil after distillation under reduced pressure (73 °C / 2.7 mbar).

<sup>1</sup>H-NMR (300 MHz, CDCl<sub>3</sub>): δ 7.40 – 7.36 (m, 1H), 7.27 – 7.15 (m, 3H), 5.19 (d, *J* = 1.5 Hz, 1H), 5.03 (d, *J* = 1.5 Hz, 1H), 2.42 (s, 3H), 2.15 (s, 3H); <sup>13</sup>C-NMR (75 MHz, CDCl<sub>3</sub>): δ 168.85, 153.80, 135.95, 135.38, 130.48, 129.10, 128.79, 125.67, 105.73, 21.05, 20.36.

**1-(4-bromophenyl)vinyl acetate (152h)**

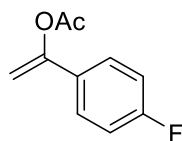
Following general procedure **GP-B** using 1-(4-bromophenyl)ethan-1-one (9.95 g, 50.0 mmol, 1.00 equiv), isopropenyl acetate (27.2 mL, 250 mmol, 5.00 equiv) and *p*-TsOH·H<sub>2</sub>O (761 mg, 4.00 mmol, 0.08 equiv) gave 1-(4-bromophenyl)vinyl acetate (7.56 g, 31.4 mmol, 63%) as slightly yellow solid after purification on SiO<sub>2</sub> (DCM / hexanes, 1:1).

**R<sub>f</sub>** (DCM / hexanes, 1:1) = 0.26; **<sup>1</sup>H-NMR** (400 MHz, CDCl<sub>3</sub>): δ 7.49 – 7.46 (m, 2H), 7.35 – 7.31 (m, 2H), 5.47 (d, *J* = 2.4 Hz, 1H), 5.06 (d, *J* = 2.4 Hz, 1H), 2.27 (s, 3H); **<sup>13</sup>C-NMR** (101 MHz, CDCl<sub>3</sub>): δ 168.96, 152.04, 133.35, 131.74, 126.51, 123.10, 102.81, 20.98.

**1-(4-chlorophenyl)vinyl acetate (152i)**

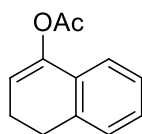
Following general procedure **GP-B** using 1-(4-chlorophenyl)ethan-1-one (6.48 mL, 50.0 mmol, 1.00 equiv), isopropenyl acetate (27.2 mL, 250 mmol, 5.00 equiv) and *p*-TsOH·H<sub>2</sub>O (761 mg, 4.00 mmol, 0.08 equiv) gave 1-(4-chlorophenyl)vinyl acetate (2.61 g, 13.3 mmol, 27%) as colorless oil after distillation under reduced pressure (95 °C / 3.0 mbar).

**<sup>1</sup>H-NMR** (300 MHz, CDCl<sub>3</sub>): δ 7.41 – 7.37 (m, 2H), 7.34 – 7.29 (m, 2H), 5.46 (d, *J* = 2.4 Hz, 1H), 5.05 (d, *J* = 2.4 Hz, 1H), 2.28 (s, 3H); **<sup>13</sup>C-NMR** (75 MHz, CDCl<sub>3</sub>): δ 169.01, 151.95, 134.86, 132.83, 128.78, 126.22, 102.74, 20.99.

**1-(4-fluorophenyl)vinyl acetate (152j)**

Following general procedure **GP-B** using 1-(4-fluorophenyl)ethan-1-one (2.42 mL, 20.0 mmol, 1.00 equiv), isopropenyl acetate (10.9 mL, 100 mmol, 5.00 equiv) and *p*-TsOH·H<sub>2</sub>O (304 mg, 1.60 mmol, 0.08 equiv) gave 1-(4-fluorophenyl)vinyl acetate (1.00 g, 5.55 mmol, 28%) as yellow oil after purification on SiO<sub>2</sub> (DCM / hexanes, 1:1).

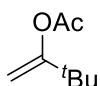
**R<sub>f</sub>** (hexanes / EA, 10:1) = 0.30; **<sup>1</sup>H-NMR** (300 MHz, CDCl<sub>3</sub>): δ 7.48 – 7.41 (m, 2H), 7.08 – 7.00 (m, 2H), 5.41 (d, *J* = 2.3 Hz, 1H), 5.01 (d, *J* = 2.3 Hz, 1H), 2.28 (s, 3H); **<sup>13</sup>C-NMR** (75 MHz, CDCl<sub>3</sub>): δ 169.08, 164.75, 161.45, 152.05, 130.54, 130.49, 126.87, 126.76, 115.72, 115.43, 102.06, 102.04, 21.02; **<sup>19</sup>F-NMR** (282 MHz, CDCl<sub>3</sub>): δ -112.80.

**3,4-dihydronaphthalen-1-yl acetate (152k)**

Following general procedure **GP-B** using 3,4-dihydronaphthalen-1(2H)-one (7.24 mL, 50.0 mmol, 1.00 equiv), isopropenyl acetate (27.2 mL, 250 mmol, 5.00 equiv) and *p*-TsOH·H<sub>2</sub>O (761 mg, 4.00 mmol, 0.08 equiv) gave 3,4-dihydronaphthalen-1-yl acetate (8.23 g, 43.7 mmol, 88%) as yellow solid after purification on SiO<sub>2</sub> (DCM / hexanes, 2:1).

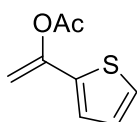
**R<sub>f</sub>** (DCM / hexanes, 2:1) = 0.42; **<sup>1</sup>H-NMR** (300 MHz, CDCl<sub>3</sub>): δ 7.20 – 7.14 (m, 3H), 7.11 – 7.07 (m, 1H), 5.71 (t, *J* = 4.7 Hz, 1H), 2.87 (t, *J* = 8.1 Hz, 2H), 2.50 – 2.41 (m, 2H), 2.30 (s, 3H); **<sup>13</sup>C-NMR** (75 MHz, CDCl<sub>3</sub>): δ 169.29, 145.61, 136.41, 130.41, 127.94, 127.61, 126.39, 120.70, 115.52, 27.45, 22.04, 20.92.



**3,3-dimethylbut-1-en-2-yl acetate (152l)**

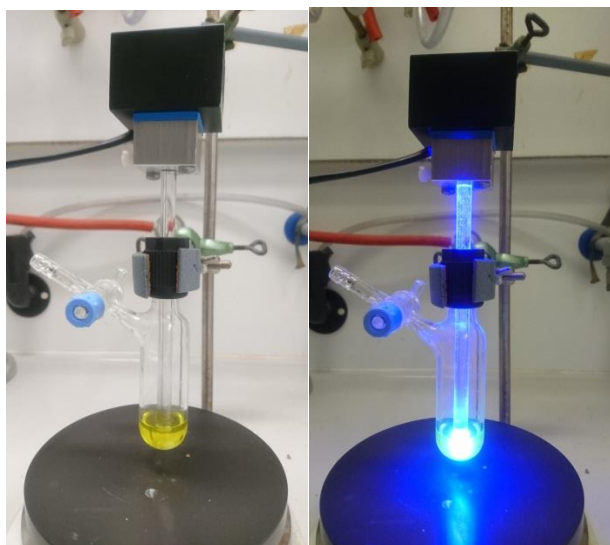
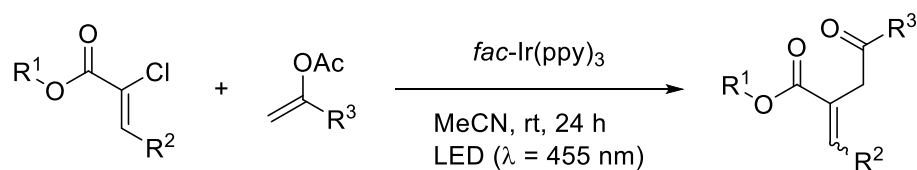
Following general procedure **GP-B** using 3,3-dimethylbutan-2-one (6.26 mL, 50.0 mmol, 1.00 equiv), isopropenyl acetate (27.2 mL, 250 mmol, 5.00 equiv) and *p*-TsOH·H<sub>2</sub>O (761 mg, 4.00 mmol, 0.08 equiv) gave 3,3-dimethylbut-1-en-2-yl acetate (3.18 g, 22.4 mmol, 45%) as colorless oil after distillation under reduced pressure (45 °C / 100 mbar).

<sup>1</sup>H-NMR (300 MHz, CDCl<sub>3</sub>): δ 4.87 (d, *J* = 2.0 Hz, 1H), 4.63 (d, *J* = 2.0 Hz, 1H), 2.17 (s, 3H), 1.09 (s, 9H); <sup>13</sup>C-NMR (75 MHz, CDCl<sub>3</sub>): δ 169.26, 162.58, 99.11, 36.07, 27.76, 21.12.

**1-(thiophen-2-yl)vinyl acetate (152m)**

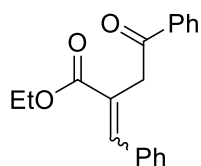
Following general procedure **GP-B** using 1-(thiophen-2-yl)ethan-1-one (5.39 mL, 50.0 mmol, 1.00 equiv), isopropenyl acetate (27.2 mL, 250 mmol, 5.00 equiv) and *p*-TsOH·H<sub>2</sub>O (761 mg, 4.00 mmol, 0.08 equiv) gave 1-(thiophen-2-yl)vinyl acetate (2.20 g, 13.1 mmol, 26%) as red oil after purification on SiO<sub>2</sub> (DCM / hexanes, 3:1 to pure DCM).

*R<sub>f</sub>* (hexanes / EA, 10:1) = 0.30; <sup>1</sup>H-NMR (300 MHz, CDCl<sub>3</sub>): δ 7.24 (dd, *J* = 5.0, 1.1 Hz, 1H), 7.10 (dd, *J* = 3.7, 1.2 Hz, 1H), 6.98 (dd, *J* = 5.0, 3.7 Hz, 1H), 5.39 (d, *J* = 2.5 Hz, 1H), 4.94 (d, *J* = 2.5 Hz, 1H), 2.28 (s, 3H); <sup>13</sup>C-NMR (75 MHz, CDCl<sub>3</sub>): δ 168.83, 147.70, 138.20, 127.51, 125.86, 124.72, 101.28, 20.95.

**5 Photochemical functionalization of  $\alpha$ -chloro cinnamates (229aa – 229ra)****General procedure (GP-C) for the photochemical functionalization of  $\alpha$ -chloro cinnamates**

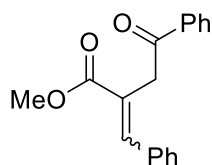
A flame dried Schlenk tube equipped with a magnetic stir bar was charged with  $\alpha$ -chloro cinnamate (500  $\mu\text{mol}$ , 1.00 equiv), enol acetate (2.50 mmol, 5.00 equiv) and *fac*-Ir(ppy)<sub>3</sub> (10.0  $\mu\text{mol}$ , 2.0 mol%). The flask was sealed with a plastic screw-cap, evacuated and backfilled with N<sub>2</sub> (3x). Dry MeCN (5 mL) was added and the reaction was magnetically stirred for roughly 5 min under N<sub>2</sub> atmosphere until a homogeneous solution was observed. The resulting mixture was degassed by freeze-pump-thaw (3 cycles) and the plastic screw-cap was replaced by another plastic screw-cap with a Teflon sealed inlet for a glass rod. A high power LED ( $\lambda = 455 \text{ nm}$ ) was attached to the top of the glass rod, which then could act as an optical fiber. After irradiation for 24 h the LED was removed, the solvent was evaporated *in vacuo* and the residue was directly purified by column chromatography on SiO<sub>2</sub> (hexanes / EA, 20:1 to 4:1) to obtain the separated *E* and *Z* isomers.

*Note: E and Z isomers were separated in all cases except for 229ma.*

**ethyl 2-benzylidene-4-oxo-4-phenylbutanoate (229aa)**

Following general procedure **GP-C** using ethyl (*Z*)-2-chloro-3-phenylacrylate (**228a-Cl**, 105 mg, 500  $\mu\text{mol}$ , 1.00 equiv), 1-phenylvinyl acetate (**152a**, 405 mg, 2.50 mmol, 5.00 equiv) and *fac*-Ir(ppy)<sub>3</sub> (6.55 mg, 10.0  $\mu\text{mol}$ , 0.02 equiv) gave (*E*)-**229aa** (68.2 mg, 231  $\mu\text{mol}$ , 46%) and (*Z*)-**229aa** (76.9 mg, 260  $\mu\text{mol}$ , 52%) as colorless oils as separated *E* and *Z* isomers after purification on SiO<sub>2</sub> (hexanes / EA, 20:1 to 12:1). *E/Z* = 47:53.

**R<sub>f</sub>** (hexanes / EA, 10:1) = 0.30 (*E* Isomer), 0.27 (*Z* Isomer); **IR** (neat): 3060, 3026, 2981, 2937, 2903, 1684, 1595, 1448, 1401, 1334, 1211, 1125, 1021, 991, 924, 842, 745, 693  $\text{cm}^{-1}$ ; **<sup>1</sup>H-NMR** (300 MHz, CDCl<sub>3</sub>, *E* Isomer):  $\delta$  8.04 – 7.98 (m, 3H), 7.63 – 7.55 (tt, *J* = 7.5, 1.3 Hz, 1H), 7.52 – 7.44 (m, 2H), 7.40 – 7.27 (m, 5H), 4.24 (q, *J* = 7.1 Hz, 2H), 4.20 (d, *J* = 0.4 Hz, 2H), 1.27 (t, *J* = 7.1 Hz, 3H); **<sup>13</sup>C-NMR** (75 MHz, CDCl<sub>3</sub>, *E* Isomer):  $\delta$  197.53, 167.47, 142.03, 136.71, 135.35, 133.27, 128.78, 128.74, 128.66, 128.62, 128.30, 127.37, 61.16, 38.05, 14.20; **<sup>1</sup>H-NMR** (300 MHz, CDCl<sub>3</sub>, *Z* Isomer):  $\delta$  8.03 – 8.00 (m, 2H), 7.63 – 7.55 (tt, *J* = 7.3, 1.3 Hz, 1H), 7.53 – 7.44 (m, 2H), 7.32 – 7.27 (m, 5H), 6.90 (s, 1H), 4.16 (d, *J* = 1.2 Hz, 2H), 4.10 (q, *J* = 7.1 Hz, 2H), 1.04 (t, *J* = 7.1 Hz, 3H); **<sup>13</sup>C-NMR** (75 MHz, CDCl<sub>3</sub>, *Z* Isomer):  $\delta$  197.07, 168.08, 139.38, 136.44, 135.94, 133.36, 128.70, 128.64, 128.30, 128.06, 127.90, 127.87, 60.78, 45.03, 13.63; **HRMS** (ESI) *m/z* calculated for C<sub>19</sub>H<sub>19</sub>O<sub>3</sub> ([M+H]<sup>+</sup>) 295.1329, found 295.1331.

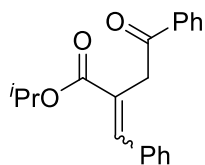
**methyl 2-benzylidene-4-oxo-4-phenylbutanoate (229ba)**

Following general procedure **GP-C** using methyl (*Z*)-2-chloro-3-phenylacrylate (**228b**, 98.3 mg, 500  $\mu\text{mol}$ , 1.00 equiv), 1-phenylvinyl acetate (**152a**, 405 mg, 2.50 mmol, 5.00 equiv) and *fac*-Ir(ppy)<sub>3</sub> (6.55 mg, 10.0  $\mu\text{mol}$ , 0.02 equiv) gave (*E*)-**229ba** (55.4 mg,

197  $\mu\text{mol}$ , 40%) and (*Z*)-**229ba** (67.6 mg, 241  $\mu\text{mol}$ , 48%) as yellowish oils as separated *E* and *Z* isomers after purification on  $\text{SiO}_2$  (hexanes / EA, 20:1 to 8:1). *E/Z* = 45:55.

**R<sub>f</sub>** (hexanes / EA, 6:1) = 0.28 (*E* Isomer), 0.21 (*Z* Isomer); **IR** (neat): 3060, 3026, 2952, 1710, 1595, 1435, 1397, 1334, 1211, 1125, 998, 924, 834, 745, 689  $\text{cm}^{-1}$ ; **<sup>1</sup>H-NMR** (400 MHz,  $\text{CDCl}_3$ , *E* Isomer):  $\delta$  8.04 – 7.99 (m, 3H), 7.61 – 7.57 (m, 1H), 7.51 – 7.46 (m, 2H), 7.36 – 7.28 (m, 5H), 4.20 (s, 2H), 3.79 (s, 3H); **<sup>13</sup>C-NMR** (101 MHz,  $\text{CDCl}_3$ , *E* Isomer):  $\delta$  197.36, 167.98, 142.32, 136.68, 135.29, 133.31, 128.80, 128.79, 128.68, 128.64, 128.31, 127.05, 52.26, 38.13; **<sup>1</sup>H-NMR** (400 MHz,  $\text{CDCl}_3$ , *Z* Isomer):  $\delta$  8.03 – 7.99 (m, 2H), 7.61 – 7.57 (m, 1H), 7.51 – 7.46 (m, 2H), 7.34 – 7.28 (m, 5H), 6.89 (s, 1H), 4.16 (d, *J* = 1.0 Hz, 2H), 3.63 (s, 3H); **<sup>13</sup>C-NMR** (101 MHz,  $\text{CDCl}_3$ , *Z* Isomer):  $\delta$  196.96, 168.58, 139.52, 136.41, 135.78, 133.40, 128.72, 128.61, 128.29, 128.19, 128.01, 127.36, 51.70, 45.10; **HRMS** (ESI) *m/z* calculated for  $\text{C}_{18}\text{H}_{17}\text{O}_3$  ( $[\text{M}+\text{H}]^+$ ) 281.1172, found 281.1176.

#### *iso*-propyl 2-benzylidene-4-oxo-4-phenylbutanoate (**229ca**)

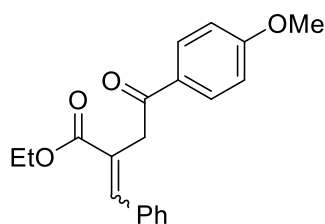


Following general procedure **GP-C** using *iso*-propyl (*Z*)-2-chloro-3-phenylacrylate (**228c**, 112 mg, 500  $\mu\text{mol}$ , 1.00 equiv), 1-phenylvinyl acetate (**152a**, 405 mg, 2.50 mmol, 5.00 equiv) and *fac*- $\text{Ir}(\text{ppy})_3$  (6.55 mg, 10.0  $\mu\text{mol}$ , 0.02 equiv) gave (*E*)-**229ca** (58.8 mg, 189  $\mu\text{mol}$ , 38%) and (*Z*)-**229ca** (66.3 mg, 214  $\mu\text{mol}$ , 43%) as colorless oils as separated *E* and *Z* isomers after purification on  $\text{SiO}_2$  (hexanes / EA, 20:1 to 8:1). *E/Z* = 47:53.

**R<sub>f</sub>** (hexanes / EA, 6:1) = 0.35 (*E* Isomer), 0.31 (*Z* Isomer); **IR** (neat): 3060, 3026, 2981, 2937, 1684, 1595, 1494, 1446, 1375, 1334, 1311, 1289, 1211, 1133, 1103, 995, 838, 745, 693  $\text{cm}^{-1}$ ; **<sup>1</sup>H-NMR** (400 MHz,  $\text{CDCl}_3$ , *E* Isomer):  $\delta$  8.01 – 8.00 (m, 3H), 7.58 (t, *J* = 7.4 Hz, 1H), 7.47 (t, *J* = 7.6 Hz, 2H), 7.37 – 7.28 (m, 5H), 5.11 (sept, *J* = 6.2 Hz, 1H), 4.18 (s, 2H), 1.25 (d, *J* = 6.3 Hz, 6H); **<sup>13</sup>C-NMR** (101 MHz,  $\text{CDCl}_3$ , *E* Isomer):  $\delta$  197.59, 166.92, 141.74, 136.87, 135.47, 133.20, 128.80, 128.68, 128.65, 128.61, 128.28, 127.89, 68.61, 38.01, 21.83; **<sup>1</sup>H-NMR** (400 MHz,  $\text{CDCl}_3$ , *Z* Isomer):  $\delta$  8.02 (d, *J* = 7.6 Hz, 2H), 7.59 (t, *J* = 7.4 Hz, 1H), 7.48 (t, *J* = 7.6 Hz, 2H), 7.32 – 7.27 (m, 5H), 6.88 (s, 1H), 4.99 (sept, *J* = 6.2 Hz, 1H), 4.14 (s,

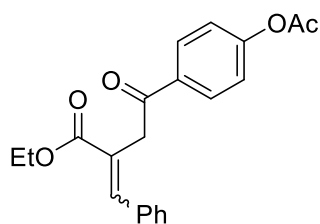
2H), 1.05 (d,  $J = 6.3$  Hz, 6H);  $^{13}\text{C-NMR}$  (101 MHz,  $\text{CDCl}_3$ , *Z* Isomer):  $\delta$  197.05, 167.53, 138.88, 136.58, 136.07, 133.29, 128.69, 128.68, 128.47, 128.31, 127.94, 127.87, 68.44, 45.07, 21.31; **HRMS** (ESI)  $m/z$  calculated for  $\text{C}_{20}\text{H}_{21}\text{O}_3$  ( $[\text{M}+\text{H}]^+$ ) 309.1485, found 309.1489.

**ethyl 2-benzylidene-4-(4-methoxyphenyl)-4-oxobutanoate (229ab)**



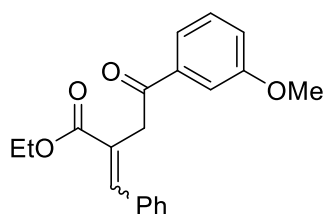
Following general procedure **GP-C** using ethyl (*Z*)-2-chloro-3-phenylacrylate (**228a-Cl**, 63.2 mg, 300  $\mu\text{mol}$ , 1.00 equiv), 1-(4-methoxyphenyl)vinyl acetate (**152b**, 288 mg, 1.50 mmol, 5.00 equiv) and *fac*- $\text{Ir}(\text{ppy})_3$  (3.93 mg, 6.00  $\mu\text{mol}$ , 0.02 equiv) gave (*E*)-**229ab** (40.7 mg, 126  $\mu\text{mol}$ , 42%) and (*Z*)-**229ab** (47.8 mg, 147  $\mu\text{mol}$ , 49%) as yellowish oils as separated *E* and *Z* isomers after purification on  $\text{SiO}_2$  (hexanes / EA, 20:1 to 6:1).  $E/Z = 46:54$ .

**R<sub>f</sub>** (hexanes / EA, 10:1) = 0.12 (*E* Isomer), 0.10 (*Z* Isomer); **IR** (neat): 3056, 2978, 2937, 2840, 1708, 1677, 1599, 1509, 1446, 1420, 1371, 1319, 1259, 1218, 1170, 1092, 1025, 931, 831, 760, 704  $\text{cm}^{-1}$ ;  $^1\text{H-NMR}$  (300 MHz,  $\text{CDCl}_3$ , *E* Isomer):  $\delta$  8.01 – 7.97 (m, 3H), 7.33 – 7.29 (m, 5H), 6.97 – 6.91 (m, 2H), 4.24 (q,  $J = 7.1$  Hz, 2H), 4.15 (s, 2H), 3.88 (s, 3H), 1.27 (t,  $J = 7.1$  Hz, 3H);  $^{13}\text{C-NMR}$  (75 MHz,  $\text{CDCl}_3$ , *E* Isomer):  $\delta$  195.99, 167.57, 163.61, 141.82, 135.41, 130.60, 129.76, 128.84, 128.69, 128.58, 127.60, 113.77, 61.11, 55.52, 37.66, 14.22;  $^1\text{H-NMR}$  (300 MHz,  $\text{CDCl}_3$ , *Z* Isomer):  $\delta$  8.02 – 7.98 (m, 2H), 7.32 – 7.28 (m, 5H), 6.97 – 6.93 (m, 2H), 6.88 (s, 1H), 4.14 – 4.06 (m, 4H), 3.87 (s, 3H), 1.03 (t,  $J = 7.1$  Hz, 3H);  $^{13}\text{C-NMR}$  (75 MHz,  $\text{CDCl}_3$ , *Z* Isomer):  $\delta$  195.58, 168.25, 163.67, 138.96, 136.02, 130.61, 129.48, 128.61, 128.22, 127.99, 127.88, 113.82, 60.75, 55.52, 44.69, 13.64; **HRMS** (ESI)  $m/z$  calculated for  $\text{C}_{20}\text{H}_{21}\text{O}_4$  ( $[\text{M}+\text{H}]^+$ ) 325.1434, found 325.1439.

**ethyl 4-(4-acetoxyphenyl)-2-benzylidene-4-oxobutanoate (229ac)**

Following general procedure **GP-C** using ethyl (*Z*)-2-chloro-3-phenylacrylate (**228a-Cl**, 105 mg, 500  $\mu\text{mol}$ , 1.00 equiv), 1-(4-acetoxyphenyl)vinyl acetate (**152c**, 551 mg, 2.50 mmol, 5.00 equiv) and *fac*-Ir(ppy)<sub>3</sub> (6.55 mg, 10.0  $\mu\text{mol}$ , 0.02 equiv) gave (*E*)-**229ac** (82.1 mg, 234  $\mu\text{mol}$ , 47%) and (*Z*)-**229ac** (88.9 mg, 252  $\mu\text{mol}$ , 50%) as yellowish oils as separated *E* and *Z* isomers after purification on SiO<sub>2</sub> (hexanes / EA, 20:1 to 6:1). *E/Z* = 48:52.

**R<sub>f</sub>** (hexanes / EA, 4:1) = 0.18 (*E* Isomer), 0.16 (*Z* Isomer); **IR** (neat): 3060, 3026, 2981, 2907, 1759, 1684, 1599, 1502, 1408, 1371, 1334, 1189, 1162, 1125, 995, 909, 849, 745, 697  $\text{cm}^{-1}$ ; **<sup>1</sup>H-NMR** (400 MHz, CDCl<sub>3</sub>, *E* Isomer):  $\delta$  8.06 – 8.01 (m, 3H), 7.35 – 7.28 (m, 5H), 7.22 – 7.18 (m, 2H), 4.24 (q, *J* = 7.1 Hz, 2H), 4.17 (s, 2H), 2.33 (s, 3H), 1.28 (t, *J* = 7.1 Hz, 3H); **<sup>13</sup>C-NMR** (101 MHz, CDCl<sub>3</sub>, *E* Isomer):  $\delta$  196.20, 168.89, 167.41, 154.48, 142.12, 135.31, 134.33, 129.94, 128.79, 128.76, 128.65, 127.21, 121.87, 61.17, 38.05, 21.18, 14.22; **<sup>1</sup>H-NMR** (300 MHz, CDCl<sub>3</sub>, *Z* Isomer):  $\delta$  8.08 – 8.03 (m, 2H), 7.33 – 7.28 (m, 5H), 7.25 – 7.21 (m, 2H), 6.90 (s, 1H), 4.14 – 4.06 (m, 4H), 2.34 (s, 3H), 1.04 (t, *J* = 7.1 Hz, 3H); **<sup>13</sup>C-NMR** (101 MHz, CDCl<sub>3</sub>, *Z* Isomer):  $\delta$  195.79, 168.83, 167.96, 154.54, 139.57, 135.91, 134.07, 129.95, 128.65, 128.08, 127.90, 127.67, 121.90, 60.80, 44.94, 21.19, 13.63; **HRMS** (ESI) *m/z* calculated for C<sub>21</sub>H<sub>21</sub>O<sub>5</sub> ([*M*+*H*]<sup>+</sup>) 353.1384, found 353.1386.

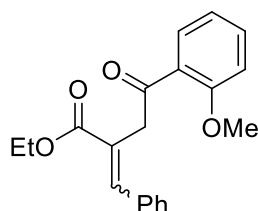
**ethyl 2-benzylidene-4-(3-methoxyphenyl)-4-oxobutanoate (229ad)**

Following general procedure **GP-C** using ethyl (*Z*)-2-chloro-3-phenylacrylate (**228a-Cl**, 105 mg, 500  $\mu\text{mol}$ , 1.00 equiv), 1-(3-methoxyphenyl)vinyl acetate (**152d**, 481 mg,

2.50 mmol, 5.00 equiv) and *fac*-Ir(ppy)<sub>3</sub> (6.55 mg, 10.0 μmol, 0.02 equiv) gave (*E*)-**229ad** (64.4 mg, 199 μmol, 40%) and (*Z*)-**229ad** (75.6 mg, 234 μmol, 47%) as slightly yellow oils as separated *E* and *Z* isomers after purification on SiO<sub>2</sub> (hexanes / EA, 20:1 to 12:1). *E/Z* = 46:54.

**R<sub>f</sub>** (hexanes / EA, 6:1) = 0.21 (*E* Isomer), 0.17 (*Z* Isomer); **IR** (neat): 3060, 2981, 2836, 1684, 1580, 1487, 1431, 1371, 1319, 1252, 1192, 1092, 1021, 981, 864, 782, 693 cm<sup>-1</sup>; **<sup>1</sup>H-NMR** (400 MHz, CDCl<sub>3</sub>, *E* Isomer): δ 8.02 (s, 1H), 7.58 (d, *J* = 7.7 Hz, 1H), 7.55 – 7.52 (m, 1H), 7.40 – 7.28 (m, 6H), 7.15 – 7.11 (m, 1H), 4.25 (q, *J* = 7.1 Hz, 2H), 4.18 (s, 2H), 3.85 (s, 3H), 1.28 (t, *J* = 7.1 Hz, 3H); **<sup>13</sup>C-NMR** (101 MHz, CDCl<sub>3</sub>, *E* Isomer): δ 197.30, 167.45, 159.89, 141.97, 138.10, 135.36, 129.65, 128.80, 128.76, 128.63, 127.41, 120.93, 119.79, 112.50, 61.14, 55.47, 38.21, 14.23; **<sup>1</sup>H-NMR** (400 MHz, CDCl<sub>3</sub>, *Z* Isomer): δ 7.60 (d, *J* = 7.7 Hz, 1H), 7.56 – 7.52 (m, 1H), 7.39 (t, *J* = 7.9 Hz, 1H), 7.33 – 7.28 (m, 5H), 7.13 (dd, *J* = 7.9, 2.3 Hz, 1H), 6.90 (s, 1H), 4.14 (d, *J* = 0.8 Hz, 2H), 4.10 (q, *J* = 7.2 Hz, 2H), 3.86 (s, 3H), 1.04 (t, *J* = 7.1 Hz, 3H); **<sup>13</sup>C-NMR** (101 MHz, CDCl<sub>3</sub>, *Z* Isomer): δ 196.87, 168.05, 159.91, 139.34, 137.83, 135.97, 129.67, 128.63, 128.05, 127.90, 120.95, 119.95, 112.44, 60.77, 55.49, 45.12, 13.64; **HRMS** (APCI) *m/z* calculated for C<sub>20</sub>H<sub>21</sub>O<sub>4</sub> ([*M*+*H*]<sup>+</sup>) 325.1434, found 325.1440.

#### ethyl 2-benzylidene-4-(2-methoxyphenyl)-4-oxobutanoate (**229ae**)

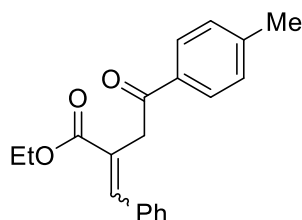


Following general procedure **GP-C** using ethyl (*Z*)-2-chloro-3-phenylacrylate (**228a-Cl**, 105 mg, 500 μmol, 1.00 equiv), 1-(2-methoxyphenyl)vinyl acetate (**152e**, 481 mg, 2.50 mmol, 5.00 equiv) and *fac*-Ir(ppy)<sub>3</sub> (6.55 mg, 10.0 μmol, 0.02 equiv) gave (*E*)-**229ae** (63.5 mg, 196 μmol, 39%) and (*Z*)-**229ae** (74.5 mg, 231 μmol, 46%) as slightly yellow oils as separated *E* and *Z* isomers after purification on SiO<sub>2</sub> (hexanes / EA, 20:1 to 12:1). *E/Z* = 46:54.

**R<sub>f</sub>** (hexanes / EA, 6:1) = 0.21 (*E* Isomer), 0.17 (*Z* Isomer); **IR** (neat): 3060, 2981, 2940, 2840, 1703, 1669, 1595, 1483, 1371, 1323, 1244, 1177, 1088, 1021, 998, 909, 823, 756, 693 cm<sup>-1</sup>; **<sup>1</sup>H-NMR** (300 MHz, CDCl<sub>3</sub>, *E* Isomer): δ 7.95 (s, 1H), 7.75 (dd, *J* = 7.7, 1.8 Hz, 1H), 7.50 –

7.43 (m, 1H), 7.37 – 7.32 (m, 5H), 7.04 – 6.93 (m, 2H), 4.28 – 4.19 (m, 4H), 3.83 (s, 3H), 1.28 (t,  $J = 7.1$  Hz, 3H);  $^{13}\text{C-NMR}$  (75 MHz,  $\text{CDCl}_3$ , *E* Isomer):  $\delta$  199.46, 167.73, 158.63, 141.31, 135.53, 133.63, 130.59, 129.04, 128.58, 128.48, 128.00, 127.97, 120.71, 111.46, 60.99, 55.47, 43.34, 14.23;  $^1\text{H-NMR}$  (300 MHz,  $\text{CDCl}_3$ , *Z* Isomer):  $\delta$  7.78 (dd,  $J = 7.7, 1.8$  Hz, 1H), 7.51 – 7.45 (m, 1H), 7.33 – 7.28 (m, 5H), 7.04 – 6.96 (m, 2H), 6.84 (s, 1H), 4.16 (s, 2H), 4.09 (q,  $J = 7.1$  Hz, 2H), 3.94 (s, 3H), 1.05 (t,  $J = 7.1$  Hz, 3H);  $^{13}\text{C-NMR}$  (75 MHz,  $\text{CDCl}_3$ , *Z* Isomer):  $\delta$  198.76, 168.38, 158.83, 138.47, 136.17, 133.93, 130.76, 128.85, 128.61, 127.86, 127.36, 120.75, 111.51, 60.60, 55.53, 50.40, 13.67; **HRMS** (APCI)  $m/z$  calculated for  $\text{C}_{20}\text{H}_{21}\text{O}_4$  ( $[\text{M}+\text{H}]^+$ ) 325.1434, found 325.1435.

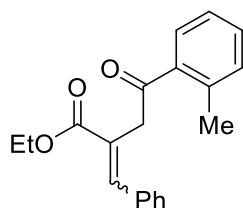
#### ethyl 2-benzylidene-4-oxo-4-(*p*-tolyl)butanoate (**229af**)



Following general procedure **GP-C** using ethyl (*Z*)-2-chloro-3-phenylacrylate (**228a-Cl**, 105 mg, 500  $\mu\text{mol}$ , 1.00 equiv), 1-(*p*-tolyl)vinyl acetate (**152f**, 441 mg, 2.50 mmol, 5.00 equiv) and *fac*- $\text{Ir}(\text{ppy})_3$  (6.55 mg, 10.0  $\mu\text{mol}$ , 0.02 equiv) gave (*E*)-**229af** (56.8 mg, 184  $\mu\text{mol}$ , 37%) and (*Z*)-**229af** (75.2 mg, 243  $\mu\text{mol}$ , 49%) as slightly yellow oils as separated *E* and *Z* isomers after purification on  $\text{SiO}_2$  (hexanes / EA, 20:1 to 10:1).  $E/Z = 43:57$ .

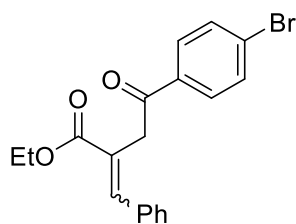
$R_f$  (hexanes / EA, 6:1) = 0.32 (*E* Isomer), 0.28 (*Z* Isomer); **IR** (neat): 3056, 3030, 2981, 2922, 1681, 1606, 1446, 1408, 1371, 1326, 1263, 1177, 1092, 1021, 909, 812, 790, 730, 700  $\text{cm}^{-1}$ ;  $^1\text{H-NMR}$  (300 MHz,  $\text{CDCl}_3$ , *E* Isomer):  $\delta$  8.02 (s, 1H), 7.94 – 7.89 (m, 2H), 7.34 – 7.26 (m, 7H), 4.24 (q,  $J = 7.1$  Hz, 2H), 4.18 (s, 2H), 2.42 (s, 3H), 1.27 (t,  $J = 7.1$  Hz, 3H);  $^{13}\text{C-NMR}$  (75 MHz,  $\text{CDCl}_3$ , *E* Isomer):  $\delta$  197.10, 167.52, 144.08, 141.89, 135.39, 134.23, 129.33, 128.81, 128.70, 128.59, 128.43, 127.52, 61.12, 37.93, 21.71, 14.21;  $^1\text{H-NMR}$  (400 MHz,  $\text{CDCl}_3$ , *Z* Isomer):  $\delta$  7.91 (d,  $J = 8.2$  Hz, 2H), 7.33 – 7.25 (m, 7H), 6.88 (s, 1H), 4.13 – 4.07 (m, 4H), 2.42 (s, 3H), 1.04 (t,  $J = 7.1$  Hz, 3H);  $^{13}\text{C-NMR}$  (101 MHz,  $\text{CDCl}_3$ , *Z* Isomer):  $\delta$  196.66, 168.13, 144.16, 139.14, 136.03, 134.03, 129.37, 128.64, 128.44, 128.11, 128.01, 127.89, 60.74, 44.90, 21.71, 13.64; **HRMS** (ESI)  $m/z$  calculated for  $\text{C}_{20}\text{H}_{21}\text{O}_3$  ( $[\text{M}+\text{H}]^+$ ) 309.1485, found 309.1488.



**ethyl 2-benzylidene-4-oxo-4-(*o*-tolyl)butanoate (229ag)**

Following general procedure **GP-C** using ethyl (*Z*)-2-chloro-3-phenylacrylate (**228a-Cl**, 105 mg, 500  $\mu\text{mol}$ , 1.00 equiv), 1-(*o*-tolyl)vinyl acetate (**152g**, 441 mg, 2.50 mmol, 5.00 equiv) and *fac*-Ir(ppy)<sub>3</sub> (6.55 mg, 10.0  $\mu\text{mol}$ , 0.02 equiv) gave (*E*)-**229ag** (35.5 mg, 115  $\mu\text{mol}$ , 23%) and (*Z*)-**229ag** (40.1 mg, 129.9  $\mu\text{mol}$ , 26%) as slightly yellow oils as separated *E* and *Z* isomers after purification on SiO<sub>2</sub> (hexanes / EA, 20:1 to 12:1). *E/Z* = 47:53.

**R<sub>f</sub>** (hexanes / EA, 6:1) = 0.38 (*E* Isomer), 0.30 (*Z* Isomer); **IR** (neat): 3060, 3026, 2981, 2929, 2903, 1684, 1602, 1446, 1401, 1323, 1289, 1237, 1207, 1121, 1021, 984, 842, 752, 697  $\text{cm}^{-1}$ ; **<sup>1</sup>H-NMR** (300 MHz, CDCl<sub>3</sub>, *E* Isomer):  $\delta$  8.02 (s, 1H), 7.70 – 7.67 (m, 1H), 7.41 – 7.32 (m, 6H), 7.28 – 7.25 (m, 2H), 4.26 (q, *J* = 7.1 Hz, 2H), 4.12 (s, 2H), 2.51 (s, 3H), 1.31 (t, *J* = 7.1 Hz, 3H); **<sup>13</sup>C-NMR** (75 MHz, CDCl<sub>3</sub>, *E* Isomer):  $\delta$  201.40, 167.47, 142.04, 138.21, 137.83, 135.41, 131.93, 131.39, 128.78, 128.75, 128.62, 128.45, 127.52, 125.67, 61.18, 41.03, 21.14, 14.25; **<sup>1</sup>H-NMR** (300 MHz, CDCl<sub>3</sub>, *Z* Isomer):  $\delta$  7.75 (d, *J* = 7.7 Hz, 1H), 7.39 (td, *J* = 7.5, 1.4 Hz, 1H), 7.33 – 7.25 (m, 7H), 6.91 (s, 1H), 4.13 – 4.05 (m, 4H), 2.52 (s, 3H), 1.05 (t, *J* = 7.1 Hz, 3H); **<sup>13</sup>C-NMR** (75 MHz, CDCl<sub>3</sub>, *Z* Isomer):  $\delta$  200.72, 167.98, 139.72, 138.55, 137.25, 135.95, 132.02, 131.56, 128.70, 128.68, 128.06, 127.97, 127.89, 125.71, 60.76, 47.92, 21.33, 13.66; **HRMS** (ESI) *m/z* calculated for C<sub>20</sub>H<sub>21</sub>O<sub>3</sub> ([M+H]<sup>+</sup>) 309.1485, found 309.1487.

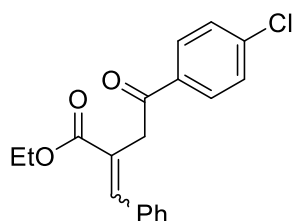
**ethyl 2-benzylidene-4-(4-bromophenyl)-4-oxobutanoate (229ah)**

Following general procedure **GP-C** using ethyl (*Z*)-2-chloro-3-phenylacrylate (**228a-Cl**, 63.2 mg, 300  $\mu\text{mol}$ , 1.00 equiv), 1-(4-bromophenyl)vinyl acetate (**152h**, 362 mg, 1.50 mmol,

5.00 equiv) and *fac*-Ir(ppy)<sub>3</sub> (3.93 mg, 6.00 μmol, 0.02 equiv) gave (*E*)-**229ah** (35.2 mg, 94.1 μmol, 32%) and (*Z*)-**229ah** (28.8 mg, 77.0 μmol, 26%) as slightly yellow oils as separated *E* and *Z* isomers after purification on SiO<sub>2</sub> (hexanes / EA, 20:1 to 12:1). *E/Z* = 55:45.

**R<sub>f</sub>** (hexanes / EA, 10:1) = 0.30 (*E* Isomer), 0.27 (*Z* Isomer); **IR** (neat): 3060, 3026, 2981, 2929, 1684, 1584, 1483, 1384, 1371, 1319, 1263, 1192, 1092, 995, 935, 812, 764, 700 cm<sup>-1</sup>; **<sup>1</sup>H-NMR** (300 MHz, CDCl<sub>3</sub>, *E* Isomer): δ 8.02 (s, 1H), 7.91 – 7.82 (m, 2H), 7.65 – 7.59 (m, 2H), 7.38 – 7.27 (m, 5H), 4.24 (q, *J* = 7.1 Hz, 2H), 4.14 (s, 2H), 1.27 (t, *J* = 7.1 Hz, 3H); **<sup>13</sup>C-NMR** (75 MHz, CDCl<sub>3</sub>, *E* Isomer): δ 196.59, 167.34, 142.23, 135.43, 135.24, 131.97, 129.83, 128.84, 128.73, 128.66, 128.46, 127.08, 61.22, 37.94, 14.22; **<sup>1</sup>H-NMR** (300 MHz, CDCl<sub>3</sub>, *Z* Isomer): δ 7.91 – 7.84 (m, 2H), 7.66 – 7.59 (m, 2H), 7.34 – 7.27 (m, 5H), 6.91 (s, 1H), 4.15 – 4.03 (m, 4H), 1.03 (t, *J* = 7.1 Hz, 3H); **<sup>13</sup>C-NMR** (75 MHz, CDCl<sub>3</sub>, *Z* Isomer): δ 196.09, 167.94, 139.73, 135.82, 135.15, 132.02, 129.83, 128.63, 128.57, 128.15, 127.92, 127.46, 60.84, 44.90, 13.62; **HRMS** (ESI) *m/z* calculated for C<sub>19</sub>H<sub>18</sub>BrO<sub>3</sub> ([M+H]<sup>+</sup>) 373.0434, found 373.0441.

#### ethyl 2-benzylidene-4-(4-chlorophenyl)-4-oxobutanoate (**229ai**)

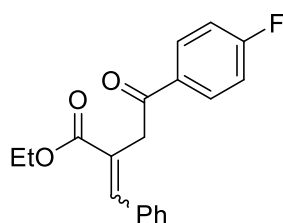


Following general procedure **GP-C** using ethyl (*Z*)-2-chloro-3-phenylacrylate (**228a-Cl**, 63.2 mg, 300 μmol, 1.00 equiv), 1-(4-chlorophenyl)vinyl acetate (**152i**, 295 mg, 1.50 mmol, 5.00 equiv) and *fac*-Ir(ppy)<sub>3</sub> (3.93 mg, 6.00 μmol, 0.02 equiv) gave (*E*)-**229ai** (34.8 mg, 106 μmol, 35%) and (*Z*)-**229ai** (26.2 mg, 80.0 μmol, 27%) as slightly yellow oils as separated *E* and *Z* isomers after purification on SiO<sub>2</sub> (hexanes / EA, 20:1 to 12:1). *E/Z* = 57:43.

**R<sub>f</sub>** (hexanes / EA, 10:1) = 0.30 (*E* Isomer), 0.26 (*Z* Isomer); **IR** (neat): 3080, 3026, 2981, 2937, 2903, 1684, 1587, 1490, 1401, 1334, 1207, 1125, 1092, 991, 838, 749, 697 cm<sup>-1</sup>; **<sup>1</sup>H-NMR** (300 MHz, CDCl<sub>3</sub>, *E* Isomer): δ 8.02 (s, 1H), 7.98 – 7.91 (m, 2H), 7.49 – 7.42 (m, 2H), 7.37 – 7.27 (m, 5H), 4.24 (q, *J* = 7.1 Hz, 2H), 4.14 (s, 2H), 1.28 (t, *J* = 7.1 Hz, 3H);

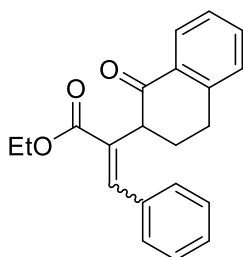
$^{13}\text{C-NMR}$  (75 MHz,  $\text{CDCl}_3$ , *E* Isomer):  $\delta$  196.41, 167.36, 142.23, 139.73, 135.24, 135.01, 129.73, 128.98, 128.84, 128.73, 128.66, 127.09, 61.23, 37.96, 14.21;  $^1\text{H-NMR}$  (300 MHz,  $\text{CDCl}_3$ , *Z* Isomer):  $\delta$  8.00 – 7.90 (m, 2H), 7.51 – 7.41 (m, 2H), 7.33 – 7.27 (m, 5H), 6.91 (s, 1H), 4.14 – 4.04 (m, 4H), 1.03 (t,  $J = 7.1$  Hz, 3H);  $^{13}\text{C-NMR}$  (75 MHz,  $\text{CDCl}_3$ , *Z* Isomer):  $\delta$  195.90, 167.97, 139.82, 139.70, 135.83, 134.73, 129.73, 129.03, 128.63, 128.15, 127.92, 127.49, 60.85, 44.94, 13.63; **HRMS** (ESI)  $m/z$  calculated for  $\text{C}_{19}\text{H}_{18}\text{ClO}_3$  ( $[\text{M}+\text{H}]^+$ ) 329.0939, found 329.0941.

### ethyl 2-benzylidene-4-(4-fluorophenyl)-4-oxobutanoate (**229aj**)



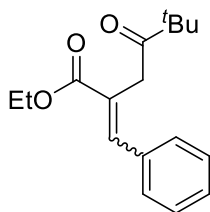
Following general procedure **GP-C** using ethyl (*Z*)-2-chloro-3-phenylacrylate (**228a-Cl**, 63.2 mg, 300  $\mu\text{mol}$ , 1.00 equiv), 1-(4-fluorophenyl)vinyl acetate (**152j**, 90.0 mg, 500  $\mu\text{mol}$ , 1.67 equiv) and *fac*-Ir(ppy)<sub>3</sub> (3.93 mg, 6.00  $\mu\text{mol}$ , 0.02 equiv) gave (*E*)-**229aj** (36.3 mg, 116  $\mu\text{mol}$ , 39%) and (*Z*)-**229aj** (37.8 mg, 121  $\mu\text{mol}$ , 40%) as slightly yellow oils as separated *E* and *Z* isomers after purification on  $\text{SiO}_2$  (hexanes / EA, 20:1 to 15:1). *E/Z* = 49:51.

**R<sub>f</sub>** (hexanes / EA, 10:1) = 0.30 (*E* Isomer), 0.26 (*Z* Isomer); **IR** (neat): 3060, 3026, 2981, 2933, 1684, 1595, 1505, 1408, 1334, 1211, 1155, 1125, 1021, 998, 842, 738, 697  $\text{cm}^{-1}$ ;  $^1\text{H-NMR}$  (300 MHz,  $\text{CDCl}_3$ , *E* Isomer):  $\delta$  8.08 – 7.99 (m, 3H), 7.37 – 7.29 (m, 5H), 7.19 – 7.10 (m, 2H), 4.24 (q,  $J = 7.1$  Hz, 2H), 4.15 (s, 2H), 1.28 (t,  $J = 7.1$  Hz, 3H);  $^{13}\text{C-NMR}$  (75 MHz,  $\text{CDCl}_3$ , *E* Isomer):  $\delta$  196.00, 167.55, 167.41, 164.18, 142.15, 135.28, 133.15, 133.11, 131.02, 130.90, 128.80, 128.75, 128.64, 127.20, 115.91, 115.62, 61.20, 37.90, 14.21;  $^{19}\text{F-NMR}$  (282 MHz,  $\text{CDCl}_3$ , *E* Isomer):  $\delta$  -105.45;  $^1\text{H-NMR}$  (300 MHz,  $\text{CDCl}_3$ , *Z* Isomer):  $\delta$  8.08 – 8.02 (m, 2H), 7.33 – 7.27 (m, 5H), 7.20 – 7.11 (m, 2H), 6.91 (s, 1H), 4.13 – 4.06 (m, 4H), 1.03 (t,  $J = 7.1$  Hz, 3H);  $^{13}\text{C-NMR}$  (75 MHz,  $\text{CDCl}_3$ , *Z* Isomer):  $\delta$  195.50, 168.04, 167.59, 164.21, 139.57, 135.86, 132.86, 132.82, 131.03, 130.91, 128.62, 128.12, 127.91, 127.63, 115.98, 115.69, 60.83, 44.89, 13.62;  $^{19}\text{F-NMR}$  (282 MHz,  $\text{CDCl}_3$ , *Z* Isomer):  $\delta$  -105.22; **HRMS** (ESI)  $m/z$  calculated for  $\text{C}_{19}\text{H}_{18}\text{FO}_3$  ( $[\text{M}+\text{H}]^+$ ) 313.1234, found 313.1243.

ethyl 2-(1-oxo-1,2,3,4-tetrahydronaphthalen-2-yl)-3-phenylacrylate (**229ak**)

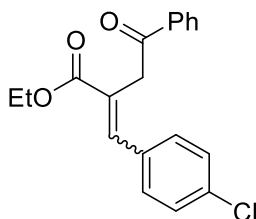
Following general procedure **GP-C** using ethyl (*Z*)-2-chloro-3-phenylacrylate (**228a-Cl**, 105 mg, 500  $\mu\text{mol}$ , 1.00 equiv), 3,4-dihydronaphthalen-1-yl acetate (**152k**, 471 mg, 2.50 mmol, 5.00 equiv) and *fac*-Ir(ppy)<sub>3</sub> (6.55 mg, 10.0  $\mu\text{mol}$ , 0.02 equiv) gave (*E*)-**229ak** (15.4 mg, 48.0  $\mu\text{mol}$ , 10%) and (*Z*)-**229ak** (23.1 mg, 72.0  $\mu\text{mol}$ , 14%) as slightly yellow oils as separated *E* and *Z* isomers after purification on SiO<sub>2</sub> (hexanes / EA, 20:1 to 9:1). *E/Z* = 40:60.

**R<sub>f</sub>** (hexanes / EA, 10:1) = 0.17 (*E* Isomer), 0.10 (*Z* Isomer); **IR** (neat): 3060, 3026, 2937, 2981, 2877, 1707, 1681, 1636, 1599, 1453, 1367, 1271, 1222, 1200, 1125, 902, 745, 700  $\text{cm}^{-1}$ ; **<sup>1</sup>H-NMR** (300 MHz, CDCl<sub>3</sub>, *E* Isomer):  $\delta$  8.08 (dd, *J* = 7.8, 1.3 Hz, 1H), 7.98 (s, 1H), 7.46 (td, *J* = 7.5, 1.5 Hz, 1H), 7.41 – 7.28 (m, 6H), 7.23 – 7.18 (m, 1H), 4.20 (qd, *J* = 7.1, 1.6 Hz, 2H), 3.88 (dd, *J* = 12.9, 4.8 Hz, 1H), 3.02 – 2.91 (m, 2H), 2.71 (ddd, *J* = 25.2, 12.7, 5.3 Hz, 1H), 2.18 – 2.07 (m, 1H), 1.21 (t, *J* = 7.1 Hz, 3H); **<sup>13</sup>C-NMR** (75 MHz, CDCl<sub>3</sub>, *E* Isomer):  $\delta$  197.36, 166.62, 143.65, 141.99, 135.50, 133.29, 132.99, 132.51, 128.64, 128.62, 128.54, 127.62, 126.74, 60.92, 48.45, 29.38, 29.23, 14.10; **<sup>1</sup>H-NMR** (300 MHz, CDCl<sub>3</sub>, *Z* Isomer):  $\delta$  8.07 (dd, *J* = 7.8, 1.3 Hz, 1H), 7.49 (td, *J* = 7.5, 1.5 Hz, 1H), 7.33 – 7.26 (m, 7H), 6.82 (s, 1H), 4.10 (qd, *J* = 7.1, 0.7 Hz, 2H), 3.74 (ddd, *J* = 12.5, 4.6, 1.1 Hz, 1H), 3.18 – 3.03 (m, 2H), 2.62 – 2.31 (m, 2H), 1.02 (t, *J* = 7.1 Hz, 3H); **<sup>13</sup>C-NMR** (75 MHz, CDCl<sub>3</sub>, *Z* Isomer):  $\delta$  197.02, 168.63, 143.87, 136.76, 136.18, 133.53, 133.32, 132.42, 128.68, 128.51, 127.93, 127.74, 126.80, 60.71, 54.23, 29.51, 29.40, 13.59; **HRMS** (ESI) *m/z* calculated for C<sub>21</sub>H<sub>20</sub>O<sub>3</sub>Na ([M+Na]<sup>+</sup>) 343.1305, found 343.1305.

**ethyl 2-benzylidene-5,5-dimethyl-4-oxohexanoate (229al)**

Following general procedure **GP-C** using ethyl (*Z*)-2-chloro-3-phenylacrylate (**228a-Cl**, 105 mg, 500  $\mu\text{mol}$ , 1.00 equiv), 3,3-dimethylbut-1-en-2-yl acetate (**152l**, 356 mg, 2.50 mmol, 5.00 equiv) and *fac*-Ir(ppy)<sub>3</sub> (6.55 mg, 10.0  $\mu\text{mol}$ , 0.02 equiv) gave (*E*)-**229al** (11.1 mg, 40.3  $\mu\text{mol}$ , 8%) and (*Z*)-**229al** (11.1 mg, 40.3  $\mu\text{mol}$ , 8%) as colorless oils as separated *E* and *Z* isomers after purification on SiO<sub>2</sub> (hexanes / EA, 20:1 to 12:1). *E/Z* = 50:50.

**R<sub>f</sub>** (hexanes / EA, 6:1) = 0.35 (*E* Isomer), 0.28 (*Z* Isomer); **IR** (neat): 3056, 3026, 2970, 2873, 1703, 1476, 1397, 1323, 1237, 1207, 1125, 1062, 1025, 935, 846, 816, 738, 697  $\text{cm}^{-1}$ ; **<sup>1</sup>H-NMR** (400 MHz, CDCl<sub>3</sub>, *E* Isomer):  $\delta$  7.95 (s, 1H), 7.38 – 7.31 (m, 3H), 7.24 – 7.21 (m, 2H), 4.24 (q, *J* = 7.1 Hz, 2H), 3.71 (s, 2H), 1.31 (t, *J* = 7.1 Hz, 3H), 1.21 (s, 9H); **<sup>13</sup>C-NMR** (101 MHz, CDCl<sub>3</sub>, *E* Isomer):  $\delta$  213.13, 167.46, 141.86, 135.54, 128.62, 128.52, 127.70, 61.04, 44.54, 36.54, 26.75, 14.29; **<sup>1</sup>H-NMR** (400 MHz, CDCl<sub>3</sub>, *Z* Isomer):  $\delta$  7.31 – 7.27 (m, 5H), 6.79 (s, 1H), 4.07 (q, *J* = 7.1 Hz, 2H), 3.68 (d, *J* = 0.9 Hz, 2H), 1.21 (s, 9H), 1.04 (t, *J* = 7.1 Hz, 3H); **<sup>13</sup>C-NMR** (101 MHz, CDCl<sub>3</sub>, *Z* Isomer):  $\delta$  212.76, 168.01, 139.28, 136.07, 128.62, 128.18, 127.94, 127.85, 60.64, 44.20, 43.42, 26.49, 13.67; **HRMS** (APCI) *m/z* calculated for C<sub>17</sub>H<sub>23</sub>O<sub>3</sub> ([*M*+*H*]<sup>+</sup>) 275.1642, found 275.1645.

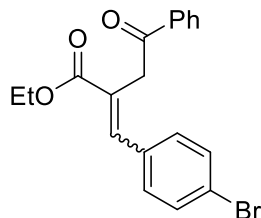
**ethyl 2-(4-chlorobenzylidene)-4-oxo-4-phenylbutanoate (229ea)**

Following general procedure **GP-C** using ethyl (*Z*)-2-chloro-3-(4-chlorophenyl)acrylate (**228e**, 123 mg, 500  $\mu\text{mol}$ , 1.00 equiv), 1-phenylvinyl acetate (**152a**, 405 mg, 2.50 mmol, 5.00 equiv) and *fac*-Ir(ppy)<sub>3</sub> (6.55 mg, 10.0  $\mu\text{mol}$ , 0.02 equiv) gave (*E*)-**229ea** (58.1 mg,

177  $\mu\text{mol}$ , 36%) and (*Z*)-**229ea** (73.9 mg, 226  $\mu\text{mol}$ , 45%) as slightly yellow oils as separated *E* and *Z* isomers after purification on  $\text{SiO}_2$  (hexanes / EA, 20:1 to 8:1). *E/Z* = 44:56.

**R<sub>f</sub>** (hexanes / EA, 6:1) = 0.24 (*E* Isomer), 0.20 (*Z* Isomer); **IR** (neat): 3056, 2974, 2907, 1707, 1677, 1591, 1487, 1379, 1341, 1297, 1241, 1125, 998, 849, 749, 685  $\text{cm}^{-1}$ ; **<sup>1</sup>H-NMR** (300 MHz,  $\text{CDCl}_3$ , *E* Isomer):  $\delta$  8.03 – 7.98 (m, 2H), 7.96 (s, 1H), 7.62 – 7.57 (m, 1H), 7.51 – 7.46 (m, 2H), 7.33 – 7.23 (m, 4H), 4.24 (q,  $J = 7.1$  Hz, 2H), 4.15 (s, 2H), 1.26 (t,  $J = 7.1$  Hz, 3H); **<sup>13</sup>C-NMR** (75 MHz,  $\text{CDCl}_3$ , *E* Isomer):  $\delta$  197.38, 167.19, 140.75, 136.58, 134.76, 133.76, 133.41, 130.07, 128.88, 128.72, 128.30, 128.01, 61.27, 37.92, 14.18; **<sup>1</sup>H-NMR** (300 MHz,  $\text{CDCl}_3$ , *Z* Isomer):  $\delta$  8.01 – 7.98 (m, 2H), 7.62 – 7.56 (m, 1H), 7.51 – 7.46 (m, 2H), 7.30 – 7.24 (m, 4H), 6.83 (s, 1H), 4.14 – 4.07 (m, 4H), 1.07 (t,  $J = 7.1$  Hz, 3H); **<sup>13</sup>C-NMR** (75 MHz,  $\text{CDCl}_3$ , *Z* Isomer):  $\delta$  196.92, 167.58, 138.34, 136.37, 134.35, 133.93, 133.44, 130.10, 128.73, 128.48, 128.26, 128.10, 60.89, 45.00, 13.71; **HRMS** (ESI)  $m/z$  calculated for  $\text{C}_{19}\text{H}_{18}\text{ClO}_3$  ( $[\text{M}+\text{H}]^+$ ) 329.0939, found 329.0944.

#### ethyl 2-(4-bromobenzylidene)-4-oxo-4-phenylbutanoate (**229fa**)

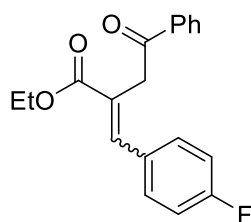


Following general procedure **GP-C** using ethyl (*Z*)-3-(4-bromophenyl)-2-chloroacrylate (**228f**, 145 mg, 500  $\mu\text{mol}$ , 1.00 equiv), 1-phenylvinyl acetate (**152a**, 405 mg, 2.50 mmol, 5.00 equiv) and *fac*- $\text{Ir}(\text{ppy})_3$  (6.55 mg, 10.0  $\mu\text{mol}$ , 0.02 equiv) gave (*E*)-**229fa** (72.2 mg, 193  $\mu\text{mol}$ , 39%) and (*Z*)-**229fa** (84.8 mg, 226  $\mu\text{mol}$ , 45%) as slightly yellow oils as separated *E* and *Z* isomers after purification on  $\text{SiO}_2$  (hexanes / EA, 20:1 to 8:1). *E/Z* = 46:54.

**R<sub>f</sub>** (hexanes / EA, 6:1) = 0.26 (*E* Isomer), 0.20 (*Z* Isomer); **IR** (neat): 3056, 2967, 2907, 1707, 1677, 1580, 1483, 1375, 1341, 1297, 1237, 1125, 1103, 998, 924, 846, 812, 749, 689  $\text{cm}^{-1}$ ; **<sup>1</sup>H-NMR** (300 MHz,  $\text{CDCl}_3$ , *E* Isomer):  $\delta$  8.03 – 7.98 (m, 2H), 7.94 (s, 1H), 7.63 – 7.57 (m, 1H), 7.52 – 7.45 (m, 4H), 7.21 – 7.15 (m, 2H), 4.24 (q,  $J = 7.1$  Hz, 2H), 4.15 (s, 2H), 1.27 (t,  $J = 7.1$  Hz, 3H); **<sup>13</sup>C-NMR** (75 MHz,  $\text{CDCl}_3$ , *E* Isomer):  $\delta$  197.35, 167.17, 140.78, 136.57, 134.22, 133.41, 131.84, 130.30, 128.71, 128.30, 128.09, 123.03, 61.28, 37.93, 14.18;

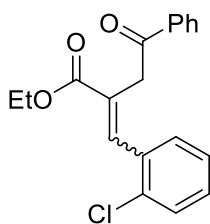
**<sup>1</sup>H-NMR** (300 MHz, CDCl<sub>3</sub>, *Z* Isomer): δ 8.04 – 7.97 (m, 2H), 7.62 – 7.56 (m, 1H), 7.52 – 7.41 (m, 4H), 7.23 – 7.14 (m, 2H), 6.81 (s, 1H), 4.16 – 4.06 (m, 4H), 1.07 (t, *J* = 7.1 Hz, 3H); **<sup>13</sup>C-NMR** (75 MHz, CDCl<sub>3</sub>, *Z* Isomer): δ 195.83, 166.49, 137.31, 135.30, 133.75, 132.38, 129.99, 129.29, 127.67, 127.50, 127.20, 121.11, 59.85, 43.93, 12.65; **HRMS** (ESI) *m/z* calculated for C<sub>19</sub>H<sub>18</sub>BrO<sub>3</sub> ([M+H]<sup>+</sup>) 373.0434, found 373.0438.

**ethyl 2-(4-fluorobenzylidene)-4-oxo-4-phenylbutanoate (229ga)**



Following general procedure **GP-C** using ethyl (*Z*)-2-chloro-3-(4-fluorophenyl)acrylate (**228g**, 114 mg, 500 μmol, 1.00 equiv), 1-phenylvinyl acetate (**152a**, 405 mg, 2.50 mmol, 5.00 equiv) and *fac*-Ir(ppy)<sub>3</sub> (6.55 mg, 10.0 μmol, 0.02 equiv) gave (*E*)-**229ga** (66.3 mg, 212 μmol, 42%) and (*Z*)-**229ga** (58.8 mg, 188 μmol, 38%) as colorless oils as separated *E* and *Z* isomers after purification on SiO<sub>2</sub> (hexanes / EA, 20:1 to 8:1). *E/Z* = 53:47.

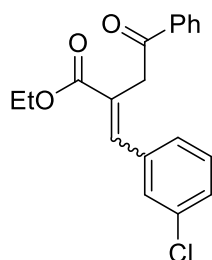
**R<sub>f</sub>** (hexanes / EA, 6:1) = 0.32 (*E* Isomer), 0.20 (*Z* Isomer); **IR** (neat): 3063, 2981, 2907, 1684, 1599, 1505, 1446, 1379, 1334, 1304, 1211, 1159, 1125, 991, 842, 752, 689 cm<sup>-1</sup>; **<sup>1</sup>H-NMR** (400 MHz, CDCl<sub>3</sub>, *E* Isomer): δ 8.02 – 7.99 (m, 2H), 7.98 (s, 1H), 7.61 – 7.58 (m, 1H), 7.50 – 7.47 (m, 2H), 7.32 – 7.29 (m, 2H), 7.06 – 7.00 (m, 2H), 4.24 (q, *J* = 7.1 Hz, 2H), 4.16 (s, 2H), 1.26 (t, *J* = 7.1 Hz, 3H); **<sup>13</sup>C-NMR** (101 MHz, CDCl<sub>3</sub>, *E* Isomer): δ 197.47, 167.31, 162.86 (d, *J* = 249.5 Hz), 140.94, 136.68, 133.37, 131.41 (d, *J* = 3.4 Hz), 130.69 (d, *J* = 8.3 Hz), 128.71, 128.31, 127.38 (d, *J* = 1.0 Hz), 115.74 (d, *J* = 21.6 Hz), 61.21, 37.91, 14.19; **<sup>19</sup>F-NMR** (376 MHz, CDCl<sub>3</sub>, *E* Isomer): δ -112.39; **<sup>1</sup>H-NMR** (400 MHz, CDCl<sub>3</sub>, *Z* Isomer): δ 8.00 (d, *J* = 7.7 Hz, 2H), 7.59 (t, *J* = 7.3 Hz, 1H), 7.49 (t, *J* = 7.5 Hz, 2H), 7.34 – 7.28 (m, 2H), 7.00 (t, *J* = 8.6 Hz, 2H), 6.85 (s, 1H), 4.17 – 4.07 (m, 4H), 1.07 (t, *J* = 7.1 Hz, 3H); **<sup>13</sup>C-NMR** (101 MHz, CDCl<sub>3</sub>, *Z* Isomer): δ 197.01, 167.70, 162.53 (d, *J* = 248.0 Hz), 138.57, 136.46, 133.40, 131.94 (d, *J* = 3.4 Hz), 130.62 (d, *J* = 8.2 Hz), 128.72, 128.28, 127.84 (d, *J* = 0.9 Hz), 114.89 (d, *J* = 21.6 Hz), 60.83, 45.00, 13.71; **<sup>19</sup>F-NMR** (376 MHz, CDCl<sub>3</sub>, *Z* Isomer): δ -113.76; **HRMS** (APCI) *m/z* calculated for C<sub>19</sub>H<sub>18</sub>FO<sub>3</sub> ([M+H]<sup>+</sup>) 313.1234, found 313.1242.

**ethyl 2-(2-chlorobenzylidene)-4-oxo-4-phenylbutanoate (229ha)**

Following general procedure **GP-C** using ethyl (*Z*)-2-chloro-3-(2-chlorophenyl)acrylate (**228h**, 123 mg, 500  $\mu\text{mol}$ , 1.00 equiv), 1-phenylvinyl acetate (**152a**, 405 mg, 2.50 mmol, 5.00 equiv) and *fac*-Ir(ppy)<sub>3</sub> (6.55 mg, 10.0  $\mu\text{mol}$ , 0.02 equiv) gave (*E*)-**229ha** (49.6 mg, 151  $\mu\text{mol}$ , 30%) and (*Z*)-**229ha** (74.4 mg, 226  $\mu\text{mol}$ , 46%) as colorless oils as separated *E* and *Z* isomers after purification on SiO<sub>2</sub> (hexanes / EA, 20:1 to 8:1). *E/Z* = 40:60.

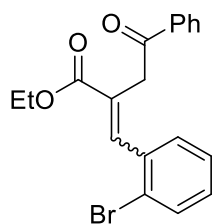
**R<sub>f</sub>** (hexanes / EA, 6:1) = 0.29 (*E* Isomer), 0.20 (*Z* Isomer); **IR** (neat): 3063, 2981, 2907, 1684, 1595, 1379, 1334, 1211, 1114, 1054, 1021, 991, 838, 752, 689  $\text{cm}^{-1}$ ; **<sup>1</sup>H-NMR** (400 MHz, CDCl<sub>3</sub>, *E* Isomer):  $\delta$  8.05 (s, 1H), 7.97 (d, *J* = 7.5 Hz, 2H), 7.57 (t, *J* = 7.4 Hz, 1H), 7.48 – 7.41 (m, 3H), 7.29 – 7.25 (m, 2H), 7.20 – 7.17 (m, 1H), 4.26 (q, *J* = 7.1 Hz, 2H), 4.07 (s, 2H), 1.28 (t, *J* = 7.1 Hz, 3H); **<sup>13</sup>C-NMR** (101 MHz, CDCl<sub>3</sub>, *E* Isomer):  $\delta$  197.46, 166.92, 139.22, 136.64, 134.05, 134.02, 133.31, 129.98, 129.75, 129.64, 129.22, 128.66, 128.29, 126.85, 61.30, 38.21, 14.17; **<sup>1</sup>H-NMR** (400 MHz, CDCl<sub>3</sub>, *Z* Isomer):  $\delta$  8.04 – 8.01 (m, 2H), 7.61 – 7.57 (m, 1H), 7.51 – 7.47 (m, 2H), 7.38 – 7.31 (m, 2H), 7.25 – 7.18 (m, 2H), 6.98 (s, 1H), 4.18 (d, *J* = 0.9 Hz, 2H), 4.03 (q, *J* = 7.1 Hz, 2H), 0.96 (t, *J* = 7.1 Hz, 3H); **<sup>13</sup>C-NMR** (101 MHz, CDCl<sub>3</sub>, *Z* Isomer):  $\delta$  196.85, 167.08, 137.29, 136.49, 135.19, 133.35, 132.93, 130.41, 129.82, 129.14, 129.01, 128.70, 128.33, 126.05, 60.78, 44.44, 13.56; **HRMS** (APCI) *m/z* calculated for C<sub>19</sub>H<sub>18</sub>ClO<sub>3</sub> ([*M*+*H*]<sup>+</sup>) 329.0939, found 329.0945.



ethyl 2-(3-chlorobenzylidene)-4-oxo-4-phenylbutanoate (**229ia**)

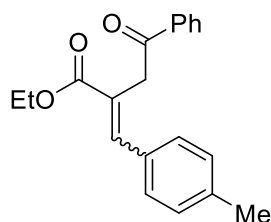
Following general procedure **GP-C** using ethyl (*Z*)-2-chloro-3-(3-chlorophenyl)acrylate (**228i**, 123 mg, 500  $\mu\text{mol}$ , 1.00 equiv), 1-phenylvinyl acetate (**152a**, 405 mg, 2.50 mmol, 5.00 equiv) and *fac*-Ir(ppy)<sub>3</sub> (6.55 mg, 10.0  $\mu\text{mol}$ , 0.02 equiv) gave (*E*)-**229ia** (70.6 mg, 215  $\mu\text{mol}$ , 43%) and (*Z*)-**229ia** (76.4 mg, 232  $\mu\text{mol}$ , 46%) as colorless oils as separated *E* and *Z* isomers after purification on SiO<sub>2</sub> (hexanes / EA, 20:1 to 8:1). *E/Z* = 48:52.

**R<sub>f</sub>** (hexanes / EA, 6:1) = 0.29 (*E* Isomer), 0.22 (*Z* Isomer); **IR** (neat): 3063, 2981, 2933, 1684, 1643, 1595, 1476, 1391, 1326, 1263, 1192, 1021, 1000, 924, 790, 685  $\text{cm}^{-1}$ ; **<sup>1</sup>H-NMR** (400 MHz, CDCl<sub>3</sub>, *E* Isomer):  $\delta$  8.01 – 7.99 (m, 2H), 7.94 (s, 1H), 7.62 – 7.57 (m, 1H), 7.50 – 7.47 (m, 2H), 7.31 – 7.26 (m, 3H), 7.20 – 7.18 (m, 1H), 4.24 (q, *J* = 7.1 Hz, 2H), 4.15 (s, 2H), 1.27 (t, *J* = 7.1 Hz, 3H); **<sup>13</sup>C-NMR** (101 MHz, CDCl<sub>3</sub>, *E* Isomer):  $\delta$  197.34, 167.09, 140.46, 137.15, 136.62, 134.57, 133.39, 129.93, 128.78, 128.76, 128.71, 128.32, 126.70, 61.34, 37.86, 14.18; **<sup>1</sup>H-NMR** (400 MHz, CDCl<sub>3</sub>, *Z* Isomer):  $\delta$  8.01 (d, *J* = 7.6 Hz, 2H), 7.60 (t, *J* = 7.4 Hz, 1H), 7.49 (t, *J* = 7.7 Hz, 2H), 7.32 – 7.25 (m, 3H), 7.20 – 7.16 (m, 1H), 6.84 (s, 1H), 4.15 (s, 2H), 4.11 (q, *J* = 7.1 Hz, 2H), 1.06 (t, *J* = 7.1 Hz, 3H); **<sup>13</sup>C-NMR** (101 MHz, CDCl<sub>3</sub>, *Z* Isomer):  $\delta$  196.85, 167.57, 137.81, 137.74, 136.35, 133.76, 133.48, 129.31, 129.18, 128.75, 128.65, 128.30, 128.03, 126.80, 60.99, 44.89, 13.63; **HRMS** (APCI) *m/z* calculated for C<sub>19</sub>H<sub>18</sub>ClO<sub>3</sub> ([*M*+*H*]<sup>+</sup>) 329.0939, found 329.0940.

ethyl 2-(2-bromobenzylidene)-4-oxo-4-phenylbutanoate (**229ja**)

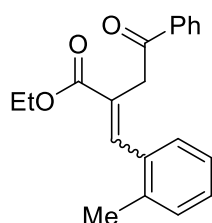
Following general procedure **GP-C** using ethyl (*Z*)-3-(2-bromophenyl)-2-chloroacrylate (**228j**, 145 mg, 500  $\mu\text{mol}$ , 1.00 equiv), 1-phenylvinyl acetate (**152a**, 405 mg, 2.50 mmol, 5.00 equiv) and *fac*-Ir(ppy)<sub>3</sub> (6.55 mg, 10.0  $\mu\text{mol}$ , 0.02 equiv) gave (*E*)-**229ja** (31.9 mg, 85.4  $\mu\text{mol}$ , 17%) and (*Z*)-**229ja** (59.2 mg, 159  $\mu\text{mol}$ , 32%) as colorless oils as separated *E* and *Z* isomers after purification on SiO<sub>2</sub> (hexanes / EA, 20:1 to 8:1). *E/Z* = 35:65.

**R<sub>f</sub>** (hexanes / EA, 6:1) = 0.27 (*E* Isomer), 0.22 (*Z* Isomer); **IR** (neat): 3060, 2981, 2903, 1684, 1595, 1446, 1401, 1375, 1334, 1274, 1241, 1211, 1110, 1021, 991, 838, 749, 600  $\text{cm}^{-1}$ ; **<sup>1</sup>H-NMR** (400 MHz, CDCl<sub>3</sub>, *E* Isomer):  $\delta$  7.99 – 7.96 (m, 3H), 7.63 – 7.55 (m, 2H), 7.48 – 7.45 (m, 2H), 7.29 – 7.23 (m, 2H), 7.22 – 7.16 (m, 1H), 4.26 (q, *J* = 7.1 Hz, 2H), 4.05 (s, 2H), 1.28 (t, *J* = 7.1 Hz, 3H); **<sup>13</sup>C-NMR** (101 MHz, CDCl<sub>3</sub>, *E* Isomer):  $\delta$  197.51, 166.93, 141.32, 136.58, 135.88, 133.35, 132.81, 130.14, 129.82, 128.89, 128.68, 128.31, 127.49, 124.01, 61.33, 38.19, 14.20; **<sup>1</sup>H-NMR** (400 MHz, CDCl<sub>3</sub>, *Z* Isomer):  $\delta$  8.05 – 8.02 (m, 2H), 7.62 – 7.55 (m, 2H), 7.49 (t, *J* = 7.6 Hz, 2H), 7.31 (dd, *J* = 7.6, 1.5 Hz, 1H), 7.28 – 7.23 (m, 1H), 7.16 (td, *J* = 7.7, 1.7 Hz, 1H), 6.94 (s, 1H), 4.18 (d, *J* = 0.8 Hz, 2H), 4.02 (q, *J* = 7.1 Hz, 2H), 0.95 (t, *J* = 7.1 Hz, 3H); **<sup>13</sup>C-NMR** (101 MHz, CDCl<sub>3</sub>, *Z* Isomer):  $\delta$  196.88, 167.00, 139.48, 137.15, 136.45, 133.39, 132.12, 130.46, 129.48, 129.29, 128.72, 128.35, 126.67, 122.84, 60.79, 44.30, 13.57; **HRMS** (APCI) *m/z* calculated for C<sub>19</sub>H<sub>18</sub>BrO<sub>3</sub> ([*M*+*H*]<sup>+</sup>) 373.0434, found 373.0438.

**ethyl 2-(4-methylbenzylidene)-4-oxo-4-phenylbutanoate (229la)**

Following general procedure **GP-C** using ethyl (*Z*)-2-chloro-3-(*p*-tolyl)acrylate (**228l**, 112 mg, 500  $\mu\text{mol}$ , 1.00 equiv), 1-phenylvinyl acetate (**152a**, 405 mg, 2.50 mmol, 5.00 equiv) and *fac*-Ir(ppy)<sub>3</sub> (6.55 mg, 10.0  $\mu\text{mol}$ , 0.02 equiv) gave (*E*)-**229la** (28.2 mg, 91.7  $\mu\text{mol}$ , 18%) and (*Z*)-**229la** (31.8 mg, 103  $\mu\text{mol}$ , 21%) as yellowish oils as separated *E* and *Z* isomers after purification on SiO<sub>2</sub> (hexanes / EA, 20:1 to 8:1). *E/Z* = 47:53.

**R<sub>f</sub>** (hexanes / EA, 10:1) = 0.20 (*E* Isomer), 0.13 (*Z* Isomer); **IR** (neat): 3056, 3026, 2981, 2922, 1684, 1599, 1513, 1446, 1371, 1326, 1267, 1211, 1177, 1088, 1021, 916, 849, 812, 756, 689  $\text{cm}^{-1}$ ; **<sup>1</sup>H-NMR** (300 MHz, CDCl<sub>3</sub>, *E* Isomer):  $\delta$  8.04 – 7.99 (m, 3H), 7.61 – 7.56 (m, 1H), 7.51 – 7.43 (m, 2H), 7.27 – 7.12 (m, 4H), 4.25 – 4.21 (m, 4H), 2.34 (s, 3H), 1.27 (t, *J* = 7.1 Hz, 3H); **<sup>13</sup>C-NMR** (75 MHz, CDCl<sub>3</sub>, *E* Isomer):  $\delta$  197.59, 167.61, 142.09, 138.92, 136.77, 133.23, 132.44, 129.34, 128.86, 128.65, 128.29, 126.52, 61.08, 38.13, 21.35, 14.22; **<sup>1</sup>H-NMR** (300 MHz, CDCl<sub>3</sub>, *Z* Isomer):  $\delta$  8.06 – 8.00 (m, 2H), 7.61 – 7.55 (m, 1H), 7.51 – 7.45 (m, 2H), 7.24 – 7.11 (m, 4H), 6.85 (s, 1H), 4.17 – 4.07 (m, 4H), 2.35 (s, 3H), 1.08 (t, *J* = 7.1 Hz, 3H); **<sup>13</sup>C-NMR** (75 MHz, CDCl<sub>3</sub>, *Z* Isomer):  $\delta$  197.17, 168.16, 139.51, 138.11, 136.49, 133.32, 132.89, 128.76, 128.68, 128.61, 128.29, 126.87, 60.73, 45.17, 21.35, 13.73; **HRMS** (ESI) *m/z* calculated for C<sub>20</sub>H<sub>20</sub>NaO<sub>3</sub> ([M+Na]<sup>+</sup>) 331.1305, found 331.1305.

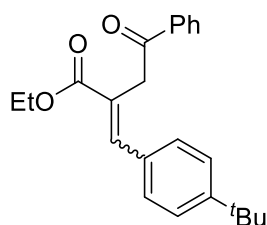
**ethyl 2-(2-methylbenzylidene)-4-oxo-4-phenylbutanoate (229ma)**

Following general procedure **GP-C** using ethyl (*Z*)-2-chloro-3-(*o*-tolyl)acrylate (**228m**, 112 mg, 500  $\mu\text{mol}$ , 1.00 equiv), 1-phenylvinyl acetate (**152a**, 405 mg, 2.50 mmol, 5.00 equiv)

and *fac*-Ir(ppy)<sub>3</sub> (6.55 mg, 10.0 μmol, 0.02 equiv) gave ethyl 2-(2-methylbenzylidene)-4-oxo-4-phenylbutanoate (46.3 mg, 150 μmol, 30%) as yellowish oil as a mixture of *E/Z* = 45:55 after purification on SiO<sub>2</sub> (hexanes / EA, 20:1 to 8:1).

**R<sub>f</sub>** (hexanes / EA, 6:1) = 0.30 (*E* Isomer), 0.24 (*Z* Isomer); **IR** (neat): 3063, 2981, 1684, 1599, 1446, 1371, 1330, 1263, 1215, 1120, 1092, 1021, 998, 916, 846, 745, 689 cm<sup>-1</sup>; **<sup>1</sup>H-NMR** (300 MHz, CDCl<sub>3</sub>, *E* Isomer): δ 8.05 – 8.02 (m, 3H), 7.62 – 7.54 (m, 1H), 7.52 – 7.43 (m, 2H), 7.23 – 7.11 (m, 4H), 4.25 (q, *J* = 7.1 Hz, 2H), 4.17 (s, 2H), 2.32 (s, 3H), 1.27 (t, *J* = 7.1 Hz, 3H); **<sup>1</sup>H-NMR** (300 MHz, CDCl<sub>3</sub>, *Z* Isomer): δ 7.96 – 7.94 (m, 2H), 7.62 – 7.56 (m, 1H), 7.52 – 7.43 (m, 2H), 7.23 – 7.11 (m, 4H), 6.99 (s, 1H), 4.06 (s, 2H), 3.99 (q, *J* = 7.1 Hz, 2H), 2.28 (s, 3H), 0.91 (t, *J* = 7.1 Hz, 3H); **<sup>13</sup>C-NMR** (75 MHz, CDCl<sub>3</sub>, both Isomers): δ 197.59, 197.21, 167.57, 167.30, 141.51, 140.11, 136.92, 136.74, 136.50, 136.30, 135.65, 134.67, 133.32, 133.16, 130.10, 129.49, 128.69, 128.61, 128.59, 128.31, 128.24, 128.21, 128.06, 127.99, 127.80, 125.89, 125.17, 61.10, 60.56, 44.32, 38.03, 19.96, 19.95, 14.19, 13.51; **HRMS** (ESI) *m/z* calculated for C<sub>20</sub>H<sub>21</sub>O<sub>3</sub> ([M+H]<sup>+</sup>) 309.1485, found 309.1487.

#### ethyl 2-(4-(*tert*-butyl)benzylidene)-4-oxo-4-phenylbutanoate (**229na**)

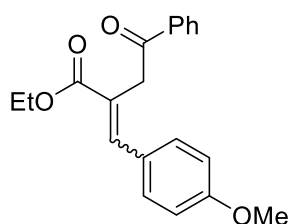


Following general procedure **GP-C** using ethyl (*Z*)-3-(4-(*tert*-butyl)phenyl)-2-chloroacrylate (**228n**, 133 mg, 500 μmol, 1.00 equiv), 1-phenylvinyl acetate (**152a**, 405 mg, 2.50 mmol, 5.00 equiv) and *fac*-Ir(ppy)<sub>3</sub> (6.55 mg, 10.0 μmol, 0.02 equiv) gave (*E*)-**229na** (35.0 mg, 99.8 μmol, 20%) and (*Z*)-**229na** (38.0 mg, 108 μmol, 22%) as yellowish oils as separated *E* and *Z* isomers after purification on SiO<sub>2</sub> (hexanes / EA, 20:1 to 8:1). *E/Z* = 48:52.

**R<sub>f</sub>** (hexanes / EA, 6:1) = 0.32 (*E* Isomer), 0.24 (*Z* Isomer); **IR** (neat): 3060, 3026, 2959, 2907, 2870, 1688, 1599, 1509, 1449, 1379, 1334, 1267, 1211, 1110, 1021, 991, 842, 752, 689cm<sup>-1</sup>; **<sup>1</sup>H-NMR** (300 MHz, CDCl<sub>3</sub>, *E* Isomer): δ 8.05 – 8.00 (m, 3H), 7.62 – 7.56 (m, 1H), 7.51 – 7.46 (m, 2H), 7.39 – 7.35 (m, 2H), 7.28 – 7.24 (m, 2H), 4.28 – 4.20 (m, 4H), 1.33 – 1.23 (m, 12H); **<sup>13</sup>C-NMR** (75 MHz, CDCl<sub>3</sub>, *E* Isomer): δ 197.53, 167.64, 152.06, 141.98, 136.80,

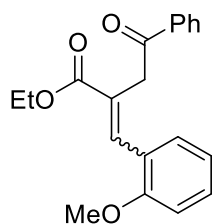
133.21, 132.42, 128.76, 128.65, 128.32, 126.53, 125.59, 61.08, 38.17, 34.75, 31.20, 14.22;  $^1\text{H-NMR}$  (300 MHz,  $\text{CDCl}_3$ , *Z* Isomer):  $\delta$  8.04 – 7.99 (m, 2H), 7.61 – 7.55 (m, 1H), 7.51 – 7.45 (m, 2H), 7.36 – 7.26 (m, 4H), 6.87 (s, 1H), 4.16 – 4.08 (m, 4H), 1.32 (s, 9H), 1.05 (t,  $J$  = 7.1 Hz, 3H);  $^{13}\text{C-NMR}$  (75 MHz,  $\text{CDCl}_3$ , *Z* Isomer):  $\delta$  197.17, 168.12, 151.32, 139.52, 136.50, 133.30, 132.91, 128.68, 128.59, 128.30, 127.00, 124.82, 60.71, 45.16, 34.66, 31.28, 13.64; **HRMS** (ESI)  $m/z$  calculated for  $\text{C}_{23}\text{H}_{27}\text{O}_3$  ( $[\text{M}+\text{H}]^+$ ) 351.1955, found 351.1964.

### ethyl 2-(4-methoxybenzylidene)-4-oxo-4-phenylbutanoate (**229oa**)



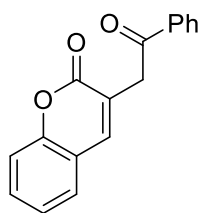
Following general procedure **GP-C** using ethyl (*Z*)-2-chloro-3-(4-methoxyphenyl)acrylate (**228o**, 120 mg, 500  $\mu\text{mol}$ , 1.00 equiv), 1-phenylvinyl acetate (**152a**, 405 mg, 2.50 mmol, 5.00 equiv) and *fac*- $\text{Ir}(\text{ppy})_3$  (6.55 mg, 10.0  $\mu\text{mol}$ , 0.02 equiv) gave (*E*)-**229oa** (25.6 mg, 79.0  $\mu\text{mol}$ , 16%) and (*Z*)-**229oa** (20.1 mg, 62.0  $\mu\text{mol}$ , 12%) as yellowish oils as separated *E* and *Z* isomers after purification on  $\text{SiO}_2$  (hexanes / EA, 20:1 to 8:1).  $E/Z$  = 56:44.

$R_f$  (hexanes / EA, 6:1) = 0.20 (*E* Isomer), 0.16 (*Z* Isomer); **IR** (neat): 3083, 2981, 2937, 2840, 1688, 1606, 1513, 1446, 1371, 1304, 1256, 1215, 1174, 1092, 1028, 916, 834, 760, 693  $\text{cm}^{-1}$ ;  $^1\text{H-NMR}$  (300 MHz,  $\text{CDCl}_3$ , *E* Isomer):  $\delta$  8.03 – 8.01 (m, 3H), 7.61 – 7.57 (m, 1H), 7.51 – 7.47 (m, 2H), 7.29 – 7.26 (m, 2H), 6.88 – 6.85 (m, 2H), 4.26 – 4.20 (m, 4H), 3.80 (s, 3H), 1.27 (t,  $J$  = 7.1 Hz, 3H);  $^{13}\text{C-NMR}$  (101 MHz,  $\text{CDCl}_3$ , *E* Isomer):  $\delta$  197.63, 167.72, 160.10, 141.80, 136.85, 133.21, 130.58, 128.65, 128.32, 127.79, 125.37, 114.09, 61.02, 55.31, 38.14, 14.23;  $^1\text{H-NMR}$  (300 MHz,  $\text{CDCl}_3$ , *Z* Isomer):  $\delta$  8.02 – 8.00 (m, 2H), 7.60 – 7.57 (m, 1H), 7.50 – 7.46 (m, 2H), 7.33 – 7.30 (m, 2H), 6.85 – 6.81 (m, 3H), 4.16 – 4.11 (m, 4H), 3.82 (s, 3H), 1.10 (t,  $J$  = 7.1 Hz, 3H);  $^{13}\text{C-NMR}$  (101 MHz,  $\text{CDCl}_3$ , *Z* Isomer):  $\delta$  197.26, 168.13, 159.66, 139.44, 136.58, 133.27, 130.57, 128.67, 128.29, 128.20, 125.65, 113.31, 60.70, 55.29, 45.26, 13.81; **HRMS** (ESI)  $m/z$  calculated for  $\text{C}_{20}\text{H}_{21}\text{O}_4$  ( $[\text{M}+\text{H}]^+$ ) 325.1434, found 325.1433.

**ethyl 2-(2-methoxybenzylidene)-4-oxo-4-phenylbutanoate (229pa)**

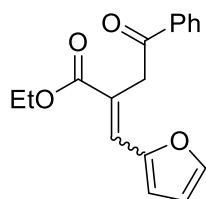
Following general procedure **GP-C** using ethyl (*Z*)-2-chloro-3-(2-methoxyphenyl)acrylate (**228p**, 120 mg, 500  $\mu\text{mol}$ , 1.00 equiv), 1-phenylvinyl acetate (**152a**, 405 mg, 2.50 mmol, 5.00 equiv) and *fac*-Ir(ppy)<sub>3</sub> (6.55 mg, 10.0  $\mu\text{mol}$ , 0.02 equiv) gave (*E*)-**229pa** (23.7 mg, 72.9  $\mu\text{mol}$ , 15%) and (*Z*)-**229pa** (40.3 mg, 124  $\mu\text{mol}$ , 25%) as yellowish oil as separated *E* and *Z* isomer after purification on SiO<sub>2</sub> (hexanes / EA, 20:1 to 6:1). *E/Z* = 37:63.

**R<sub>f</sub>** (hexanes / EA, 6:1) = 0.18 (*E* Isomer), 0.10 (*Z* Isomer); **IR** (neat): 3063, 2981, 2903, 2840, 1684, 1599, 1487, 1326, 1300, 1287, 1211, 1092, 1021, 946, 916, 846, 790, 752, 689  $\text{cm}^{-1}$ ; **<sup>1</sup>H-NMR** (300 MHz, CDCl<sub>3</sub>, *E* Isomer):  $\delta$  8.08 (s, 1H), 8.01 – 7.97 (m, 2H), 7.60 – 7.54 (m, 1H), 7.50 – 7.43 (m, 2H), 7.34 – 7.27 (m, 1H), 7.21 – 7.17 (m, 1H), 6.92 – 6.84 (m, 2H), 4.24 (q, *J* = 7.1 Hz, 2H), 4.13 (s, 2H), 3.82 (s, 3H), 1.28 (t, *J* = 7.1 Hz, 3H); **<sup>13</sup>C-NMR** (75 MHz, CDCl<sub>3</sub>, *E* Isomer):  $\delta$  197.84, 167.45, 157.45, 138.34, 136.85, 133.12, 130.35, 129.49, 128.59, 128.24, 127.47, 124.35, 120.48, 110.58, 61.02, 55.47, 38.51, 14.21; **<sup>1</sup>H-NMR** (300 MHz, CDCl<sub>3</sub>, *Z* Isomer):  $\delta$  8.05 – 8.00 (m, 2H), 7.62 – 7.54 (m, 1H), 7.52 – 7.44 (m, 2H), 7.31 – 7.23 (m, 2H), 6.97 (s, 1H), 6.93 – 6.83 (m, 2H), 4.17 (d, *J* = 1.1 Hz, 2H), 4.07 (q, *J* = 7.1 Hz, 2H), 3.80 (s, 3H), 1.02 (t, *J* = 7.1 Hz, 3H); **<sup>13</sup>C-NMR** (75 MHz, CDCl<sub>3</sub>, *Z* Isomer):  $\delta$  196.16, 167.06, 155.77, 135.54, 134.67, 132.15, 129.18, 128.51, 127.85, 127.57, 127.25, 126.80, 126.73, 124.14, 118.86, 109.20, 59.50, 54.34, 43.98, 12.61; **HRMS** (EI) *m/z* calculated for C<sub>20</sub>H<sub>20</sub>O<sub>4</sub> ([M]<sup>+</sup>) 324.1356, found 324.1350.

**3-(2-oxo-2-phenylethyl)-2H-chromen-2-one (229qa)**

Following general procedure **GP-C** using 3-chloro-2H-chromen-2-one (90.3 mg, 500  $\mu\text{mol}$ , 1.00 equiv), 1-phenylvinyl acetate (**152a**, 405 mg, 2.50 mmol, 5.00 equiv) and *fac*-Ir(ppy)<sub>3</sub> (6.55 mg, 10.0  $\mu\text{mol}$ , 0.02 equiv) gave 3-(2-oxo-2-phenylethyl)-2H-chromen-2-one (34.1 mg, 129  $\mu\text{mol}$ , 26%) as white solid after purification on SiO<sub>2</sub> (hexanes / EA, 10:1 to 6:1).

**R<sub>f</sub>** (hexanes / EA, 6:1) = 0.10; **mp**: 128 °C; **IR** (neat): 3071, 2926, 2855, 1710, 1606, 1449, 1401, 1375, 1334, 1252, 1181, 1073, 991, 957, 924, 827, 752, 685 cm<sup>-1</sup>; **<sup>1</sup>H-NMR** (300 MHz, CDCl<sub>3</sub>):  $\delta$  8.07 – 8.03 (m, 2H), 7.68 (s, 1H), 7.62 – 7.56 (m, 1H), 7.53 – 7.44 (m, 4H), 7.35 – 7.23 (m, 2H), 4.26 (d, *J* = 0.7 Hz, 2H); **<sup>13</sup>C-NMR** (75 MHz, CDCl<sub>3</sub>):  $\delta$  196.01, 161.61, 153.52, 142.14, 136.32, 133.73, 133.62, 131.29, 130.19, 128.78, 128.47, 127.63, 124.49, 123.11, 119.29, 116.61, 39.57; **HRMS** (APCI) *m/z* calculated for C<sub>17</sub>H<sub>13</sub>O<sub>3</sub> ([M+H]<sup>+</sup>) 265.0859, found 265.0862.

**ethyl 2-(furan-2-ylmethylene)-4-oxo-4-phenylbutanoate (229ra)**

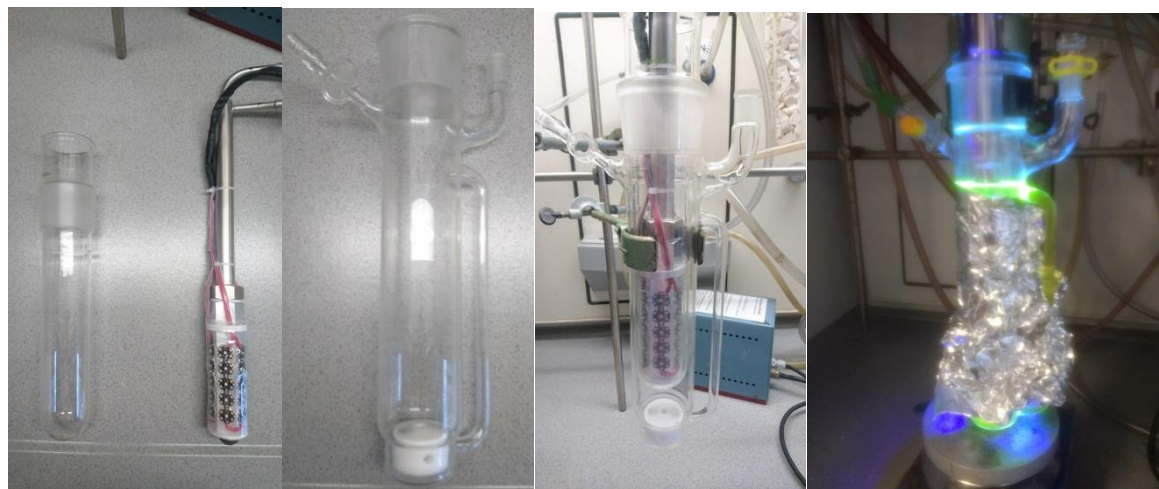
Following general procedure **GP-C** using ethyl (*Z*)-2-chloro-3-(furan-2-yl)acrylate (**228r**, 100 mg, 500  $\mu\text{mol}$ , 1.00 equiv), 1-phenylvinyl acetate (**152a**, 405 mg, 2.50 mmol, 5.00 equiv) and *fac*-Ir(ppy)<sub>3</sub> (3.27 mg, 5.00  $\mu\text{mol}$ , 0.01 equiv) gave (*E*)-**229ra** (3.25 mg, 11.4  $\mu\text{mol}$ , 2.6%) and (*Z*)-**229ra** (1.75 mg, 6.16  $\mu\text{mol}$ , 1.4%) as dark yellow oils as separated *E* and *Z* isomers after purification on SiO<sub>2</sub> (hexanes / EA, 20:1 to 8:1). *E/Z* = 65:35.

**R<sub>f</sub>** (hexanes / EA, 6:1) = 0.24 (*E* Isomer), 0.20 (*Z* Isomer); **IR** (neat): 3063, 3123, 2981, 2933, 1688, 1640, 1599, 1476, 1371, 1328, 1263, 1196, 1088, 1021, 916, 883, 797, 745, 689 cm<sup>-1</sup>;

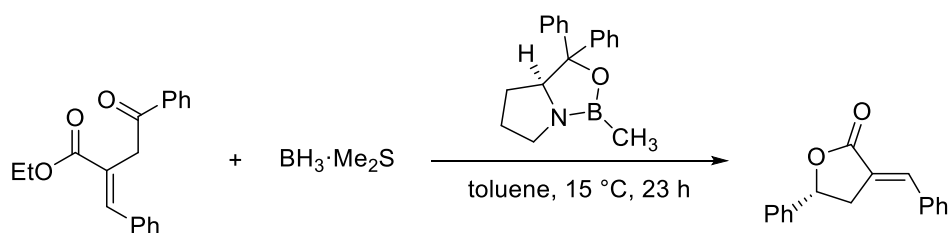
**<sup>1</sup>H-NMR** (300 MHz, CDCl<sub>3</sub>, *E* Isomer): δ 8.08 – 8.04 (m, 2H), 7.66 (s, 1H), 7.63 – 7.57 (m, 1H), 7.53 – 7.47 (m, 2H), 7.38 (d, *J* = 1.7 Hz, 1H), 6.60 (d, *J* = 3.4 Hz, 1H), 6.43 (dd, *J* = 3.4, 1.8 Hz, 1H), 4.53 (s, 2H), 4.24 (q, *J* = 7.1 Hz, 2H), 1.29 (t, *J* = 7.1 Hz, 3H); **<sup>13</sup>C-NMR** (75 MHz, CDCl<sub>3</sub>, *E* Isomer): δ 197.15, 150.31, 143.35, 133.29, 128.68, 128.42, 128.25, 122.27, 115.10, 112.26, 60.77, 45.11, 14.10; **<sup>1</sup>H-NMR** (300 MHz, CDCl<sub>3</sub>, *Z* Isomer): δ 8.01 – 7.98 (m, 2H), 7.62 – 7.56 (m, 1H), 7.51 – 7.43 (m, 4H), 6.69 (s, 1H), 6.47 – 6.46 (m, 1H), 4.23 (q, *J* = 7.1 Hz, 2H), 4.10 (s, 2H), 1.21 (t, *J* = 7.1 Hz, 3H); **<sup>13</sup>C-NMR** (75 MHz, CDCl<sub>3</sub>, *Z* Isomer): δ 195.92, 166.71, 150.21, 143.67, 135.98, 131.98, 127.55, 127.19, 126.72, 121.39, 115.38, 110.98, 60.10, 37.24, 13.21; **HRMS** (ESI) *m/z* calculated for C<sub>17</sub>H<sub>17</sub>O<sub>4</sub> ([M+H]<sup>+</sup>) 285.1121, found 285.1126.



## 6 Photochemical reaction setup for big scale synthesis of **229aa**

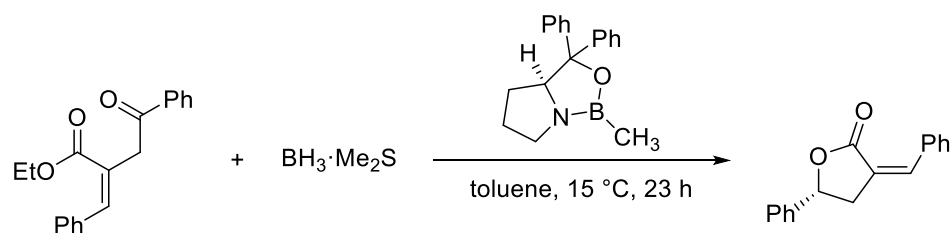


A 200 mL flame dried Schlenk tube equipped with a magnetic stir bar was charged with  $\alpha$ -chloro ethyl cinnamate (**228a**, 4.21 g, 20.0 mmol, 1.00 equiv), 1-phenylvinyl acetate (**152a**, 16.2 g, 100 mmol, 5.00 equiv) and *fac*-Ir(ppy)<sub>3</sub> (65.5 mg, 100  $\mu$ mol, 0.5 mol%). The tube was evacuated, backfilled with N<sub>2</sub> (3x) and subsequently completely filled with freshly degassed dry MeCN (~180 mL). The reaction mixture was magnetically stirred for roughly 15 min under N<sub>2</sub> atmosphere until a homogeneous solution was observed. The tube was sealed with the photoapparatus, which was completely immersed in the reaction mixture. The photoapparatus consisted of a hollow glass cylinder containing a water-cooled metal block wrapped with 30 high power LEDs ( $\lambda = 455$  nm). After irradiation for 48 h, the solvent was evaporated under reduced pressure and 1-phenylvinyl acetate was removed by distillation. The resulting residue was subsequently purified by column chromatography on SiO<sub>2</sub> (hexanes / EA, 20:1 to 12:1) to obtain the separated *E* and *Z* isomers of (*E*)-**229aa** (1.73 g, 5.86 mmol, 29%) and (*Z*)-**229aa** (1.87 g, 6.34 mmol, 32%). *E/Z* = 48:52.

7 Enantioselective synthesis of  $\alpha$ -alkylidene- $\gamma$ -aryl- $\gamma$ -butyrolactone (238)*(R,E)*-3-benzylidene-5-phenyldihydrofuran-2(3*H*)-one (*(R,E)*-238)

A flame dried 10 mL Schlenk flask equipped with a magnetic stir bar was charged with (*S*)-(-)-2-Methyl-CBS-oxazaborolidine (10.4 mg, 37.4 mmol, 10 mol%) and ethyl (*E*)-2-benzylidene-4-oxo-4-phenylbutanoate (*(E)*-**229aa**, 110 mg, 374  $\mu$ mol, 1.00 equiv), sealed with a septum and subsequently evacuated and backfilled with  $N_2$  (3x). Toluene (2 mL) was added and the solution was cooled to  $-15$  °C.  $BH_3 \cdot Me_2S$  (2 M in THF, 243  $\mu$ L, 486  $\mu$ mol, 1.30 equiv) was added and the reaction mixture was magnetically stirred for 23 h at  $-15$  °C. Subsequently, MeOH (1 mL) was added and the mixture was acidified with HCl (1 M) to pH 1-2. After stirring for additional 30 minutes, the reaction mixture was diluted with  $H_2O$  (15 mL) and washed with DCM (3 x 15 mL). The combined organic layers were dried over  $Na_2SO_4$  and evaporated under reduced pressure. The residue was dissolved in DCM (3 mL) and TFA (46.9 mg, 411  $\mu$ mol, 1.10 equiv) was added. After 2 h full lactonization was observed and the reaction was quenched with sat.  $NaHCO_3$  (10 mL) and washed with DCM (3 x 30 mL). The combined organic layers were dried over  $Na_2SO_4$  and evaporated under reduced pressure. The residue was purified by column chromatography on  $SiO_2$  (hexanes / EA, 6:1) to obtain (*R,E*)-3-benzylidene-5-phenyldihydrofuran-2(3*H*)-one as white solid (48.8 mg, 195  $\mu$ mol, 52%).

**R<sub>f</sub>** (hexanes / EA, 4:1) = 0.28; **mp**: 85 °C; **IR** (neat): 3090, 3056, 3030, 2970, 1729, 1647, 1494, 1319, 1226, 1189, 1066, 1021, 984, 764, 685  $cm^{-1}$ ; **<sup>1</sup>H-NMR** (300 MHz,  $CDCl_3$ ):  $\delta$  7.64 (t,  $J$  = 2.9 Hz, 1H), 7.52 – 7.31 (m, 10H), 5.61 (dd,  $J$  = 8.3, 6.0 Hz, 1H), 3.70 (ddd,  $J$  = 17.6, 8.3, 2.7 Hz, 1H), 3.16 (ddd,  $J$  = 17.6, 6.0, 3.1 Hz, 1H); **<sup>13</sup>C-NMR** (75 MHz,  $CDCl_3$ ):  $\delta$  172.04, 140.31, 137.02, 134.56, 130.09, 130.01, 128.98, 128.93, 128.59, 125.41, 124.11, 78.20, 36.57; **HRMS** (EI)  $m/z$  calculated for  $C_{17}H_{14}O_2$  ( $[M]^+$ ) 250.0988, found 250.0992; **Chiral HPLC** performed on Chiralpak AS-H (*n*-heptane / *i*-PrOH = 70:30,  $\lambda$  = 215 nm, 0.5 mL/min).  $t_r$  (minor) = 40.0 min,  $t_r$  (major) = 28.8 min; enantiomeric excess: 79%;  **$[\alpha]_D^{20}$** : -15.4 ( $c$  = 1.00,  $CHCl_3$ ).

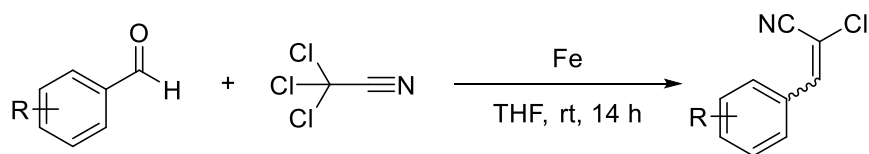
**(*R,Z*)-3-benzylidene-5-phenyldihydrofuran-2(3*H*)-one (*R,Z*)-238)**

A flame dried 25 mL Schlenk flask equipped with a magnetic stir bar was charged with (*S*)-(-)-2-Methyl-CBS-oxazaborolidine (27.7 mg, 100  $\mu\text{mol}$ , 10 mol%) and ethyl (*Z*)-2-benzylidene-4-oxo-4-phenylbutanoate ((*Z*)-**229aa**, 294 mg, 1.00 mmol, 1.00 equiv), sealed with a septum and subsequently evacuated and backfilled with  $\text{N}_2$  (3x). Toluene (6 mL) was added and the solution was cooled to  $-15\text{ }^\circ\text{C}$ .  $\text{BH}_3\cdot\text{Me}_2\text{S}$  (2 M in THF, 650  $\mu\text{L}$ , 1.30 mmol, 1.30 equiv) was added and the reaction mixture was magnetically stirred for 23 h at  $-15\text{ }^\circ\text{C}$ . Subsequently, MeOH (3 mL) was added and the mixture was acidified with HCl (1 M) to pH 1-2. After stirring for additional 30 minutes, the reaction mixture was diluted with  $\text{H}_2\text{O}$  (40 mL) and washed with DCM (3 x 40 mL). The combined organic layers were dried over  $\text{Na}_2\text{SO}_4$  and evaporated under reduced pressure. The residue was dissolved in DCM (8 mL) and TFA (125 mg, 1.10 mmol, 1.10 equiv) was added. After 2 h full lactonization was observed and the reaction was quenched with sat.  $\text{NaHCO}_3$  (20 mL) and washed with DCM (3 x 20 mL). The combined organic layers were dried over  $\text{Na}_2\text{SO}_4$  and evaporated under reduced pressure. The residue was purified by column chromatography on  $\text{SiO}_2$  (hexanes / EA, 8:1) to obtain (*R,Z*)-3-benzylidene-5-phenyldihydrofuran-2(3*H*)-one as white solid (175 mg, 700  $\mu\text{mol}$ , 70%).

**$R_f$**  (hexanes / EA, 4:1) = 0.30; **mp**:  $123\text{ }^\circ\text{C}$ ; **IR** (neat): 3034, 2922, 1751, 1654, 1494, 1349, 1215, 1170, 1099, 1023, 928, 730, 693  $\text{cm}^{-1}$ ;  **$^1\text{H-NMR}$**  (400 MHz,  $\text{CDCl}_3$ ):  $\delta$  7.87 (d,  $J = 7.3$  Hz, 2H), 7.44 – 7.33 (m, 8H), 7.01 (s, 1H), 5.57 (t,  $J = 7.3$  Hz, 1H), 3.52 (dd,  $J = 16.6, 7.1$  Hz, 1H), 3.12 (dd,  $J = 16.6, 7.1$  Hz, 1H);  **$^{13}\text{C-NMR}$**  (101 MHz,  $\text{CDCl}_3$ ):  $\delta$  168.31, 139.88, 139.79, 133.59, 130.72, 129.65, 128.85, 128.54, 128.21, 125.54, 124.38, 77.86, 40.32; **HRMS** (ESI)  $m/z$  calculated for  $\text{C}_{17}\text{H}_{14}\text{O}_2$  ( $[\text{M}]^+$ ) 250.0988, found 250.0993. **Chiral HPLC** performed on Phenomenex Lux Cellulose-1 (*n*-heptane / *i*-PrOH = 98:2,  $\lambda = 215$  nm, 0.5 mL/min).  $t_r$  (minor) = 77.5 min,  $t_r$  (major) = 72.9 min; enantiomeric excess: 89%;  **$[\alpha]_D^{20}$** : +78.4 ( $c = 1.00, \text{CHCl}_3$ ).

## 8 Synthesis of $\alpha$ -chloro cinnamitriles (248a – 248h)

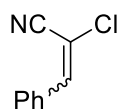
### General procedure (GP-D) for the synthesis of $\alpha$ -chloro cinnamitriles<sup>[198]</sup>



A flame dried 250 mL two-neck-flask equipped with a magnetic stir bar was charged with aromatic aldehyde (10.0 mmol, 1.00 equiv), 2,2,2-trichloroacetonitrile (11.0 mmol, 1.10 equiv) and Fe powder (100 mmol, 10.0 equiv) and dry THF (100 mL) under nitrogen atmosphere. The reaction mixture was magnetically stirred for 14 h. Upon completion, the reaction was filtered, THF was removed *in vacuo* and the crude product was purified by column chromatography on SiO<sub>2</sub> (hexanes / EA, 15:1) to obtain the pure product as *E/Z* mixture.

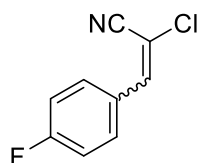
*Note: Following this procedure gives the E isomer as major diastereomer which is in accordance to analytical data of the literature.*<sup>[198,261]</sup>

### 2-chloro-3-phenylacrylonitrile (248a)



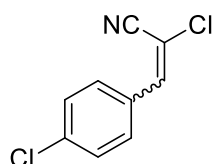
Following general procedure **GP-D** using benzaldehyde (2.02 mL, 20.0 mmol, 1.00 equiv), 2,2,2-trichloroacetonitrile (2.21 mL, 22.0 mmol, 1.10 equiv) and Fe powder (11.2 g, 200 mmol, 10.0 equiv) gave 2-chloro-3-phenylacrylonitrile (1.51 g, 9.23 mmol, 46%) as colorless oil after purification on SiO<sub>2</sub> (hexanes / EA, 15:1). *E/Z* = 83:17.

**R<sub>f</sub>** (hexanes / EA, 10:1) = 0.40; **<sup>1</sup>H-NMR** (300 MHz, CDCl<sub>3</sub>, *E* Isomer):  $\delta$  7.70 – 7.67 (m, 2H), 7.48 – 7.43 (m, 3H), 7.37 (s, 1H); **<sup>1</sup>H-NMR** (300 MHz, CDCl<sub>3</sub>, *Z* Isomer):  $\delta$  7.76 – 7.73 (m, 2H), 7.48 – 7.43 (m, 3H), 7.35 (s, 1H); **<sup>13</sup>C-NMR** (75 MHz, CDCl<sub>3</sub>, both Isomers):  $\delta$  145.35, 142.33, 131.38, 131.28, 130.42, 129.21, 128.89, 128.68, 115.12, 100.26.

**2-chloro-3-(4-fluorophenyl)acrylonitrile (248b)**

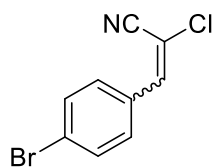
Following general procedure **GP-D** using 4-fluorobenzaldehyde (1.05 mL, 10.0 mmol, 1.00 equiv), 2,2,2-trichloroacetonitrile (1.10 mL, 11.0 mmol, 1.10 equiv) and Fe powder (5.58 g, 100 mmol, 10.0 equiv) gave 2-chloro-3-(4-fluorophenyl)acrylonitrile (665 mg, 3.66 mmol, 37%) as yellow solid after purification on SiO<sub>2</sub> (hexanes / EA, 15:1). *E/Z* = 74:26.

**R<sub>f</sub>** (hexanes / EA, 10:1) = 0.40; **IR** (neat): 3078, 3041, 2929, 2217, 1602, 1509, 1356, 1289, 1241, 1207, 1166, 1107, 1058, 1017, 827, 711 cm<sup>-1</sup>; **<sup>1</sup>H-NMR** (400 MHz, CDCl<sub>3</sub>, *E* Isomer): δ 7.72 – 7.68 (m, 2H), 7.32 (s, 1H), 7.17 – 7.11 (m, 2H); **<sup>1</sup>H-NMR** (400 MHz, CDCl<sub>3</sub>, *Z* Isomer): δ 7.80 – 7.74 (m, 2H), 7.31 (s, 1H), 7.19 – 7.10 (m, 2H); **<sup>13</sup>C-NMR** (101 MHz, CDCl<sub>3</sub>, both Isomers): δ 165.38, 162.86, 144.02, 140.98, 132.73, 132.64, 130.93, 130.84, 127.70, 127.66, 116.63, 116.41, 116.34, 116.12, 115.01, 100.05, 100.02; **<sup>19</sup>F-NMR** (376 MHz, CDCl<sub>3</sub>, both Isomers): δ -106.91, -107.36; **HRMS** (ESI) *m/z* calculated for C<sub>9</sub>H<sub>5</sub>NFCl ([M]<sup>+</sup>) 181.0089, found 181.0093.

**2-chloro-3-(4-chlorophenyl)acrylonitrile (248c)**

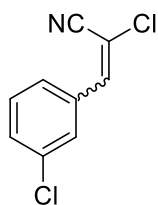
Following general procedure **GP-D** using 4-chlorobenzaldehyde (1.41 g, 10.0 mmol, 1.00 equiv), 2,2,2-trichloroacetonitrile (1.10 mL, 11.0 mmol, 1.10 equiv) and Fe powder (5.58 g, 100 mmol, 10.0 equiv) gave 2-chloro-3-(4-chlorophenyl)acrylonitrile (1.25 g, 6.31 mmol, 63%) as white solid after purification on SiO<sub>2</sub> (hexanes / EA, 15:1). *E/Z* = 71:29.

**R<sub>f</sub>** (hexanes / EA, 10:1) = 0.30; **<sup>1</sup>H-NMR** (300 MHz, CDCl<sub>3</sub>, *E* Isomer): δ 7.65 – 7.60 (m, 2H), 7.45 – 7.40 (m, 2H), 7.32 (s, 1H); **<sup>1</sup>H-NMR** (300 MHz, CDCl<sub>3</sub>, *Z* Isomer): δ 7.71 – 7.67 (m, 2H), 7.45 – 7.40 (m, 2H), 7.30 (s, 1H); **<sup>13</sup>C-NMR** (75 MHz, CDCl<sub>3</sub>, both Isomers): δ 143.95, 140.97, 137.37, 131.59, 130.14, 129.88, 129.78, 129.55, 129.25, 116.17, 114.87, 102.03, 100.87.

**3-(4-bromophenyl)-2-chloroacrylonitrile (248d)**

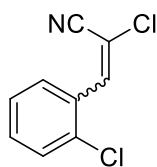
Following general procedure **GP-D** using 4-bromobenzaldehyde (1.85 g, 10.0 mmol, 1.00 equiv), 2,2,2-trichloroacetonitrile (1.10 mL, 11.0 mmol, 1.10 equiv) and Fe powder (5.58 g, 100 mmol, 10.0 equiv) gave 3-(4-bromophenyl)-2-chloroacrylonitrile (1.60 g, 6.60 mmol, 66%) as yellow solid after purification on SiO<sub>2</sub> (hexanes / EA, 15:1). *E/Z* = 71:29.

**R<sub>f</sub>** (hexanes / EA, 10:1) = 0.36; **<sup>1</sup>H-NMR** (400 MHz, CDCl<sub>3</sub>, *E* Isomer): δ 7.62 – 7.54 (m, 4H), 7.30 (s, 1H); **<sup>1</sup>H-NMR** (400 MHz, CDCl<sub>3</sub>, *Z* Isomer): δ 7.76 – 7.68 (m, 1H), 7.62 – 7.54 (m, 3H), 7.28 (s, 1H); **<sup>13</sup>C-NMR** (101 MHz, CDCl<sub>3</sub>, both Isomers): δ 144.07, 141.09, 132.53, 132.49, 132.24, 131.72, 131.02, 130.56, 130.21, 130.03, 125.90, 125.81, 116.20, 114.88, 102.18, 101.00.

**2-chloro-3-(3-chlorophenyl)acrylonitrile (248e)**

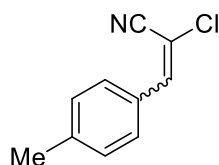
Following general procedure **GP-D** using 3-chlorobenzaldehyde (1.13 mL, 10.0 mmol, 1.00 equiv), 2,2,2-trichloroacetonitrile (1.10 mL, 11.0 mmol, 1.10 equiv) and Fe powder (5.58 g, 100 mmol, 10.0 equiv) gave 2-chloro-3-(3-chlorophenyl)acrylonitrile (1.23 g, 6.21 mmol, 62%) as colorless oil after purification on SiO<sub>2</sub> (hexanes / EA, 15:1). *E/Z* = 76:24.

**R<sub>f</sub>** (hexanes / EA, 10:1) = 0.40; **IR** (neat): 3063, 2221, 1561, 1479, 1416, 1341, 1282, 1207, 1103, 1013, 920, 875, 779, 674 cm<sup>-1</sup>; **<sup>1</sup>H-NMR** (400 MHz, CDCl<sub>3</sub>, *E* Isomer): δ 7.61 – 7.57 (m, 2H), 7.44 – 7.36 (m, 2H), 7.29 (s, 1H); **<sup>1</sup>H-NMR** (400 MHz, CDCl<sub>3</sub>, *Z* Isomer): δ 7.73 – 7.72 (m, 1H), 7.61 – 7.57 (m, 1H), 7.44 – 7.36 (m, 2H), 7.28 (s, 1H); **<sup>13</sup>C-NMR** (101 MHz, CDCl<sub>3</sub>, both isomers): δ 143.74, 140.87, 135.23, 134.91, 133.24, 132.98, 131.23, 130.52, 130.19, 129.95, 128.68, 128.56, 126.53, 116.01, 114.66, 102.95, 101.88; **HRMS** (EI) *m/z* calculated for C<sub>9</sub>H<sub>5</sub>NCl<sub>2</sub> ([M]<sup>+</sup>) 196.9794, found 196.9798.

**2-chloro-3-(2-chlorophenyl)acrylonitrile (248f)**

Following general procedure **GP-D** using 2-chlorobenzaldehyde (1.12 mL, 10.0 mmol, 1.00 equiv), 2,2,2-trichloroacetonitrile (1.10 mL, 11.0 mmol, 1.10 equiv) and Fe powder (5.58 g, 100 mmol, 10.0 equiv) gave 2-chloro-3-(2-chlorophenyl)acrylonitrile (1.39 g, 7.02 mmol, 70%) as white solid after purification on SiO<sub>2</sub> (hexanes / EA, 15:1). *E/Z* = 75:25.

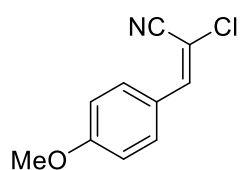
**R<sub>f</sub>** (hexanes / EA, 10:1) = 0.40; **IR** (neat): 3194, 3097, 3071, 3041, 2221, 1587, 1464, 1431, 1282, 1207, 1159, 1051, 1010, 950, 887, 864, 831, 745, 693 cm<sup>-1</sup>; **<sup>1</sup>H-NMR** (400 MHz, CDCl<sub>3</sub>, *E* Isomer): δ 7.92 – 7.89 (m, 1H), 7.72 (s, 1H), 7.48 – 7.45 (m, 1H), 7.41 – 7.33 (m, 2H); **<sup>1</sup>H-NMR** (400 MHz, CDCl<sub>3</sub>, *Z* Isomer): δ 7.92 – 7.89 (m, 1H), 7.69 (s, 1H), 7.48 – 7.45 (m, 1H), 7.41 – 7.33 (m, 2H); **<sup>13</sup>C-NMR** (101 MHz, CDCl<sub>3</sub>, both Isomers): δ 142.01, 139.14, 134.71, 134.27, 132.15, 131.94, 130.49, 130.14, 130.05, 129.95, 129.82, 128.91, 127.50, 126.86, 115.88, 114.46, 104.05, 103.20; **HRMS** (EI) *m/z* calculated for C<sub>9</sub>H<sub>5</sub>NCl<sub>2</sub> ([M]<sup>+</sup>) 196.9794, found 196.9794.

**2-chloro-3-(*p*-tolyl)acrylonitrile (248g)**

Following general procedure **GP-D** using 4-methylbenzaldehyde (1.18 mL, 10.0 mmol, 1.00 equiv), 2,2,2-trichloroacetonitrile (1.10 mL, 11.0 mmol, 1.10 equiv) and Fe powder (5.58 g, 100 mmol, 10.0 equiv) gave 2-chloro-3-(*p*-tolyl)acrylonitrile (1.07 g, 6.02 mmol, 60%) as colorless oil after purification on SiO<sub>2</sub> (hexanes / EA, 15:1). *E/Z* = 74:26.

**R<sub>f</sub>** (hexanes / EA, 10:1) = 0.40; **<sup>1</sup>H-NMR** (300 MHz, CDCl<sub>3</sub>, *E* Isomer): δ 7.60 – 7.57 (m, 2H), 7.32 (s, 1H), 7.26 – 7.23 (m, 2H), 2.40 (s, 3H); **<sup>1</sup>H-NMR** (300 MHz, CDCl<sub>3</sub>, *Z* Isomer): δ 7.67 – 7.64 (m, 2H), 7.30 (s, 1H), 7.26 – 7.23 (m, 2H), 2.40 (s, 3H); **<sup>13</sup>C-NMR** (75 MHz, CDCl<sub>3</sub>, both Isomers): δ 145.34, 142.25, 142.09, 142.02, 130.50, 129.91, 129.62, 128.69, 115.36, 99.01, 21.66, 21.62.

**(E)-2-chloro-3-(4-methoxyphenyl)acrylonitrile (248h)**



*Note: Reaction had to be heated to 55 °C.*

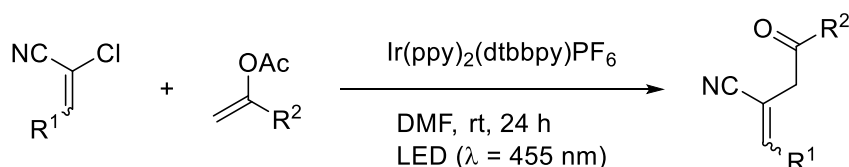
Following general procedure **GP-D** at 55 °C using 4-methoxybenzaldehyde (1.22 mL, 10.0 mmol, 1.00 equiv), 2,2,2-trichloroacetonitrile (1.10 mL, 11.0 mmol, 1.10 equiv) and Fe powder (5.58 g, 100 mmol, 10.0 equiv) gave (*E*)-2-chloro-3-(4-methoxyphenyl)acrylonitrile (440 mg, 2.27 mmol, 23%) as yellow solid after purification on SiO<sub>2</sub> (hexanes / EA, 15:1).

**R<sub>f</sub>** (hexanes / EA, 10:1) = 0.14; **<sup>1</sup>H-NMR** (300 MHz, CDCl<sub>3</sub>, *E* Isomer): δ 7.70 – 7.64 (m, 2H), 7.27 (s, 1H), 6.97 – 6.92 (m, 2H), 3.86 (s, 3H); **<sup>13</sup>C-NMR** (75 MHz, CDCl<sub>3</sub>, *E* Isomer): δ 161.90, 144.87, 130.61, 124.07, 114.60, 97.24, 55.49.



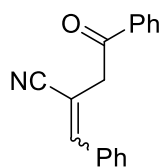
## 9 Photochemical functionalization of $\alpha$ -chloro cinnamitriles (249aa – 249ga)

### General procedure (GP-E) for the photochemical functionalization of $\alpha$ -chloro cinnamates



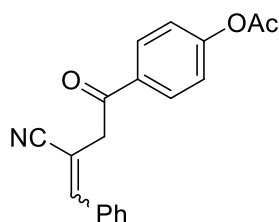
A flame dried Schlenk tube equipped with a magnetic stir bar was charged with  $\alpha$ -chloro cinnamitrile (500  $\mu$ mol, 1.00 equiv), enol acetate (2.50 mmol, 5.00 equiv) and Ir(ppy)<sub>2</sub>(dtbbpy)PF<sub>6</sub> (10.0  $\mu$ mol, 2.0 mol%). The flask was sealed with a plastic screw-cap, evacuated and backfilled with N<sub>2</sub> (3x). DMF (2.5 mL) was added and the reaction was magnetically stirred for roughly 5 min under N<sub>2</sub> atmosphere until a homogeneous solution was observed. The resulting mixture was degassed by freeze-pump-thaw (3 cycles) and the plastic screw-cap was replaced by another plastic screw-cap with a Teflon sealed inlet for a glass rod. A high power LED ( $\lambda = 455$  nm) was attached to the top of the glass rod, which then could act as an optical fiber. After irradiation for 24 h the LED was removed, the mixture was diluted with H<sub>2</sub>O (30 mL) and washed with DCM (3 x 25 mL). The combined organic layers were dried over Na<sub>2</sub>SO<sub>4</sub>, the solvent was removed *in vacuo* and the residue was purified by column chromatography on SiO<sub>2</sub> (hexanes / EA, 8:1) to obtain the separated *E* and *Z* isomers.

*Note: In some cases it was not possible to separate both isomers completely.*

**2-benzylidene-4-oxo-4-phenylbutanenitrile (249aa)**

Following general procedure **GP-E** using 2-chloro-3-phenylacrylonitrile (**248a**, 32.7 mg, 200  $\mu\text{mol}$ , 1.00 equiv), 1-phenylvinyl acetate (**152a**, 162 mg, 1.00 mmol, 5.00 equiv) and  $\text{Ir}(\text{ppy})_2(\text{dtbbpy})\text{PF}_6$  (3.66 mg, 4.00  $\mu\text{mol}$ , 0.02 equiv) gave (*E*)-**249aa** (20.2 mg, 81.2  $\mu\text{mol}$ , 41%) as yellow solid and (*Z*)-**249aa** (12.4 mg, 49.8  $\mu\text{mol}$ , 25%) as yellow oil as separated *E* and *Z* isomers after purification on  $\text{SiO}_2$  (hexanes / EA, 8:1 to 4:1). *E/Z* = 62:38.

**R<sub>f</sub>** (hexanes / EA, 6:1) = 0.18 (*E* Isomer), 0.13 (*Z* Isomer); **mp** (*E* Isomer): 90 °C; **IR** (neat): 3060, 3030, 2212, 1751, 1684, 1625, 1446, 1328, 1215, 991, 749, 689  $\text{cm}^{-1}$ ; **<sup>1</sup>H-NMR** (300 MHz,  $\text{CDCl}_3$ , *E* Isomer):  $\delta$  7.98 – 7.94 (m, 2H), 7.66 – 7.59 (m, 1H), 7.57 (s, 1H), 7.54 – 7.47 (m, 2H), 7.39 – 7.34 (m, 3H), 7.27 – 7.22 (m, 2H), 4.14 (d, *J* = 0.7 Hz, 2H); **<sup>13</sup>C-NMR** (75 MHz,  $\text{CDCl}_3$ , *E* Isomer):  $\delta$  194.50, 147.83, 135.72, 134.00, 133.45, 129.74, 128.94, 128.93, 128.63, 128.33, 119.97, 108.63, 39.78; **<sup>1</sup>H-NMR** (300 MHz,  $\text{CDCl}_3$ , *Z* Isomer):  $\delta$  8.03 – 7.98 (m, 2H), 7.81 – 7.76 (m, 2H), 7.66 – 7.59 (m, 1H), 7.55 – 7.48 (m, 2H), 7.45 – 7.40 (m, 3H), 7.05 (s, 1H), 4.08 (d, *J* = 1.0 Hz, 2H); **<sup>13</sup>C-NMR** (75 MHz,  $\text{CDCl}_3$ , *Z* Isomer):  $\delta$  194.59, 147.41, 135.81, 133.92, 133.30, 130.53, 128.93, 128.91, 128.87, 128.33, 118.50, 104.07, 44.71; **HRMS** (ESI) *m/z* calculated for  $\text{C}_{17}\text{H}_{13}\text{NO}$  ( $[\text{M}]^+$ ) 247.0992, found 247.0985.

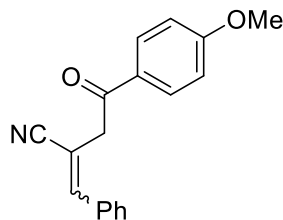
**4-(3-cyano-4-phenylbut-3-enoyl)phenyl acetate (249ab)**

Following general procedure **GP-E** using 2-chloro-3-phenylacrylonitrile (**248a**, 81.8 mg, 500  $\mu\text{mol}$ , 1.00 equiv), 1-(4-acetoxyphenyl)vinyl acetate (**152c**, 551 mg, 2.50 mmol, 5.00 equiv) and  $\text{Ir}(\text{ppy})_2(\text{dtbbpy})\text{PF}_6$  (9.14 mg, 10.0  $\mu\text{mol}$ , 0.02 equiv) gave (*E*)-**249ab** (71.7 mg, 216  $\mu\text{mol}$ , 47%) as yellow solid and (*Z*)-**249ab** (40.3 mg, 121  $\mu\text{mol}$ , 26%) as yellow oil

as separated *E* and *Z* isomers after purification on SiO<sub>2</sub> (hexanes / EA, 8:1 to 2:1). *E/Z* = 64:36.

**R<sub>f</sub>** (hexanes / EA, 2:1) = 0.40 (*E* Isomer), 0.30 (*Z* Isomer); **mp** (*E* Isomer): 115 °C; **IR** (neat): 3063, 2937, 2214, 1769, 1684, 1599, 1502, 1446, 1412, 1367, 1326, 1189, 1162, 998, 909, 853, 740, 697 cm<sup>-1</sup>; **<sup>1</sup>H-NMR** (300 MHz, CDCl<sub>3</sub>, *E* Isomer): δ 8.02 – 7.97 (m, 2H), 7.57 (s, 1H), 7.40 – 7.36 (m, 3H), 7.26 – 7.20 (m, 4H), 4.11 (d, *J* = 0.7 Hz, 2H), 2.34 (s, 3H); **<sup>13</sup>C-NMR** (75 MHz, CDCl<sub>3</sub>, *E* Isomer): δ 193.25, 168.82, 154.99, 147.92, 133.38, 133.23, 130.01, 129.80, 128.98, 128.60, 122.18, 119.92, 108.43, 39.78, 21.19; **<sup>1</sup>H-NMR** (300 MHz, CDCl<sub>3</sub>, *Z* Isomer): δ 8.06 – 8.01 (m, 2H), 7.81 – 7.76 (m, 2H), 7.44 – 7.41 (m, 3H), 7.27 – 7.23 (m, 2H), 7.04 (s, 1H), 4.06 (d, *J* = 1.0 Hz, 2H), 2.34 (s, 3H); **<sup>13</sup>C-NMR** (75 MHz, CDCl<sub>3</sub>, *Z* Isomer): δ 193.36, 168.78, 154.94, 147.50, 133.34, 133.24, 130.57, 129.99, 128.92, 128.88, 122.17, 118.46, 103.87, 44.67, 21.20; **HRMS** (EI) *m/z* calculated for C<sub>19</sub>H<sub>15</sub>NO<sub>3</sub> ([M]<sup>+</sup>) 305.1046, found 305.1043.

## 2-benzylidene-4-(4-methoxyphenyl)-4-oxobutanenitrile (**249ac**)

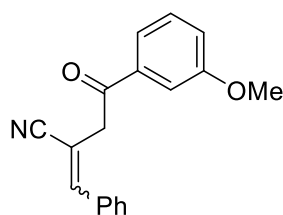


Following general procedure **GP-E** using 2-chloro-3-phenylacrylonitrile (**248a**, 81.8 mg, 500 μmol, 1.00 equiv), 1-(4-methoxyphenyl)vinyl acetate (**152b**, 481 mg, 2.50 mmol, 5.00 equiv) and Ir(ppy)<sub>2</sub>(dtbbpy)PF<sub>6</sub> (9.14 mg, 10.0 μmol, 0.02 equiv) gave (*E*)-**249ac** (55.7 mg, 200 μmol, 40%) as yellow solid and (*Z*)-**249ac** (38.7 mg, 139 μmol, 28%) as yellow oil as separated *E* and *Z* isomers after purification on SiO<sub>2</sub> (hexanes / EA, 6:1 to 4:1). *E/Z* = 59:41.

**R<sub>f</sub>** (hexanes / EA, 6:1) = 0.10 (*E* Isomer), 0.08 (*Z* Isomer); **mp** (*E* Isomer): 110 °C; **IR** (neat): 3056, 3011, 2963, 2840, 2214, 1763, 1673, 1595, 1505, 1446, 1420, 1319, 1259, 1218, 1170, 1114, 1028, 831, 745, 697 cm<sup>-1</sup>; **<sup>1</sup>H-NMR** (300 MHz, CDCl<sub>3</sub>, *E* Isomer): δ 7.95 – 7.90 (m, 2H), 7.53 (s, 1H), 7.38 – 7.33 (m, 3H), 7.27 – 7.22 (m, 2H), 6.98 – 6.92 (m, 2H), 4.08 (d, *J* = 0.8 Hz, 2H), 3.87 (s, 3H); **<sup>13</sup>C-NMR** (75 MHz, CDCl<sub>3</sub>, *E* Isomer): δ 192.99, 164.17, 147.58,

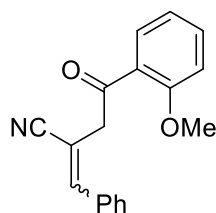
133.50, 130.70, 129.71, 128.91, 128.77, 128.70, 120.13, 114.08, 108.94, 55.62, 39.42;  $^1\text{H-NMR}$  (300 MHz,  $\text{CDCl}_3$ , *Z* Isomer):  $\delta$  8.01 – 7.95 (m, 2H), 7.80 – 7.75 (m, 2H), 7.45 – 7.38 (m, 3H), 7.04 (s, 1H), 7.00 – 6.94 (m, 2H), 4.02 (d,  $J = 1.0$  Hz, 2H), 3.88 (s, 3H);  $^{13}\text{C-NMR}$  (75 MHz,  $\text{CDCl}_3$ , *Z* Isomer):  $\delta$  193.09, 164.10, 147.19, 133.37, 130.72, 130.45, 128.88, 128.85, 118.61, 114.08, 104.41, 55.59, 44.37; **HRMS** (ESI)  $m/z$  calculated for  $\text{C}_{18}\text{H}_{16}\text{NO}_2$  ( $[\text{M}+\text{H}]^+$ ) 278.1176, found 278.1178.

### 2-benzylidene-4-(3-methoxyphenyl)-4-oxobutanenitrile (**249ad**)



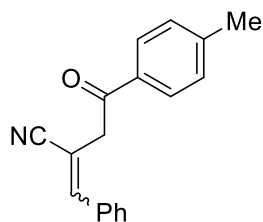
Following general procedure **GP-E** using 2-chloro-3-phenylacrylonitrile (**248a**, 81.8 mg, 500  $\mu\text{mol}$ , 1.00 equiv), 1-(3-methoxyphenyl)vinyl acetate (**152d**, 481 mg, 2.50 mmol, 5.00 equiv) and  $\text{Ir}(\text{ppy})_2(\text{dtbbpy})\text{PF}_6$  (9.14 mg, 10.0  $\mu\text{mol}$ , 0.02 equiv) gave (*E*)-**249ad** (61.6 mg, 222  $\mu\text{mol}$ , 45%) and (*Z*)-**249ad** (27.7 mg, 99.8  $\mu\text{mol}$ , 20%) as yellow oils as separated *E* and *Z* isomers after purification on  $\text{SiO}_2$  (hexanes / EA, 10:1 to 4:1).  $E/Z = 69:31$ .

$R_f$  (hexanes / EA, 4:1) = 0.24 (*E* Isomer), 0.20 (*Z* Isomer); **IR** (neat): 3060, 3004, 2940, 2836, 2214, 1684, 1580, 1487, 1431, 1319, 1256, 1102, 1080, 1043, 1013, 928, 875, 775, 685  $\text{cm}^{-1}$ ;  $^1\text{H-NMR}$  (400 MHz,  $\text{CDCl}_3$ , *E* Isomer):  $\delta$  7.55 (s, 1H), 7.51 – 7.48 (m, 2H), 7.41 – 7.35 (m, 4H), 7.26 – 7.22 (m, 2H), 7.16 (ddd,  $J = 8.2, 2.5, 0.9$  Hz, 1H), 4.12 (d,  $J = 0.5$  Hz, 2H), 3.85 (s, 3H);  $^{13}\text{C-NMR}$  (101 MHz,  $\text{CDCl}_3$ , *E* Isomer):  $\delta$  194.36, 160.05, 147.77, 137.08, 133.46, 129.91, 129.77, 128.96, 128.66, 120.87, 120.51, 119.98, 112.55, 108.67, 55.54, 39.91;  $^1\text{H-NMR}$  (400 MHz,  $\text{CDCl}_3$ , *Z* Isomer):  $\delta$  7.80 – 7.76 (m, 2H), 7.58 – 7.52 (m, 2H), 7.44 – 7.39 (m, 4H), 7.16 (ddd,  $J = 8.2, 2.5, 0.7$  Hz, 1H), 7.04 (s, 1H), 4.06 (s, 2H), 3.87 (s, 3H);  $^{13}\text{C-NMR}$  (101 MHz,  $\text{CDCl}_3$ , *Z* Isomer):  $\delta$  194.46, 160.06, 147.37, 137.17, 133.33, 130.53, 129.91, 128.92, 128.89, 120.90, 120.45, 118.51, 112.54, 104.14, 55.54, 44.84; **HRMS** (APCI)  $m/z$  calculated for  $\text{C}_{18}\text{H}_{19}\text{N}_2\text{O}_2$  ( $[\text{M}+\text{NH}_4]^+$ ) 295.1441, found 295.1448.

**2-benzylidene-4-(2-methoxyphenyl)-4-oxobutanenitrile (249ae)**

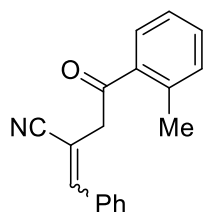
Following general procedure **GP-E** using 2-chloro-3-phenylacrylonitrile (**248a**, 81.8 mg, 500  $\mu\text{mol}$ , 1.00 equiv), 1-(2-methoxyphenyl)vinyl acetate (**152e**, 481 mg, 2.50 mmol, 5.00 equiv) and  $\text{Ir}(\text{ppy})_2(\text{dtbbpy})\text{PF}_6$  (9.14 mg, 10.0  $\mu\text{mol}$ , 0.02 equiv) gave **249ae** (113 mg, 407  $\mu\text{mol}$ , 82%) as orange oil as combined mixture of *E* and *Z* isomers after purification on  $\text{SiO}_2$  (hexanes / EA, 10:1 to 4:1). *E/Z* = 64:36.

**R<sub>f</sub>** (hexanes / EA, 4:1) = 0.32; **IR** (neat): 3060, 3026, 2944, 2840, 2214, 1669, 1595, 1483, 1435, 1244, 1223, 1192, 1110, 1054, 1021, 995, 928, 894, 816, 152, 693  $\text{cm}^{-1}$ ; **<sup>1</sup>H-NMR** (400 MHz,  $\text{CDCl}_3$ , *E* Isomer):  $\delta$  7.80 (dd,  $J = 7.7, 1.7$  Hz, 1H), 7.76 (dd,  $J = 7.4, 1.8$  Hz, 1H), 7.55 – 7.49 (m, 1H), 7.47 (s, 1H), 7.42 – 7.40 (m, 1H), 7.38 – 7.35 (m, 2H), 7.29 – 7.27 (m, 1H), 7.07 – 6.99 (m, 2H), 4.17 (s, 2H), 3.86 (s, 3H); **<sup>1</sup>H-NMR** (400 MHz,  $\text{CDCl}_3$ , *Z* Isomer):  $\delta$  7.85 (dd,  $J = 7.8, 1.7$  Hz, 1H), 7.55 – 7.49 (m, 1H), 7.42 – 7.40 (m, 1H), 7.38 – 7.35 (m, 2H), 7.29 – 7.27 (m, 1H), 7.07 – 6.99 (m, 3H), 6.96 (s, 1H), 4.08 (d,  $J = 0.8$  Hz, 2H), 3.98 (s, 3H); **<sup>13</sup>C-NMR** (75 MHz,  $\text{CDCl}_3$ , both Isomers):  $\delta$  196.23, 196.16, 159.03, 158.93, 147.10, 146.65, 134.67, 134.61, 133.70, 133.57, 131.07, 130.99, 130.25, 129.57, 128.87, 128.84, 128.80, 128.77, 126.58, 126.42, 120.97, 120.41, 118.85, 111.63, 111.56, 109.31, 105.10, 55.62, 55.53, 49.65, 44.97; **HRMS** (APCI)  $m/z$  calculated for  $\text{C}_{18}\text{H}_{16}\text{NO}_2$  ( $[\text{M}+\text{H}]^+$ ) 278.1176, found 278.1179.

**2-benzylidene-4-oxo-4-(*p*-tolyl)butanenitrile (249af)**

Following general procedure **GP-E** using 2-chloro-3-phenylacrylonitrile (**248a**, 81.8 mg, 500  $\mu\text{mol}$ , 1.00 equiv), 1-(*p*-tolyl)vinyl acetate (**152f**, 441 mg, 2.50 mmol, 5.00 equiv) and  $\text{Ir}(\text{ppy})_2(\text{dtbbpy})\text{PF}_6$  (9.14 mg, 10.0  $\mu\text{mol}$ , 0.02 equiv) gave (*E*)-**249af** (57.8 mg, 221  $\mu\text{mol}$ , 44%) and (*Z*)-**249af** (24.8 mg, 94.8  $\mu\text{mol}$ , 19%) as yellow oils as separated *E* and *Z* isomers after purification on  $\text{SiO}_2$  (hexanes / EA, 10:1 to 4:1). *E/Z* = 70:30.

**R<sub>f</sub>** (hexanes / EA, 4:1) = 0.31 (*E* Isomer), 0.25 (*Z* Isomer); **IR** (neat): 3030, 2922, 2214, 1677, 1602, 1494, 1446, 1408, 1364, 1326, 1222, 1181, 1110, 1077, 1032, 998, 931, 894, 812, 779, 745, 697  $\text{cm}^{-1}$ ; **<sup>1</sup>H-NMR** (400 MHz,  $\text{CDCl}_3$ , *E* Isomer):  $\delta$  7.85 (d, *J* = 8.2 Hz, 2H), 7.55 (s, 1H), 7.39 – 7.34 (m, 3H), 7.29 (d, *J* = 8.0 Hz, 2H), 7.26 – 7.23 (m, 2H), 4.10 (d, *J* = 0.6 Hz, 2H), 2.43 (s, 3H); **<sup>13</sup>C-NMR** (101 MHz,  $\text{CDCl}_3$ , *E* Isomer):  $\delta$  194.09, 147.67, 145.00, 133.52, 133.32, 129.71, 129.61, 128.93, 128.67, 128.47, 120.05, 108.85, 39.69, 21.77; **<sup>1</sup>H-NMR** (400 MHz,  $\text{CDCl}_3$ , *Z* Isomer):  $\delta$  7.90 (d, *J* = 8.1 Hz, 2H), 7.80 – 7.76 (m, 2H), 7.45 – 7.40 (m, 3H), 7.31 (d, *J* = 8.0 Hz, 2H), 7.04 (s, 1H), 4.04 (s, 2H), 2.44 (s, 3H); **<sup>13</sup>C-NMR** (101 MHz,  $\text{CDCl}_3$ , *Z* Isomer):  $\delta$  194.19, 147.27, 144.90, 133.40, 133.37, 130.48, 129.62, 128.91, 128.86, 128.49, 118.55, 104.30, 44.59, 21.76; **HRMS** (EI) *m/z* calculated for  $\text{C}_{18}\text{H}_{15}\text{NO}$  ( $[\text{M}]^+$ ) 261.1148, found 261.1141.

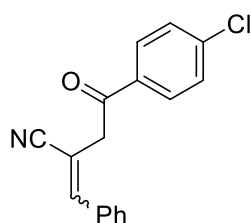
**2-benzylidene-4-oxo-4-(*o*-tolyl)butanenitrile (249ag)**

Following general procedure **GP-E** using 2-chloro-3-phenylacrylonitrile (**248a**, 81.8 mg, 500  $\mu\text{mol}$ , 1.00 equiv), 1-(*o*-tolyl)vinyl acetate (**152g**, 441 mg, 2.50 mmol, 5.00 equiv) and

Ir(ppy)<sub>2</sub>(dtbbpy)PF<sub>6</sub> (9.14 mg, 10.0 μmol, 0.02 equiv) gave (*E*)-**249ag** (47.2 mg, 181 μmol, 36%) and (*Z*)-**249ag** (31.4 mg, 120 μmol, 24%) as yellow oils as separated *E* and *Z* isomers after purification on SiO<sub>2</sub> (hexanes / EA, 15:1 to 8:1). *E/Z* = 60:40.

**R<sub>f</sub>** (hexanes / EA, 4:1) = 0.31 (*E* Isomer), 0.25 (*Z* Isomer); **IR** (neat): 3063, 3026, 2967, 2929, 2214, 1684, 1602, 1572, 1487, 1449, 1312, 1211, 1138, 984, 909, 730, 697, 667 cm<sup>-1</sup>; **<sup>1</sup>H-NMR** (300 MHz, CDCl<sub>3</sub>, *E* Isomer): δ 7.63 – 7.59 (m, 1H), 7.54 (s, 1H), 7.47 – 7.36 (m, 4H), 7.32 – 7.24 (m, 4H), 4.08 (s, 2H), 2.55 (s, 3H); **<sup>13</sup>C-NMR** (75 MHz, CDCl<sub>3</sub>, *E* Isomer): δ 197.70, 147.68, 139.43, 136.00, 133.50, 132.47, 132.35, 129.77, 128.94, 128.80, 128.64, 125.93, 120.02, 108.85, 42.25, 21.63; **<sup>1</sup>H-NMR** (300 MHz, CDCl<sub>3</sub>, *Z* Isomer): δ 7.81 – 7.76 (m, 2H), 7.75 – 7.71 (m, 1H), 7.47 – 7.37 (m, 4H), 7.35 – 7.27 (m, 2H), 7.04 (s, 1H), 4.02 (d, *J* = 1.0 Hz, 2H), 2.56 (s, 3H); **<sup>13</sup>C-NMR** (75 MHz, CDCl<sub>3</sub>, *Z* Isomer): δ 197.81, 147.36, 139.39, 136.07, 133.32, 132.45, 132.29, 130.51, 128.90, 128.87, 128.84, 125.96, 118.53, 104.36, 47.23, 21.70; **HRMS** (APCI) *m/z* calculated for C<sub>18</sub>H<sub>19</sub>N<sub>2</sub>O ([M+NH<sub>4</sub>]<sup>+</sup>) 279.1492, found 279.1497.

### 2-benzylidene-4-(4-chlorophenyl)-4-oxobutanenitrile (**249ah**)

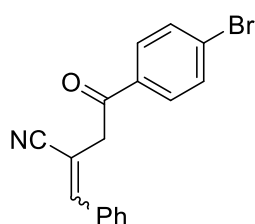


Following general procedure **GP-E** using 2-chloro-3-phenylacrylonitrile (**248a**, 81.8 mg, 500 μmol, 1.00 equiv), 1-(4-chlorophenyl)vinyl acetate (**152i**, 491 mg, 2.50 mmol, 5.00 equiv) and Ir(ppy)<sub>2</sub>(dtbbpy)PF<sub>6</sub> (9.14 mg, 10.0 μmol, 0.02 equiv) gave (*E*)-**249ah** (47.5 mg, 168 μmol, 34%) and (*Z*)-**249ah** (25.5 mg, 90.7 μmol, 18%) as orange oils as separated *E* and *Z* isomers after purification on SiO<sub>2</sub> (hexanes / EA, 20:1 to 10:1). *E/Z* = 65:35.

**R<sub>f</sub>** (hexanes / EA, 4:1) = 0.31 (*E* Isomer), 0.25 (*Z* Isomer); **IR** (neat): 3060, 3026, 2926, 2855, 2214, 1751, 1684, 1625, 1587, 1487, 1449, 1401, 1367, 1330, 1289, 1211, 995, 943, 902, 812, 752, 682 cm<sup>-1</sup>; **<sup>1</sup>H-NMR** (300 MHz, CDCl<sub>3</sub>, *E* Isomer): δ 7.92 – 7.86 (m, 2H), 7.57 (s, 1H), 7.49 – 7.44 (m, 2H), 7.40 – 7.35 (m, 3H), 7.25 – 7.21 (m, 2H), 4.10 (d, *J* = 0.8 Hz, 2H); **<sup>13</sup>C-NMR** (75 MHz, CDCl<sub>3</sub>, *E* Isomer): δ 193.36, 148.00, 140.58, 133.99, 133.34, 129.84,

129.73, 129.28, 128.99, 128.60, 119.84, 108.29, 39.71; **<sup>1</sup>H-NMR** (400 MHz, CDCl<sub>3</sub>, *Z* Isomer): δ 7.95 (d, *J* = 8.6 Hz, 2H), 7.78 (dd, *J* = 6.5, 2.9 Hz, 2H), 7.49 (d, *J* = 8.6 Hz, 2H), 7.43 (dd, *J* = 5.0, 1.8 Hz, 3H), 7.05 (s, 1H), 4.04 (s, 2H); **<sup>13</sup>C-NMR** (101 MHz, CDCl<sub>3</sub>, *Z* Isomer): δ 193.39, 147.58, 140.51, 134.13, 133.20, 130.65, 129.74, 129.31, 128.92, 118.40, 103.69, 44.68; **HRMS** (APCI) *m/z* calculated for C<sub>17</sub>H<sub>16</sub>ClN<sub>2</sub>O ([M+NH<sub>4</sub>]<sup>+</sup>) 299.0946, found 299.0946.

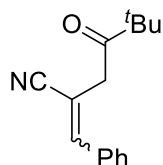
### 2-benzylidene-4-(4-bromophenyl)-4-oxobutanenitrile (**249ai**)



Following general procedure **GP-E** using 2-chloro-3-phenylacrylonitrile (**248a**, 81.8 mg, 500 μmol, 1.00 equiv), 1-(4-bromophenyl)vinyl acetate (**152h**, 603 mg, 2.50 mmol, 5.00 equiv) and Ir(ppy)<sub>2</sub>(dtbbpy)PF<sub>6</sub> (9.14 mg, 10.0 μmol, 0.02 equiv) gave (*E*)-**249ai** (46.8 mg, 144 μmol, 29%) and (*Z*)-**249ai** (38.3 mg, 118 μmol, 23%) as orange oils as separated *E* and *Z* isomers after purification on SiO<sub>2</sub> (hexanes / EA, 15:1 to 10:1). *E/Z* = 55:45.

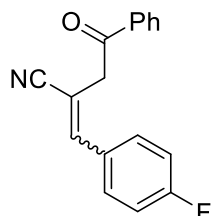
**R<sub>f</sub>** (hexanes / EA, 4:1) = 0.31 (*E* Isomer), 0.25 (*Z* Isomer); **IR** (neat): 3060, 3030, 2922, 2855, 2214, 1684, 1584, 1487, 1446, 1397, 1323, 1211, 1069, 991, 909, 808, 730, 697 cm<sup>-1</sup>; **<sup>1</sup>H-NMR** (400 MHz, CDCl<sub>3</sub>, *E* Isomer): δ 7.83 – 7.78 (m, 2H), 7.65 – 7.62 (m, 2H), 7.56 (s, 1H), 7.40 – 7.35 (m, 3H), 7.25 – 7.21 (m, 2H), 4.09 (d, *J* = 0.7 Hz, 2H); **<sup>13</sup>C-NMR** (101 MHz, CDCl<sub>3</sub>, *E* Isomer): δ 193.54, 148.00, 134.43, 133.37, 132.29, 129.84, 129.80, 129.36, 128.99, 128.60, 119.81, 108.30, 39.70; **<sup>1</sup>H-NMR** (400 MHz, CDCl<sub>3</sub>, *Z* Isomer): δ 7.88 – 7.84 (m, 2H), 7.80 – 7.76 (m, 2H), 7.68 – 7.64 (m, 2H), 7.45 – 7.41 (m, 3H), 7.04 (s, 1H), 4.04 (d, *J* = 1.0 Hz, 2H); **<sup>13</sup>C-NMR** (101 MHz, CDCl<sub>3</sub>, *Z* Isomer): δ 193.61, 147.59, 134.53, 133.19, 132.30, 130.65, 129.81, 129.26, 128.92, 128.60, 118.39, 103.66, 44.65; **HRMS** (APCI) *m/z* calculated for C<sub>17</sub>H<sub>16</sub>BrN<sub>2</sub>O ([M+NH<sub>4</sub>]<sup>+</sup>) 343.0441, found 343.0448.



**2-benzylidene-5,5-dimethyl-4-oxohexanenitrile (249aj)**

Following general procedure **GP-E** using 2-chloro-3-phenylacrylonitrile (**248a**, 81.8 mg, 500  $\mu\text{mol}$ , 1.00 equiv), 3,3-dimethylbut-1-en-2-yl acetate (**152l**, 356 mg, 2.50 mmol, 5.00 equiv) and  $\text{Ir}(\text{ppy})_2(\text{dtbbpy})\text{PF}_6$  (9.14 mg, 10.0  $\mu\text{mol}$ , 0.02 equiv) gave (*E*)-**249aj** (35.6 mg, 157  $\mu\text{mol}$ , 32%) and (*Z*)-**249aj** (18.3 mg, 80.9  $\mu\text{mol}$ , 16%) as colorless oils as separated *E* and *Z* isomers after purification on  $\text{SiO}_2$  (hexanes / EA, 20:1 to 12:1). *E/Z* = 66:34.

**R<sub>f</sub>** (hexanes / EA, 4:1) = 0.40 (*E* Isomer), 0.30 (*Z* Isomer); **IR** (neat): 3060, 3030, 2967, 2873, 2214, 1736, 1707, 1625, 1476, 1367, 1312, 1237, 1062, 1006, 931, 894, 782, 745, 697  $\text{cm}^{-1}$ ; **<sup>1</sup>H-NMR** (300 MHz,  $\text{CDCl}_3$ , *E* Isomer):  $\delta$  7.48 (s, 1H), 7.40 – 7.35 (m, 3H), 7.21 – 7.17 (m, 2H), 3.63 (d, *J* = 0.8 Hz, 2H), 1.19 (s, 9H); **<sup>13</sup>C-NMR** (75 MHz,  $\text{CDCl}_3$ , *E* Isomer):  $\delta$  210.45, 147.50, 133.55, 129.63, 128.82, 128.41, 119.88, 109.32, 44.61, 38.05, 26.30; **<sup>1</sup>H-NMR** (300 MHz,  $\text{CDCl}_3$ , *Z* Isomer):  $\delta$  7.77 – 7.73 (m, 2H), 7.44 – 7.39 (m, 3H), 6.94 (s, 1H), 3.59 (d, *J* = 1.0 Hz, 2H), 1.23 (s, 9H); **<sup>13</sup>C-NMR** (101 MHz,  $\text{CDCl}_3$ , *Z* Isomer):  $\delta$  210.26, 147.18, 133.37, 130.40, 128.86, 128.82, 118.47, 104.55, 44.47, 42.89, 26.23; **HRMS** (EI) *m/z* calculated for  $\text{C}_{15}\text{H}_{17}\text{NO}$  ( $[\text{M}]^+$ ) 227.1305, found 227.1302.

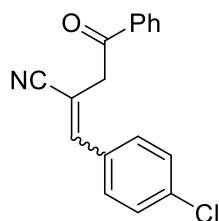
**2-(4-fluorobenzylidene)-4-oxo-4-phenylbutanenitrile (249ba)**

Following general procedure **GP-E** using 2-chloro-3-(4-fluorophenyl)acrylonitrile (**248b**, 90.8 mg, 500  $\mu\text{mol}$ , 1.00 equiv), 1-phenylvinyl acetate (**152a**, 405 mg, 2.50 mmol, 5.00 equiv) and  $\text{Ir}(\text{ppy})_2(\text{dtbbpy})\text{PF}_6$  (9.14 mg, 10.0  $\mu\text{mol}$ , 0.02 equiv) gave (*E*)-**249ba** (43.3 mg, 163  $\mu\text{mol}$ , 33%) as yellow solid and (*Z*)-**249ba** (20.4 mg, 76.8  $\mu\text{mol}$ , 15%) as

yellow oil as separated *E* and *Z* isomers after purification on SiO<sub>2</sub> (hexanes / EA, 6:1 to 4:1). *E/Z* = 68:32.

**R<sub>f</sub>** (hexanes / EA, 4:1) = 0.30 (*E* Isomer), 0.20 (*Z* Isomer); **mp** (*E* Isomer): 95 °C; **IR** (neat): 3067, 2952, 2922, 2214, 1751, 1681, 1599, 1505, 1446, 1401, 1334, 1237, 1211, 1159, 1099, 998, 827, 752, 689 cm<sup>-1</sup>; **<sup>1</sup>H-NMR** (300 MHz, CDCl<sub>3</sub>, *E* Isomer): δ 7.94 – 7.89 (m, 2H), 7.62 – 7.56 (m, 1H), 7.50 – 7.43 (m, 3H), 7.23 – 7.17 (m, 2H), 7.05 – 6.98 (m, 2H), 4.06 (d, *J* = 0.8 Hz, 2H); **<sup>13</sup>C-NMR** (75 MHz, CDCl<sub>3</sub>, *E* Isomer): δ 194.41, 164.98, 161.65, 146.69, 135.64, 134.12, 130.75, 130.64, 129.57, 129.52, 128.98, 128.35, 119.85, 116.32, 116.03, 108.57, 108.55, 39.72; **<sup>19</sup>F-NMR** (282 MHz, CDCl<sub>3</sub>, *E* Isomer): δ -110.28; **<sup>1</sup>H-NMR** (300 MHz, CDCl<sub>3</sub>, *Z* Isomer): δ 8.02 – 7.98 (m, 2H), 7.82 – 7.76 (m, 2H), 7.66 – 7.60 (m, 1H), 7.55 – 7.48 (m, 2H), 7.15 – 7.08 (m, 2H), 7.01 (s, 1H), 4.07 (d, *J* = 1.0 Hz, 2H); **<sup>13</sup>C-NMR** (75 MHz, CDCl<sub>3</sub>, *Z* Isomer): δ 194.52, 165.38, 162.04, 146.07, 135.75, 133.98, 131.08, 130.97, 129.59, 129.54, 128.95, 128.31, 118.42, 116.20, 115.91, 103.79, 103.76, 44.58; **<sup>19</sup>F-NMR** (282 MHz, CDCl<sub>3</sub>, *Z* Isomer): δ -109.02; **HRMS** (ESI) *m/z* calculated for C<sub>17</sub>H<sub>13</sub>FNO ([M+H]<sup>+</sup>) 266.0976, found 266.0981.

## 2-(4-chlorobenzylidene)-4-oxo-4-phenylbutanenitrile (**249ca**)

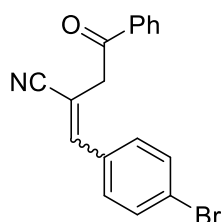


Following general procedure **GP-E** using 2-chloro-3-(4-chlorophenyl)acrylonitrile (**248c**, 99.0 mg, 500 μmol, 1.00 equiv), 1-phenylvinyl acetate (**152a**, 405 mg, 2.50 mmol, 5.00 equiv) and Ir(ppy)<sub>2</sub>(dtbbpy)PF<sub>6</sub> (9.14 mg, 10.0 μmol, 0.02 equiv) gave (*E*)-**249ca** (71.7 mg, 255 μmol, 51%) as yellow oil and (*Z*)-**249ca** (45.9 mg, 163 μmol, 33%) as yellow solid as separated *E* and *Z* isomers after purification on SiO<sub>2</sub> (hexanes / EA, 15:1 to 4:1). *E/Z* = 61:39.

**R<sub>f</sub>** (hexanes / EA, 4:1) = 0.20 (*E* Isomer), 0.16 (*Z* Isomer); **mp**: 110 °C (*Z* Isomer); **IR** (neat): 3086, 3034, 2967, 2914, 2221, 1681, 1591, 1487, 1435, 1356, 1326, 1211, 1092, 995, 894, 834, 752, 685 cm<sup>-1</sup>; **<sup>1</sup>H-NMR** (400 MHz, CDCl<sub>3</sub>, *E* Isomer): δ 7.97 – 7.94 (m, 2H), 7.66 –

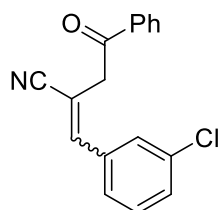
7.61 (m, 1H), 7.53 – 7.48 (m, 3H), 7.36 – 7.32 (m, 2H), 7.20 – 7.18 (m, 2H), 4.10 (s, 2H);  $^{13}\text{C-NMR}$  (101 MHz,  $\text{CDCl}_3$ , *E* Isomer):  $\delta$  194.35, 146.55, 135.92, 135.60, 134.17, 131.83, 129.95, 129.26, 129.01, 128.36, 119.74, 109.30, 39.77;  $^1\text{H-NMR}$  (400 MHz,  $\text{CDCl}_3$ , *Z* Isomer):  $\delta$  8.00 – 7.97 (m, 2H), 7.73 – 7.70 (m, 2H), 7.65 – 7.60 (m, 1H), 7.53 – 7.48 (m, 2H), 7.40 – 7.36 (m, 2H), 6.99 (s, 1H), 4.08 (d,  $J = 0.8$  Hz, 2H);  $^{13}\text{C-NMR}$  (101 MHz,  $\text{CDCl}_3$ , *Z* Isomer):  $\delta$  194.47, 146.00, 136.43, 135.72, 134.03, 131.74, 130.17, 129.16, 128.98, 128.31, 118.29, 104.82, 44.67; **HRMS** (APCI)  $m/z$  calculated for  $\text{C}_{17}\text{H}_{16}\text{ClN}_2\text{O}$  ( $[\text{M}+\text{NH}_4]^+$ ) 299.0946, found 299.0945.

### 2-(4-bromobenzylidene)-4-oxo-4-phenylbutanenitrile (**249da**)



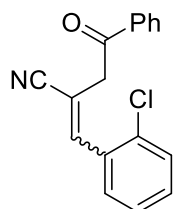
Following general procedure **GP-E** using 3-(4-bromophenyl)-2-chloroacrylonitrile (**248d**, 121 mg, 500  $\mu\text{mol}$ , 1.00 equiv), 1-phenylvinyl acetate (**152a**, 405 mg, 2.50 mmol, 5.00 equiv) and  $\text{Ir}(\text{ppy})_2(\text{dtbbpy})\text{PF}_6$  (9.14 mg, 10.0  $\mu\text{mol}$ , 0.02 equiv) gave (*E*)-**249da** (55.6 mg, 171  $\mu\text{mol}$ , 34%) as yellow solid and (*Z*)-**249da** (27.4 mg, 84.1  $\mu\text{mol}$ , 17%) as yellow solid as separated *E* and *Z* isomers after purification on  $\text{SiO}_2$  (hexanes / EA, 15:1 to 4:1).  $E/Z = 67:33$ .

**R<sub>f</sub>** (hexanes / EA, 4:1) = 0.24 (*E* Isomer), 0.17 (*Z* Isomer); **mp** (*E* Isomer): 133 °C; **mp** (*Z* Isomer): 120 °C; **IR** (neat): 3090, 3034, 2967, 2911, 2221, 1681, 1580, 1483, 1405, 1356, 1326, 1211, 1073, 995, 916, 834, 752, 685  $\text{cm}^{-1}$ ;  $^1\text{H-NMR}$  (300 MHz,  $\text{CDCl}_3$ , *E* Isomer):  $\delta$  7.97 – 7.93 (m, 2H), 7.66 – 7.60 (m, 1H), 7.53 – 7.46 (m, 5H), 7.13 – 7.10 (m, 2H), 4.10 (s, 2H);  $^{13}\text{C-NMR}$  (75 MHz,  $\text{CDCl}_3$ , *E* Isomer):  $\delta$  194.25, 146.57, 135.64, 134.14, 132.28, 132.23, 130.11, 129.00, 128.34, 124.23, 119.67, 109.42, 39.78;  $^1\text{H-NMR}$  (300 MHz,  $\text{CDCl}_3$ , *Z* Isomer):  $\delta$  8.02 – 7.97 (m, 2H), 7.68 – 7.60 (m, 3H), 7.58 – 7.48 (m, 4H), 6.98 (s, 1H), 4.07 (d,  $J = 1.0$  Hz, 2H);  $^{13}\text{C-NMR}$  (75 MHz,  $\text{CDCl}_3$ , *Z* Isomer):  $\delta$  194.33, 146.04, 135.75, 134.01, 132.15, 130.33, 128.98, 128.32, 124.87, 118.21, 104.97, 44.64; **HRMS** (APCI)  $m/z$  calculated for  $\text{C}_{17}\text{H}_{16}\text{BrN}_2\text{O}$  ( $[\text{M}+\text{NH}_4]^+$ ) 343.0441, found 343.0445.

**2-(3-chlorobenzylidene)-4-oxo-4-phenylbutanenitrile (249ea)**

Following general procedure **GP-E** using 2-chloro-3-(3-chlorophenyl)acrylonitrile (**248e**, 99.0 mg, 500  $\mu\text{mol}$ , 1.00 equiv), 1-phenylvinyl acetate (**152a**, 405 mg, 2.50 mmol, 5.00 equiv) and  $\text{Ir}(\text{ppy})_2(\text{dtbbpy})\text{PF}_6$  (9.14 mg, 10.0  $\mu\text{mol}$ , 0.02 equiv) gave (*E*)-**249ea** (67.3 mg, 239  $\mu\text{mol}$ , 48%) and (*Z*)-**249ea** (34.7 mg, 123  $\mu\text{mol}$ , 24%) as yellow oils as separated *E* and *Z* isomers after purification on  $\text{SiO}_2$  (hexanes / EA, 15:1 to 4:1). *E/Z* = 66:34.

**R<sub>f</sub>** (hexanes / EA, 4:1) = 0.22 (*E* Isomer), 0.17 (*Z* Isomer); **IR** (neat): 3063, 2918, 2217, 1684, 1595, 1565, 1476, 1416, 1329, 1215, 1080, 998, 898, 782, 685  $\text{cm}^{-1}$ ; **<sup>1</sup>H-NMR** (400 MHz,  $\text{CDCl}_3$ , *E* Isomer):  $\delta$  7.96 – 7.93 (m, 2H), 7.65 – 7.61 (m, 1H), 7.52 – 7.48 (m, 3H), 7.36 – 7.28 (m, 2H), 7.25 – 7.23 (m, 1H), 7.13 – 7.11 (m, 1H), 4.10 (s, 2H); **<sup>13</sup>C-NMR** (101 MHz,  $\text{CDCl}_3$ , *E* Isomer):  $\delta$  194.30, 146.24, 135.62, 135.07, 134.98, 134.14, 130.27, 129.78, 128.99, 128.59, 128.35, 126.58, 119.51, 110.24, 39.67; **<sup>1</sup>H-NMR** (400 MHz,  $\text{CDCl}_3$ , *Z* Isomer):  $\delta$  8.00 (d,  $J = 7.6$  Hz, 2H), 7.73 – 7.63 (m, 3H), 7.52 (t,  $J = 7.6$  Hz, 2H), 7.41 – 7.31 (m, 2H), 6.99 (s, 1H), 4.09 (s, 2H); **<sup>13</sup>C-NMR** (101 MHz,  $\text{CDCl}_3$ , *Z* Isomer):  $\delta$  194.30, 145.74, 135.71, 134.96, 134.84, 134.04, 130.46, 130.19, 128.99, 128.32, 126.71, 117.99, 105.98, 44.66; **HRMS** (APCI)  $m/z$  calculated for  $\text{C}_{17}\text{H}_{16}\text{ClN}_2\text{O}$  ( $[\text{M}+\text{NH}_4]^+$ ) 299.0946, found 299.0945.

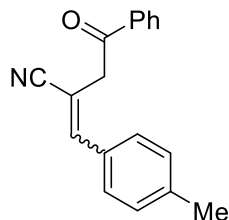
**2-(2-chlorobenzylidene)-4-oxo-4-phenylbutanenitrile (249fa)**

Following general procedure **GP-E** using 2-chloro-3-(2-chlorophenyl)acrylonitrile (**248f**, 99.0 mg, 500  $\mu\text{mol}$ , 1.00 equiv), 1-phenylvinyl acetate (**152a**, 405 mg, 2.50 mmol, 5.00 equiv) and  $\text{Ir}(\text{ppy})_2(\text{dtbbpy})\text{PF}_6$  (9.14 mg, 10.0  $\mu\text{mol}$ , 0.02 equiv) gave (*E*)-**248fa**

(73.7 mg, 261  $\mu\text{mol}$ , 52%) and (*Z*)-**248fa** (36.3 mg, 129  $\mu\text{mol}$ , 26%) as yellow oils as separated *E* and *Z* isomers after purification on  $\text{SiO}_2$  (hexanes / EA, 15:1 to 4:1). *E/Z* = 67:33.

**R<sub>f</sub>** (hexanes / EA, 4:1) = 0.25 (*E* Isomer), 0.20 (*Z* Isomer); **IR** (neat): 3063, 2918, 2221, 1755, 1684, 1595, 1468, 1326, 1278, 1215, 1181, 1129, 1054, 998, 954, 909, 752, 685  $\text{cm}^{-1}$ ; **<sup>1</sup>H-NMR** (300 MHz,  $\text{CDCl}_3$ , *E* Isomer):  $\delta$  8.11 – 8.06 (m, 1H), 8.04 – 7.99 (m, 2H), 7.67 – 7.61 (m, 1H), 7.56 – 7.48 (m, 2H), 7.46 – 7.34 (m, 4H), 4.15 (d,  $J$  = 1.0 Hz, 2H); **<sup>13</sup>C-NMR** (75 MHz,  $\text{CDCl}_3$ , *E* Isomer):  $\delta$  194.27, 143.99, 135.72, 134.12, 133.98, 131.75, 131.37, 129.75, 129.51, 128.95, 128.31, 127.26, 117.79, 107.72, 44.58; **<sup>1</sup>H-NMR** (300 MHz,  $\text{CDCl}_3$ , *Z* Isomer):  $\delta$  7.94 – 7.90 (m, 2H), 7.65 – 7.59 (m, 2H), 7.51 – 7.43 (m, 3H), 7.36 – 7.29 (m, 1H), 7.25 – 7.15 (m, 2H), 4.03 (d,  $J$  = 0.8 Hz, 2H); **<sup>13</sup>C-NMR** (75 MHz,  $\text{CDCl}_3$ , *Z* Isomer):  $\delta$  194.42, 144.98, 135.58, 134.07, 133.92, 131.84, 130.99, 130.06, 129.54, 128.93, 128.30, 127.06, 119.29, 110.72, 39.88; **HRMS** (APCI)  $m/z$  calculated for  $\text{C}_{17}\text{H}_{16}\text{ClN}_2\text{O}$  ( $[\text{M}+\text{NH}_4]^+$ ) 299.0946, found 299.0954.

## 2-(4-methylbenzylidene)-4-oxo-4-phenylbutanenitrile (**249ga**)



Following general procedure **GP-E** using 2-chloro-3-(*p*-tolyl)acrylonitrile (**248g**, 88.8 mg, 500  $\mu\text{mol}$ , 1.00 equiv), 1-phenylvinyl acetate (**152a**, 405 mg, 2.50 mmol, 5.00 equiv) and  $\text{Ir}(\text{ppy})_2(\text{dtbbpy})\text{PF}_6$  (9.14 mg, 10.0  $\mu\text{mol}$ , 0.02 equiv) gave (*E*)-**249ga** (33.6 mg, 129  $\mu\text{mol}$ , 26%) as yellow solid and (*Z*)-**249ga** (18.1 mg, 69.3  $\mu\text{mol}$ , 14%) as yellow oil as separated *E* and *Z* isomers after purification on  $\text{SiO}_2$  (hexanes / EA, 15:1 to 4:1). *E/Z* = 65:35.

**R<sub>f</sub>** (hexanes / EA, 4:1) = 0.22 (*E* Isomer), 0.16 (*Z* Isomer); **mp** (*E* Isomer): 101  $^\circ\text{C}$ ; **IR** (neat): 3030, 2963, 2217, 1684, 1621, 1509, 1446, 1405, 1360, 1326, 1211, 1110, 1021, 998, 902, 831, 752, 682  $\text{cm}^{-1}$ ; **<sup>1</sup>H-NMR** (400 MHz,  $\text{CDCl}_3$ , *E* Isomer):  $\delta$  7.98 – 7.94 (m, 2H), 7.65 – 7.60 (m, 1H), 7.53 – 7.47 (m, 3H), 7.19 – 7.13 (m, 4H), 4.14 (s, 2H), 2.35 (s, 3H); **<sup>13</sup>C-NMR** (101 MHz,  $\text{CDCl}_3$ , *E* Isomer):  $\delta$  194.56, 147.85, 140.17, 135.82, 133.95, 130.69, 129.66, 128.93, 128.73, 128.34, 120.23, 107.60, 39.87, 21.40; **<sup>1</sup>H-NMR** (400 MHz,  $\text{CDCl}_3$ , *Z*

## Experimental part

---

Isomer):  $\delta$  8.01 – 7.99 (m, 2H), 7.70 – 7.68 (m, 2H), 7.64 – 7.60 (m, 1H), 7.53 – 7.49 (m, 1H), 7.24 – 7.22 (m, 2H), 7.18 – 7.13 (m, 1H), 7.01 (s, 1H), 4.05 (s, 2H), 2.39 (s, 3H);  **$^{13}\text{C-NMR}$**  (101 MHz,  $\text{CDCl}_3$ , Z Isomer):  $\delta$  194.73, 147.38, 141.04, 135.88, 133.87, 130.64, 129.58, 128.94, 128.92, 128.35, 118.75, 102.71, 44.70, 21.54; **HRMS** (APCI)  $m/z$  calculated for  $\text{C}_{18}\text{H}_{19}\text{N}_2\text{O}$  ( $[\text{M}+\text{NH}_4]^+$ ) 279.1492, found 279.1496.

## F References

- [1] Gomberg, M. *J. Am. Chem. Soc.* **1900**, *22*, 757-771.
- [2] Matsubara, H.; Kawamoto, T.; Fukuyama, T.; Ryu, I. *Acc. Chem. Res.* **2018**, *51*, 2023-2035.
- [3] Huang, M.-H.; Hao, W.-J.; Li, G.; Tu, S.-J.; Jiang, B. *Chem. Commun.* **2018**, *54*, 10791-10811.
- [4] Yi, H.; Zhang, G.; Wang, H.; Huang, Z.; Wang, J.; Singh, A. K.; Lei, A. *Chem. Rev.* **2017**, *117*, 9016-9085.
- [5] Dénès, F.; Pichowicz, M.; Povie, G.; Renaud, P. *Chem. Rev.* **2014**, *114*, 2587-2693.
- [6] Dénès, F.; Schiesser, C. H.; Renaud, P. *Chem. Soc. Rev.* **2013**, *40*, 7900-7942.
- [7] Wille, U. *Chem. Rev.* **2013**, *113*, 813-853.
- [8] van der Kerk, G. J. M.; Noltes, J. G.; Luijten, J. G. A. *J. Appl. Chem.* **1957**, *7*, 356-365.
- [9] Kuivila, H. G. *Acc. Chem. Res.* **1968**, *1*, 299-305.
- [10] Curran, D. P. *Synthesis* **1988**, *6*, 417-439.
- [11] Curran, D. P. *Synthesis* **1988**, *7*, 489-513.
- [12] Neumann, W. P. *Synthesis* **1987**, *8*, 665-683.
- [13] Stork, G.; Baine, N. H. *J. Am. Chem. Soc.* **1982**, *104*, 2321-2323.
- [14] Curran, D. P.; Kim, D.; Liu, H. T.; Shen, W. *J. Am. Chem. Soc.* **1988**, *110*, 5900-5902.
- [15] Curran, D. P.; Liu, H. *J. Am. Chem. Soc.* **1991**, *113*, 2127-2132.
- [16] Curran, D. P.; Shen, W. *J. Am. Chem. Soc.* **1993**, *115*, 6051-6059.
- [17] Laarhoven, L. J. J.; Mulder, P.; Wayner, D. D. M. *Acc. Chem. Res.* **1999**, *32*, 342-349.
- [18] Liu, Q.; Han, B.; Zhang, W.; Yang, L.; Liu, Z.-L.; Yu, W. *Synlett* **2005**, *14*, 2248-2250.
- [19] Kippo, T.; Hamaoka, K.; Ueda, M.; Fukuyama, T.; Ryu, I. *Tetrahedron* **2016**, *72*, 7866-7874.
- [20] Yan, M.; Kawamata, Y.; Baran, P. S. *Chem. Rev.* **2017**, *117*, 13230-13319.
- [21] Marzo, L.; Pagire, S. K.; Reiser, O.; König, B. *Angew. Chem. Int. Ed.* **2018**, *57*, 10034-10072.
- [22] Teegardin, K. A.; Day, J. I.; Chan, J.; Weaver, J. D. *Org. Process Res. Dev.* **2016**, *20*, 1156-1163.
- [23] Skubi, K. L.; Blum, T. R.; Yoon, T. P. *Chem. Rev.* **2016**, *116*, 10035-10074.
- [24] Shaw, M. H.; Twilton, J.; MacMillan, D. W. C. *J. Org. Chem.* **2016**, *81*, 6898-6926.
- [25] Twilton, J.; Le, C.; Zhang, P.; Shaw, M. H.; Evans, R. W.; MacMillan, D. W. C. *Nat. Rev. Chem.* **2017**, *1*, 0052.
- [26] Corey, E. J.; Mehrotra, M. M. *Tetrahedron Lett.* **1988**, *29*, 57-60.
- [27] Curran, D. P.; Rakiewicz, D. M. *J. Am. Chem. Soc.* **1985**, *107*, 1448-1449.
- [28] Tsai, Y.-M.; Ke, B.-W.; Yang, C.-T.; Lin, C.-H. *Tetrahedron Lett.* **1992**, *33*, 7895-9898.
- [29] Bosch, E.; Bachi, M. D. *J. Org. Chem.* **1993**, *58*, 5581-5582.
- [30] Clive, D. L. J.; Yeh, V. S. C. *Tetrahedron Lett.* **1998**, *39*, 4789-4792.
- [31] Majumdar, K. C.; Mondal, S.; Ghosh, D. *Tetrahedron Lett.* **2010**, *51*, 5273-5276.
- [32] Dinesh, T. K.; Palani, N.; Balasubramanian, S. *Synlett* **2015**, *26*, 1055-1058.
- [33] Jezek, E.; Schall, A.; Reiser, O. *Synlett* **2005**, *6*, 915-918.
- [34] Zhan, Z.-P.; Lang, K. *Org. Biomol. Chem.* **2005**, *3*, 727-728.
- [35] Padwa, A.; Nimmegern, H.; Wong, G. S. K. *J. Org. Chem.* **1985**, *50*, 5620-5627.

- [36] Bencivenni, G.; Lanza, T.; Leardini, R.; Minozzi, M.; Nanni, D.; Spagnolo, P.; Zanardi, G. *Org. Lett.* **2008**, *10*, 1127-1130.
- [37] Robertson, J.; Pillai, J.; Lush, R. K. *Chem. Soc. Rev.* **2001**, *30*, 94-103.
- [38] Lathbury, D. C.; Parsons, P. J.; Pinto, I. *J. Chem. Soc., Chem. Commun.* **1988**, *0*, 81-82.
- [39] Borthwick, A. D.; Caddick, S.; Parsons, P. J. *Tetrahedron* **1992**, *48*, 10655-10666.
- [40] Burke, S. D.; Jung, K. W. *Tetrahedron Lett.* **1994**, *35*, 5837-5840.
- [41] Stien, D.; Crich, D.; Bertrand, M. P. *Tetrahedron* **1998**, *54*, 10779-10788.
- [42] Gloor, C. S.; Dénès, F.; Renaud, P. *Angew. Chem. Int. Ed.* **2017**, *56*, 133329-113332.
- [43] Lin, H.; Schall, A.; Reiser, O. *Synlett* **2005**, *17*, 2603-2606.
- [44] Prediger, I.; Weiss, T.; Reiser, O. *Synthesis* **2008**, *14*, 2191-2198.
- [45] Crick, P. J.; Simpkins, N. S.; Highton, A. *Org. Lett.* **2011**, *13*, 6472-6475.
- [46] Robertson, J.; Peplow, M. A.; Pillai, J. *Tetrahedron Lett.* **1996**, *37*, 5825-5828.
- [47] Uenoyama, Y.; Fukuyama, T.; Nobuta, O.; Matsubara, H.; Ryu, I. *Angew. Chem. Int. Ed.* **2005**, *44*, 1075-1078.
- [48] Jones, S. B.; Simmons, B.; MacMillan, D. W. C. *J. Am. Chem. Soc.* **2009**, *131*, 13606-13607.
- [49] Baguley, P. A.; Walton, J. C. *Angew. Chem. Int. Ed.* **1998**, *37*, 3072-3082.
- [50] Stork, G.; Sher, P. M. *J. Am. Chem. Soc.* **1986**, *108*, 303-304.
- [51] Grogneç, E. L.; Chrétien, J.-M.; Zammattio, F.; Quintard, J.-P. *Chem. Rev.* **2015**, *115*, 10207-10260.
- [52] Studer, A.; Amrein, S. *Synthesis* **2002**, *7*, 835-849.
- [53] Hedstrand, D. M.; Kruizinga, W. H.; Kellogg, R. M. *Tetrahedron Lett.* **1978**, *19*, 1255-1258.
- [54] Van Bergen, T. J.; Hedstrand, D. M.; Kruizinga, W. H.; Kellogg, R. M. *J. Org. Chem.* **1979**, *44*, 4953-4962.
- [55] Cano-Yelo, H.; Deronizer, A. *Tetrahedron Lett.* **1984**, *25*, 5517-5520.
- [56] Okada, K.; Okamoto, K.; Morita, N.; Okubo, K.; Oda, M. *J. Am. Chem. Soc.* **1991**, *113*, 9401-9402.
- [57] Hironaka, K.; Fukuzumi, S.; Tonaka, T. *J. Chem. Soc., Perkin Trans. 2* **1984**, *0*, 1705-1709.
- [58] Pac, C.; Ihama, M.; Yasuda, M.; Miyauchi, Y.; Sakurai, H. *J. Am. Chem. Soc.* **1981**, *103*, 6495-6497.
- [59] Ishitani, O.; Pac, C.; Sakurai, H. *J. Org. Chem.* **1983**, *48*, 2941-2942.
- [60] Ischay, M. A.; Anzovino, M. E.; Du, J.; Yoon, T. P. *J. Am. Chem. Soc.* **2008**, *130*, 12886-12887.
- [61] Nicewicz, D. A.; MacMillan, D. W. C. *Science* **2008**, *322*, 77-80.
- [62] Narayanam, J. M. R.; Tucker, J. W.; Stephenson, C. R. J. *J. Am. Chem. Soc.* **2009**, *131*, 8756-8757.
- [63] Schultz, D. M.; Yoon, T. P. *Science* **2014**, *343*, 985-993.
- [64] Fagnoni, M.; Dondi, D.; Ravelli, D.; Albini, A. *Chem. Rev.* **2007**, *107*, 2725-2756.
- [65] Teplý, F. *Collect. Czech. Chem. Commun.* **2011**, *76*, 859-917.
- [66] Narayanam, J. M. R.; Stephenson, C. R. J. *Chem. Soc. Rev.* **2011**, *40*, 102-113.
- [67] Neumann, M.; Földner, S.; König, B.; Zeitler, K. *Angew. Chem. Int. Ed.* **2011**, *50*, 951-954.
- [68] Nicewicz, D. A.; Nguyen, T. M. *ACS Catal.* **2014**, *4*, 355-360.
- [69] Romero, N. A.; Nicewicz, D. A. *Chem. Rev.* **2016**, *116*, 10075-10166.
- [70] Prier, C. K.; Rankic, D. A.; MacMillan, D. W. C. *Chem. Rev.* **2013**, *113*, 5322-5363.
- [71] Xuan, J.; Xiao, W.-J. *Angew. Chem. Int. Ed.* **2012**, *51*, 6828-6838.
- [72] Koike, T.; Akita, M. *Inorg. Chem. Front.* **2014**, *1*, 562-576.



- [73] Kern, J.-M.; Sauvage, J.-P. *J. Chem. Soc., Chem. Commun.* **1987**, 546-548.
- [74] Pirtsch, M.; Paria, S.; Matsuno, T.; Isobe, H.; Reiser, O. *Chem. Eur. J.* **2012**, *18*, 7336-7340.
- [75] Bagal, D. B.; Kachkovskiy, G.; Knorn, M.; Rawner, T.; Bhanage, B. M.; Reiser, O. *Angew. Chem. Int. Ed.* **2015**, *54*, 6999-7002.
- [76] Reiser, O. *Acc. Chem. Res.* **2016**, *49*, 1990-1996.
- [77] Hossain, A.; Vidyasagar, A.; Eichinger, C.; Lankes, C.; Phan, J.; Rehbein, J.; Reiser, O. *Angew. Chem. Int. Ed.* **2018**, *57*, 8288-8292.
- [78] Rawner, T.; Lutsker, E.; Kaiser, C. A.; Reiser, O. *ACS Catal.* **2018**, *8*, 3950-3956.
- [79] Beatty, J. W.; Stephenson, C. R. J. *Acc. Chem. Res.* **2015**, *48*, 1474-1484.
- [80] Peon, J.; Tan, X.; Hoerner, J. D.; Xia, C.; Luk, Y. F.; Kohler, B. *J. Phys. Chem. A* **2001**, *105*, 5768-5777.
- [81] Bockmann, T. M.; Kochi, J. K. *J. Org. Chem.* **1990**, *55*, 4127-4135.
- [82] Wallentin, C.-J.; Nguyen, J. D.; Finkbeiner, P.; Stephenson, C. R. J. *J. Am. Chem. Soc.* **2012**, *134*, 8875-8884.
- [83] Ghosh, I.; Ghosh, T.; Bardagi, J. I.; König, B. *Science* **2014**, *346*, 725-728.
- [84] Juris, A.; Balzani, V.; Belser, P.; Zelewsky, A. v. *Helv. Chim. Acta* **1981**, *64*, 2175-2182.
- [85] Kalyanasundaram, K. *Coord. Chem. Rev.* **1982**, *46*, 159-244.
- [86] Juris, A.; Balzani, V.; Campagna, S.; Belser, P.; Zelewsky, A. v. *Coord. Chem. Rev.* **1988**, *84*, 85-277.
- [87] Balzani, V.; Juris, A. *Coord. Chem. Rev.* **2001**, *211*, 97-115.
- [88] Slinker, J. D.; Gorodetsky, A. A.; Lowry, M. S.; Wang, J.; Parker, S.; Rohl, R.; Bernhard, S.; Malliaras, G. G. *J. Am. Chem. Soc.* **2004**, *126*, 2763-2767.
- [89] Lowry, M. S.; Goldsmith, J. I.; Slinker, J. D.; Rohl, R.; Pascal, R. A.; Malliaras, G. G.; Bernhard, S. *Chem. Mater.* **2005**, *17*, 5712-5719.
- [90] Balzani, V.; Bergamini, G.; Marchioni, F.; Ceroni, P. *Coord. Chem. Rev.* **2006**, *250*, 1254-1266.
- [91] Flamigni, L.; Barbieri, A.; Sabatini, C.; Ventura, B.; Barigelletti, F. *Top. Curr. Chem.* **2007**, *281*, 143-204.
- [92] Tucker, J. W.; Stephenson, C. R. J. *J. Org. Chem.* **2012**, *77*, 1617-1622.
- [93] Tucker, J. W.; Nguyen, J. D.; Narayanam, J. M. R.; Krabbe, S. W.; Stephenson, C. R. J. *Chem. Commun.* **2010**, *46*, 4985-4987.
- [94] Nguyen, J. D.; D'Amato, E. M.; Narayanam, J. M. R.; Stephenson, C. R. J. *Nat. Chem.* **2012**, *4*, 854-859.
- [95] Maji, T.; Karmakar, A.; Reiser, O. *J. Org. Chem.* **2011**, *76*, 736-739.
- [96] Reina, D. F.; Dauncey, E. M.; Morcillo, S. P.; Svejstrup, T. D.; Popescu, M. V.; Douglas, J. J.; Sheikh, N. S.; Leonori, D. *Eur. J. Org. Chem.* **2017**, 2108-2111.
- [97] Lin, X.; Gan, Z.; Lu, J.; Su, Z.; Hu, C.; Zhang, Y.; Wu, Y.; Gao, L.; Song, Z. *Chem. Commun.* **2016**, *52*, 6189-6192.
- [98] Tucker, J. W.; Stephenson, C. R. J. *Org. Lett.* **2011**, *13*, 5468-5471.
- [99] Deng, G.-B.; Wang, Z.-Q.; Xia, J.-D.; Qian, P.-C.; Song, R.-J.; Hu, M.; Gong, L.-B.; Li, J.-H. *Angew. Chem. Int. Ed.* **2013**, *52*, 1535-1538.
- [100] Xiao, T.; Dong, X.; Tang, Y.; Zhou, L. *Adv. Synth. Catal.* **2012**, *354*, 3195-3199.
- [101] Dong, X.; Xu, Y.; Liu, J. J.; Hu, Y.; Xiao, T.; Zhou, L. *Chem. Eur. J.* **2013**, *19*, 16928-16933.
- [102] Fu, W.; Zhu, M.; Zou, G.; Xu, C.; Wang, Z.; Ji, B. *J. Org. Chem.* **2015**, *80*, 4766-4770.
- [103] Nagode, S. B.; Chaturvedi, A. K.; Rastogi, N. *Asian J. Chem.* **2017**, *6*, 453-457.

- [104] Feng, S.; Xie, X.; Zhang, W.; Liu, L.; Zhong, Z.; Xu, D.; She, X. *Org. Lett.* **2016**, *18*, 3846-3849.
- [105] Hari, D. P.; Hering, T.; König, B. *Org. Lett.* **2012**, *14*, 5334-5337.
- [106] Huang, L.; Ye, L.; Li, X.-H.; Li, Z.-L.; Lin, J.-S.; Liu, X.-Y. *Org. Lett.* **2016**, *18*, 5284-5287.
- [107] An, X.-D.; Jiao, Y.-Y.; Zhang, H.; Gao, Y.; Yu, S. *Org. Lett.* **2018**, *20*, 401-404.
- [108] Pagire, S. K.; Reiser, O. *Green Chem.* **2017**, *19*, 1721-1725.
- [109] Han, H. S.; Lee, Y. J.; Jung, Y.-S.; Han, S. B. *Org. Lett.* **2017**, *19*, 1962-1965.
- [110] Chakrasali, P.; Kim, K.; Jung, Y.-S.; Kim, H.; Han, S. B. *Org. Lett.* **2018**, *20*, 7509-7513.
- [111] Malpani, Y. R.; Biswas, B. K.; Han, H. S.; Jung, Y.-S.; Han, S. B. *Org. Lett.* **2018**, *20*, 1693-1697.
- [112] Wang, H.; Li, Y.; Tang, Z.; Wang, S.; Zhang, H.; Cong, H.; Lei, A. *ACS Catal.* **2018**, *8*, 10599-10605.
- [113] Zhang, P.; Xiao, T.; Xiong, S.; Dong, X.; Zhou, L. *Org. Lett.* **2014**, *16*, 3264-3267.
- [114] Pagire, S. K.; Kreitmeier, P.; Reiser, O. *Angew. Chem. Int. Ed.* **2017**, *56*, 10928-10932.
- [115] Gao, F.; Wang, J.-T.; Liu, L.-L.; Ma, N.; Yang, C.; Gao, Y.; Xia, W. *Chem. Commun.* **2017**, *53*, 8533-8536.
- [116] Xia, X.-F.; Zhang, G.-W.; Wang, D.; Zhu, S.-L. *J. Org. Chem.* **2017**, *82*, 8455-8463.
- [117] Brachet, E.; Marzo, L.; Selkti, M.; König, B.; Belmont, P. *Chem. Sci.* **2016**, *7*, 5002-5006.
- [118] Li, H.; Cheng, Z.; Tung, C.-H.; Xu, Z. *ACS Catal.* **2018**, *8*, 8237-8243.
- [119] Wang, L.; Lear, J. M.; Rafferty, S. M.; Fosu, S. C.; Nagib, D. A. *Science* **2018**, *362*, 225-229.
- [120] Ravelli, D.; Protti, S.; Fagnoni, M. *Chem. Rev.* **2016**, *116*, 9850-9913.
- [121] Wang, C.-S.; Dixneuf, P. H.; Soulé, J.-F. *Chem. Rev.* **2018**, *118*, 7532-7585.
- [122] Beletskaya, I. P.; Cheprakov, A. V. *Chem. Rev.* **2000**, *100*, 3009-3066.
- [123] Haas, D.; Hammann, J. M.; Greiner, R.; Knochel, P. *ACS Catal.* **2016**, *6*, 1540-1552.
- [124] Miyaura, N.; Suzuki, A. *Chem. Rev.* **1995**, *95*, 2457-2483.
- [125] Dounay, A. B.; Overman, L. E. *Chem. Rev.* **2003**, *103*, 2945-2963.
- [126] Oestreich, M. *Angew. Chem. Int. Ed.* **2014**, *53*, 2282-2285.
- [127] Pinson, J.; Savéant, J.-M. *J. Chem. Soc., Chem. Commun.* **1974**, *22*, 933-934.
- [128] Costentin, C.; Robert, M.; Savéant, J.-M. *J. Am. Chem. Soc.* **2004**, *126*, 16051-16057.
- [129] Pause, L.; Robert, M.; Savéant, J.-M. *J. Am. Chem. Soc.* **1999**, *121*, 7158-7159.
- [130] Zhang, X.-M. *J. Chem. Soc., Perkin Trans. 2* **1993**, 2275-2279.
- [131] Savéant, J.-M. *J. Phys. Chem.* **1994**, *98*, 3716-3724.
- [132] Andrieux, C. P.; Gorande, A. L.; Savéant, J.-M. *J. Am. Chem. Soc.* **1992**, *114*, 6892-6904.
- [133] Savéant, J.-M. *Acc. Chem. Res.* **1993**, *26*, 455-461.
- [134] Andrieux, C. P.; Gallardo, I.; Savéant, J.-M.; Su, K.-B. *J. Am. Chem. Soc.* **1986**, *108*, 638-647.
- [135] Andrieux, C. P.; Merz, A.; Savéant, J.-M. *J. Am. Chem. Soc.* **1985**, *107*, 6097-6103.
- [136] Andrieux, C. P.; Blocman, C.; Dumas-Bouchiat, J. M.; M'Halla, F.; Savéant, J.-M. *J. Am. Chem. Soc.* **1980**, *102*, 3806-3813.
- [137] Savéant, J.-M. *Acc. Chem. Res.* **1980**, *13*, 323-329.
- [138] Paria, S.; Reiser, O. *Adv. Synth. Catal.* **2014**, *356*, 557-562.
- [139] Paria, S.; Kais, V.; Reiser, O. *Adv. Synth. Catal.* **2014**, *356*, 2853-2858.
- [140] Zhang, X.-M.; Bordwell, F. G. *J. Am. Chem. Soc.* **1992**, *114*, 9787-9792.
- [141] Pierini, A. B.; Vera, D. M. A. *J. Org. Chem.* **2003**, *68*, 9191-9199.

- [142] Jiang, Y.; Xu, K.; Zeng, C. *Chem. Rev.* **2018**, *118*, 4485-4540.
- [143] Tyson, E. L.; Farney, E. P.; Yoon, T. P. *Org. Lett.* **2012**, *14*, 1110-1113.
- [144] Pelagalli, R.; Chiarotto, I.; Feroci, M.; Vecchio, S. *Green Chem.* **2012**, *14*, 2251-2255.
- [145] Myers, M. C.; Bharadwaj, A. R.; Milgram, B. C.; Scheidt, K. A. *J. Am. Chem. Soc.* **2005**, *127*, 14675-14680.
- [146] Benedetti, E.; Duchemin, N.; Bethge, L.; Vonhoff, S.; Klussmann, S.; Vasseur, J.-J.; Cossy, J.; Smietana, M.; Arseniyadis, S. *Chem. Commun.* **2015**, *51*, 6076-6079.
- [147] Watson, S. P. *Synth. Commun.* **1992**, *22*, 2971-2977.
- [148] Hering, T.; Hari, D. P.; König, B. *J. Org. Chem.* **2012**, *77*, 10347-10352.
- [149] Jiang, H.; Cheng, Y.; Zhang, Y.; Yu, S. *Eur. J. Org. Chem.* **2013**, *2013*, 5485-5492.
- [150] Paria, S., *Dissertation*, Universität Regensburg, **2014**.
- [151] Föll, T., *Master Thesis*, Universität Regensburg, **2015**.
- [152] Nguyen, J. D.; Reiss, B.; Dai, C.; Stephenson, C. R. J. *Chem. Commun.* **2013**, *49*, 4352-4354.
- [153] Saito, I.; Ikehira, H.; Kasatani, R.; Watanabe, M.; Matsuura, T. *J. Am. Chem. Soc.* **1986**, *108*, 3115-3117.
- [154] Rackl, D.; Kais, V.; Kreitmeier, P.; Reiser, O. *Beilstein J. Org. Chem.* **2014**, *10*, 2157-2165.
- [155] Fife, T. H.; Przystas, T. J.; Pujari, M. P. *J. Am. Chem. Soc.* **1988**, *110*, 8157-8163.
- [156] Porwisiak, J.; Schlosser, M. *Chem. Ber.* **1996**, *129*, 233-235.
- [157] Smith, J. R. L.; Masheder, D. *J. Chem. Soc., Perkin Trans. 2* **1976**, *0*, 47-51.
- [158] Lewis, F. D.; Ho, T.-I. *J. Am. Chem. Soc.* **1980**, *102*, 1751-1752.
- [159] Furst, L.; Matsuura, B. S.; Narayanam, J. M. R.; Tucker, J. W.; Stephenson, C. R. J. *Org. Lett.* **2010**, *12*, 3104-3107.
- [160] Tucker, J. W.; Narayanam, J. M. R.; Krabbe, S. W.; Stephenson, C. R. J. *Org. Lett.* **2010**, *12*, 368-371.
- [161] Taylor, M. J. W.; Eckenhoff, W. T.; Pintauer, T. *Dalton Trans.* **2010**, *39*, 11475-11482.
- [162] Arora, A.; Teegardin, K. A.; Weaver, J. D. *Org. Lett.* **2015**, *17*, 3722-3725.
- [163] Arora, A.; Weaver, J. D. *Org. Lett.* **2016**, *18*, 3996-3999.
- [164] Kotani, S.; Osakama, K.; Sugiura, M.; Nakajima, M. *Org. Lett.* **2011**, *13*, 3968-3971.
- [165] Dömling, A. *Chem. Rev.* **2006**, *106*, 17-89.
- [166] Touré, B. B.; Hall, D. G. *Chem. Rev.* **2009**, *109*, 4439-4486.
- [167] Estévez, V.; Villacampa, M.; Menéndez, J. C. *Chem. Soc. Rev.* **2010**, *39*, 4402-4421.
- [168] Dömling, A.; Wang, W.; Wang, K. *Chem. Rev.* **2012**, *112*, 3083-3135.
- [169] Rotstein, B. H.; Zaretsky, S.; Rai, V.; Yudin, A. K. *Chem. Rev.* **2014**, *114*, 8323-8359.
- [170] Estévez, V.; Villacampa, M.; Menéndez, J. C. *Chem. Soc. Rev.* **2014**, *43*, 4633-4657.
- [171] Godineau, E.; Landais, Y. *Chem. Eur. J.* **2009**, *15*, 3044-3055.
- [172] Liu, Z.; Liu, Z.-Q. *Org. Lett.* **2017**, *19*, 5649-5652.
- [173] Hartmann, M.; Li, Y.; Studer, A. *Org. Biomol. Chem.* **2016**, *14*, 206-210.
- [174] Tu, H.-Y.; Zhu, S.; Qing, F.-L.; Chu, L. *Chem. Commun.* **2018**, *54*, 12710-12713.
- [175] Courant, T.; Masson, G. *Chem. Eur. J.* **2012**, *18*, 423-427.
- [176] Carboni, A.; Dagousset, G.; Magnier, E.; Masson, G. *Org. Lett.* **2014**, *16*, 1240-1243.
- [177] Majek, M.; Jacobi von Wangelin, A. *Angew. Chem. Int. Ed.* **2015**, *54*, 2270-2274.
- [178] Yin, Z.-B.; Ye, J.-H.; Zhou, W.-J.; Zhang, Y.-H.; Ding, L.; Gui, Y.-Y.; Yan, S.-S.; Li, J.; Yu, D.-G. *Org. Lett.* **2018**, *20*, 190-193.
- [179] Petterson, F.; Bergonzini, G.; Cassani, C.; Wallentin, C.-J. *Chem. Eur. J.* **2017**, *23*, 7444-7447.
- [180] Hari, D. P.; Schroll, P.; König, B. *J. Am. Chem. Soc.* **2012**, *134*, 2958-2961.
- [181] Schroll, P.; Hari, D. P.; König, B. *Chemistry Open* **2012**, *1*, 130-133.

- [182] Majek, M.; Filace, F.; Jacobi von Wangelin, A. *Chem. Eur. J.* **2015**, *21*, 4518-4522.
- [183] Ghosh, I.; Marzo, L.; Das, A.; Shaikh, R.; König, B. *Acc. Chem. Res.* **2016**, *49*, 1566-1577.
- [184] Yao, C.-J.; Sun, Q.; Rastogi, N.; König, B. *ACS Catal.* **2015**, *5*, 2935-2938.
- [185] Tlahuext-Aca, A.; Hopkinson, M. N.; Sahoo, B.; Glorius, F. *Chem. Sci.* **2016**, *7*, 89-93.
- [186] Luo, Y.-R., *Handbook of Bond Dissociation Energies in Organic Compounds*, CRC Press LLC, **2003**.
- [187] Johansson Seechurn, C. C. C.; DeAngelis, A.; Colacot, T. J., *New Trends in Cross-Coupling: Theory and Applications*, RSC Publishing: Cambridge, **2015**.
- [188] Hicks, J. D.; Hyde, A. M.; Cuezva, A. M.; Buchwald, S. L. *J. Am. Chem. Soc.* **2009**, *131*, 16720-16734.
- [189] Vinogradova, E. V.; Fors, B. P.; Buchwald, S. L. *J. Am. Chem. Soc.* **2012**, *134*, 11132-11135.
- [190] Mitsudo, K.; Nakagawa, Y.; Mizukawa, J.-i.; Tanaka, H.; Akaba, R.; Okada, T.; Suga, S. *Electrochim. Acta* **2012**, *82*, 444-449.
- [191] Daasbjerg, K. *J. Chem. Soc. Perkin Trans. 2* **1994**, 1275-1277.
- [192] Singh, A.; Arora, A.; Weaver, J. D. *Org. Lett.* **2013**, *15*, 5390-5393.
- [193] Zhao, Y.; Li, Z.; Yang, C.; Lin, R.; Xia, W. *Beilstein J. Org. Chem.* **2014**, *10*, 622-627.
- [194] Lin, R.; Sun, H.; Yang, C.; Yang, Y.; Zhao, X.; Xia, W. *Beilstein J. Org. Chem.* **2015**, *11*, 31-36.
- [195] Tripathi, S.; Yadav, L. D. S. *New J. Chem.* **2018**, *42*, 3765-3769.
- [196] Franz, J. F.; Kraus, W. B.; Zeitler, K. *Chem. Commun.* **2015**, *51*, 8280-8283.
- [197] Augustine, J. K.; Bombrun, A.; Venkatachaliah, S.; Jothi, A. *Org. Biomol. Chem.* **2013**, *11*, 8065-8072.
- [198] Falck, J. R.; Bejot, R.; Barma, D. K.; Bandyopadhyay, A.; Joseph, S.; Mioskowski, C. *J. Org. Chem.* **2006**, *71*, 8178-8182.
- [199] Macharla, A. K.; Nappunni, R. C.; Nama, N. *Tetrahedron Lett.* **2012**, *53*, 1401-1405.
- [200] Berkessel, A.; Sebastian, L.; Müller, T. N. *Angew. Chem. Int. Ed.* **2006**, *45*, 6567-6570.
- [201] Galli, C.; Guarnieri, A.; Koch, H.; Mencarelli, P.; Rappoport, Z. *J. Org. Chem.* **1997**, *62*, 4072-4077.
- [202] Goumans, T. P. M.; van Alem, K.; Lodder, G. *Eur. J. Org. Chem.* **2008**, 435-443.
- [203] Zhang, F.; Du, P.; Chen, J.; Wang, H.; Luo, Q.; Wan, X. *Org. Lett.* **2014**, *16*, 1932-1935.
- [204] Zhang, L.; Zhang, J.; Ma, J.; Cheng, D.-J.; Tan, B. *J. Am. Chem. Soc.* **2017**, *139*, 1714-1717.
- [205] Knorr, L. *Ber. Dtsch. Chem. Ges.* **1884**, *17*, 1635-1642.
- [206] Knorr, L. *Ber. Dtsch. Chem. Ges.* **1884**, *17*, 2863-2870.
- [207] Paal, C. *Ber. Dtsch. Chem. Ges.* **1884**, *17*, 2756-2767.
- [208] Paal, C. *Ber. Dtsch. Chem. Ges.* **1885**, *18*, 367-371.
- [209] Kim, J. M.; Lee, S.; Kim, S. H.; Lee, H. S.; Kim, J. N. *Bull. Korean Chem. Soc.* **2008**, *29*, 2215-2220.
- [210] Minetto, G.; Raveglia, L. F.; Sega, A.; Taddei, M. *Eur. J. Org. Chem.* **2005**, *2005*, 5277-5288.
- [211] Reddy, G. S.; Salahuddin, S.; Neelakantan, P.; Iyengar, D. S. *Heterocycl. Commun.* **2002**, *8*, 361-364.
- [212] Wu, Y.-L.; Wang, D.-L.; Guo, E.-H.; Song, S.; Feng, J.-T.; Zhang, X. *Bioorg. Med. Chem. Lett.* **2017**, *27*, 1284-1290.

- [213] Lai, L.; Li, A.-N.; Zhou, J.; Guo, Y.; Lin, L.; Chen, W.; Wang, R. *Org. Biomol. Chem.* **2017**, *15*, 2185-2190.
- [214] Dong, Y.; Guo, X.; Yu, Y.; Liu, G. *Mol. Diversity* **2013**, *17*, 1-7.
- [215] Elford, T. G.; Ulaczyk-Lesanko, A.; De Pascale, G.; Wright, G. D.; Hall, D. G. *J. Comb. Chem.* **2009**, *11*, 155-168.
- [216] Albrecht, A.; Koszuk, J. F.; Modranka, J.; Rozalski, M.; Krajewska, U.; Janecka, A.; Studzian, K.; Janecki, T. *Bioorg. Med. Chem. Lett.* **2008**, *16*, 4872-4882.
- [217] Lei, A.; He, M.; Zhang, X. *J. Am. Chem. Soc.* **2002**, *124*, 8198-8199.
- [218] Garlets, Z. J.; Nguyen, J. D.; Stephenson, C. R. *J. Isr. J. Chem.* **2014**, *54*, 351-360.
- [219] Bou-Hamdan, F. R.; Seeberger, P. H. *Chem. Sci.* **2012**, *3*, 1612-1616.
- [220] Andrews, R. S.; Becker, J. J.; Gagné, M. R. *Angew. Chem. Int. Ed.* **2012**, *51*, 4140-4143.
- [221] Tucker, J. W.; Zhang, Y.; Jamison, T. F.; Stephenson, C. R. *J. Angew. Chem. Int. Ed.* **2012**, *51*, 4144-4147.
- [222] Douglas, J. J.; Sevrin, M. J.; Cole, K. P.; Stephenson, C. R. *J. Org. Process Res. Dev.* **2016**, *20*, 1148-1155.
- [223] Yayla, H. G.; Peng, F.; Mangion, I. K.; McLaughlin, M.; Campeau, L.-C.; Davies, I. W.; DiRocco, D. A.; Knowles, R. R. *Chem. Sci.* **2016**, *7*, 2066-2073.
- [224] Beatty, J. W.; Douglas, J. J.; Miller, R.; McAtee, R. C.; Cole, K. P.; Stephenson, C. R. *J. Chem* **2016**, *1*, 456-472.
- [225] Beatty, J. W.; Douglas, J. J.; Cole, K. P.; Stephenson, C. R. *J. Nat. Commun.* **2015**, *6*, 7919-7924.
- [226] Gemal, A. L.; Luche, J.-L. *J. Am. Chem. Soc.* **1981**, *103*, 5454-5459.
- [227] Ramachandran, P. V.; Garner, G.; Pratihari, D. *Org. Lett.* **2007**, *9*, 4753-4756.
- [228] Luche, J.-L. *J. Am. Chem. Soc.* **1978**, *100*, 2226-2227.
- [229] He, P.; Liu, X.; Zheng, H.; Li, W.; Lin, L.; Feng, X. *Org. Lett.* **2012**, *14*, 5134-5137.
- [230] Itsuno, S.; Sakurai, Y.; Shimizu, K.; Ito, K. *J. Chem. Soc., Perkin Trans. 1* **1990**, *0*, 1859-1863.
- [231] Apsimon, J. W.; Collier, T. L. *Tetrahedron* **1986**, *42*, 5157-5254.
- [232] Yamada, S.; Mori, Y.; Morimatsu, K.; Ishizu, Y.; Ozaki, Y.; Yoshioka, R.; Nakatani, T.; Seko, H. *J. Org. Chem.* **1996**, *61*, 8586-8590.
- [233] Hajipour, A. R.; Hantehzadeh, M. *J. Org. Chem.* **1999**, *64*, 8475-8478.
- [234] Morrison, J. D.; Grandbois, E. R.; Howard, S. I. *J. Org. Chem.* **1980**, *45*, 4229-4231.
- [235] Hirao, A.; Nakahama, S.; Mochizuki, H.; Itsuno, S.; Yamazaki, N. *J. Org. Chem.* **1980**, *45*, 4231-4233.
- [236] Hirao, A.; Itsuno, S.; Nakahama, S.; Yamazaki, N. *J. Chem. Soc., Chem. Commun.* **1981**, 315-317.
- [237] Itsuno, S.; Hirao, A.; Nakahama, S.; Yamazaki, N. *J. Chem. Soc., Perkin Trans. 1* **1983**, *0*, 1673-1676.
- [238] Corey, E. J.; Bakshi, R. K.; Shibata, S. *J. Am. Chem. Soc.* **1987**, *109*, 5551-5553.
- [239] Corey, E. J.; Bakshi, R. K.; Shibata, S.; Chen, C. P.; Singh, V. K. *J. Am. Chem. Soc.* **1987**, *109*, 7925-7926.
- [240] Corey, E. J.; Helal, C. J. *Angew. Chem. Int. Ed.* **1998**, *37*, 1986-2012.
- [241] Corey, E. J.; Shibata, S.; Bakshi, R. K. *J. Org. Chem.* **1988**, *53*, 2861-2863.
- [242] Cho, B. T. *Tetrahedron* **2006**, *62*, 7621-7643.
- [243] Föll, T.; Rehbein, J.; Reiser, O. *Org. Lett.* **2018**, *20*, 5794-5798.
- [244] Schmidbauer, S.; Hohenleutner, A.; König, B. *Beilstein J. Org. Chem.* **2013**, *9*, 2088-2096.
- [245] Devery, J. J.; Douglas, J. J.; Nguyen, J. D.; Cole, K. P.; Flowers, R. A.; Stephenson, C. R. *J. Chem. Sci.* **2015**, *6*, 537-541.

- [246] Obora, Y.; Okabe, Y.; Ishii, Y. *Org. Biomol. Chem.* **2010**, *8*, 4071-4073.
- [247] Saha, D.; Adak, L.; Mukherjee, M.; Ranu, B. C. *Org. Biomol. Chem.* **2012**, *10*, 952-957.
- [248] Bose, D. S.; Jayalakshmi, B. *J. Org. Chem.* **1999**, *64*, 1713-1714.
- [249] Nakajima, N.; Saito, M.; Ubukata, M. *Tetrahedron* **2002**, *58*, 3561-3577.
- [250] Movassagh, B.; Fazeli, A. *Synth. Commun.* **2007**, *37*, 623-628.
- [251] Singh, M. K.; Lakshman, M. K. *J. Org. Chem.* **2009**, *74*, 3079-3084.
- [252] Reddy, K. R.; Maheswari, C. U.; Venkateshwar, M.; Prashanthi, S.; Kantam, M. L. *Tetrahedron Lett.* **2009**, *50*, 2050-2053.
- [253] Oishi, T.; Yamaguchi, K.; Mizuno, N. *Angew. Chem. Int. Ed.* **2009**, *48*, 6286-6288.
- [254] Chao, H. S. I. *Synth. Commun.* **1988**, *18*, 1641-1650.
- [255] Rounds, W. D.; Eaton, J. T.; Urbanowicz, J. H.; Gribble, G. W. *Tetrahedron Lett.* **1988**, *29*, 6557-6560.
- [256] Möltgen, E.; Tinapp, P. *Liebigs Ann. Chem.* **1979**, *12*, 1952-1959.
- [257] Xi, F.; Kamal, F.; Schenerman, M. A. *Tetrahedron Lett.* **2002**, *43*, 1395-1396.
- [258] Kang, H.-Y.; Song, S.-E. *Tetrahedron Lett.* **2000**, *41*, 937-939.
- [259] Bornschein, C.; Werkmeister, S.; Wendt, B.; Jiao, H.; Alberico, E.; Baumann, W.; Junge, H.; Junge, K.; Beller, M. *Nat. Commun.* **2014**, *5*, 4111-4121.
- [260] Lange, S.; Elangovan, S.; Cordes, C.; Spannenberg, A.; Jiao, H.; Junge, H.; Bachmann, S.; Scalone, M.; Topf, C.; Junge, K.; Beller, M. *Catal. Sci. Technol.* **2016**, *6*, 4768-4772.
- [261] Matveeva, E. D.; Erin, A. S.; Osetrov, A. G.; Leshcheva, I. F.; Kurts, A. L. *Russ. J. Org. Chem.* **2006**, *42*, 388-392.
- [262] Armarego, W. L. F.; Chai, C. L. L., *Purification of Laboratory Chemicals*, 6th ed., Butterworth Heinemann: Oxford, **2009**.

## G Appendix

### 1 Reduction potentials of $\alpha$ -halo cinnamates

Cyclic voltammetry measurements were carried out on an Autolab PGSTAT 302N set-up at 20 °C in MeCN, containing tetrabutyl ammonium tetrafluoroborate as supporting electrolyte. A conventional undivided electrochemical cell equipped with a glassy carbon working electrode, platinum wire as the counter electrode and silver wire as the reference electrode was used. The solvent was degassed by vigorous nitrogen bubbling prior to the measurement. Redox potentials were referenced against ferrocene as an internal standard. All values are reported in reference to the SCE electrode.

**Table 15.** Reduction potentials of  $\alpha$ -halo cinnamates.

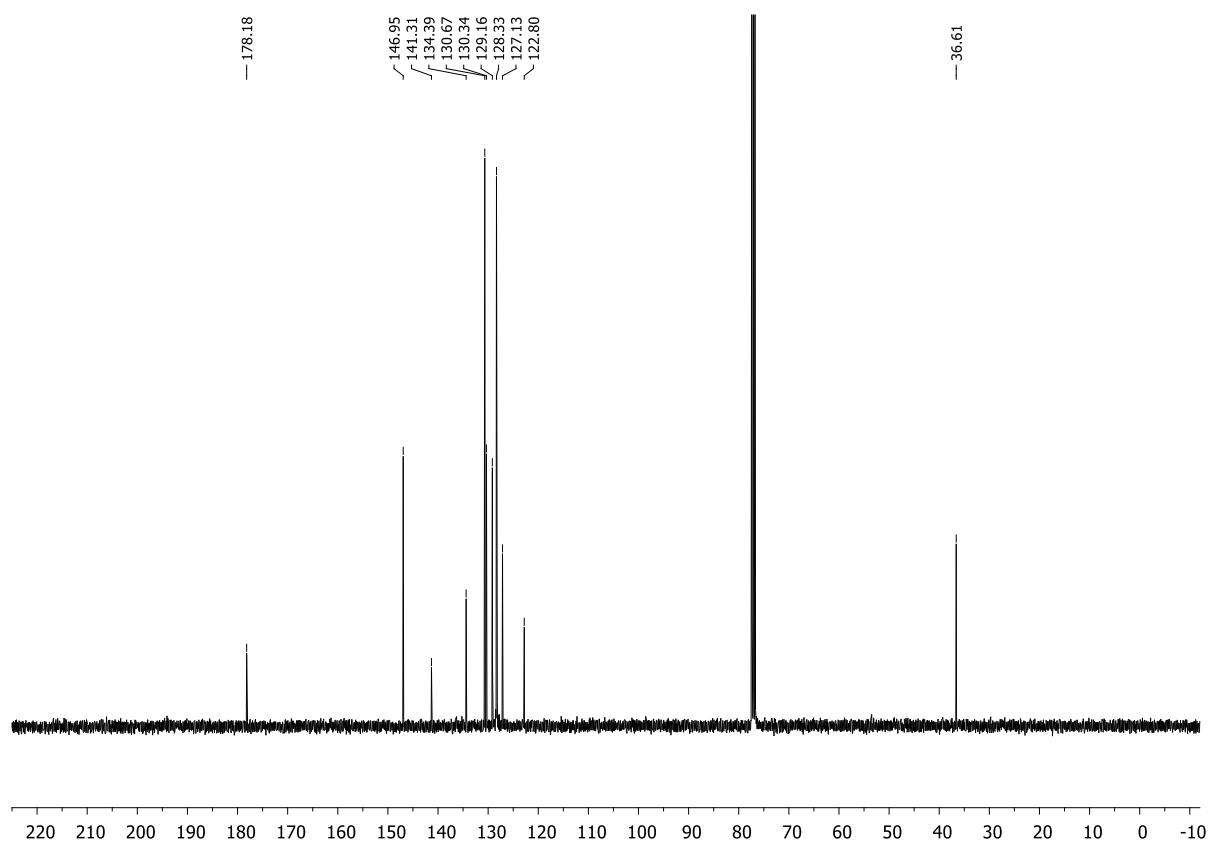
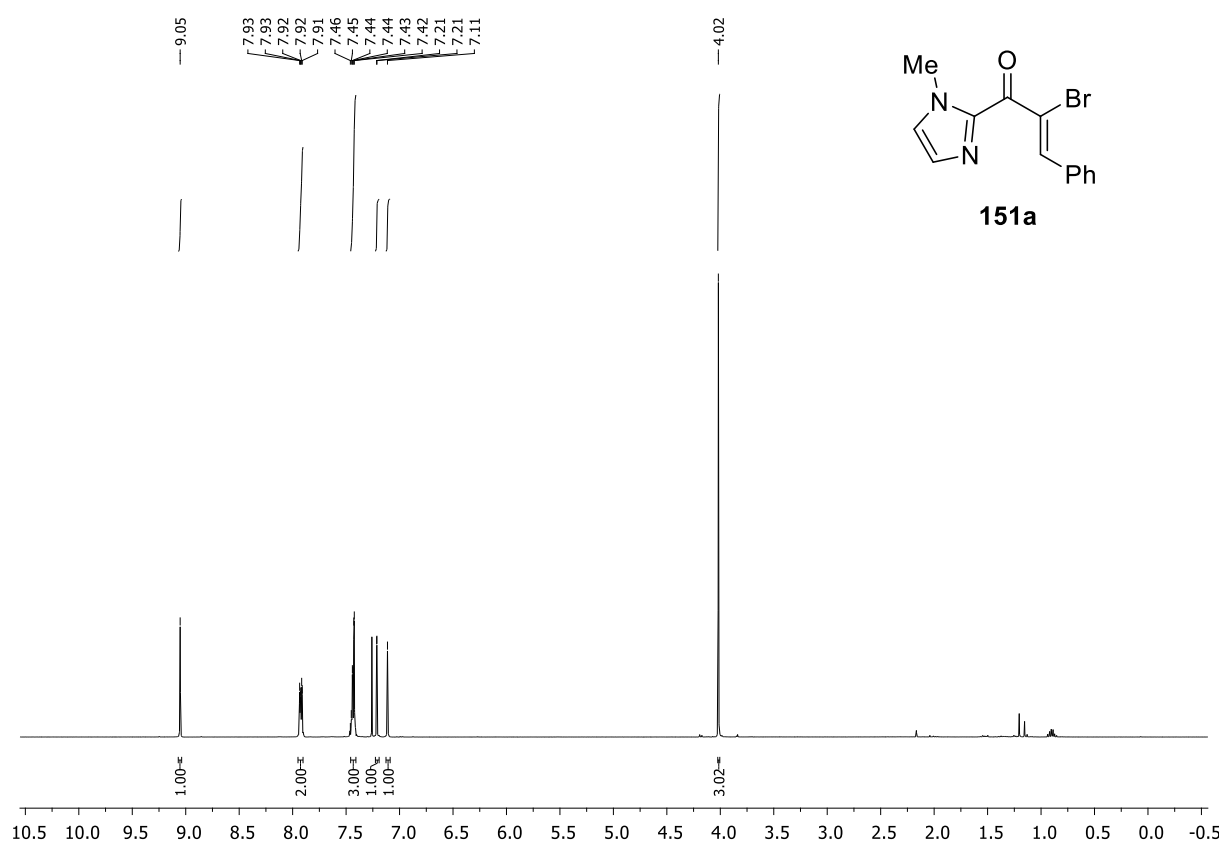
Entry	Compound	Reduction potential vs SCE [V] in MeCN
1	<b>228a-F</b>	-1.93
2	<b>228a-Cl</b>	-1.64
3	<b>228a-Br</b>	-1.54
4	<b>228b</b>	-1.66
5	<b>228c</b>	-1.66
6	<b>228d</b>	-1.71
7	<b>228e</b>	-1.54
8	<b>228f</b>	-1.56
9	<b>228g</b>	-1.67
10	<b>228h</b>	-1.56
11	<b>228i</b>	-1.56
12	<b>228j</b>	-1.55
13	<b>228k</b>	-1.01
14	<b>228l</b>	-1.67
15	<b>228m</b>	-1.65
16	<b>228n</b>	-1.71
17	<b>228o</b>	-1.73
18	<b>228p</b>	-1.70
19	<b>228q</b>	-1.60
20	<b>228r</b>	n.d.
21	<b>228s</b>	n.d.
22	<b>228t</b>	n.d.
23	<b>228u</b>	-2.09

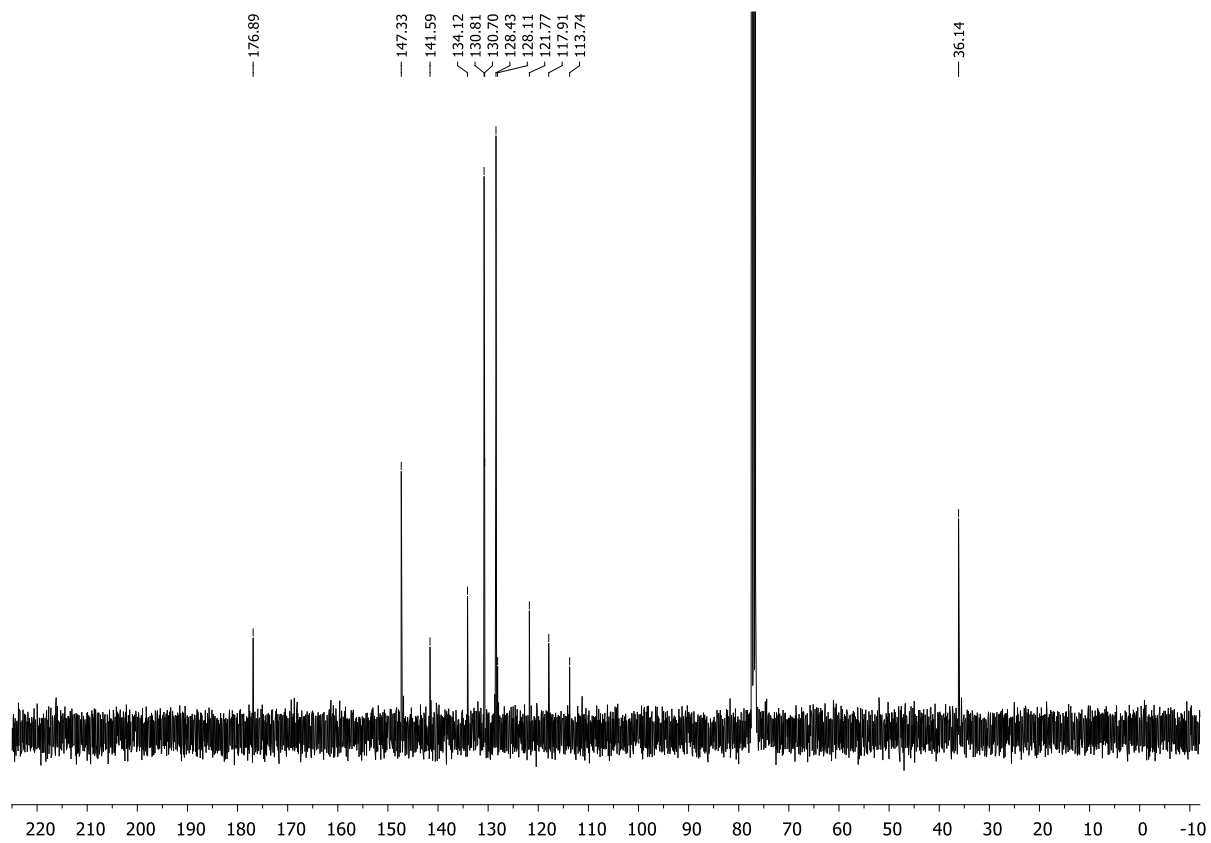
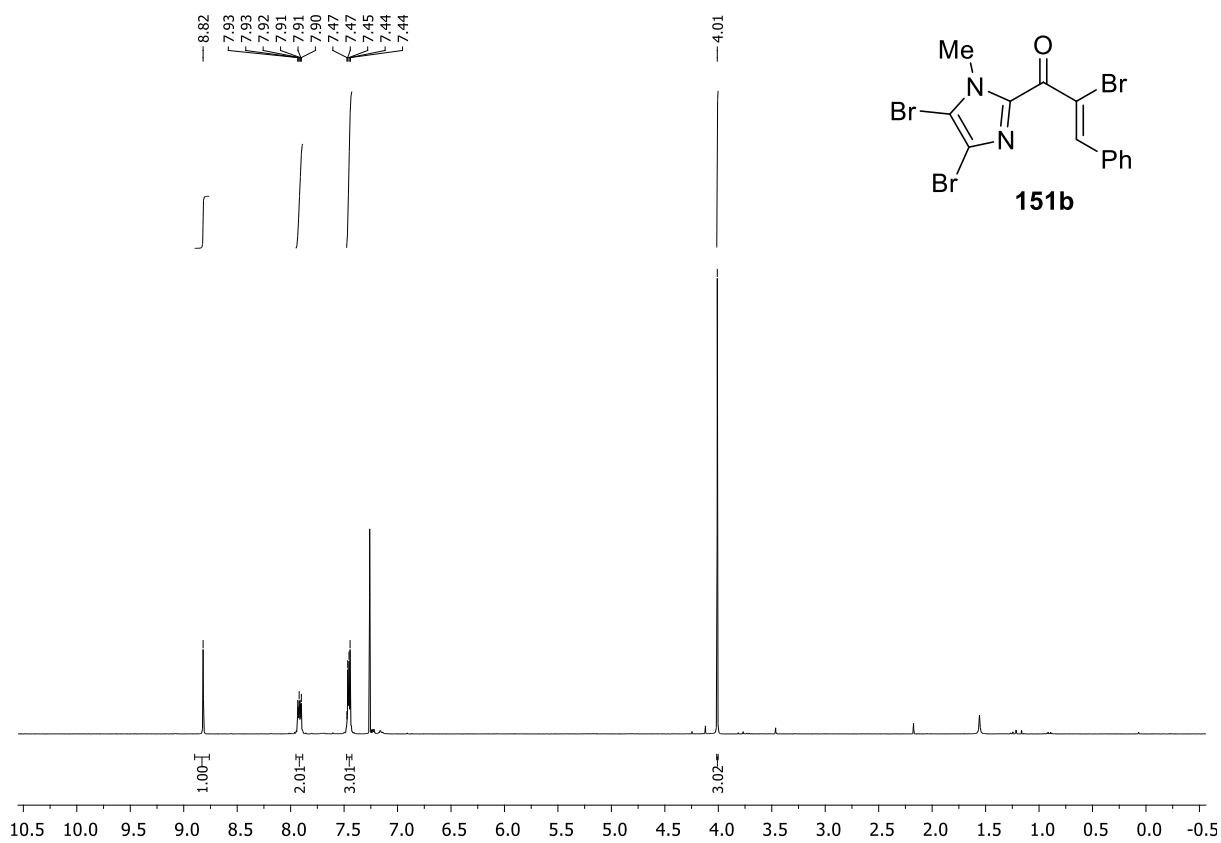
## 2 NMR spectra of new compounds

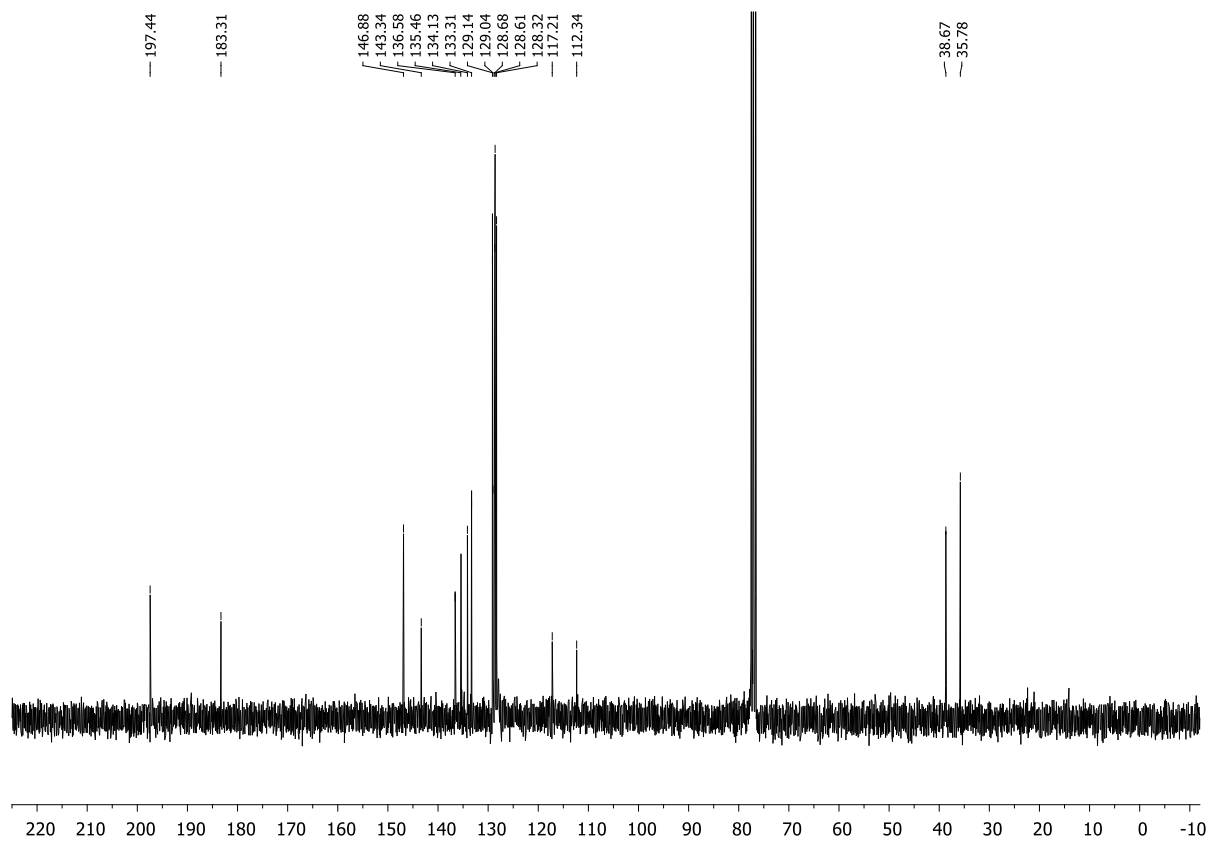
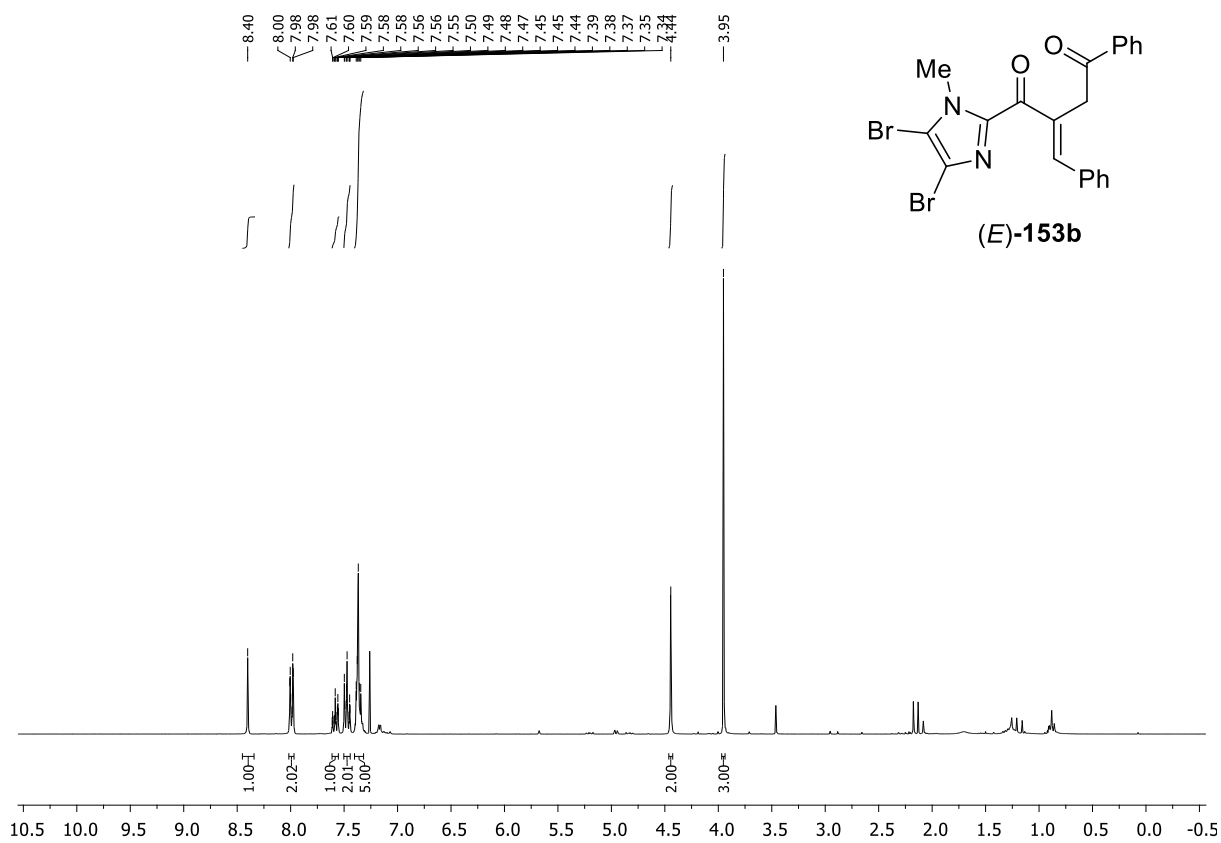
The upper images show the  $^1\text{H}$ -NMR spectra whereas the lower images describe the  $^{13}\text{C}$ -NMR spectra.

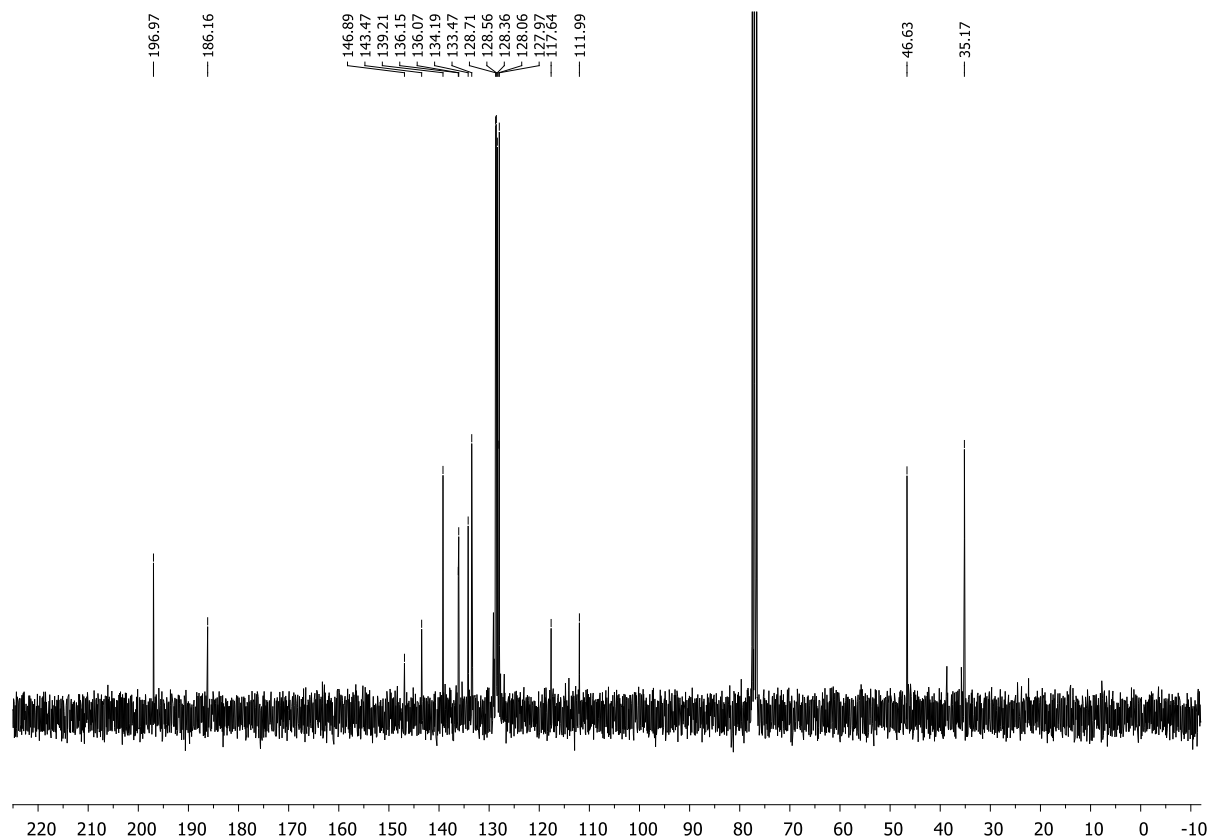
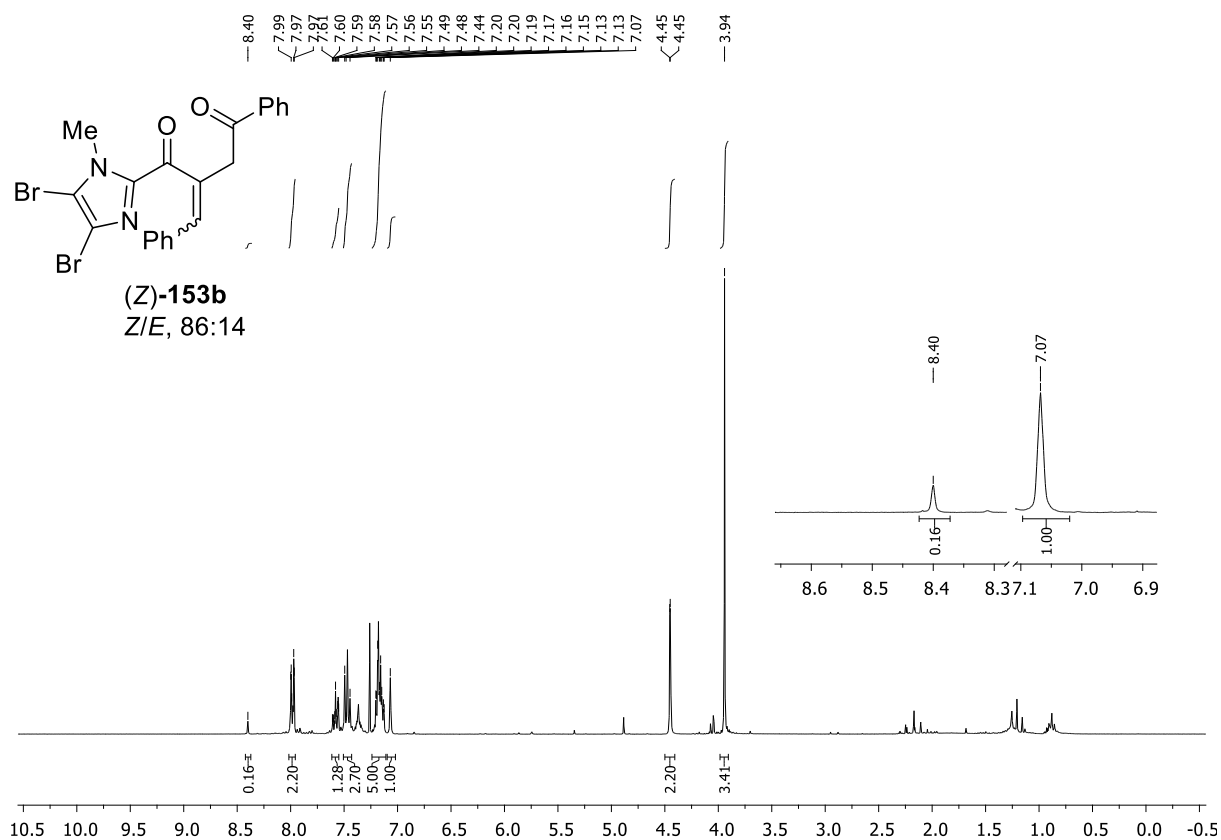
All compounds were dissolved in  $\text{CDCl}_3$  unless otherwise stated.

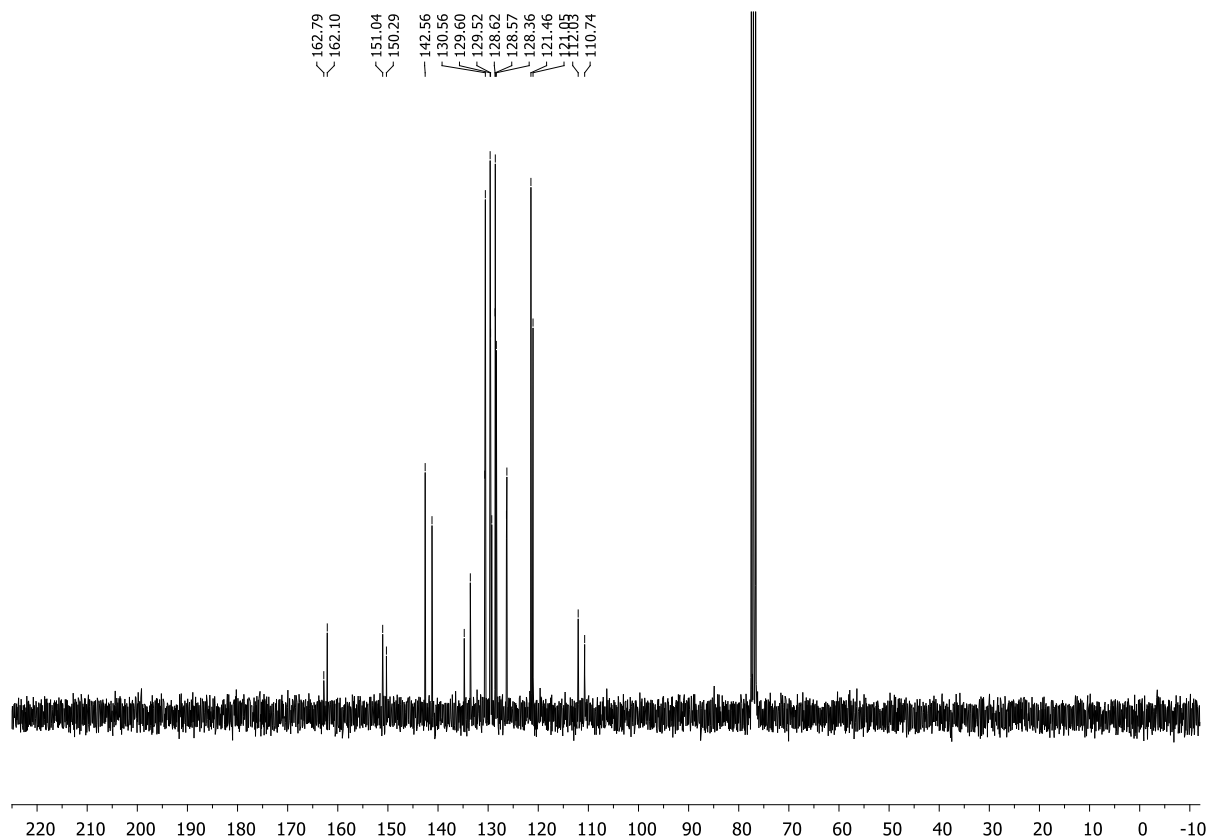
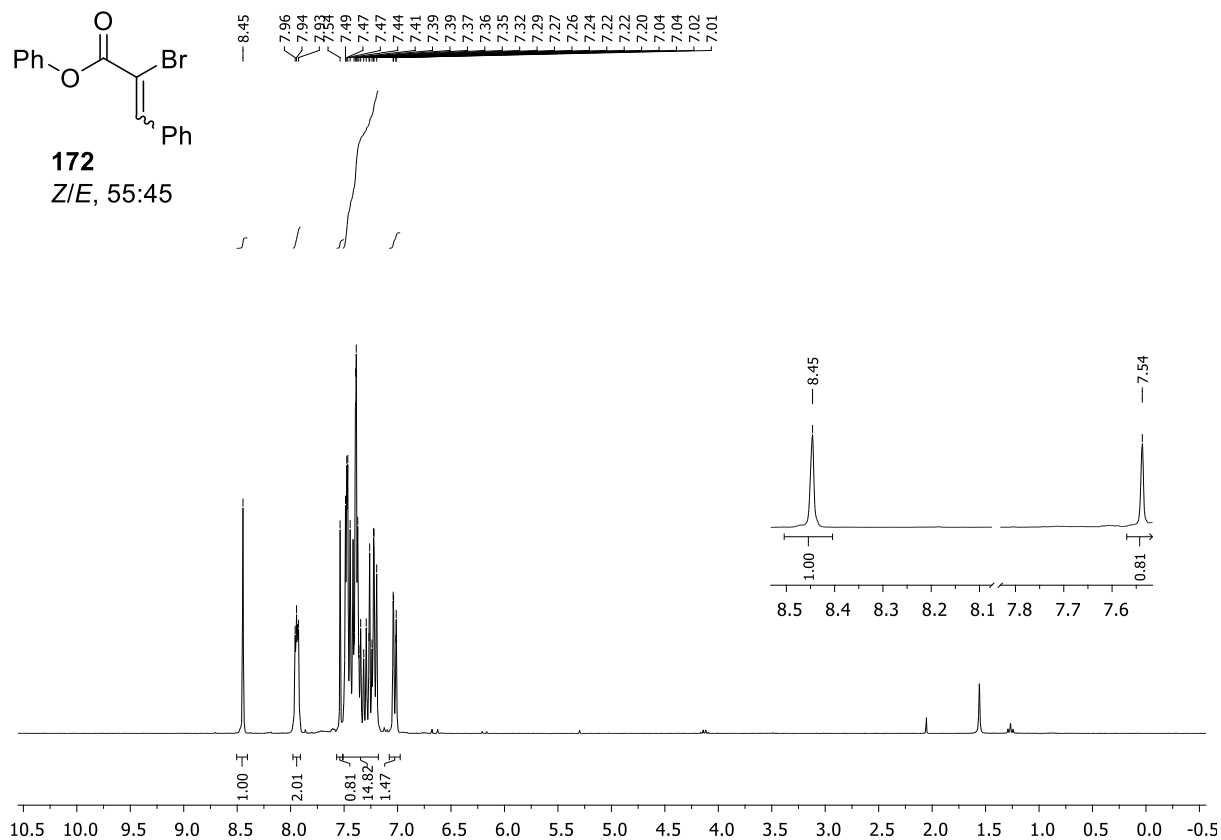
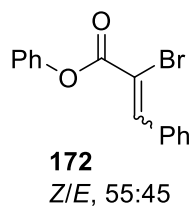


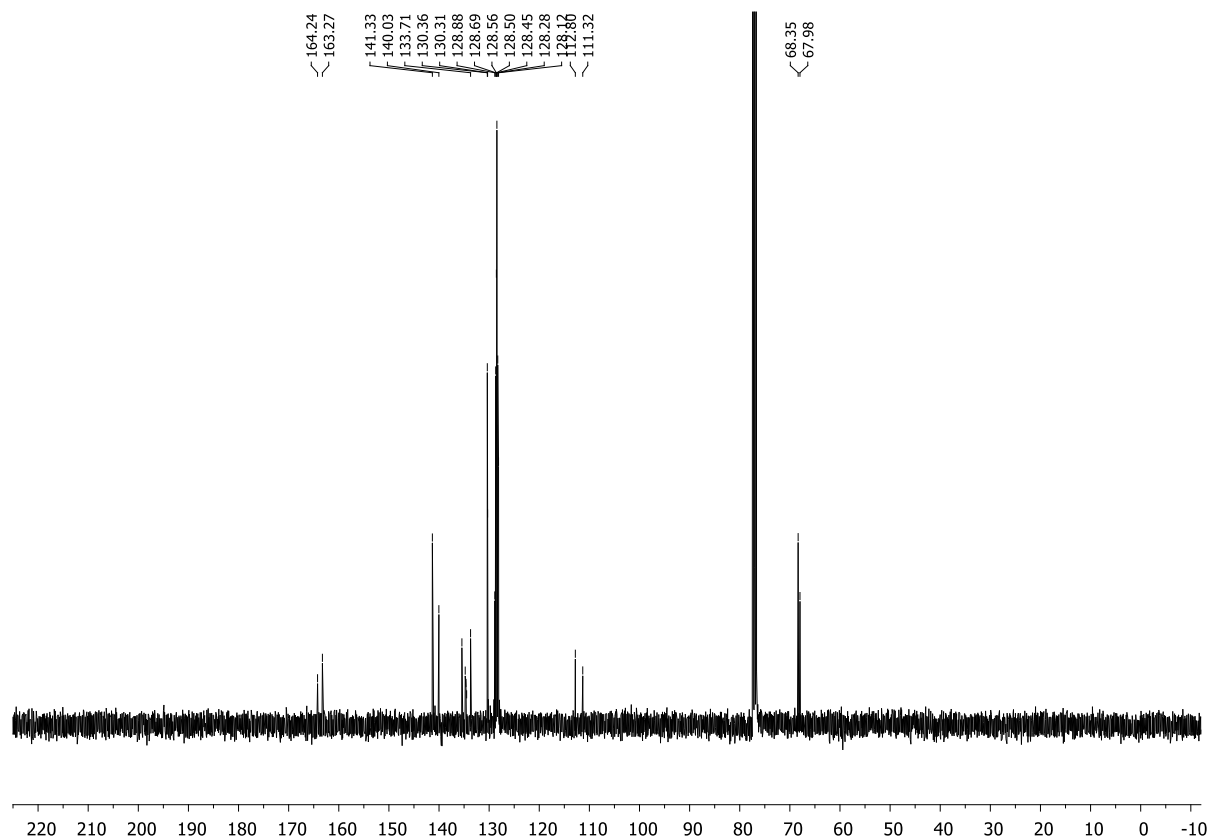
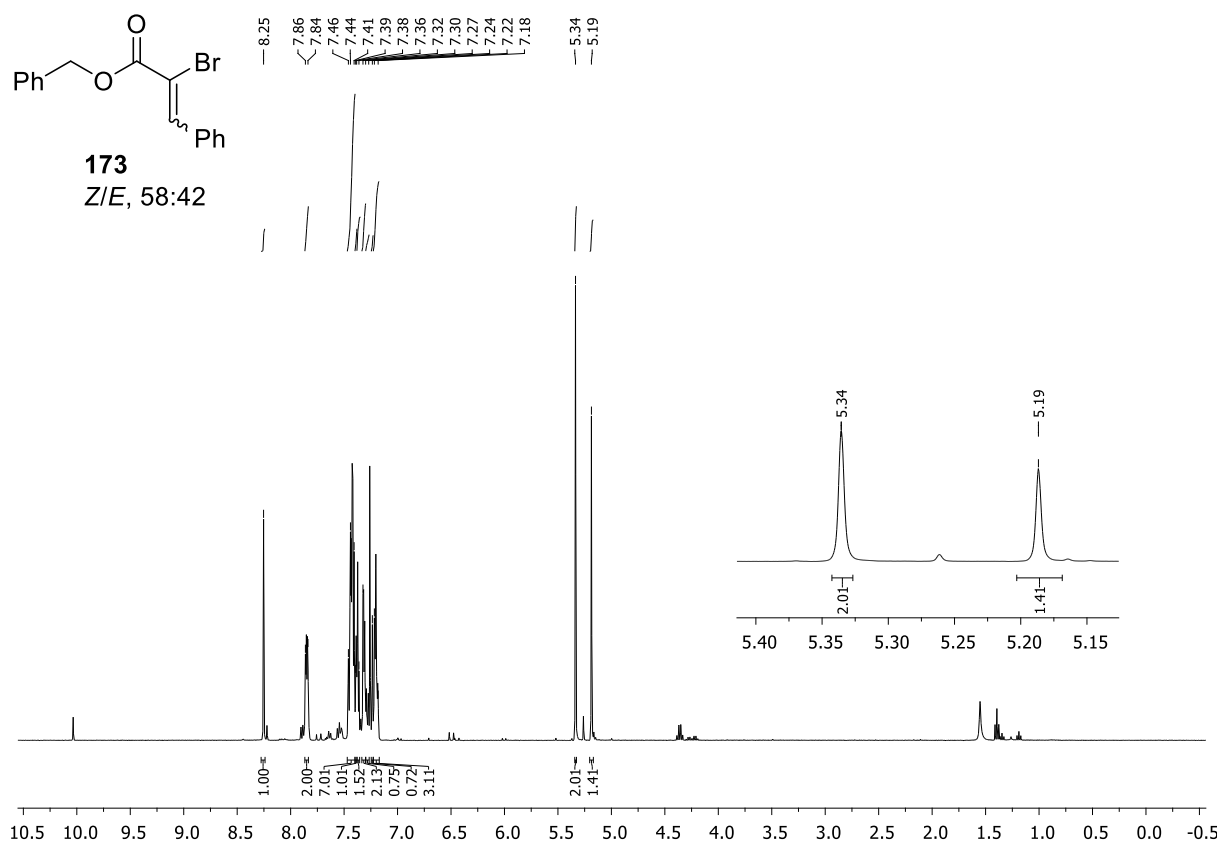


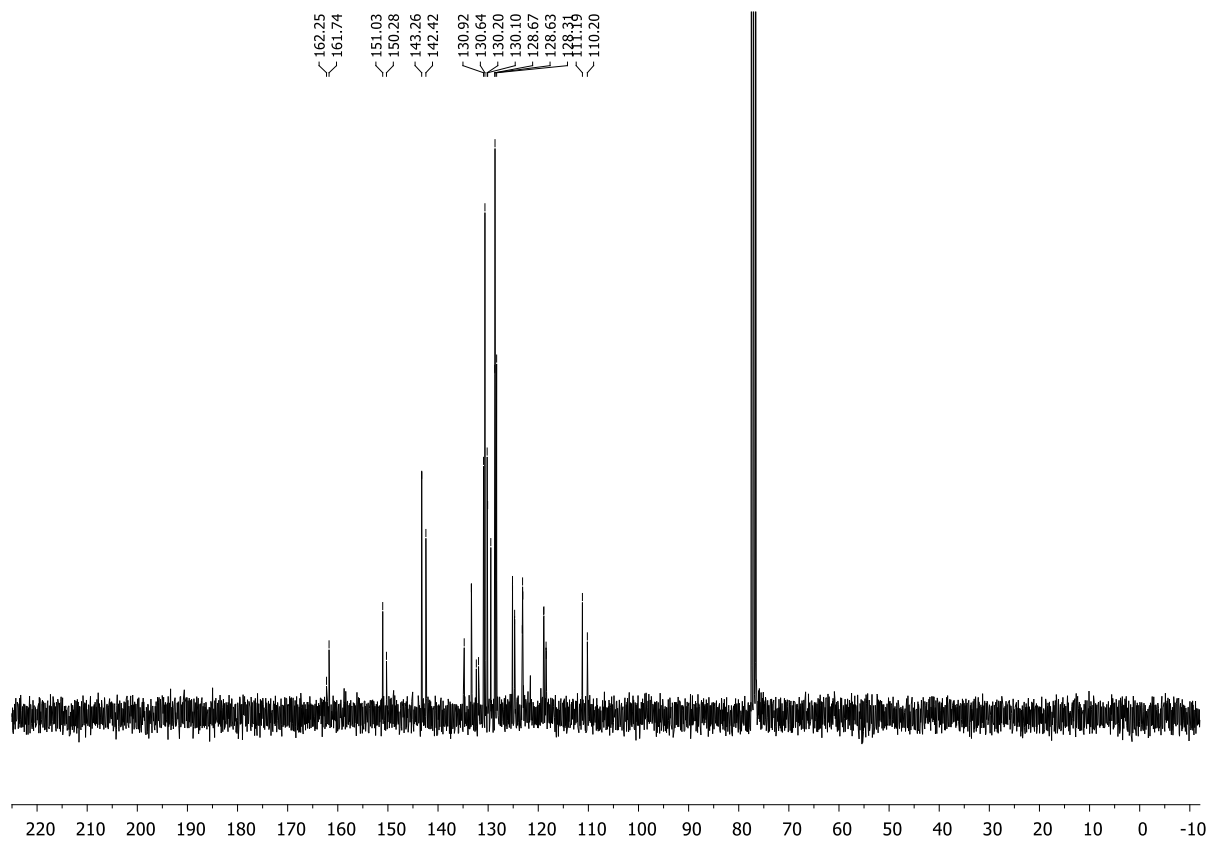
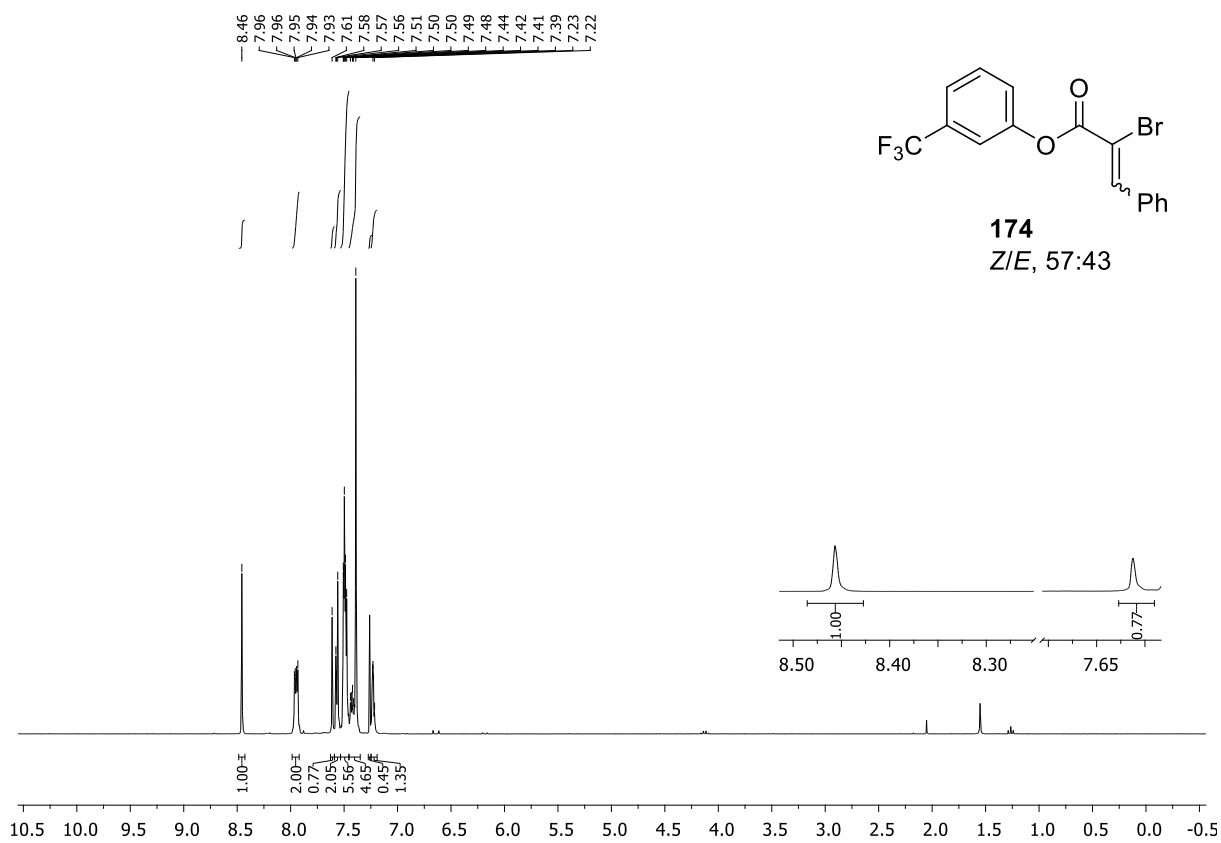


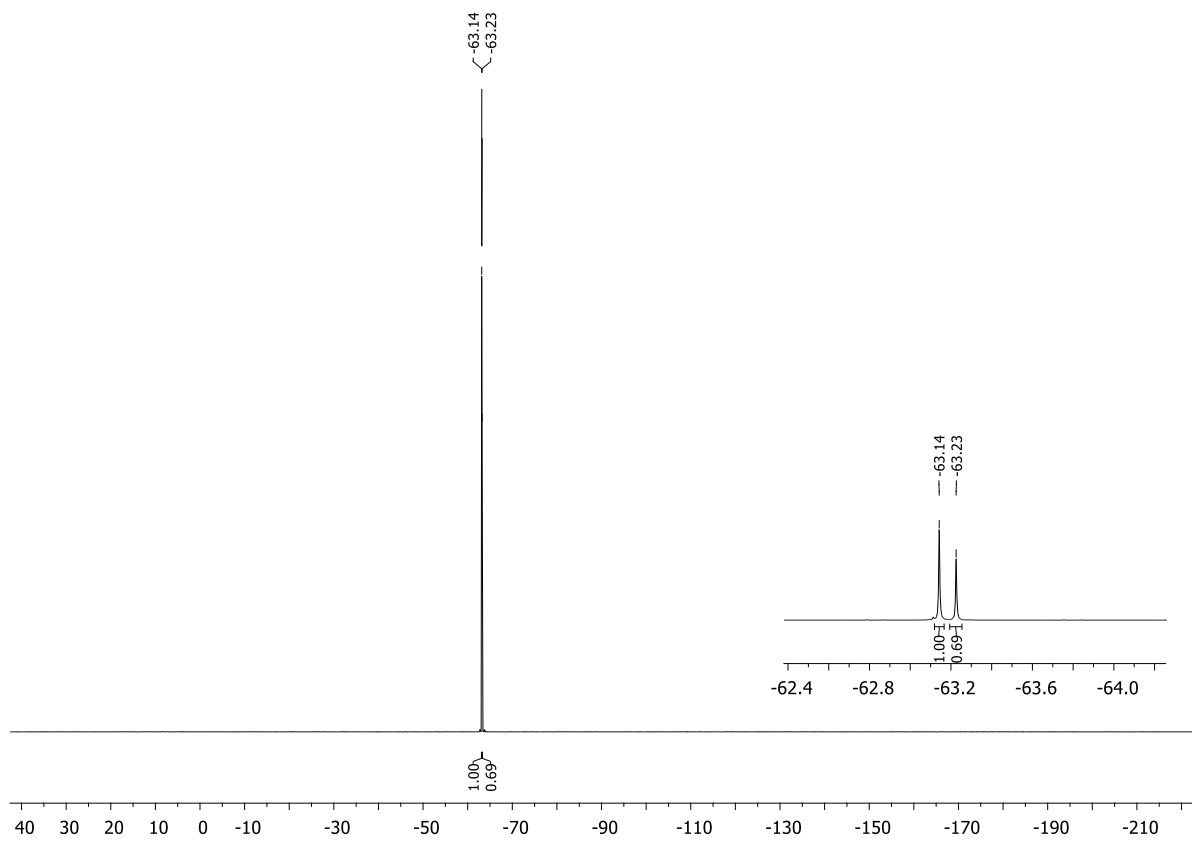




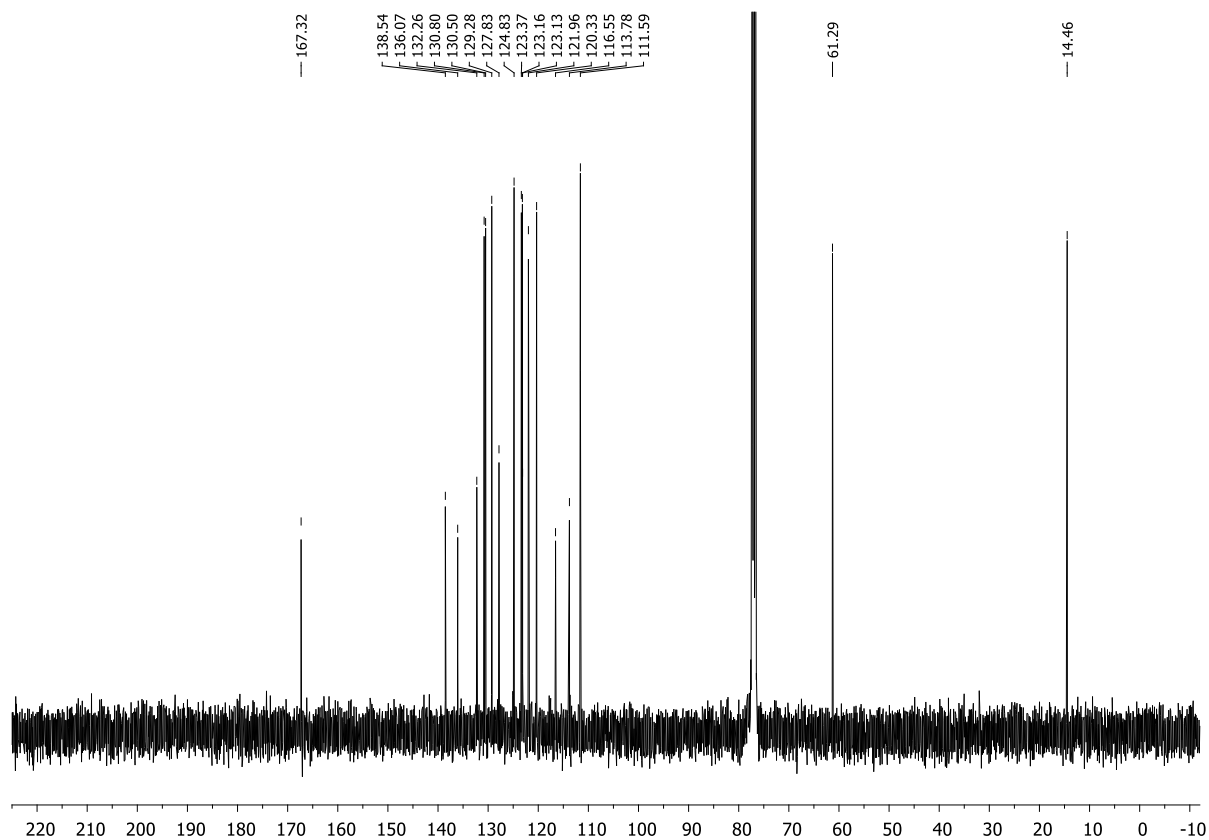
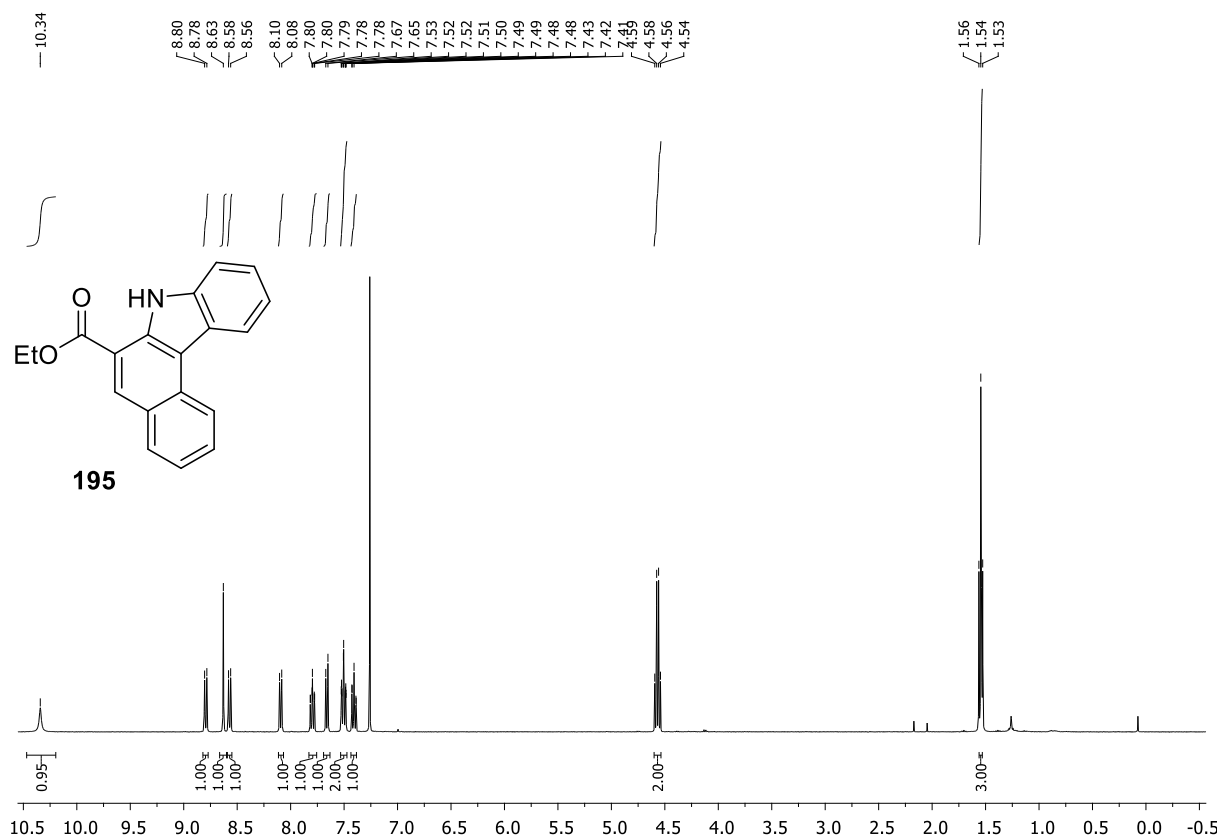


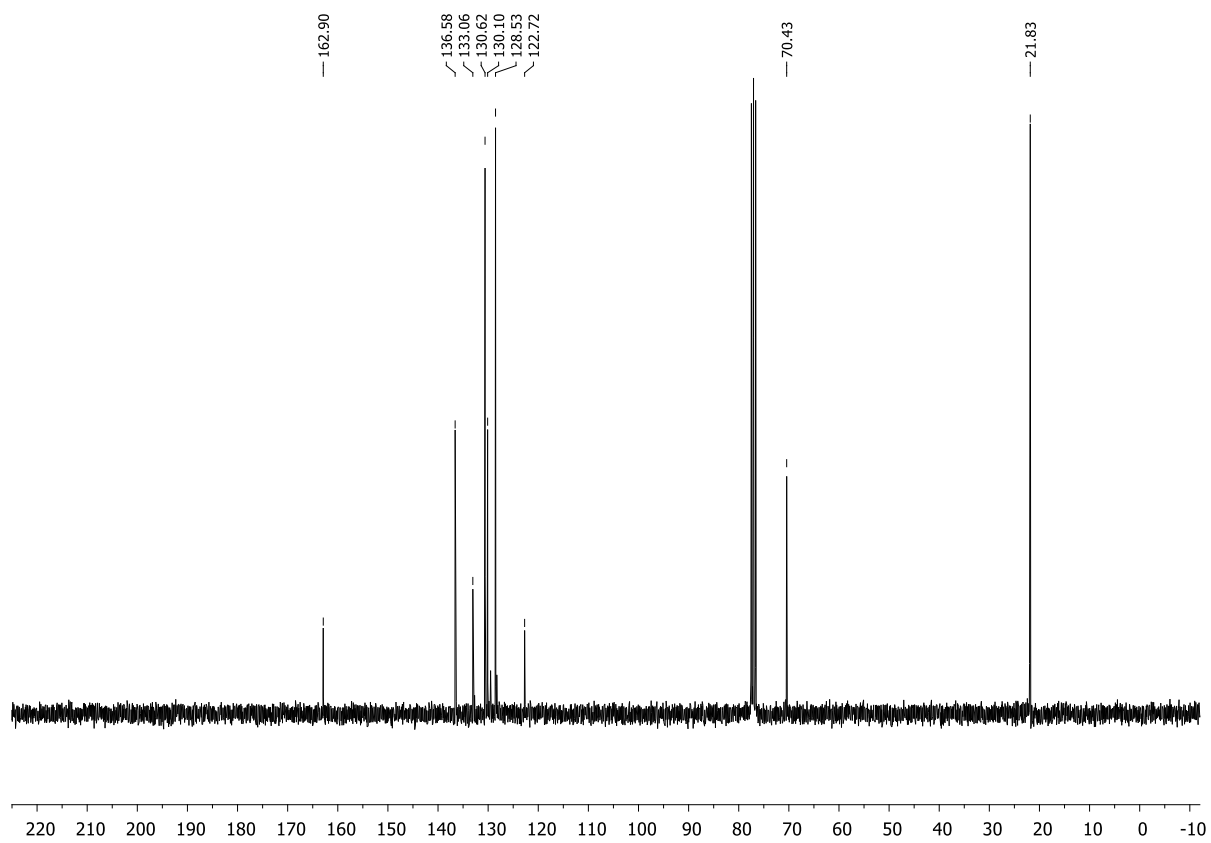
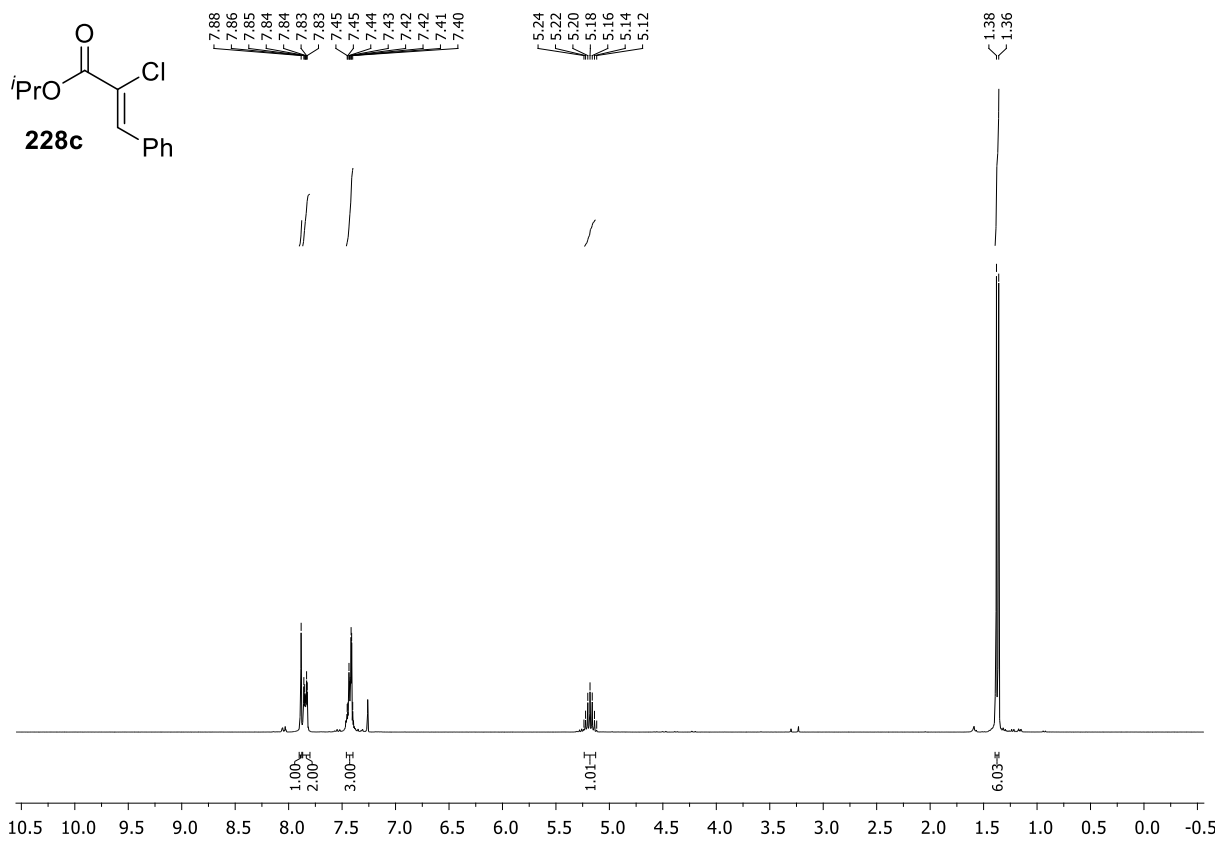


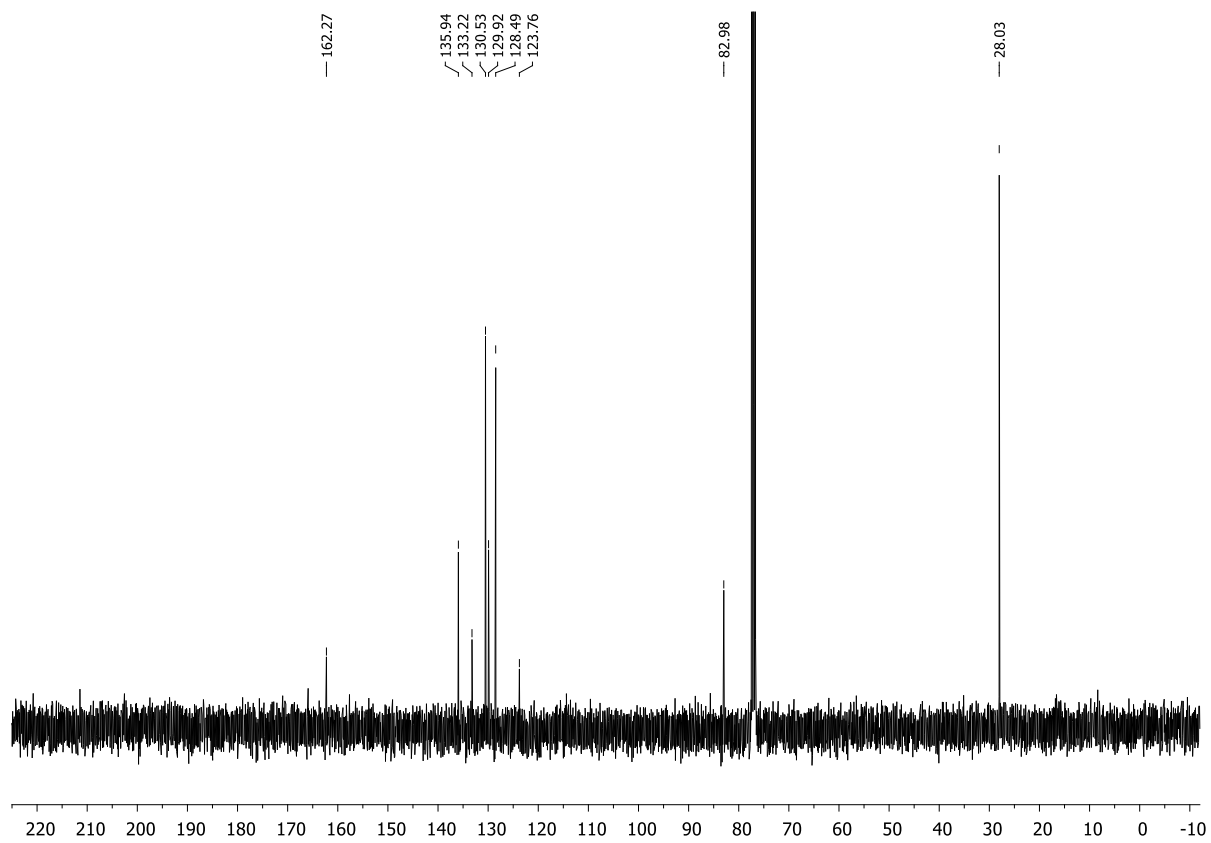
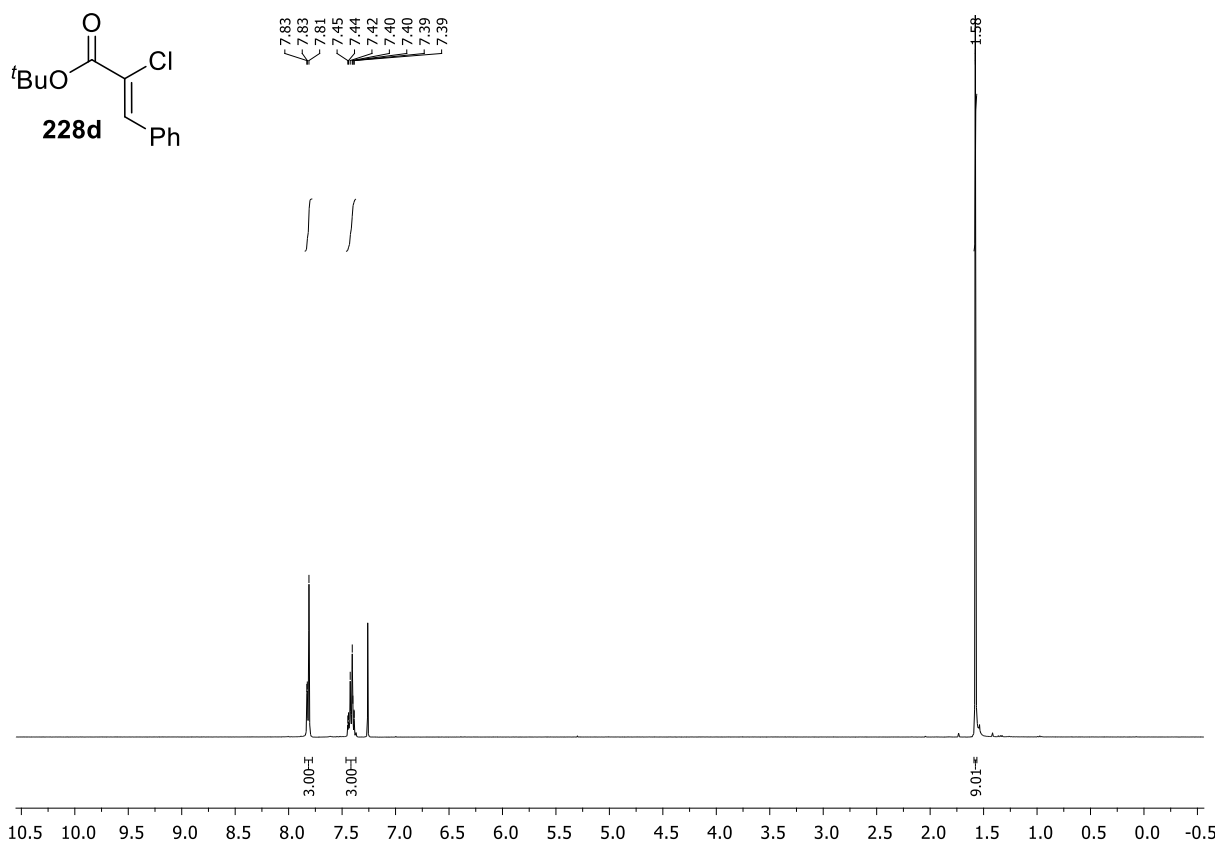


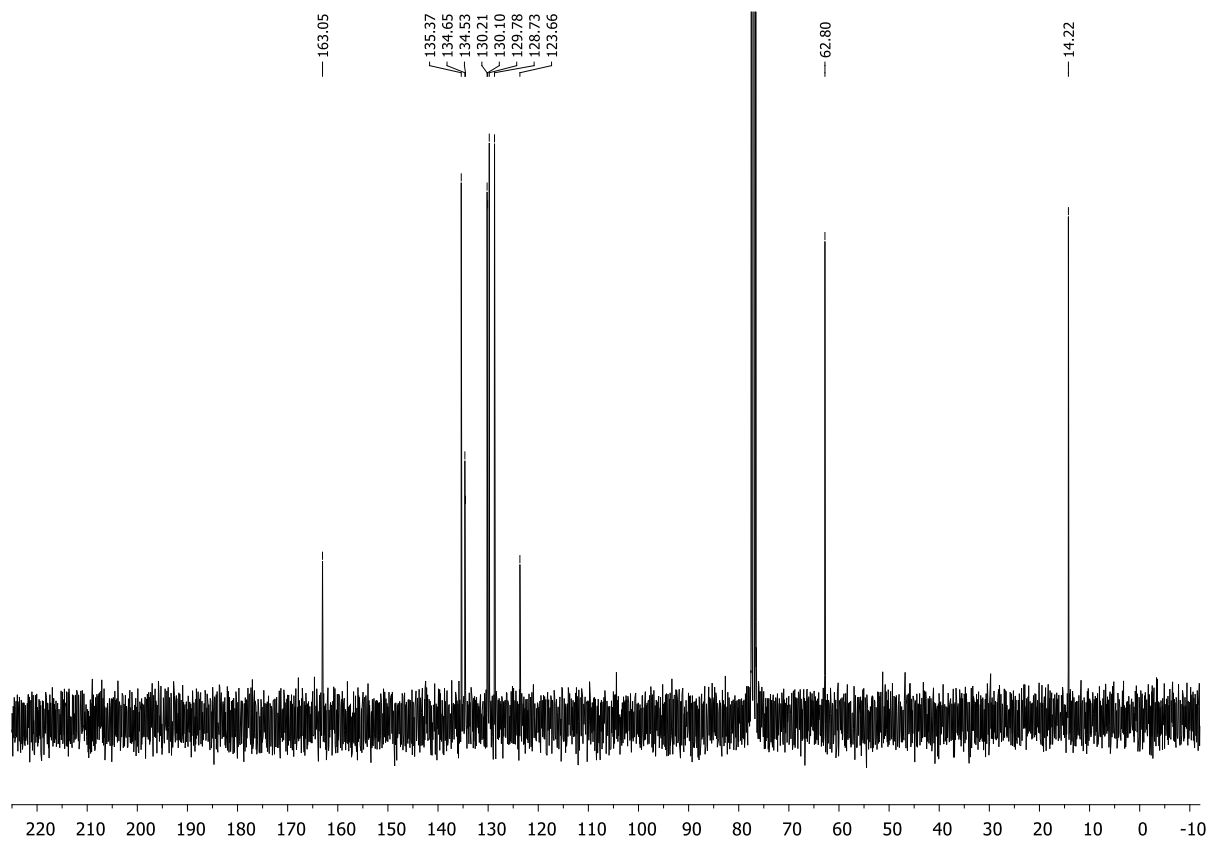
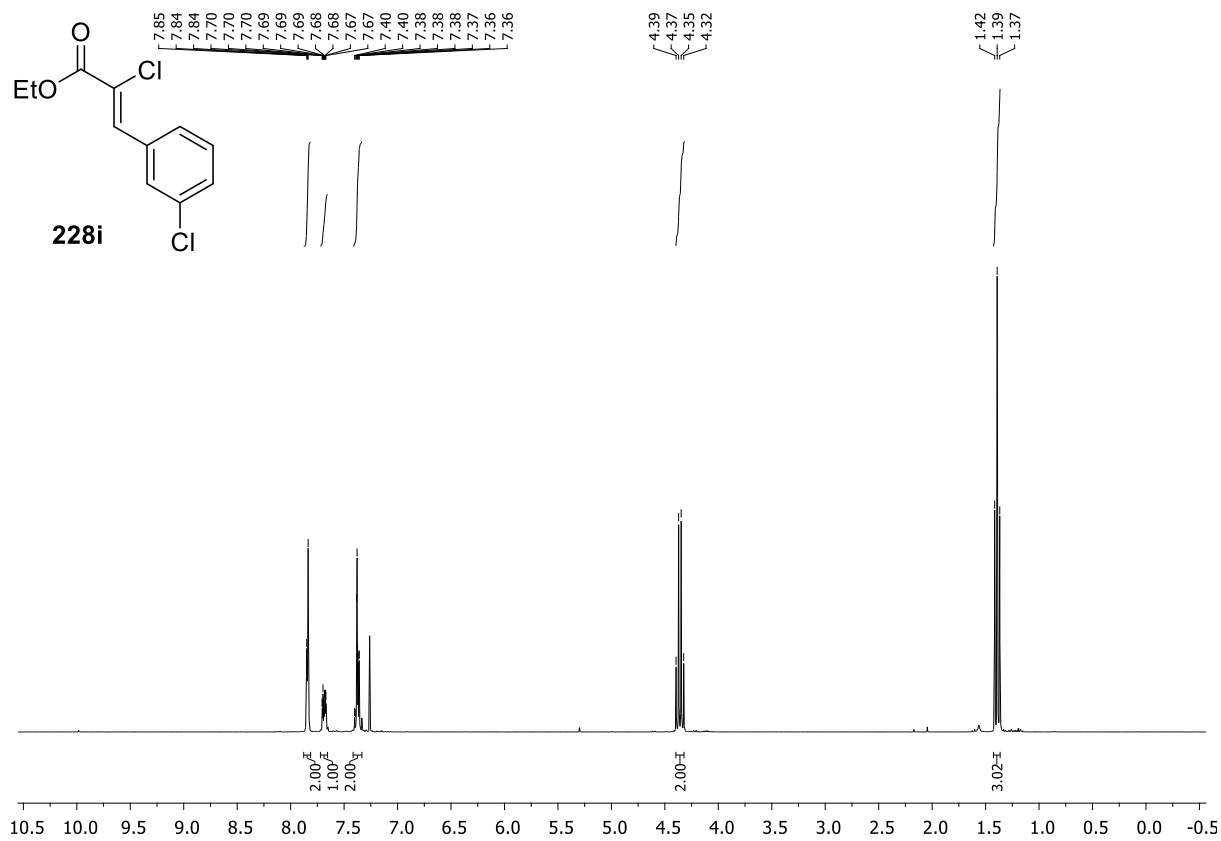


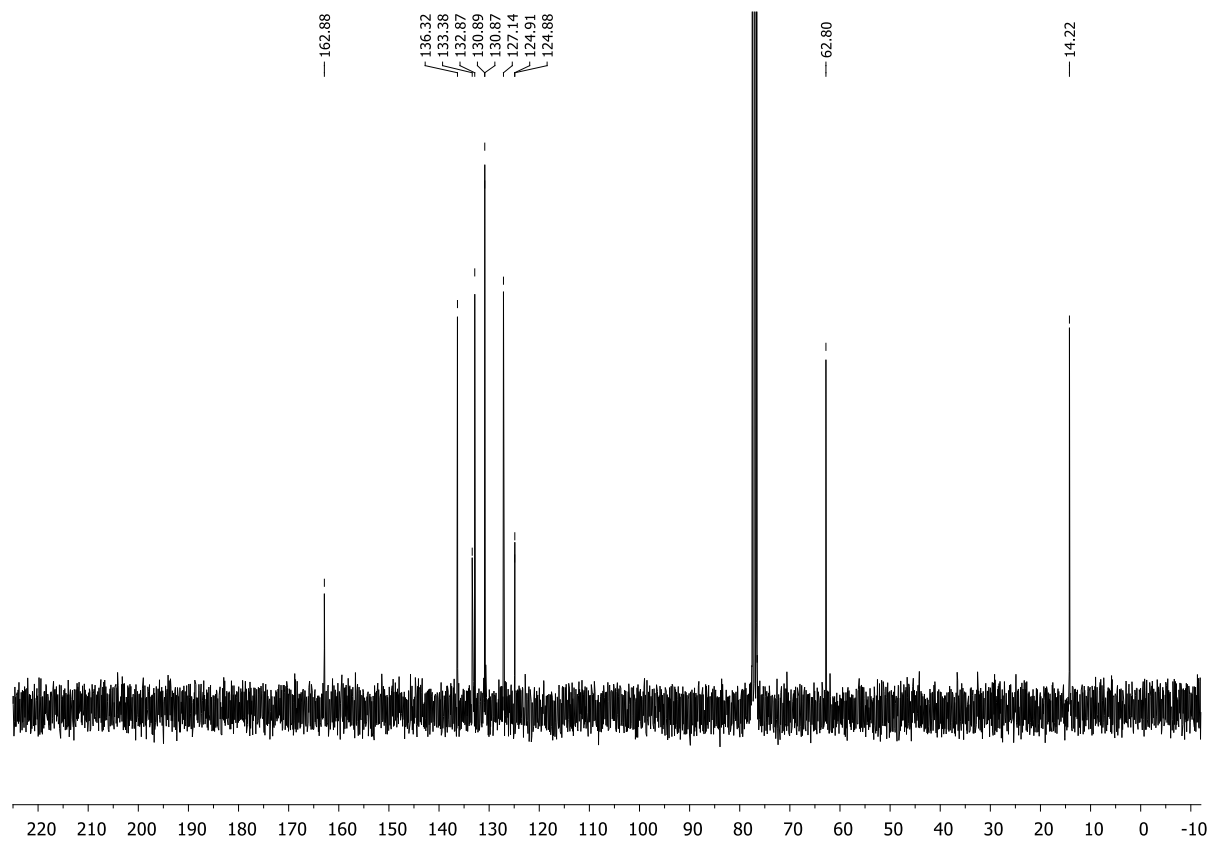
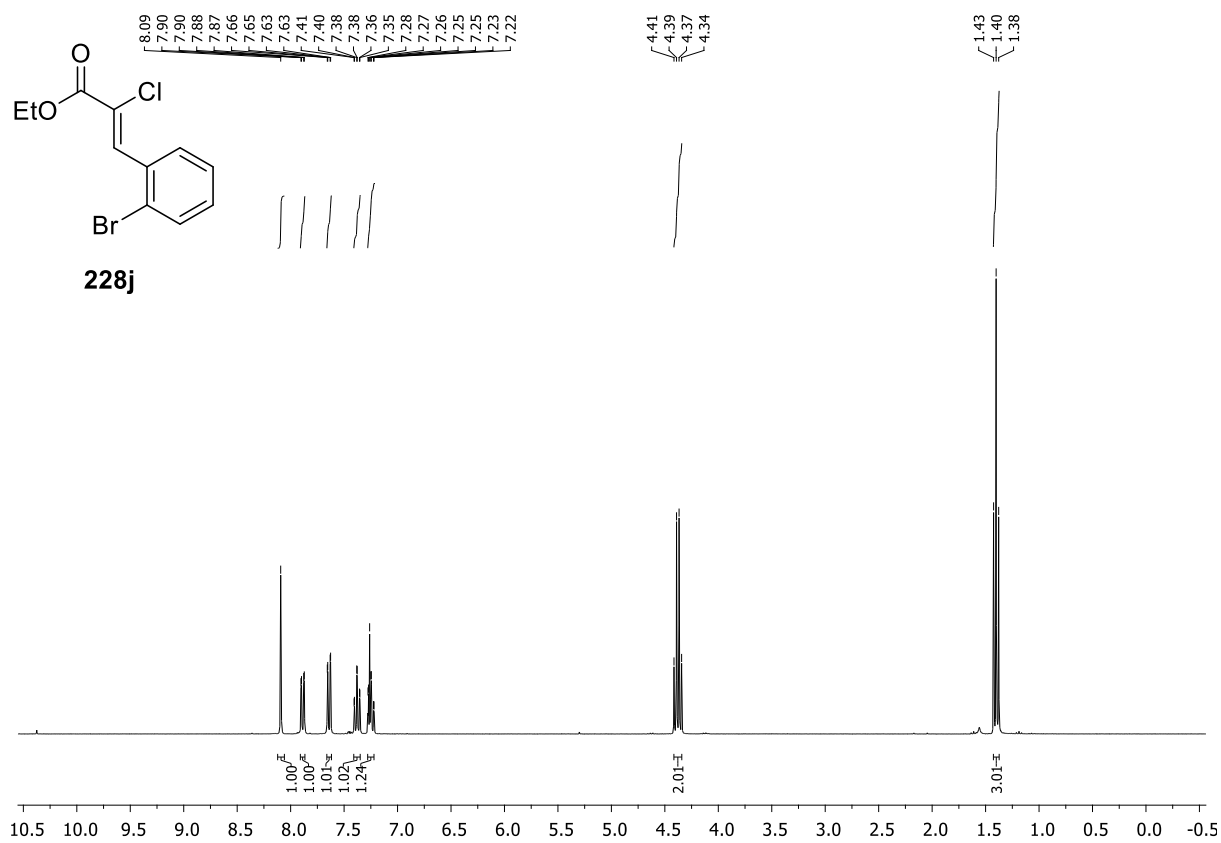


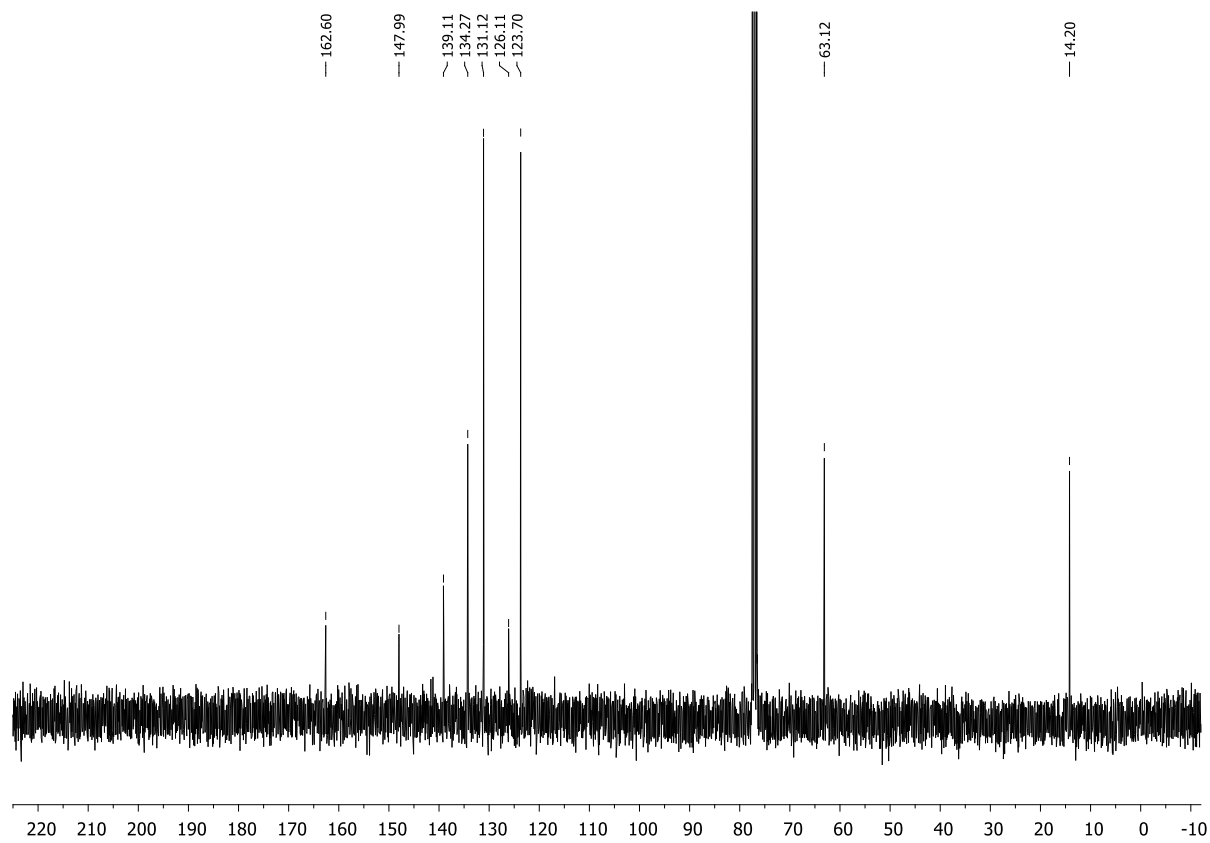
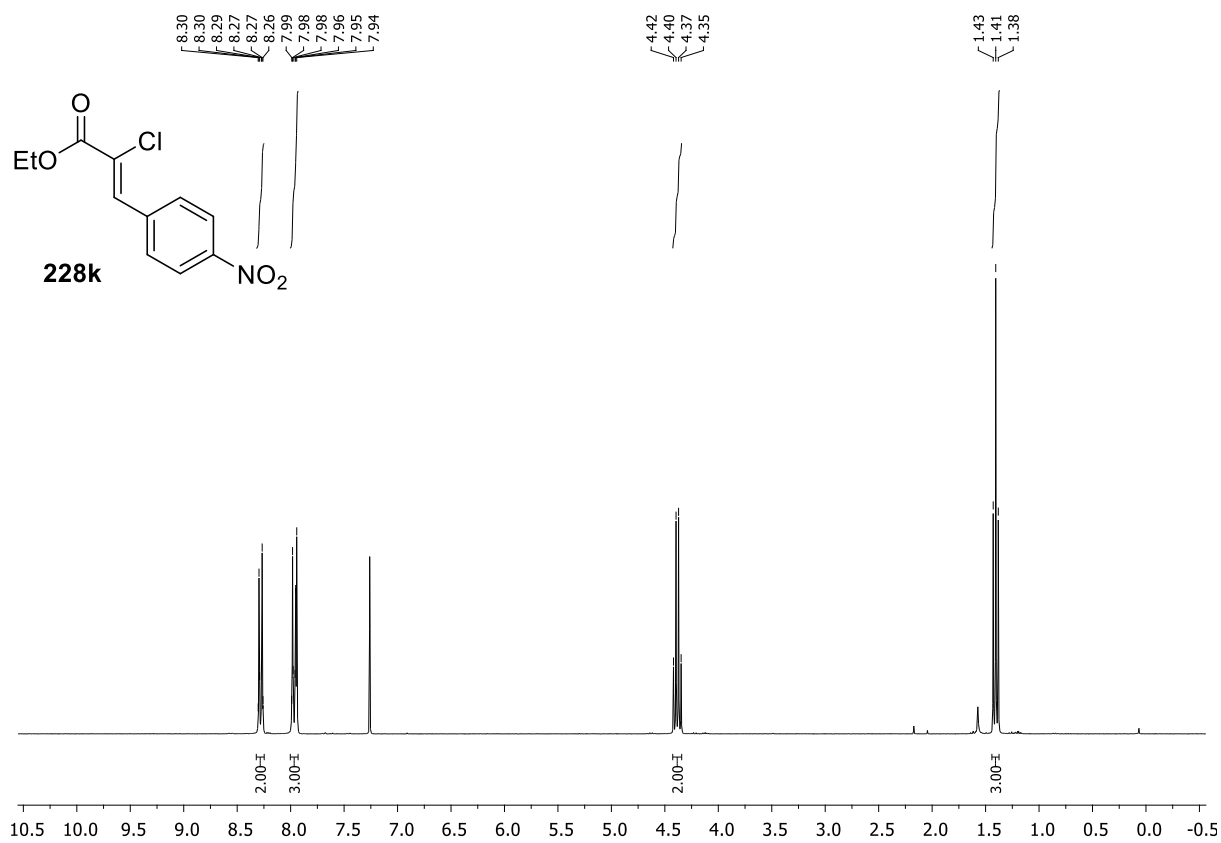


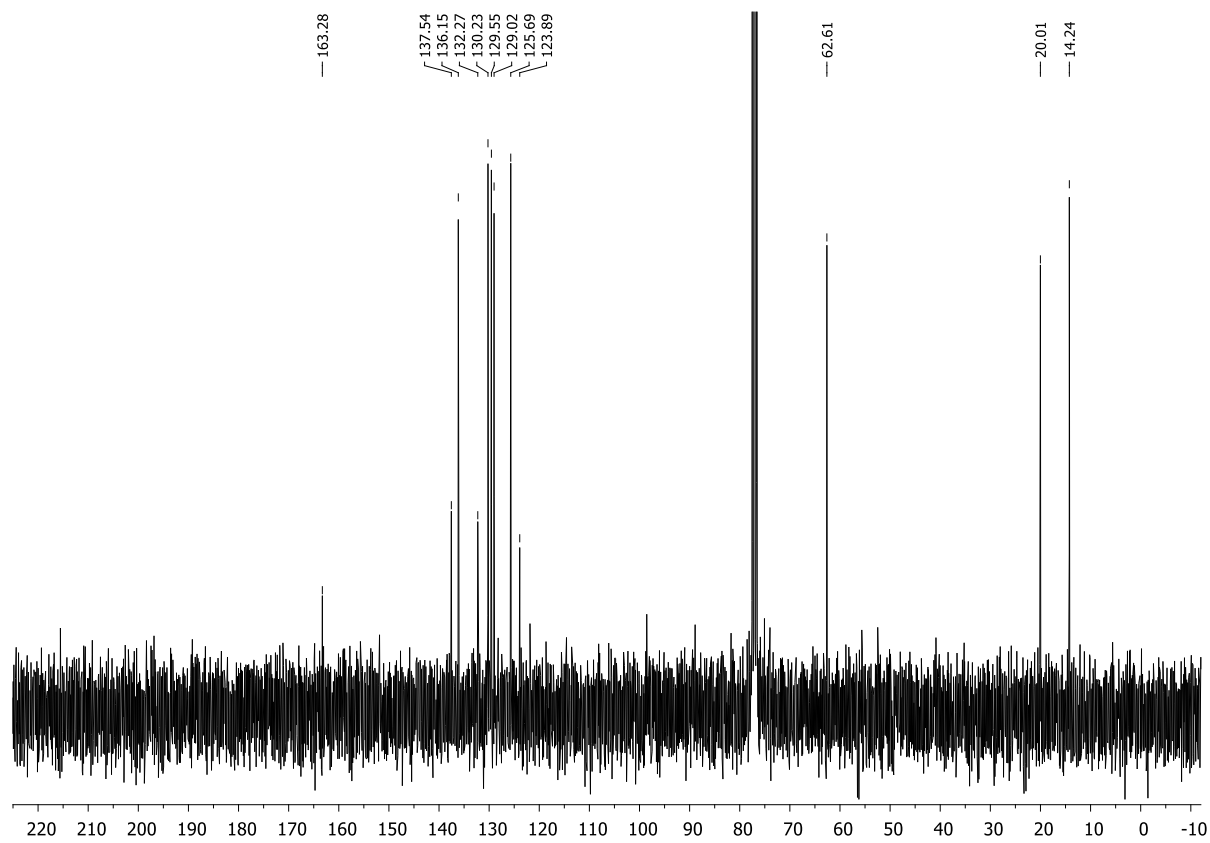
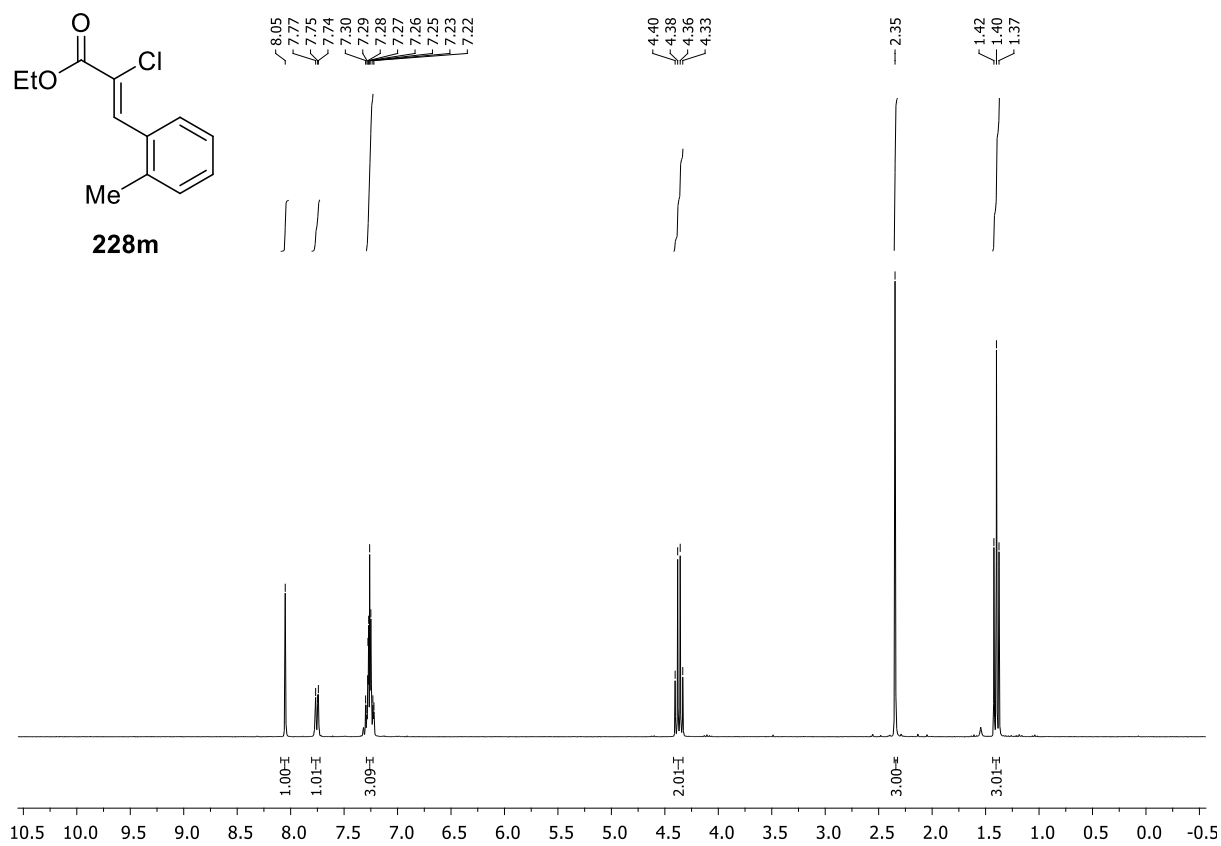
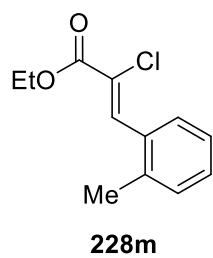




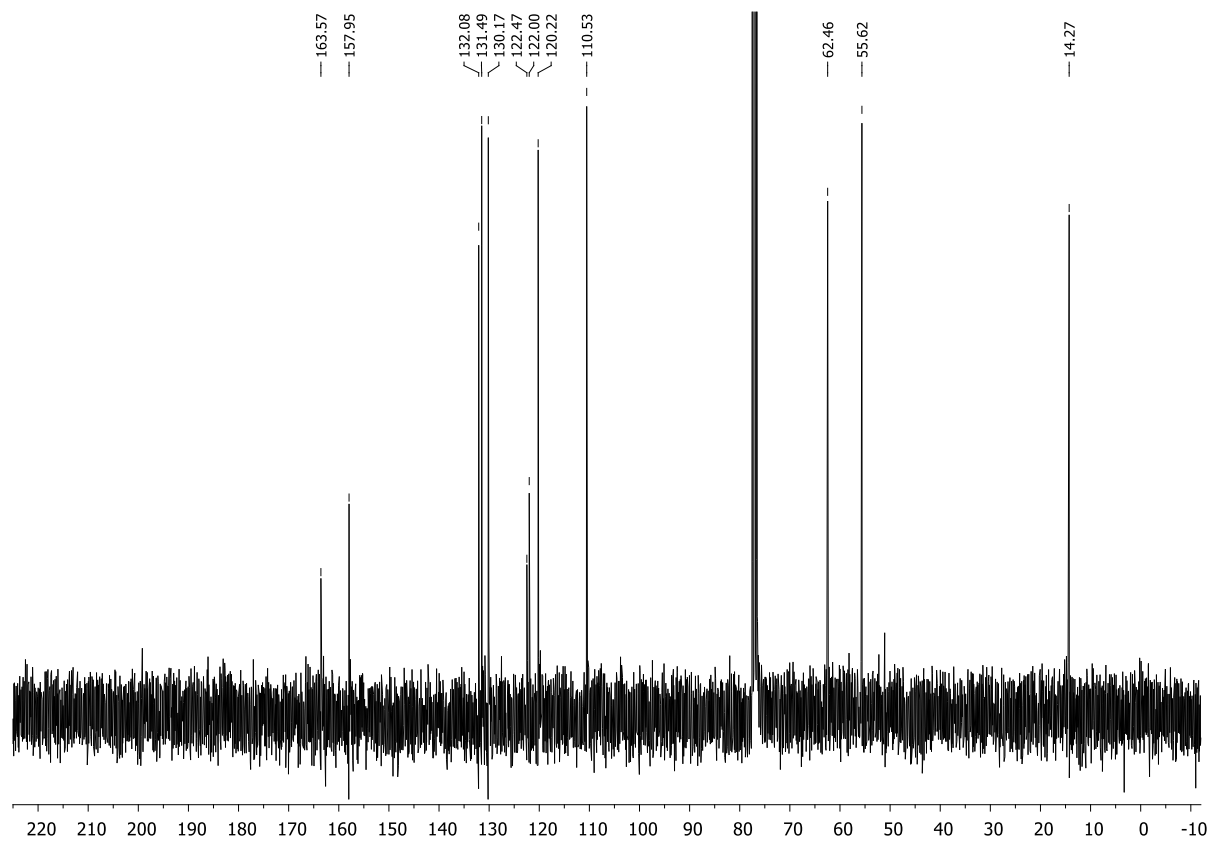
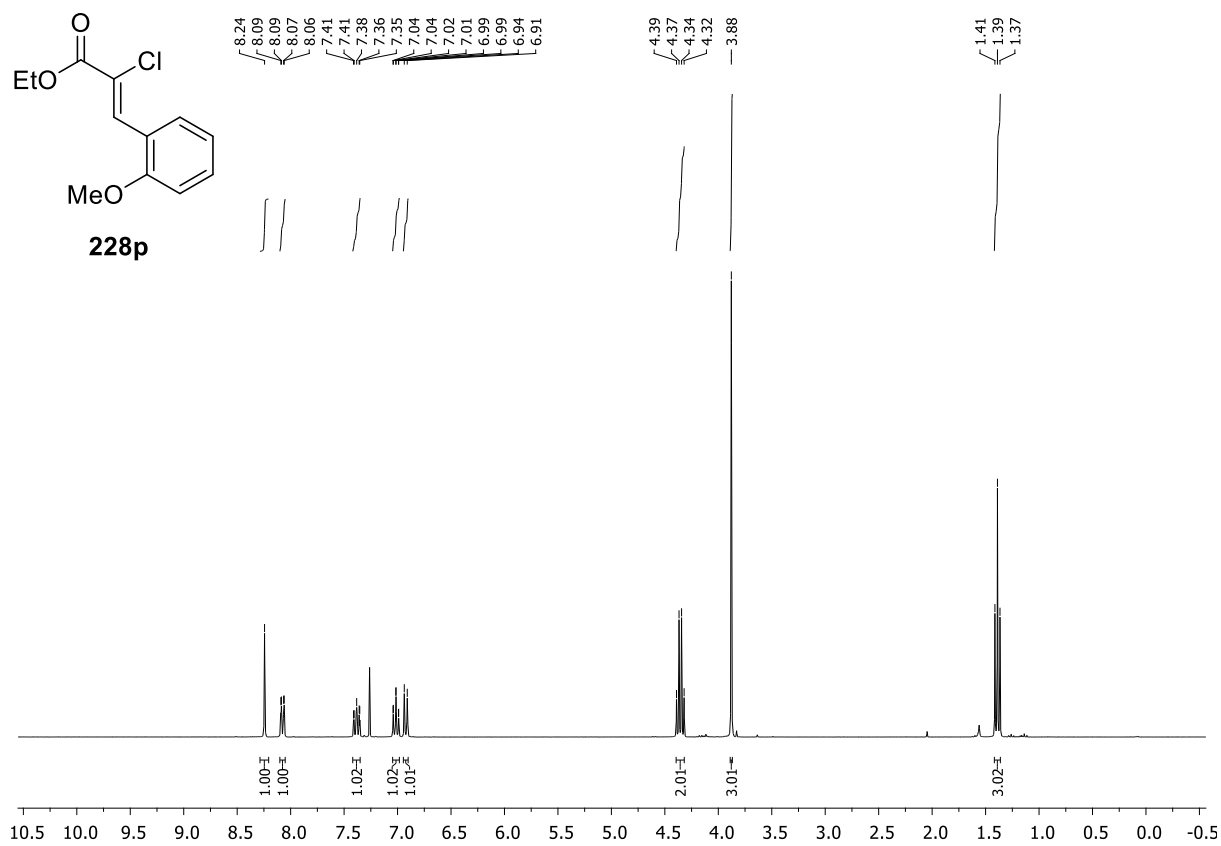




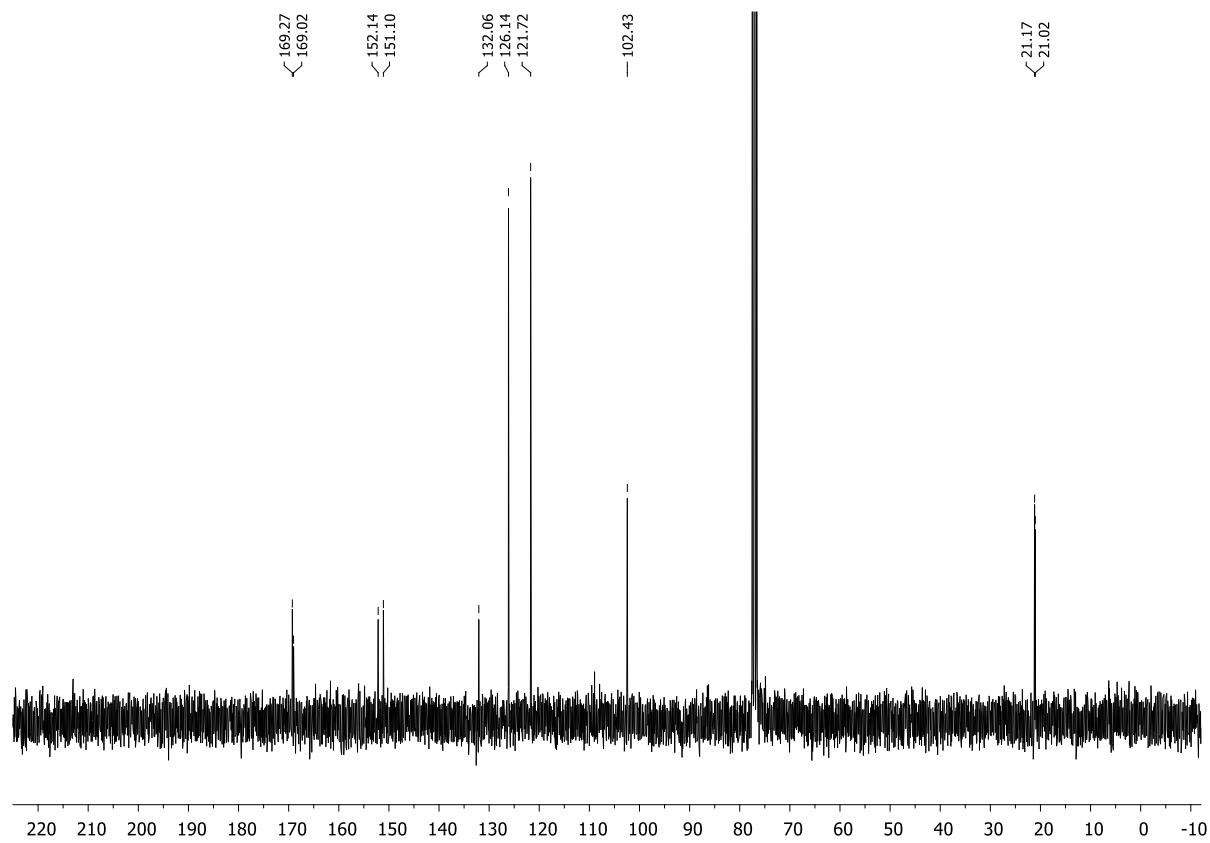
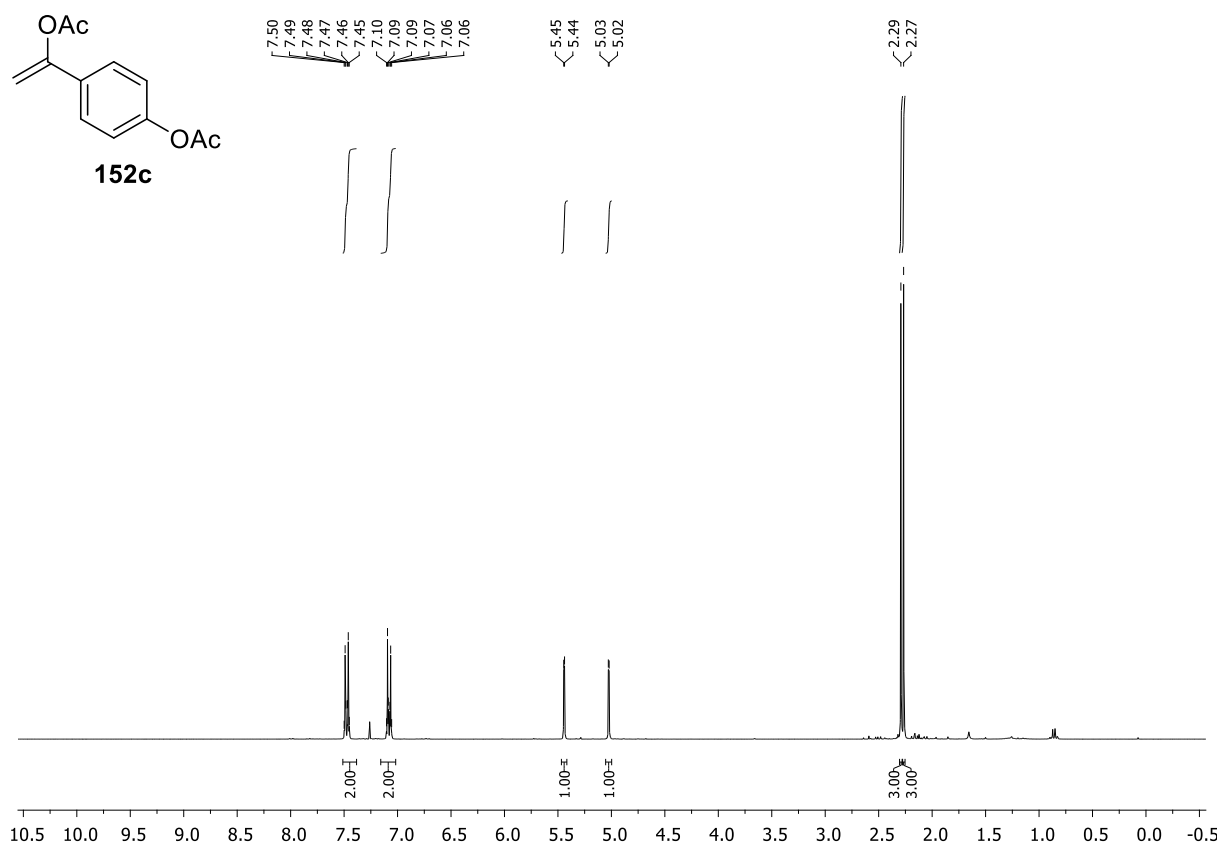


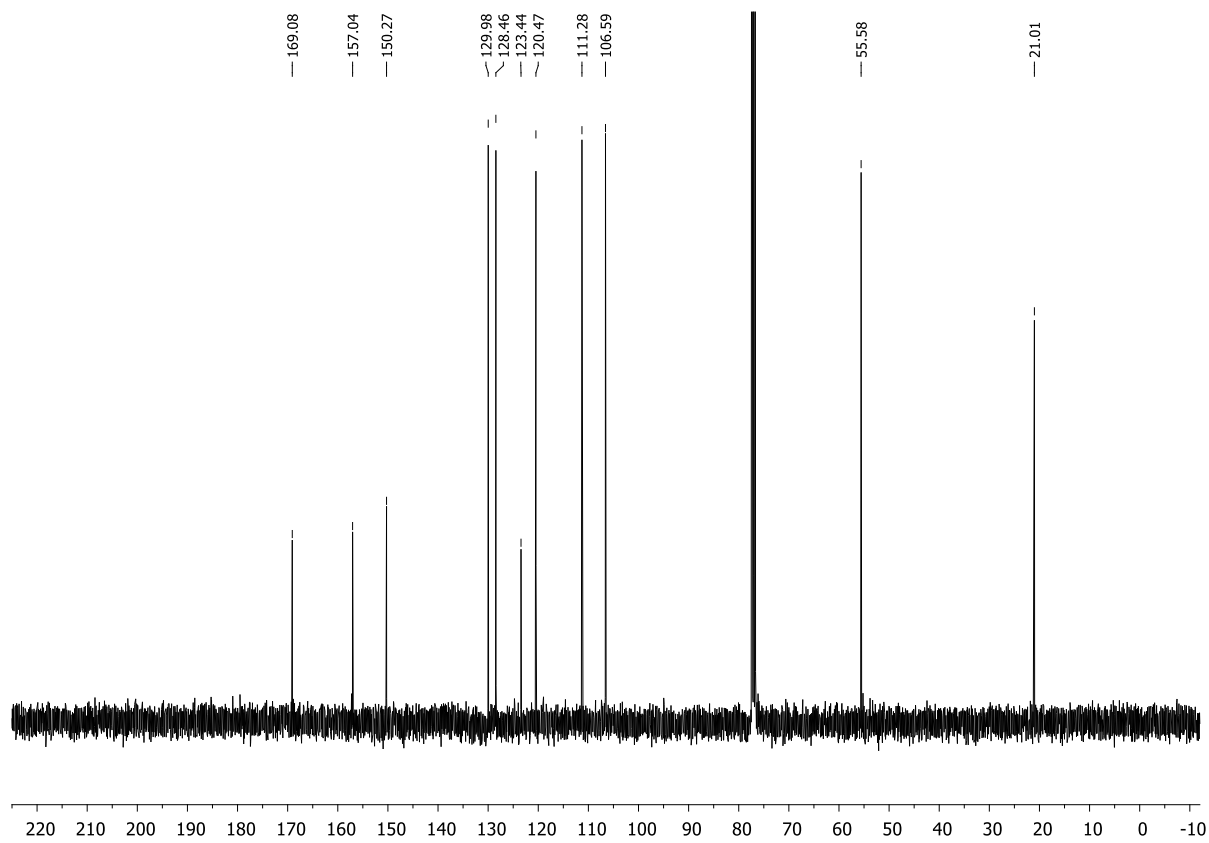
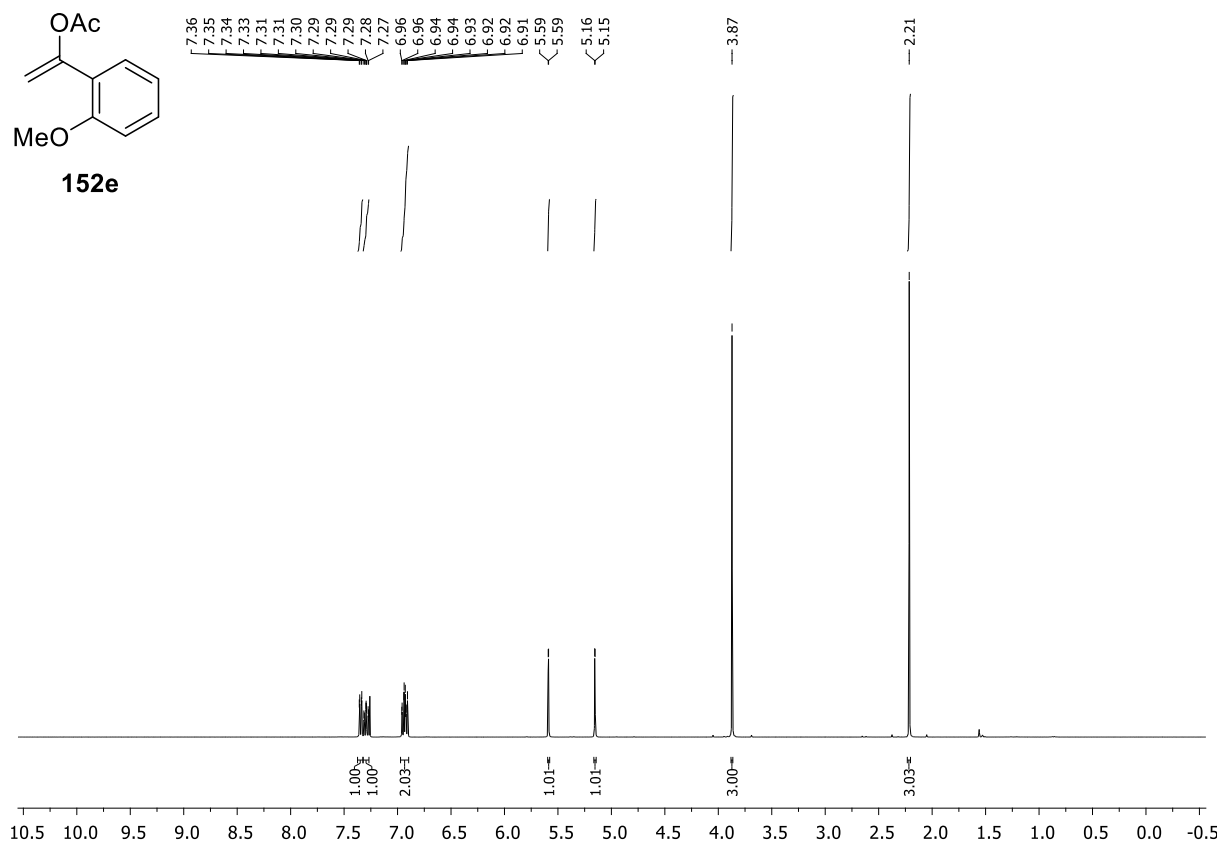
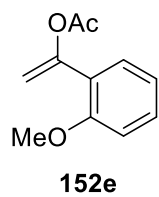


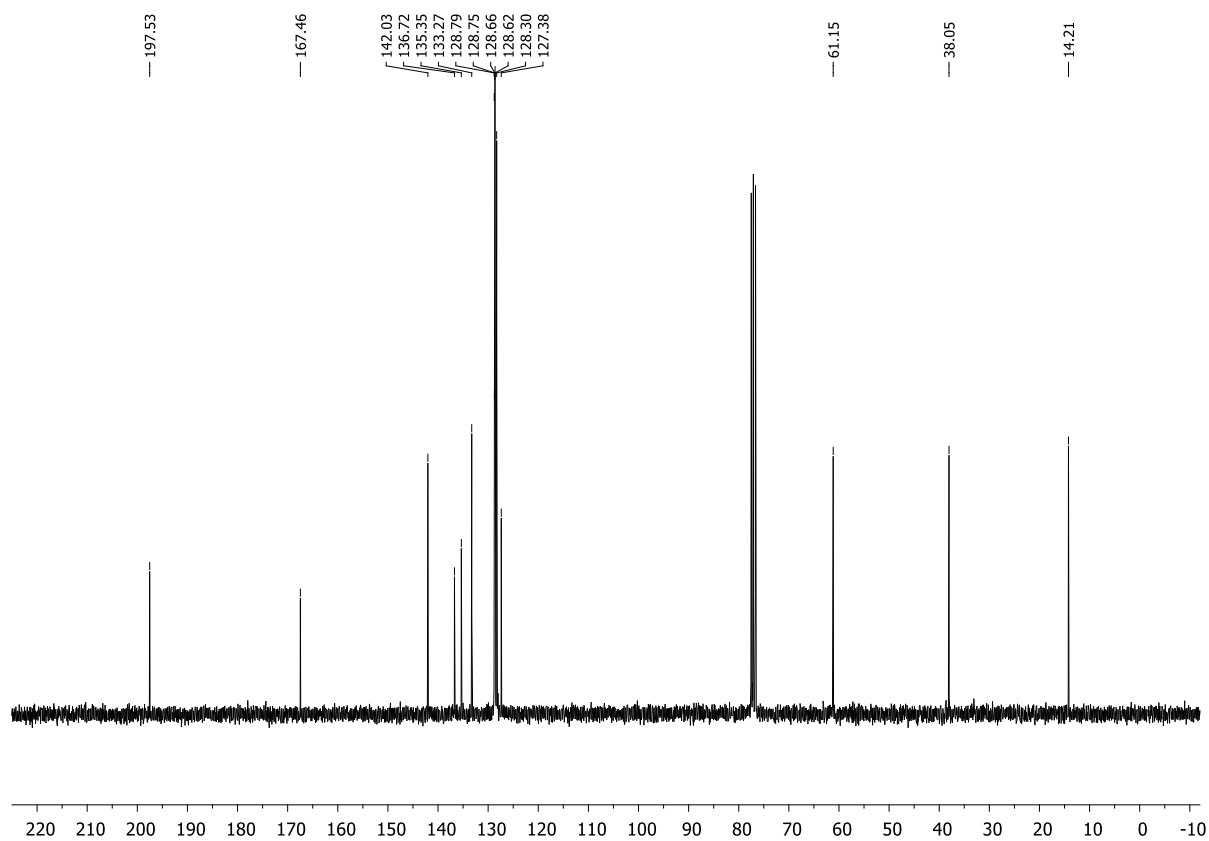
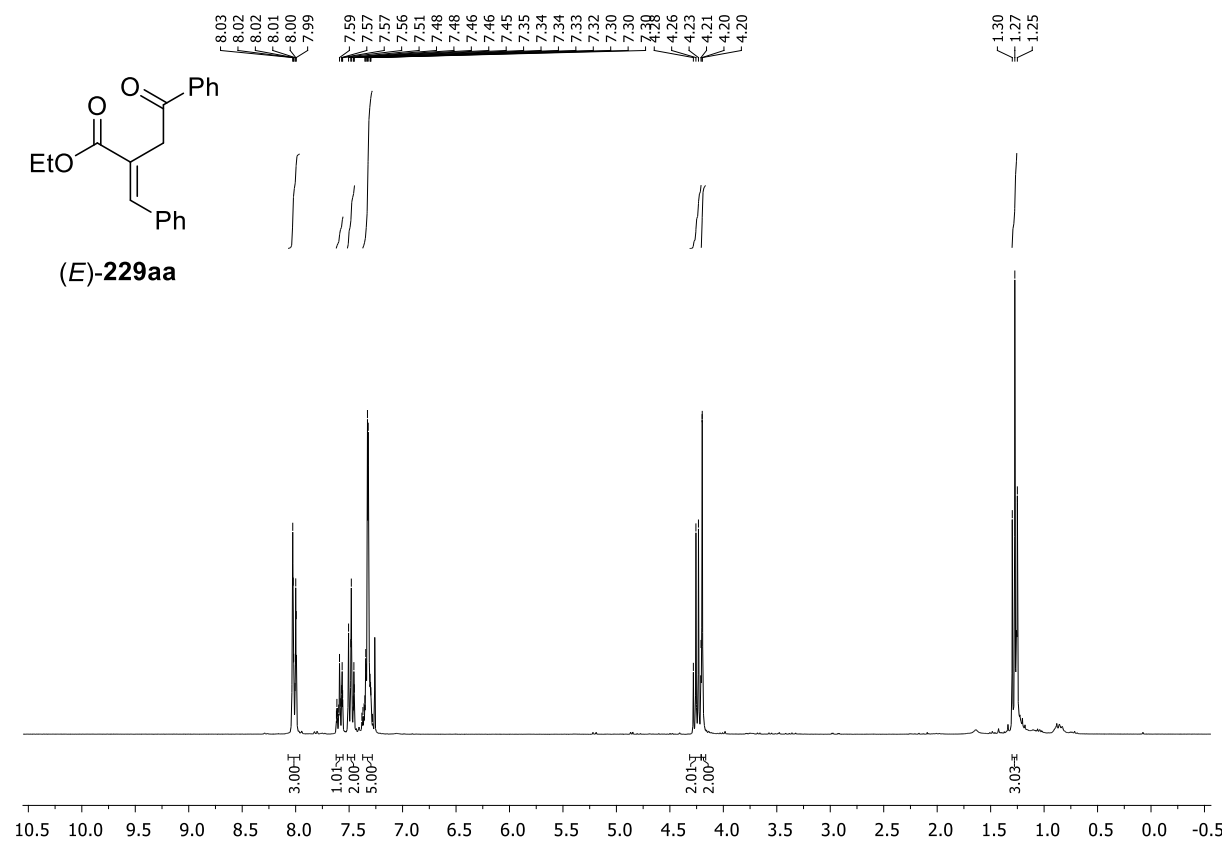
# Appendix

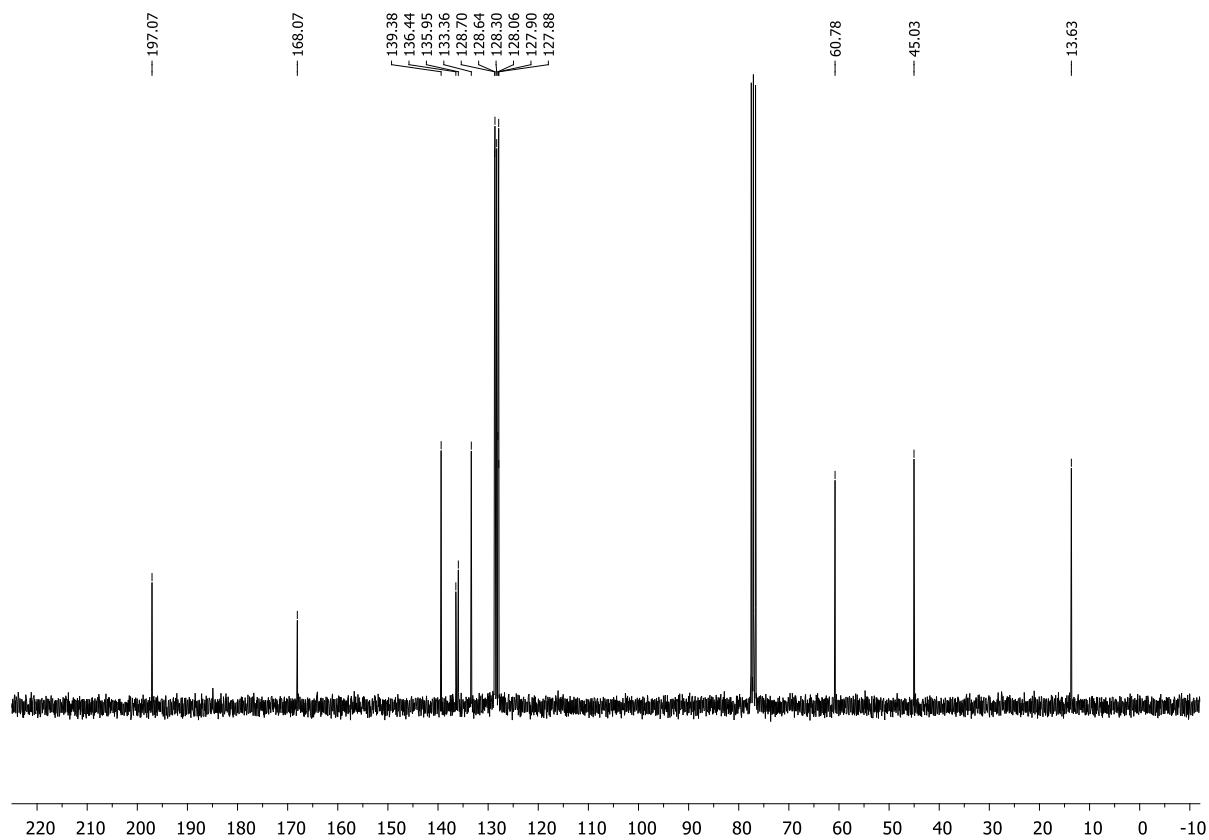
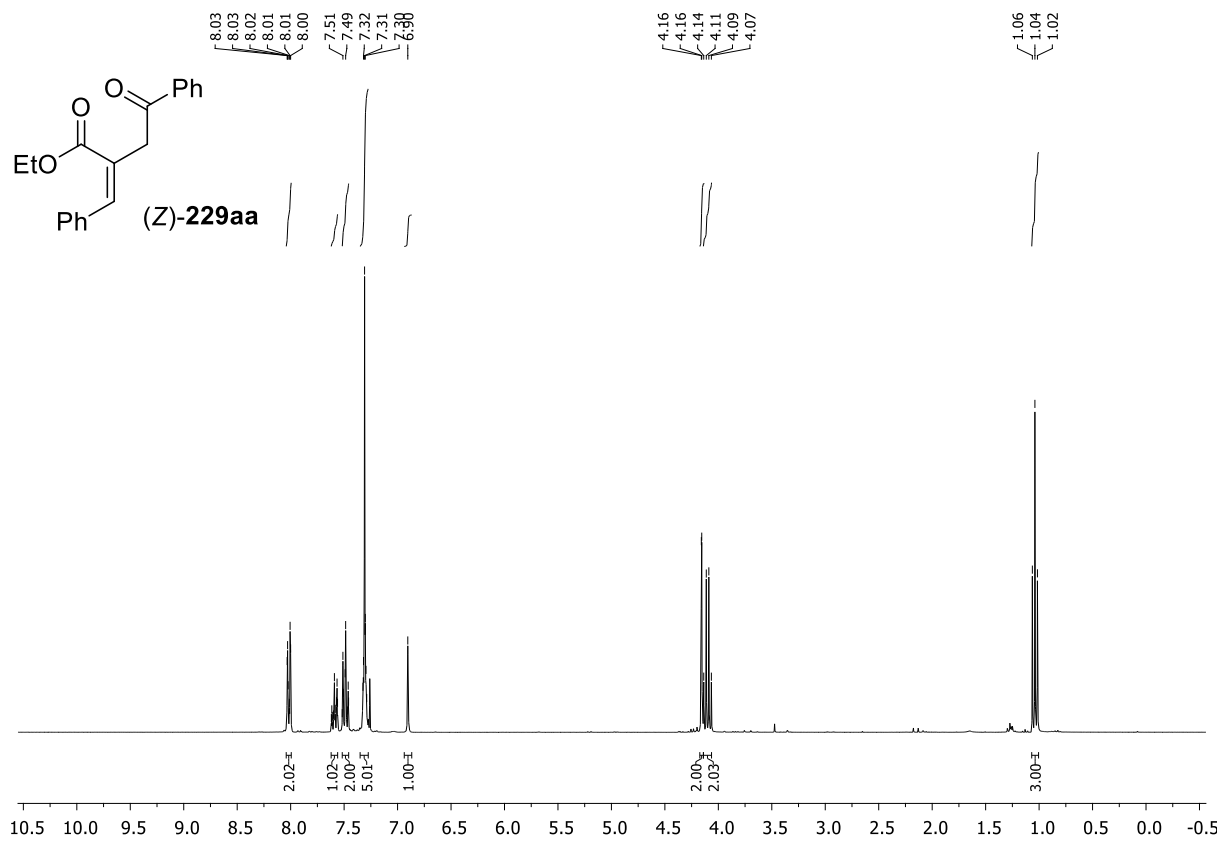


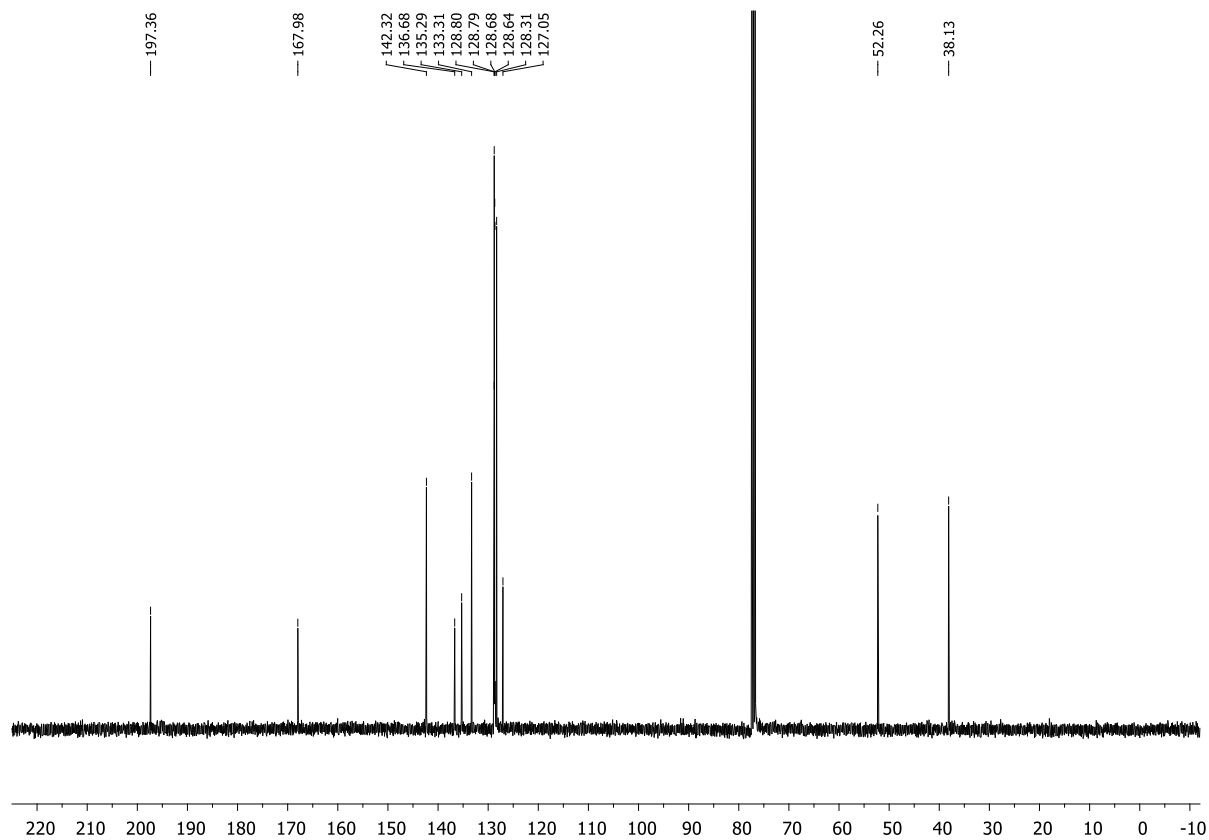
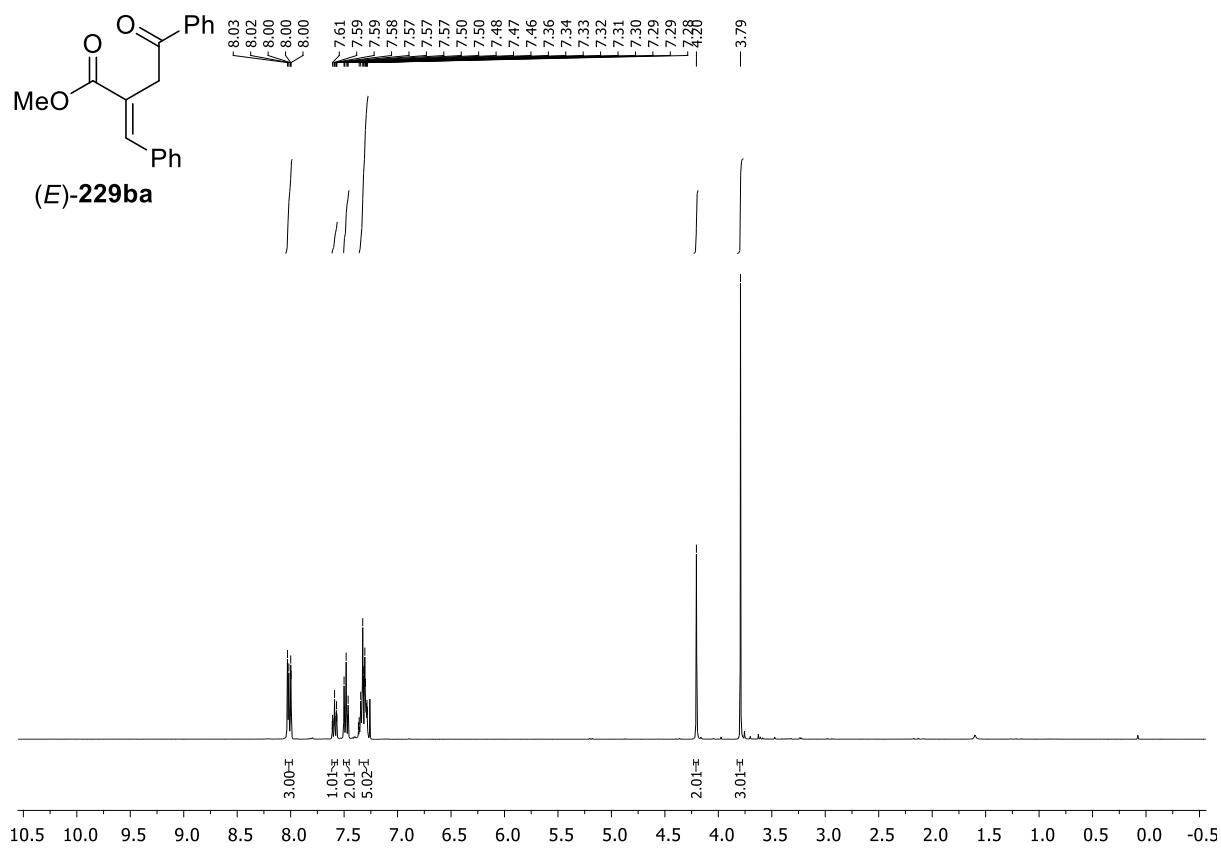


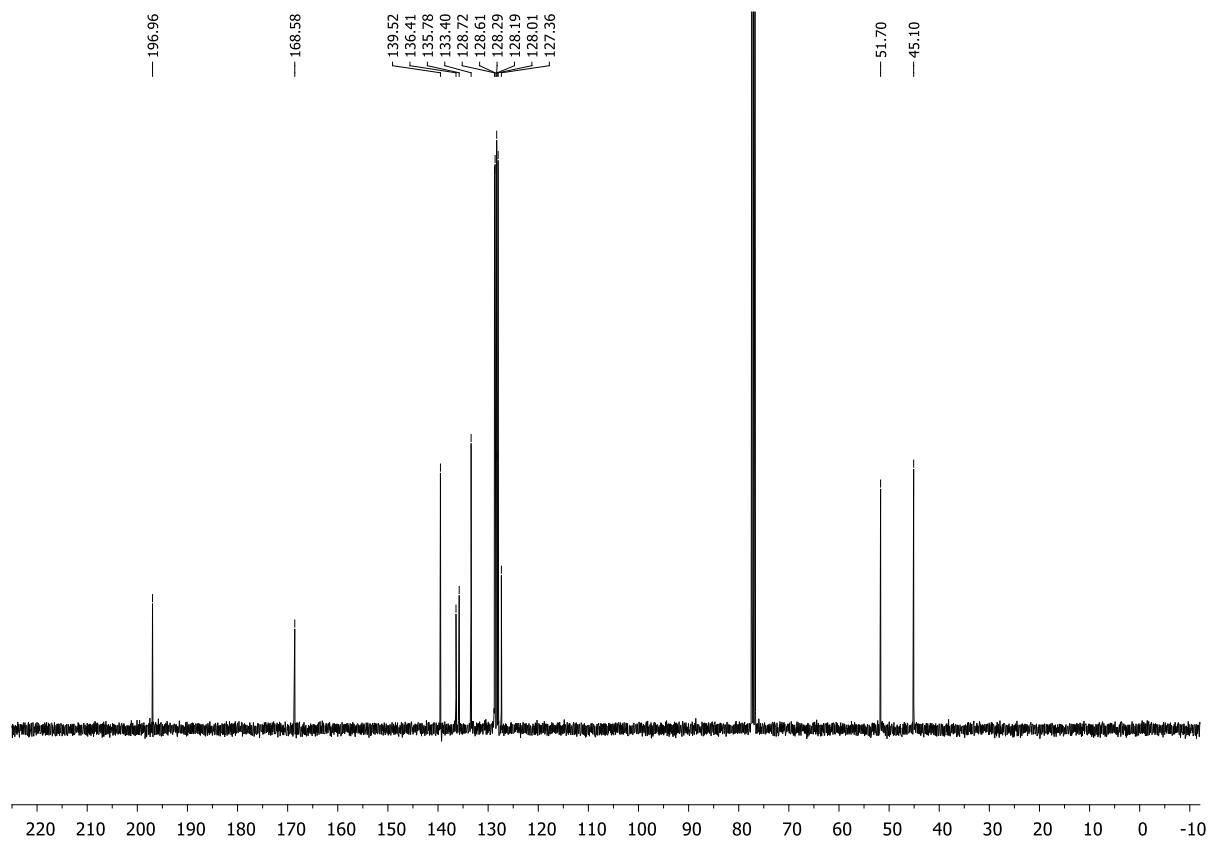
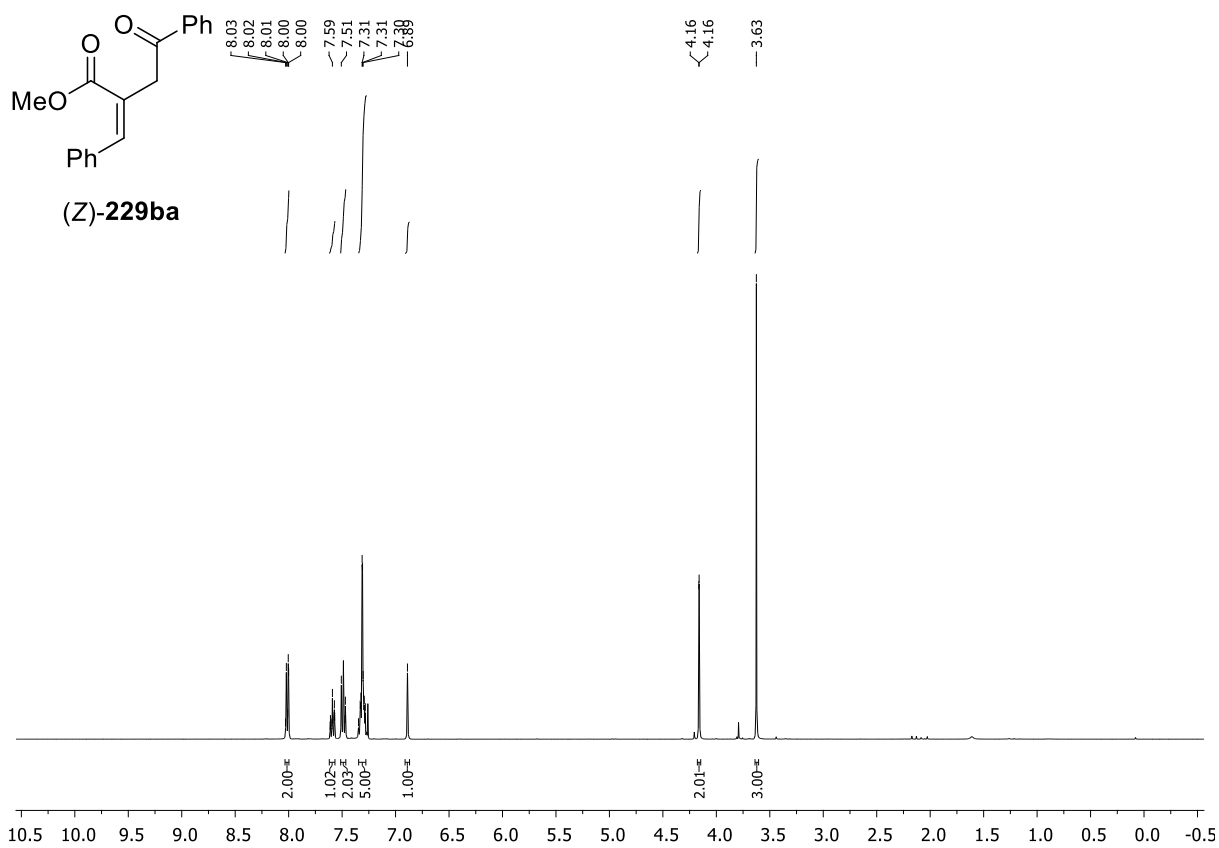


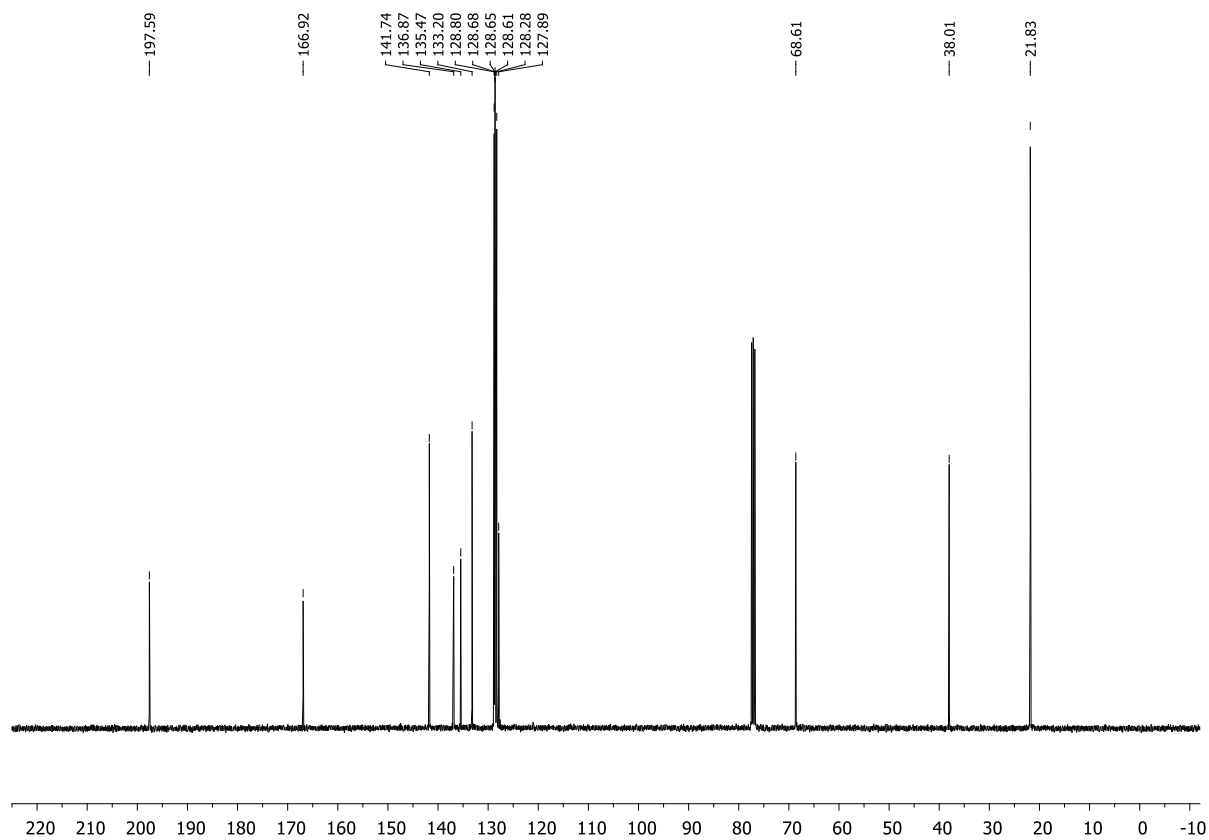
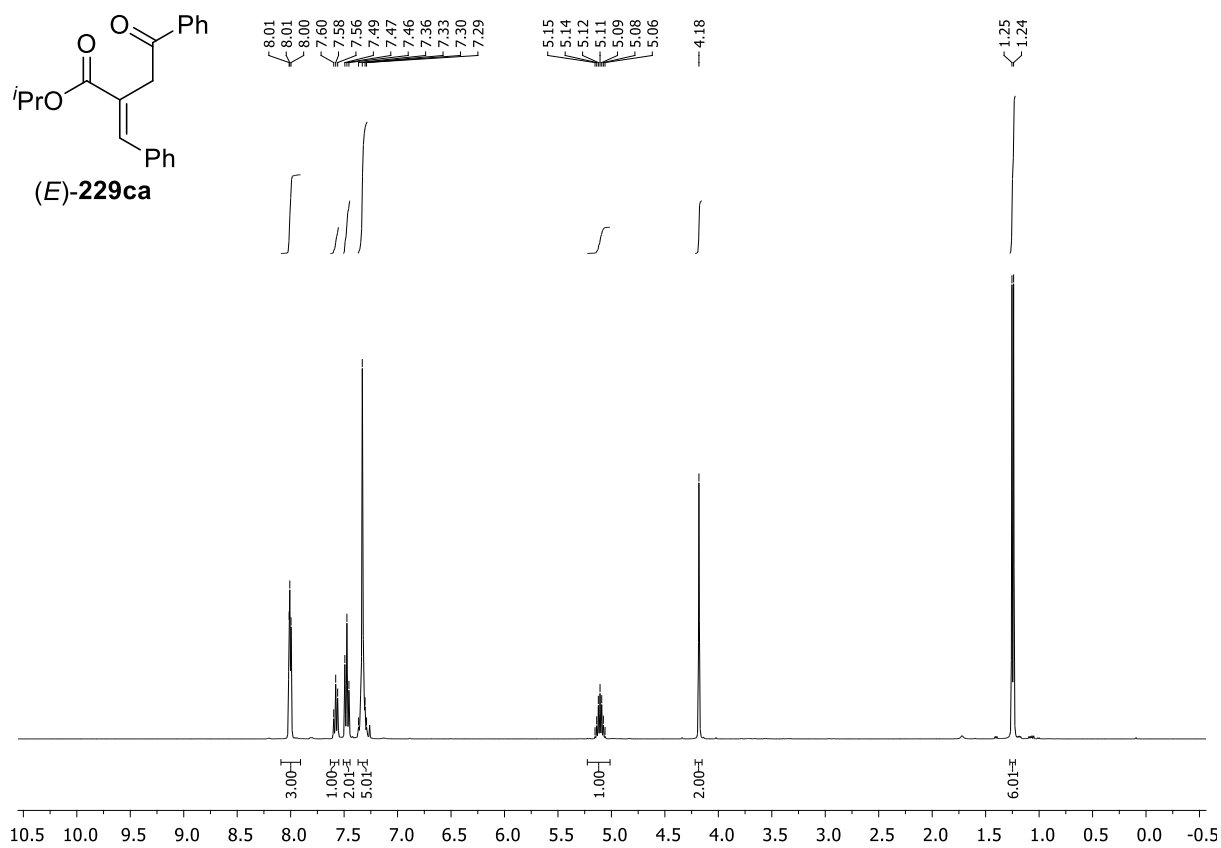


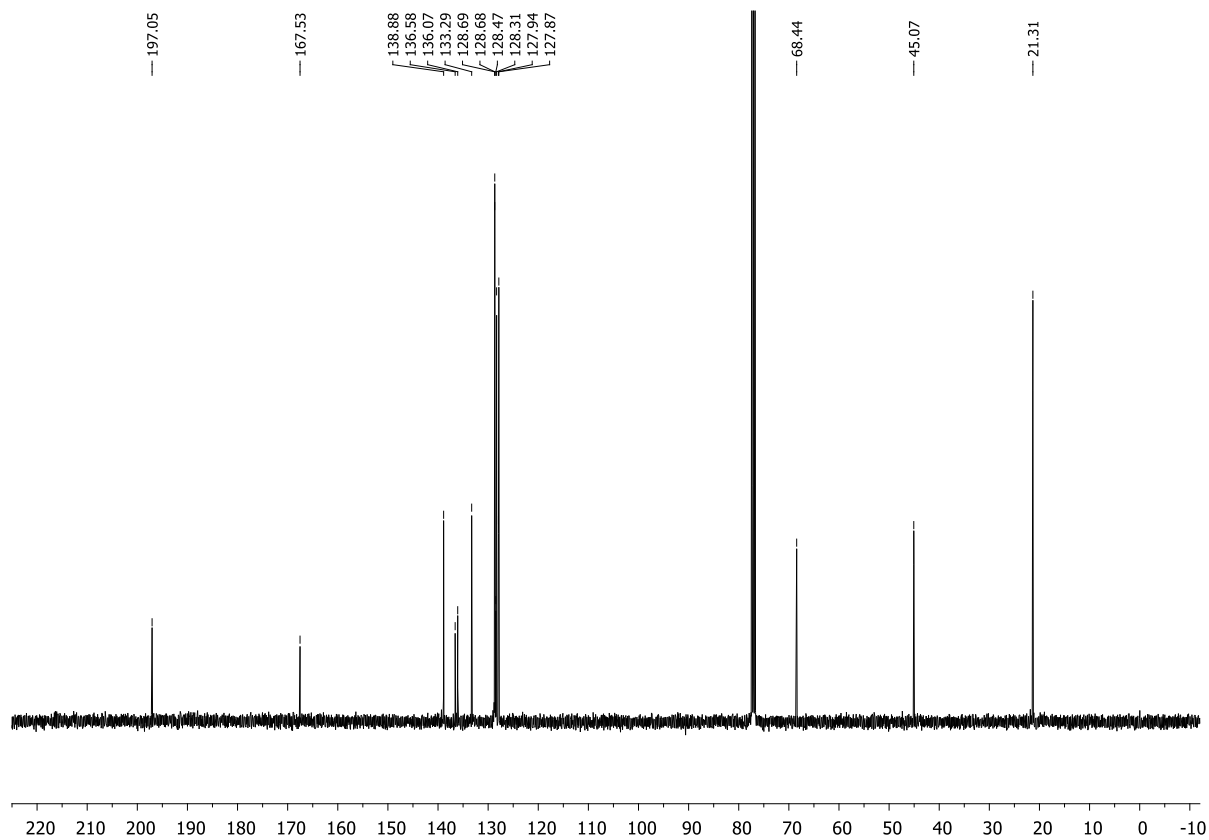
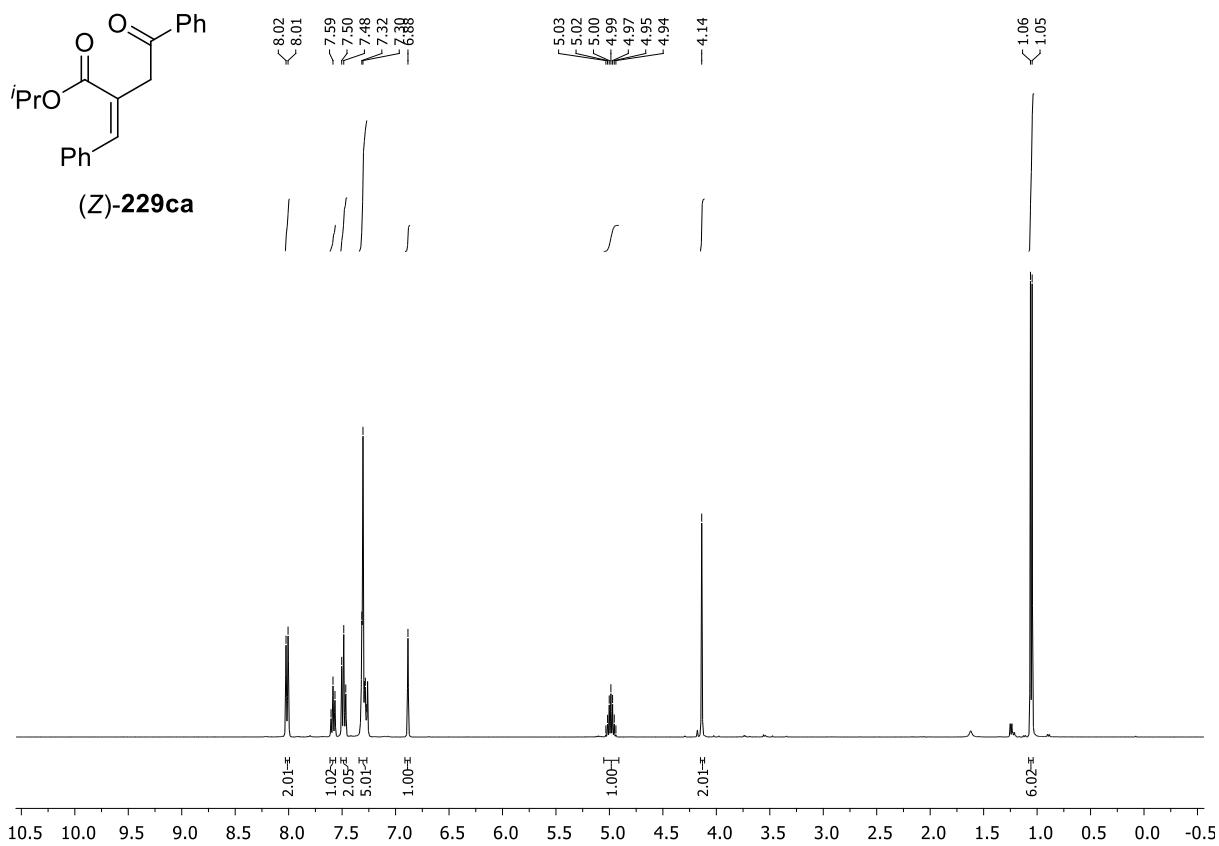




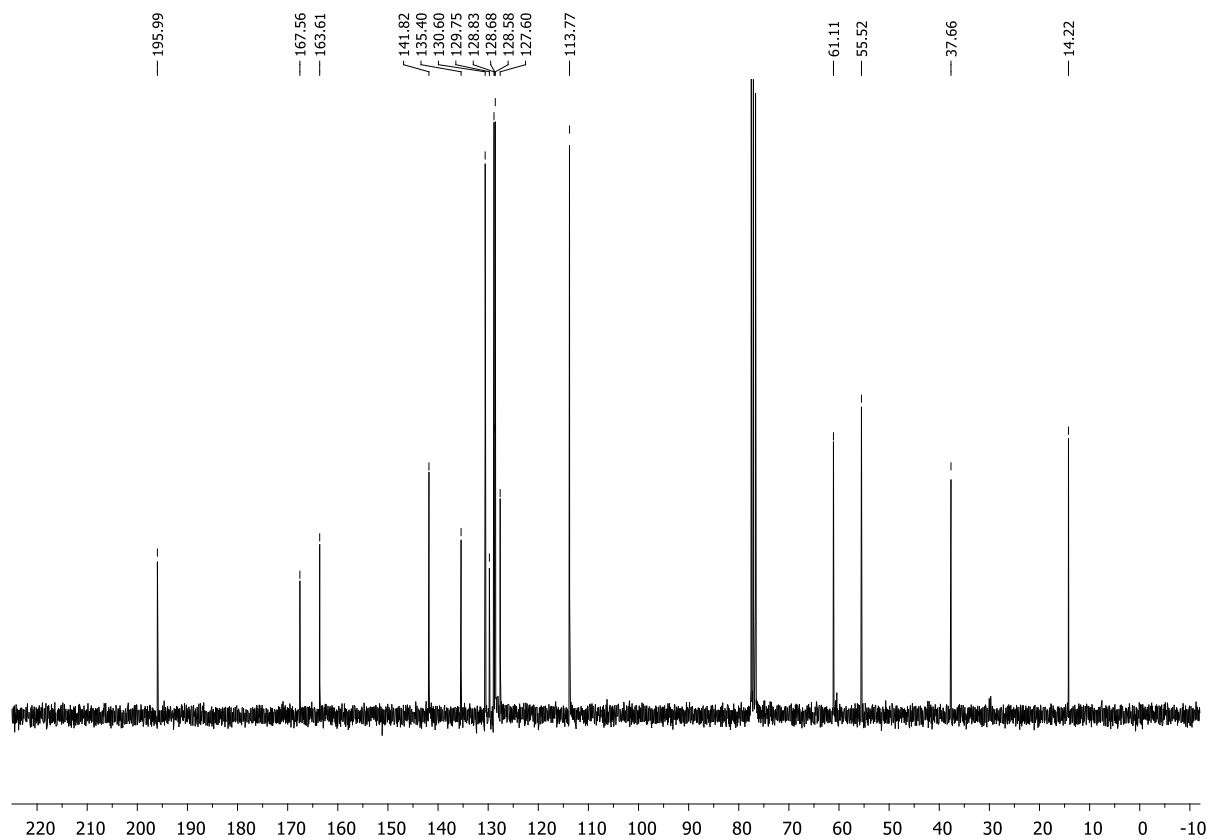
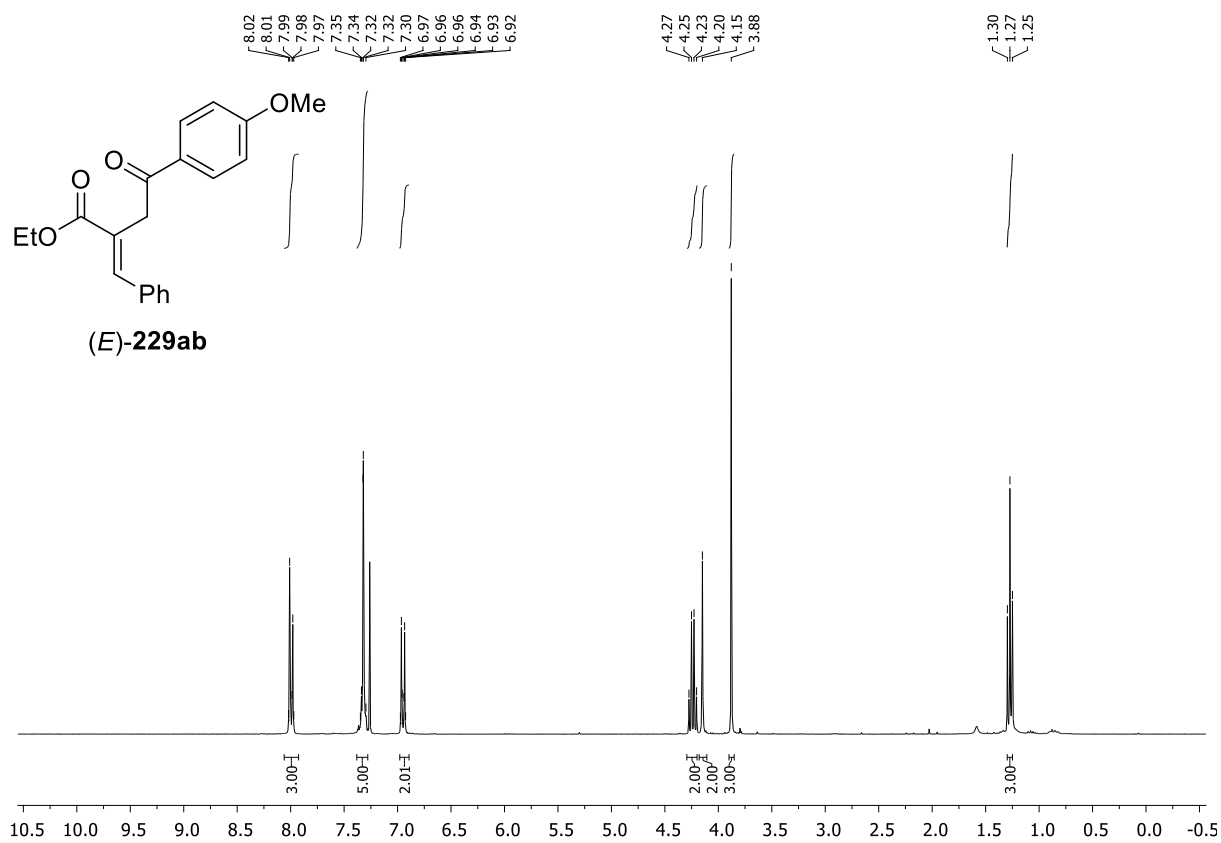


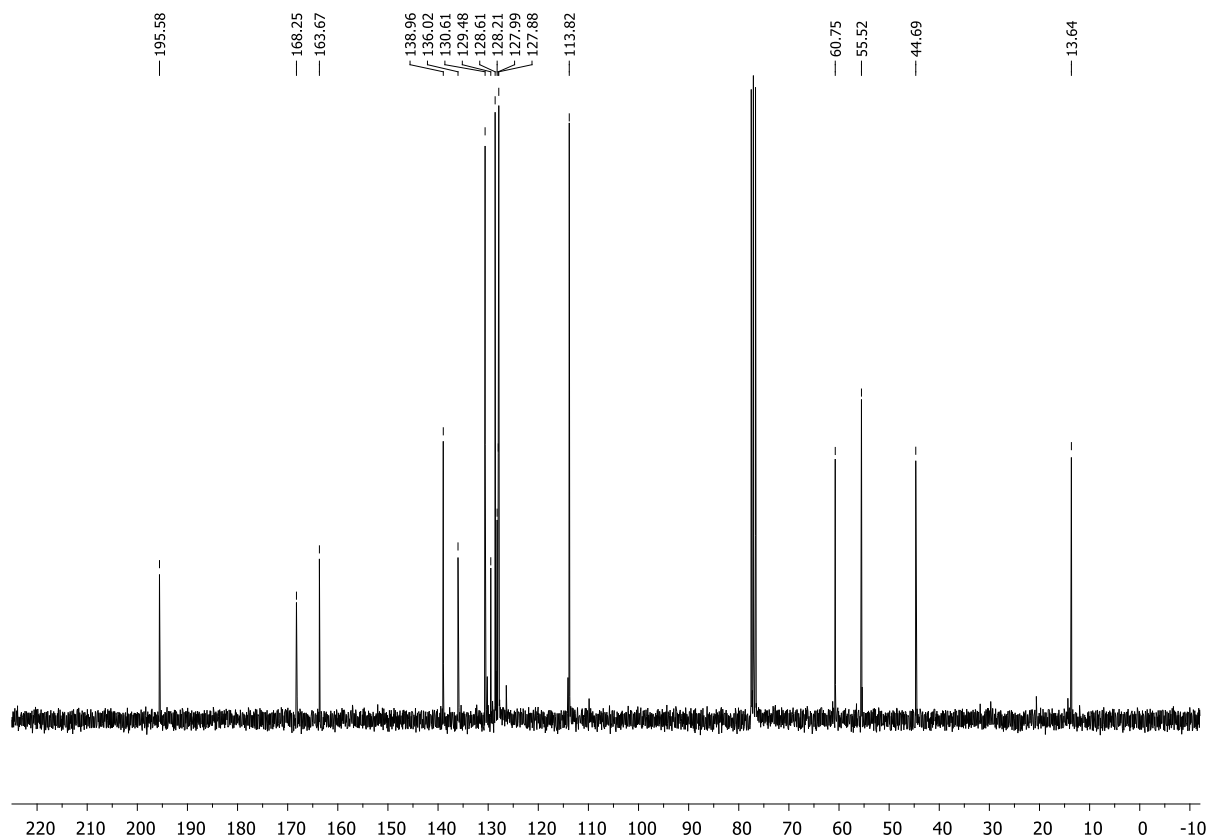
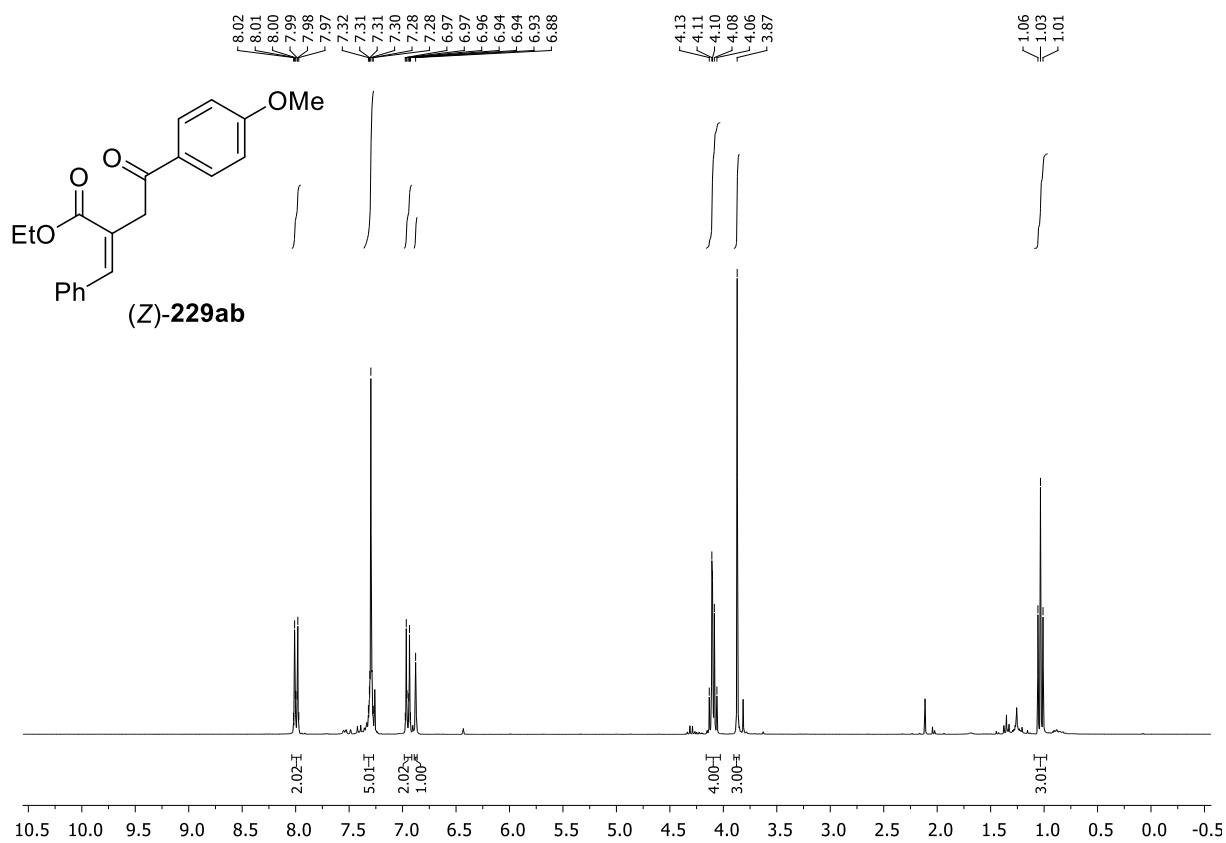


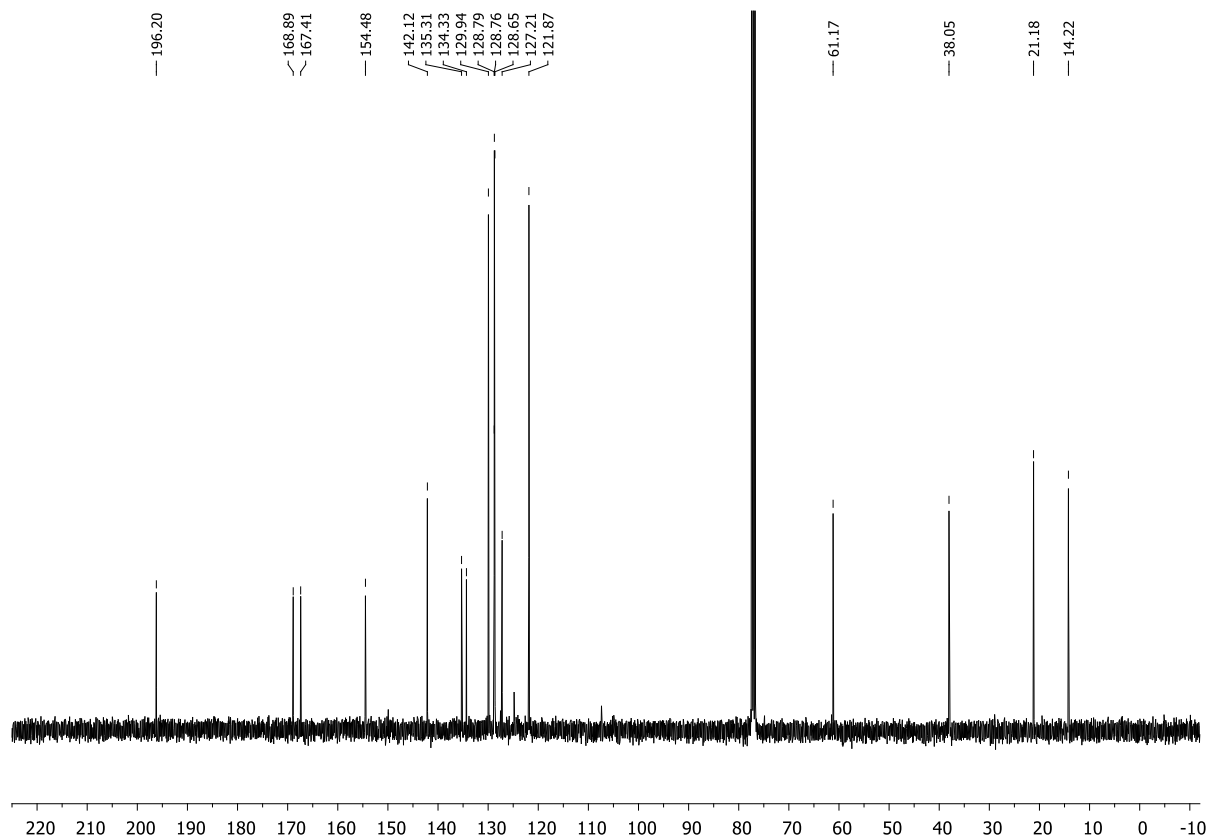
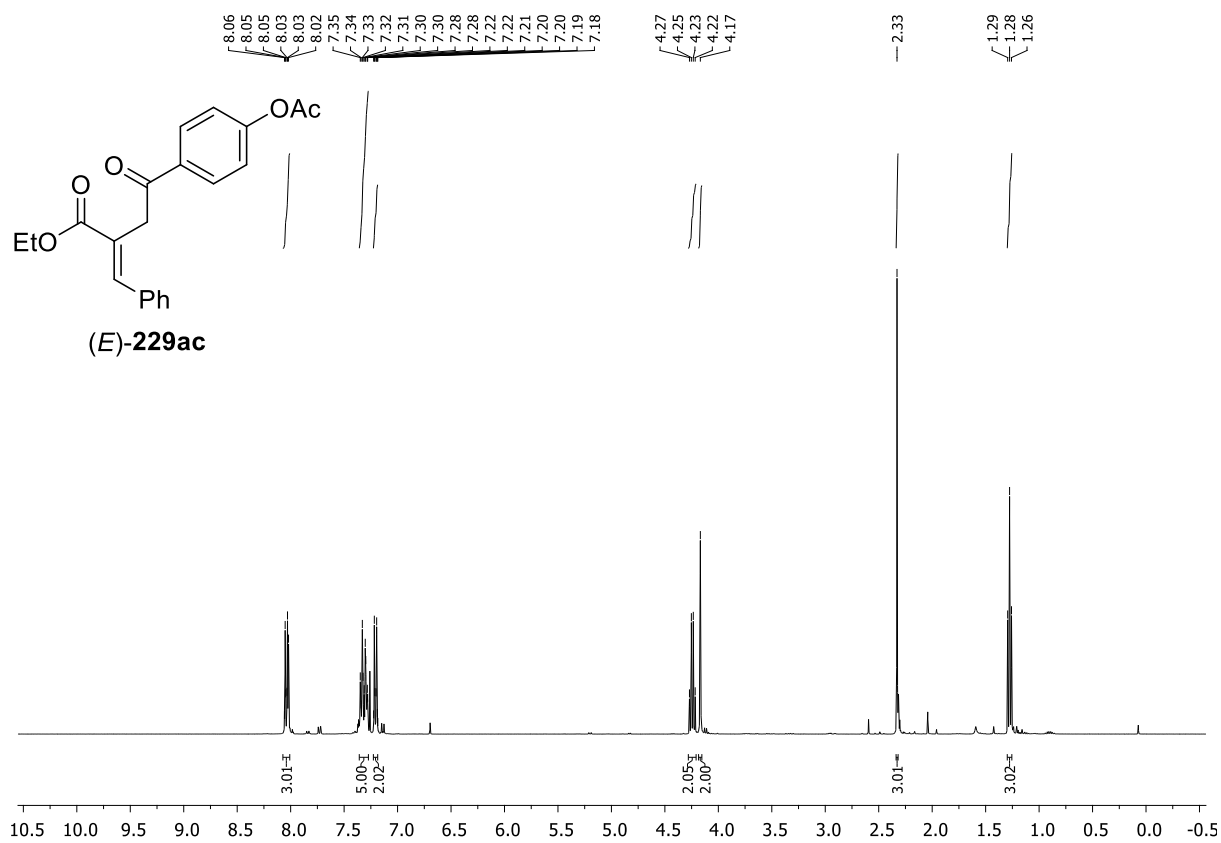


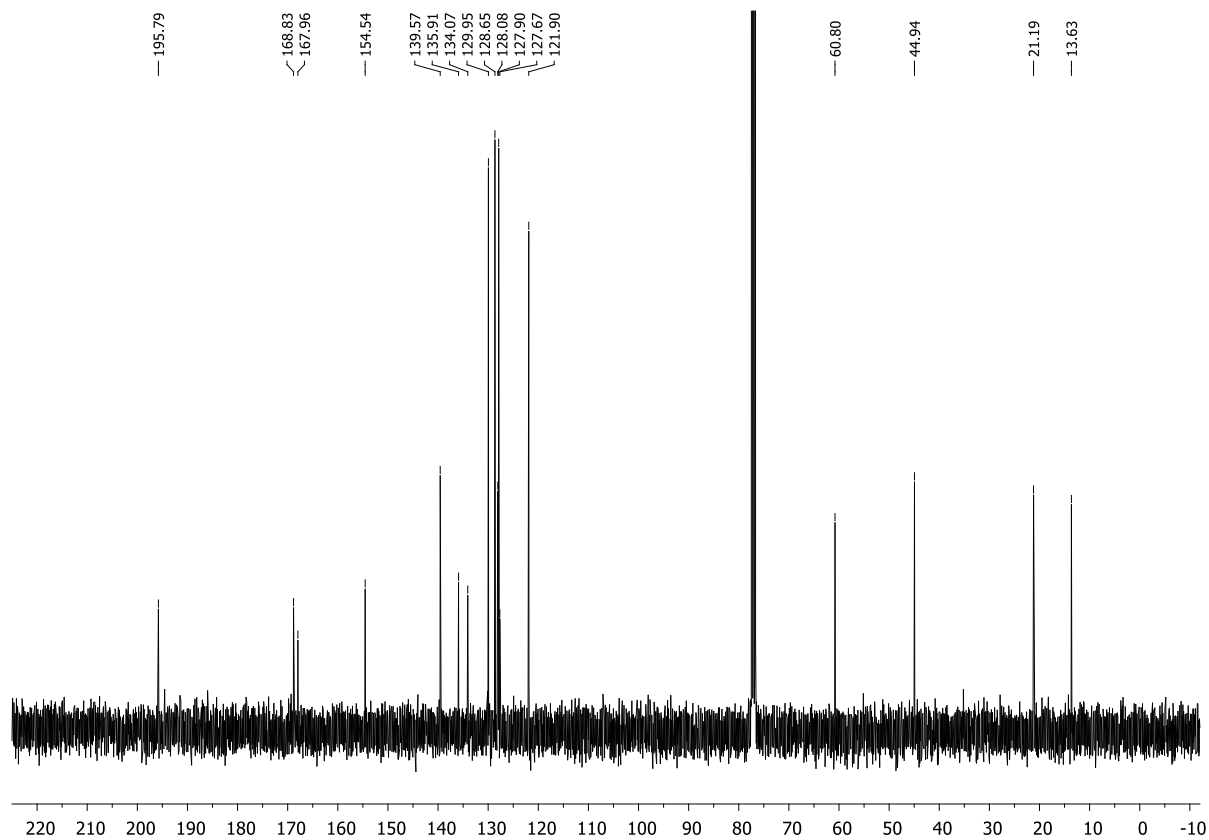
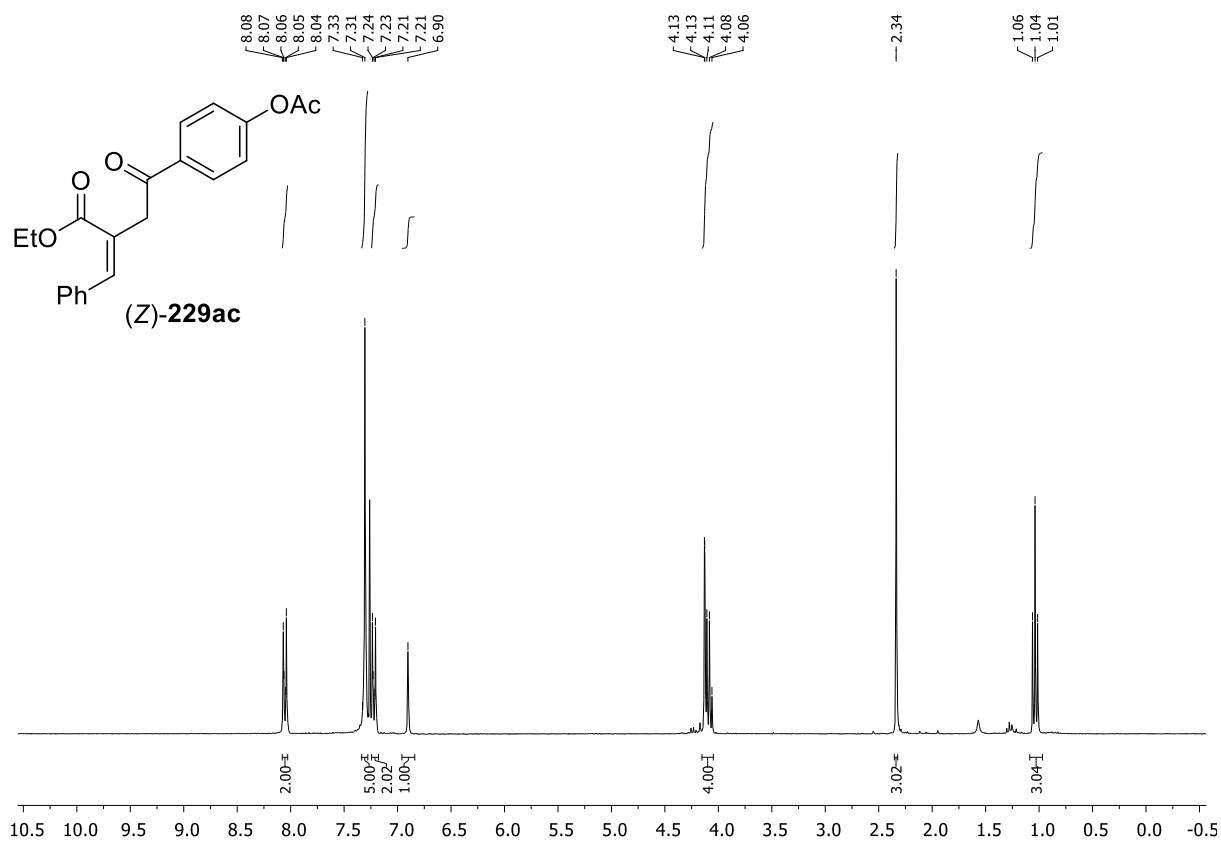


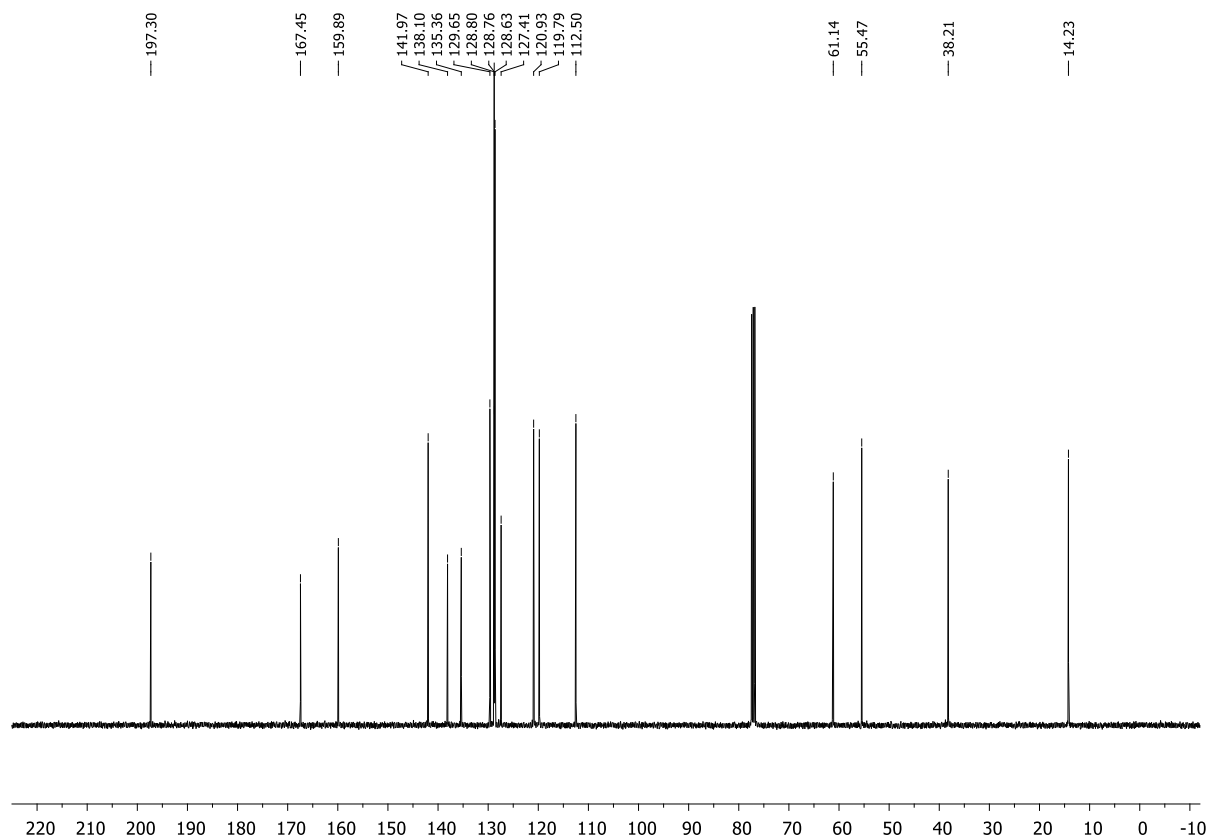
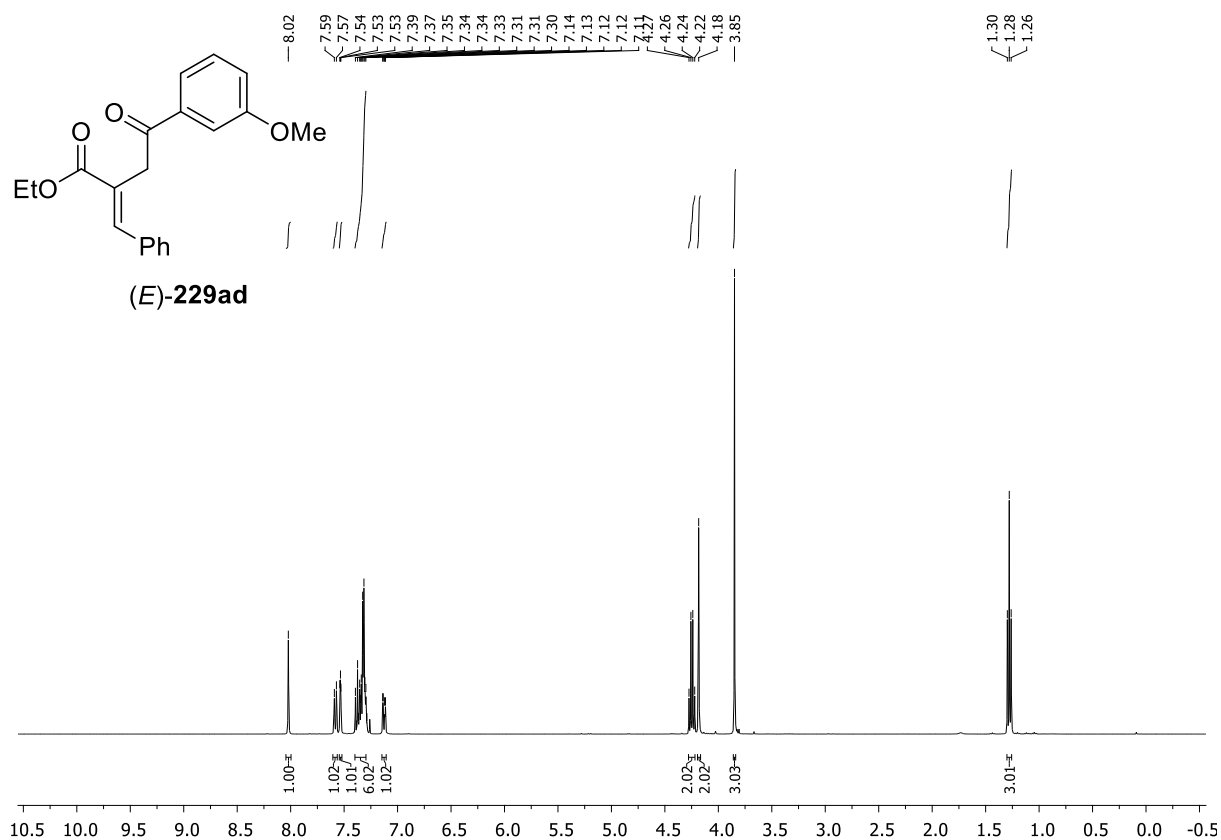


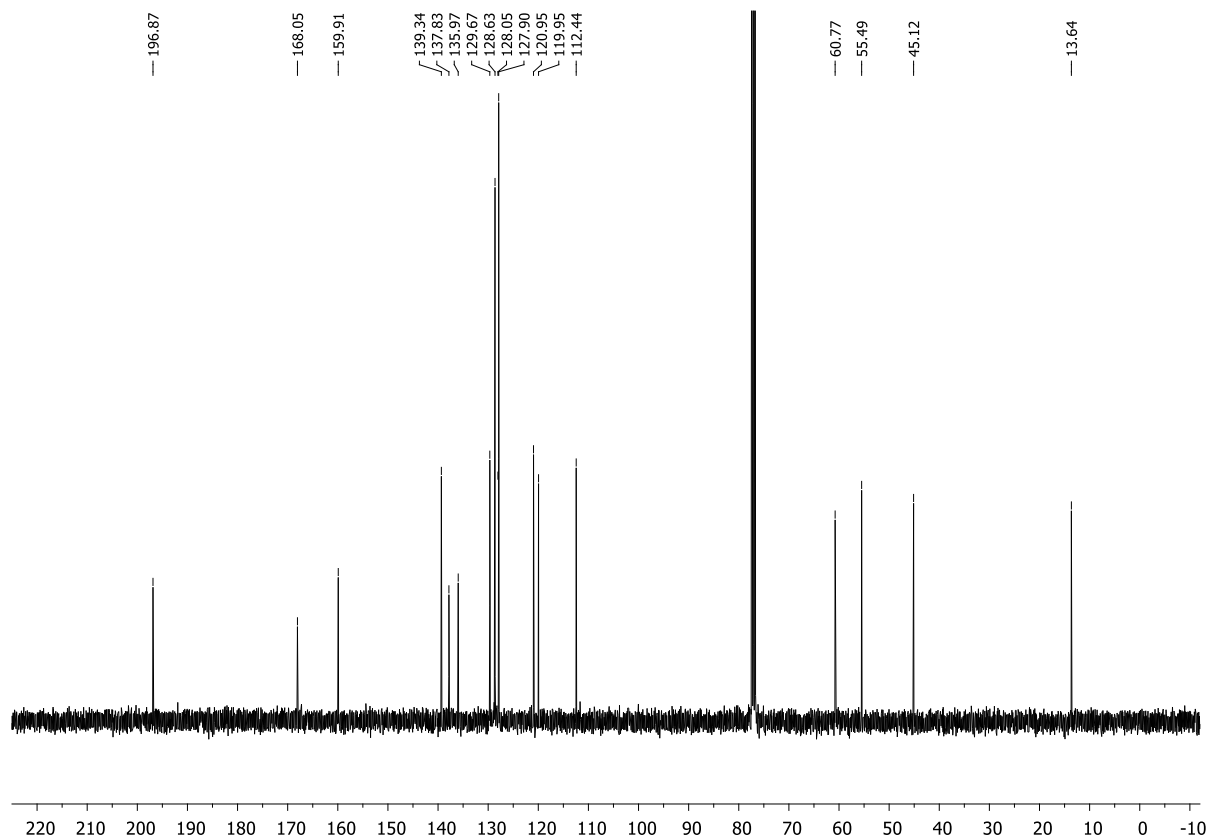
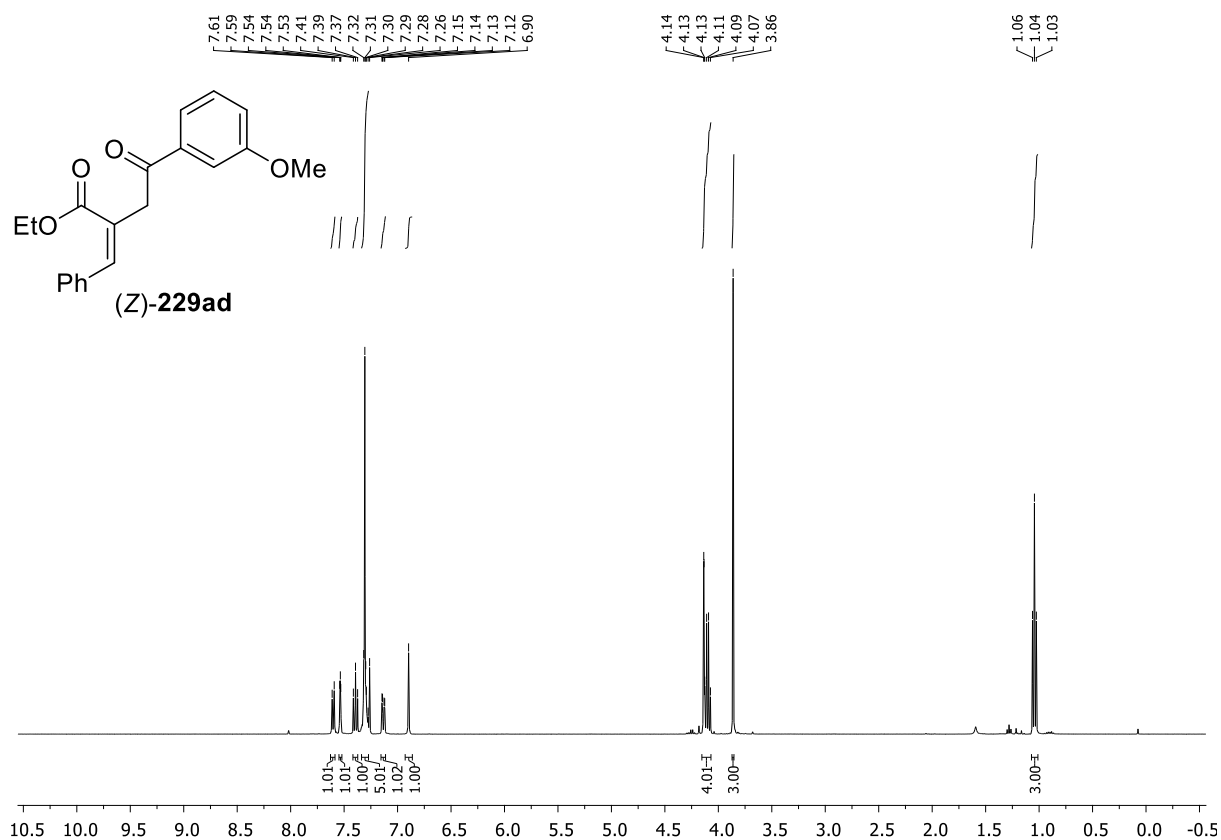


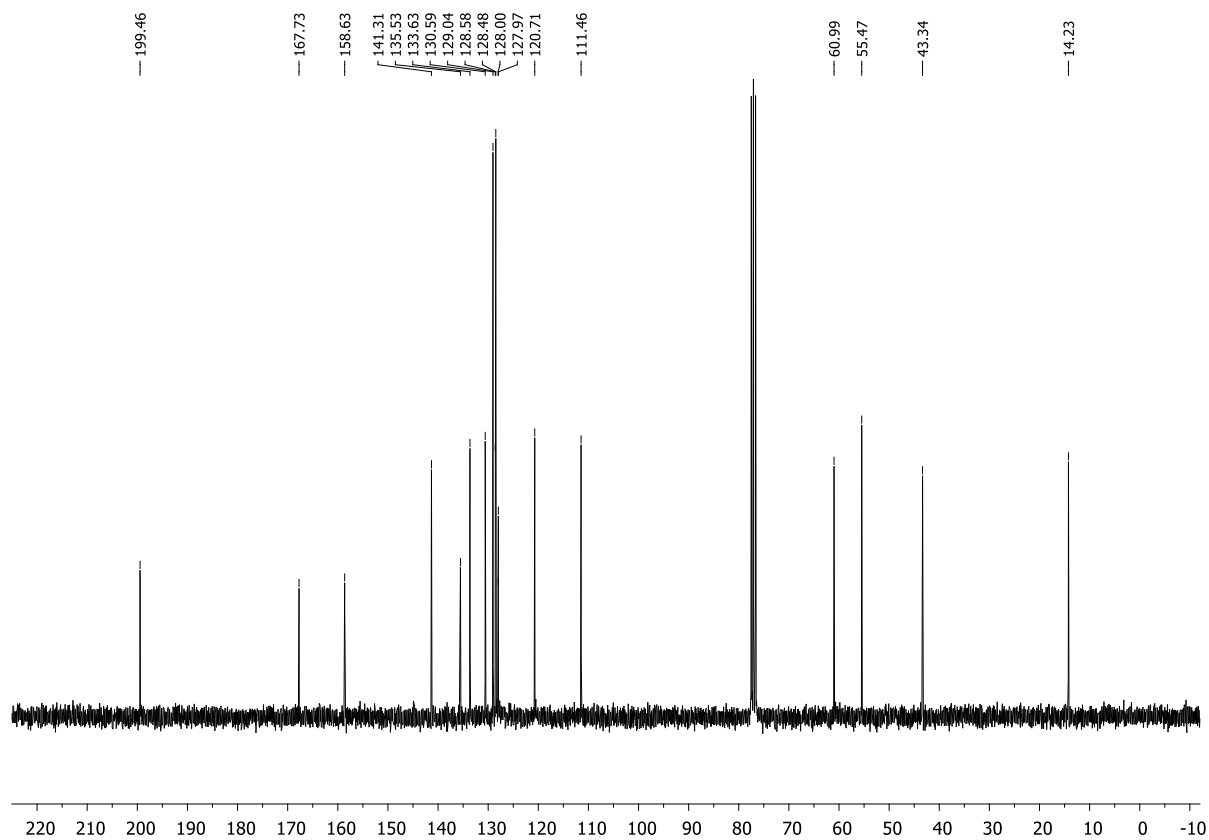
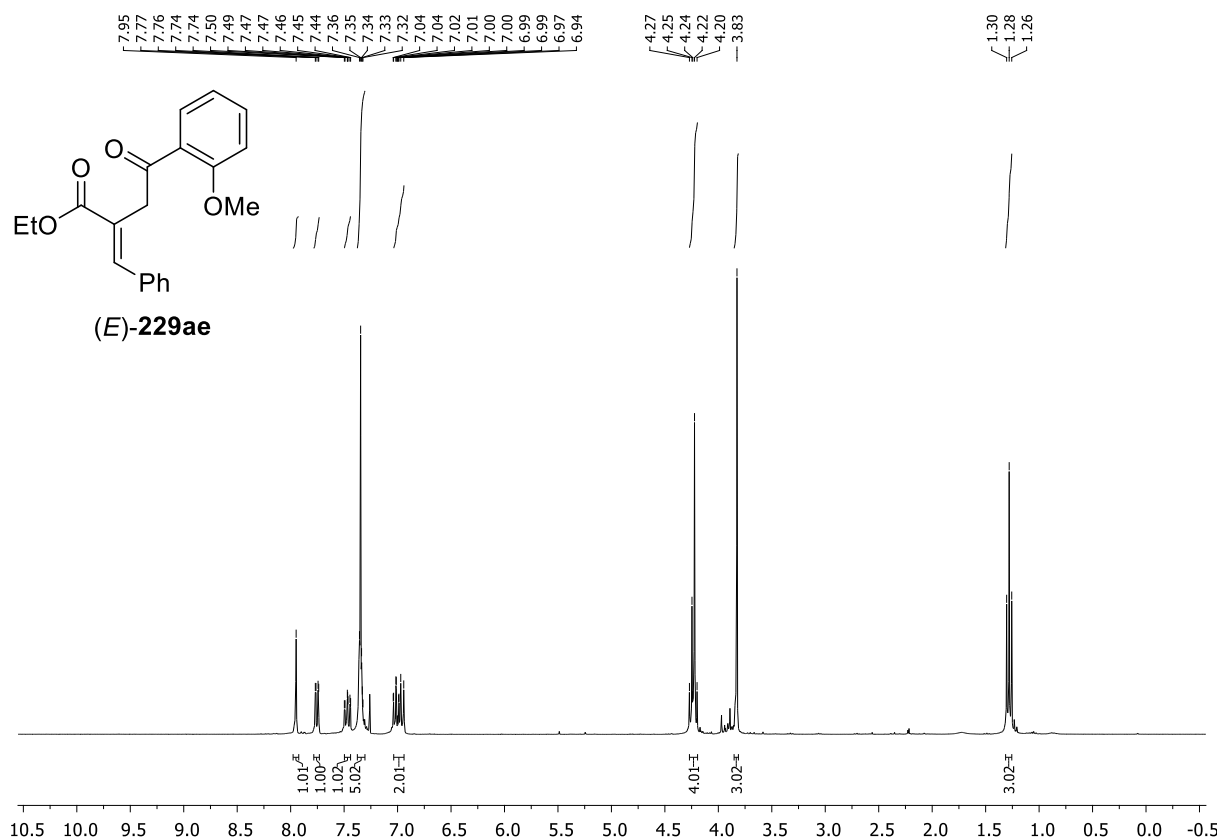


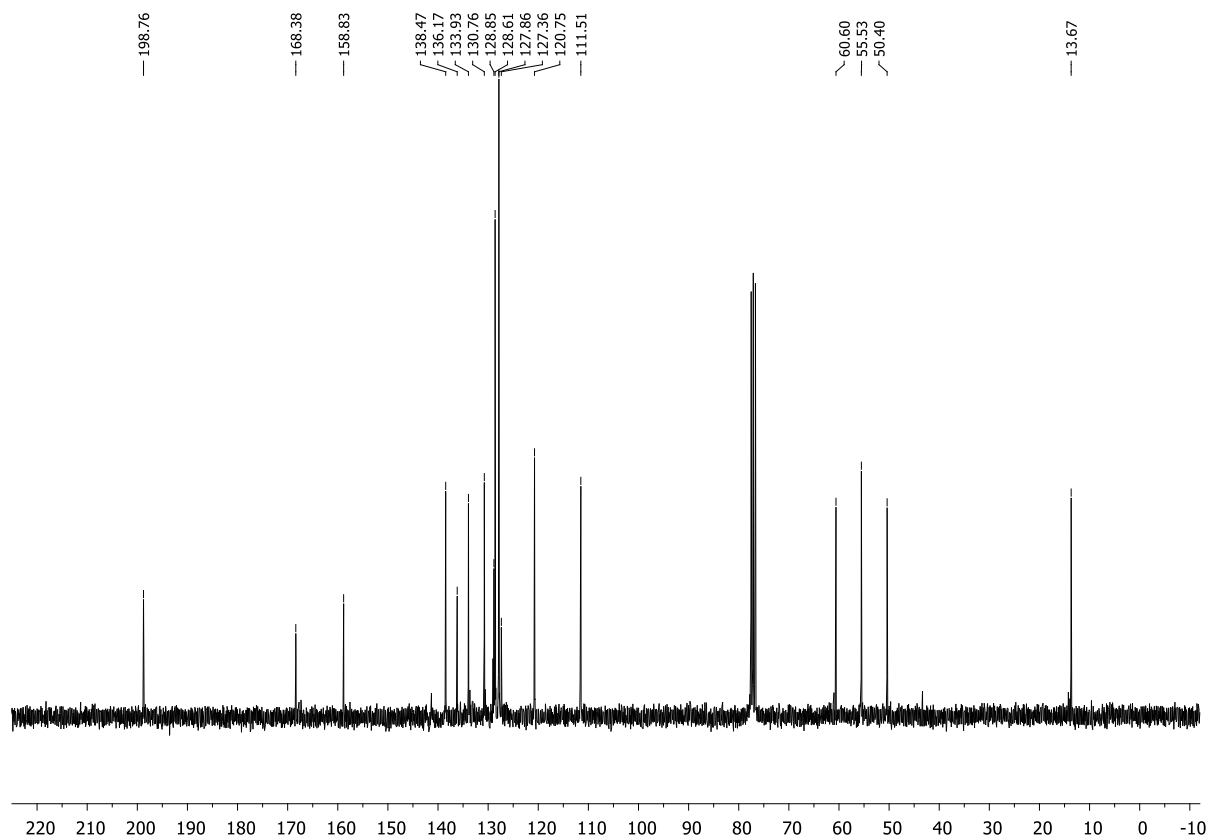
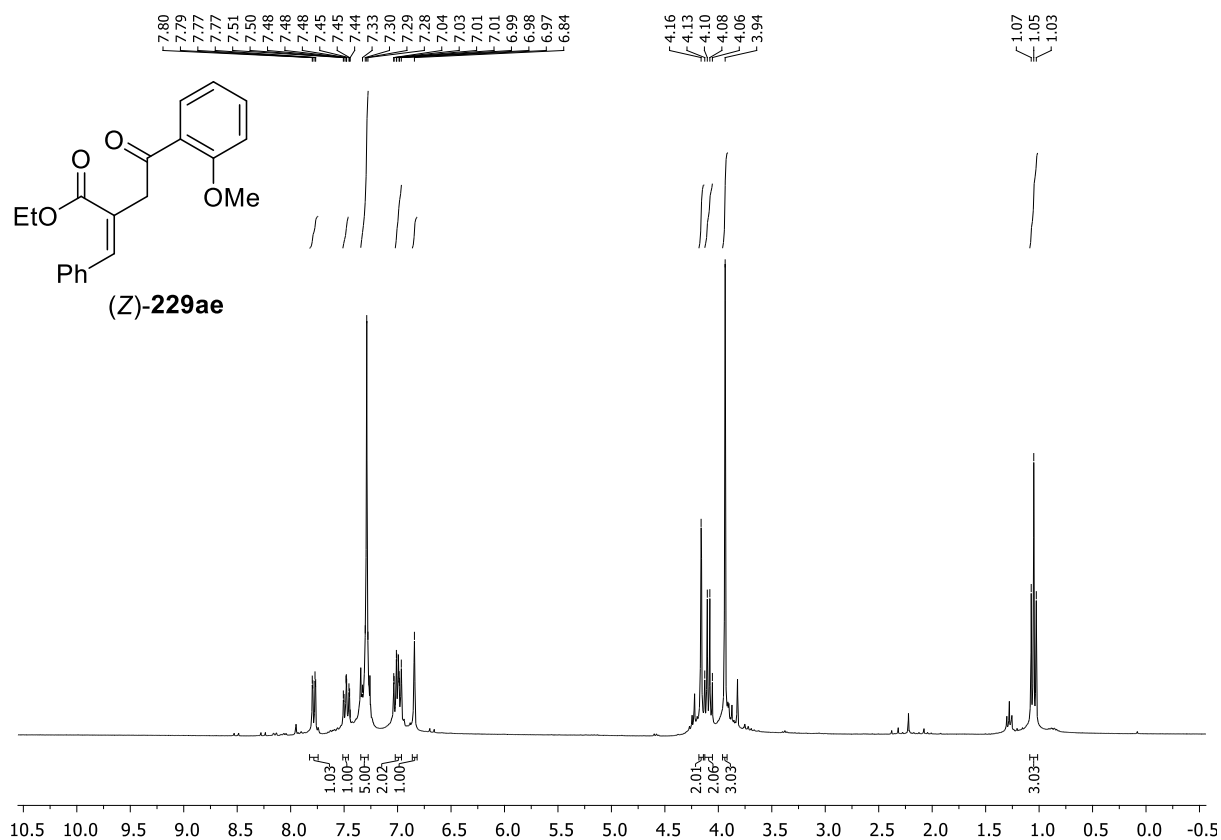




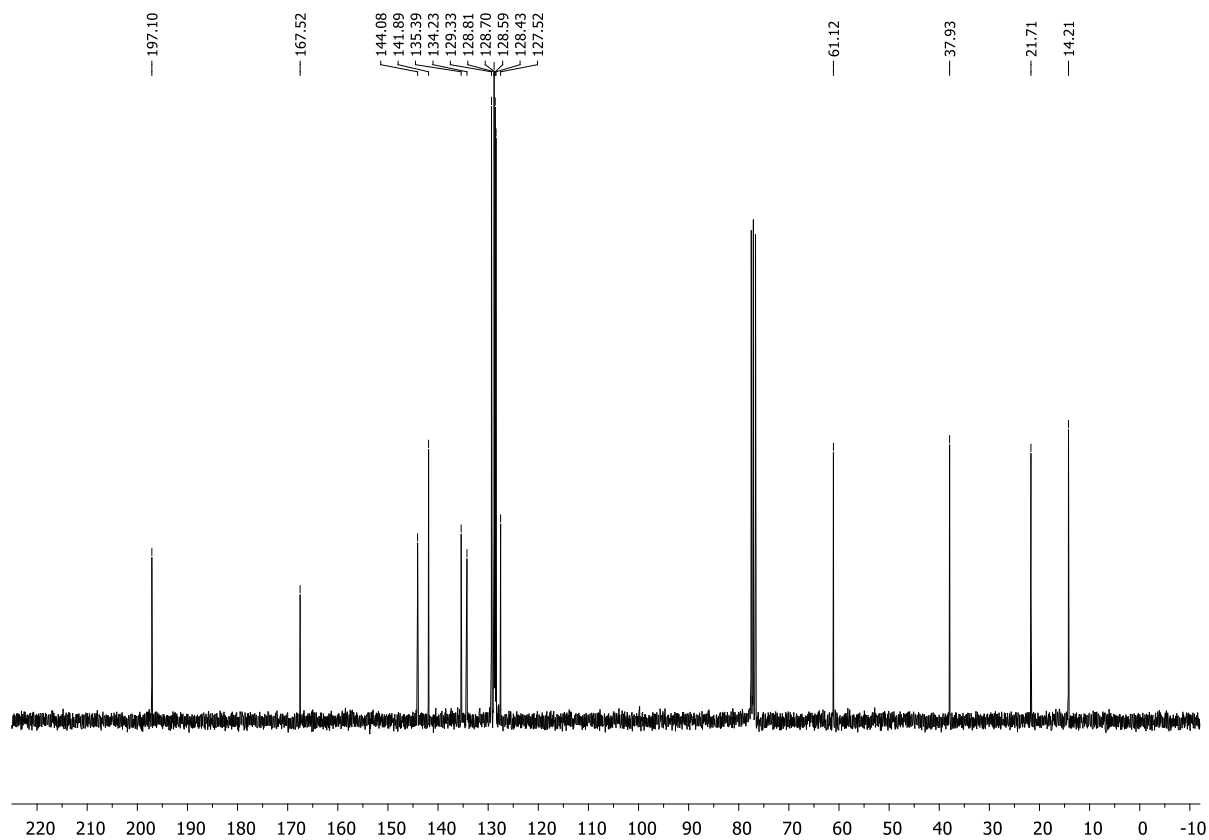
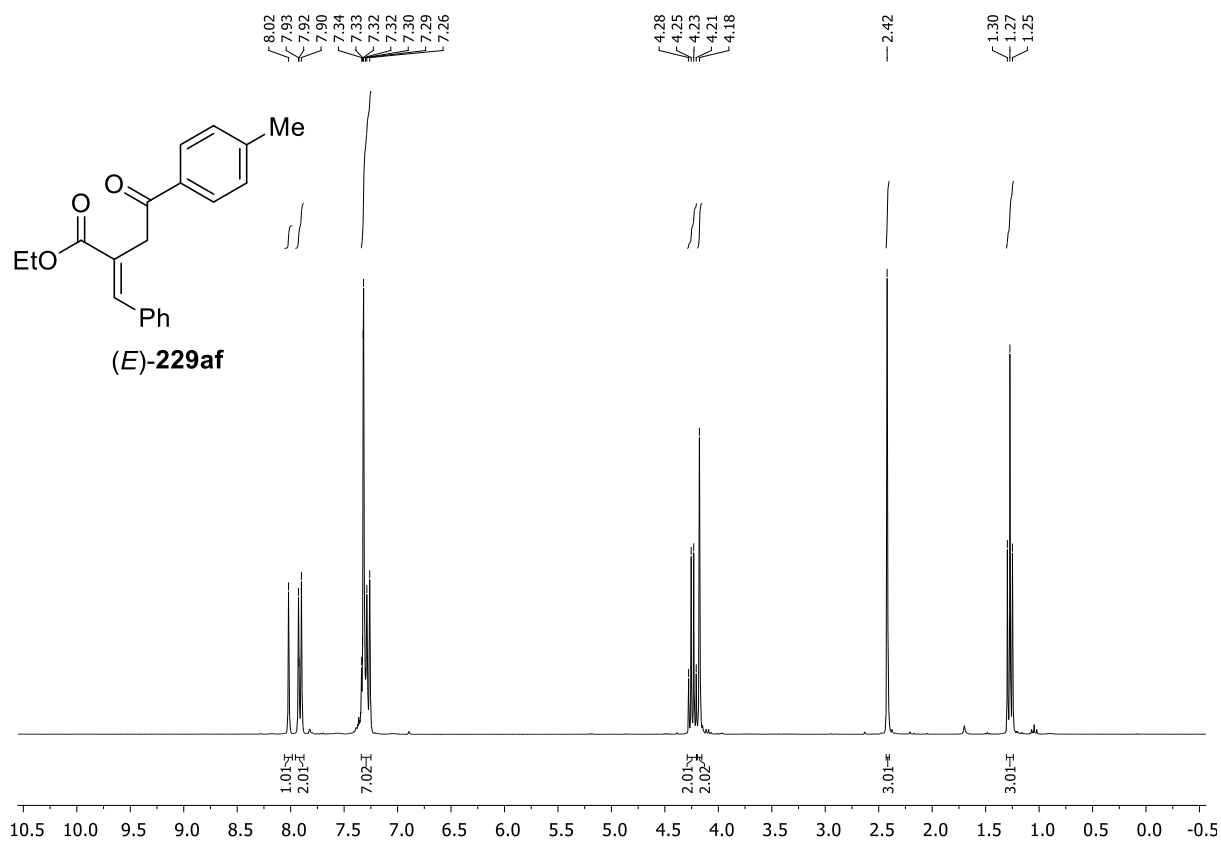


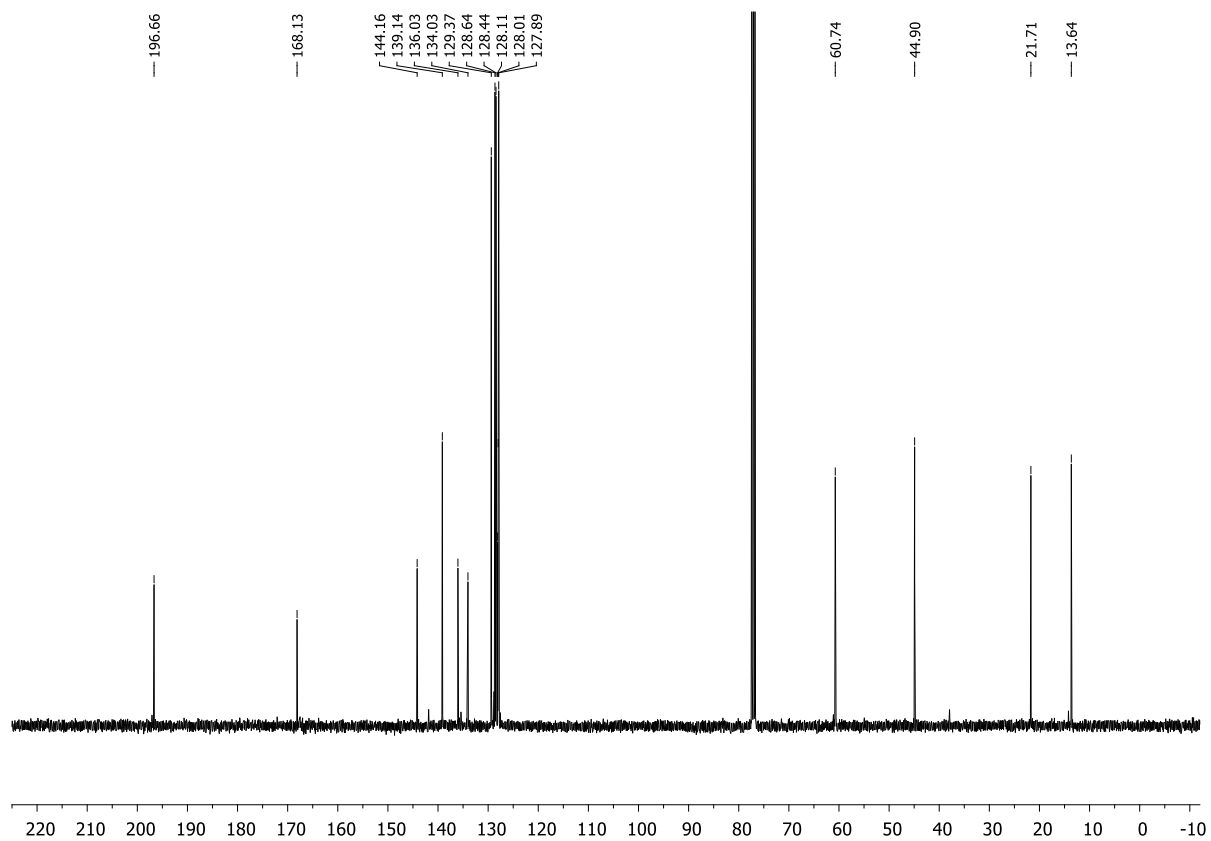
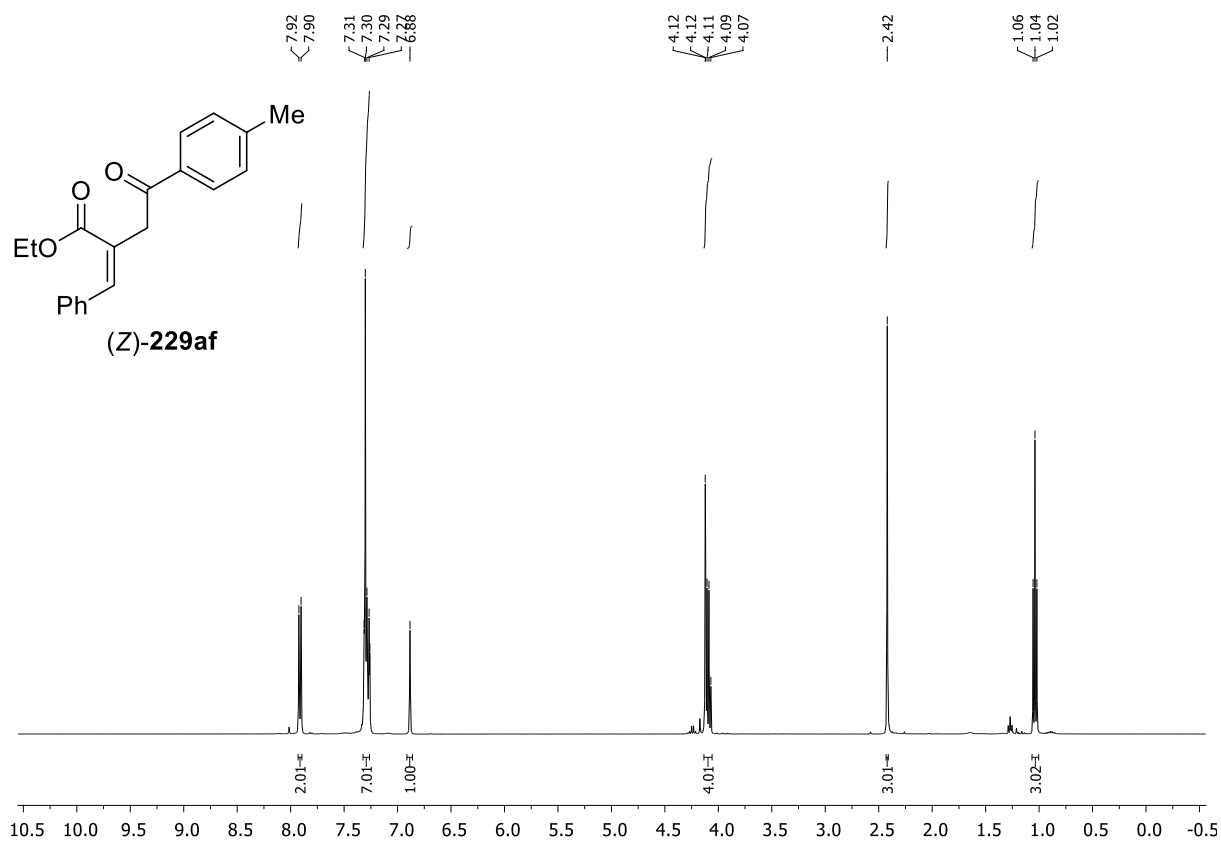


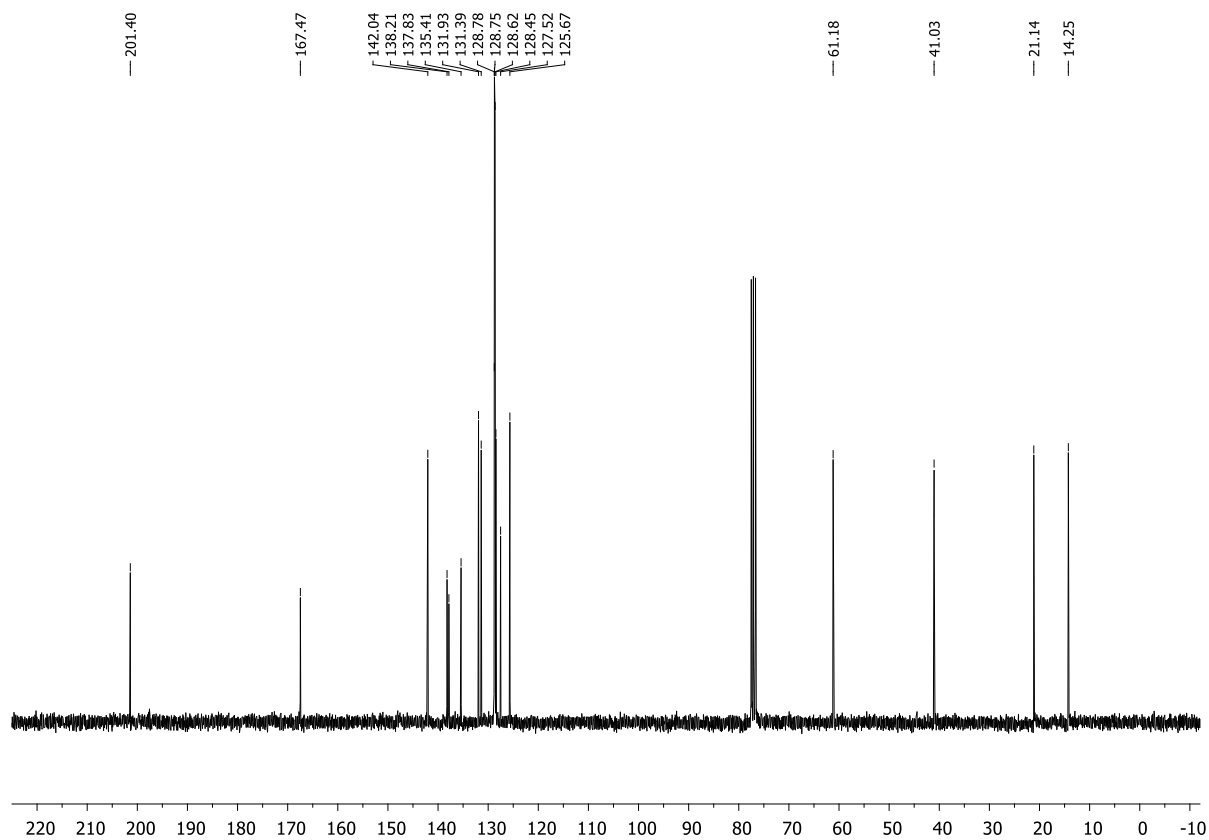
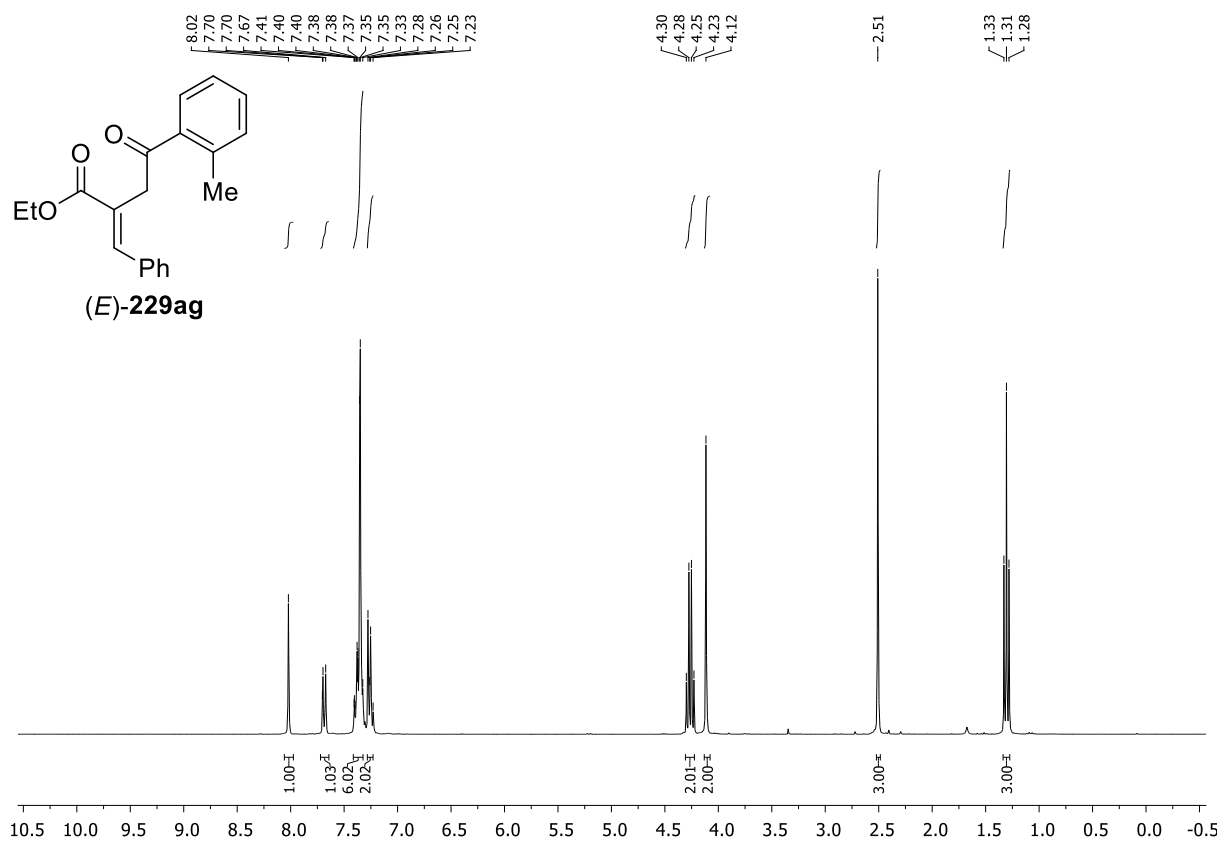


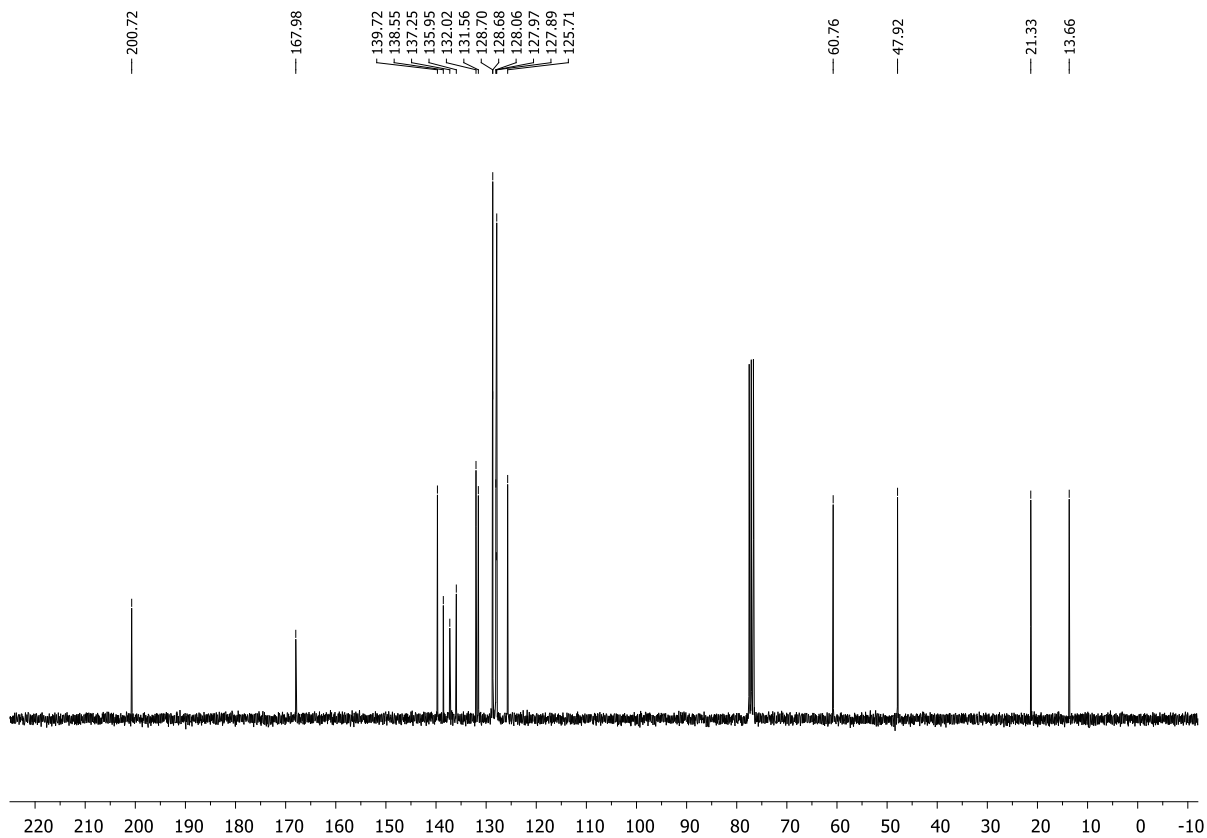
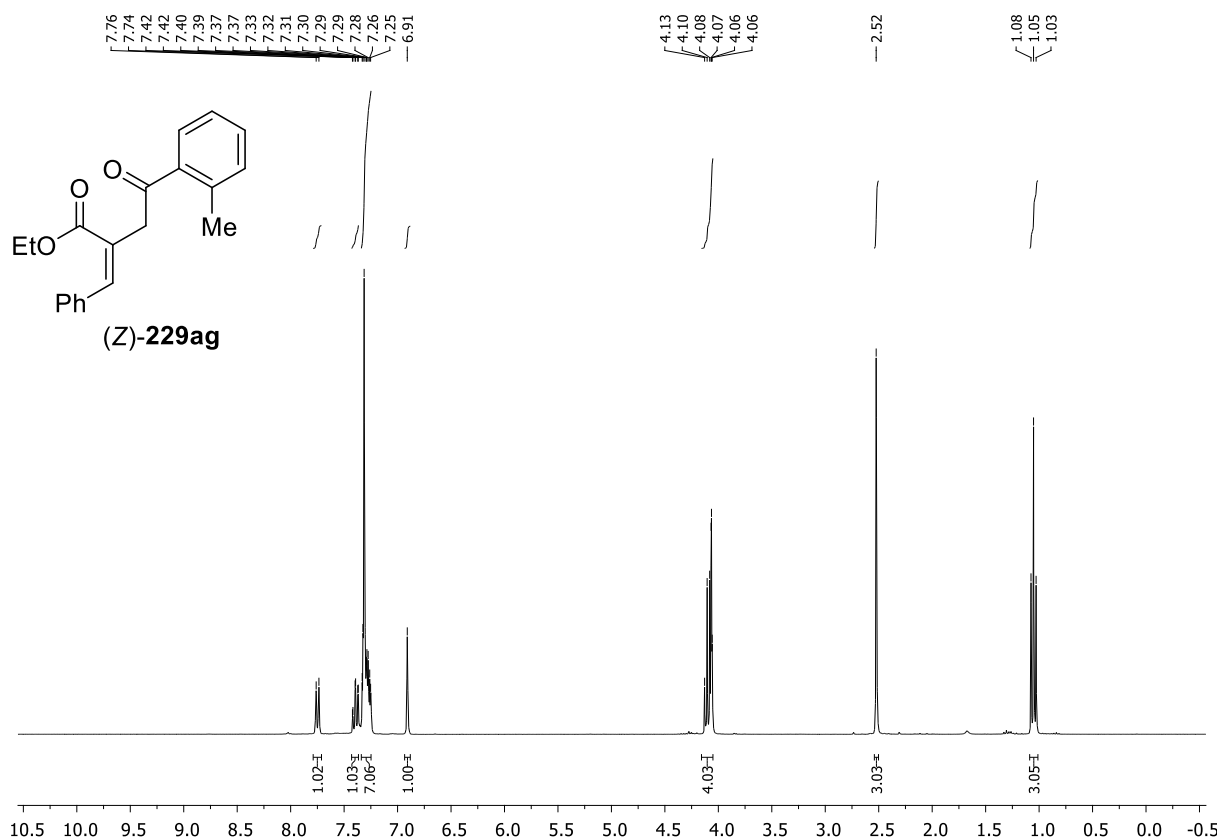


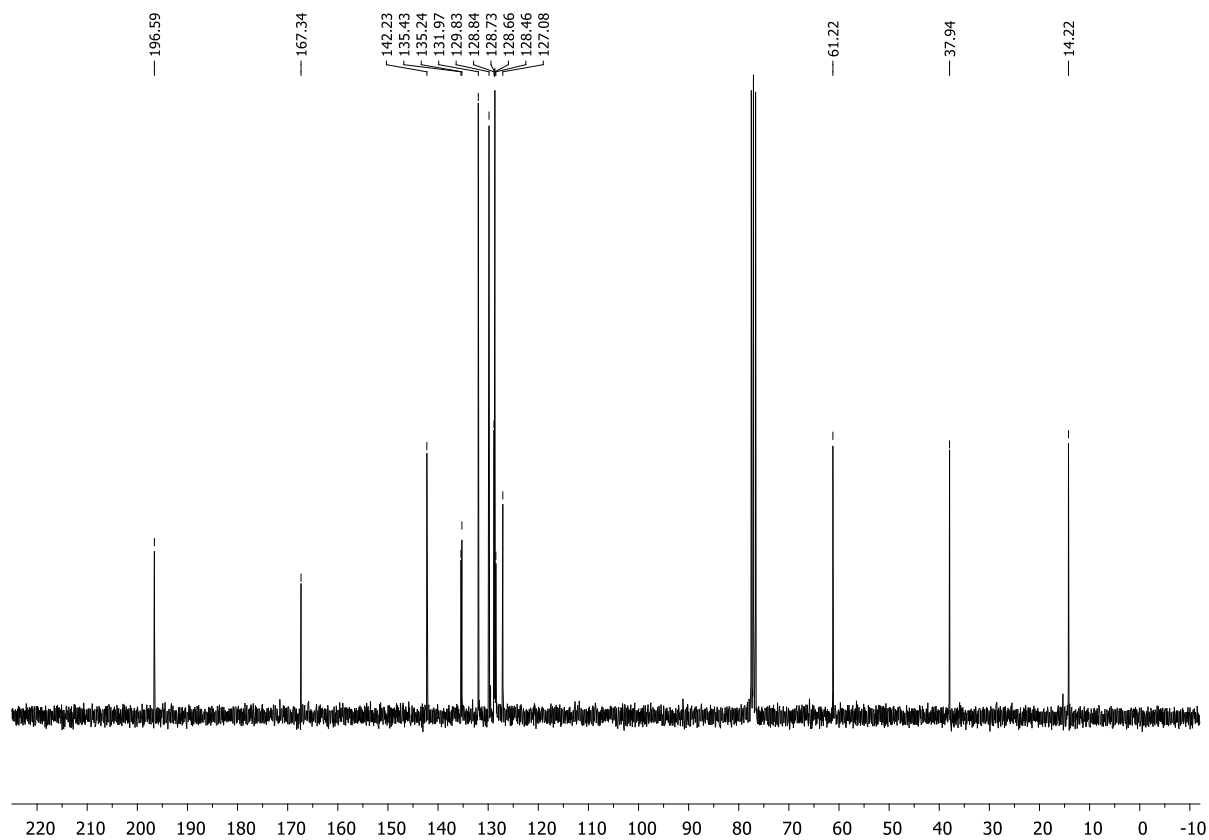
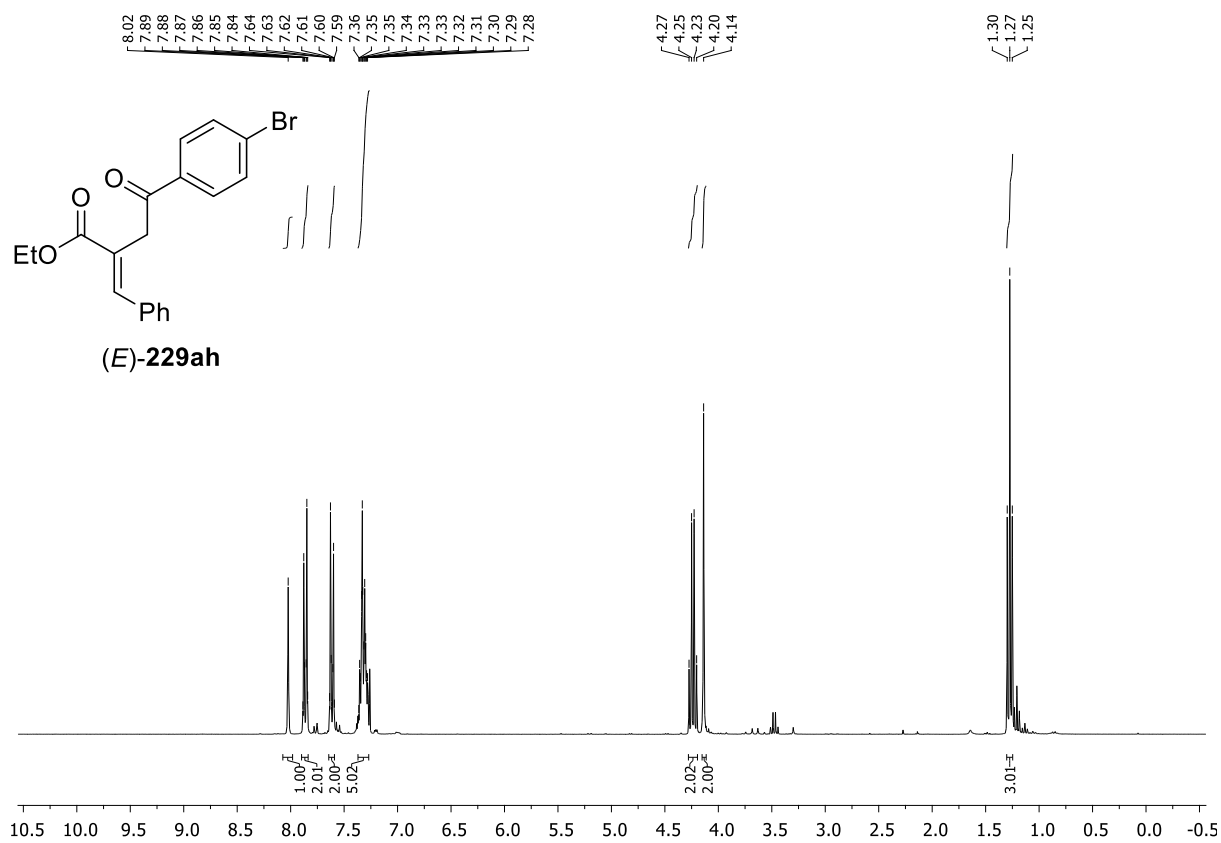


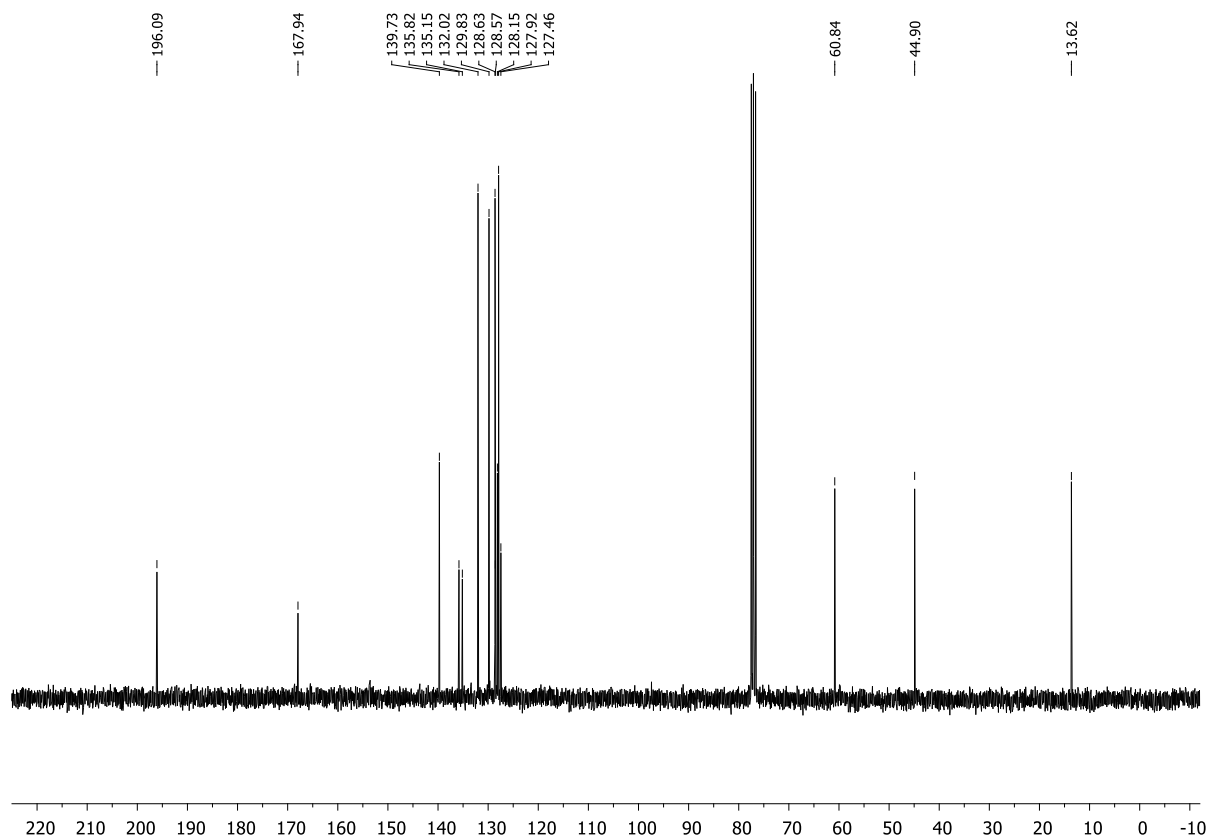
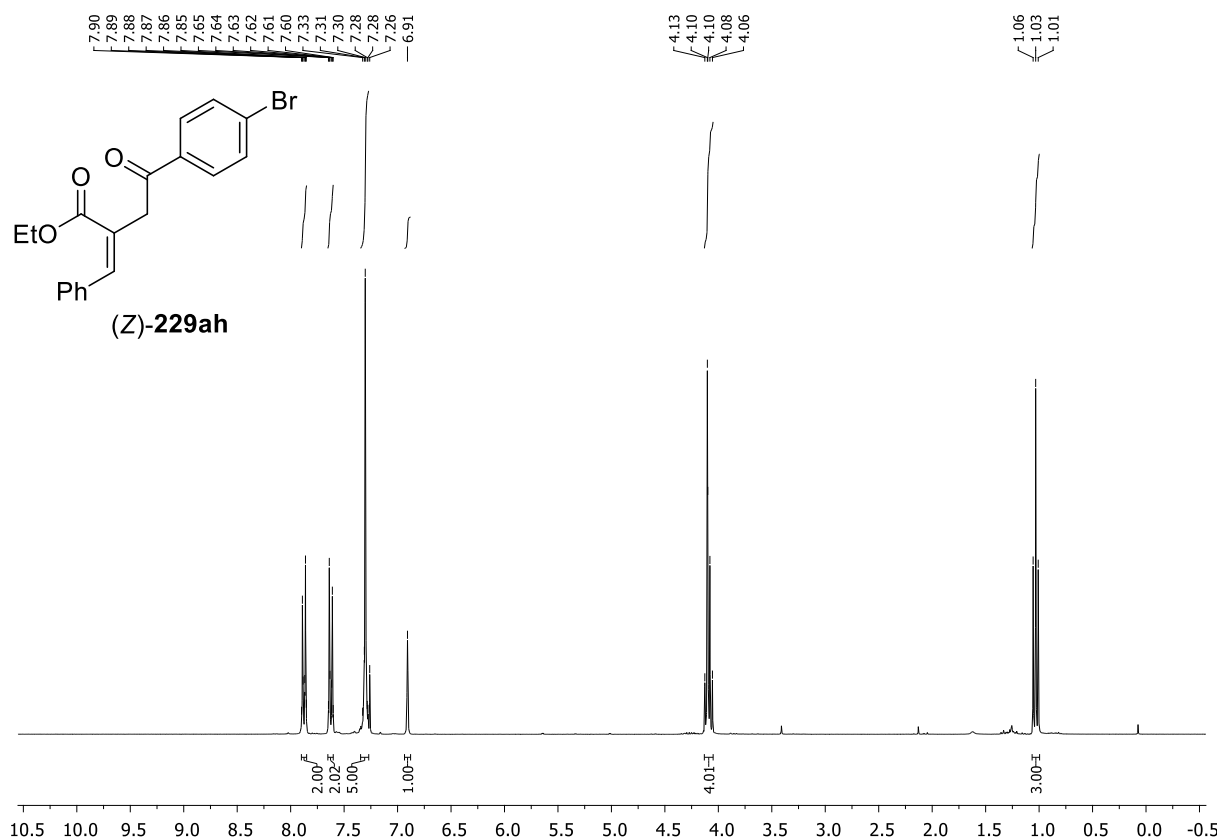


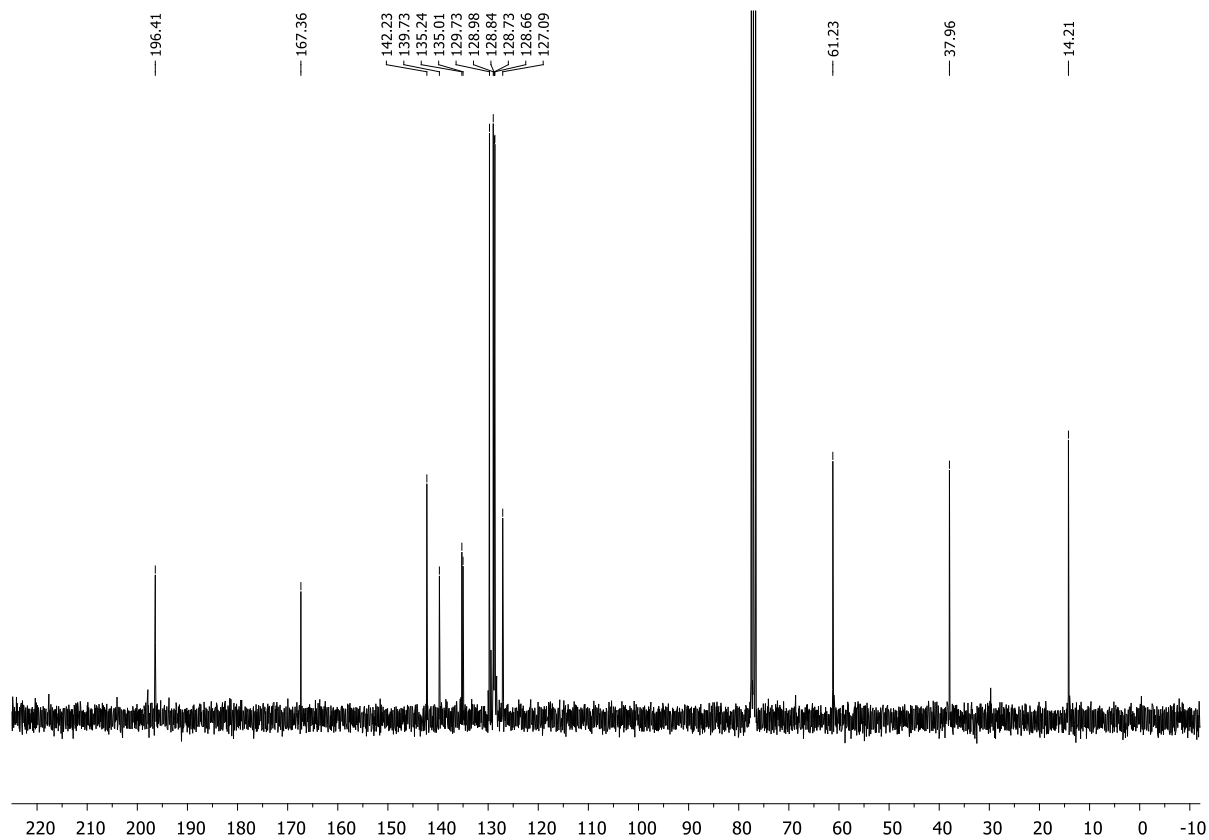
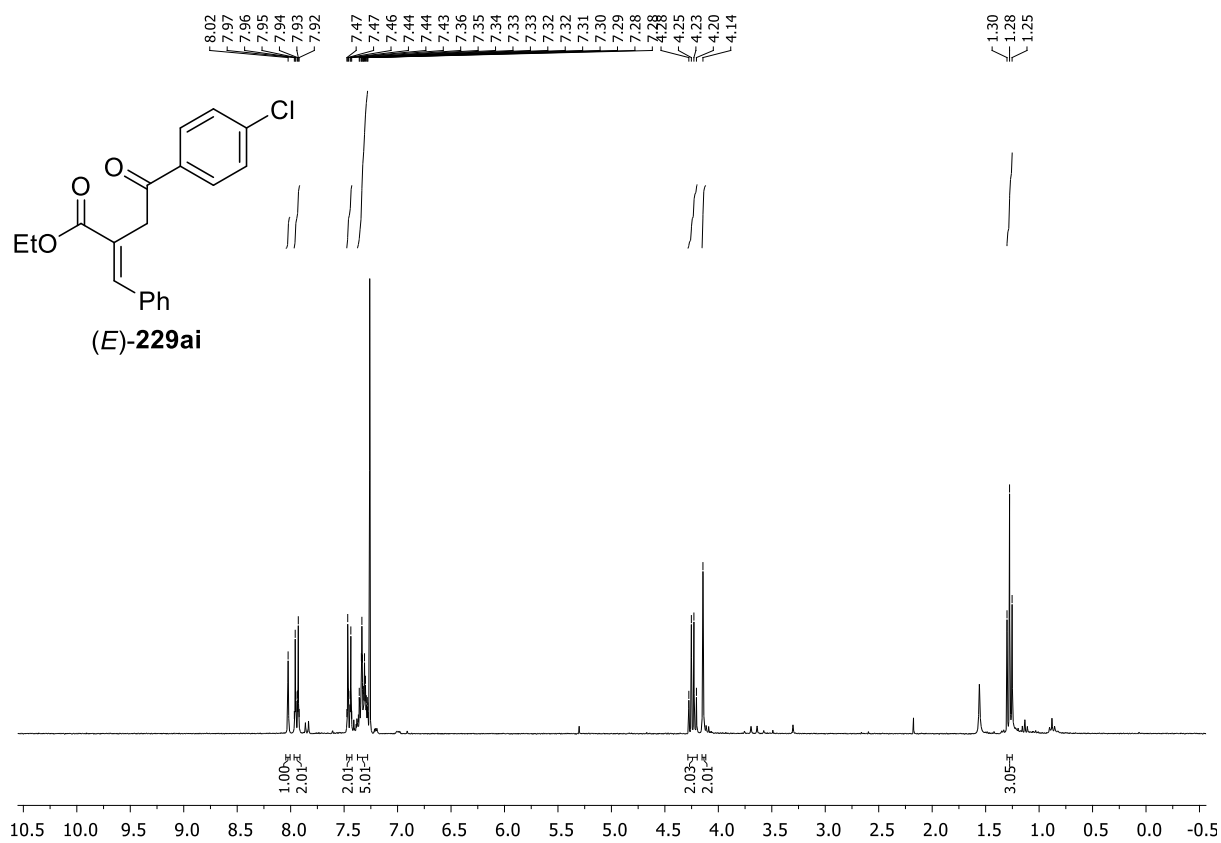


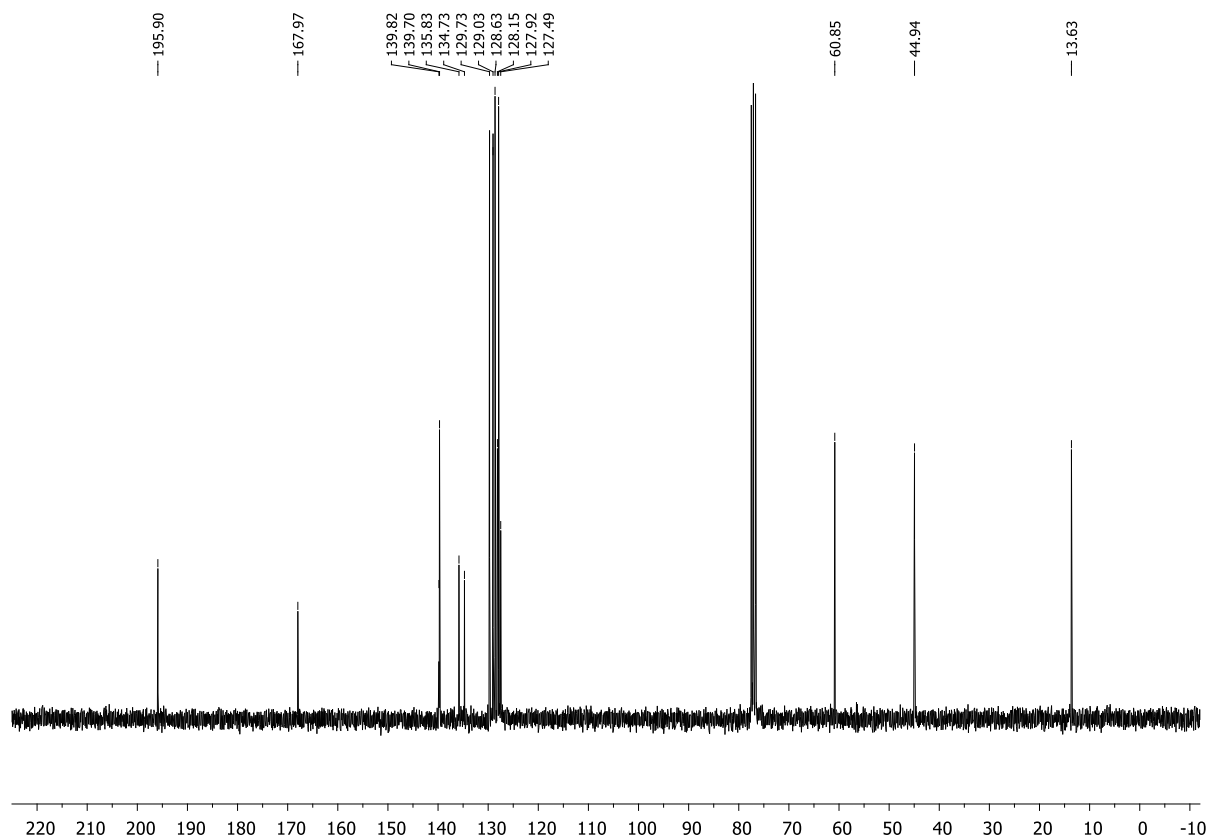
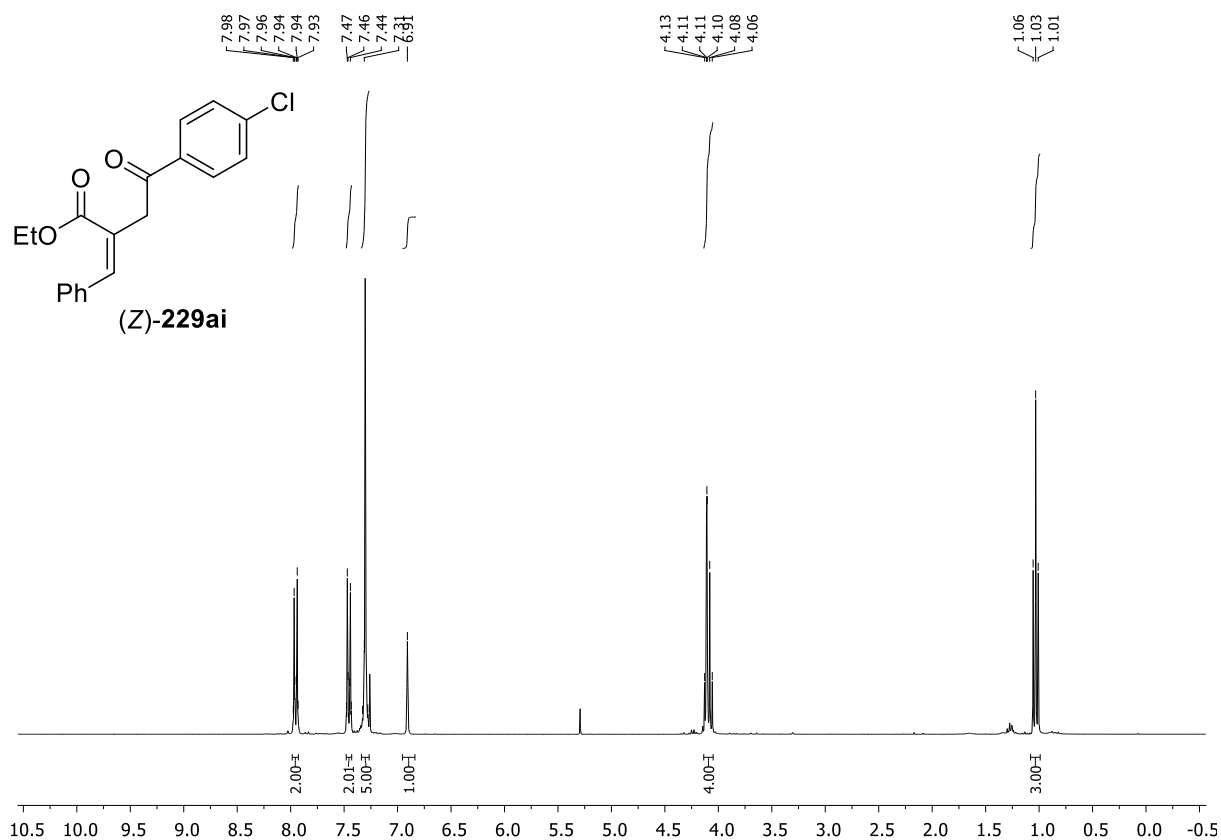




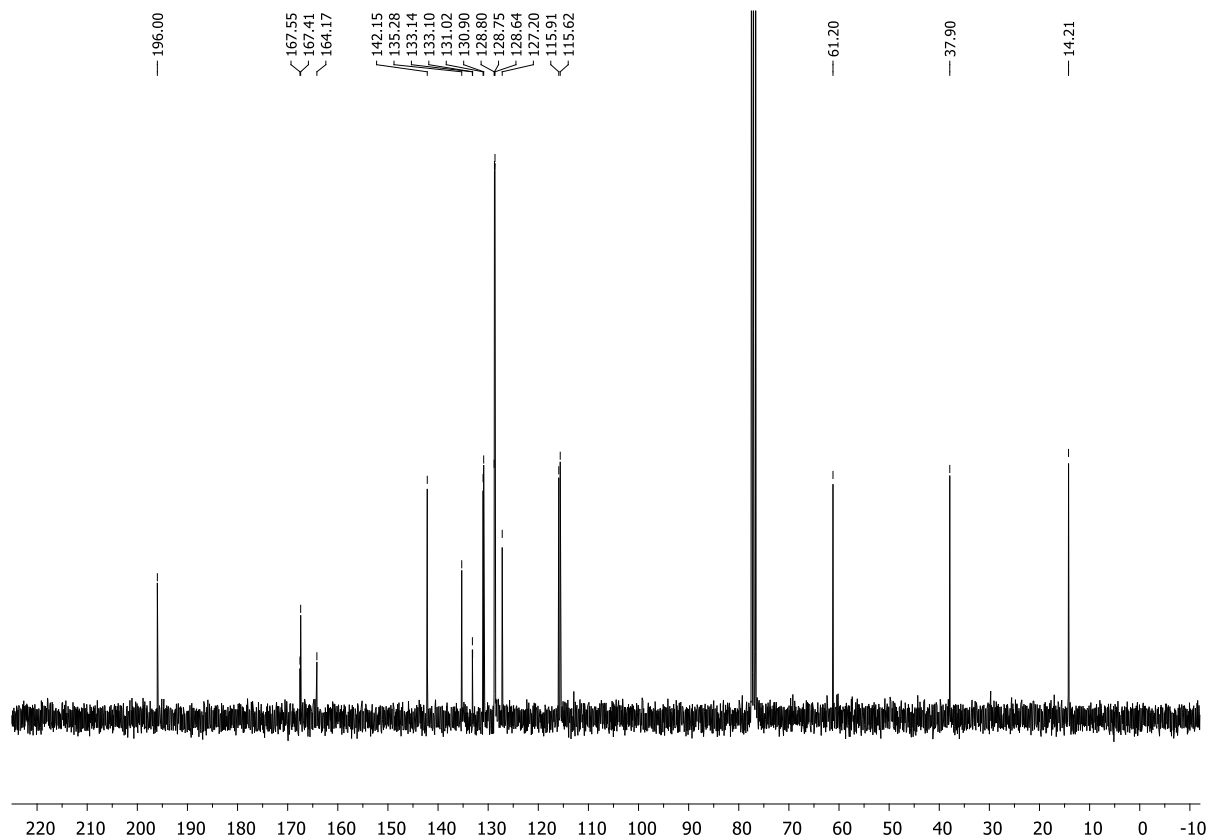
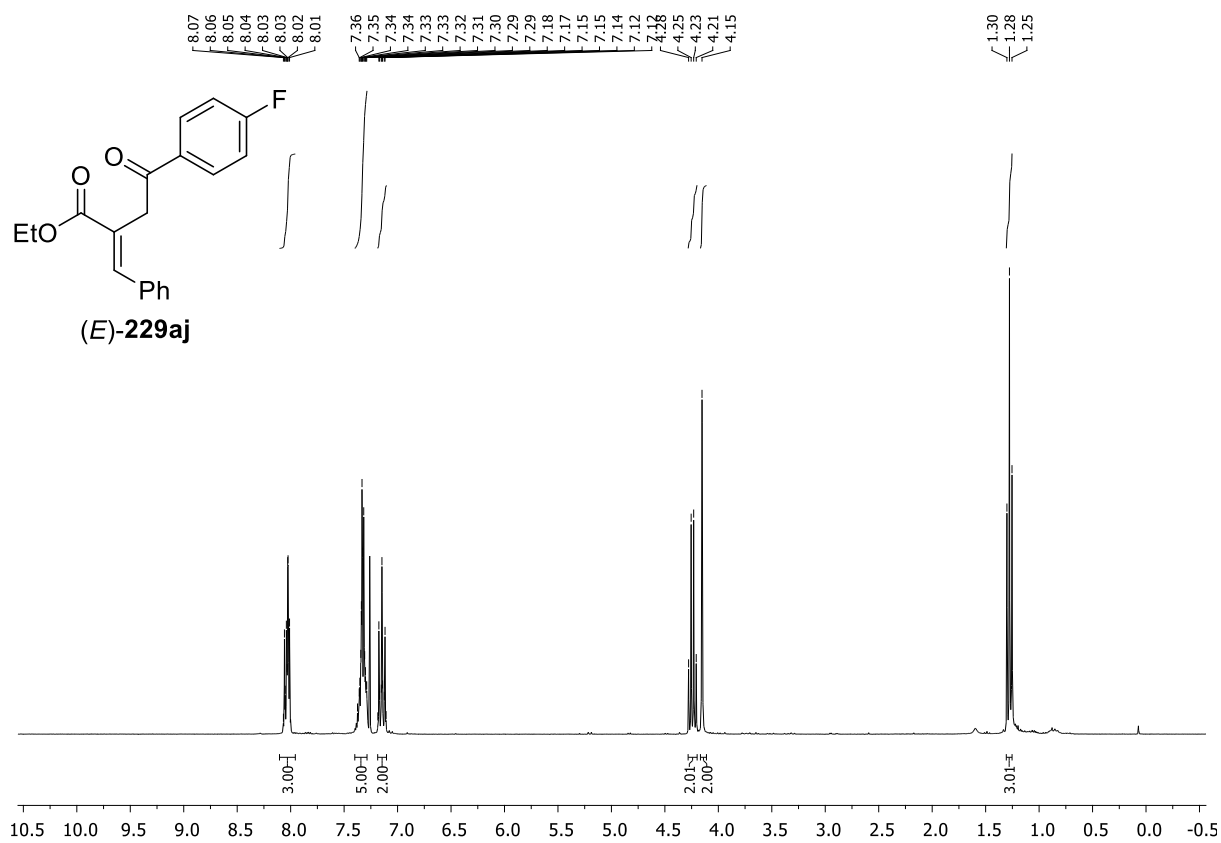


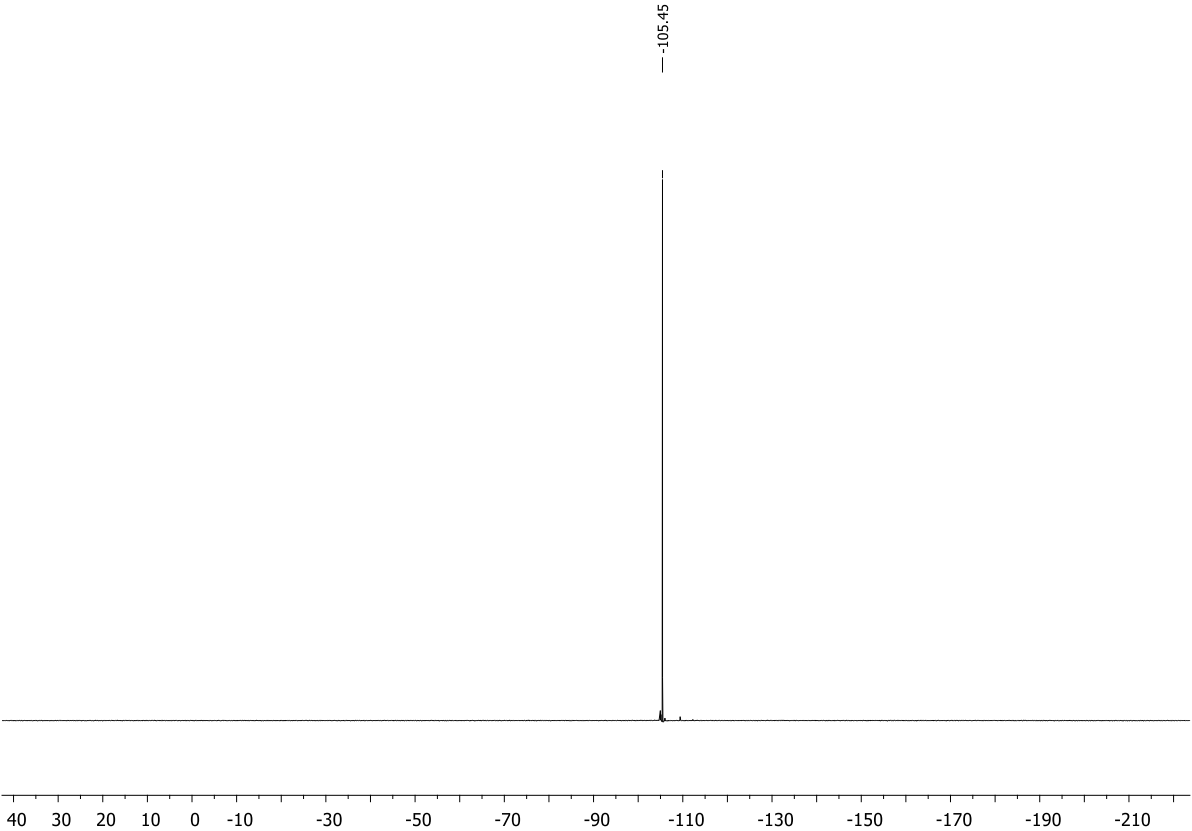


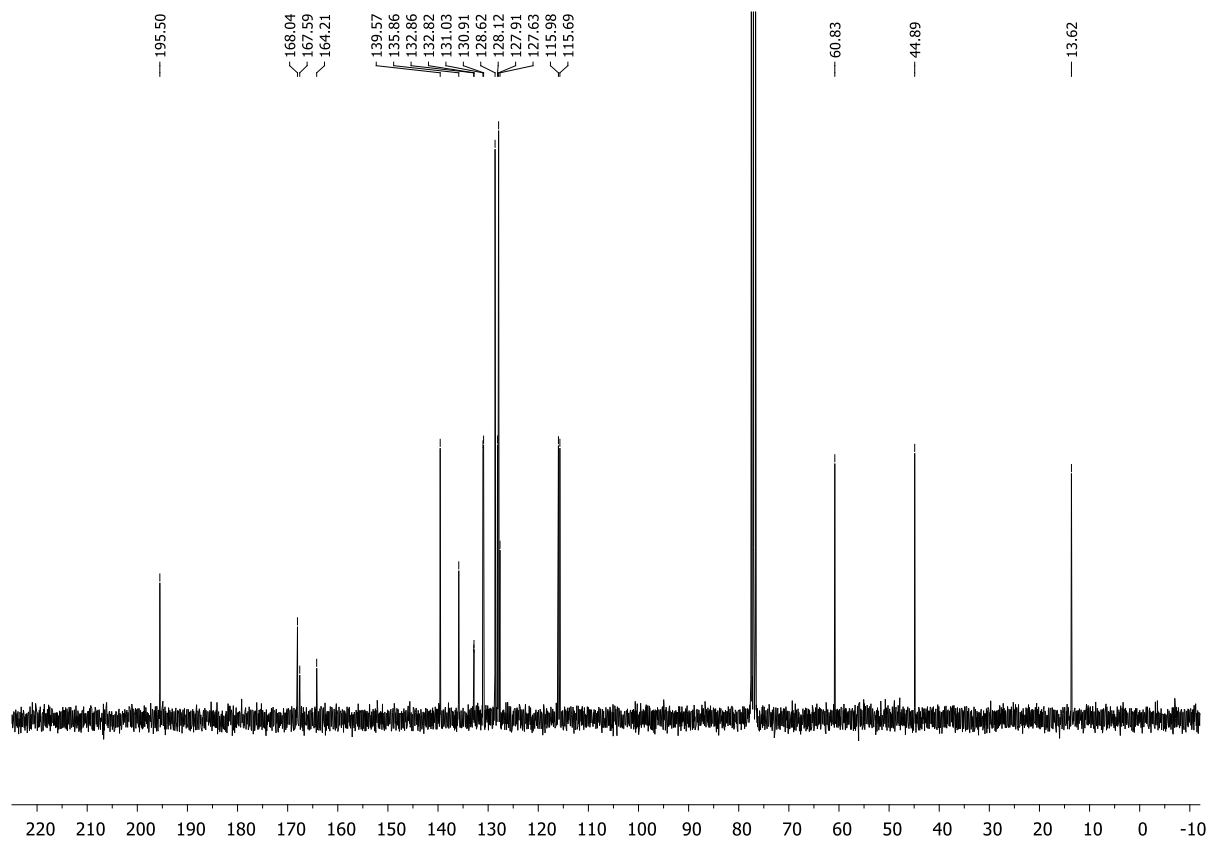
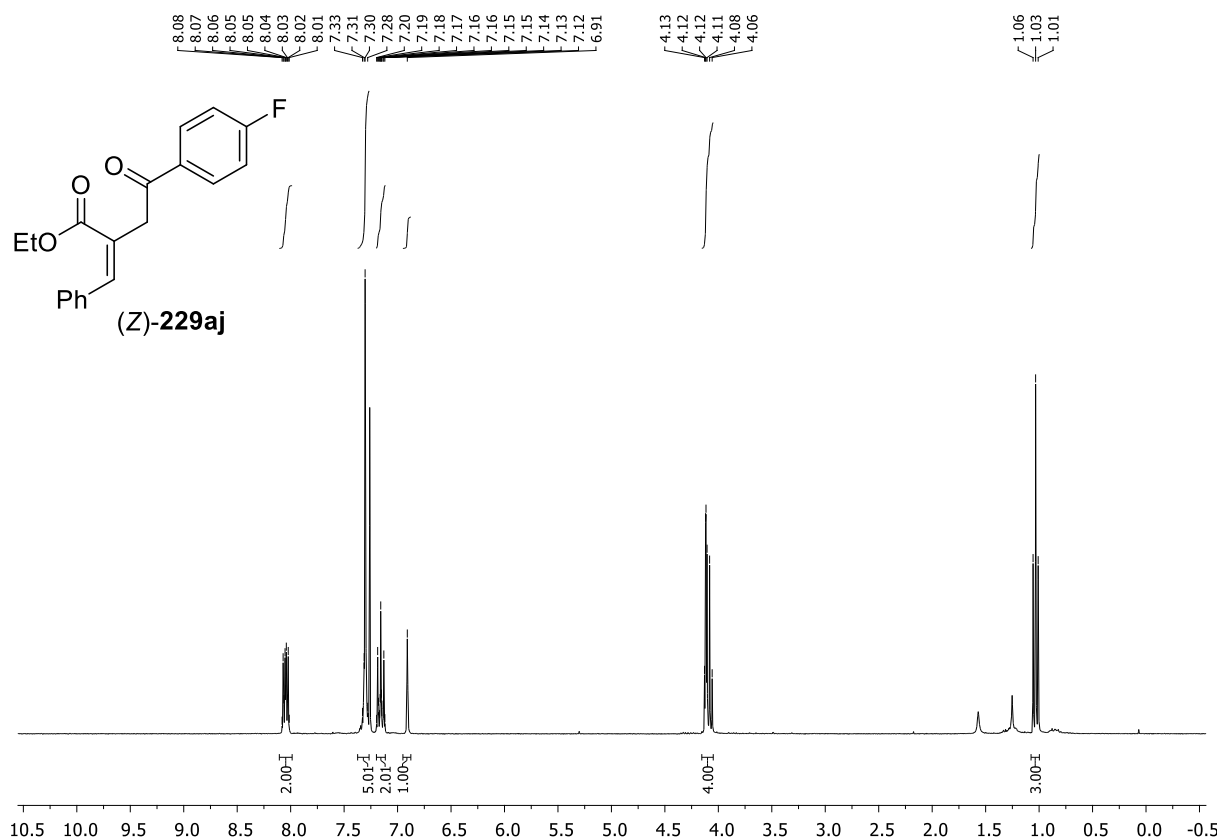


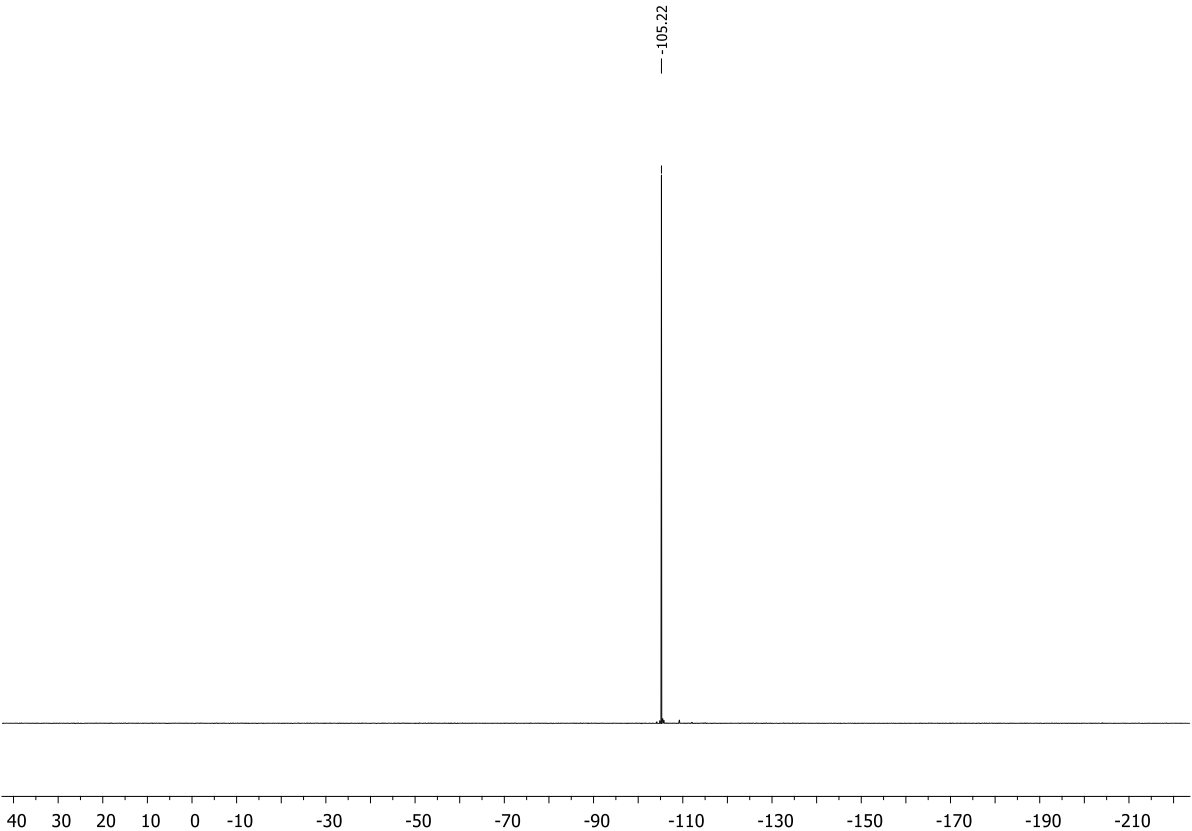


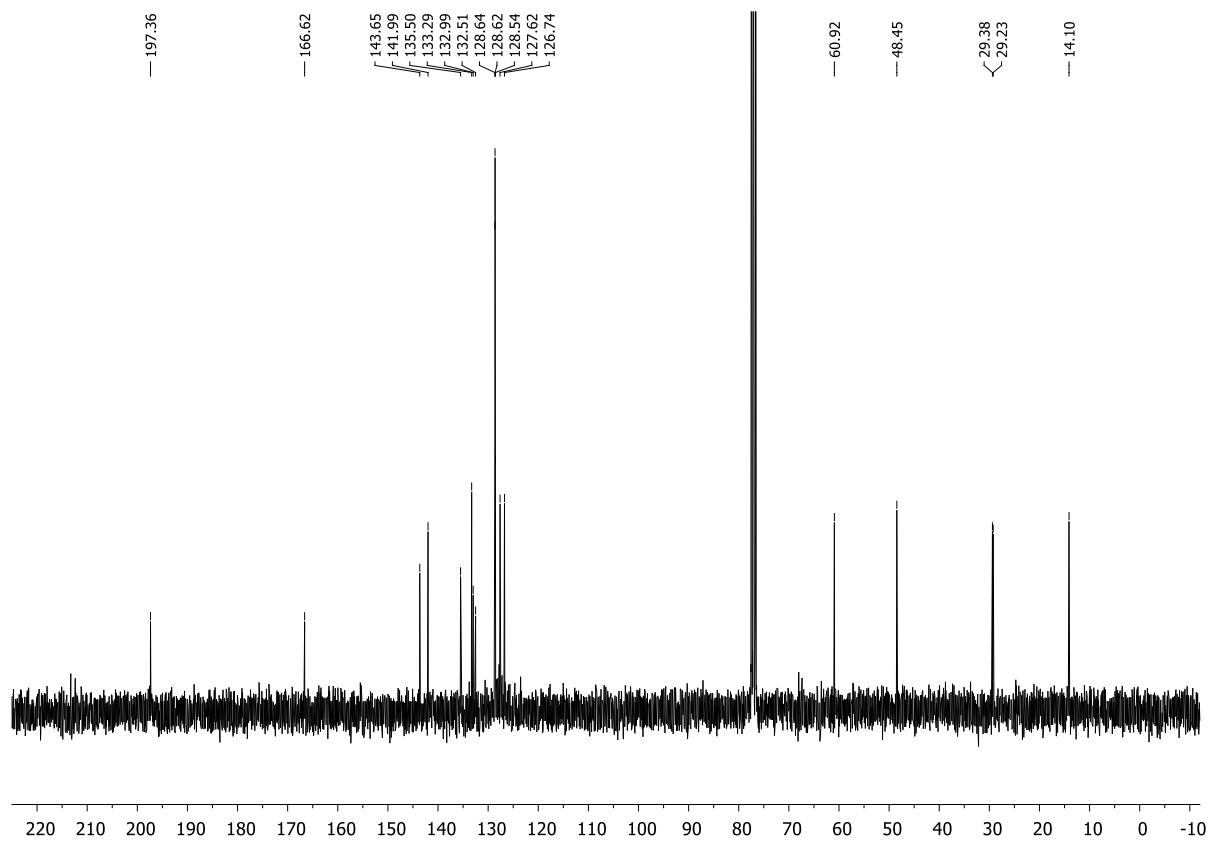
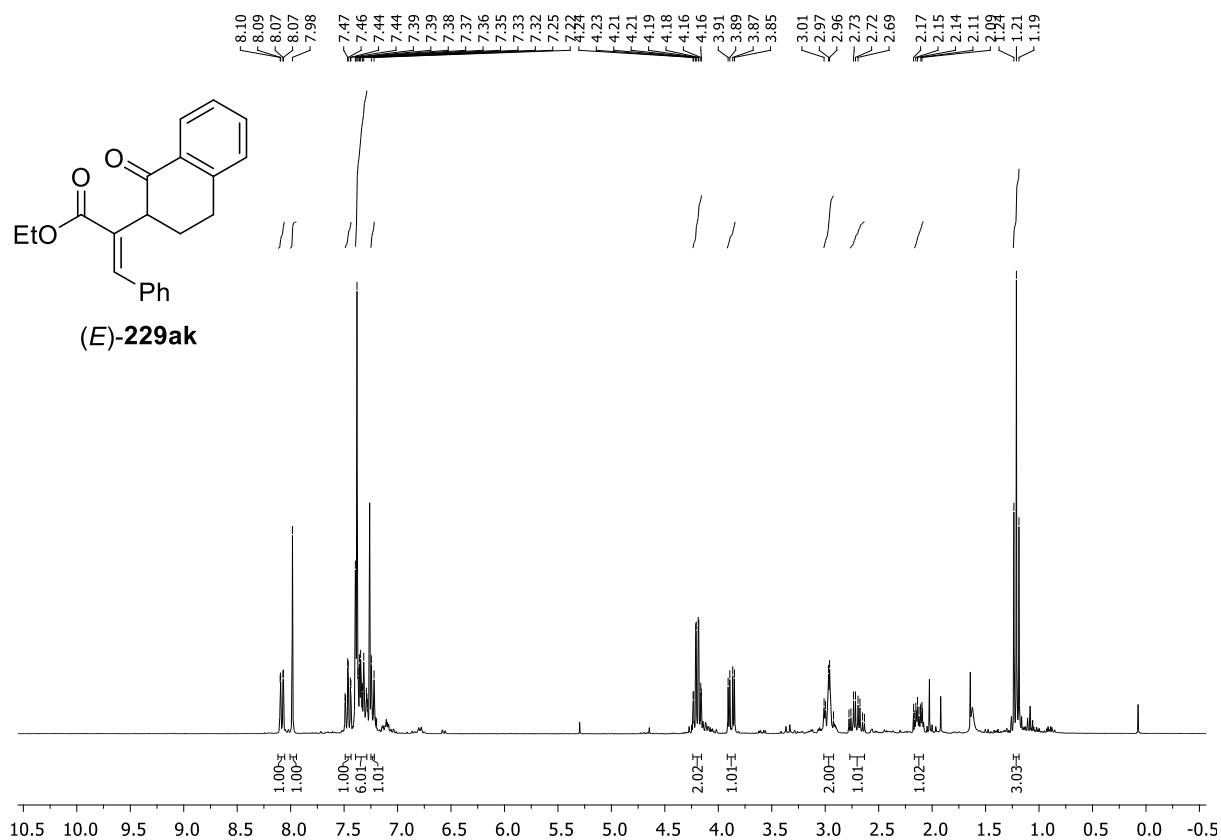


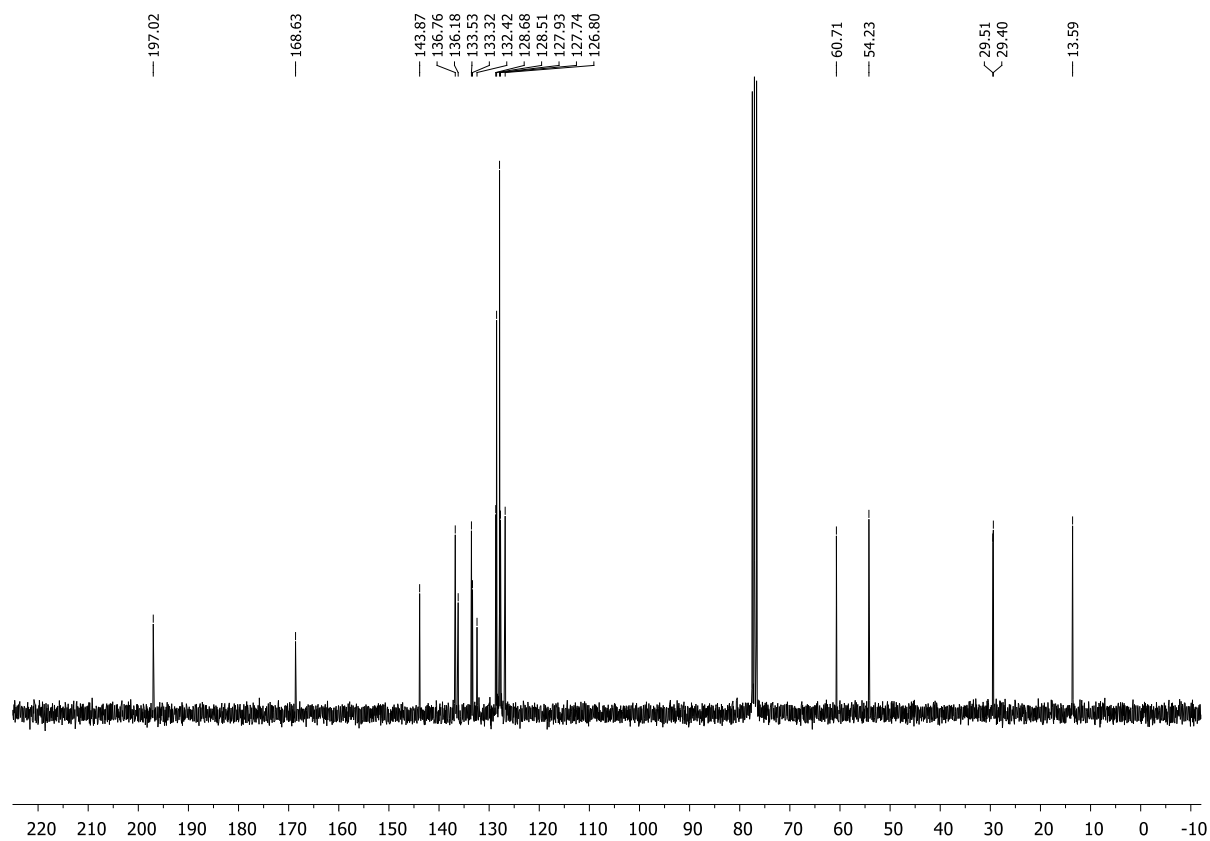
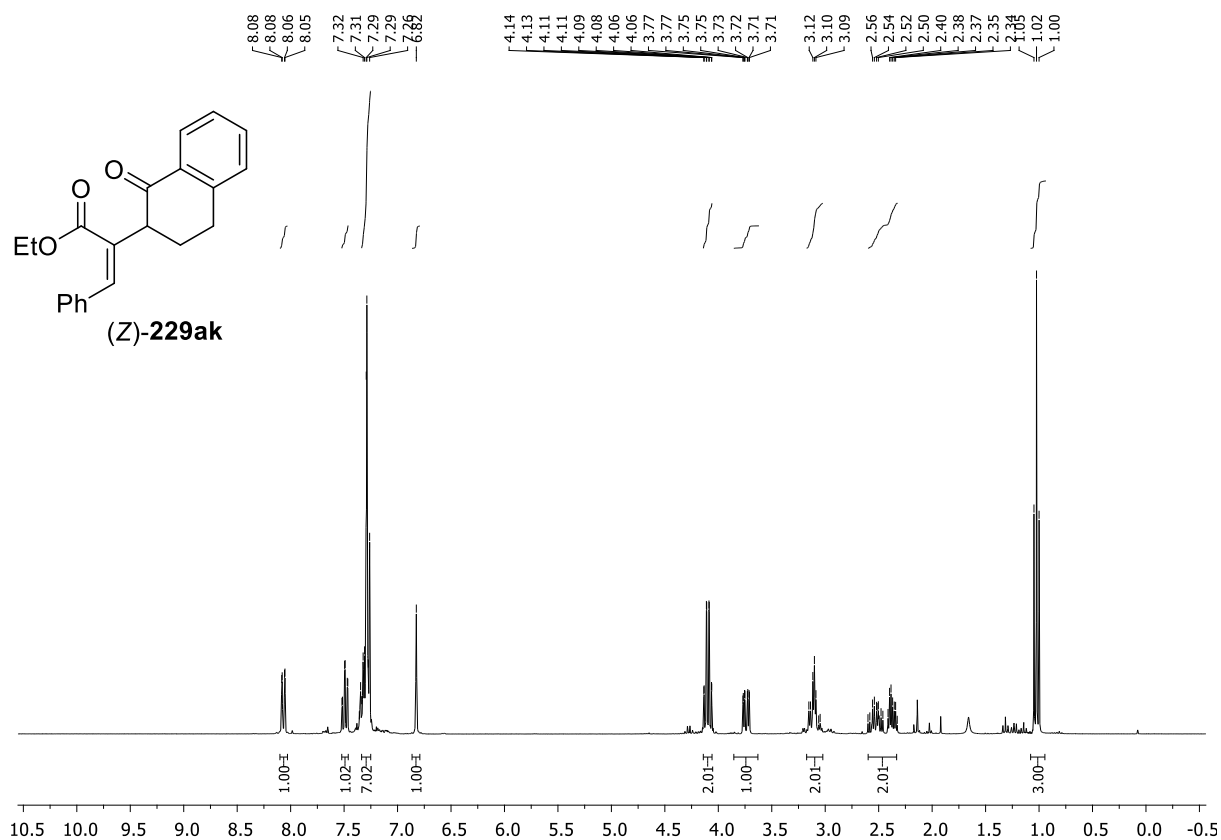


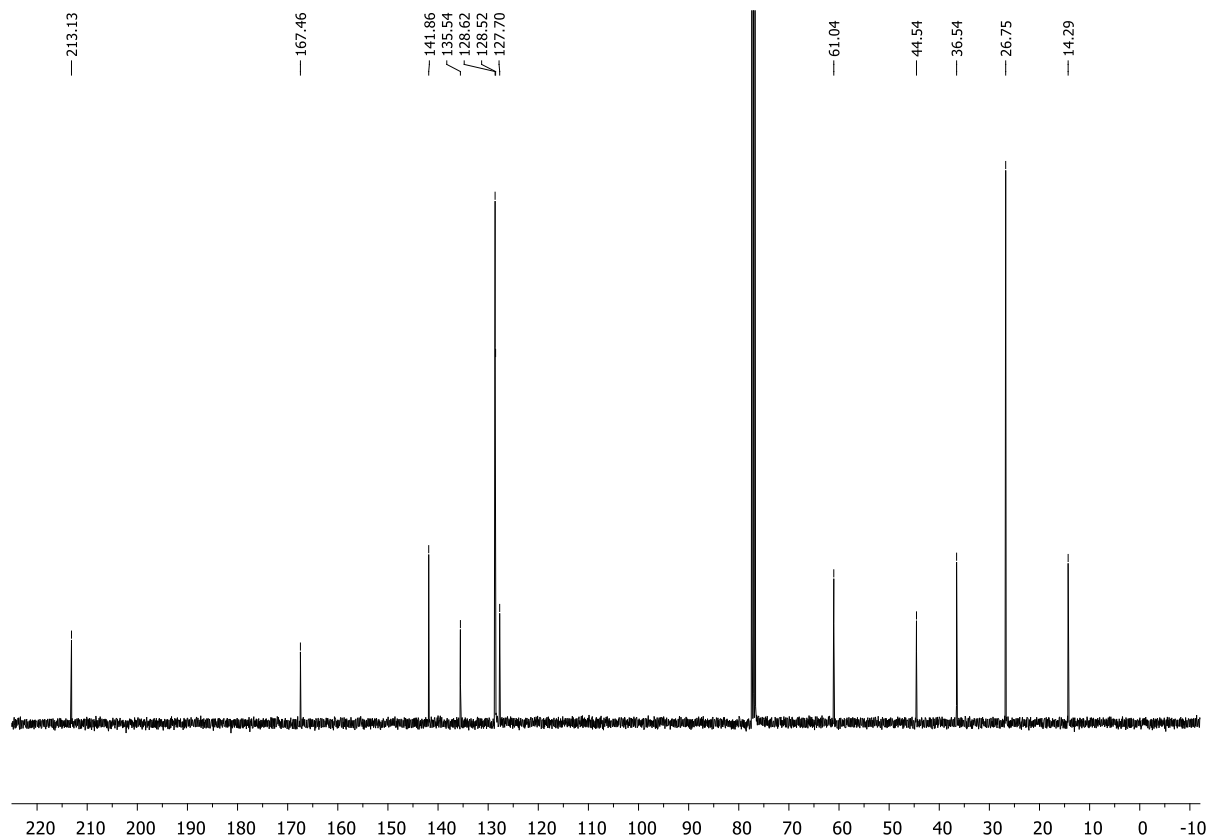
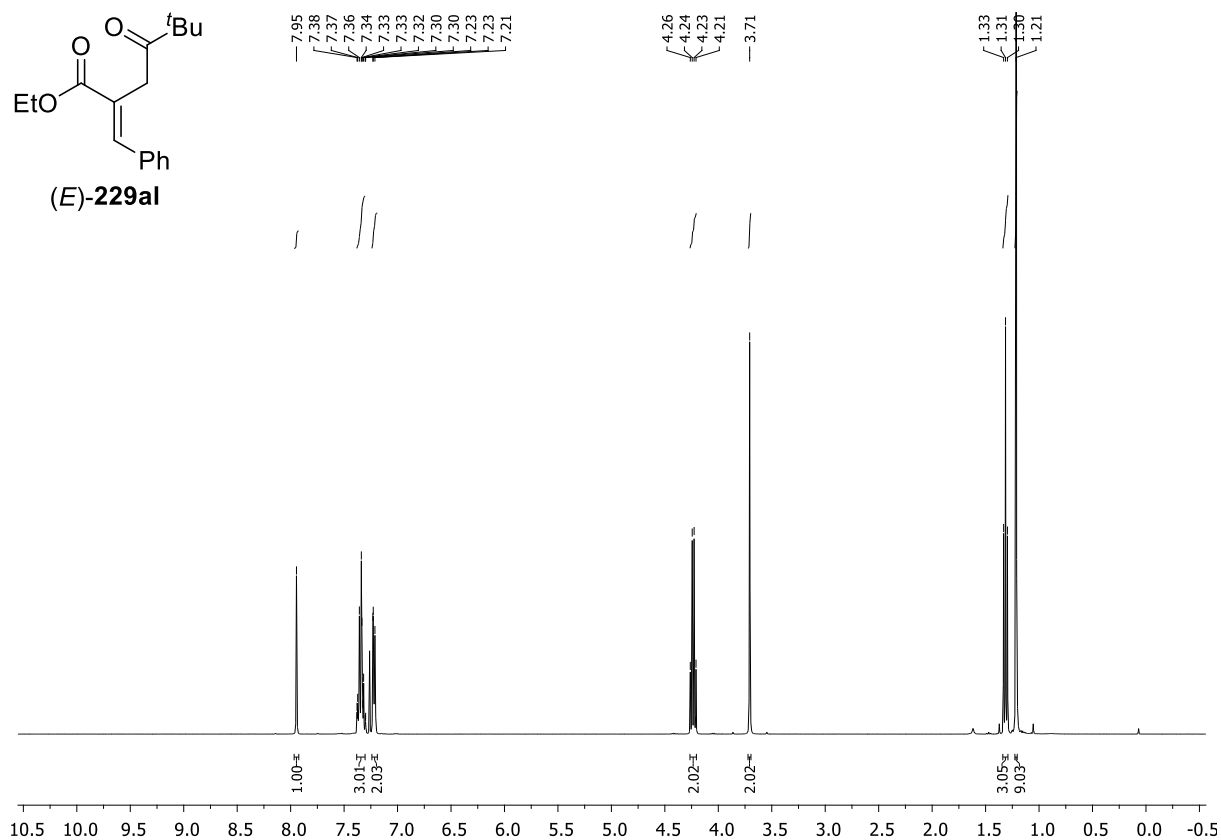
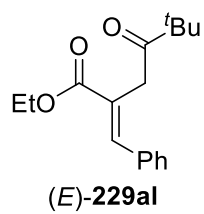


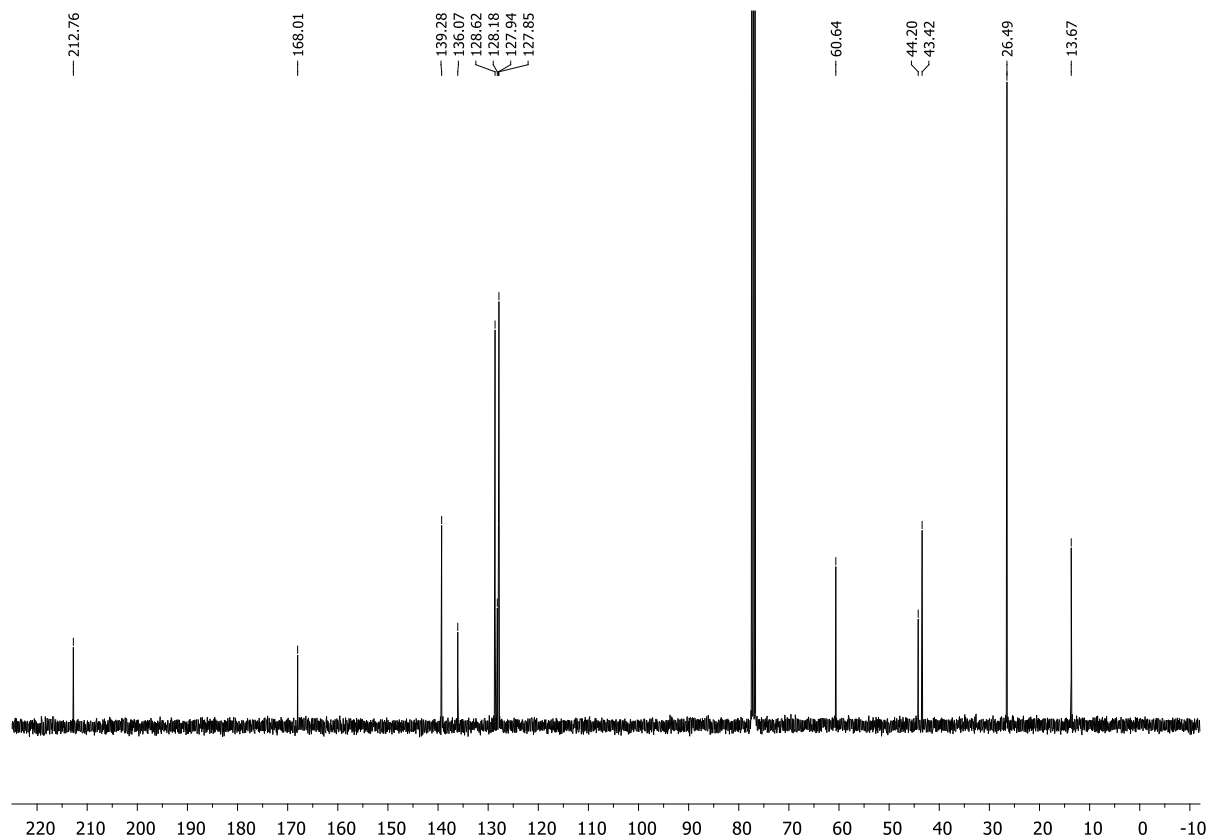
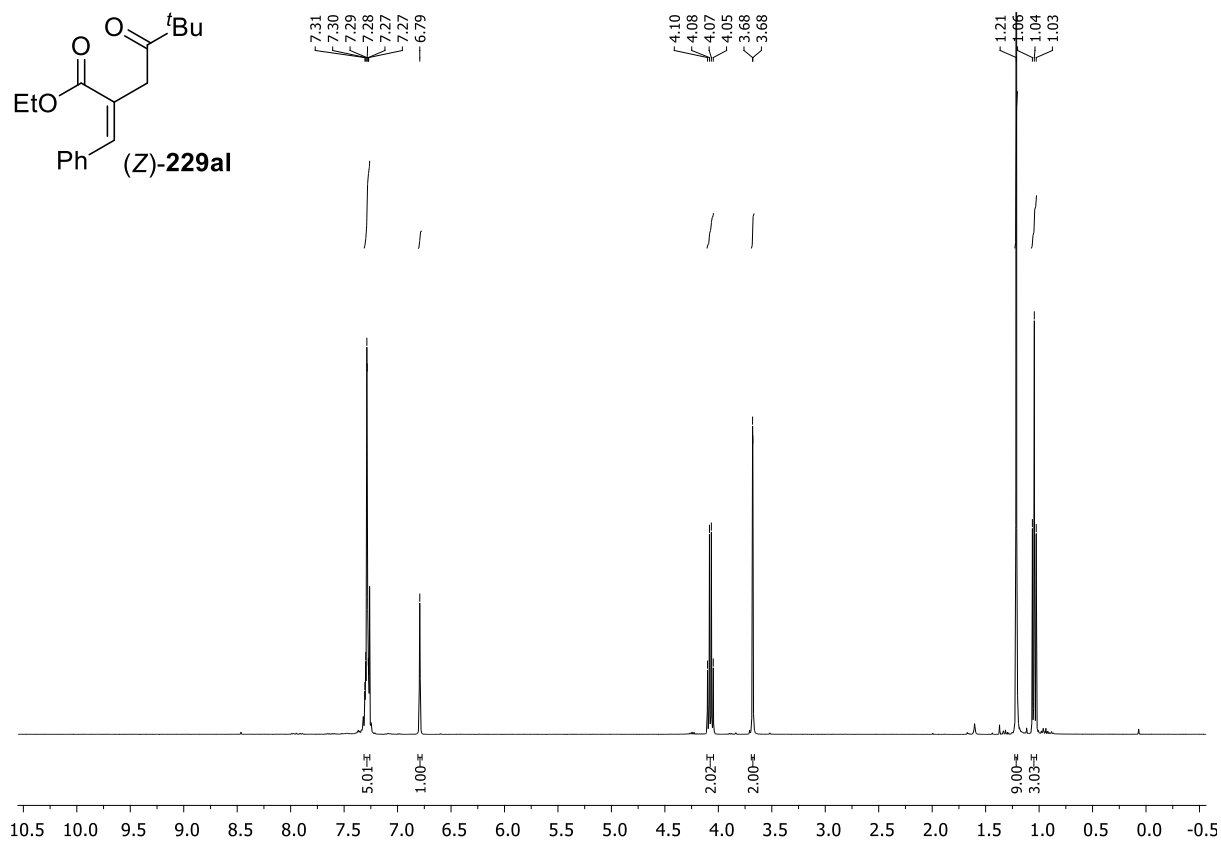




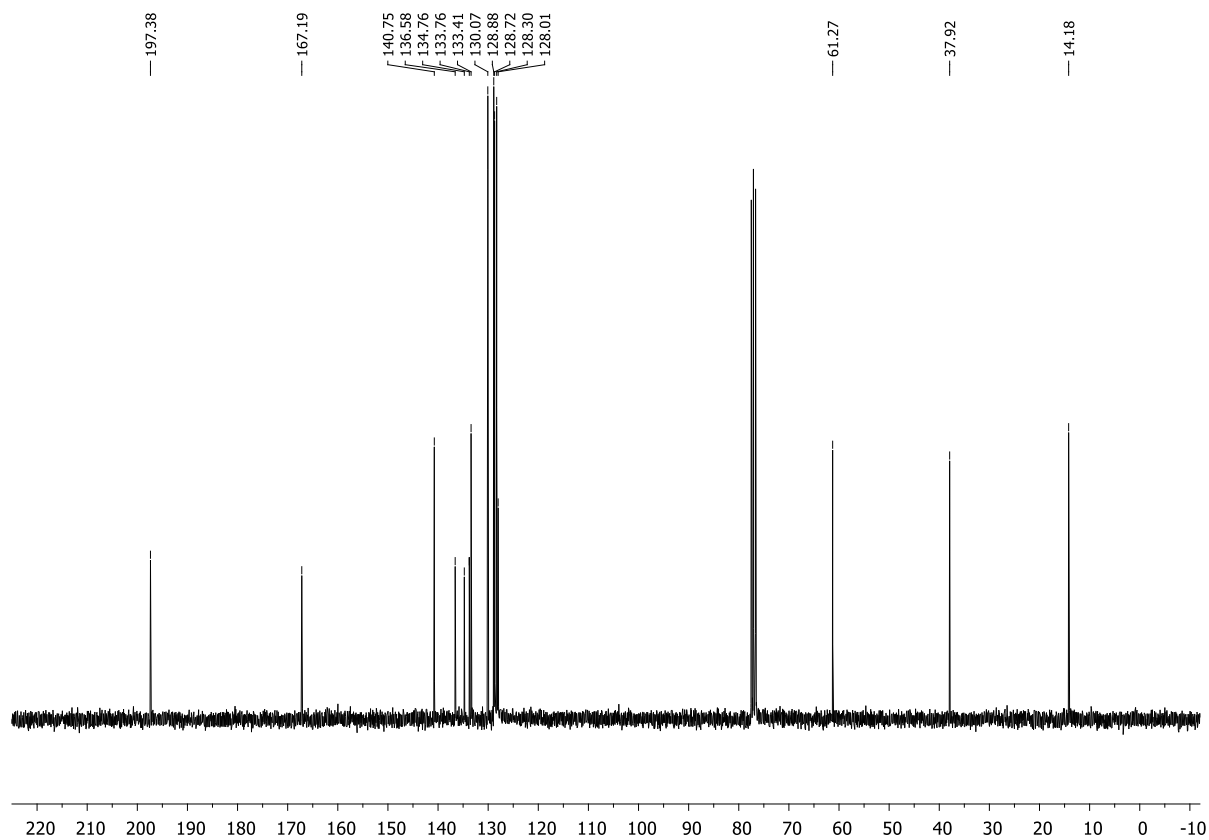
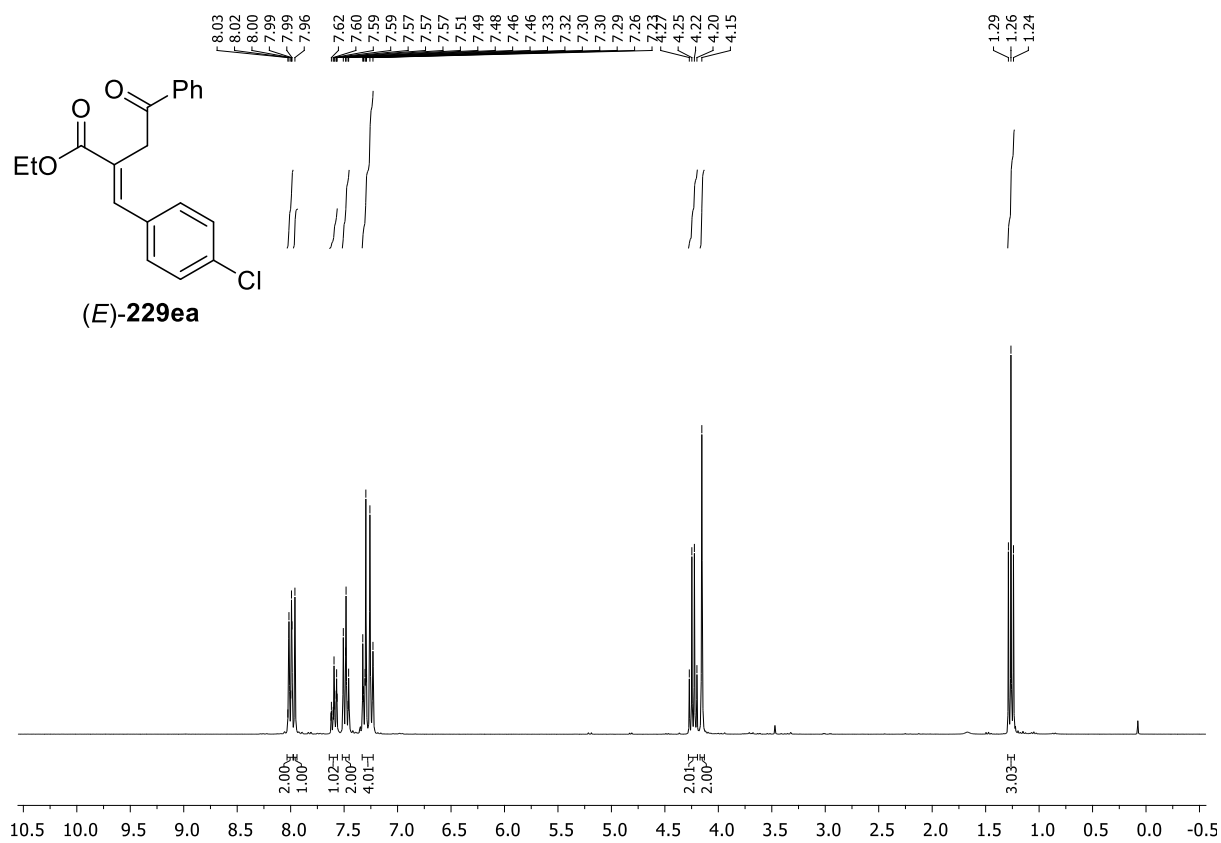


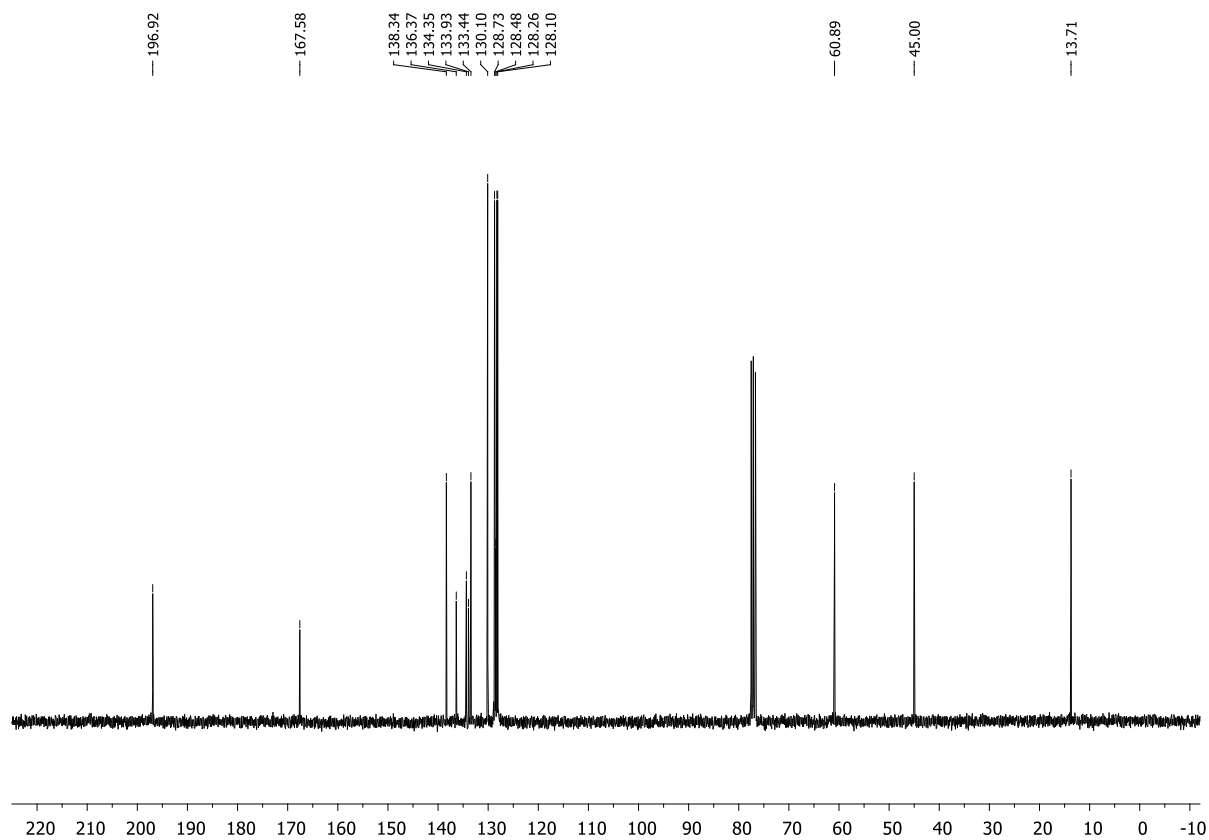
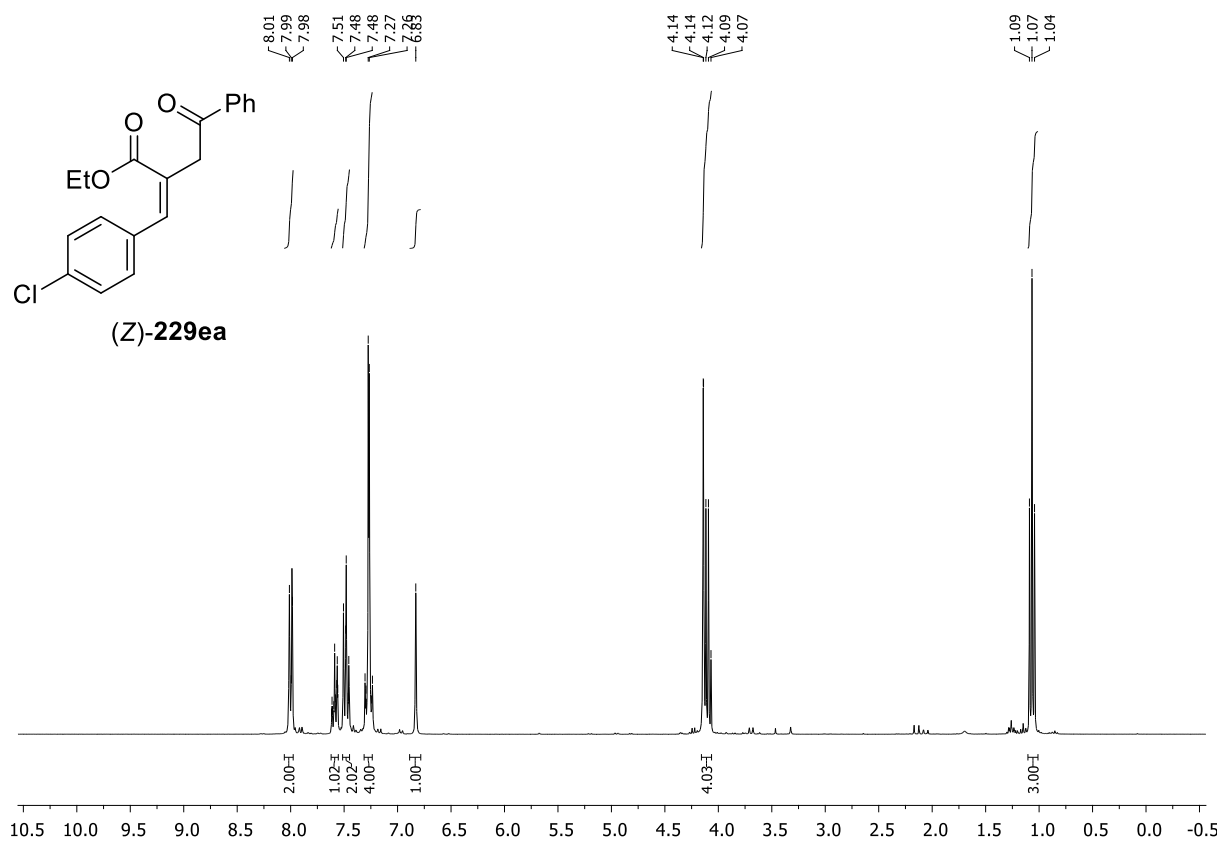


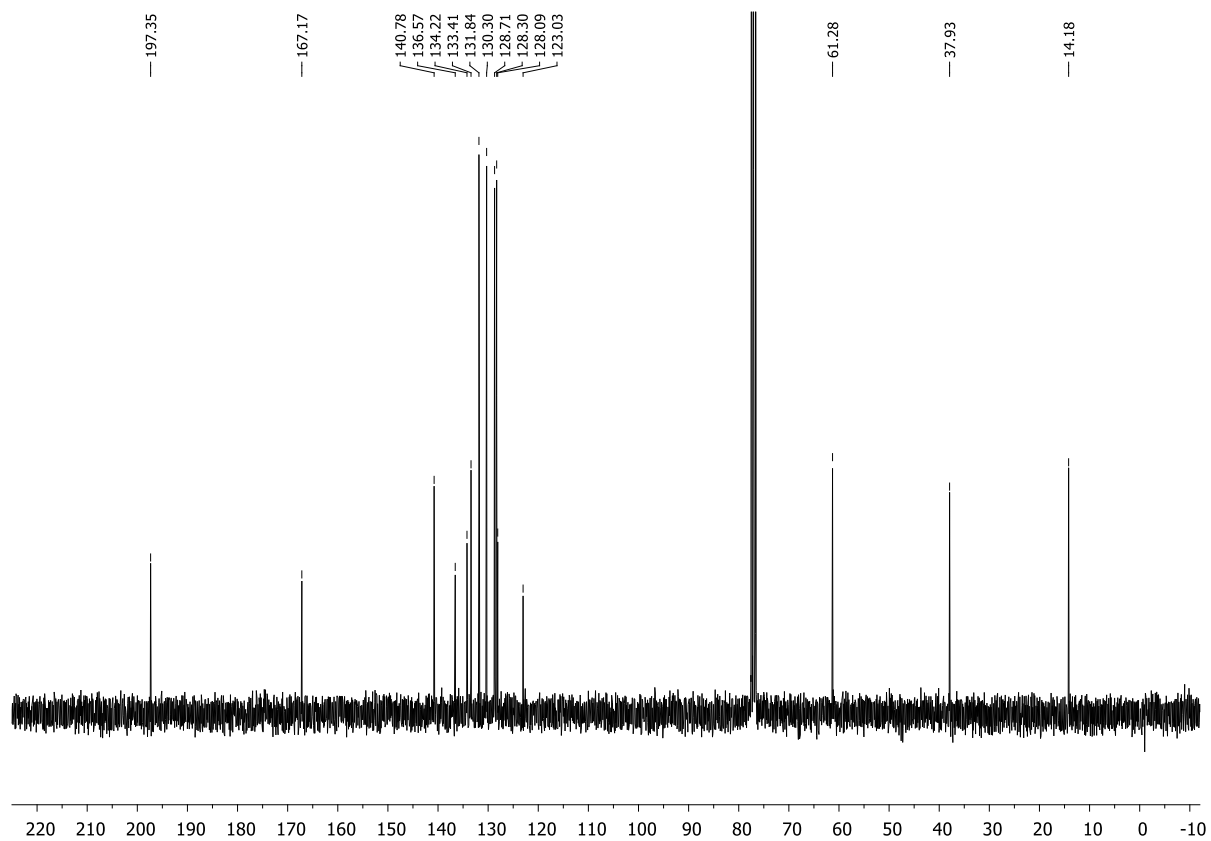
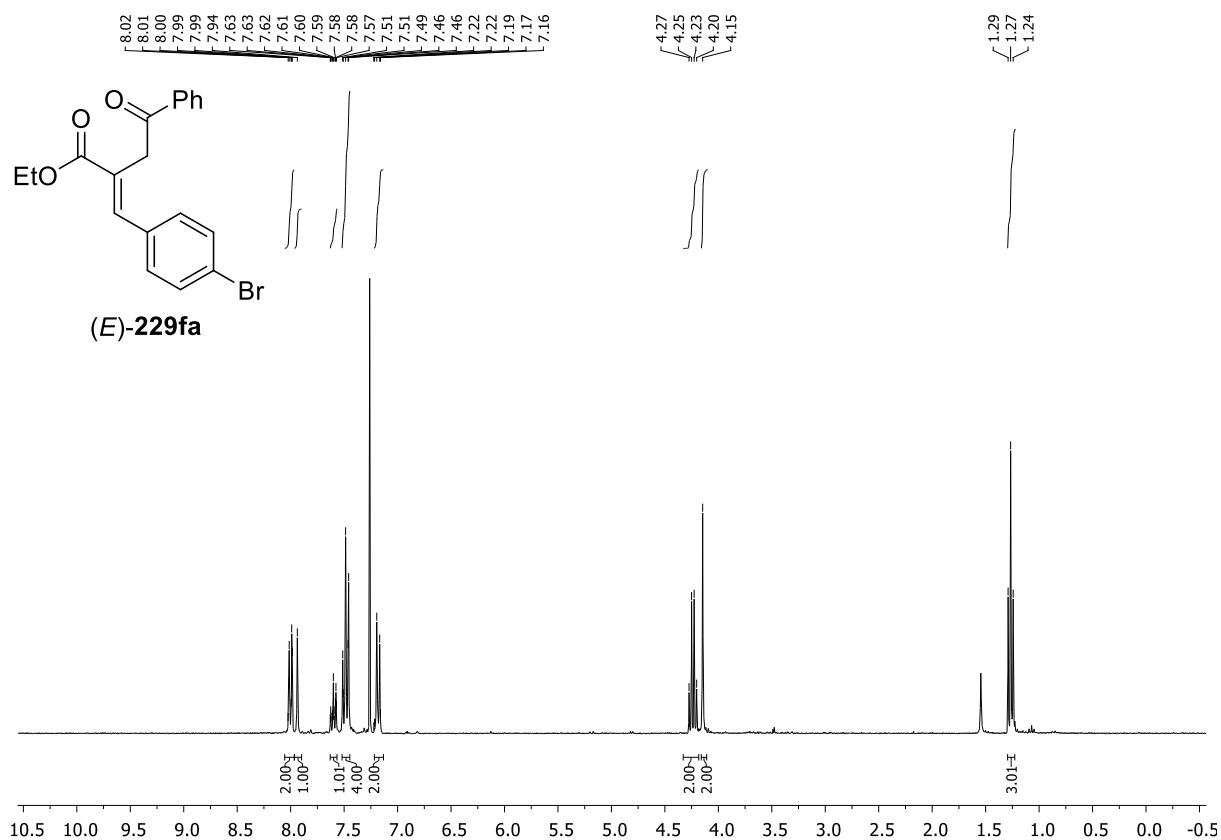


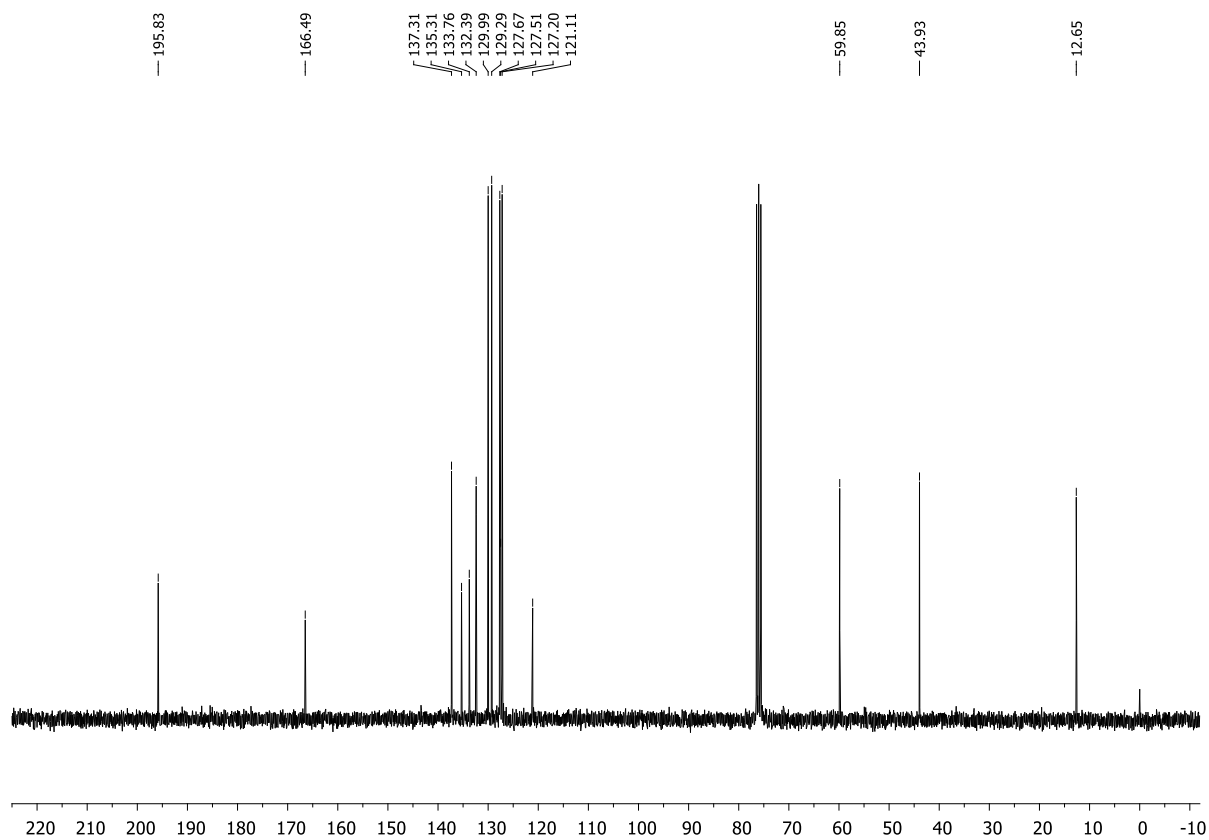
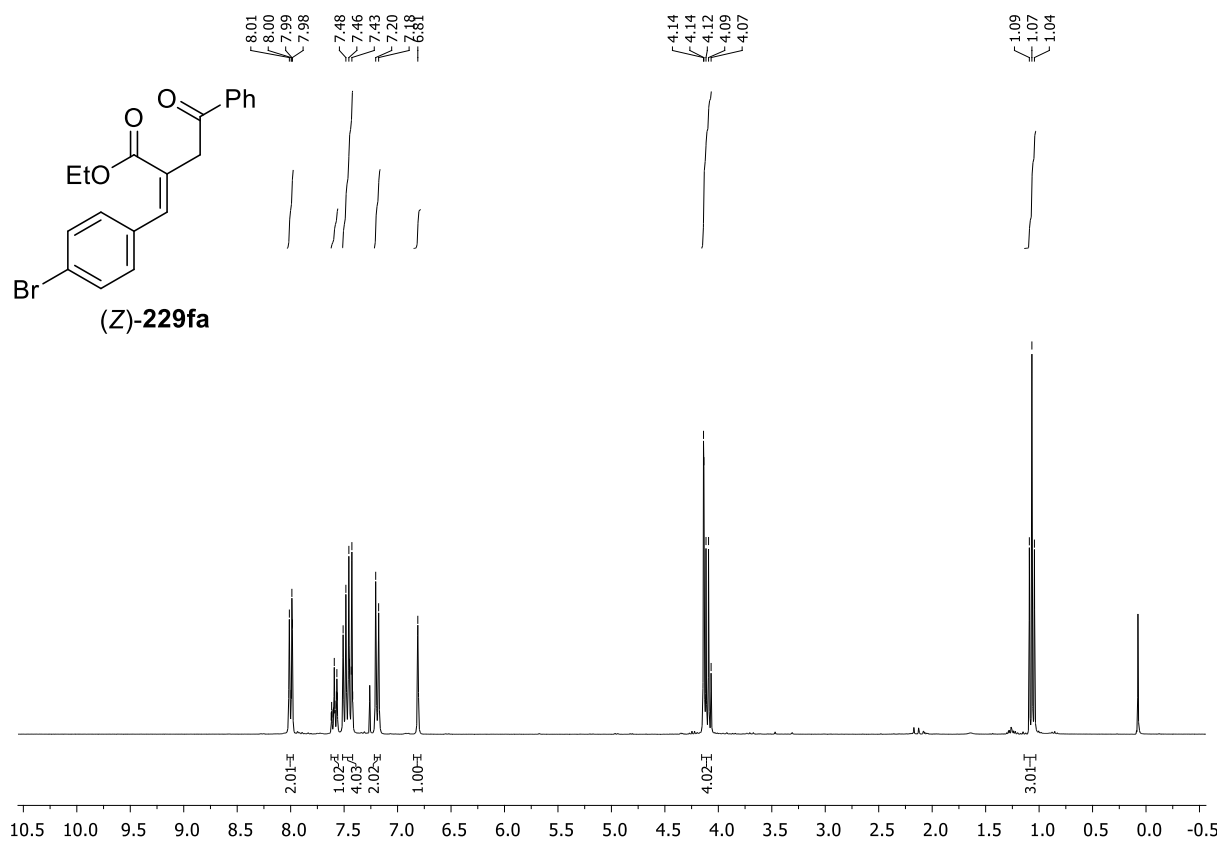


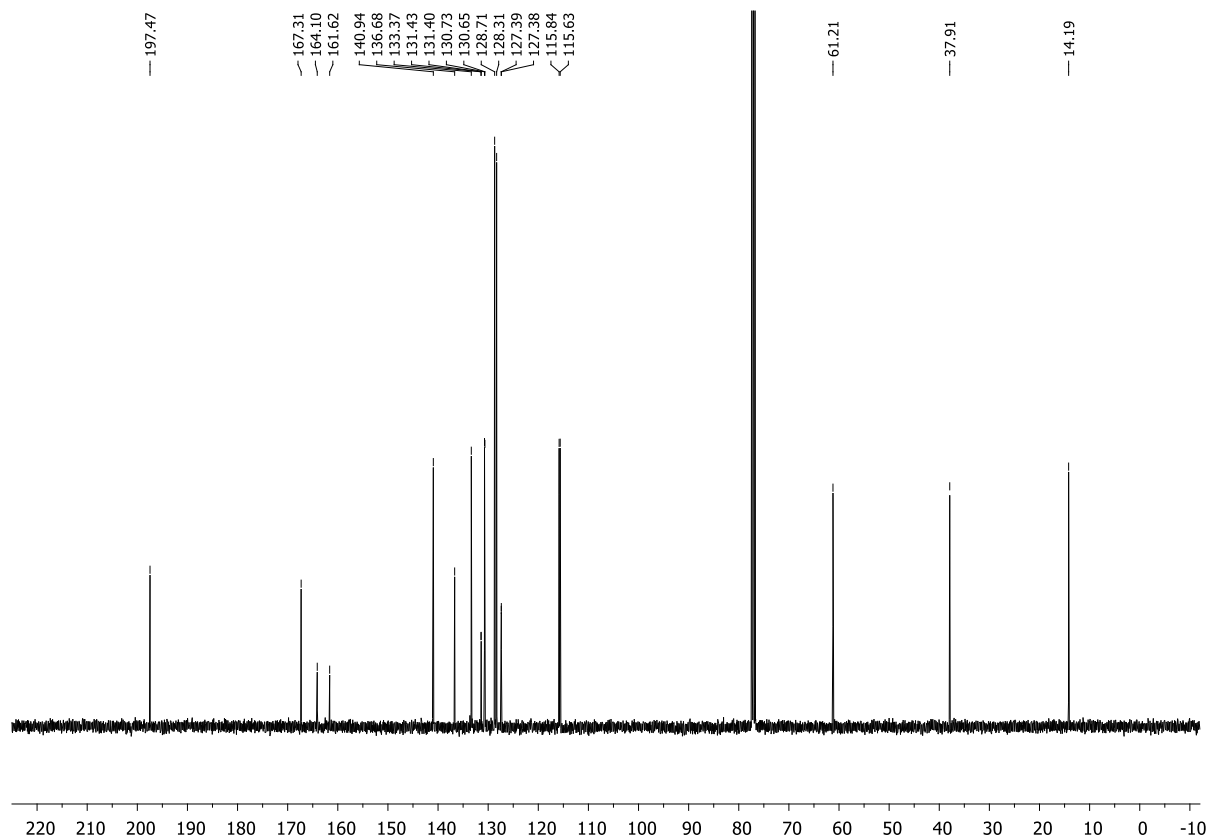
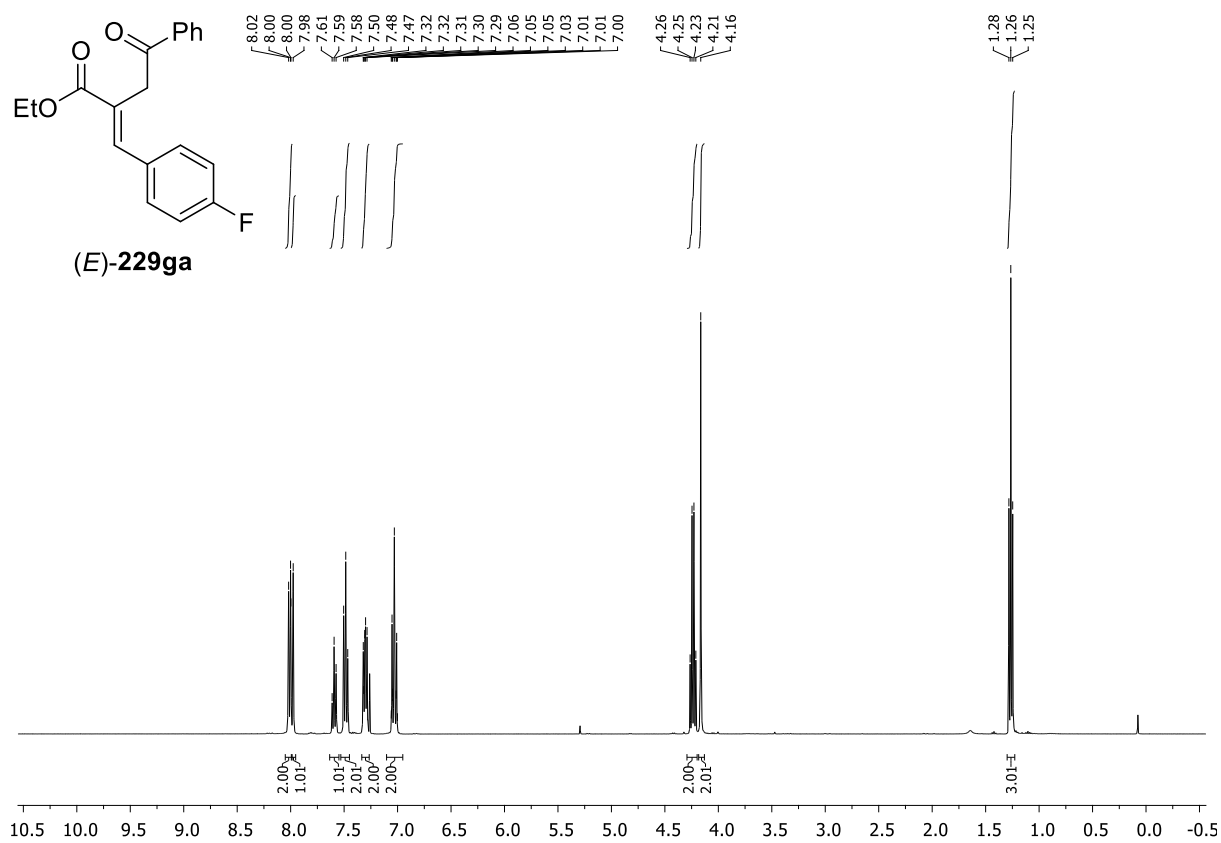


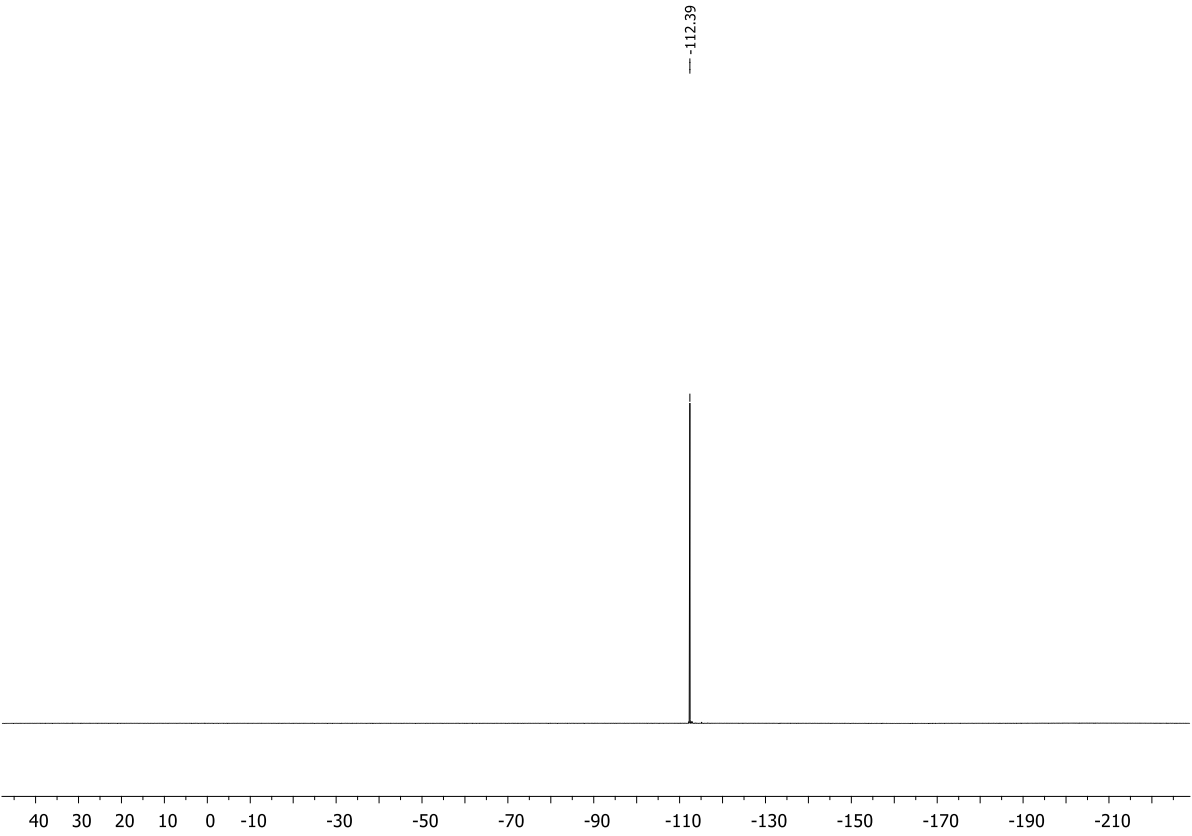




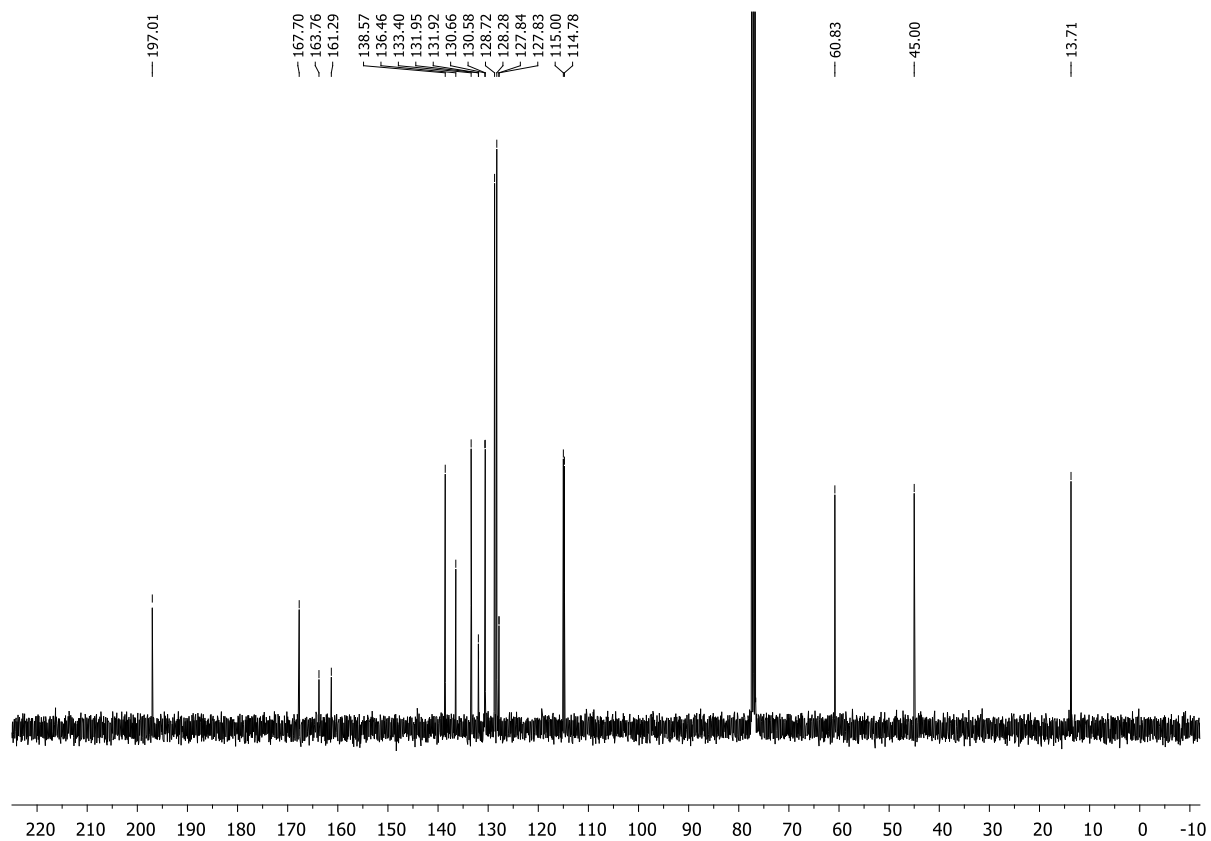
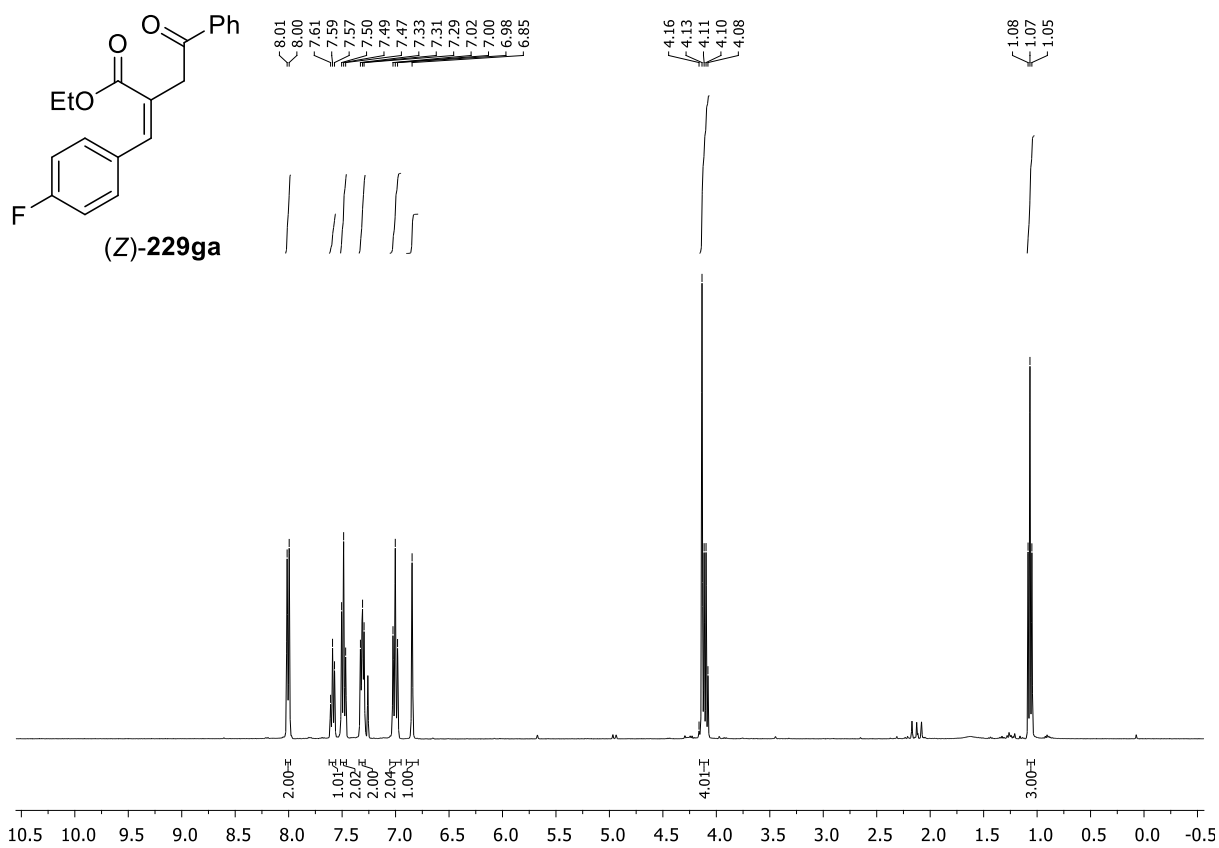


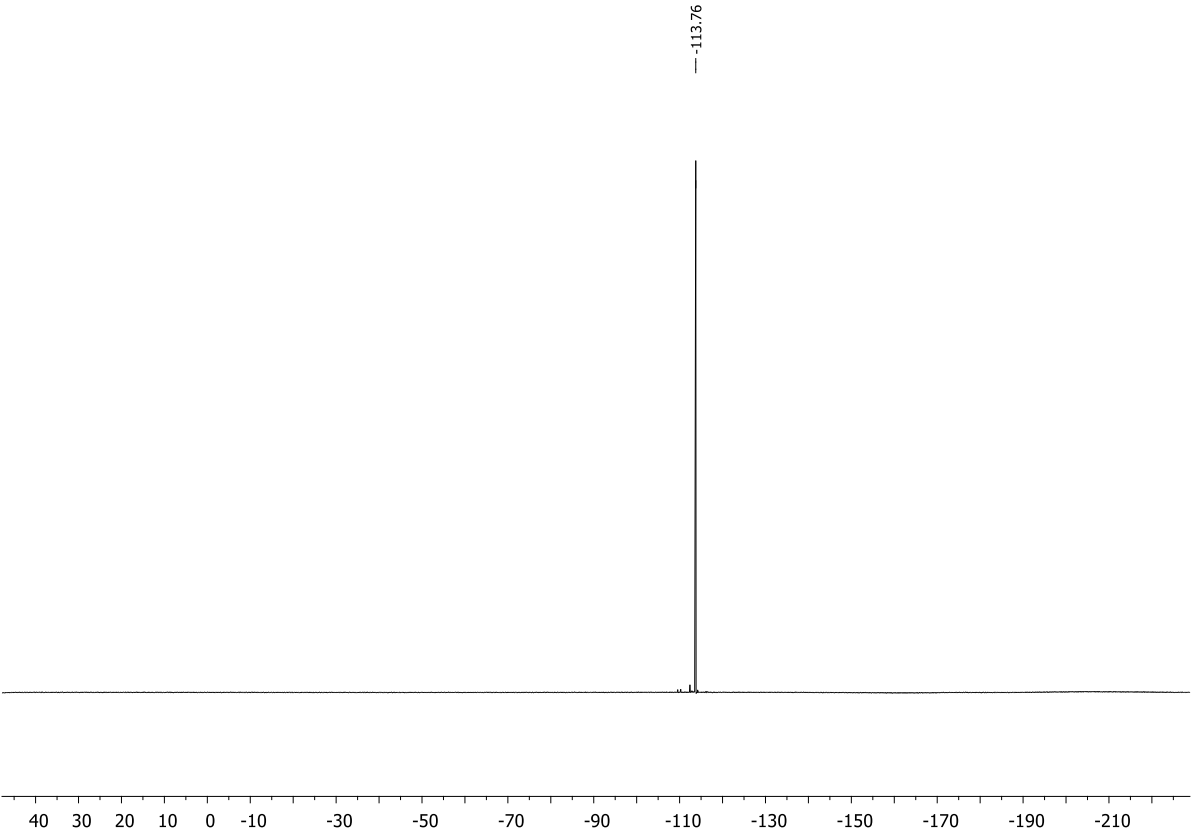




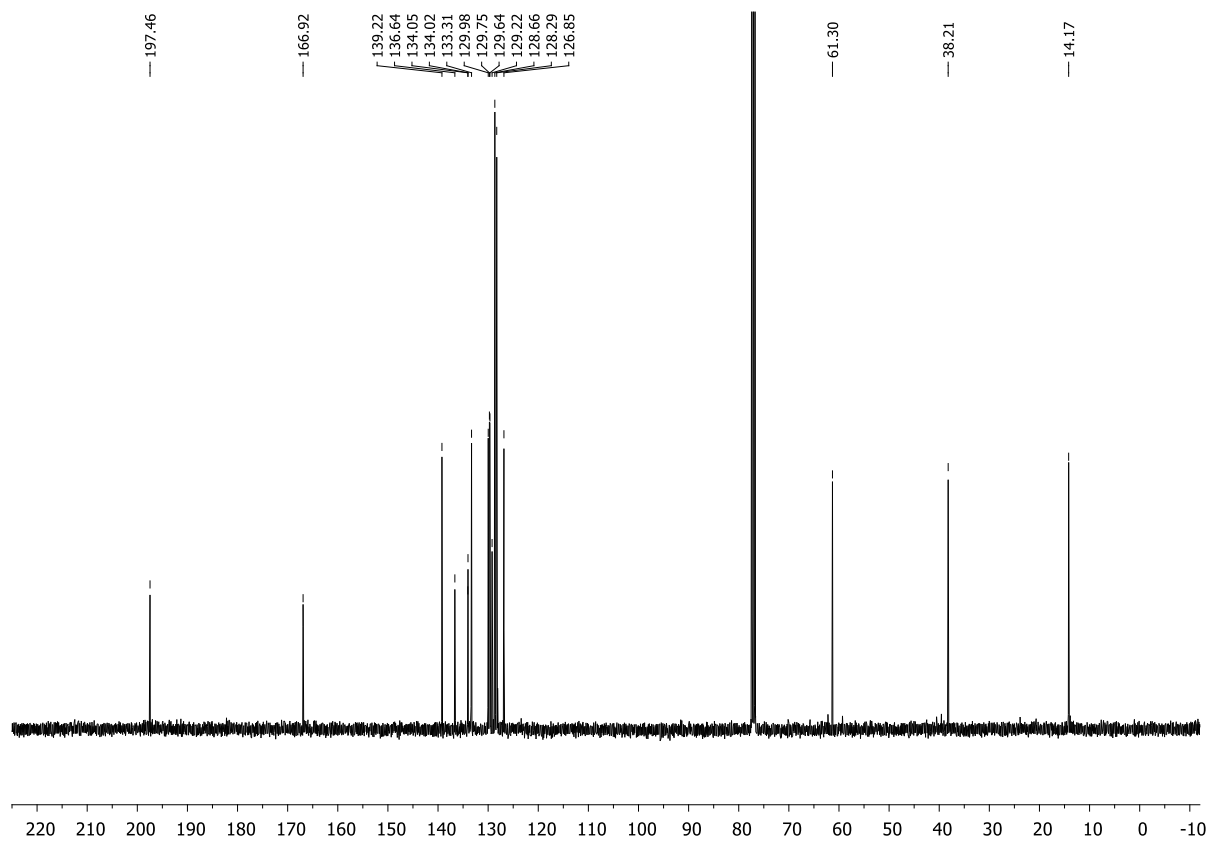
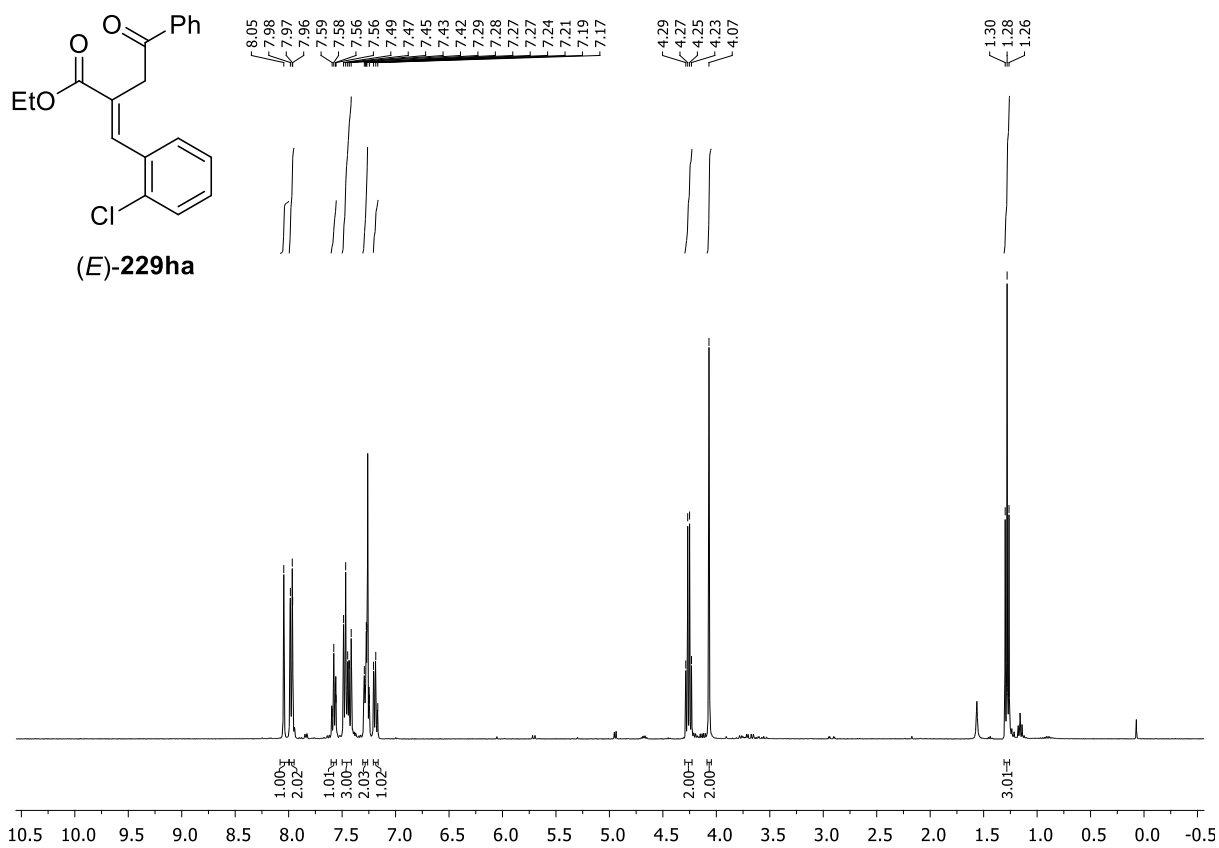


Appendix

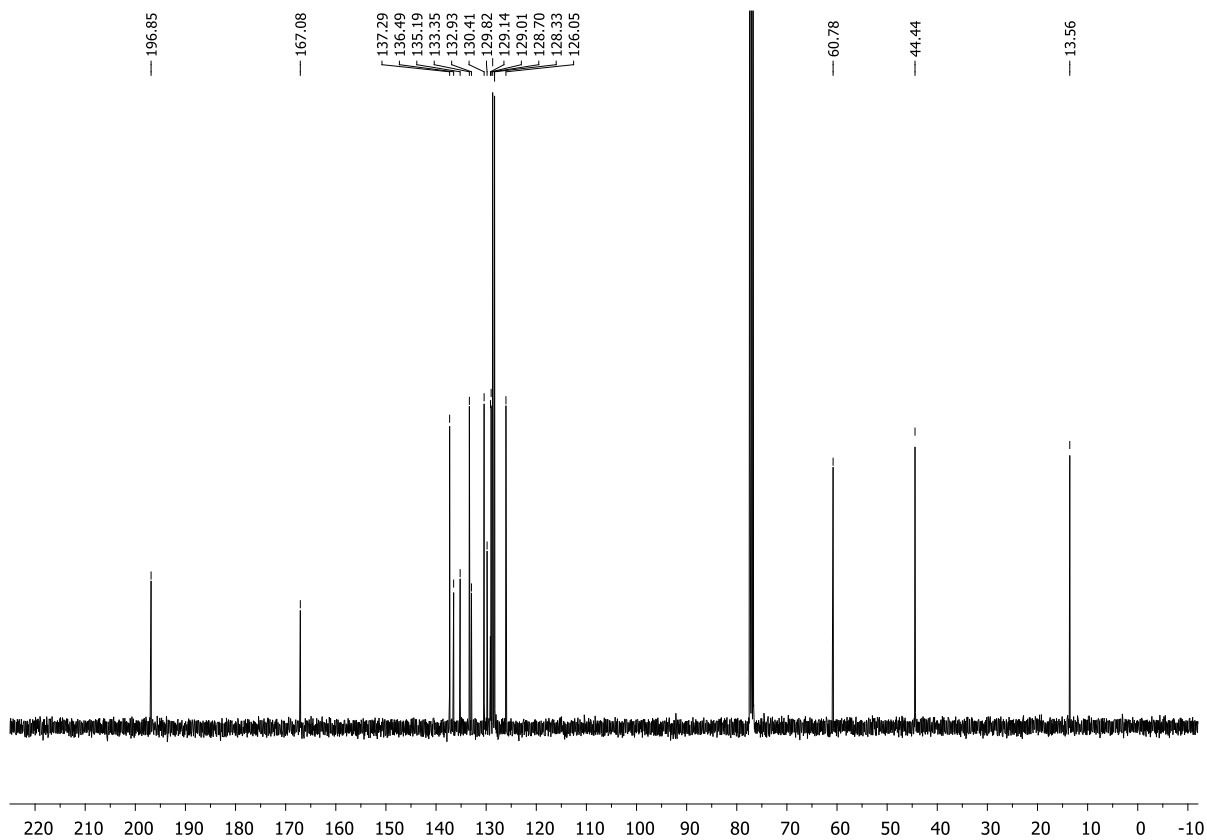
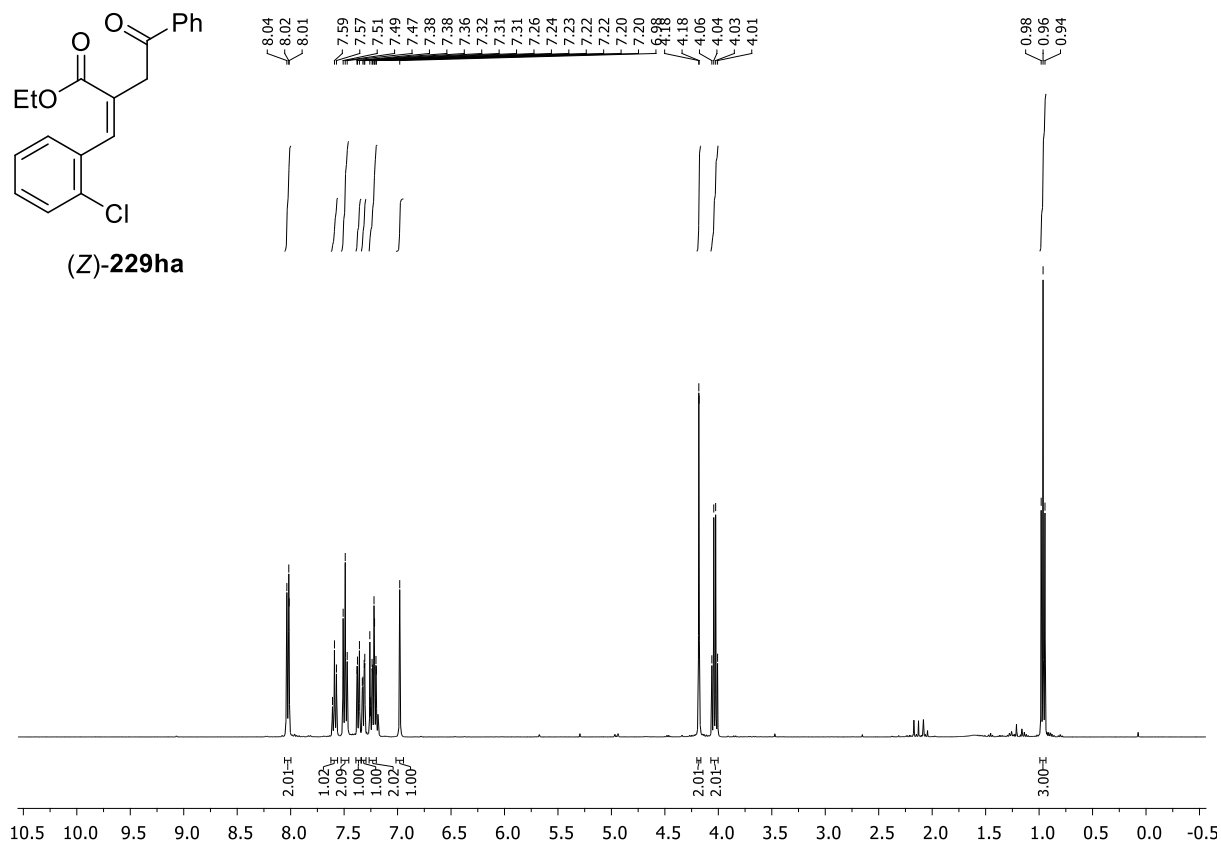
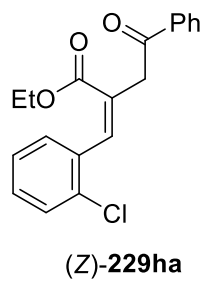


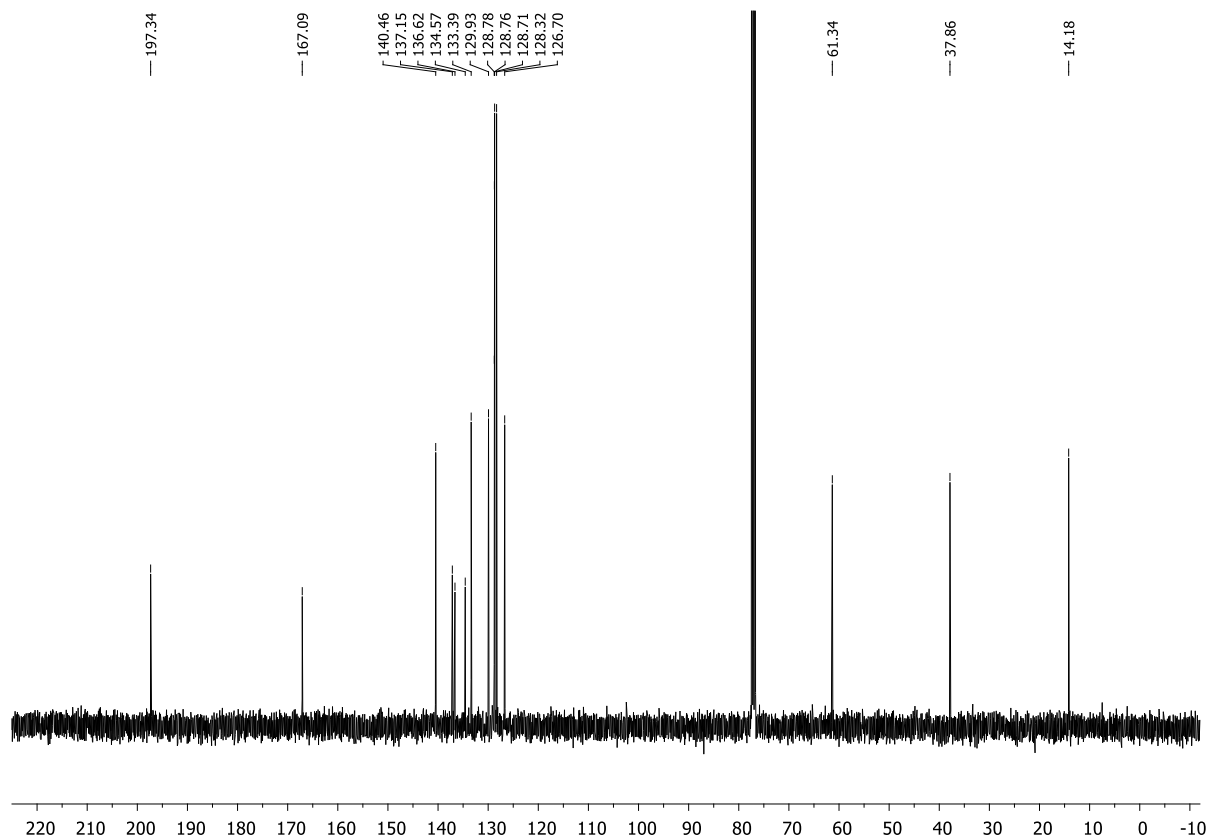
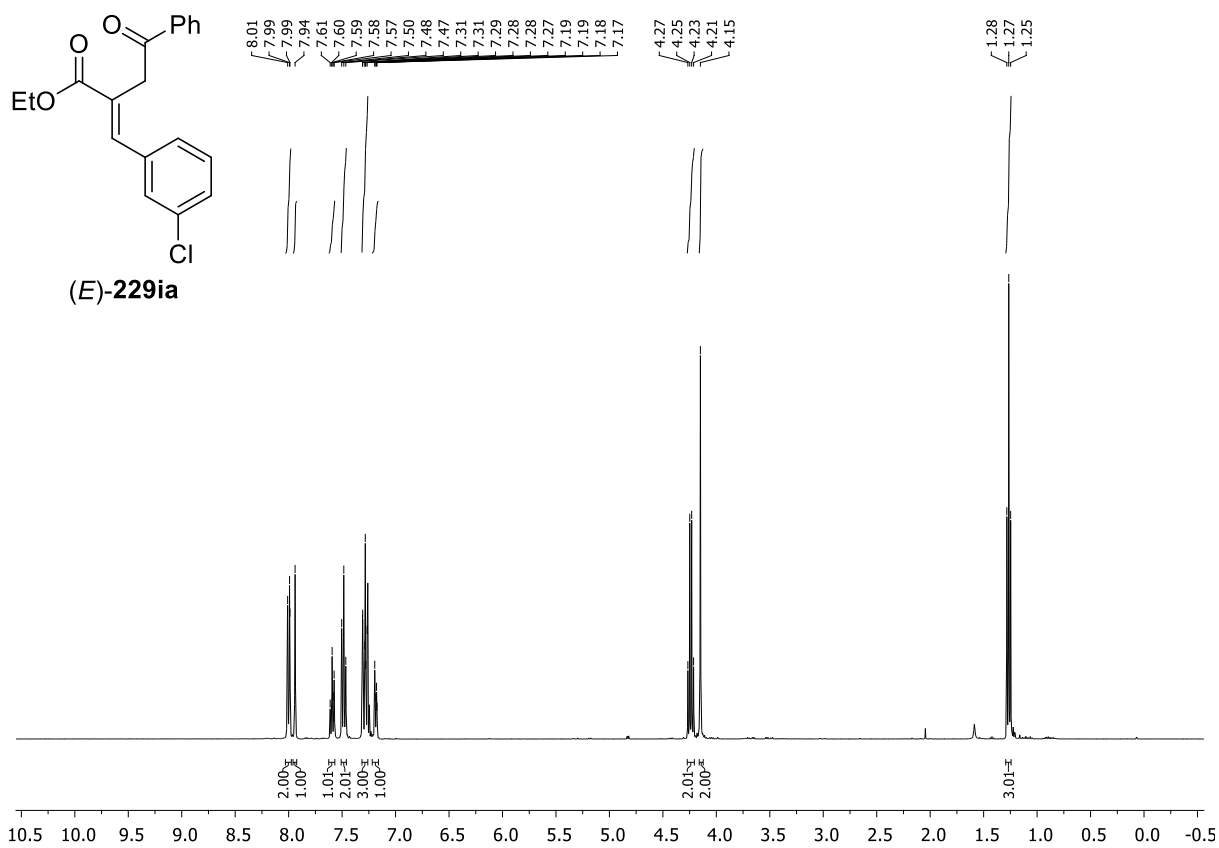


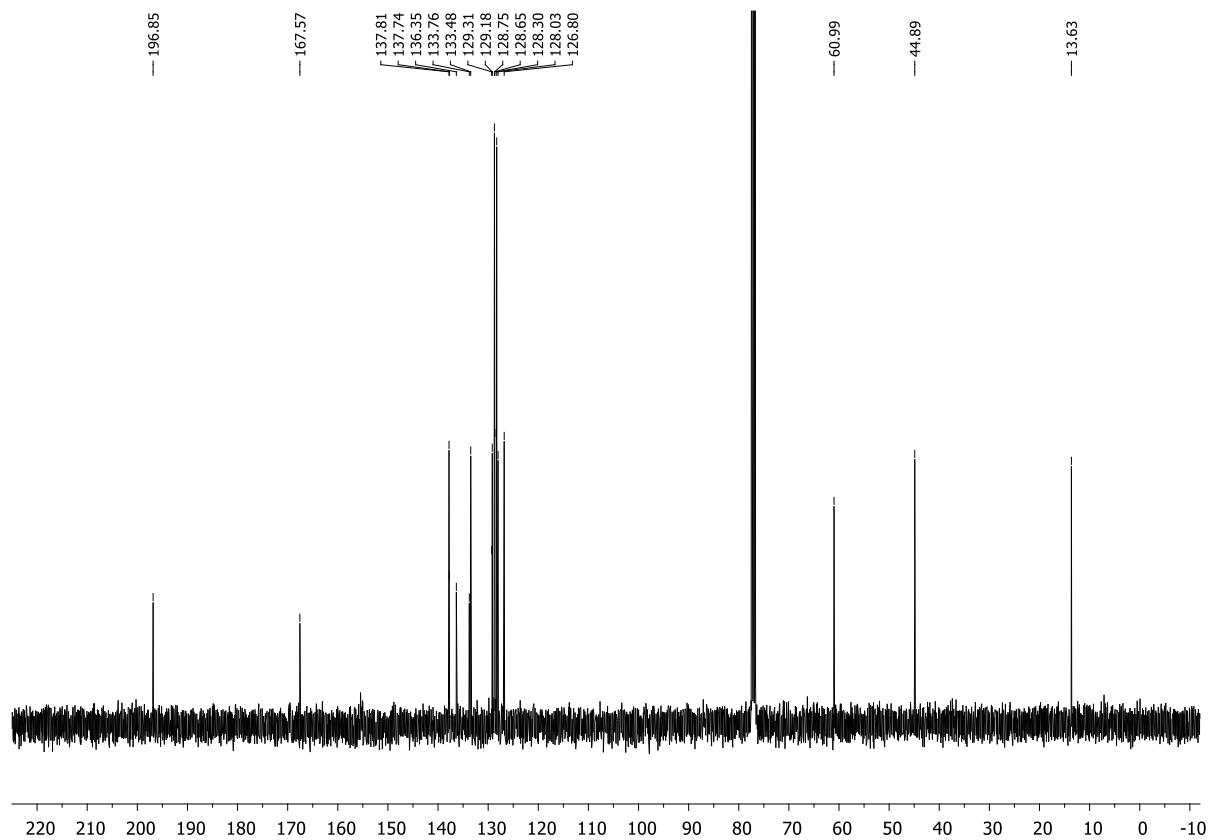
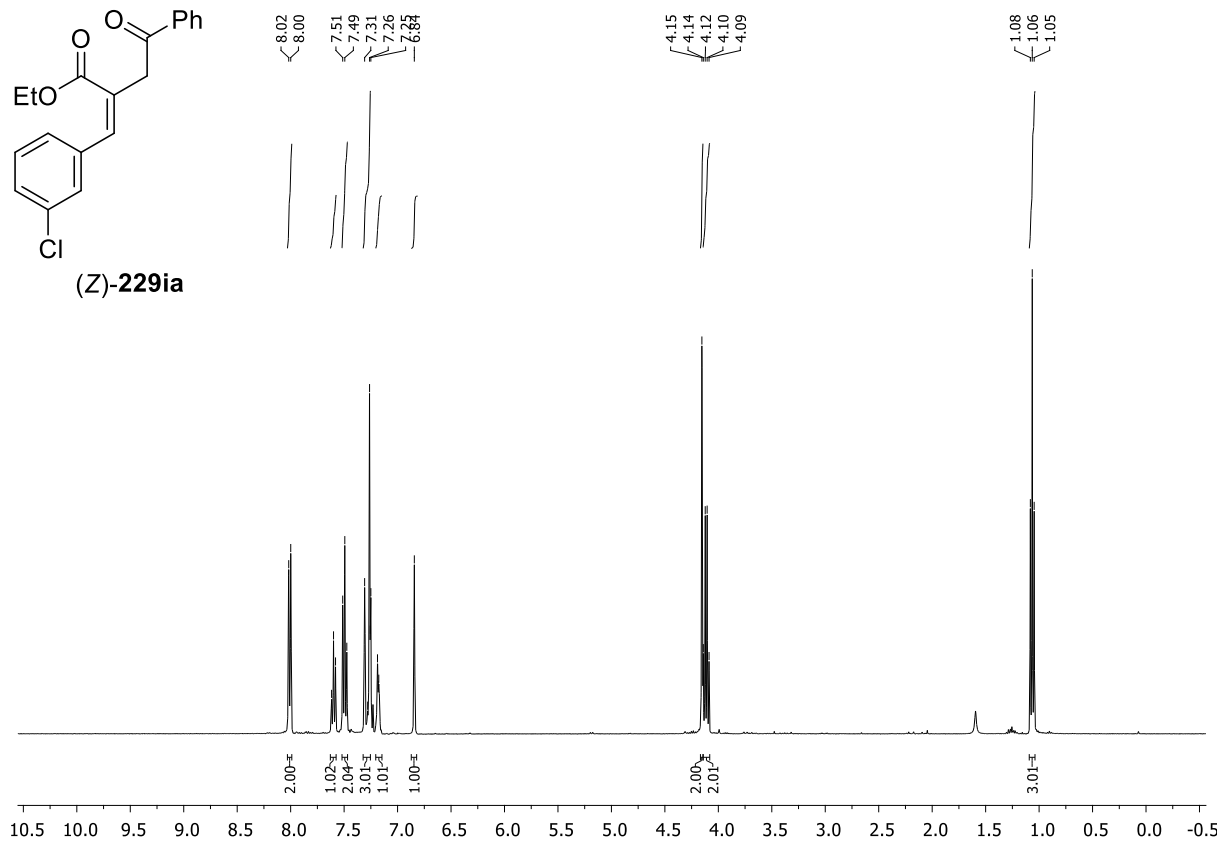
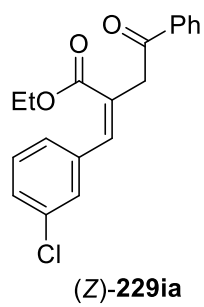


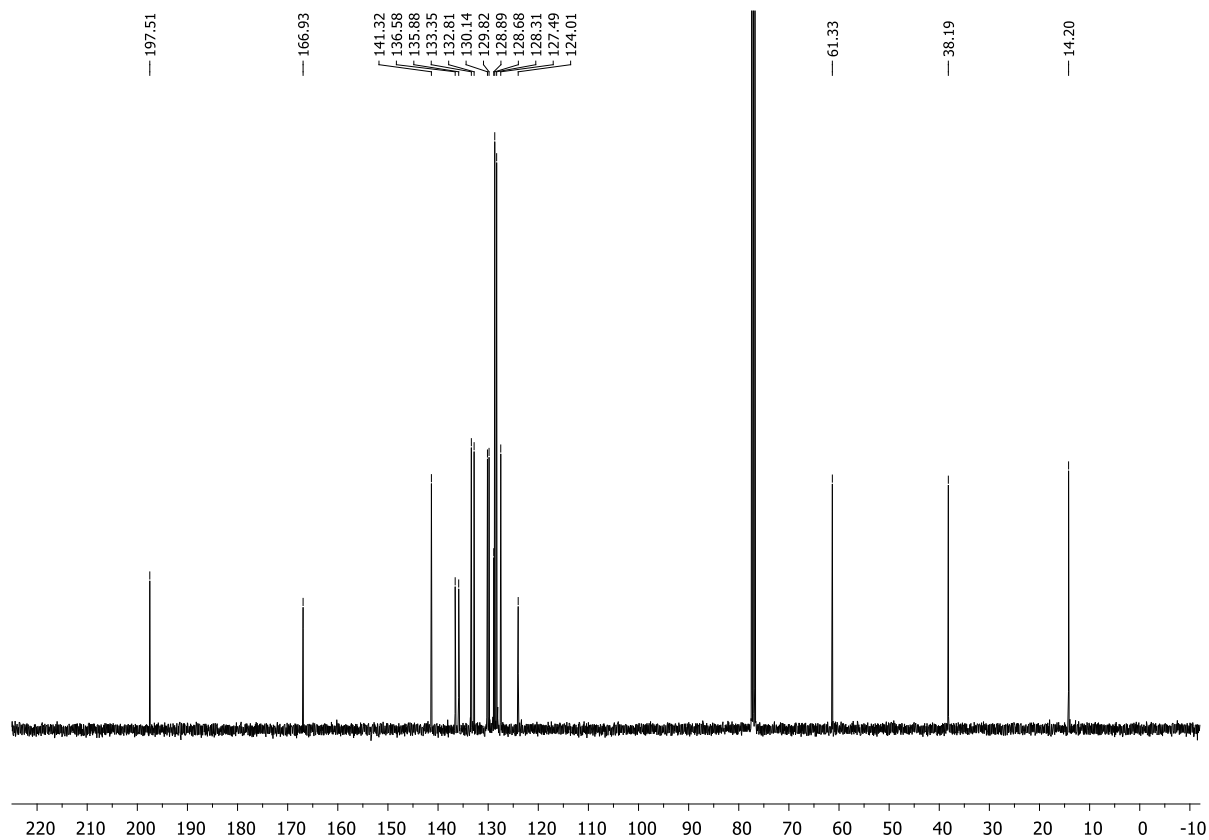
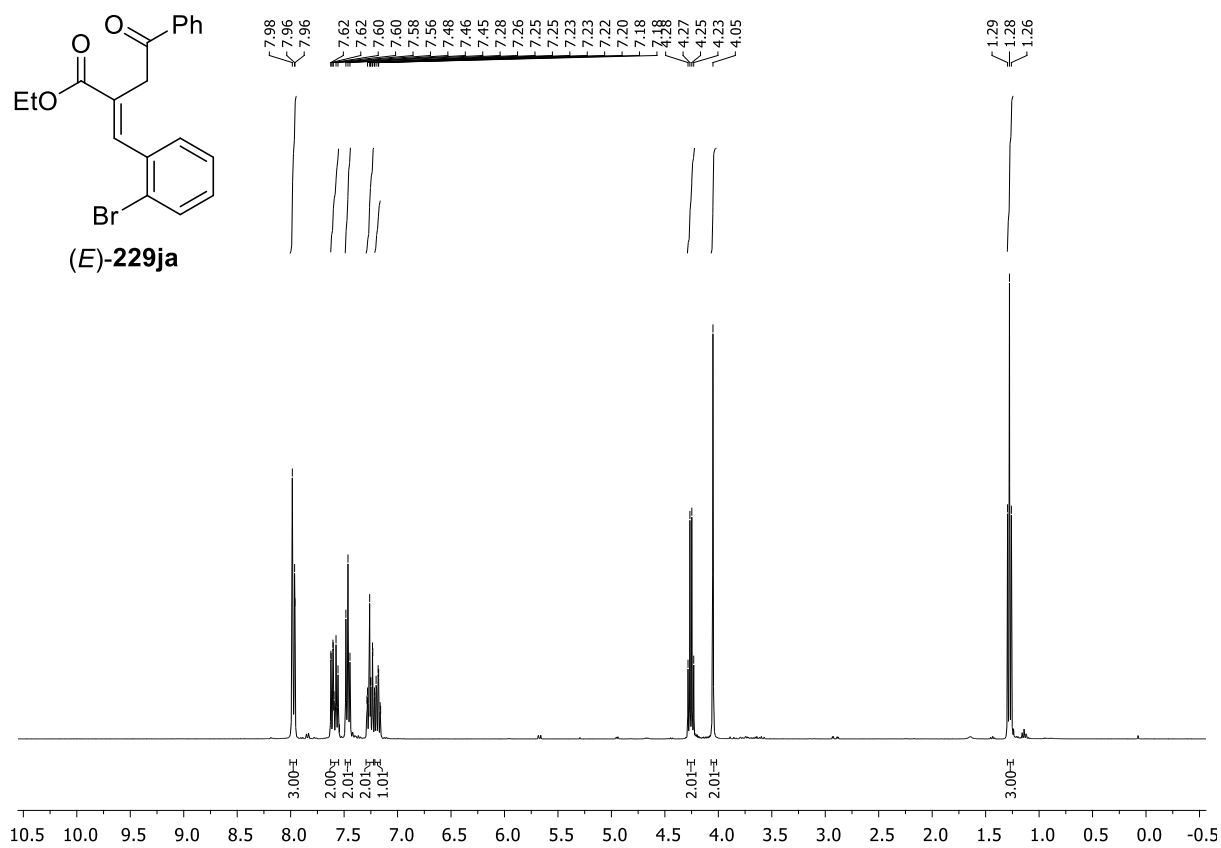
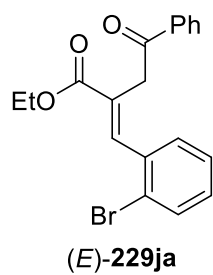


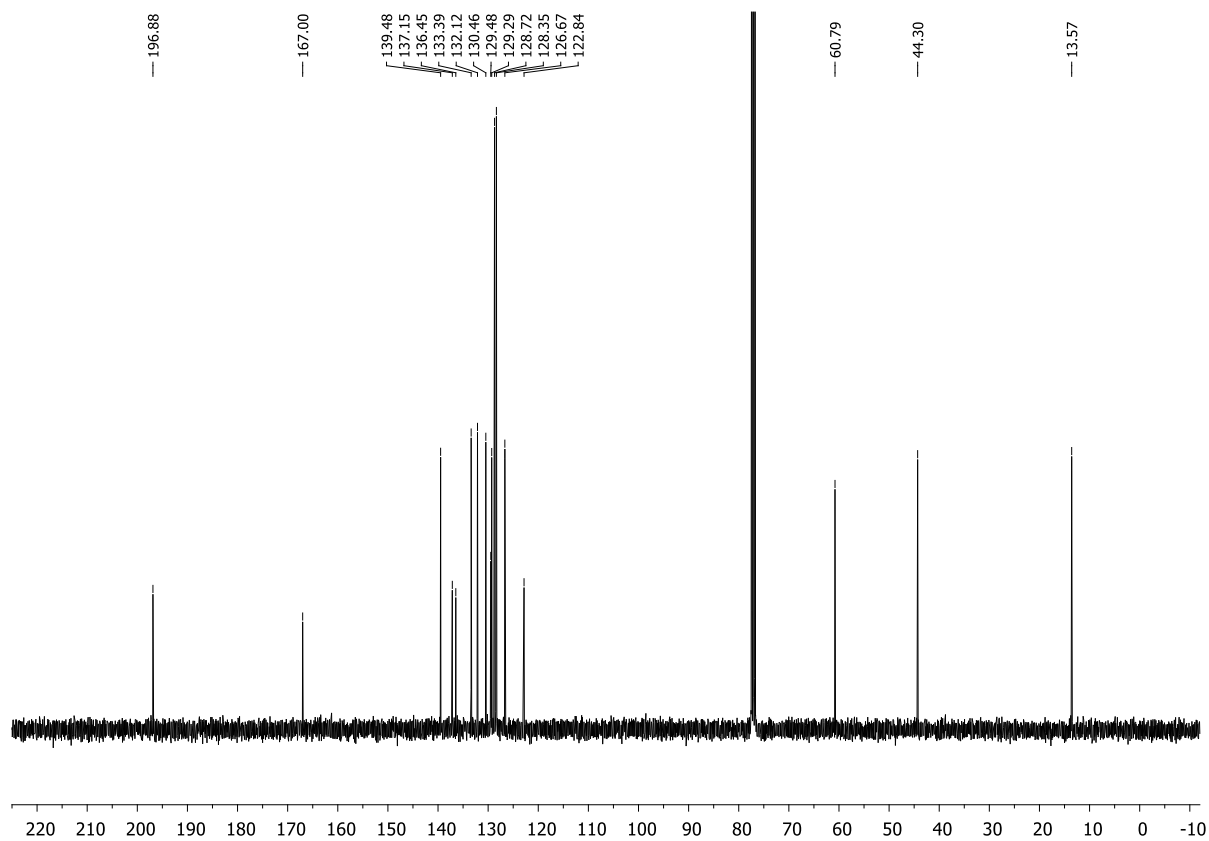
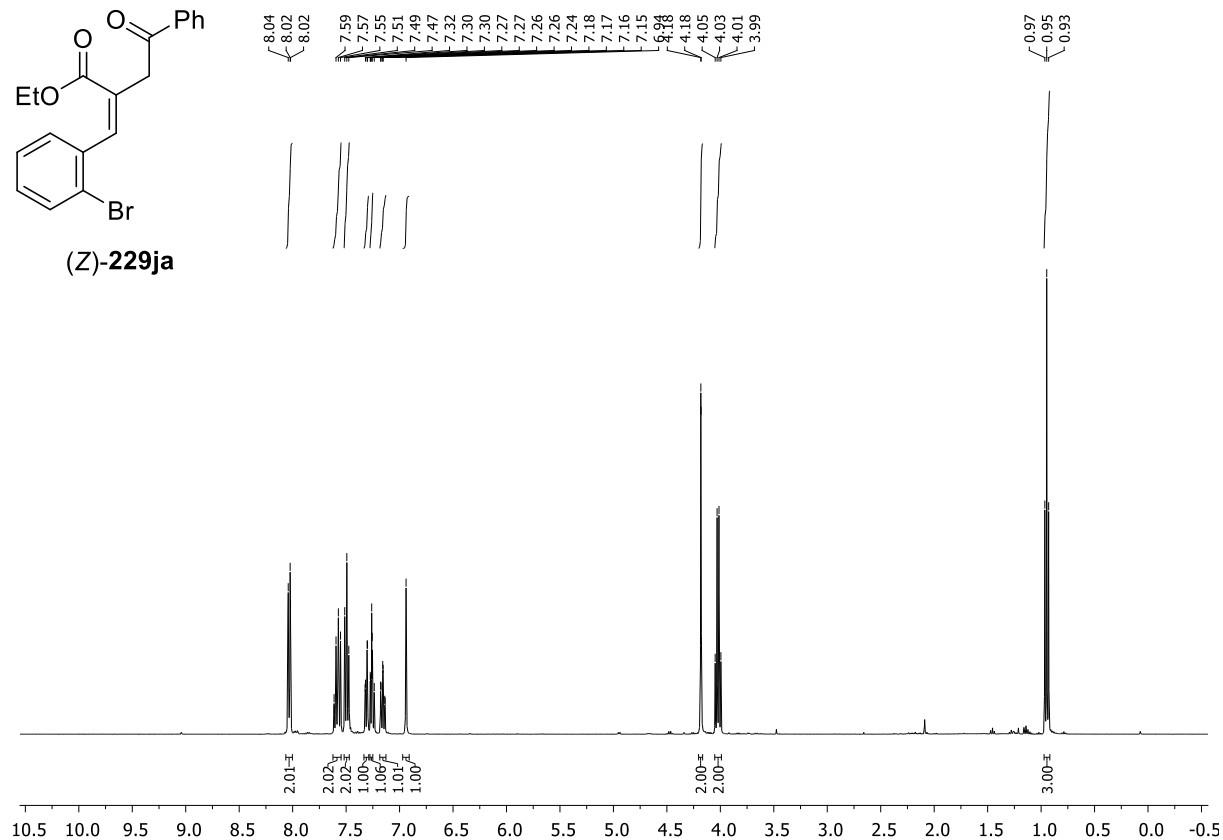
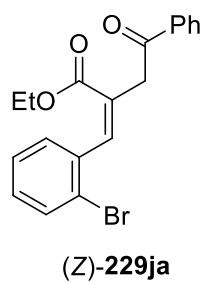
# Appendix

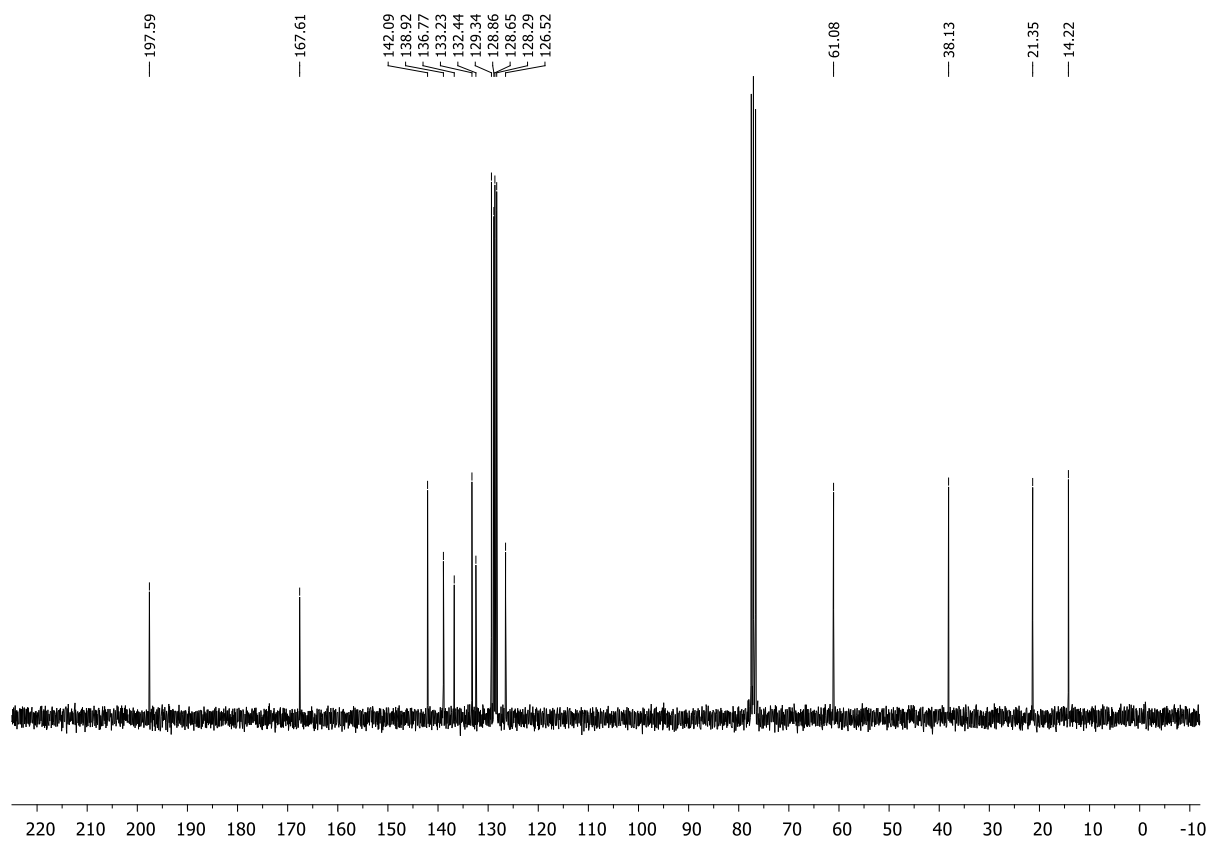
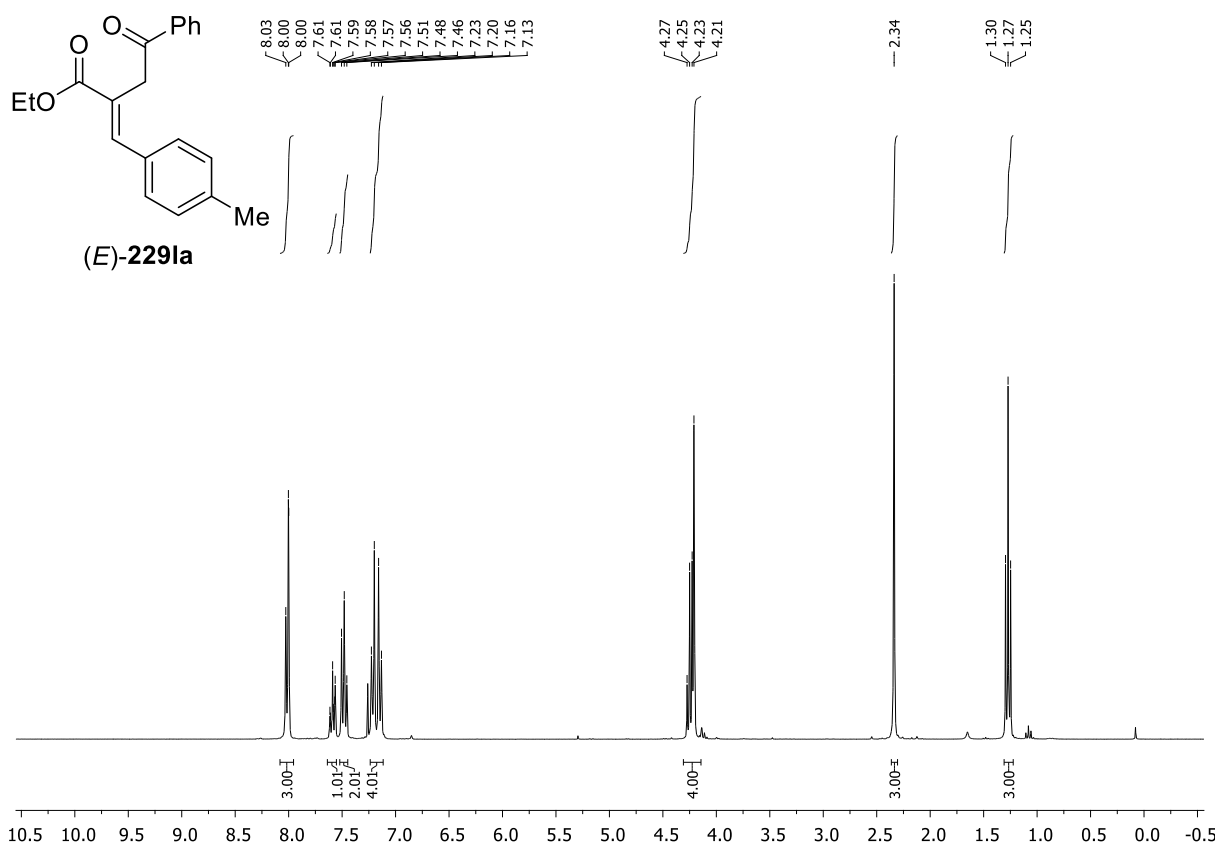


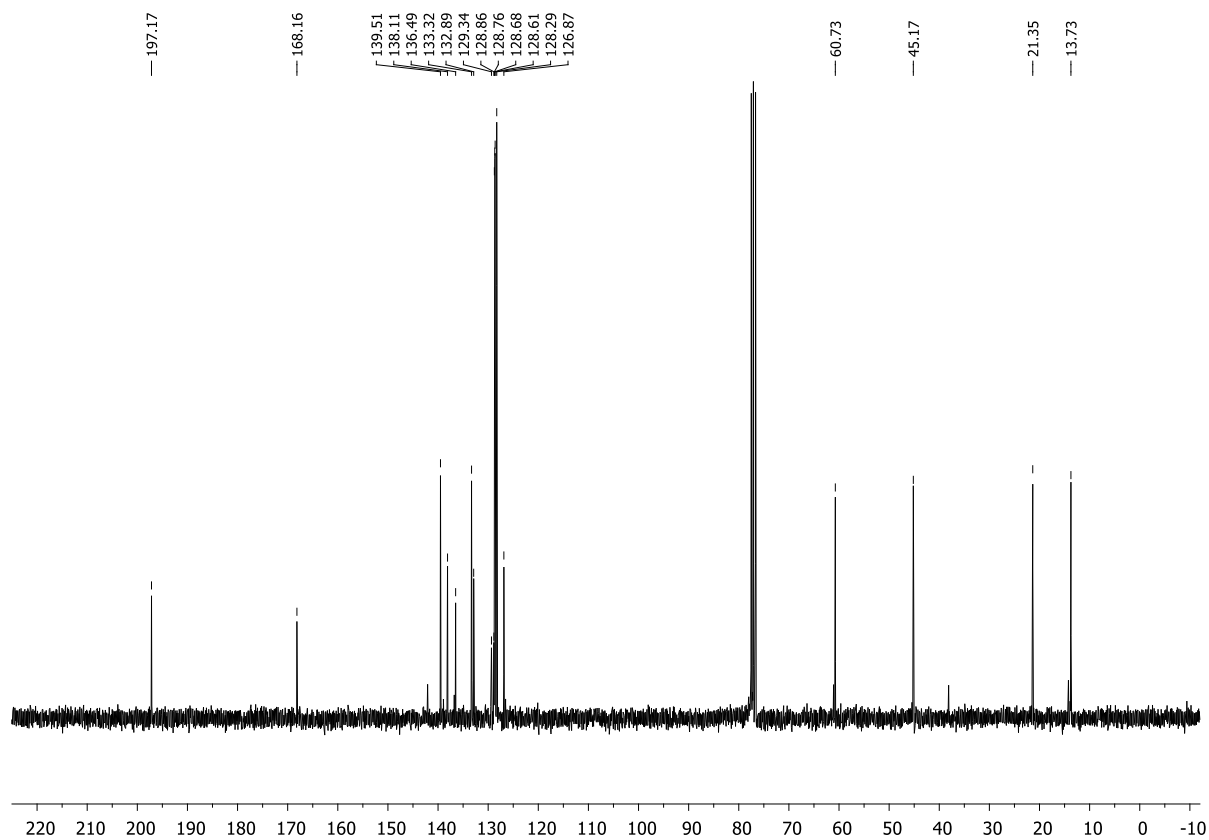
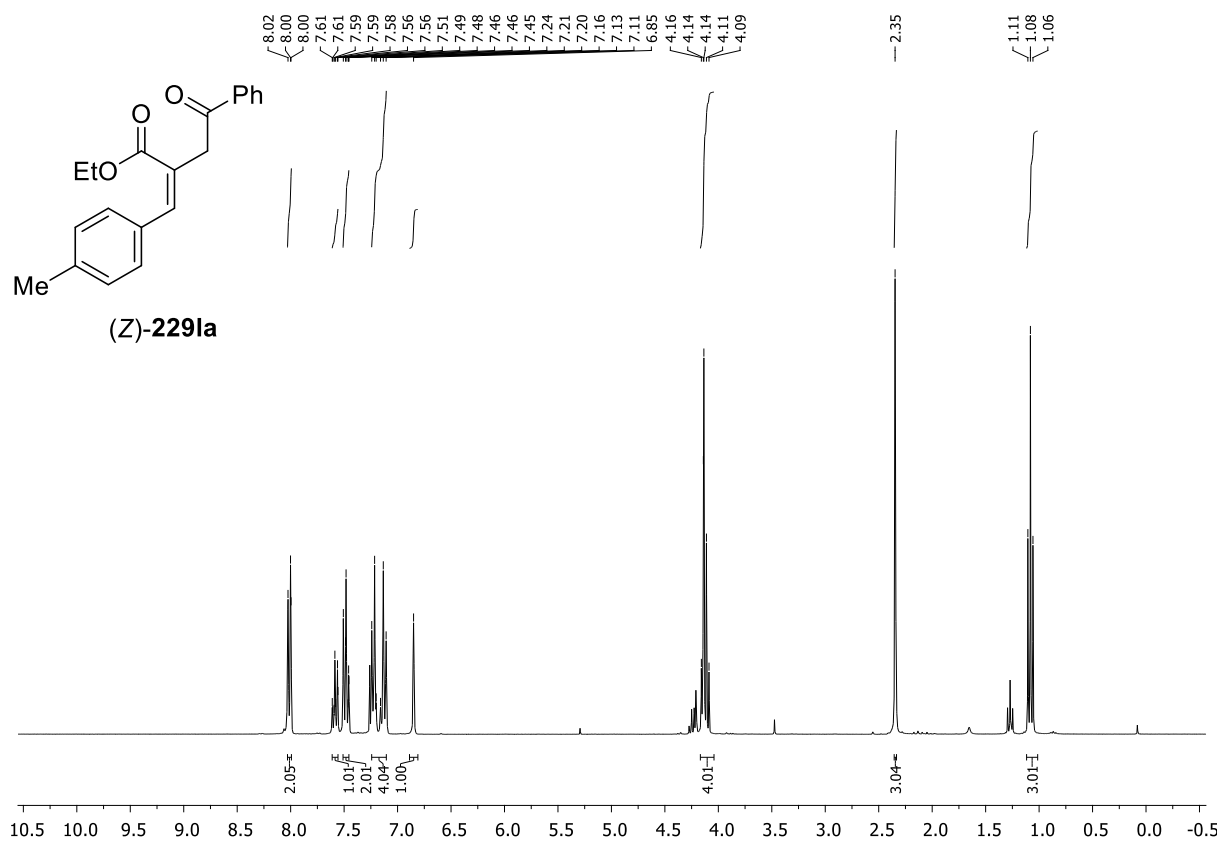




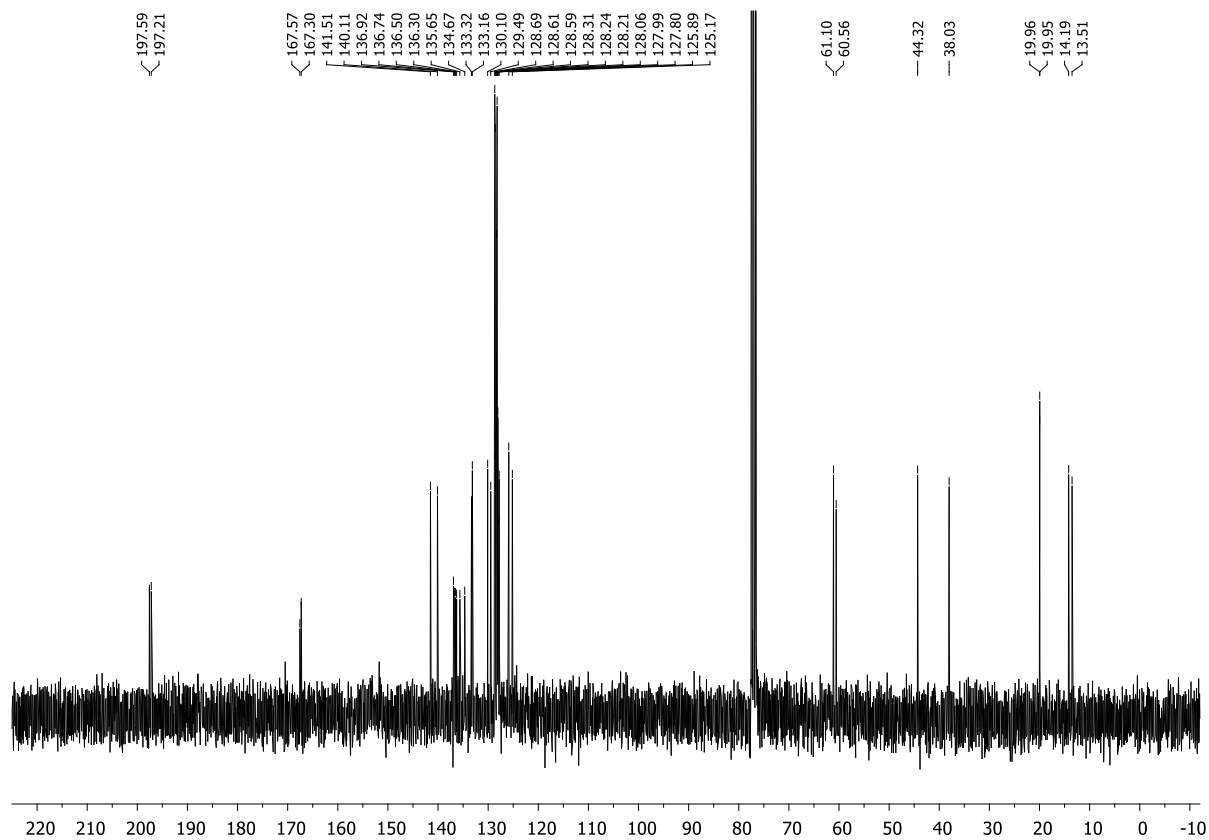
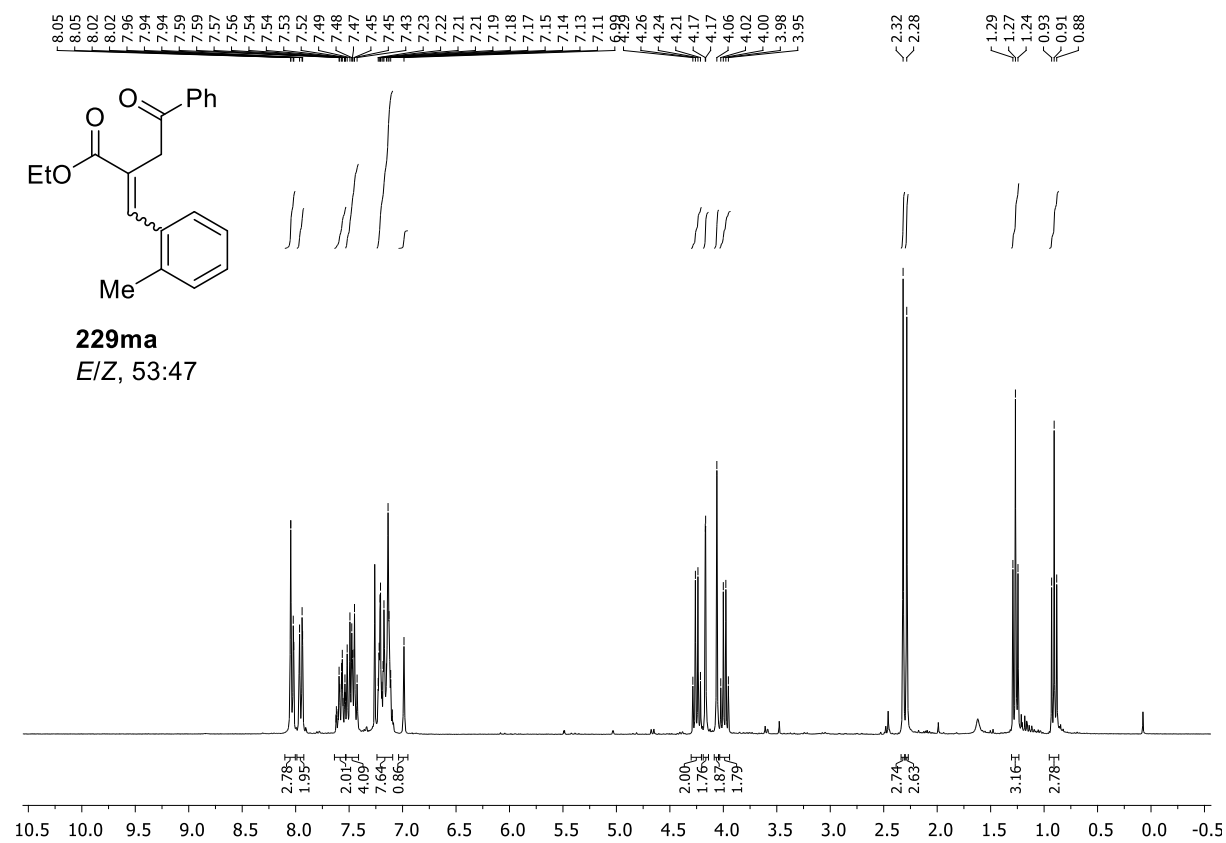


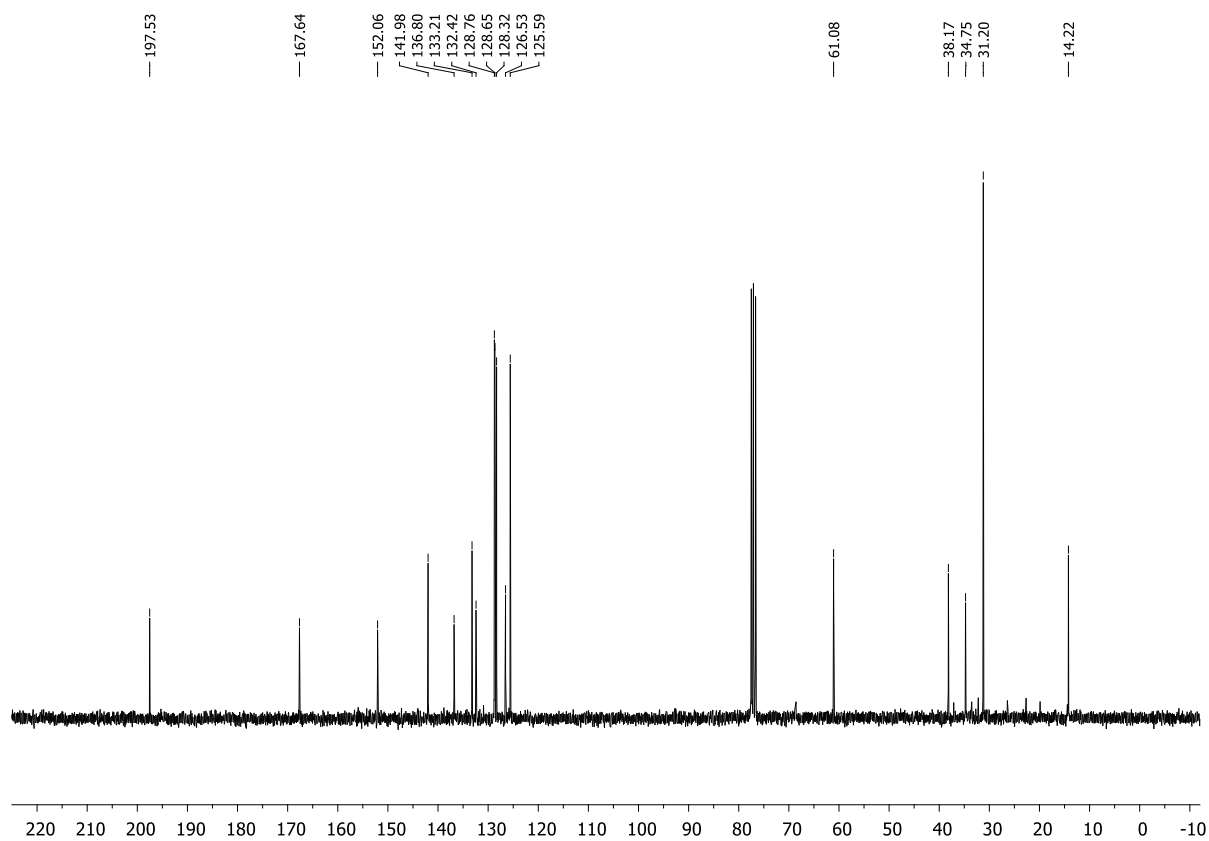
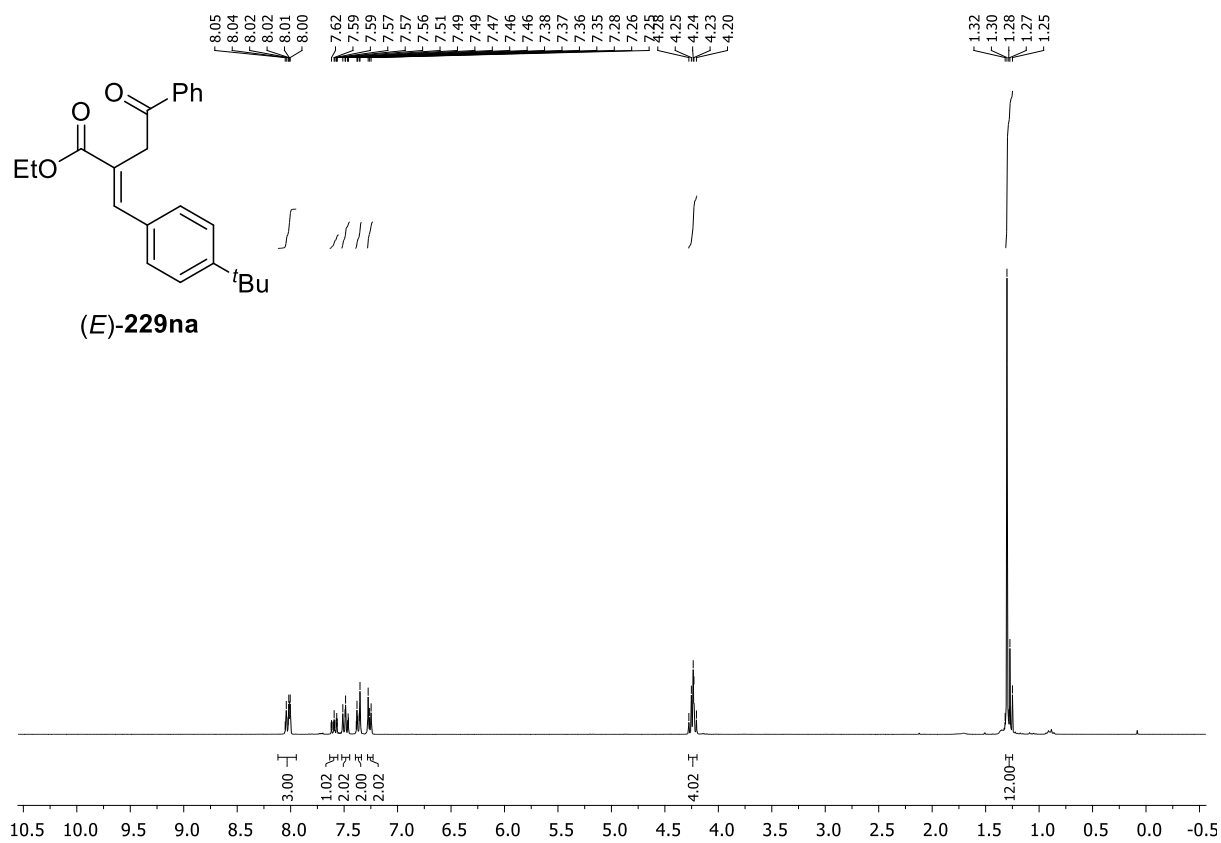


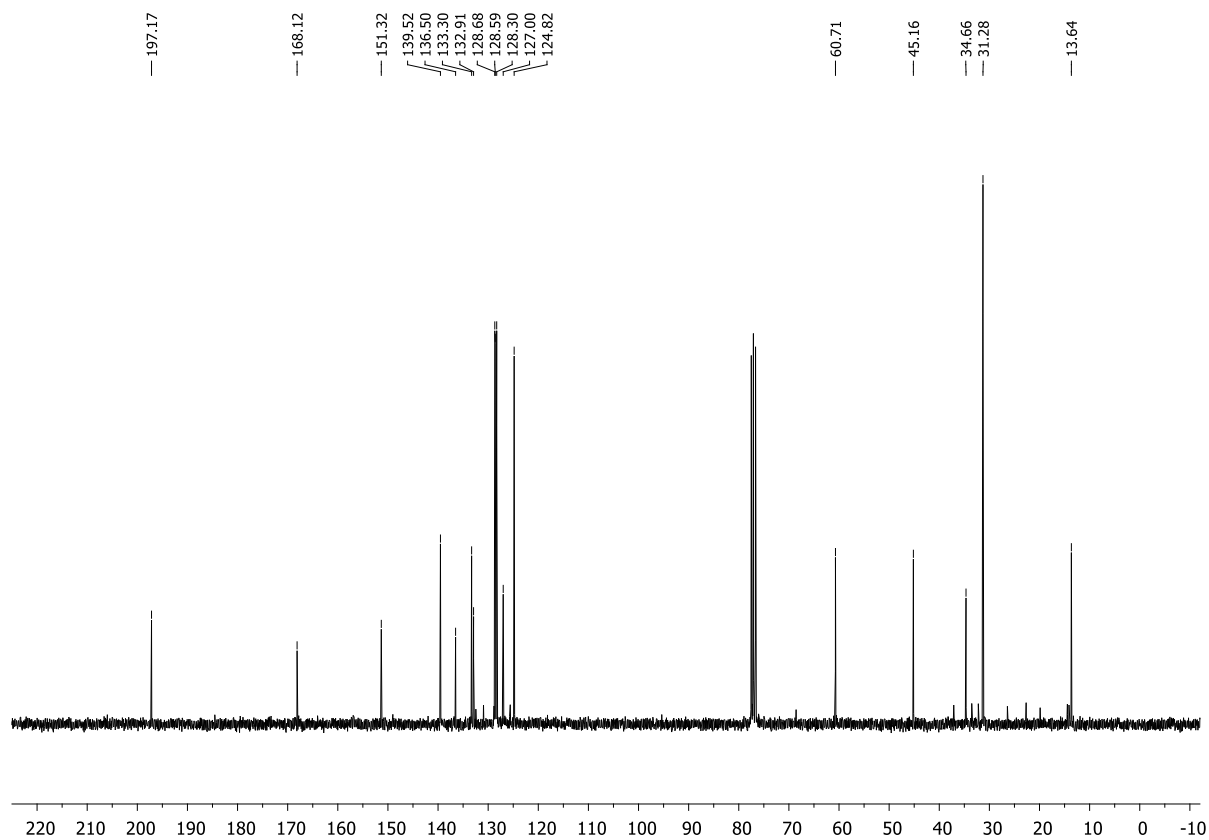
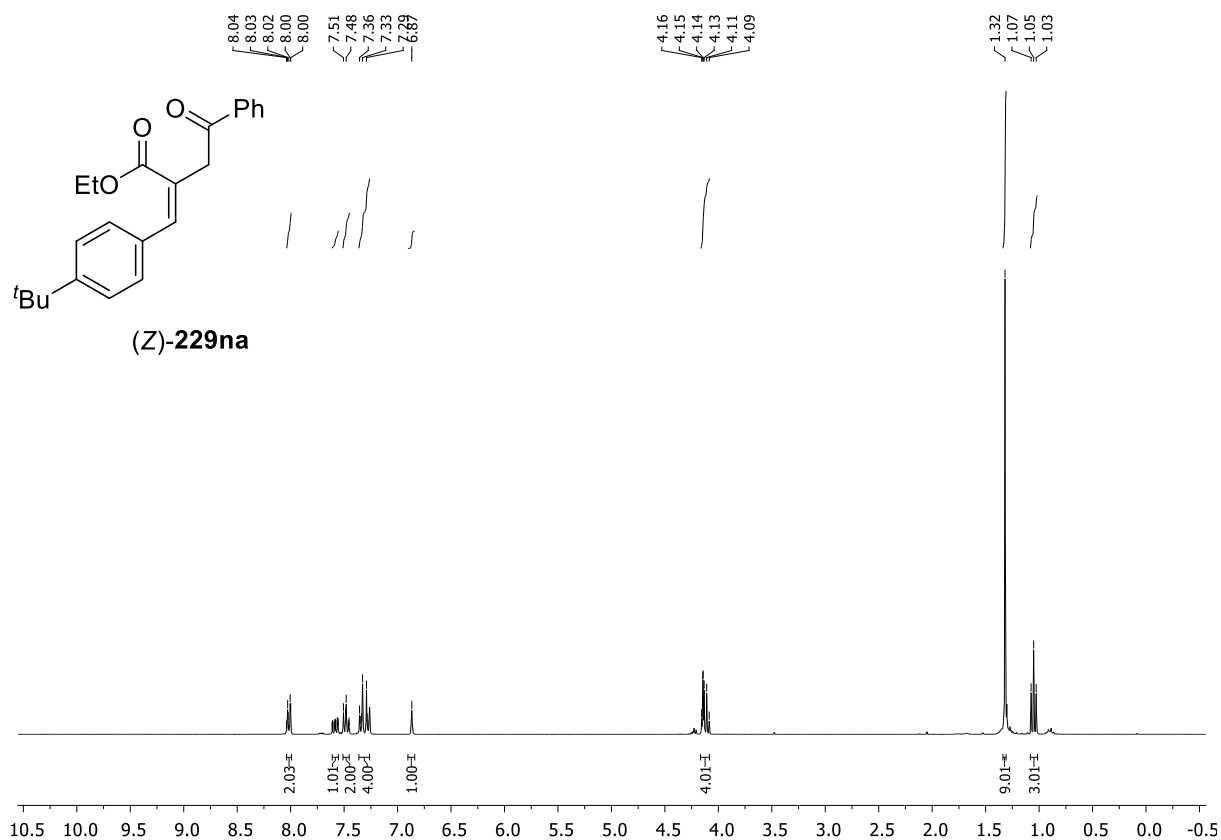


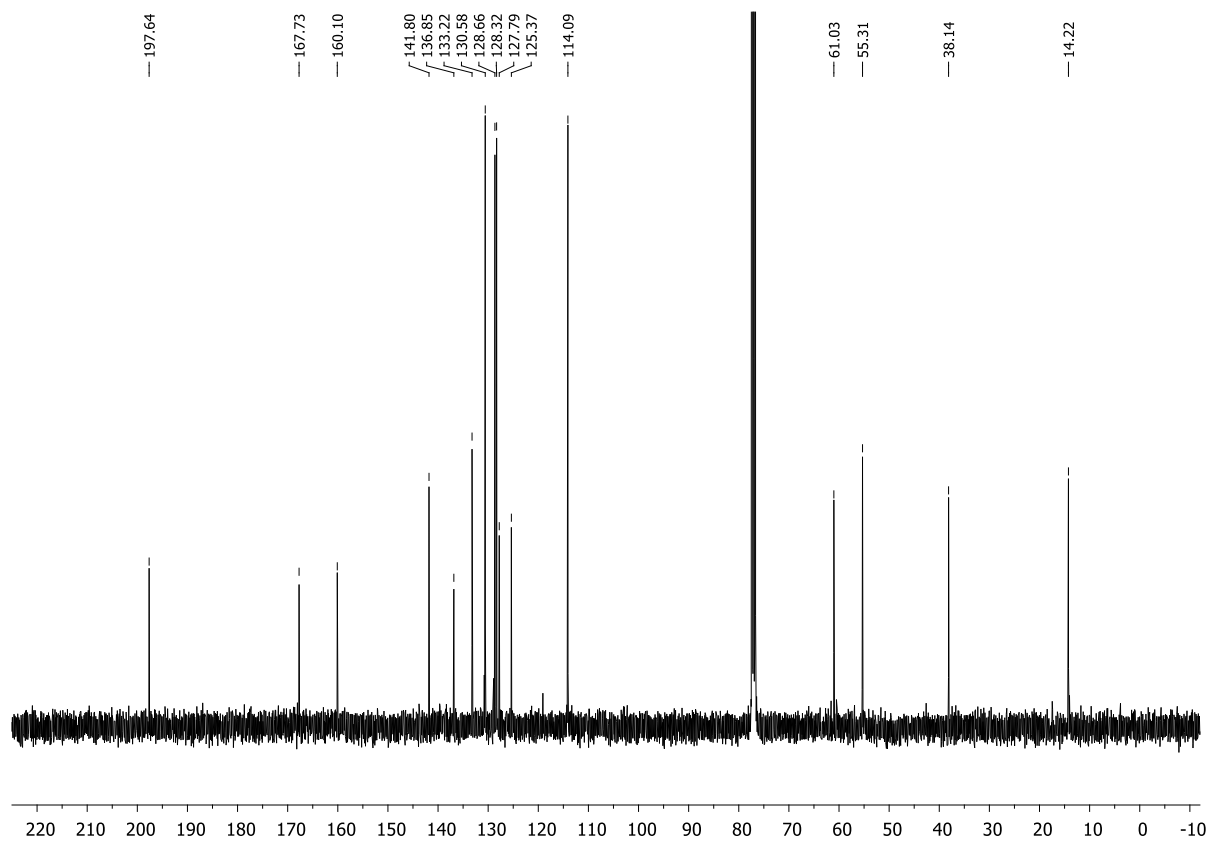
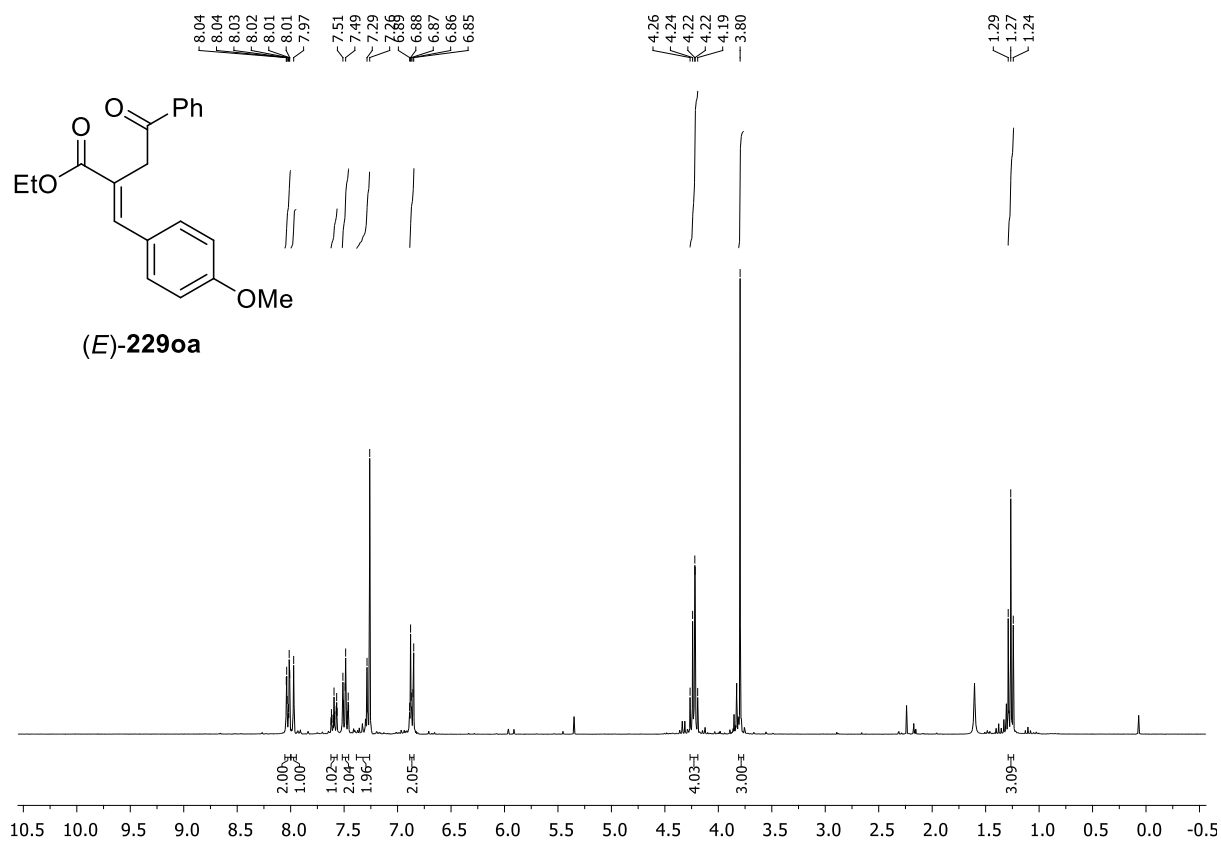


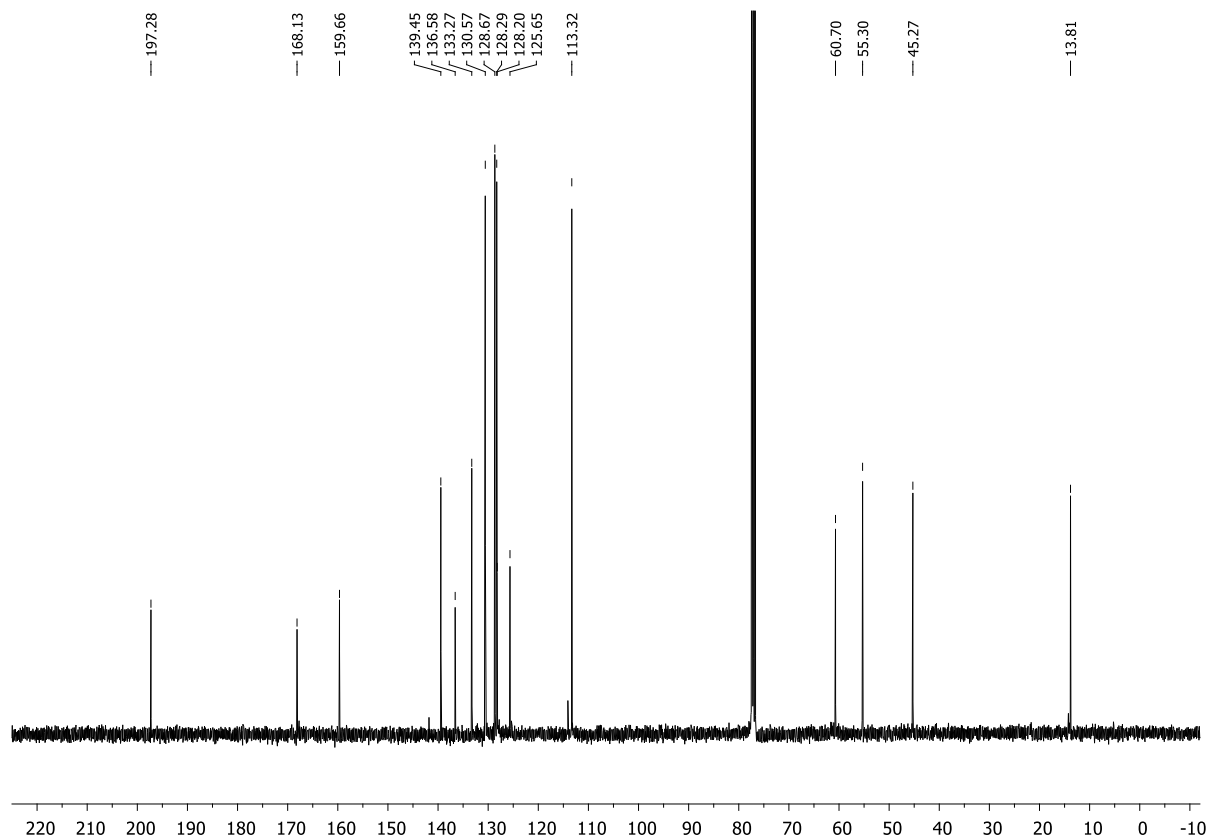
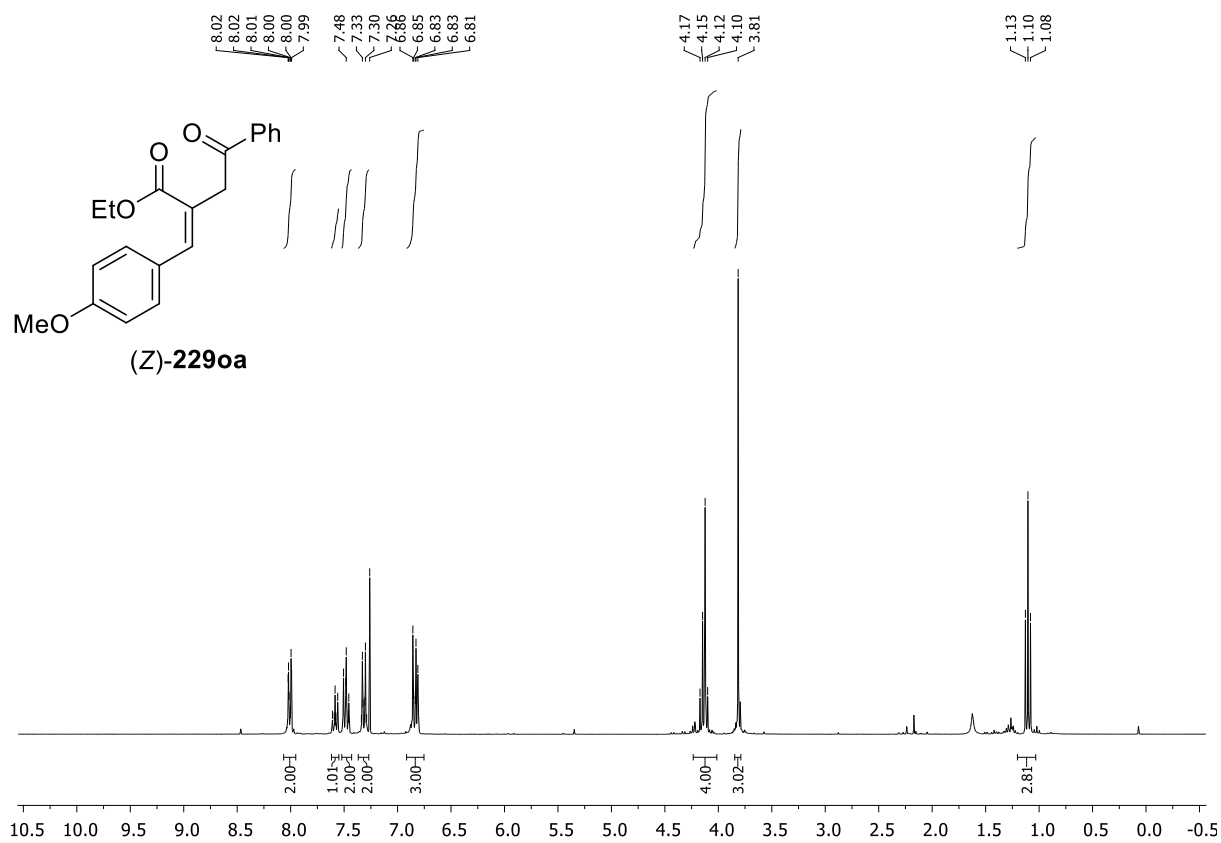


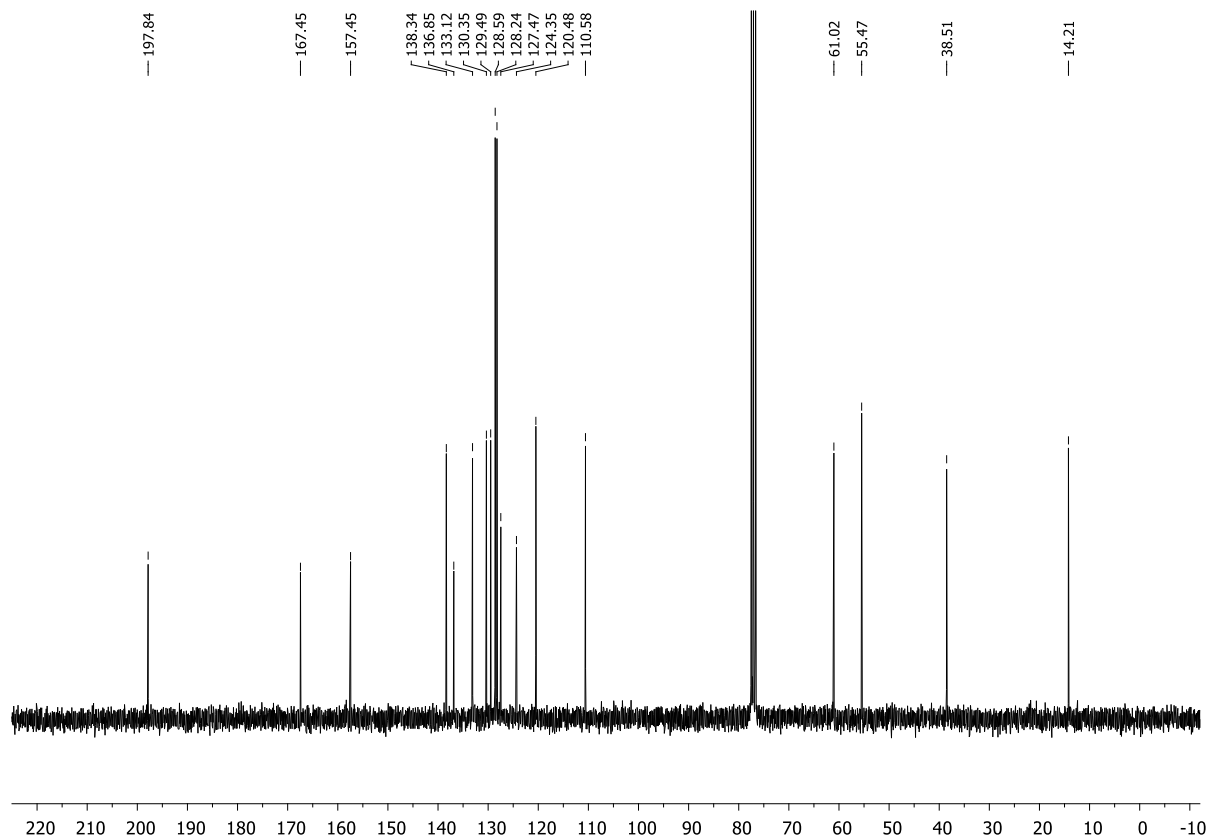
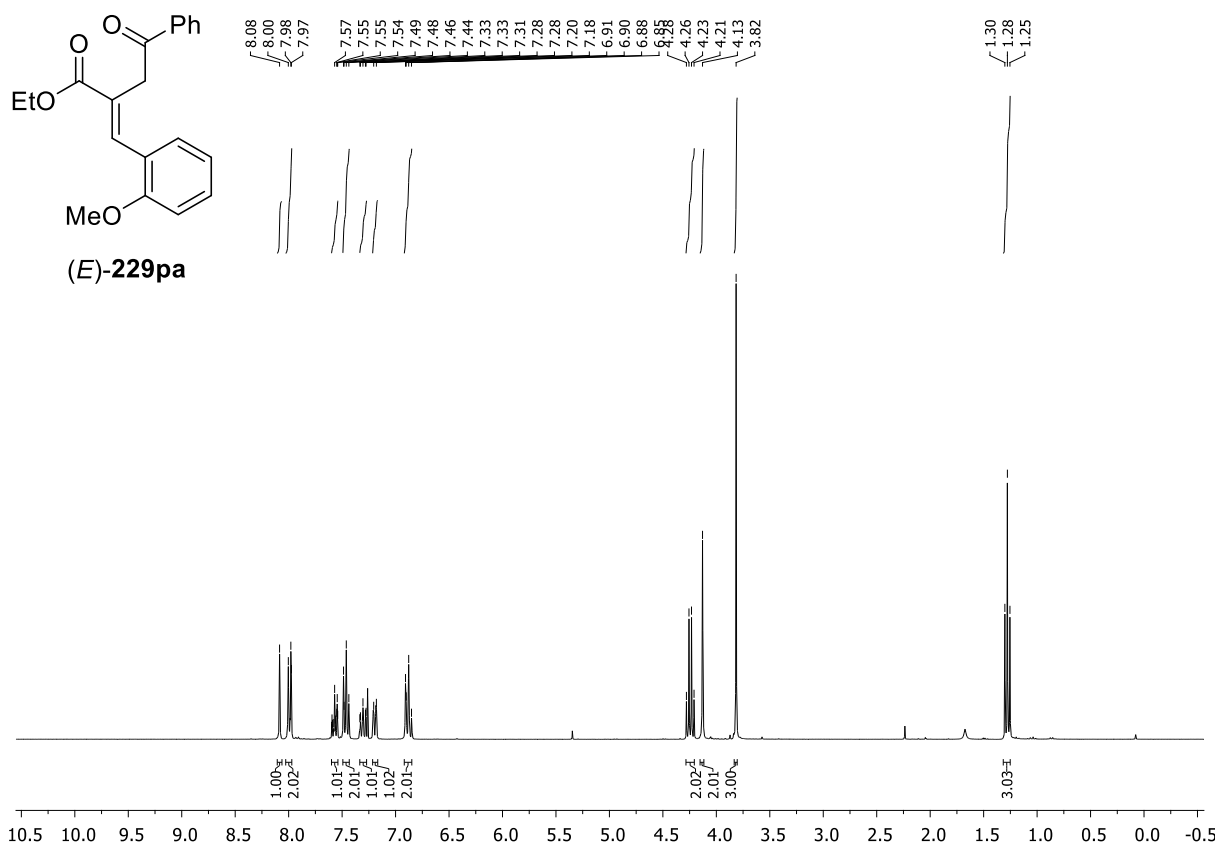


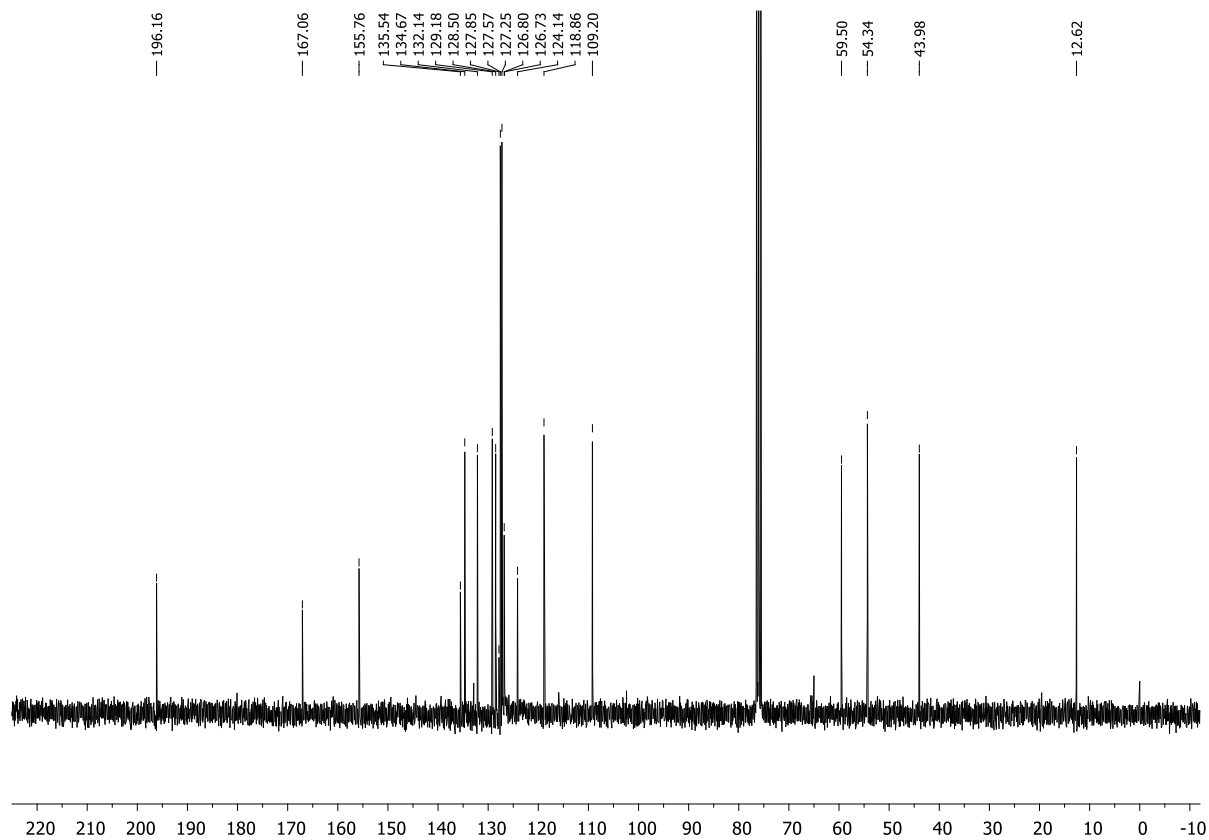
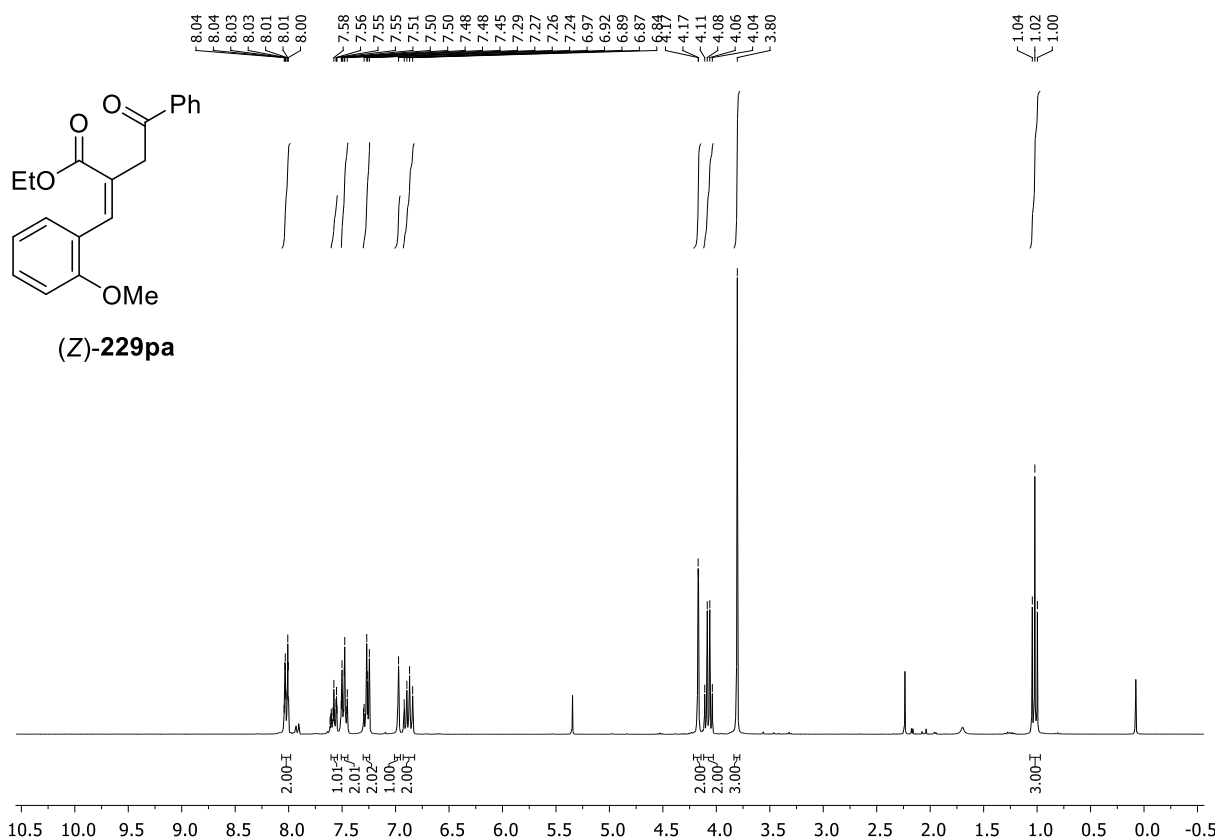


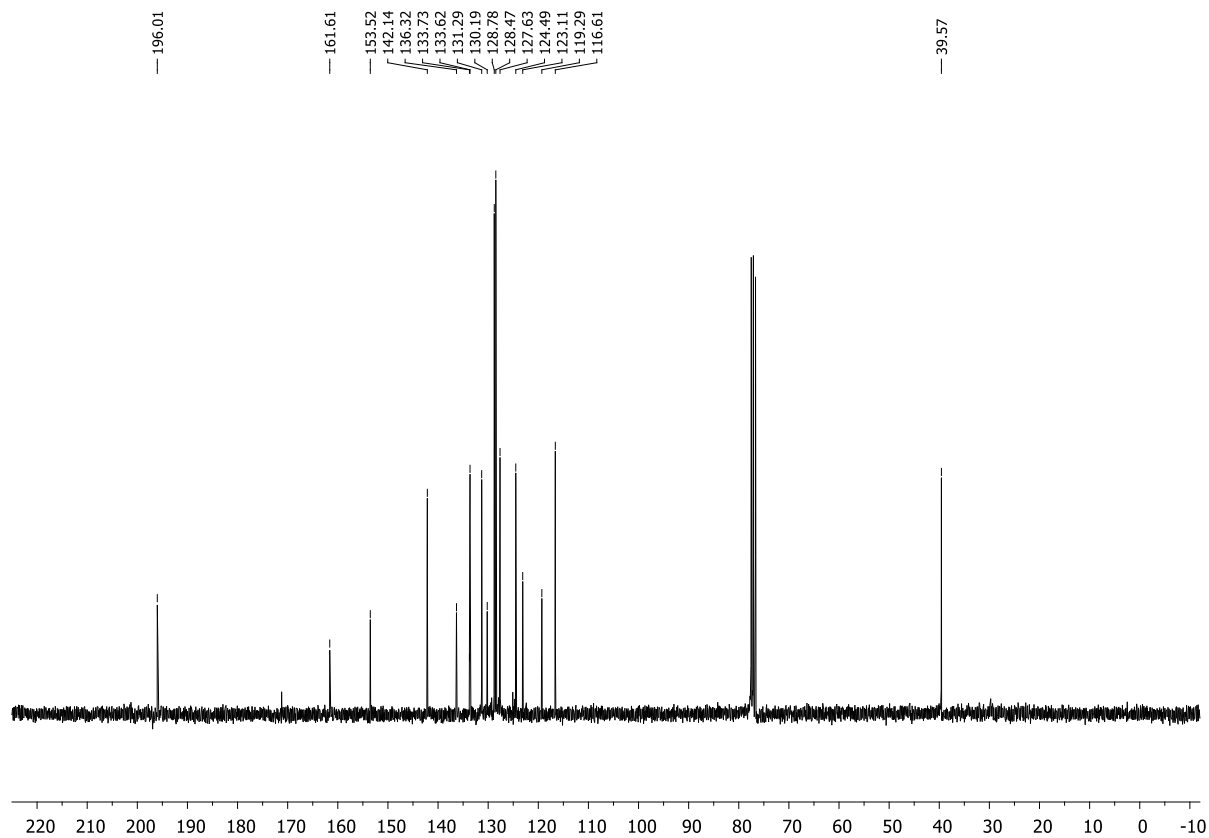
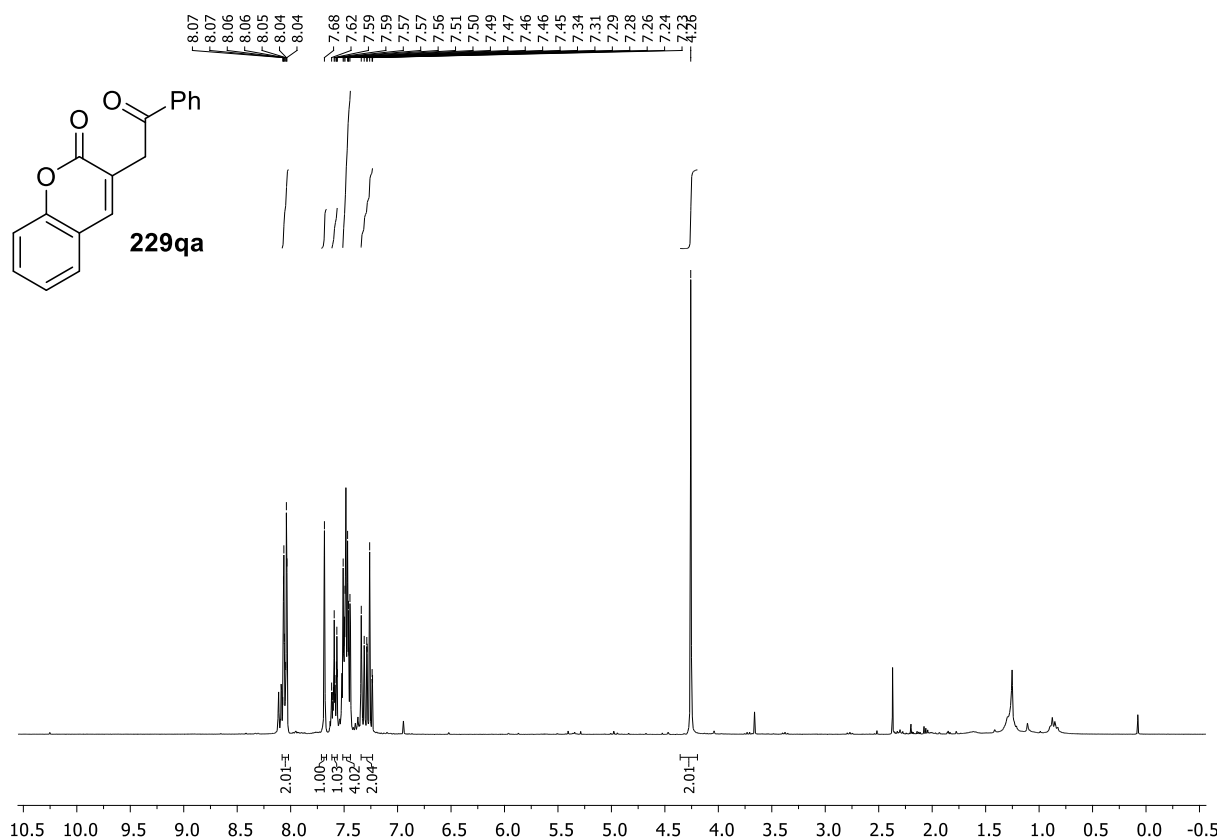




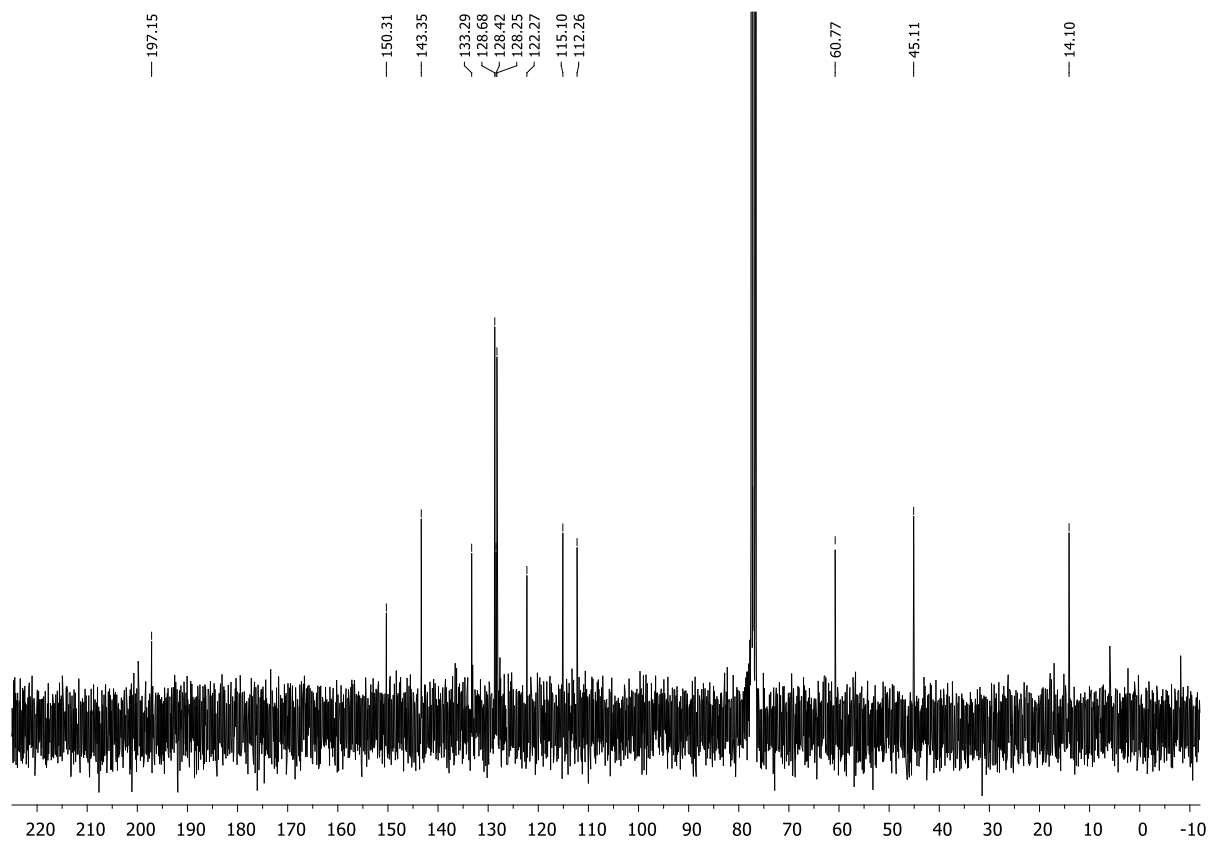
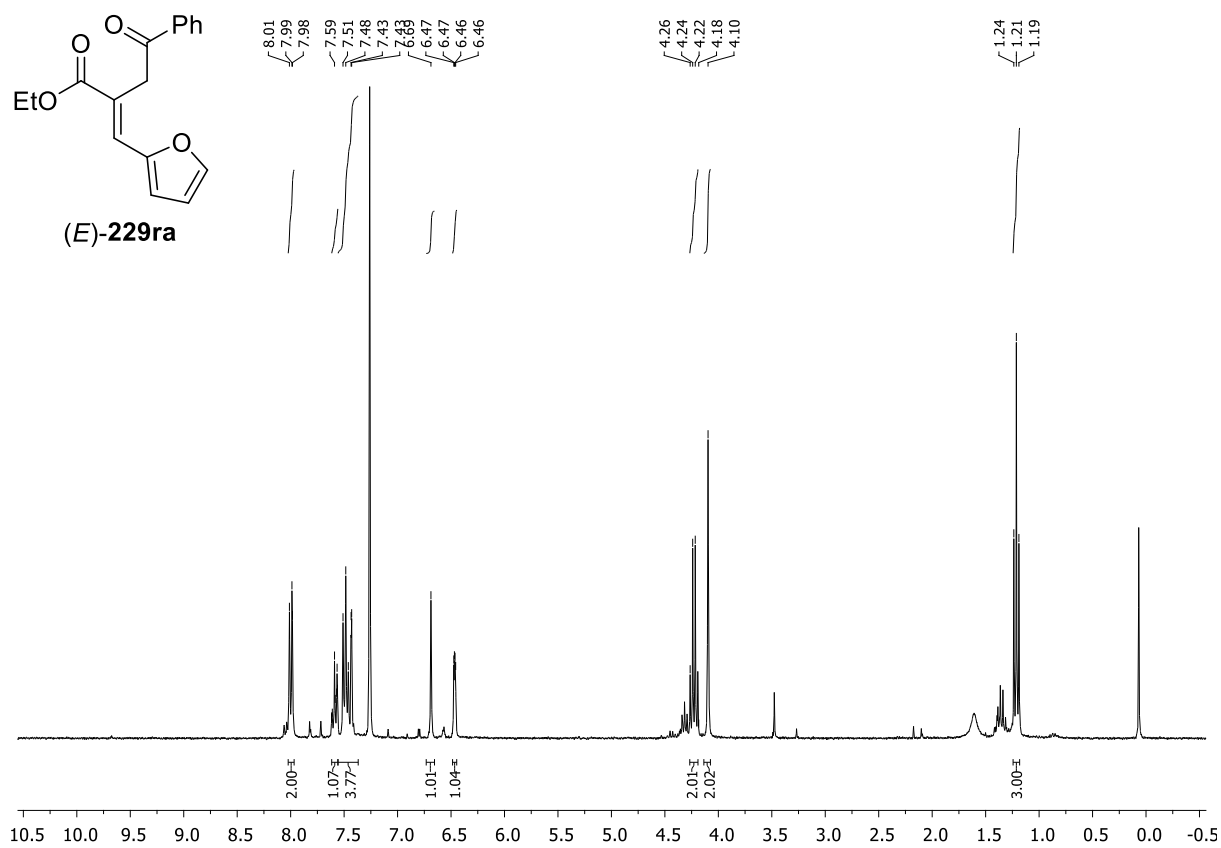


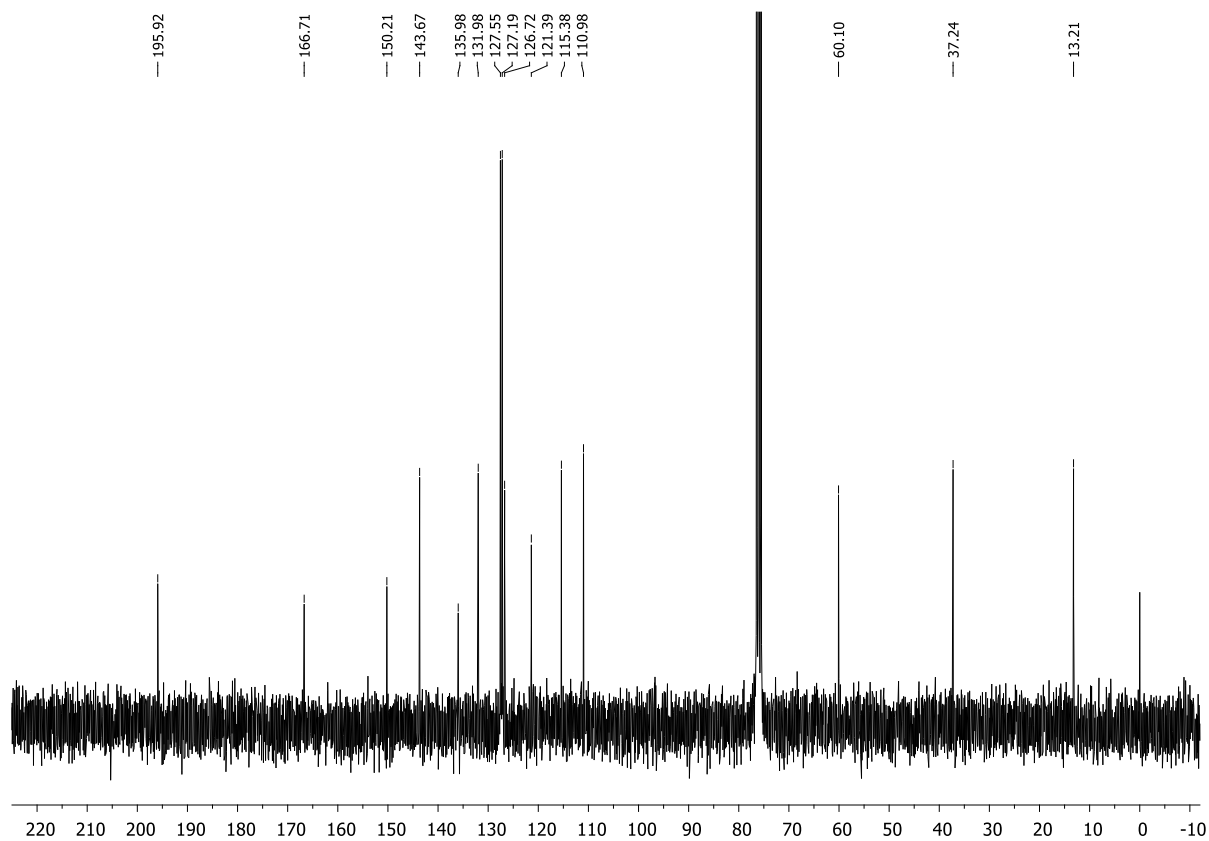
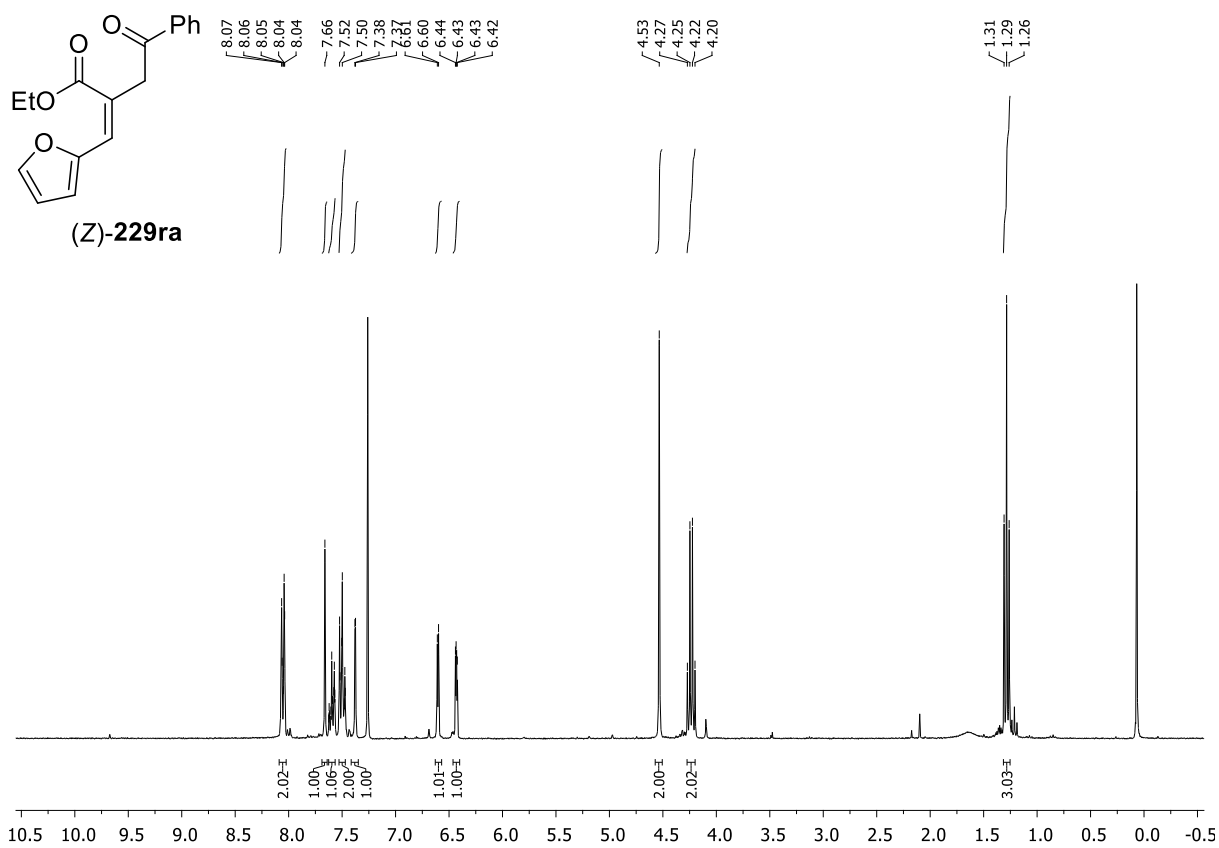




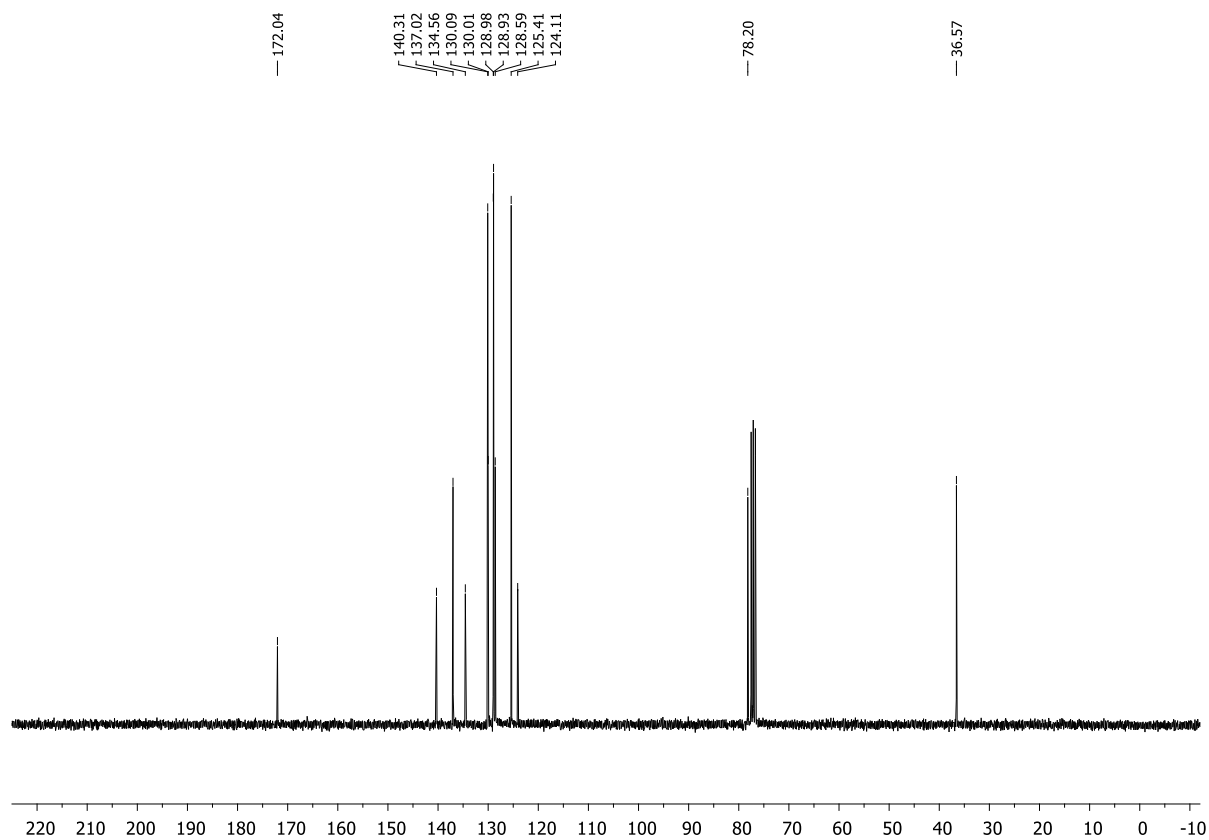
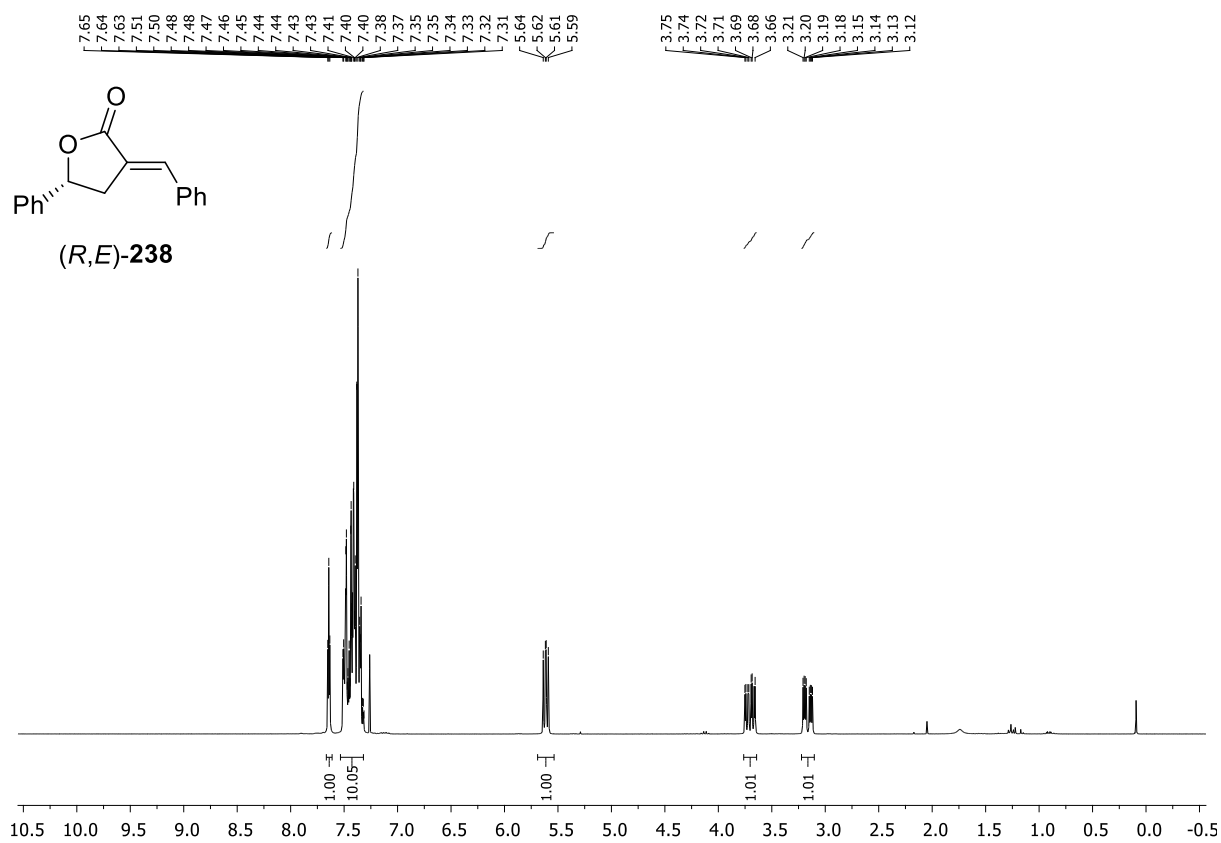


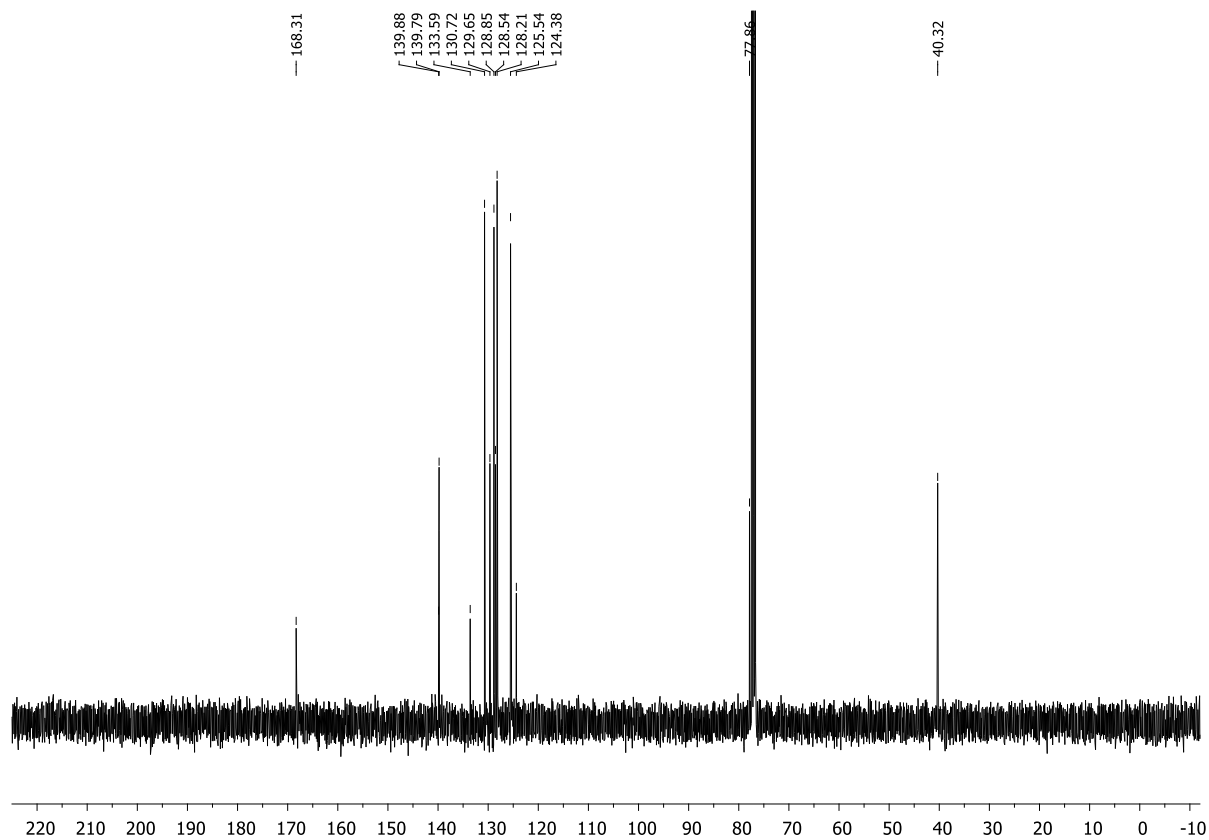
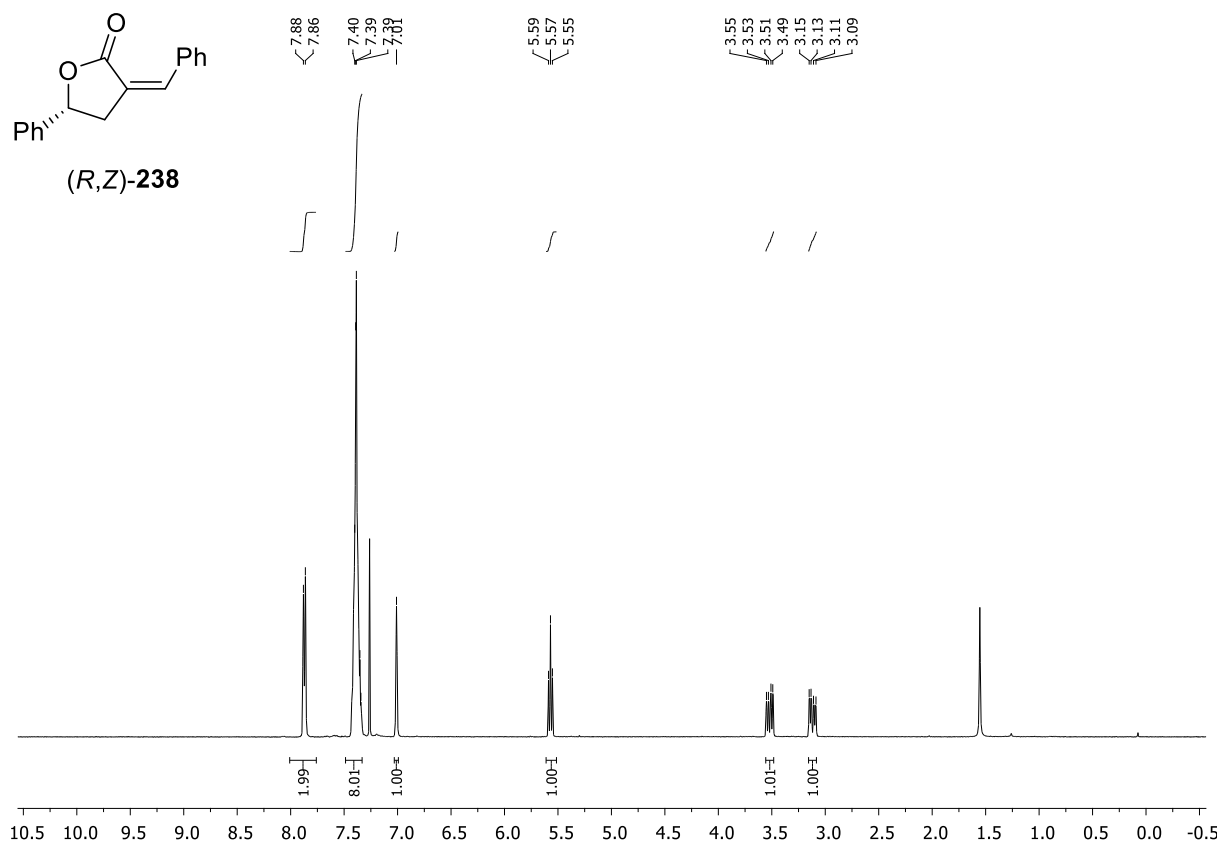




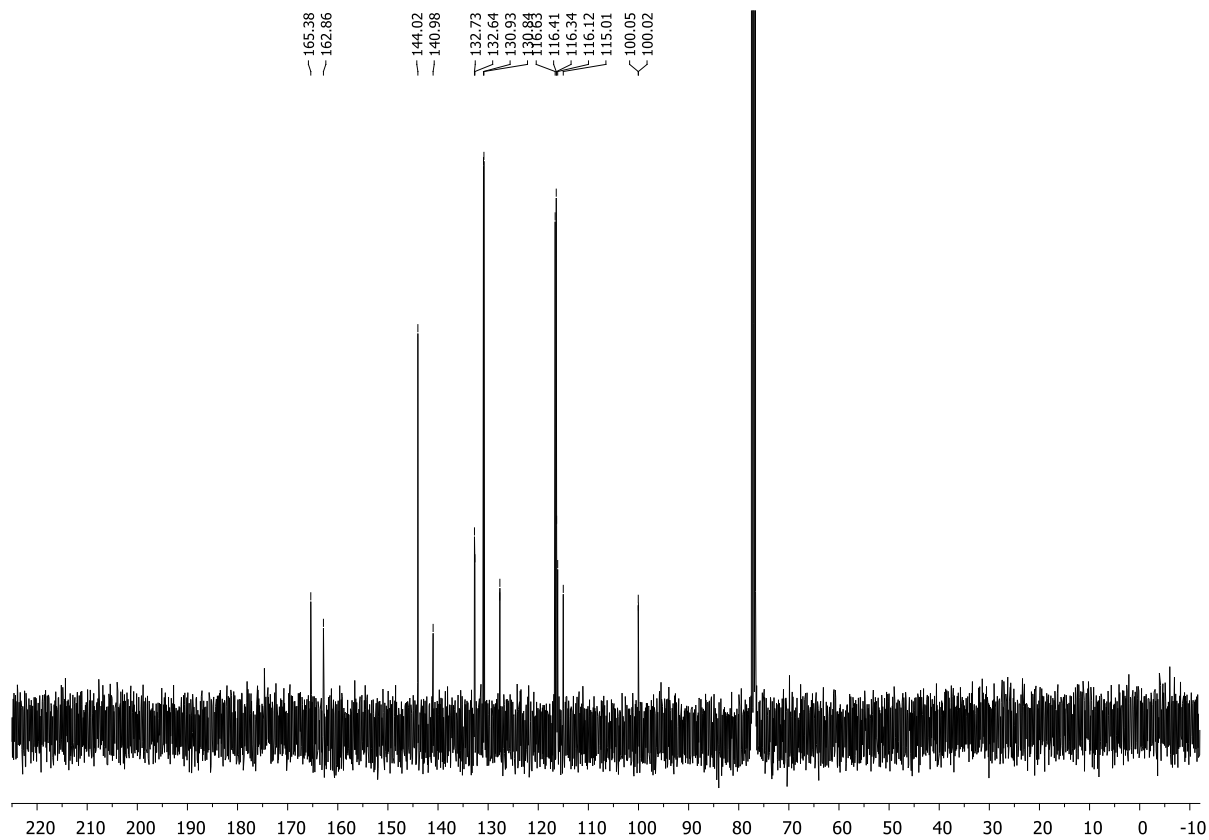
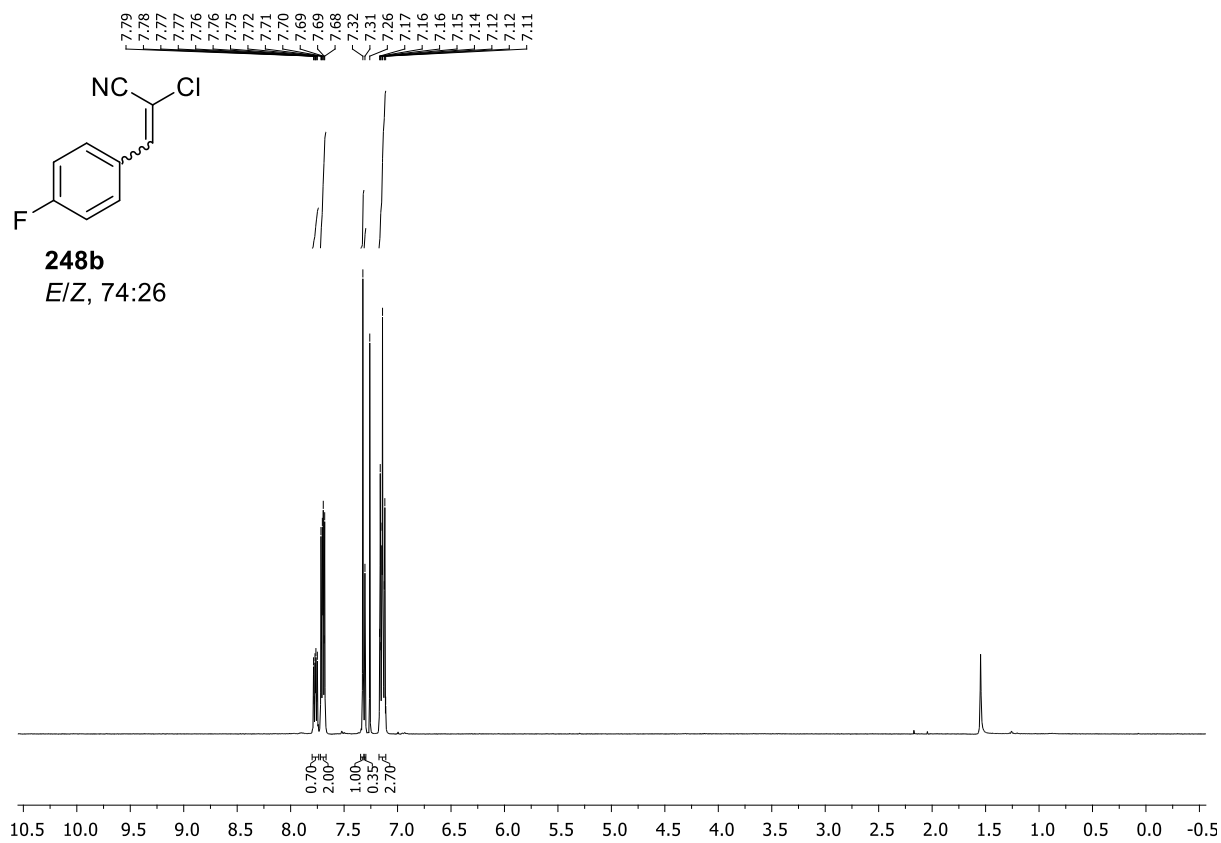


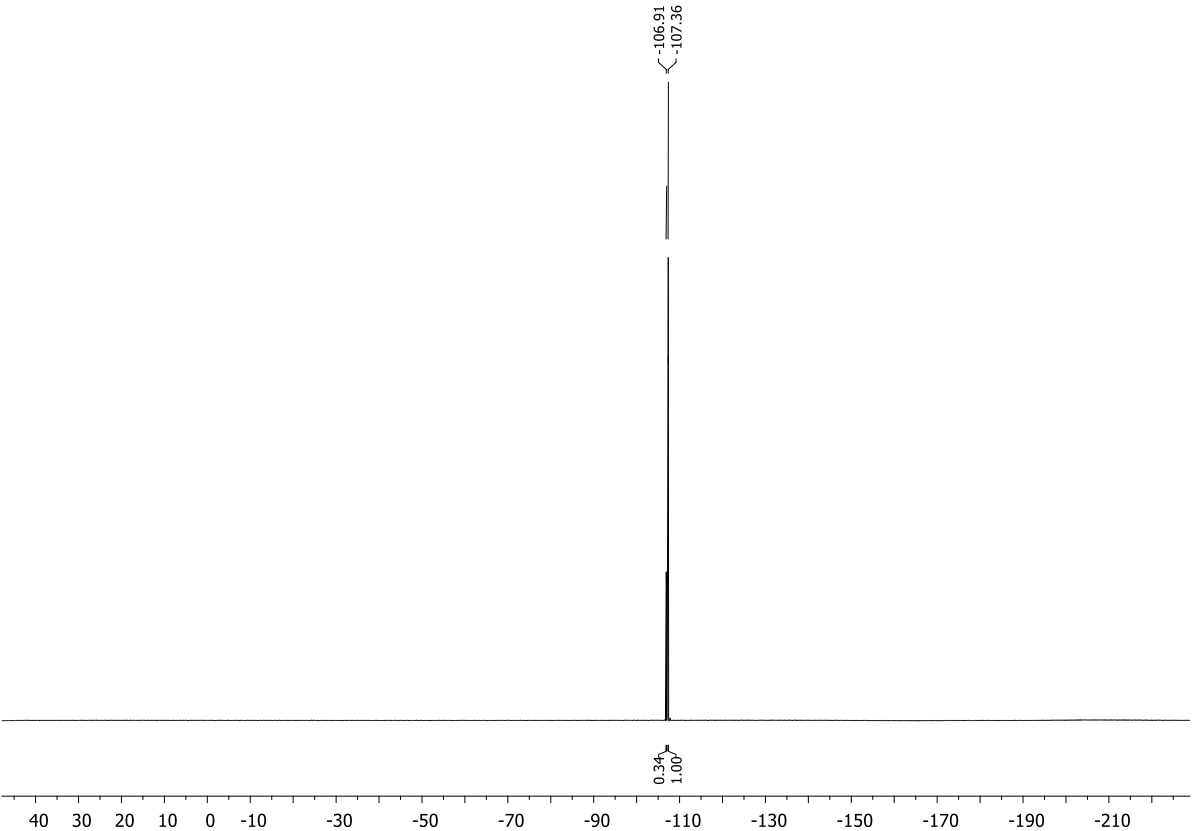
# Appendix

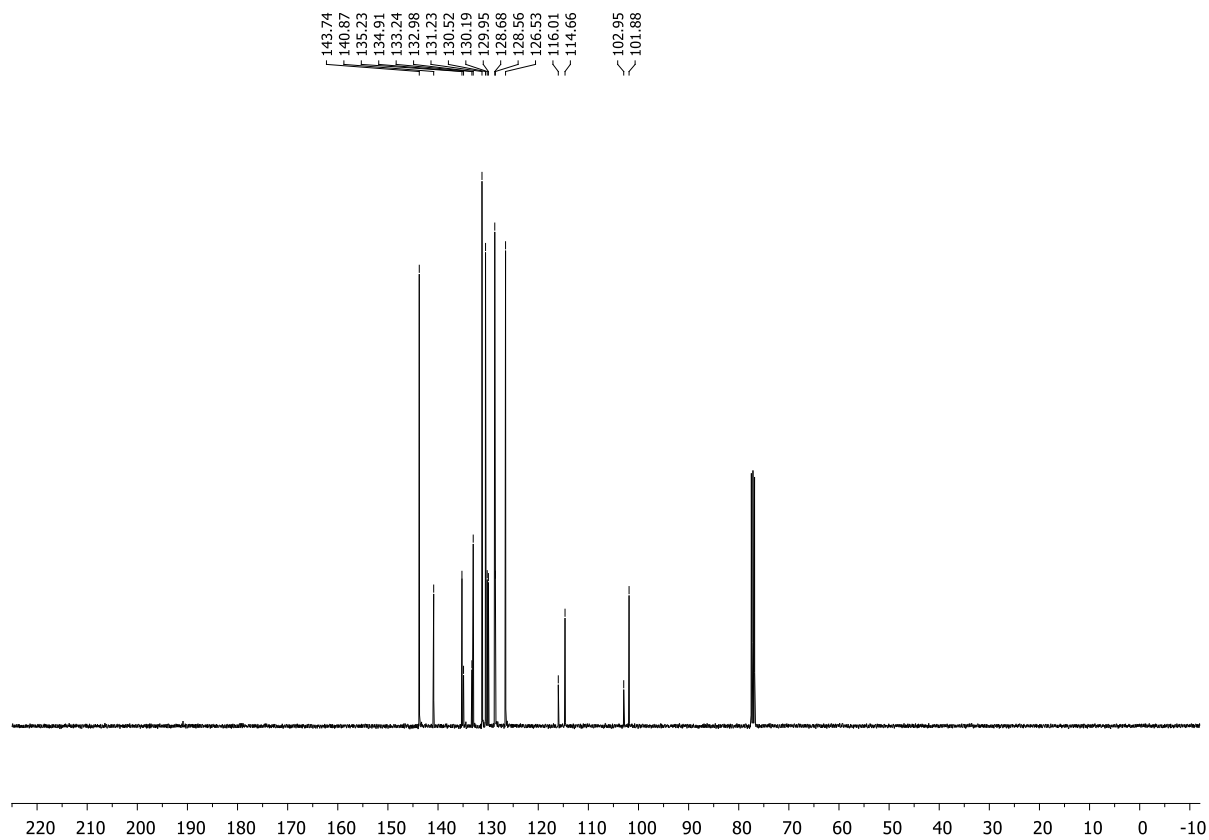
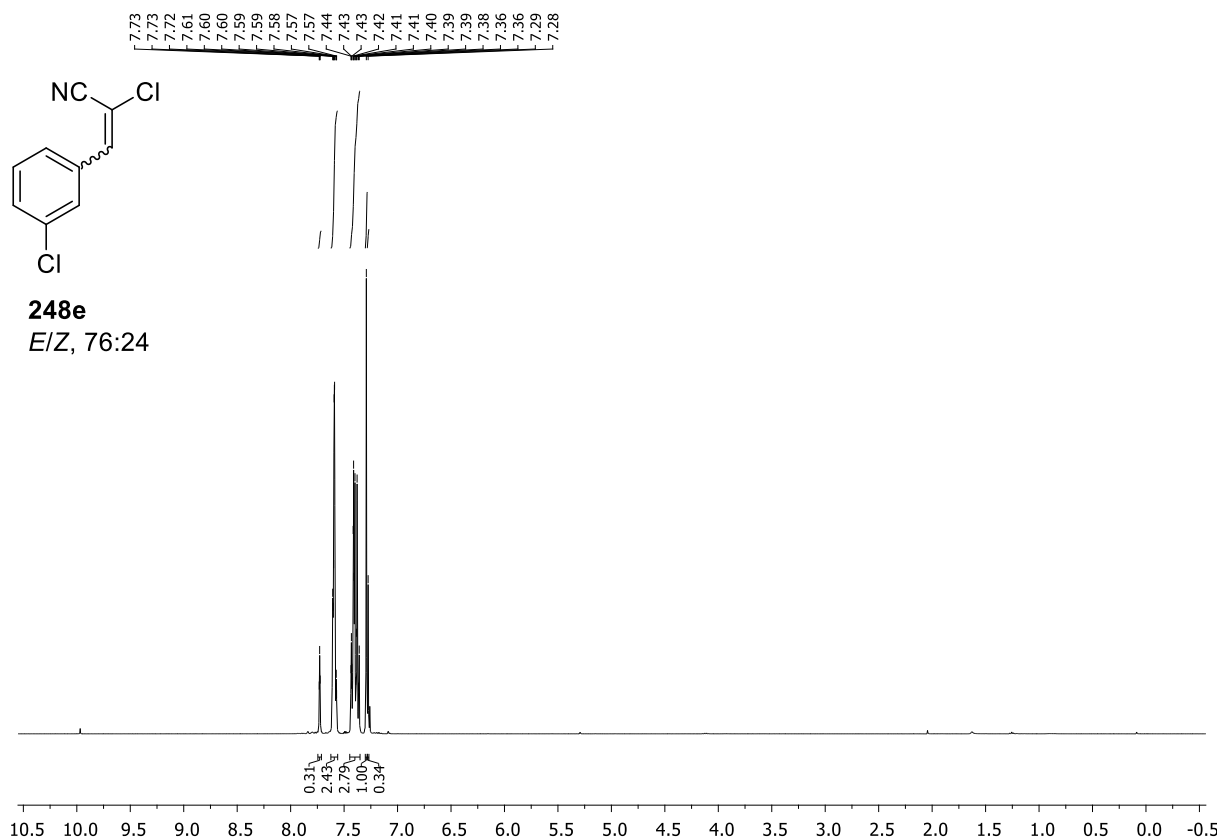




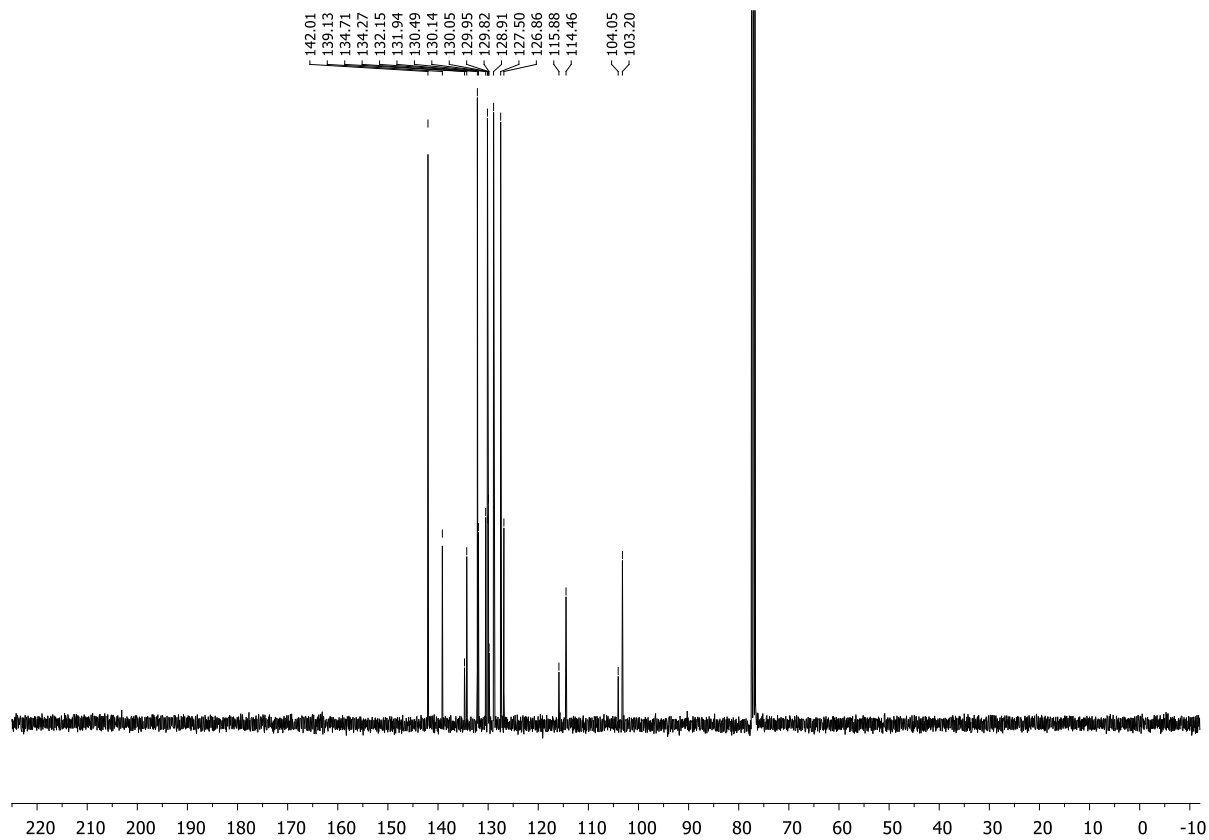
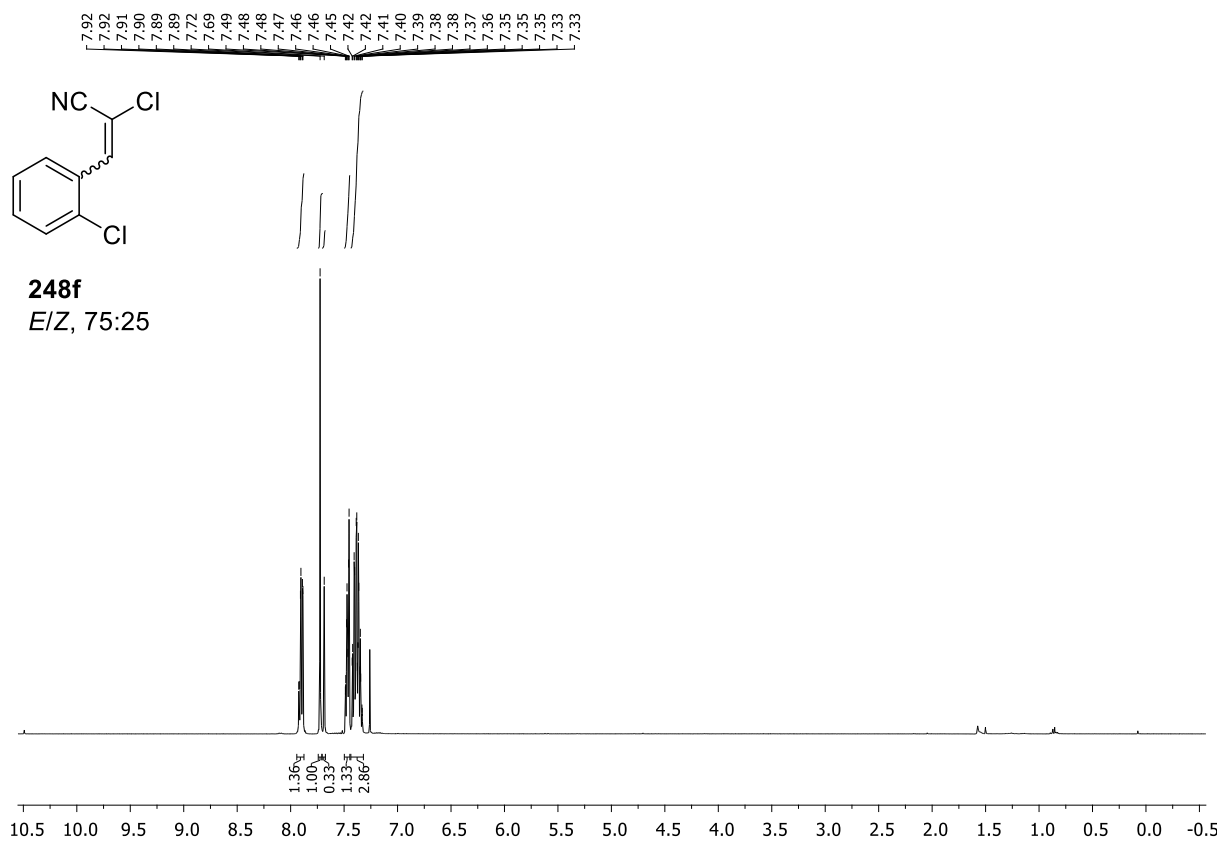
Appendix



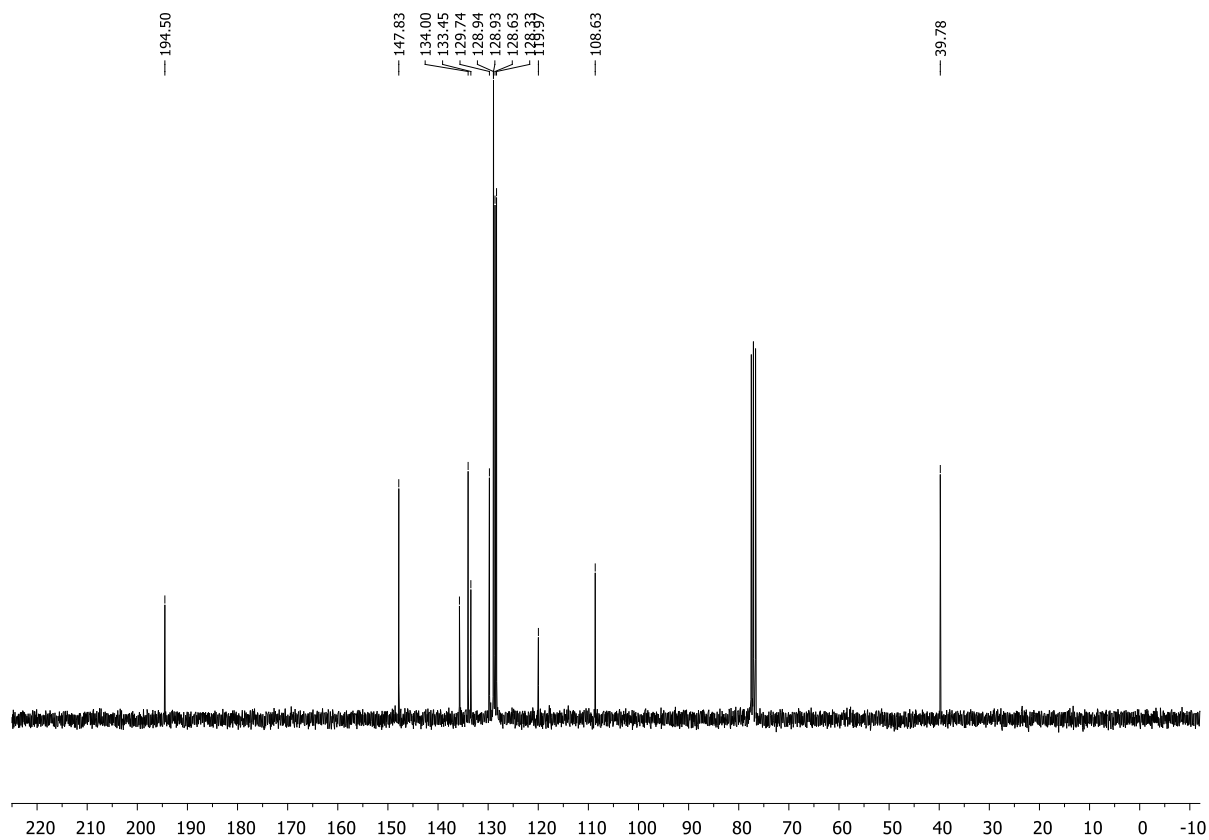
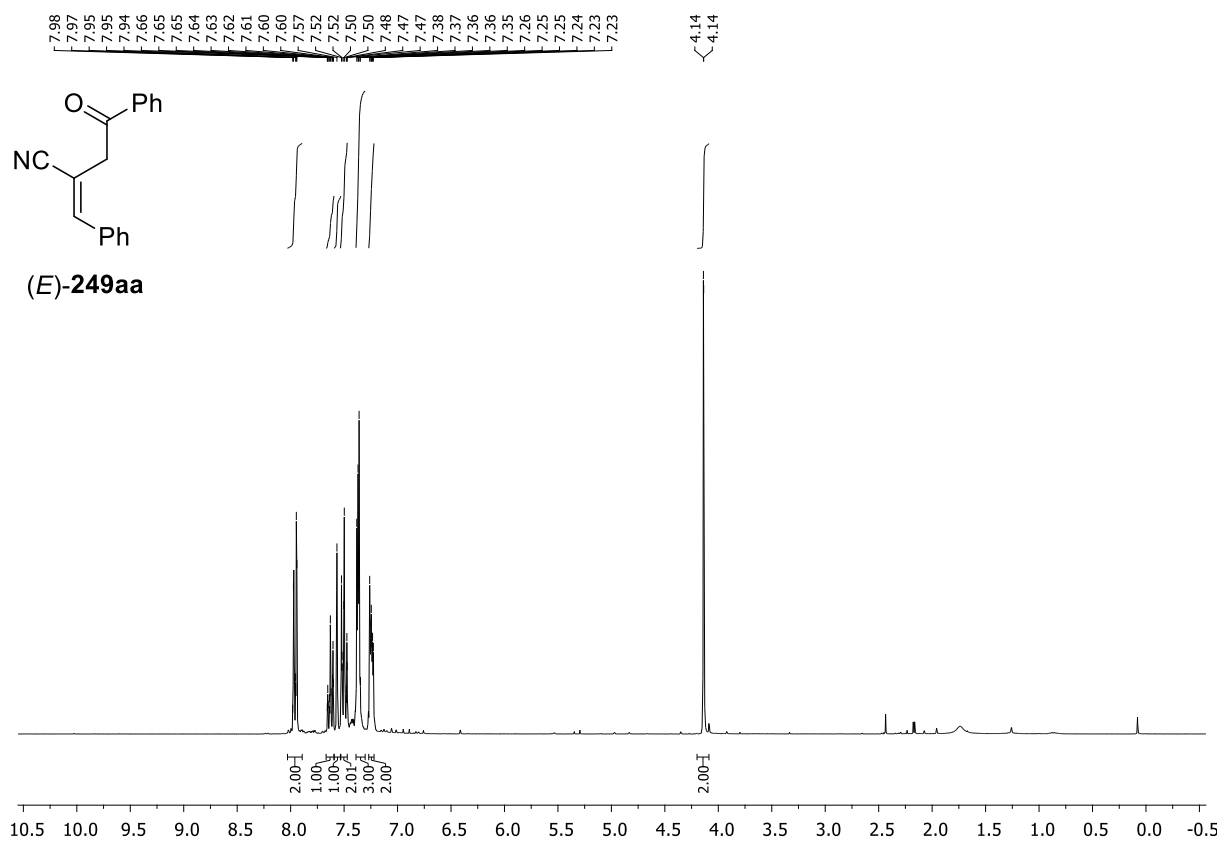


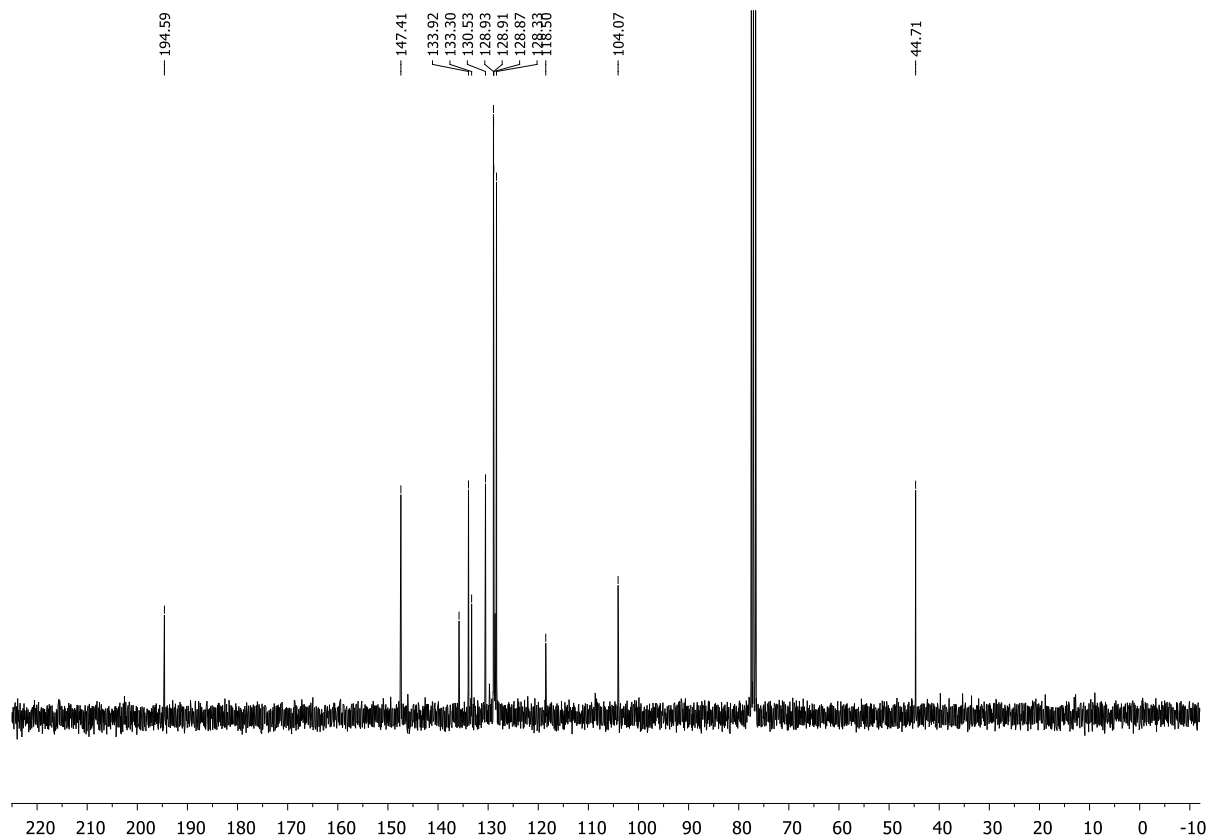
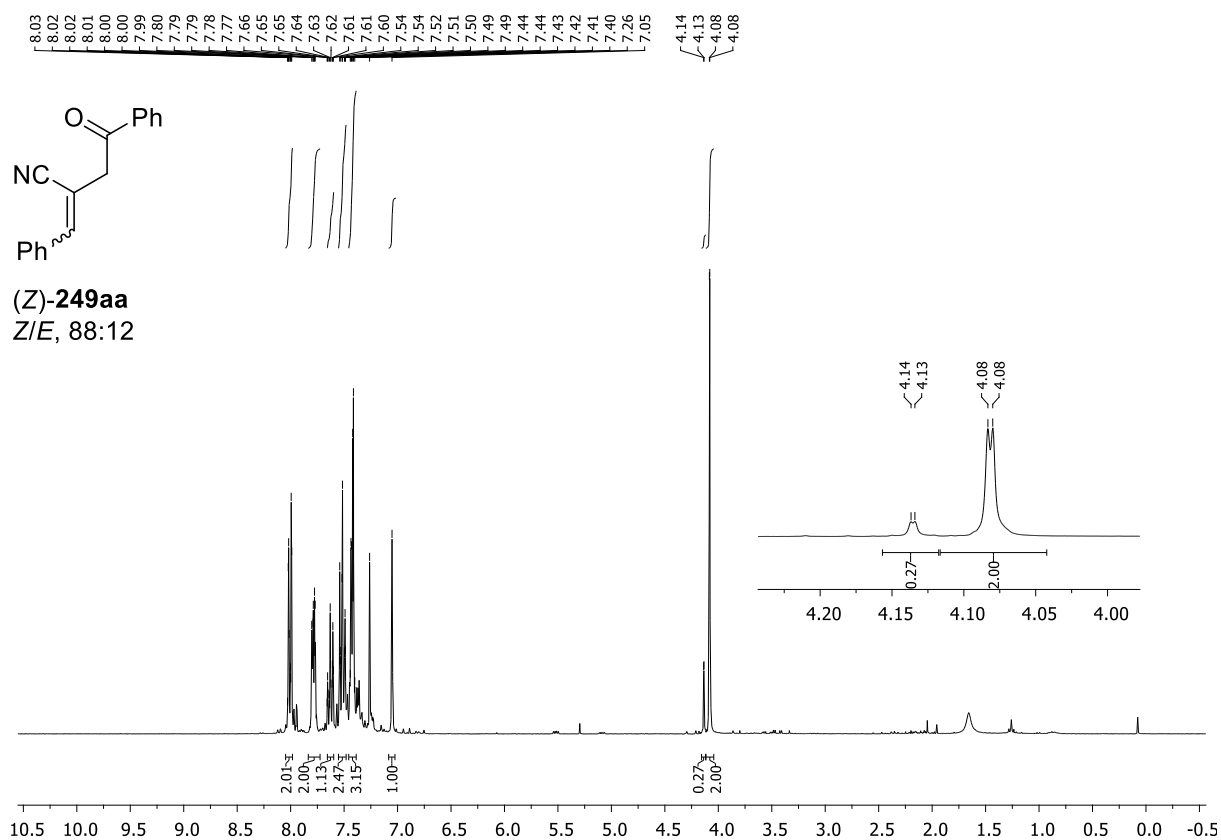


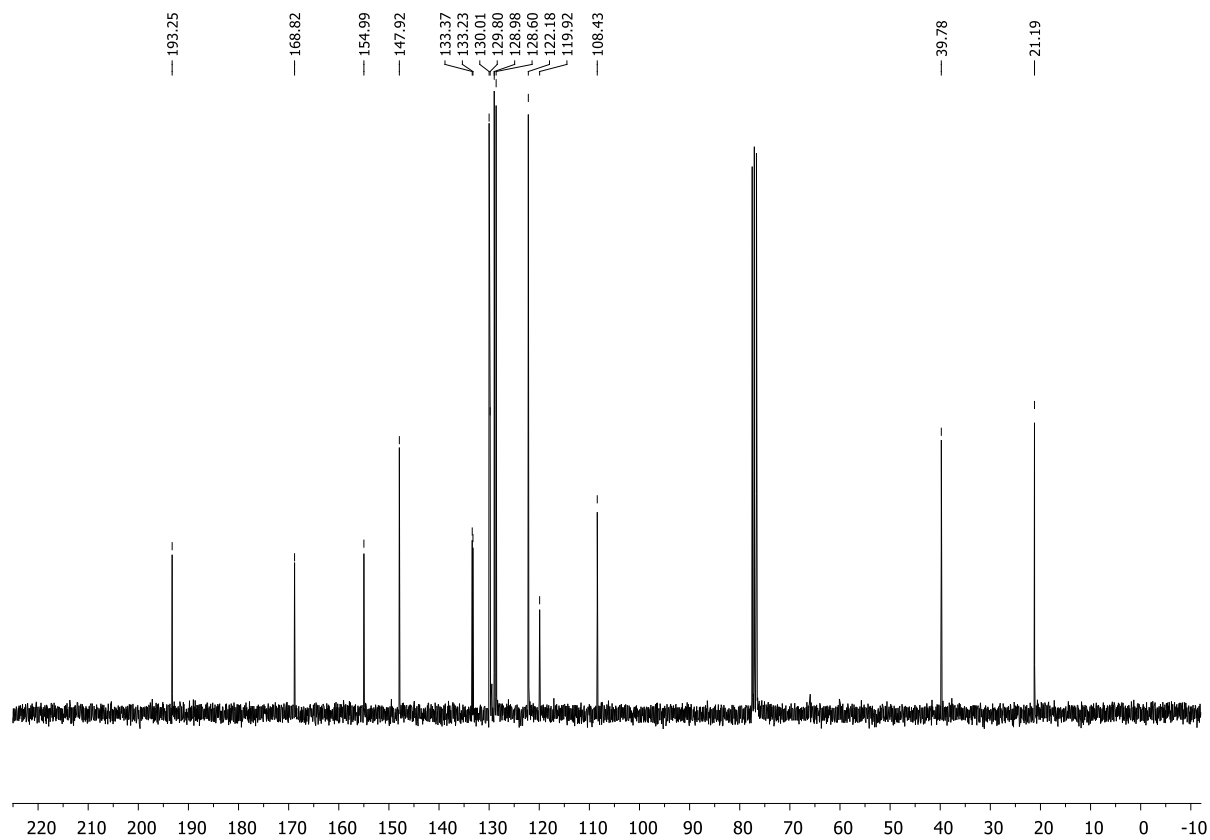
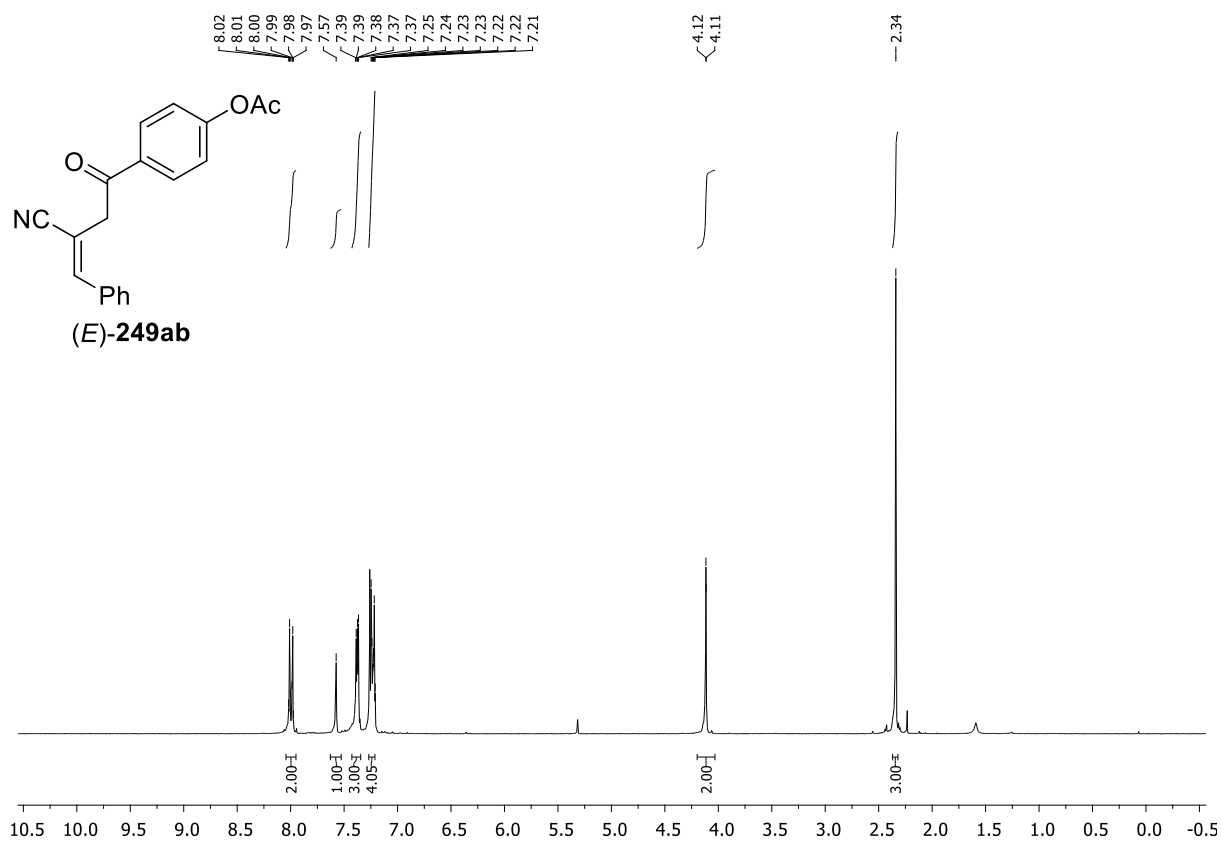
# Appendix



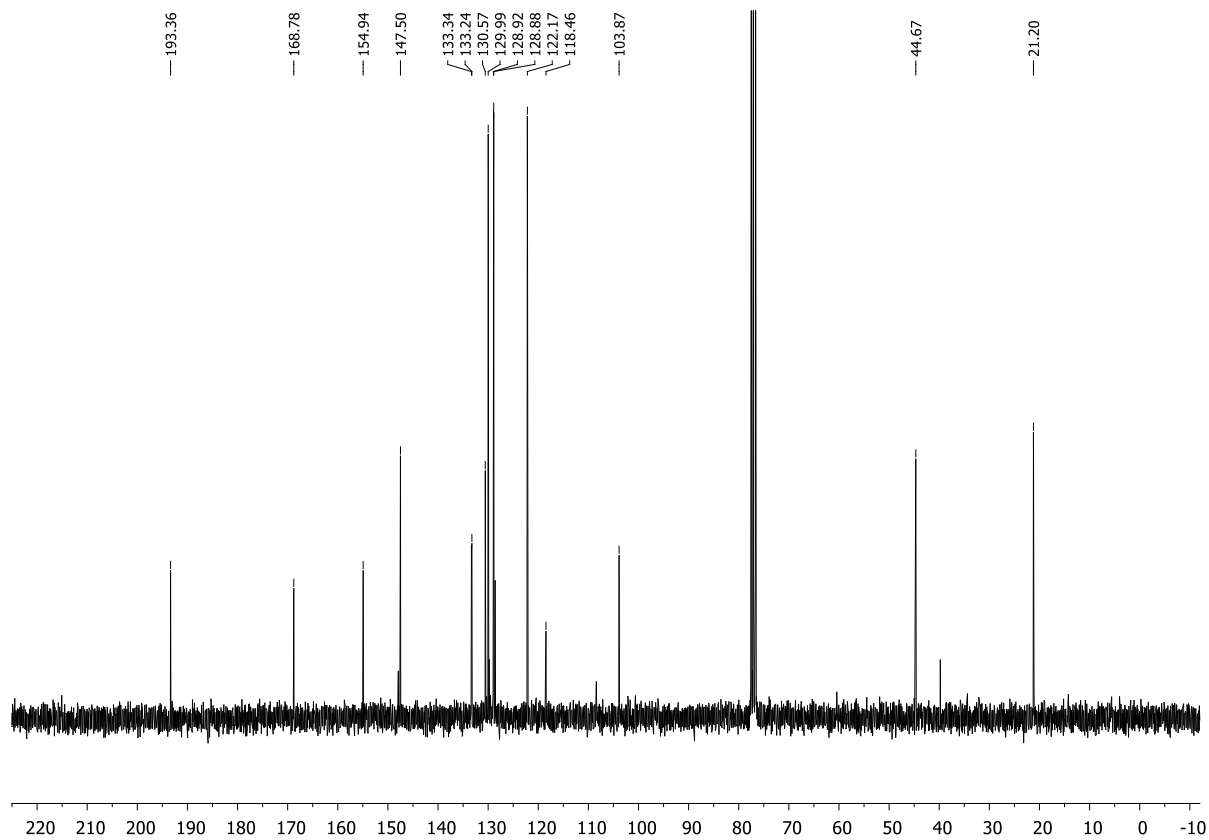
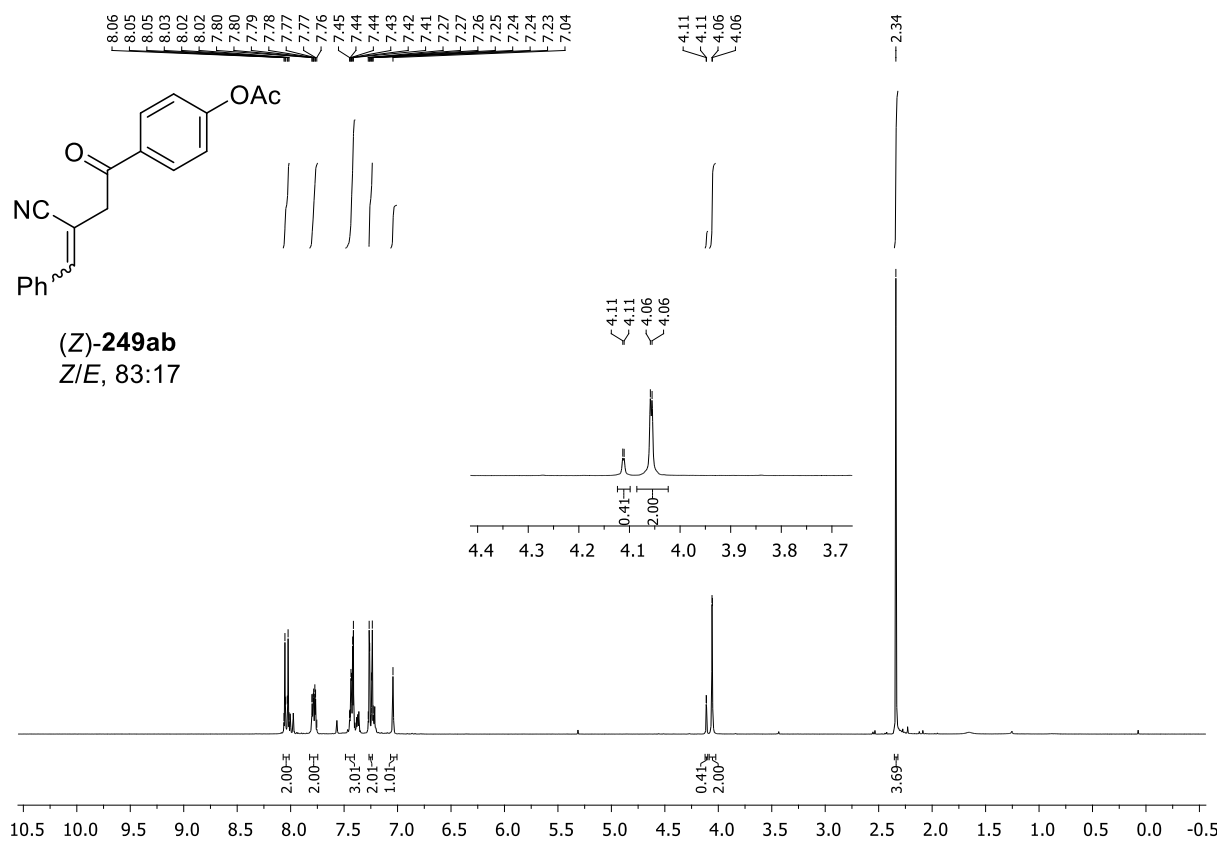


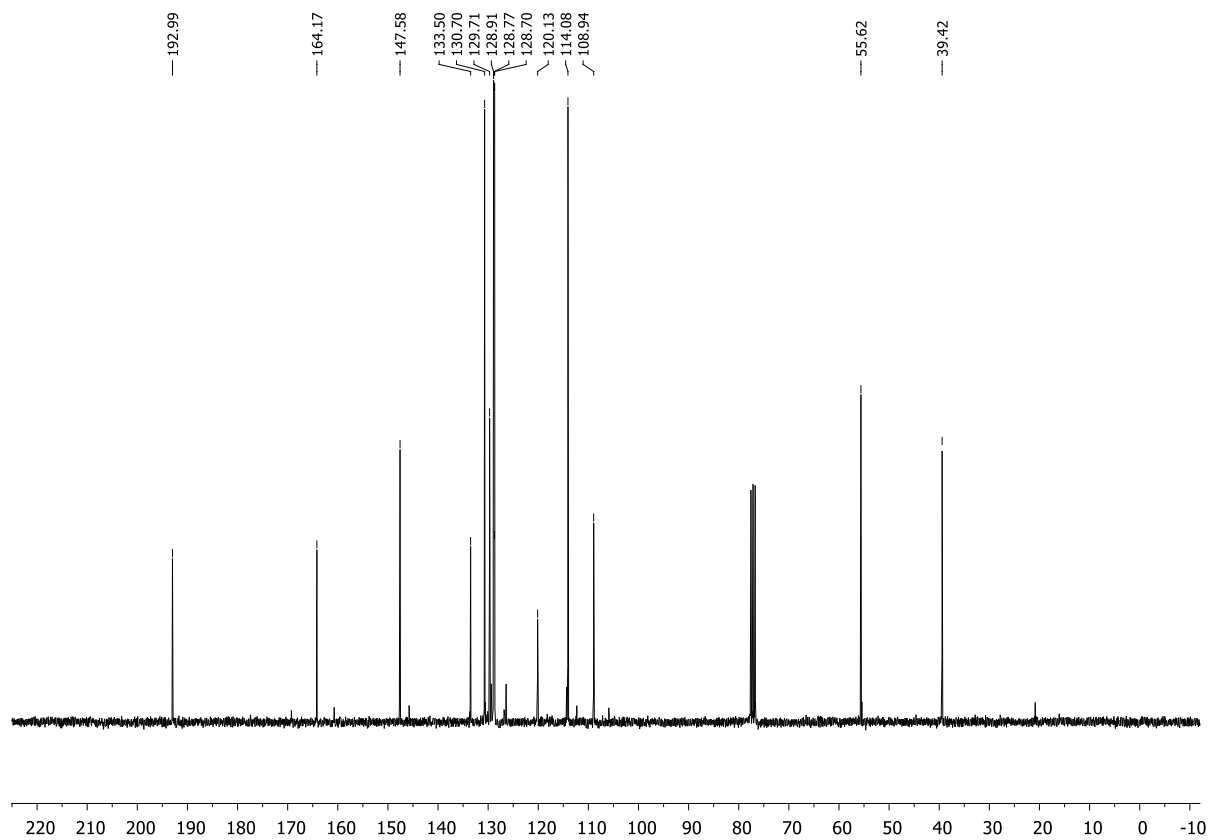
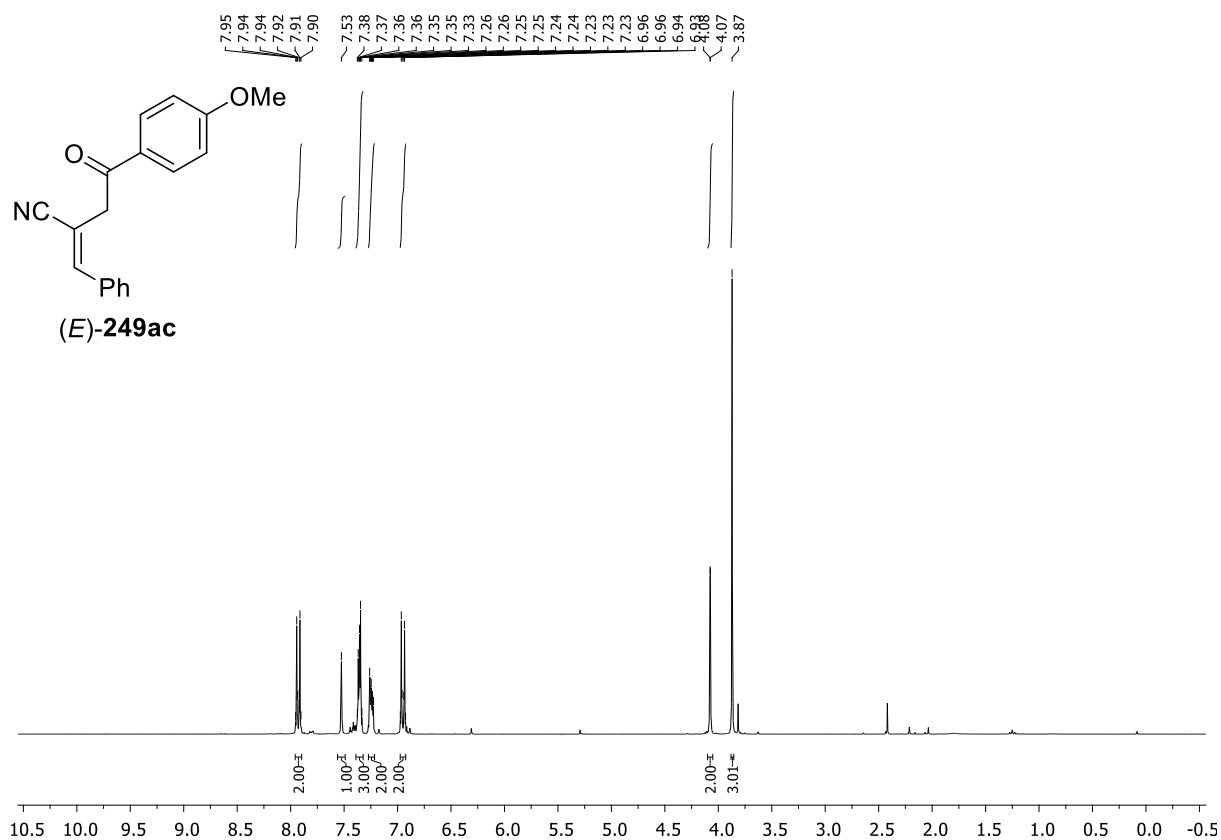


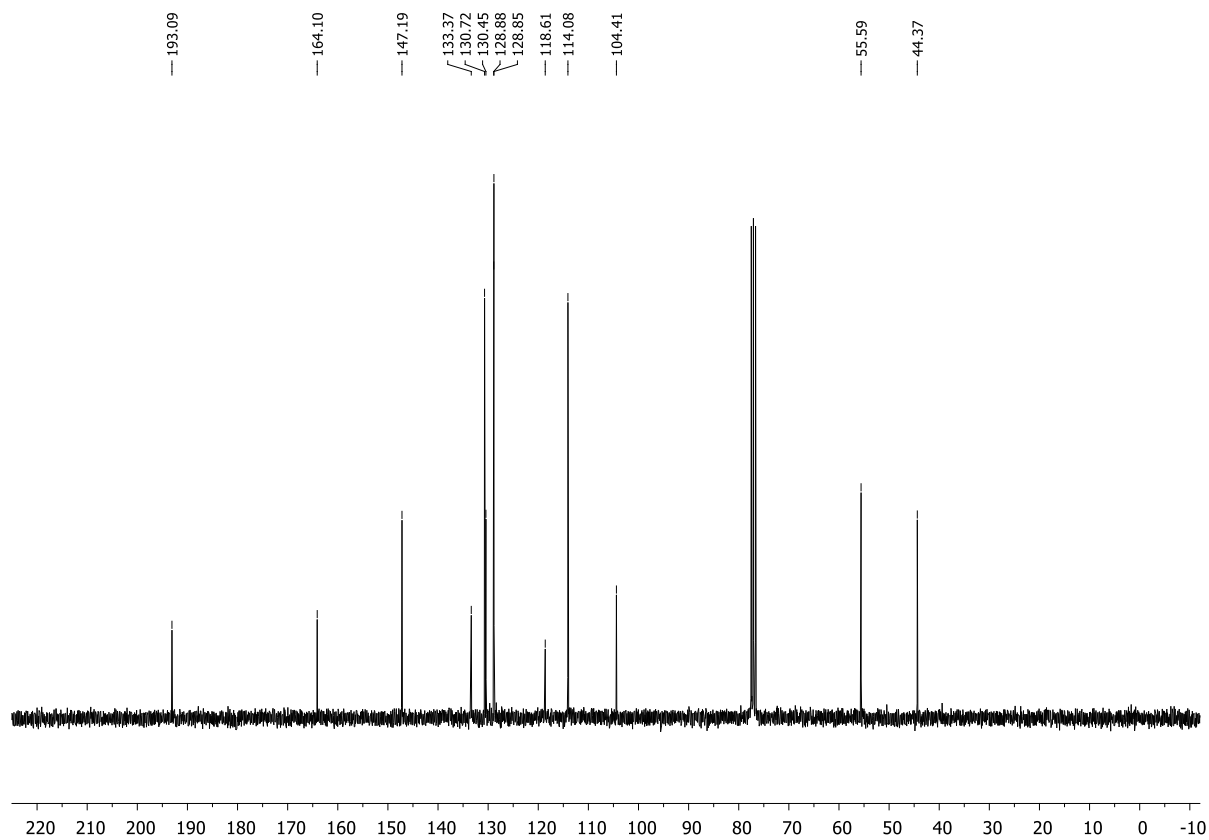
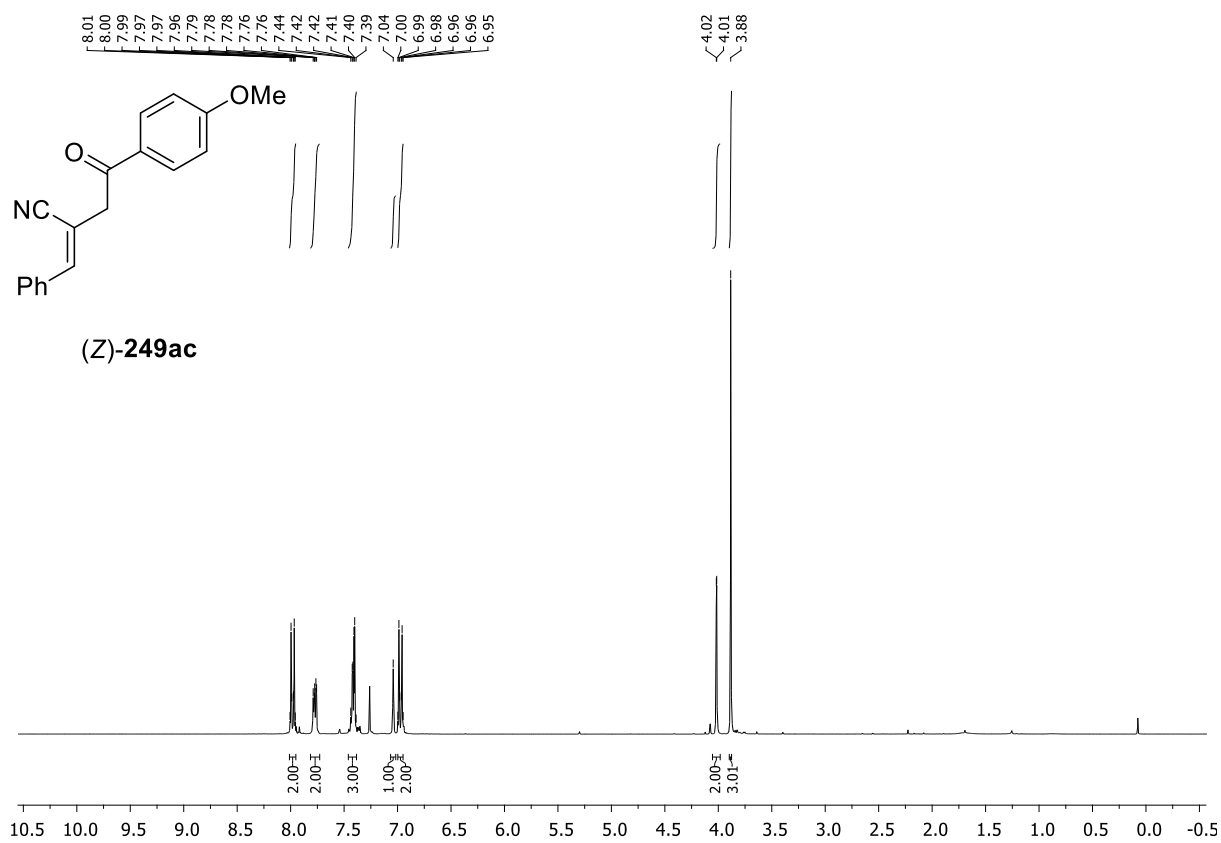


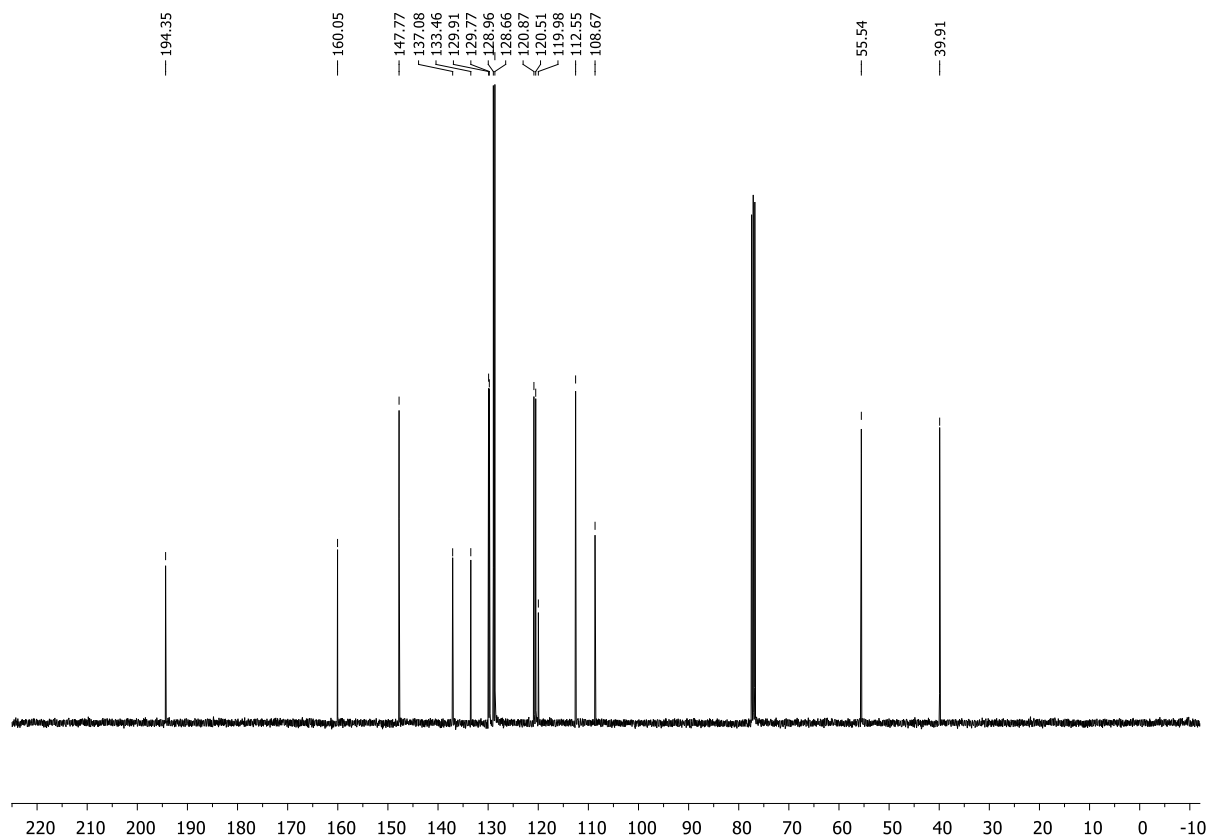
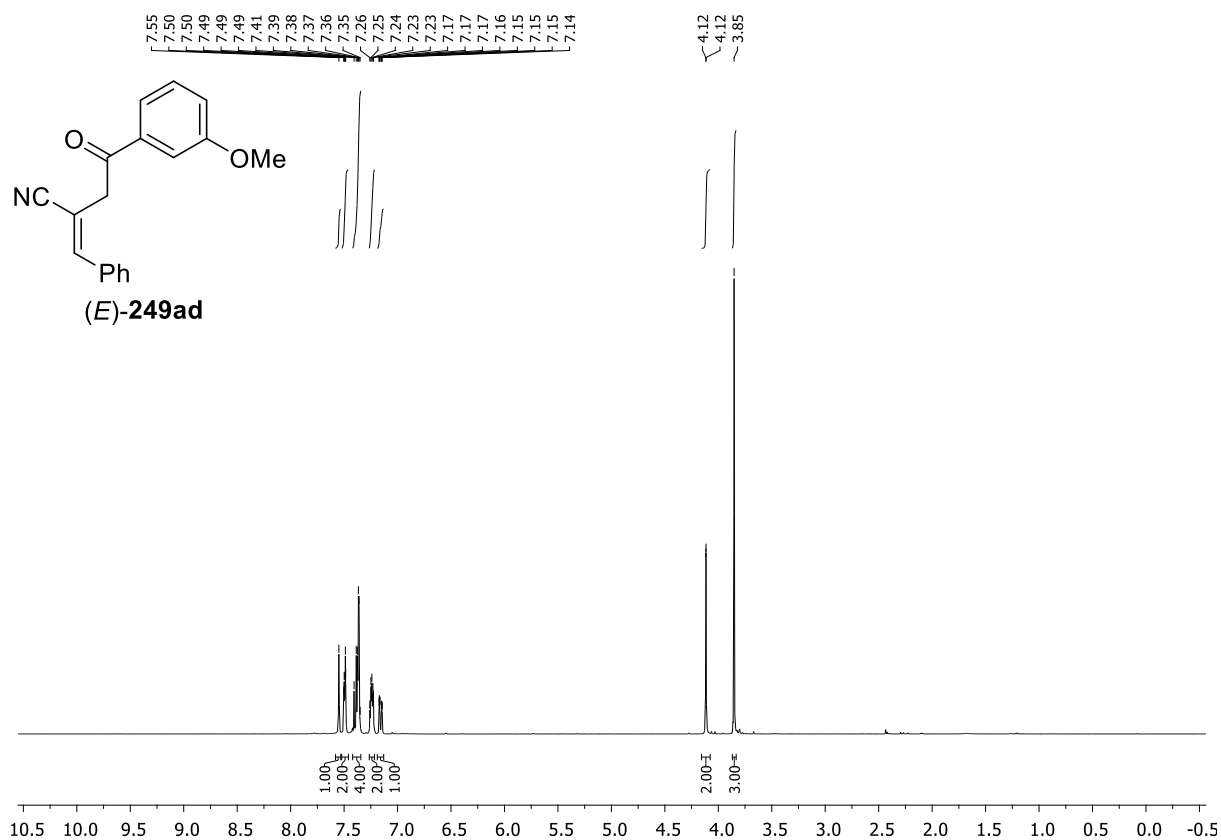


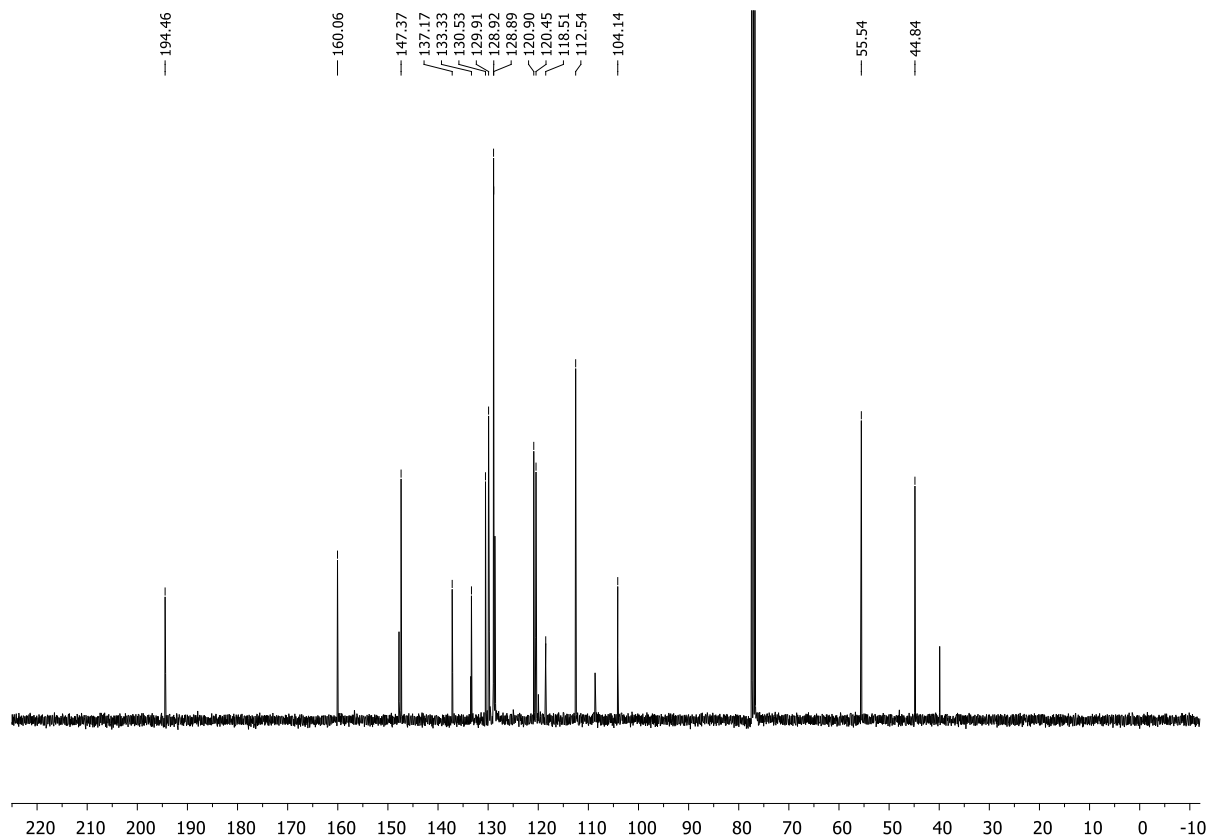
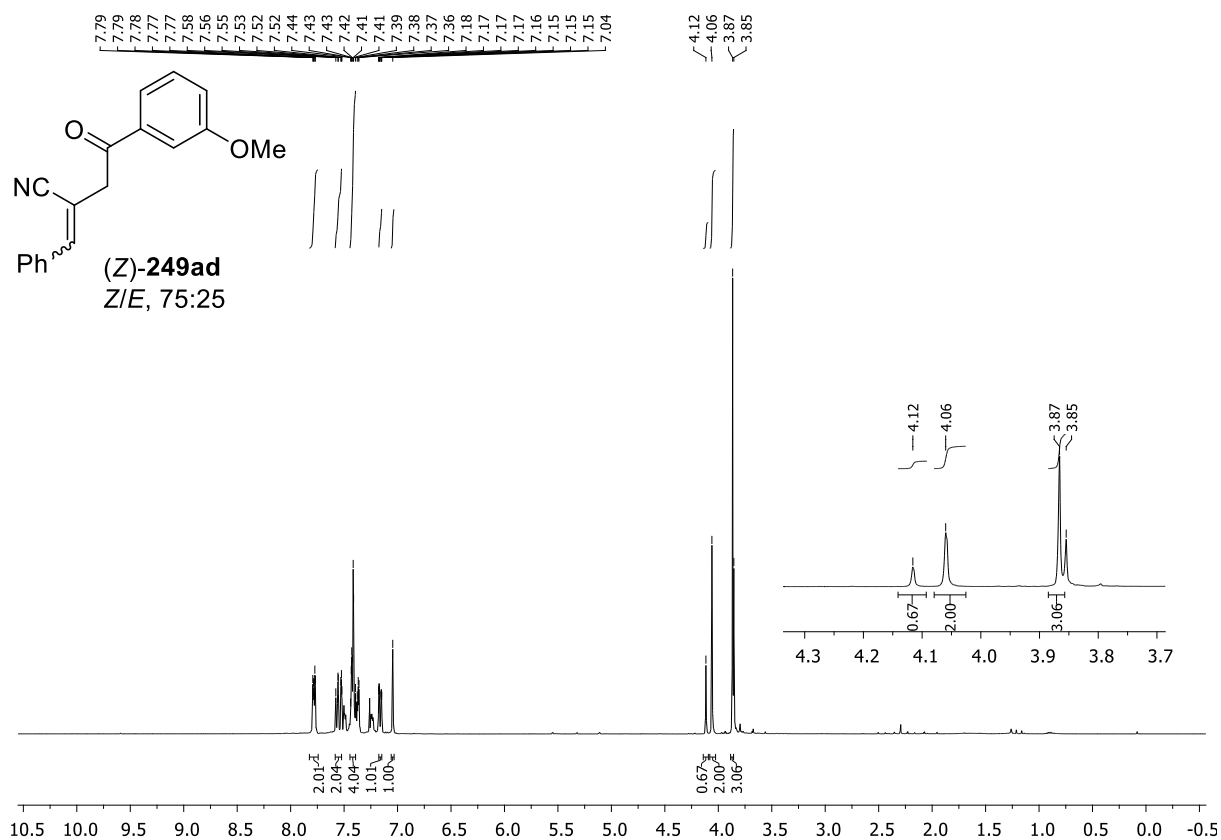
# Appendix



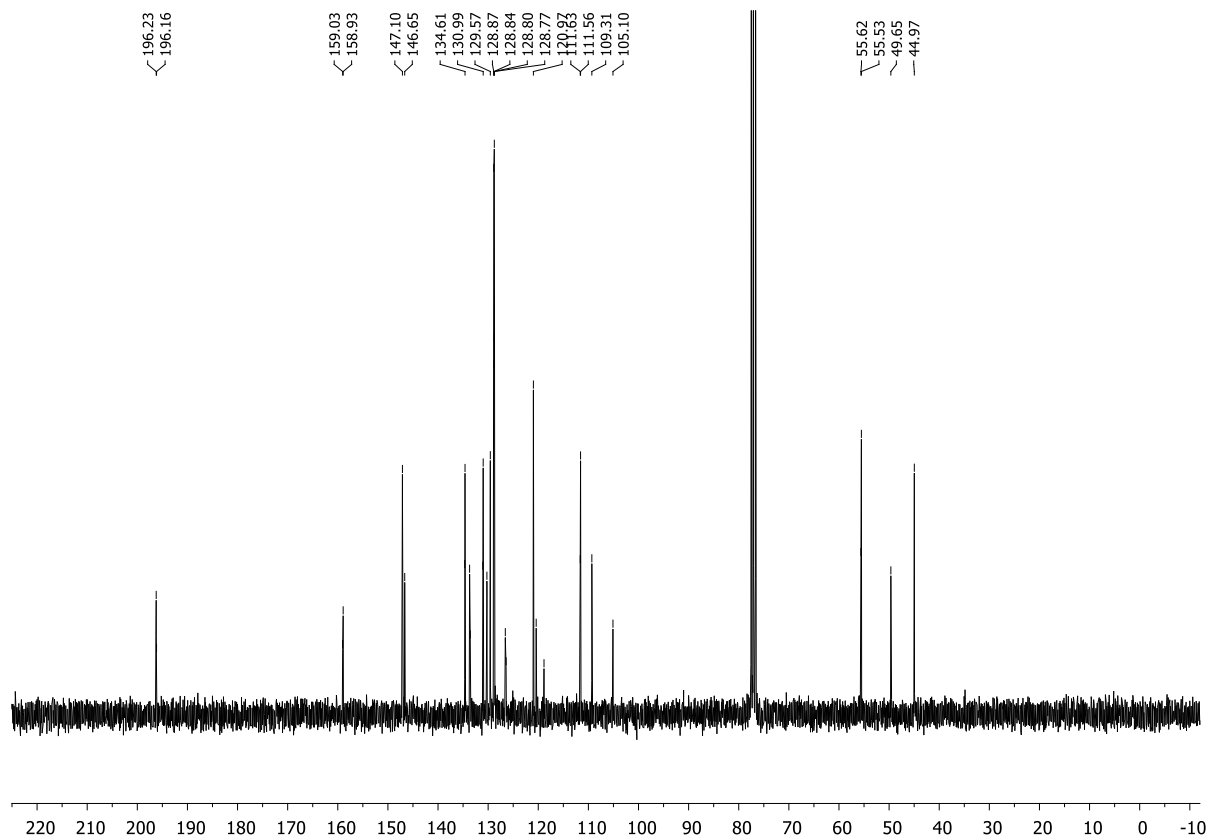
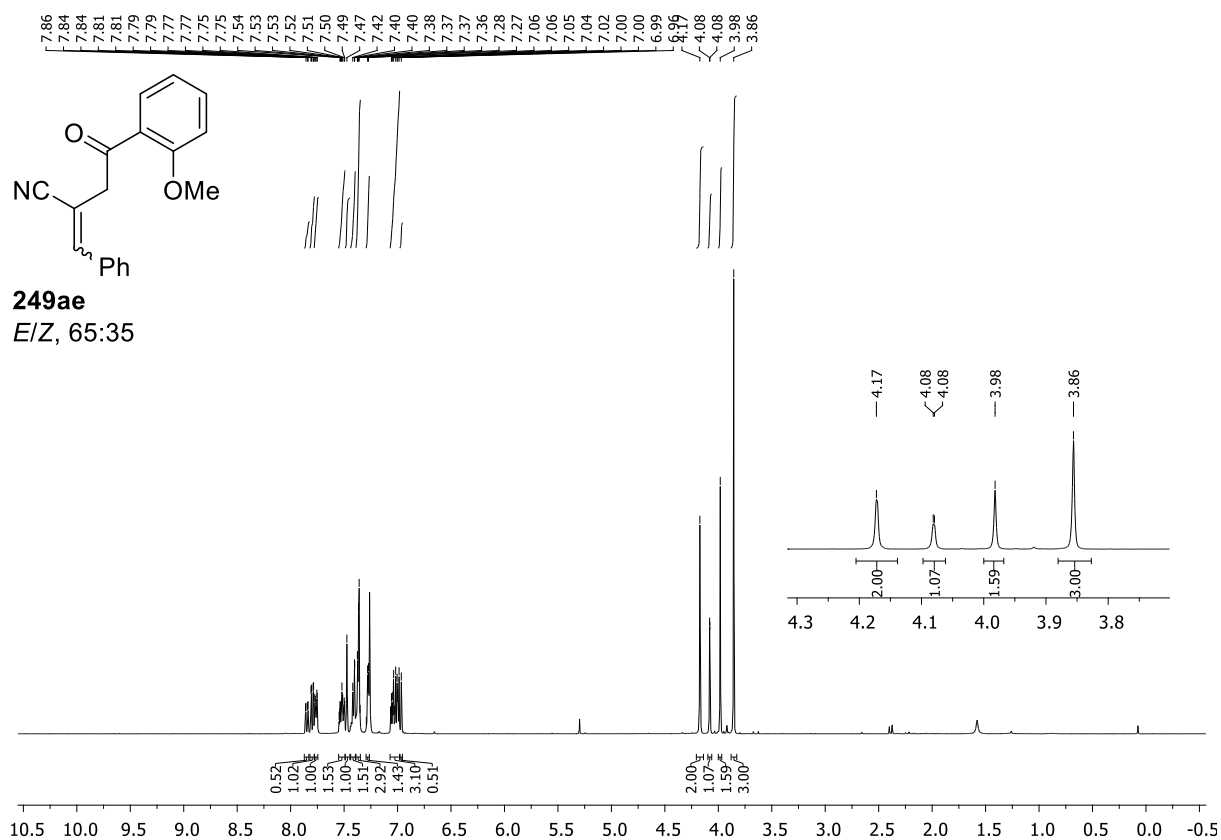


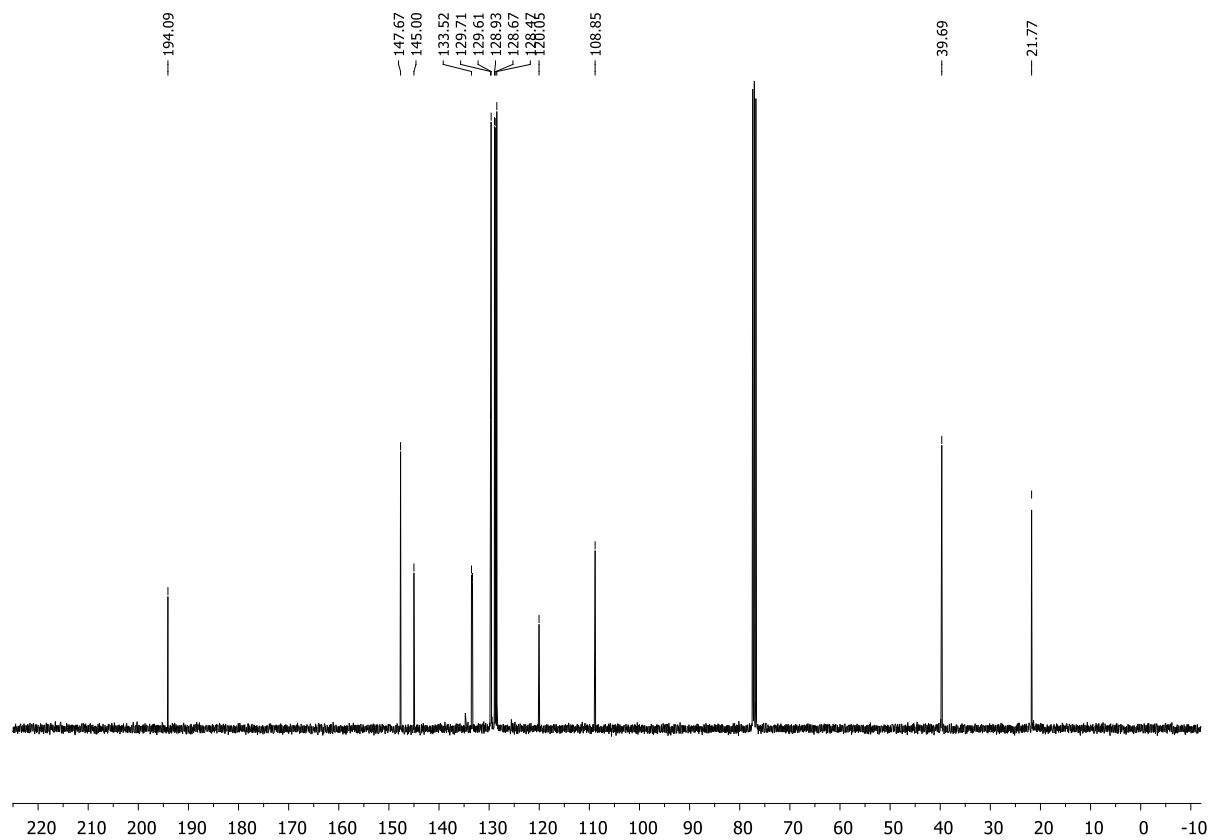
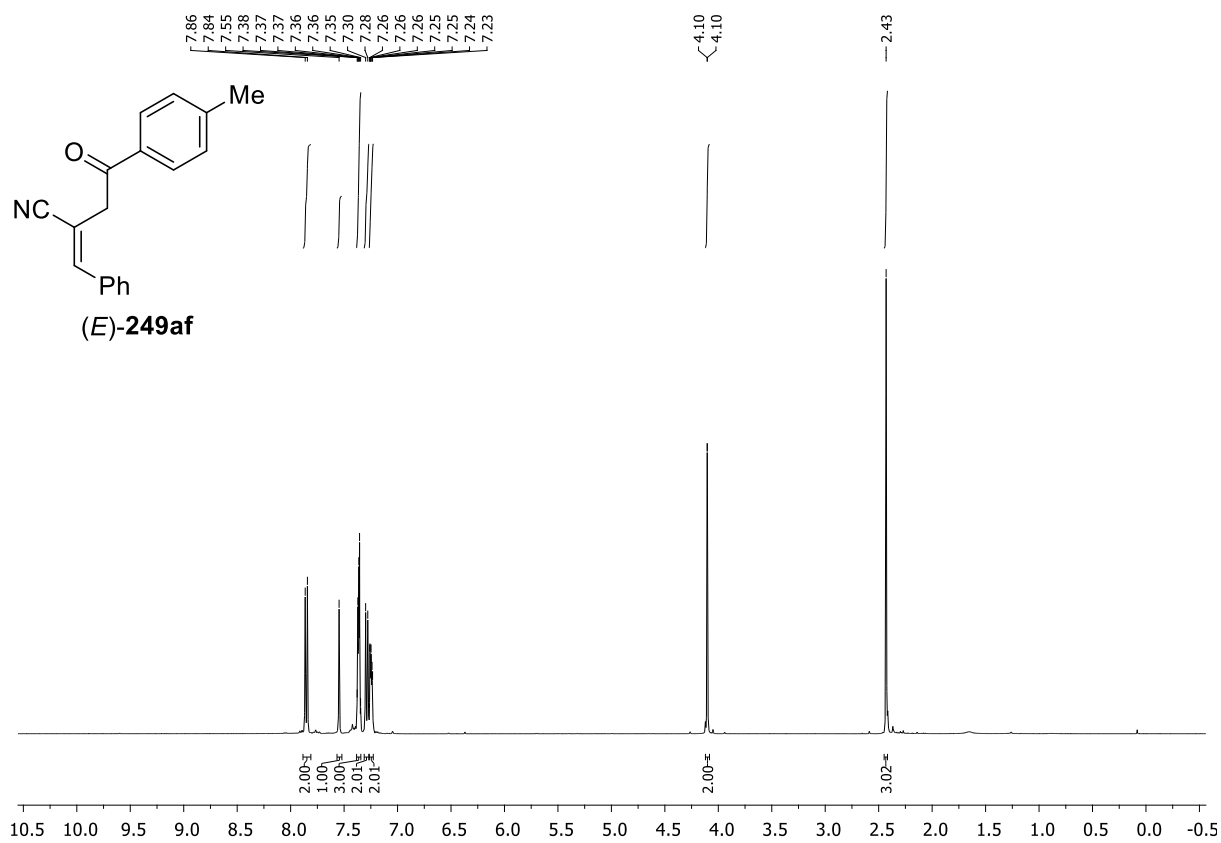


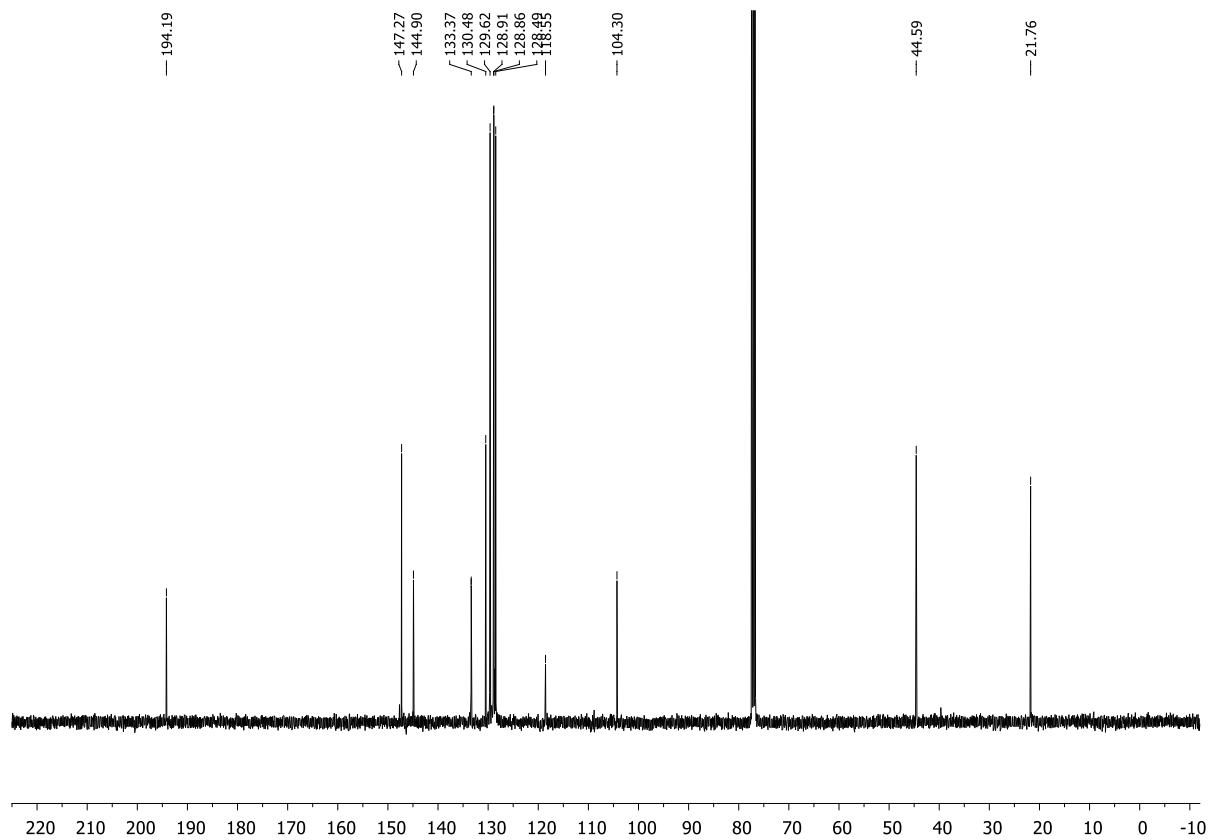
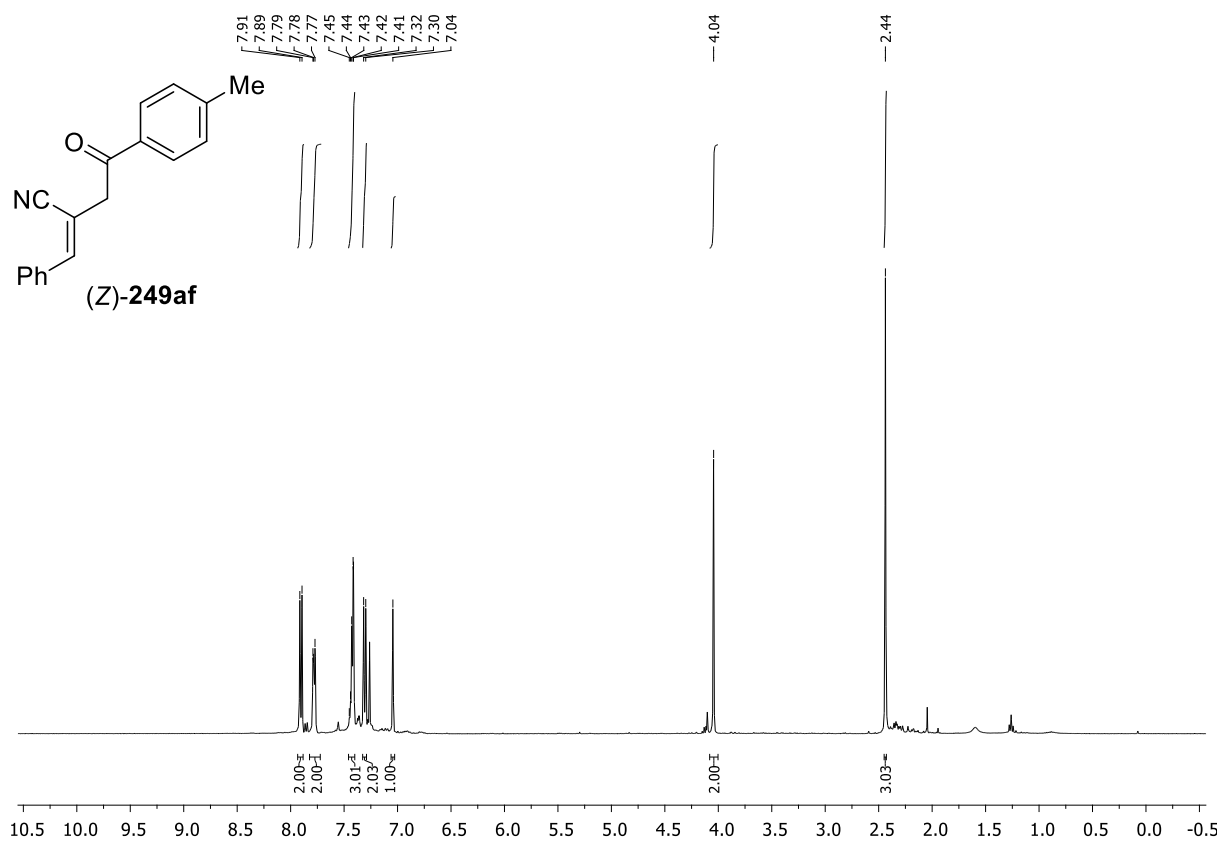


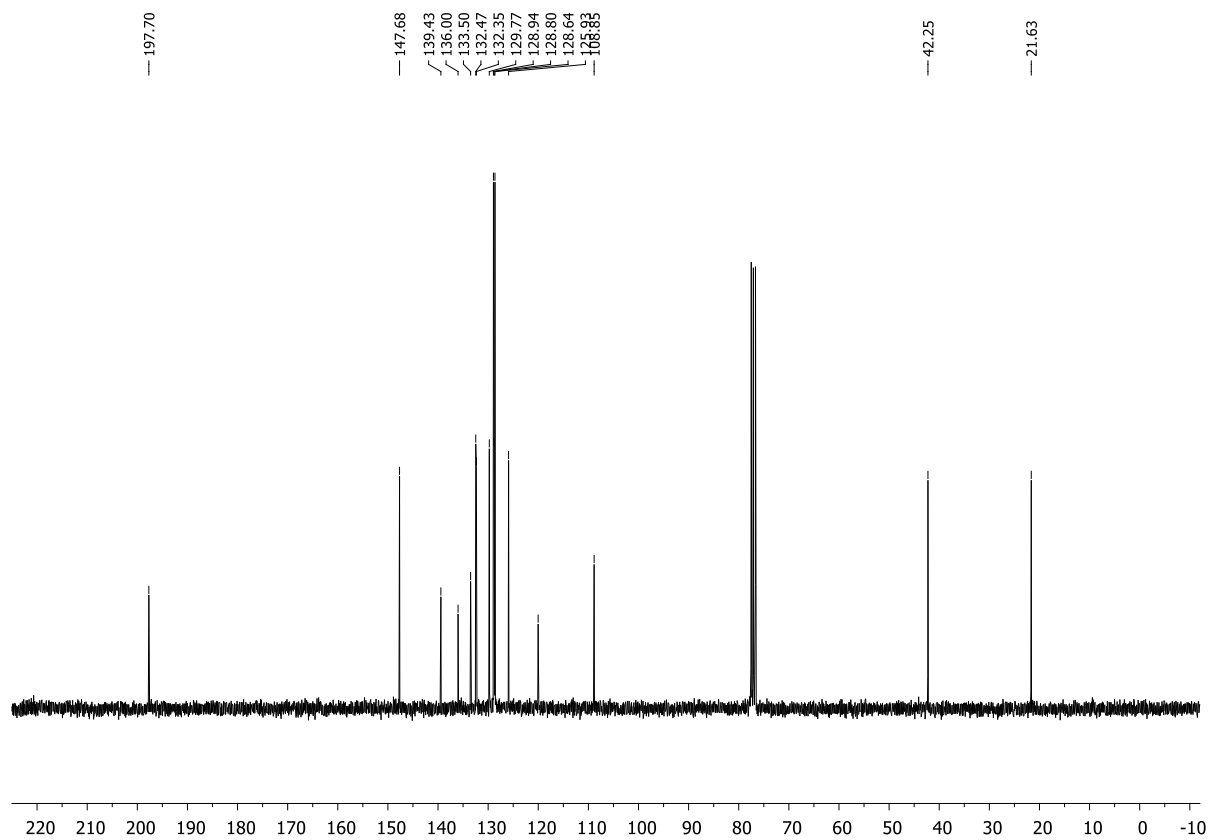
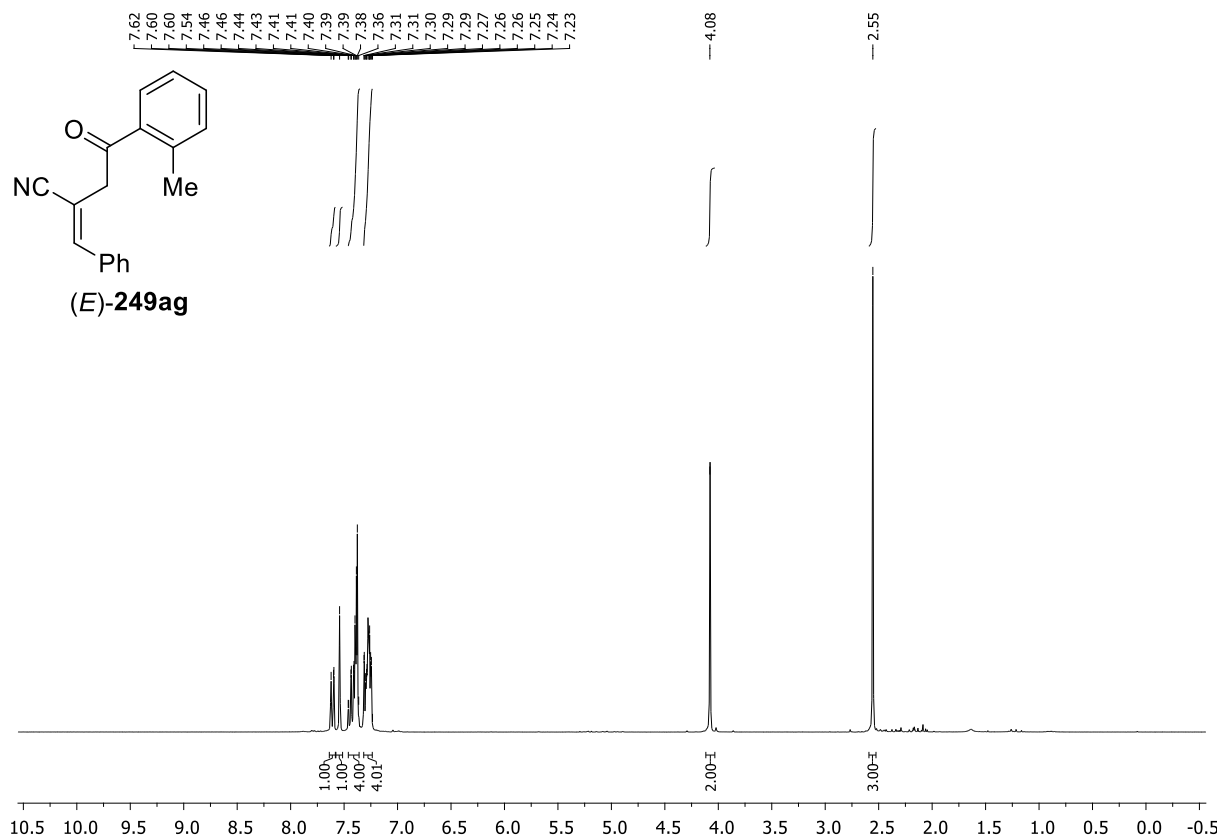


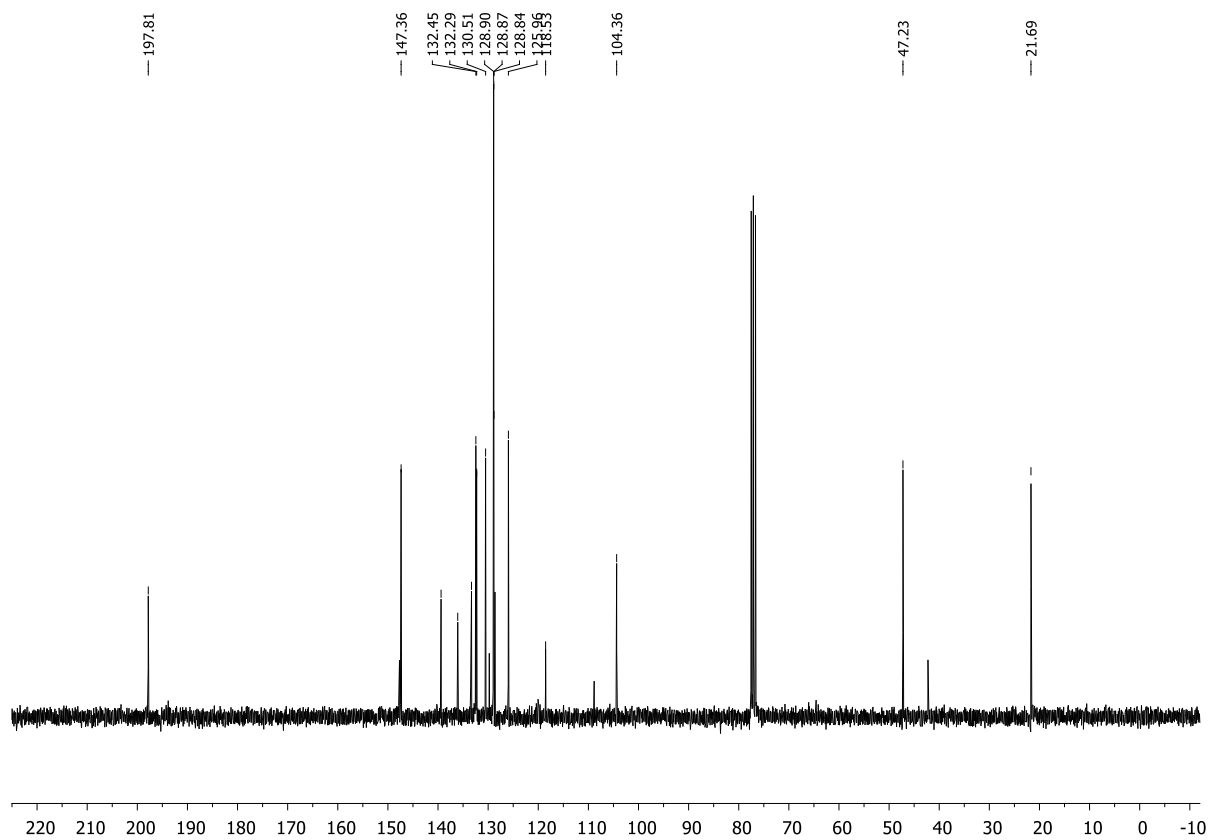
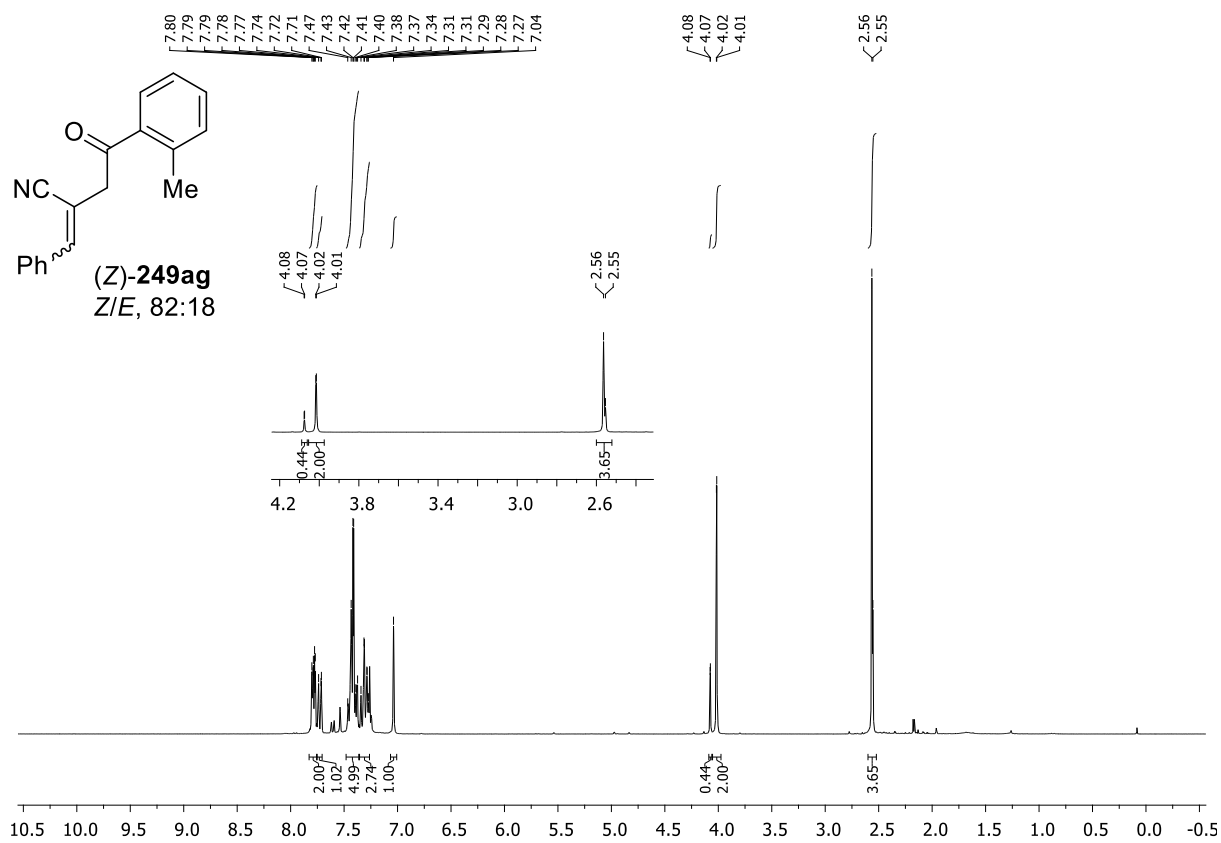


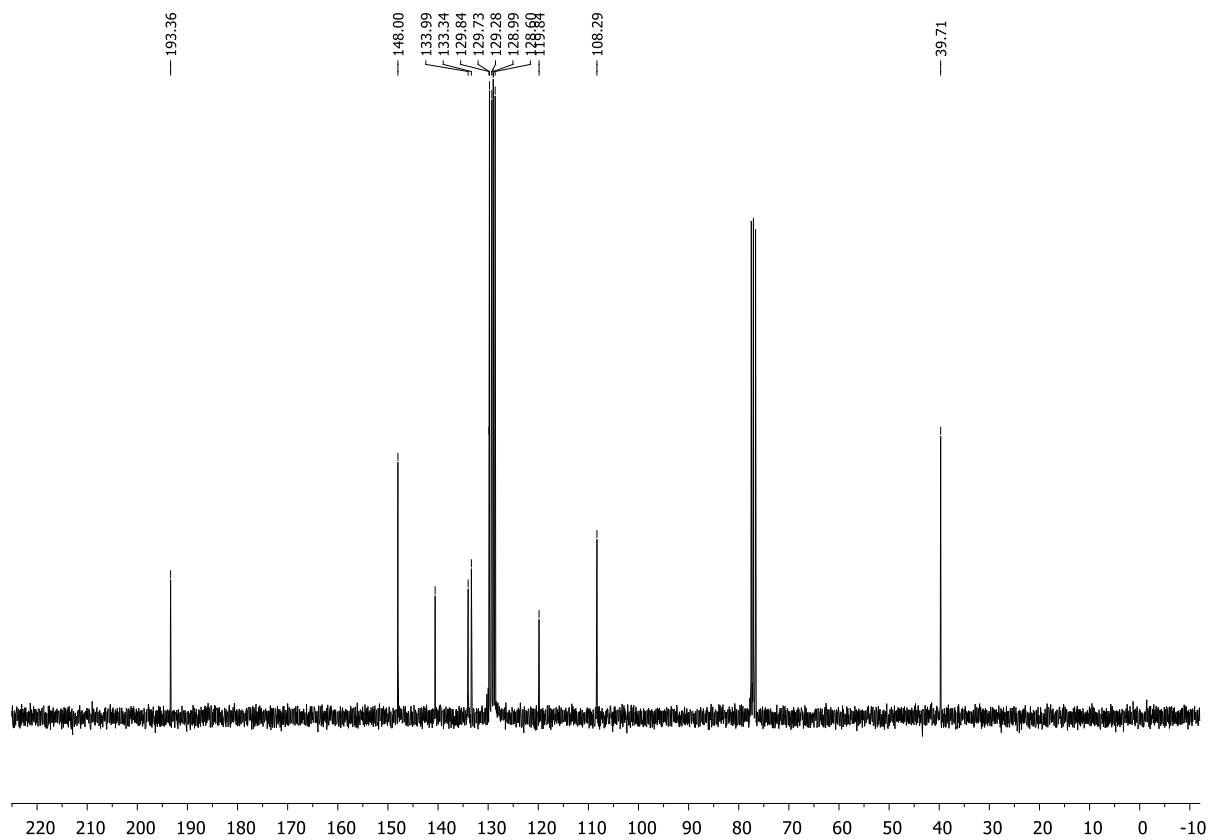
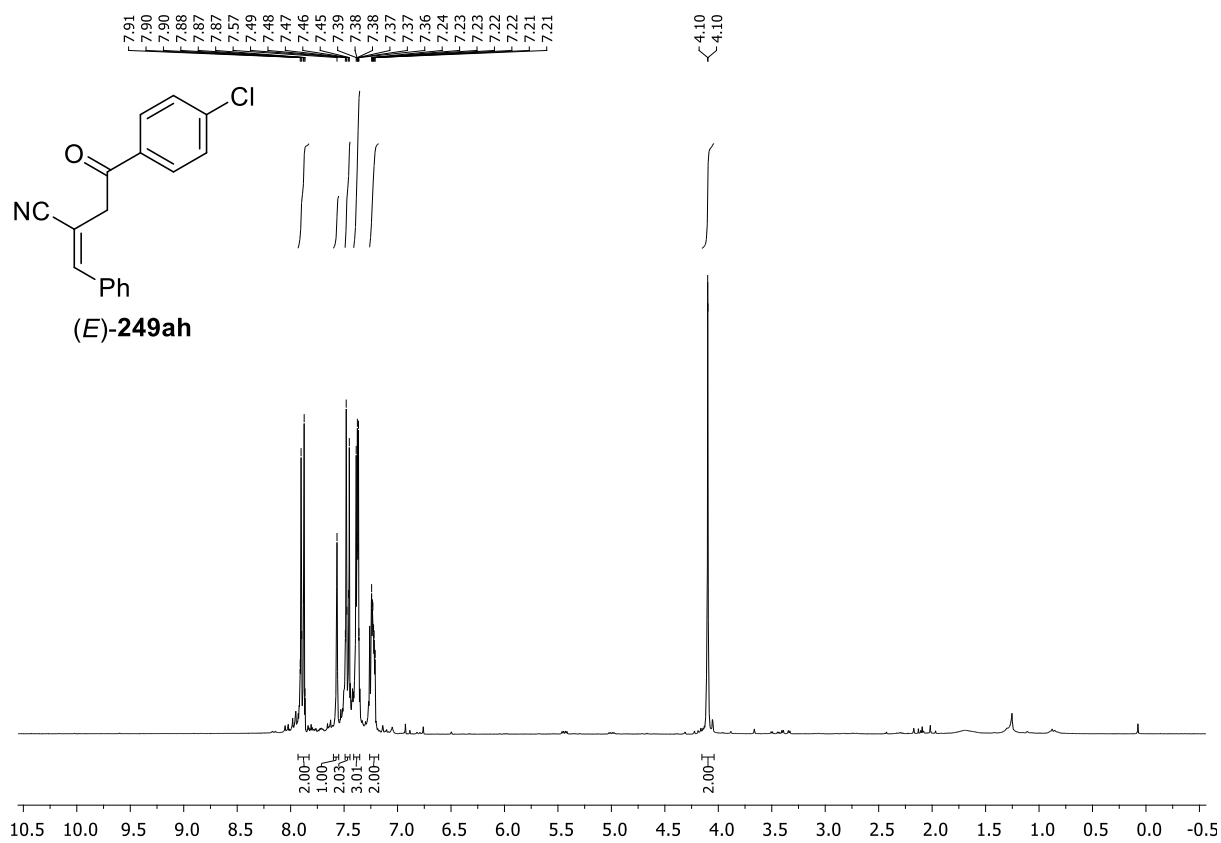


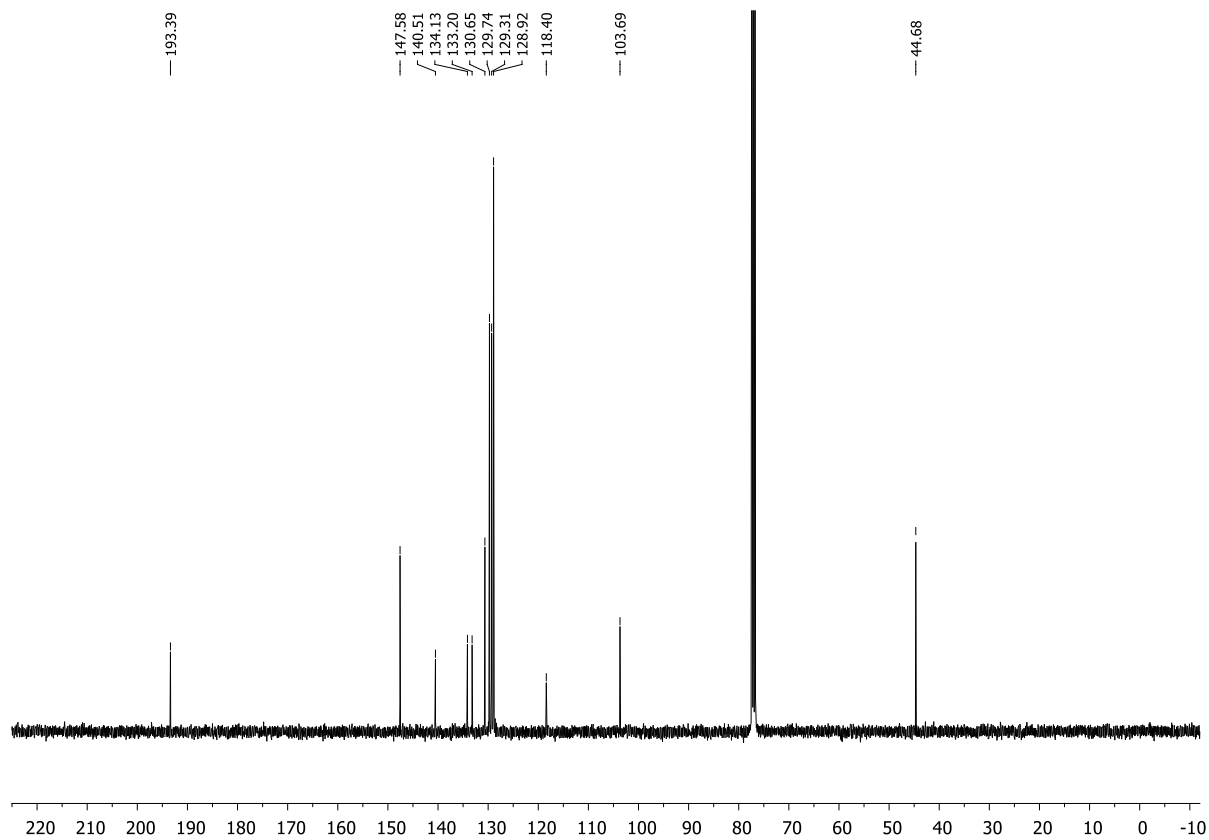
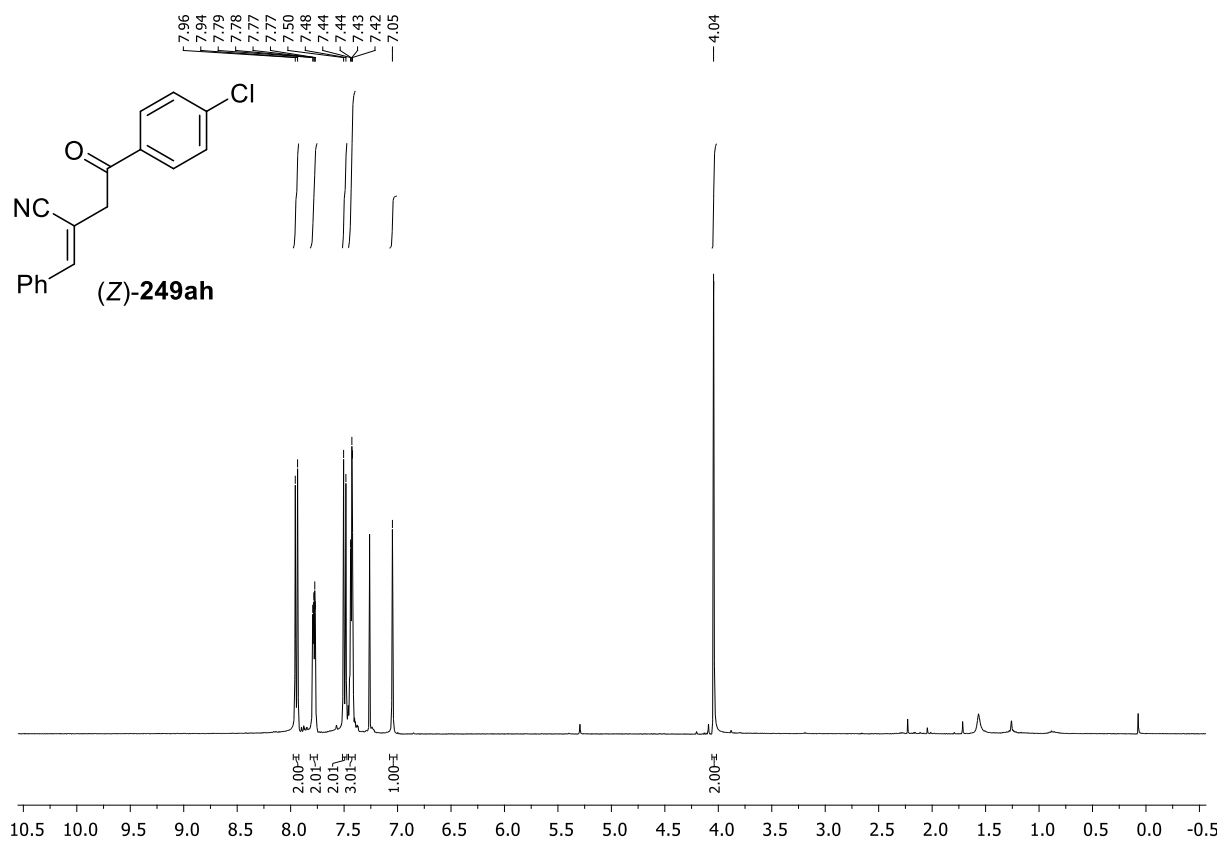


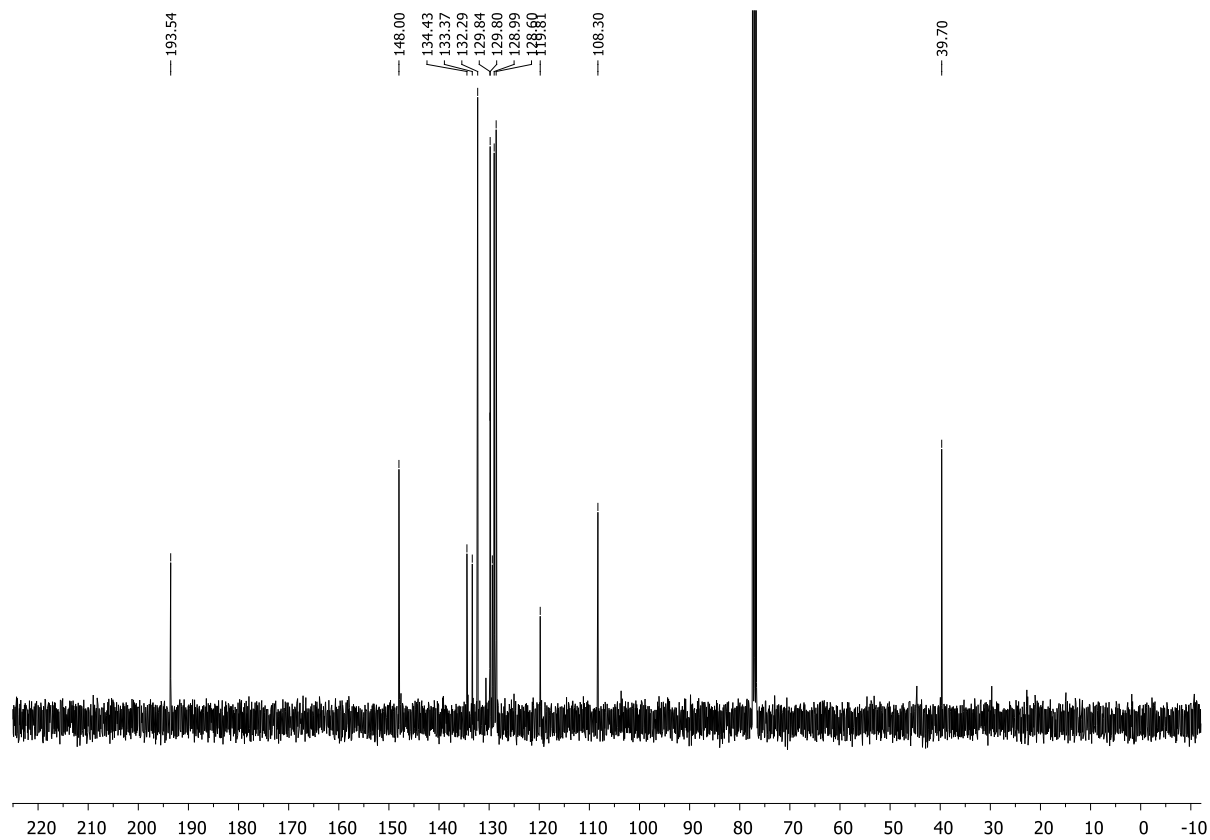
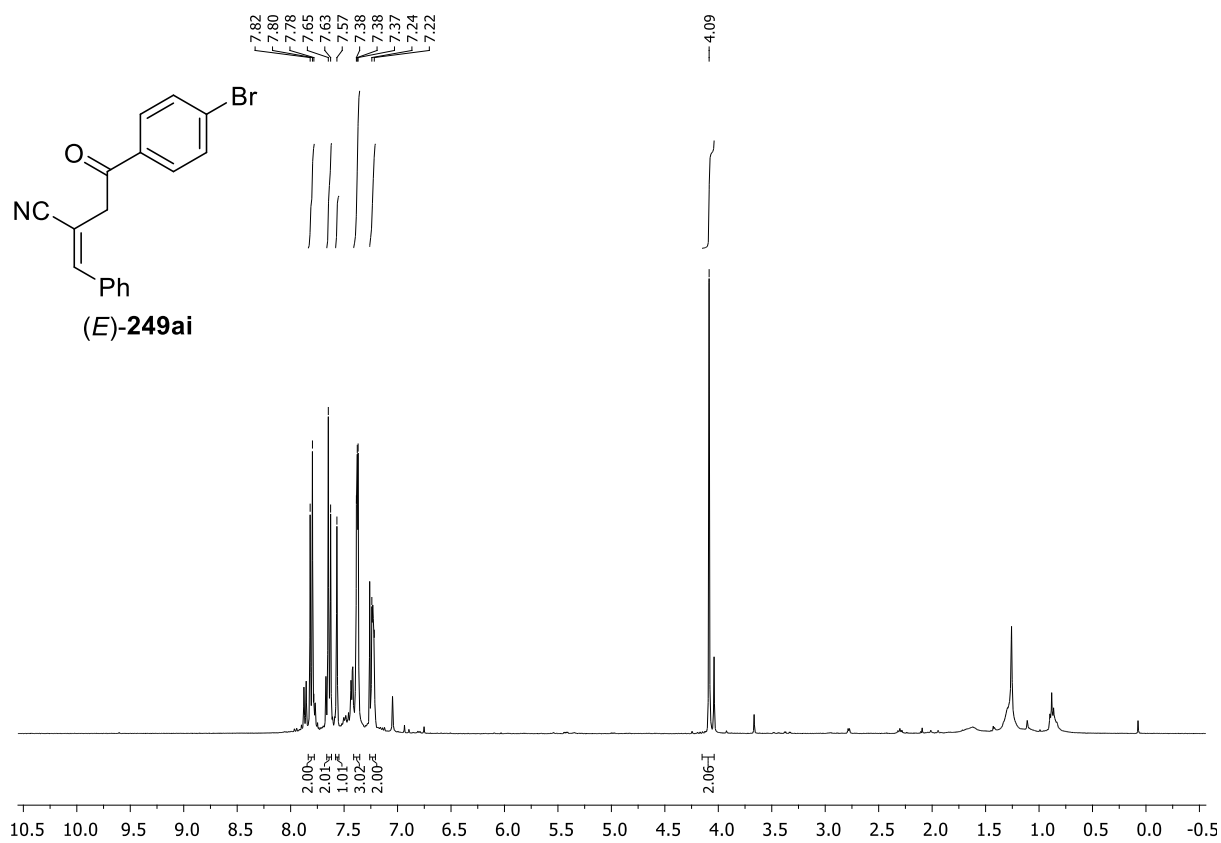




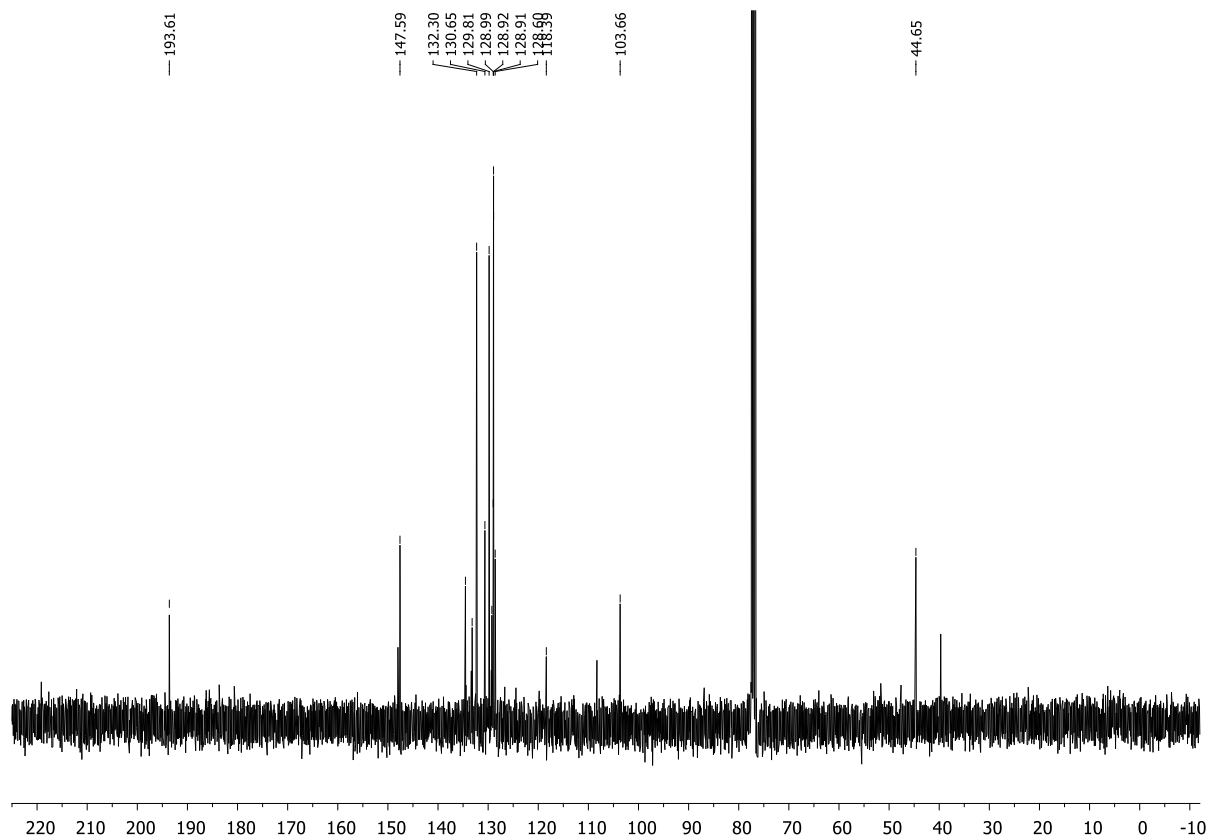
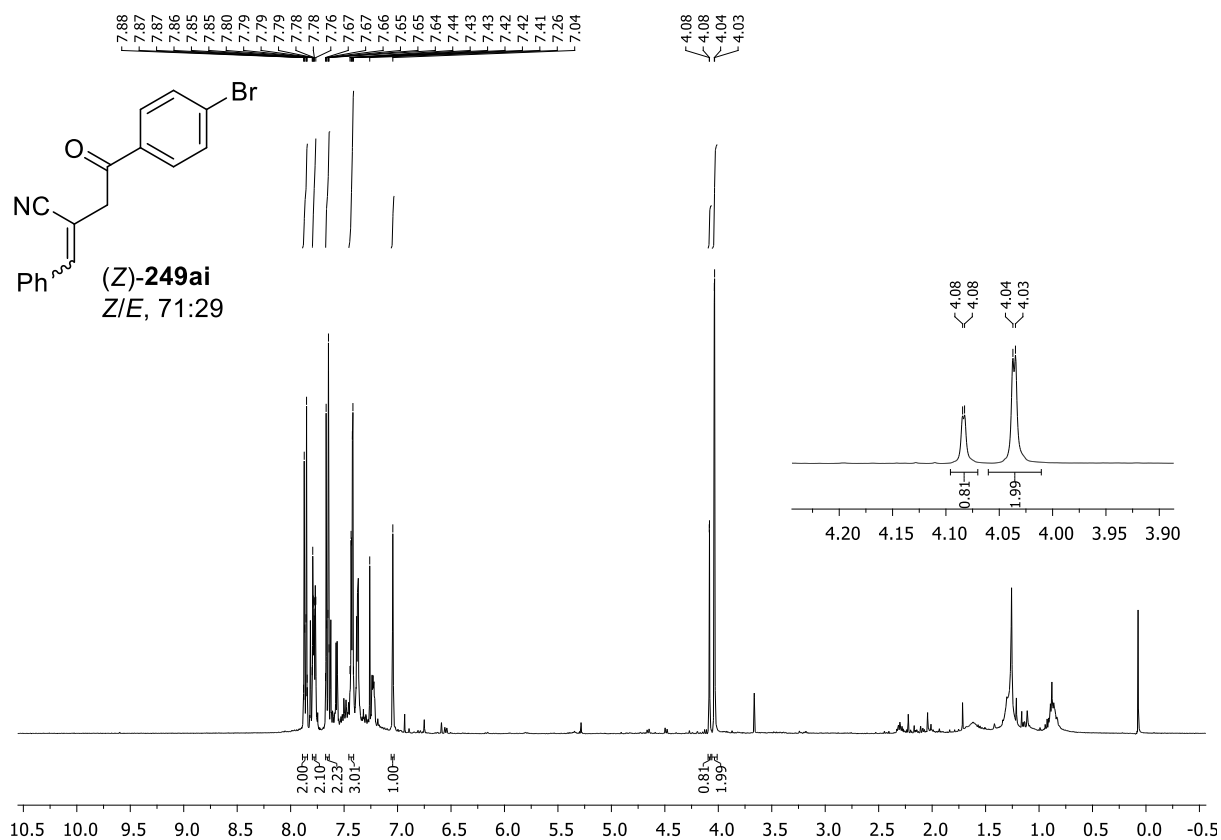


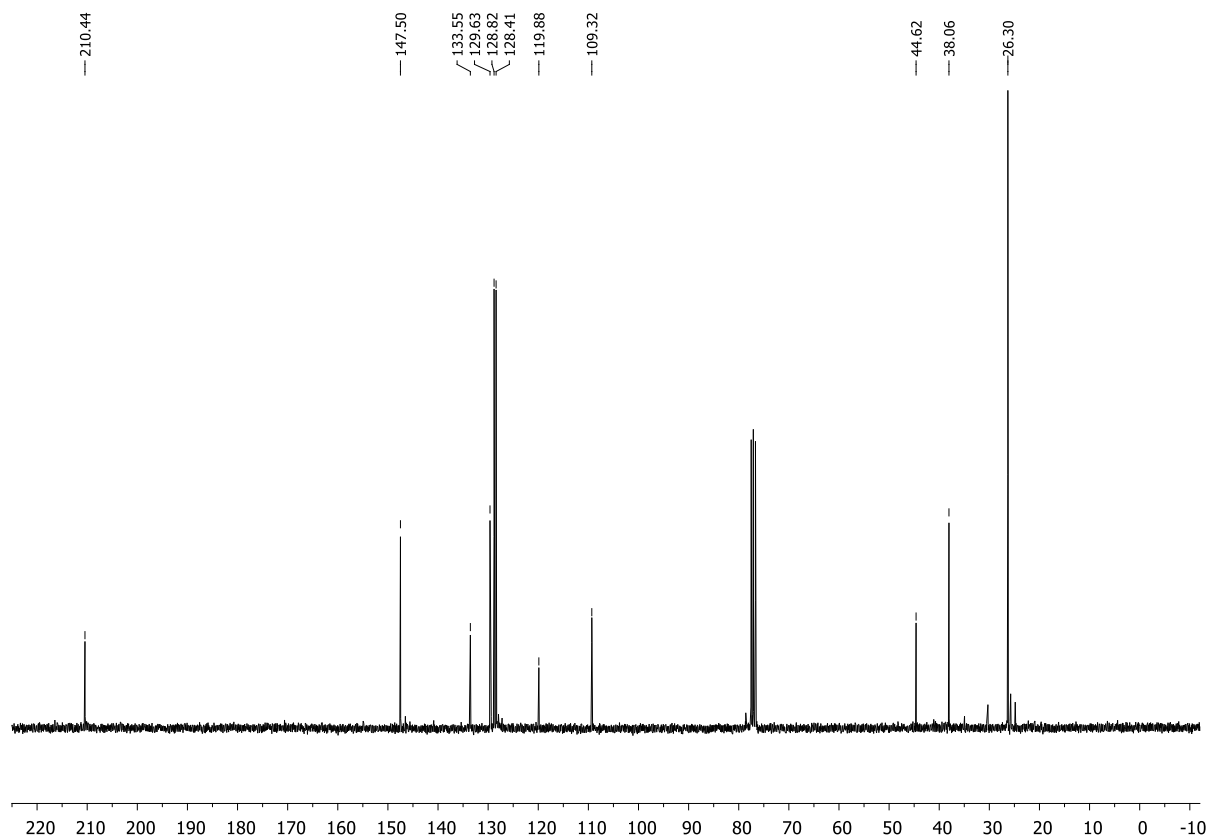
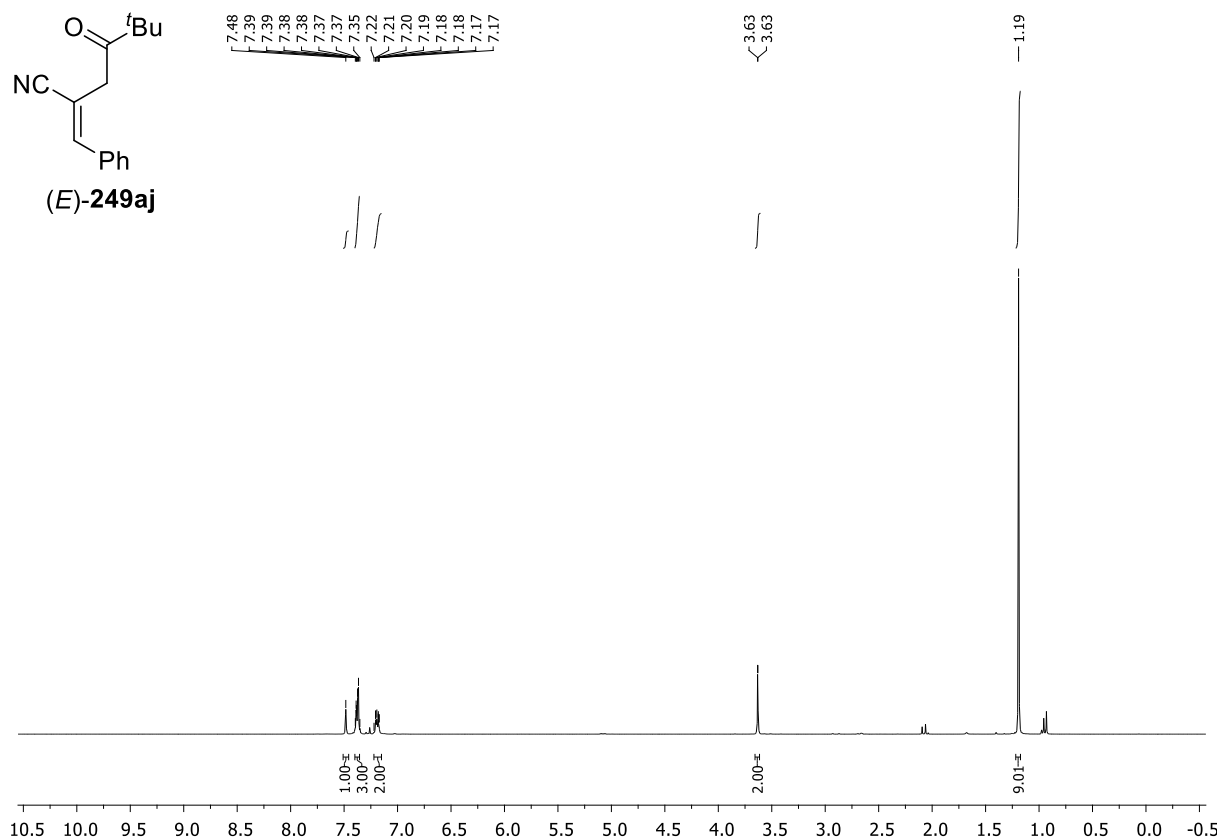
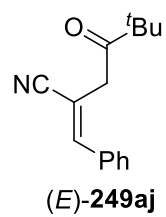


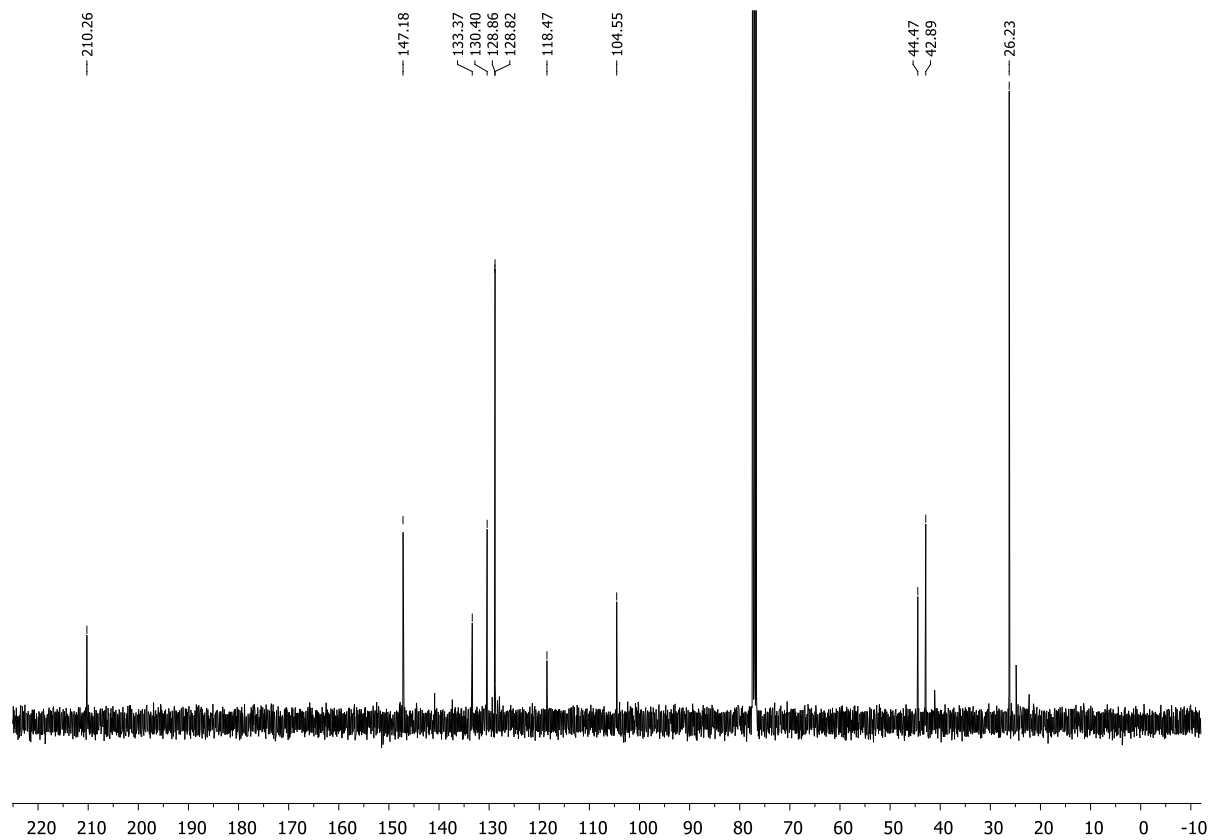
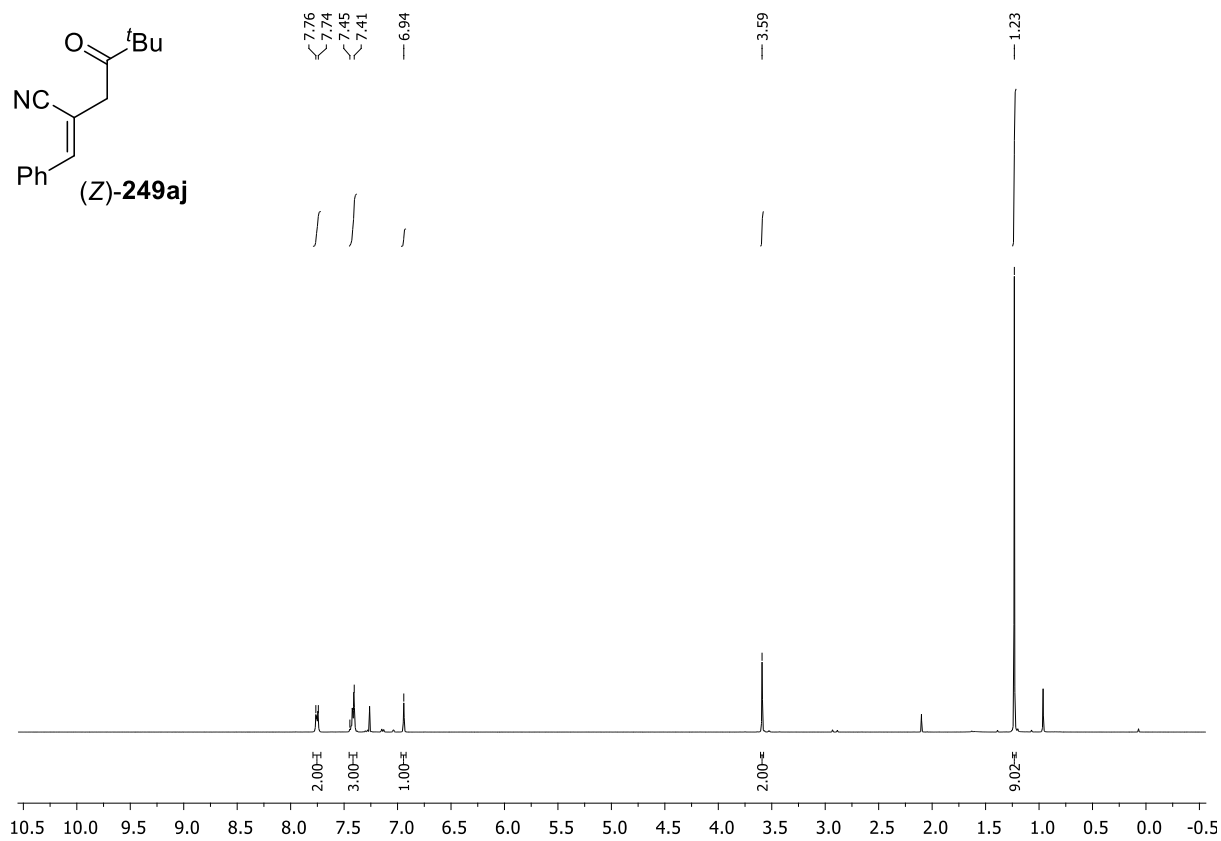


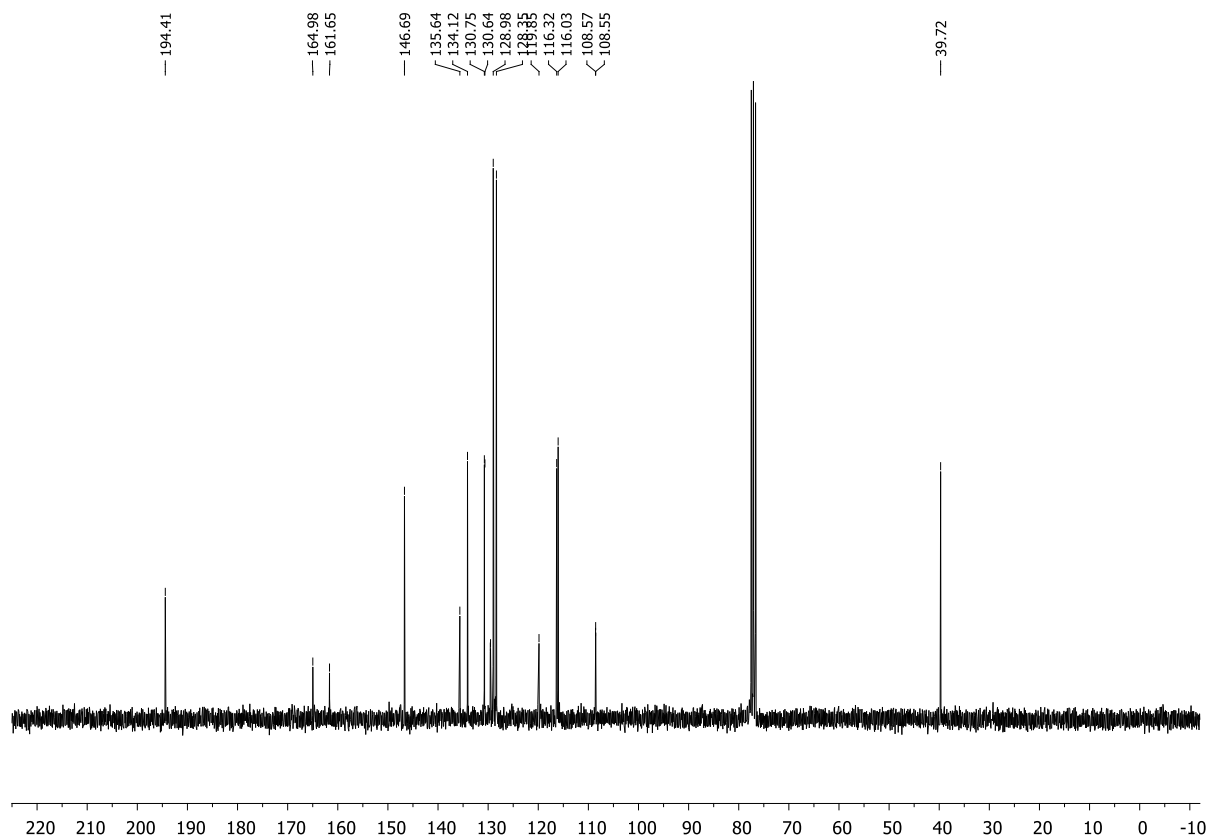
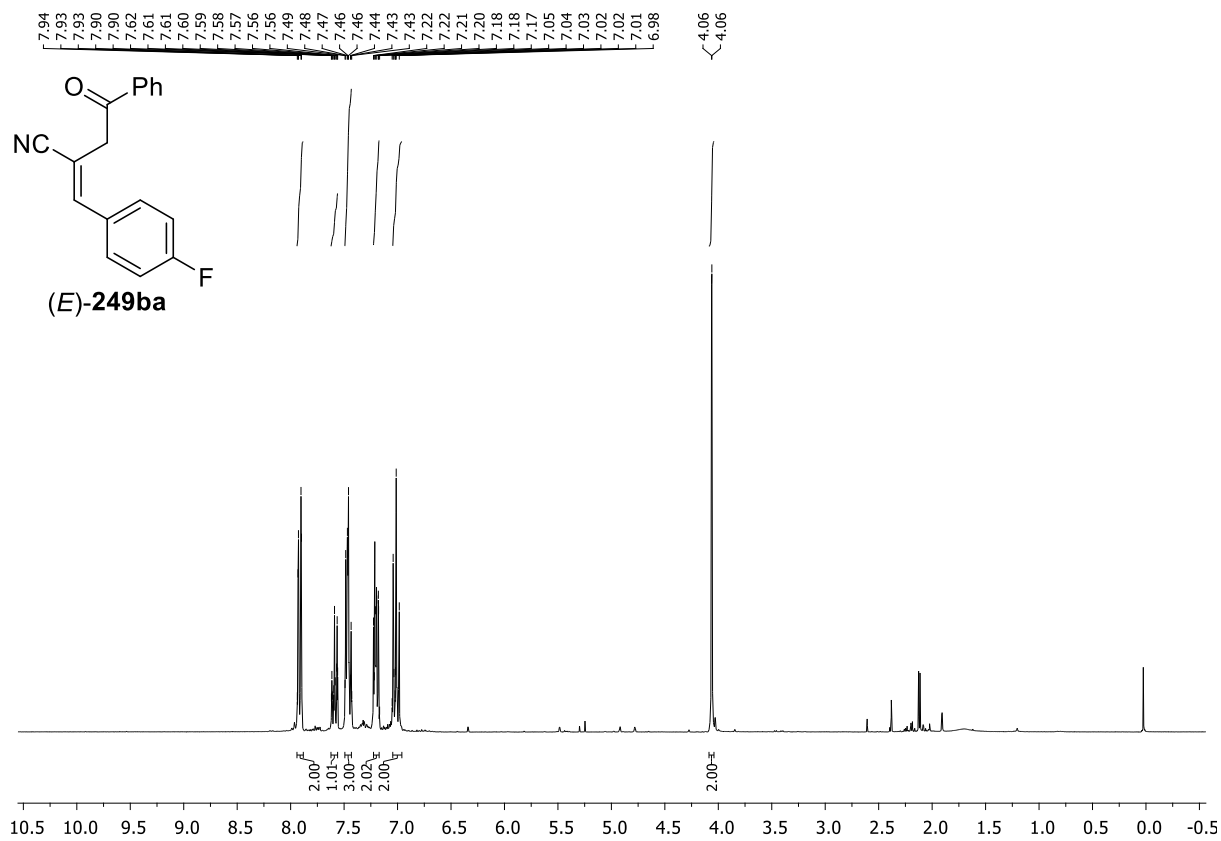


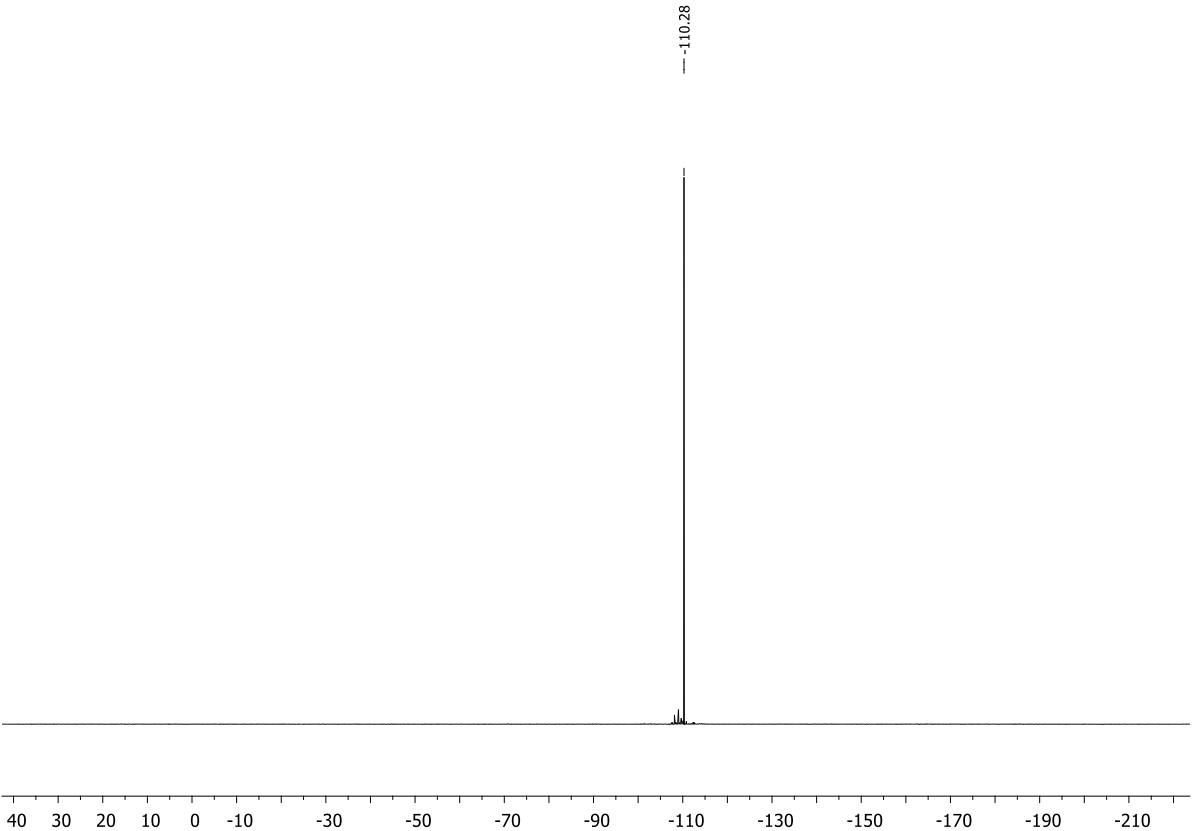


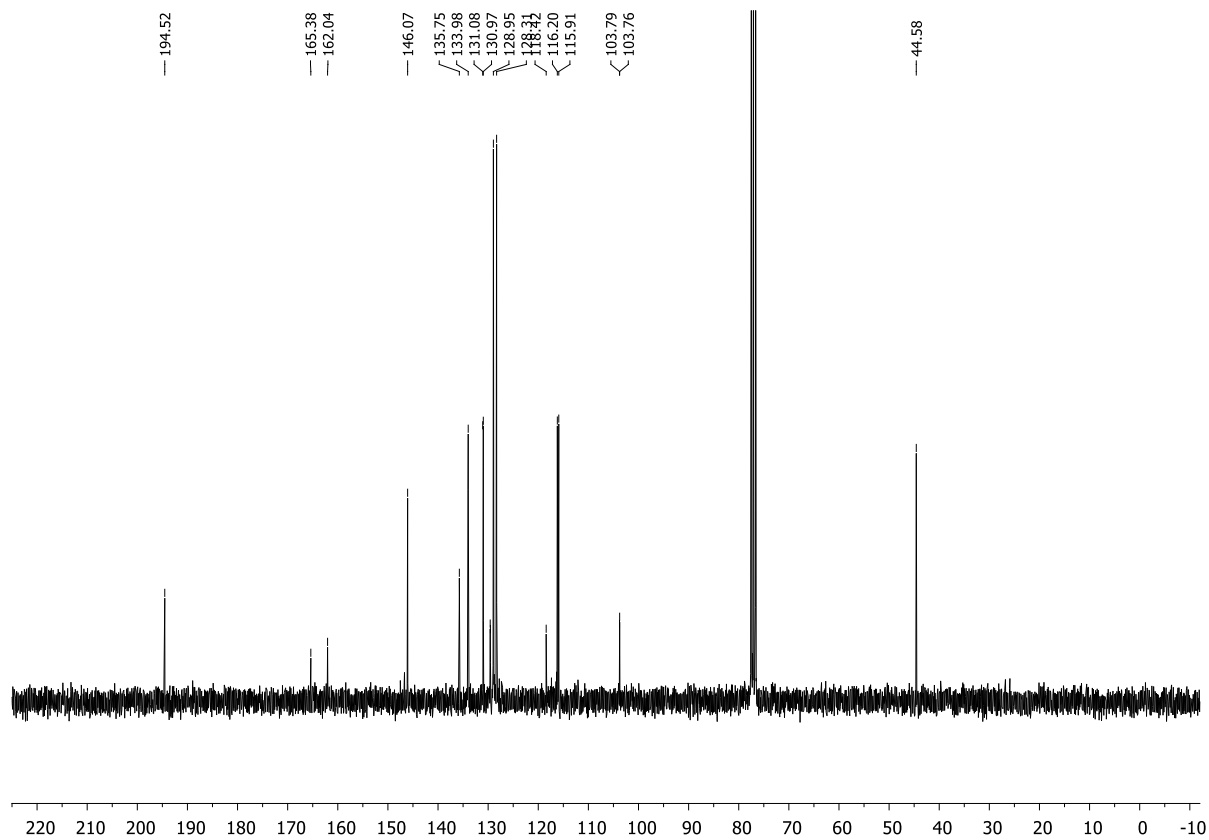
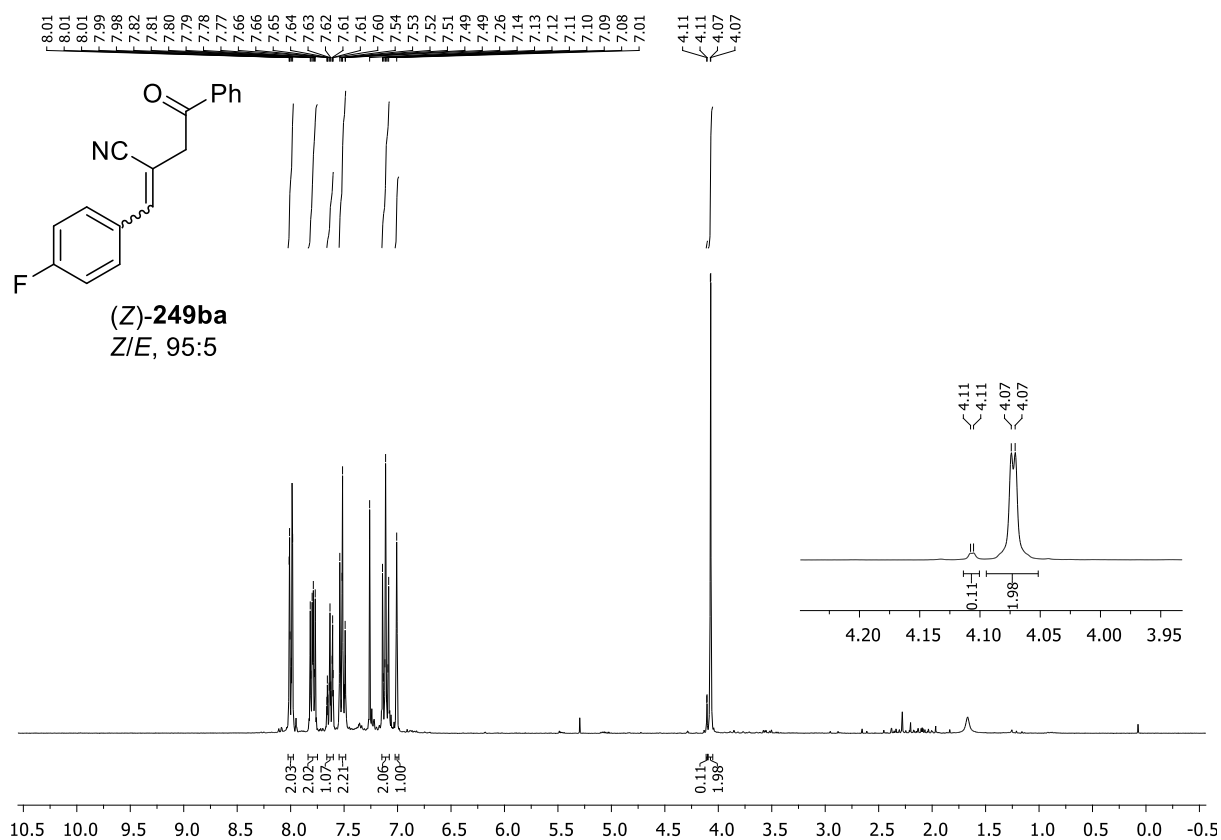


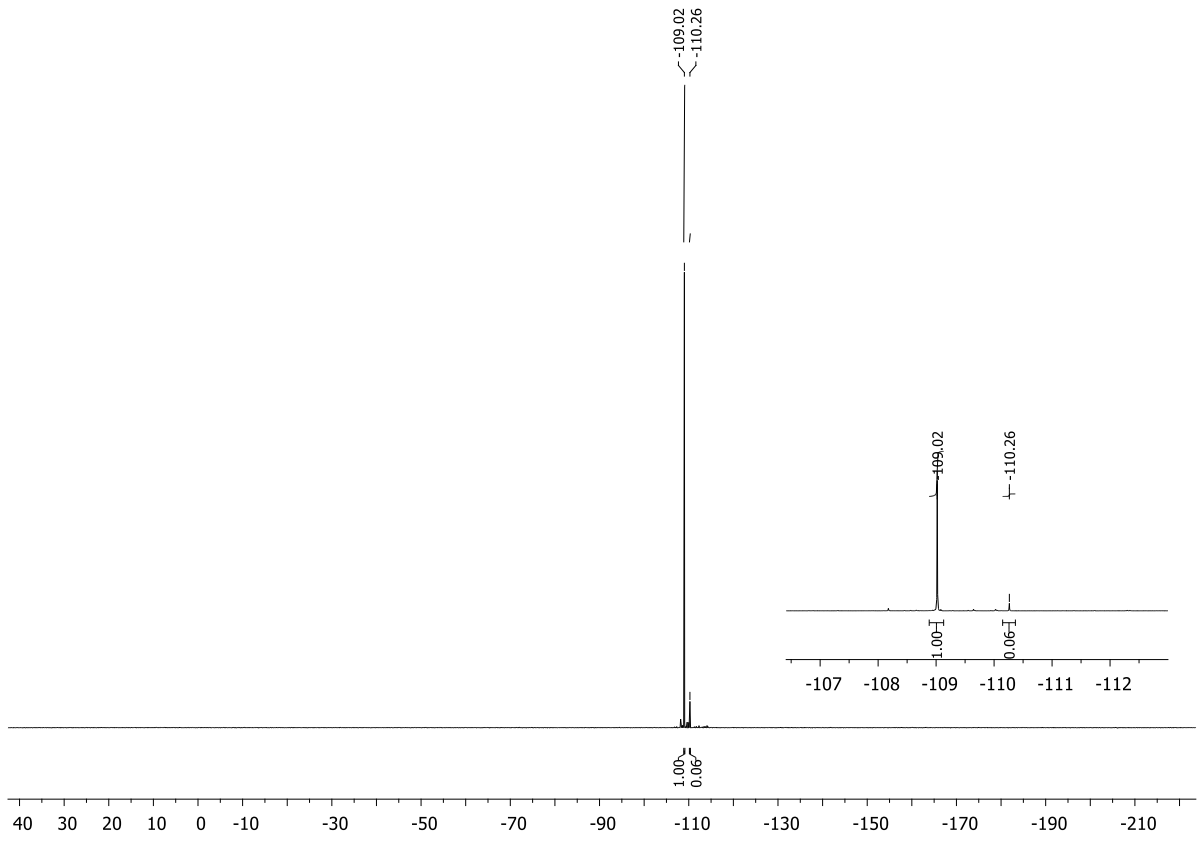


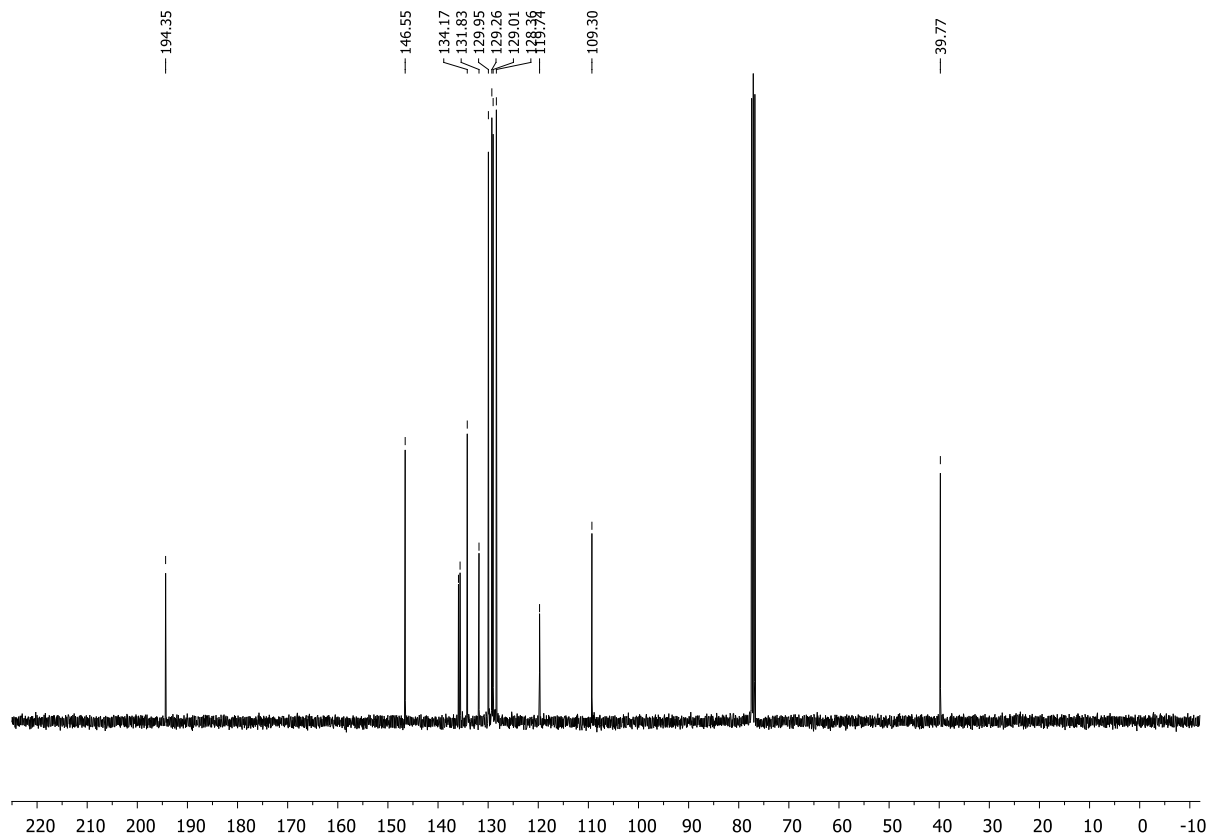
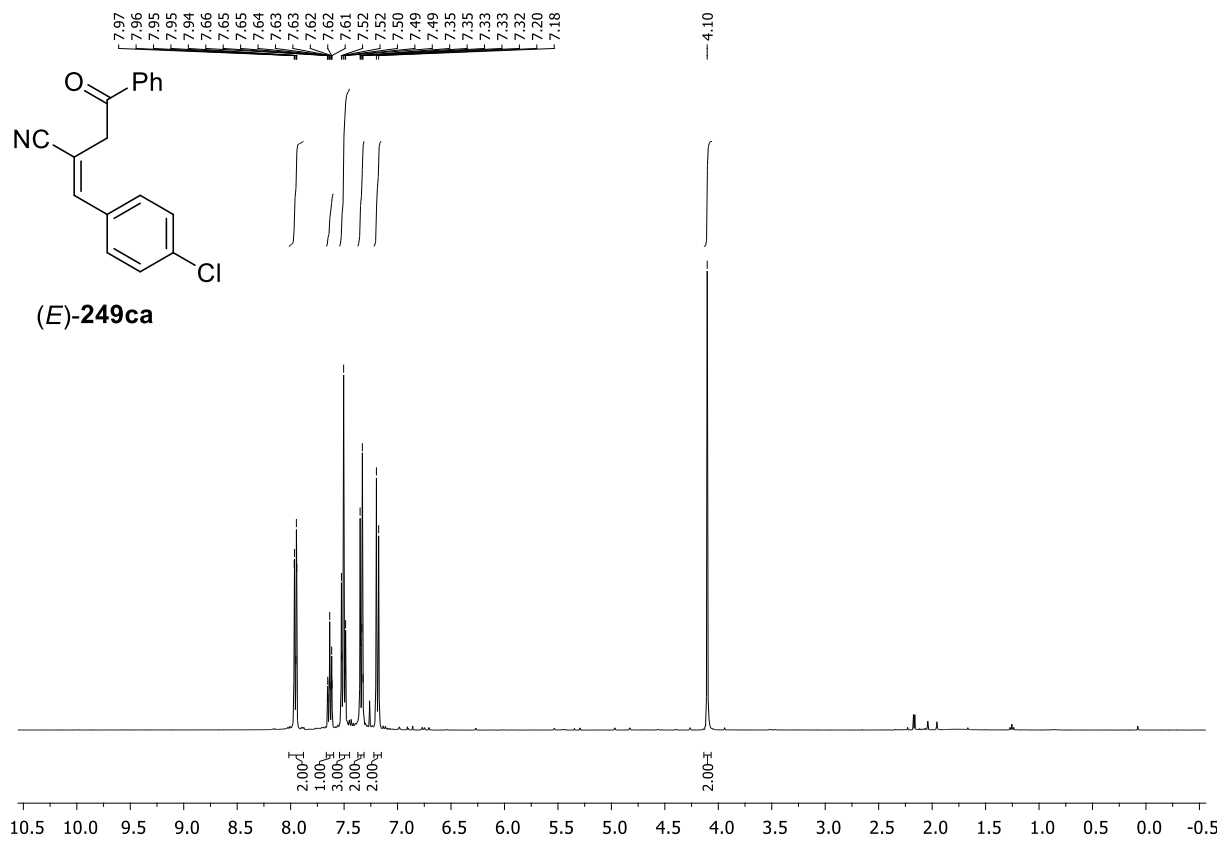




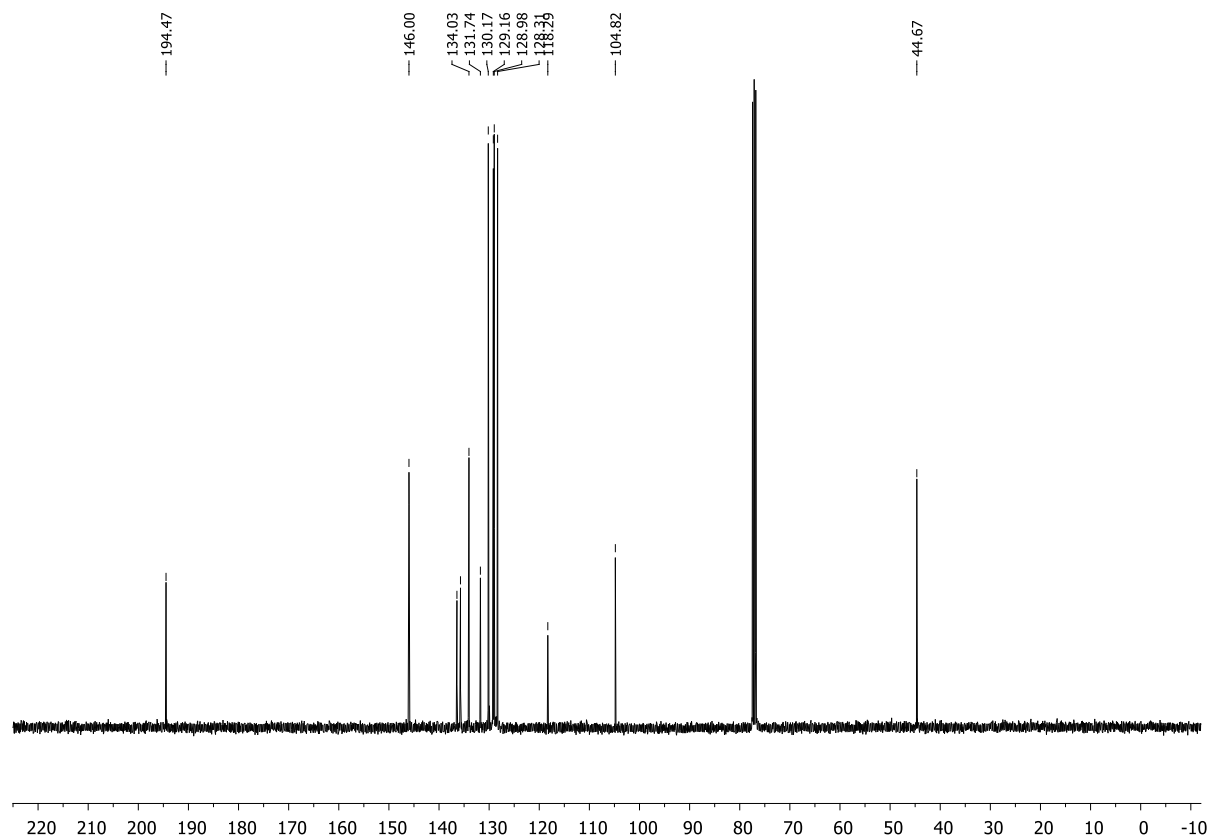
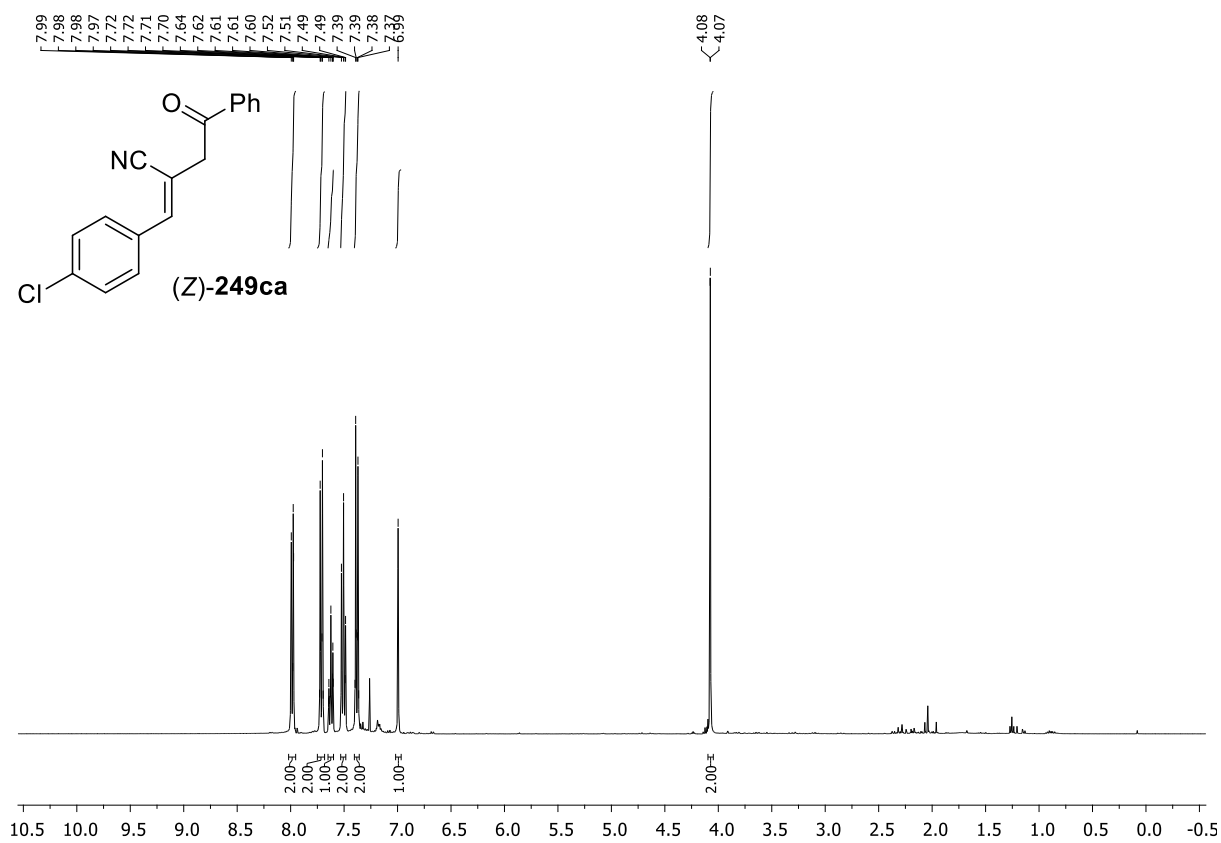


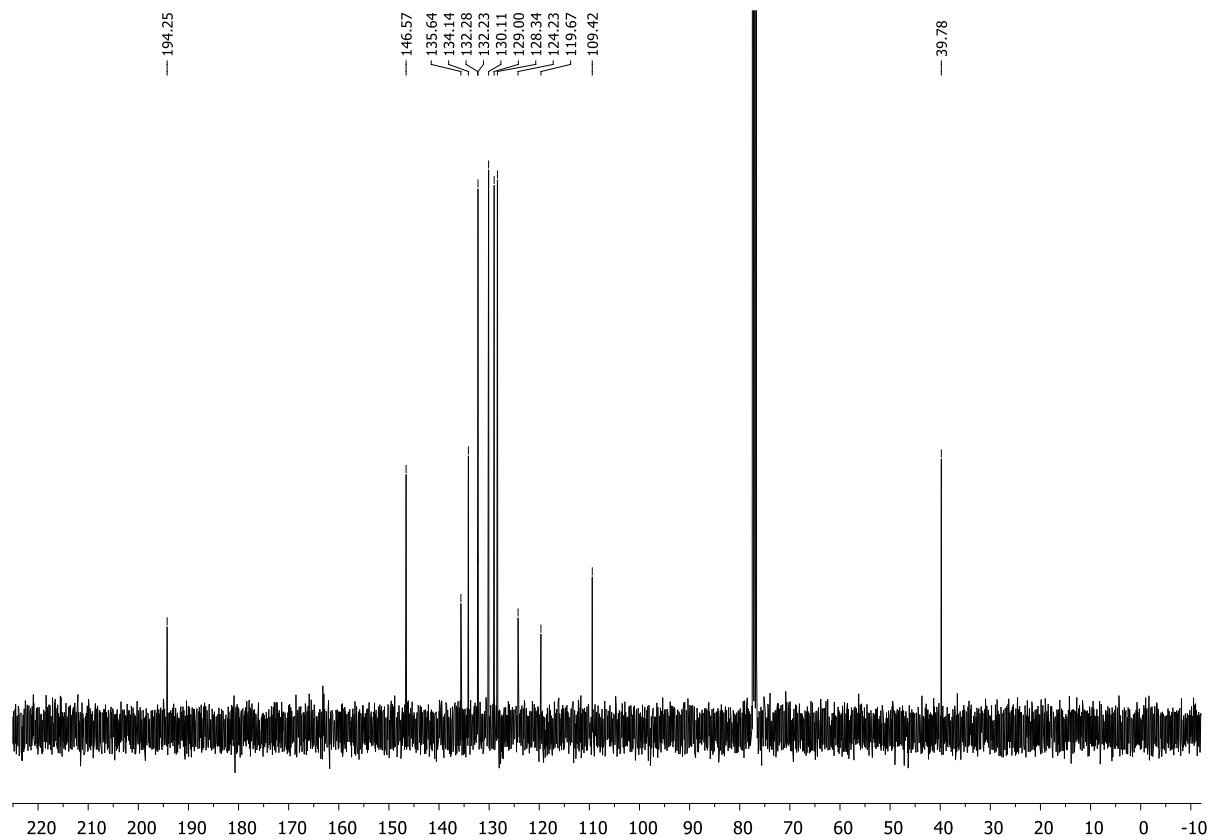
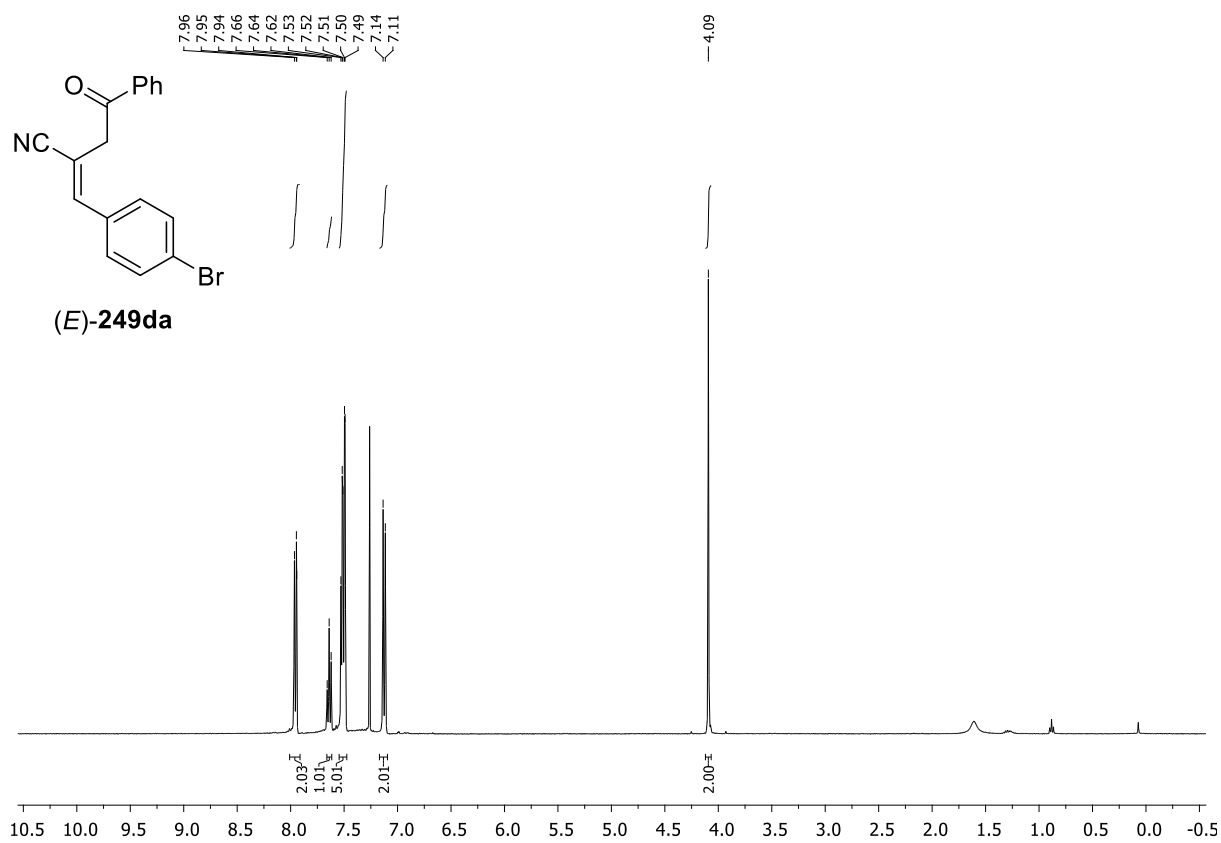


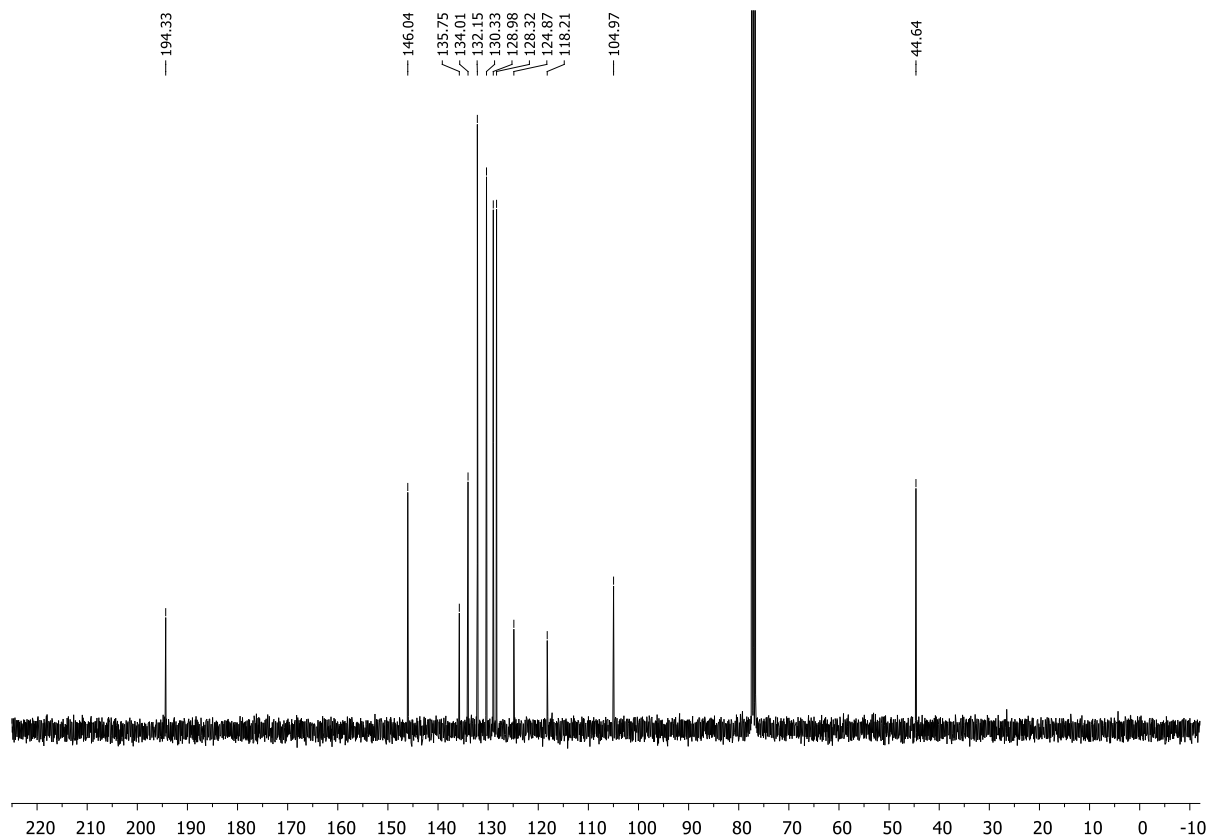
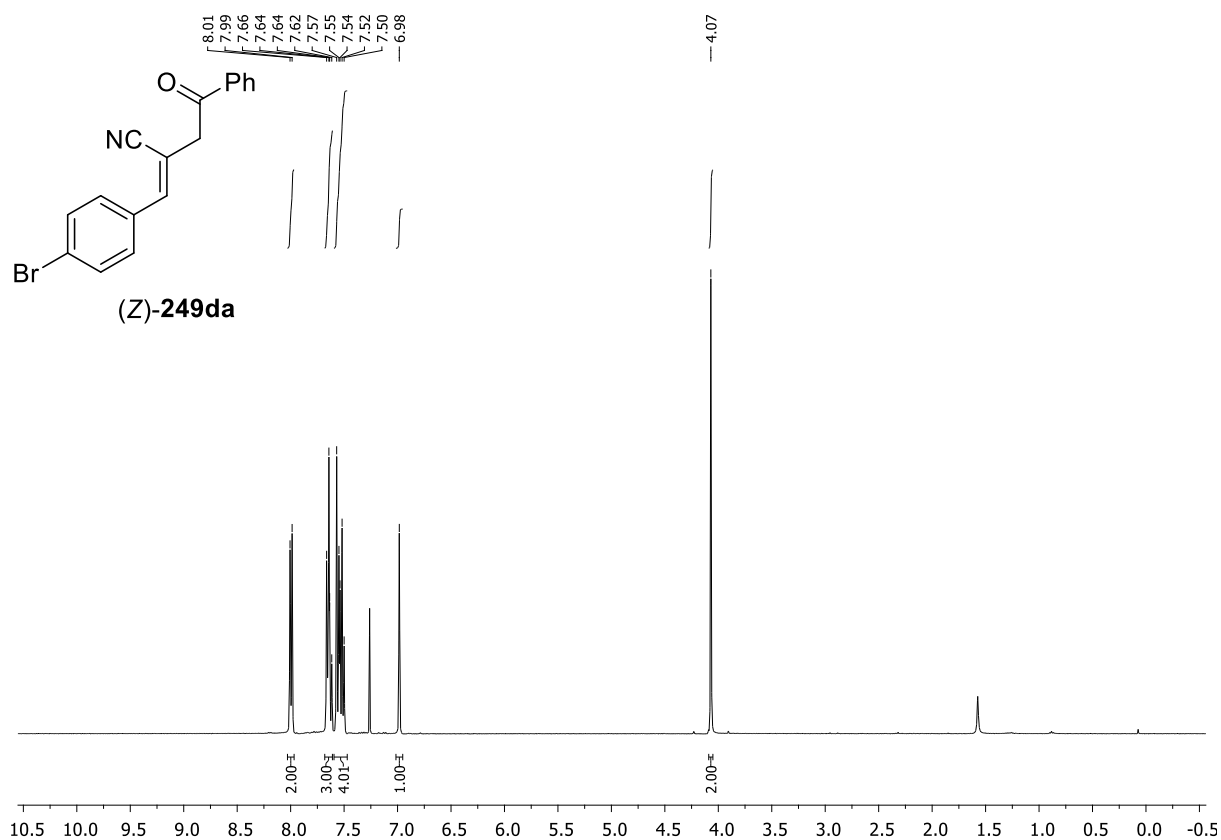


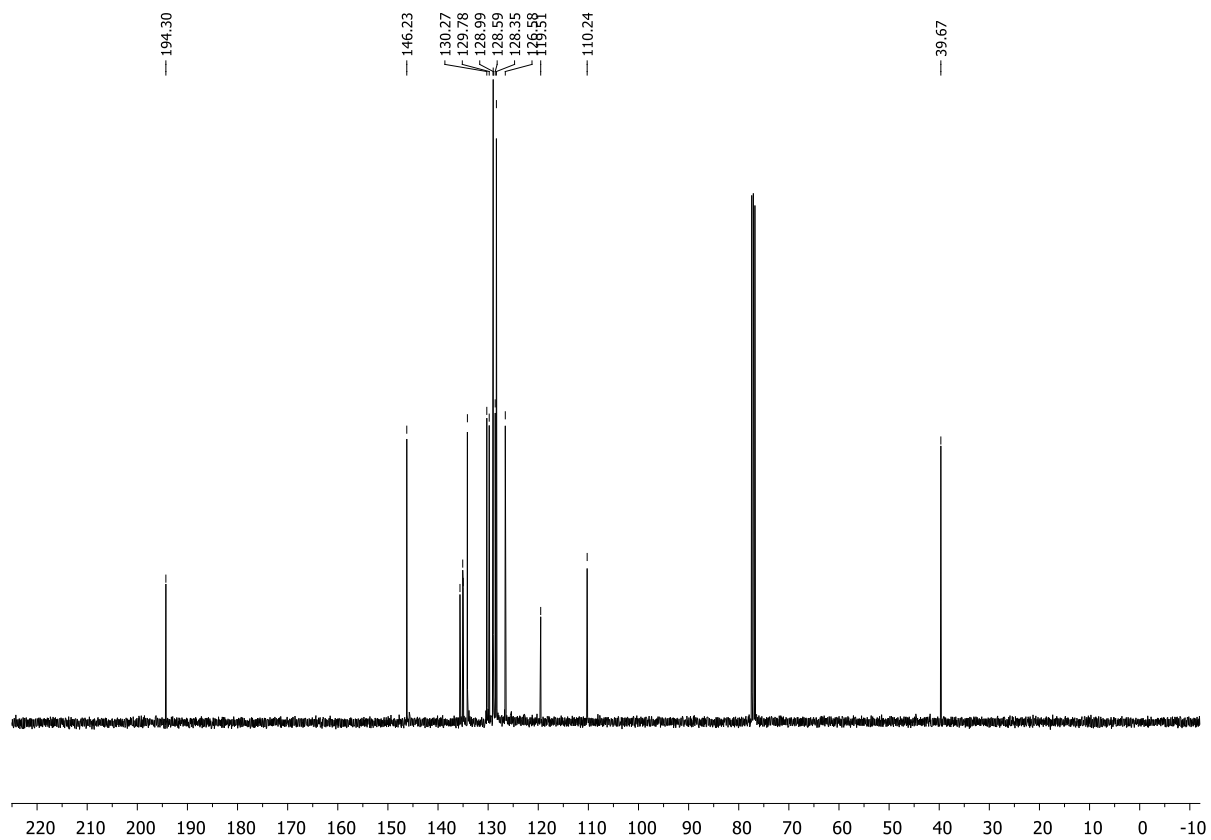
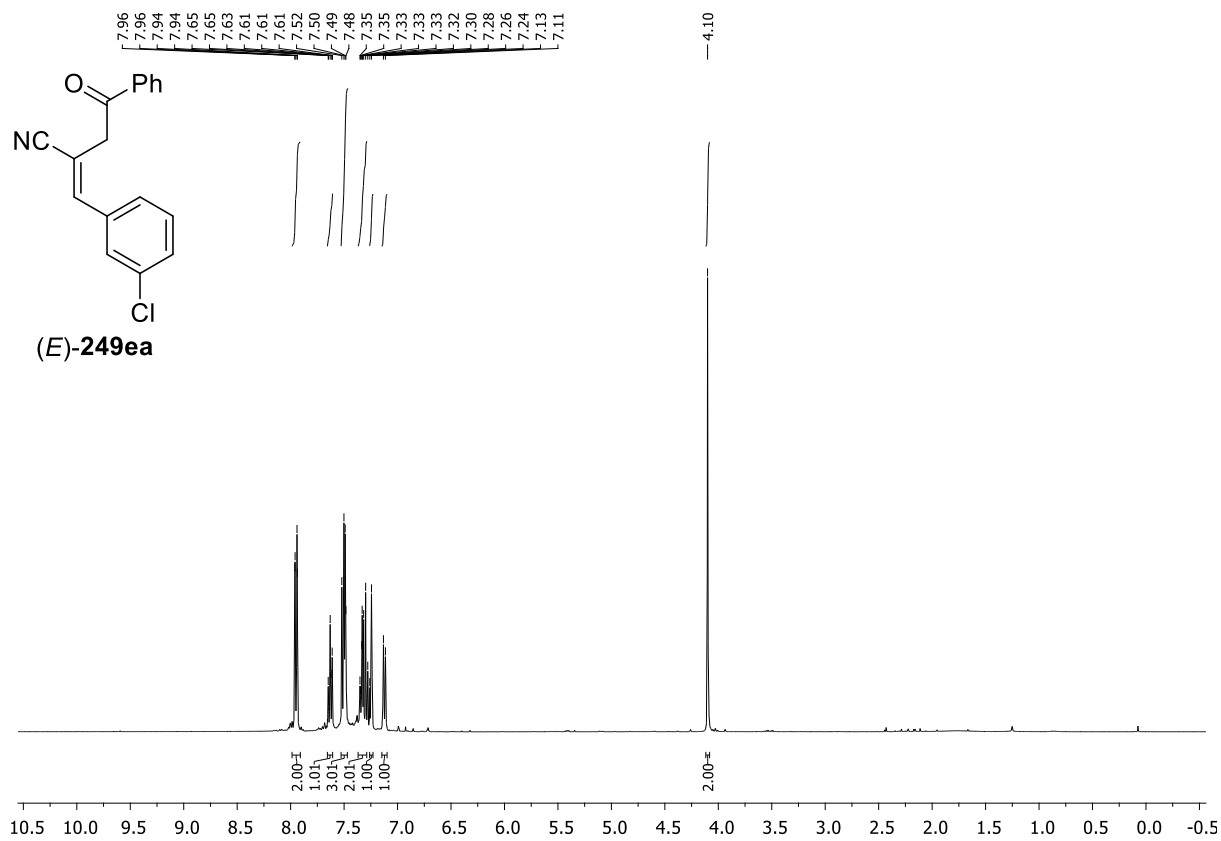


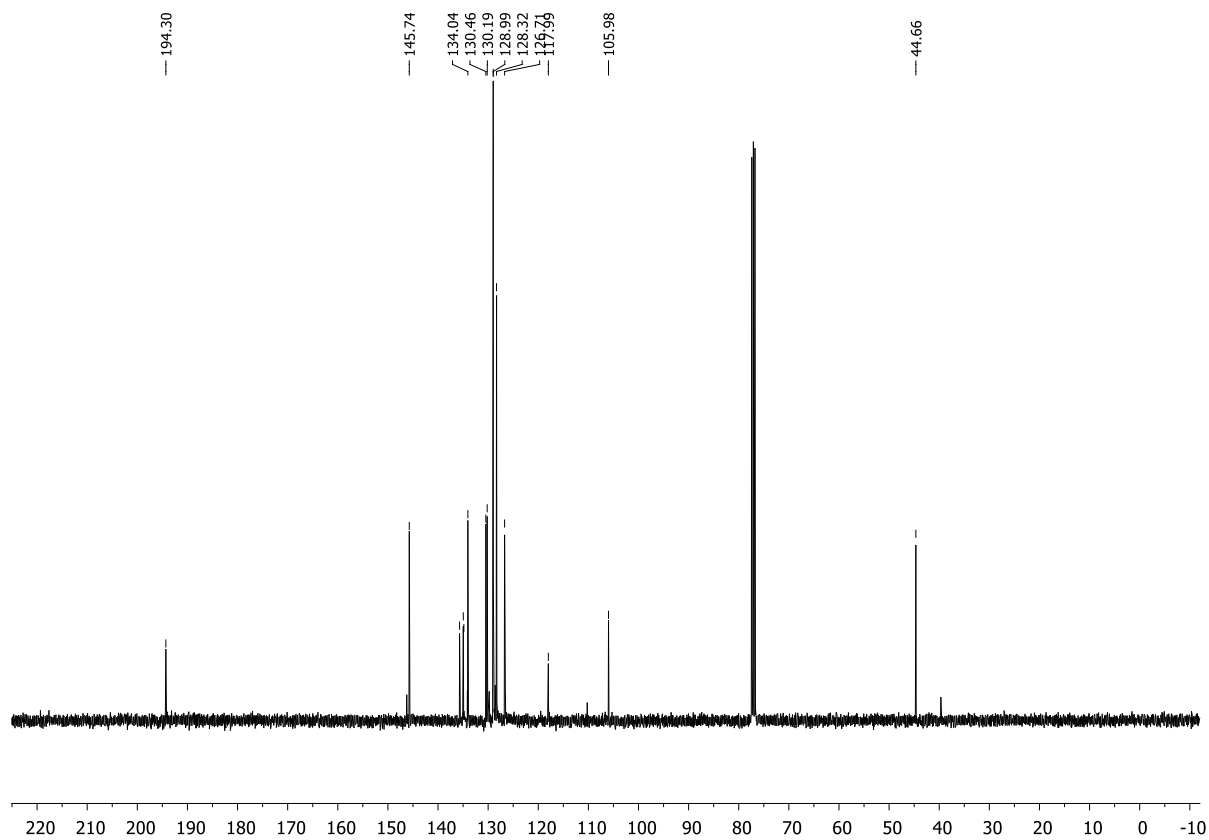
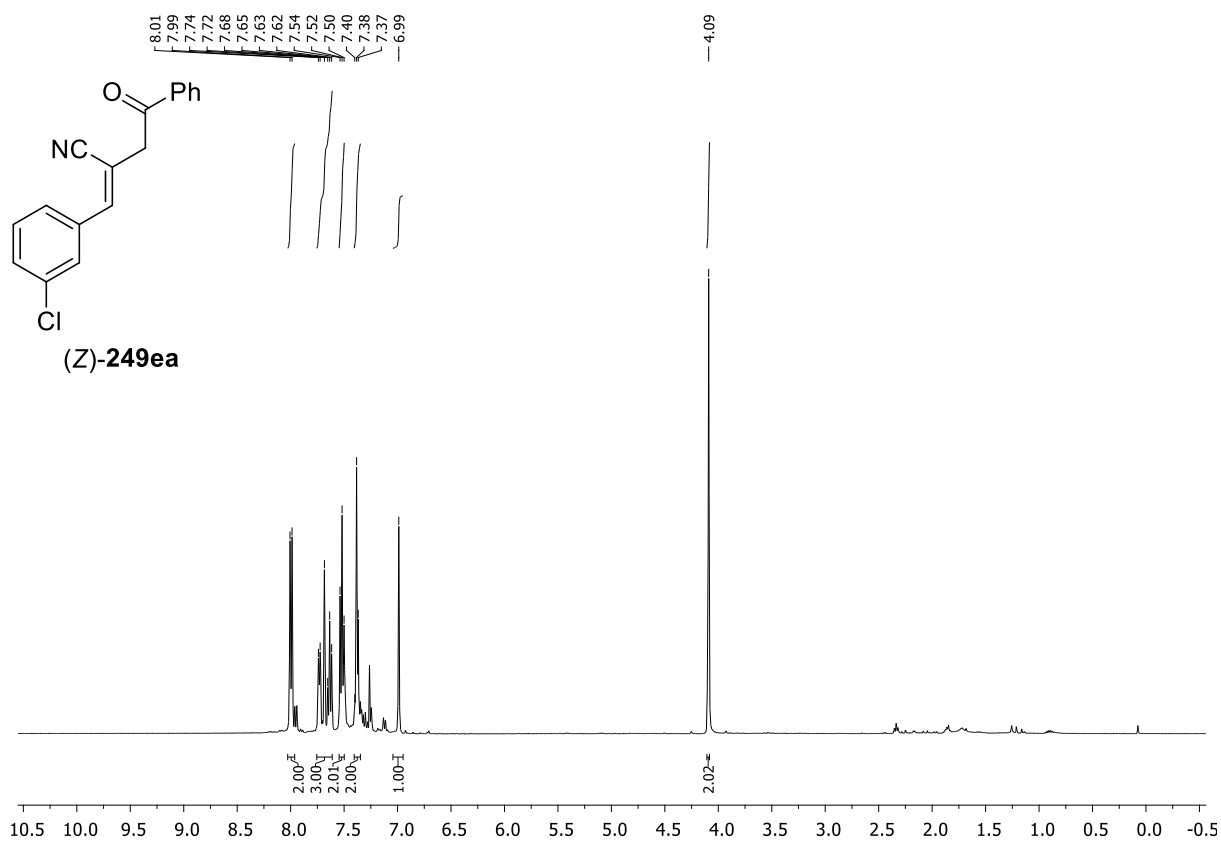


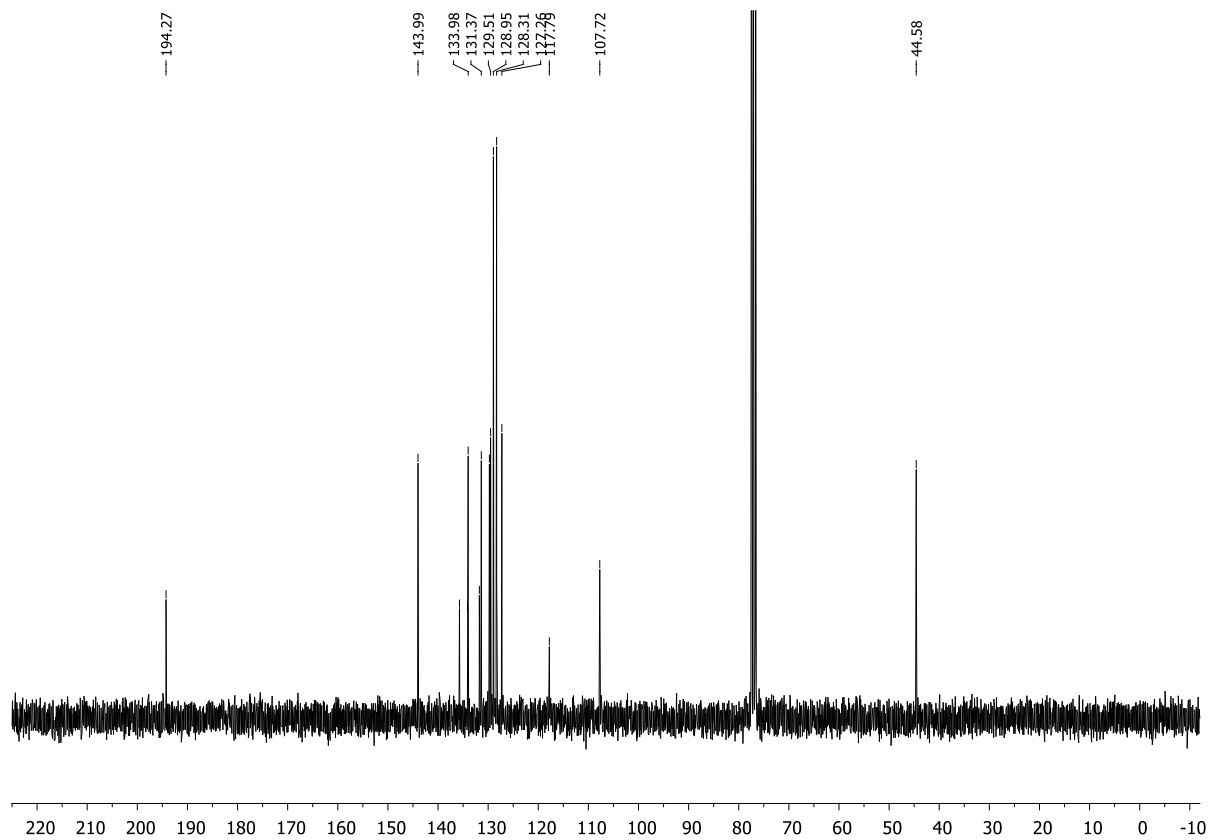
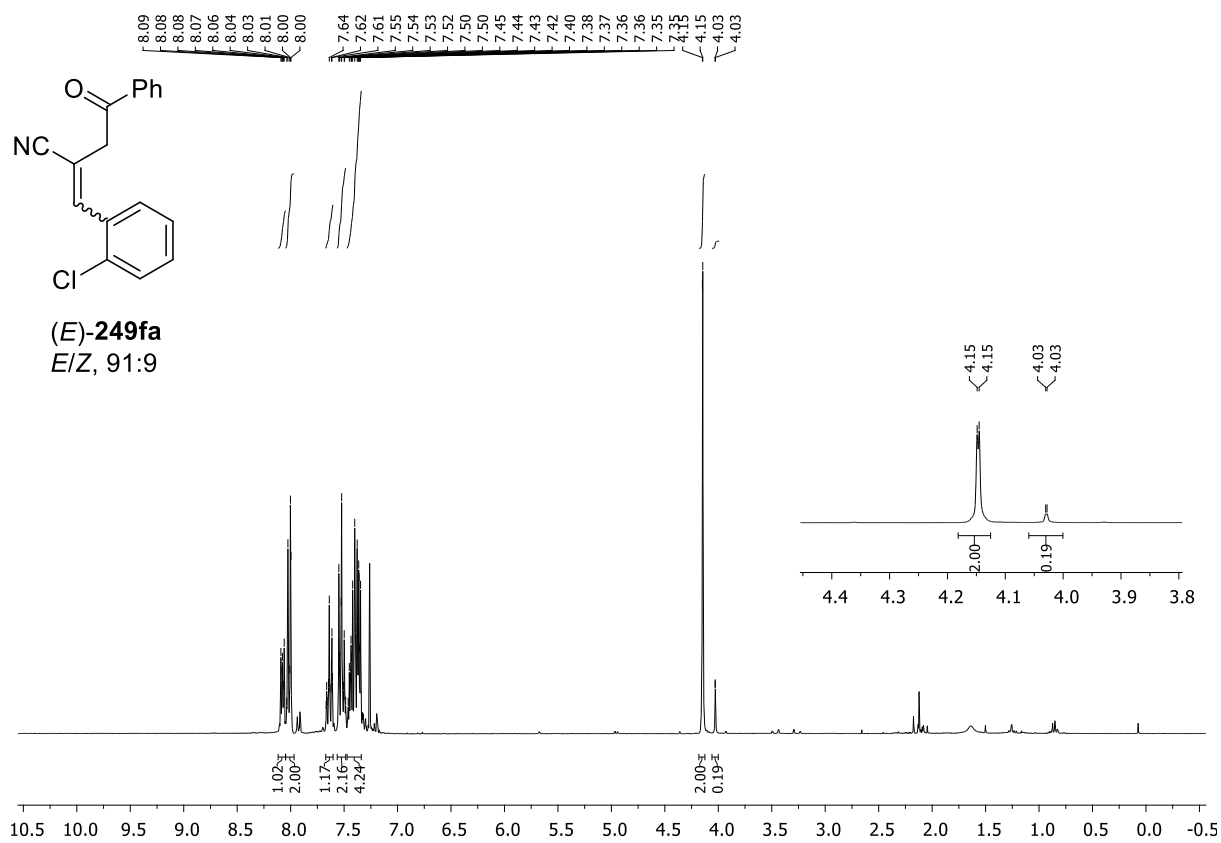


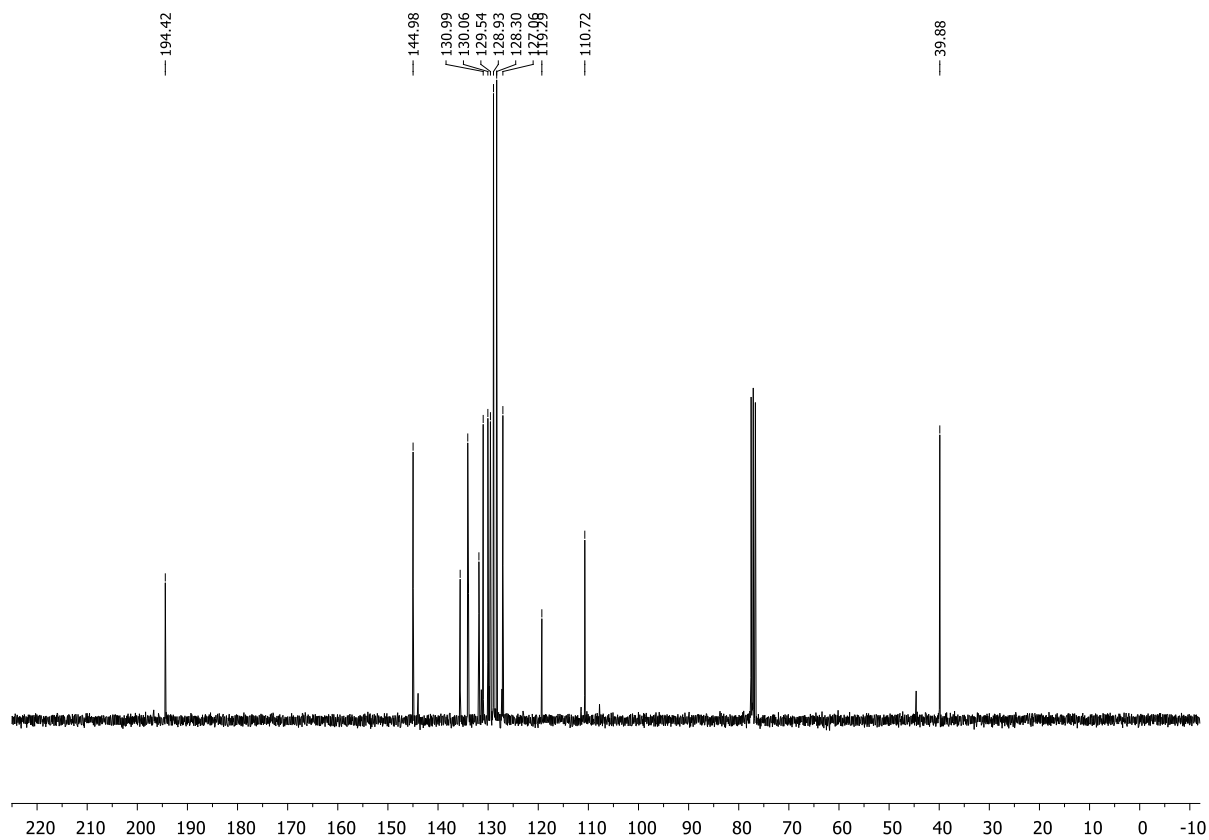
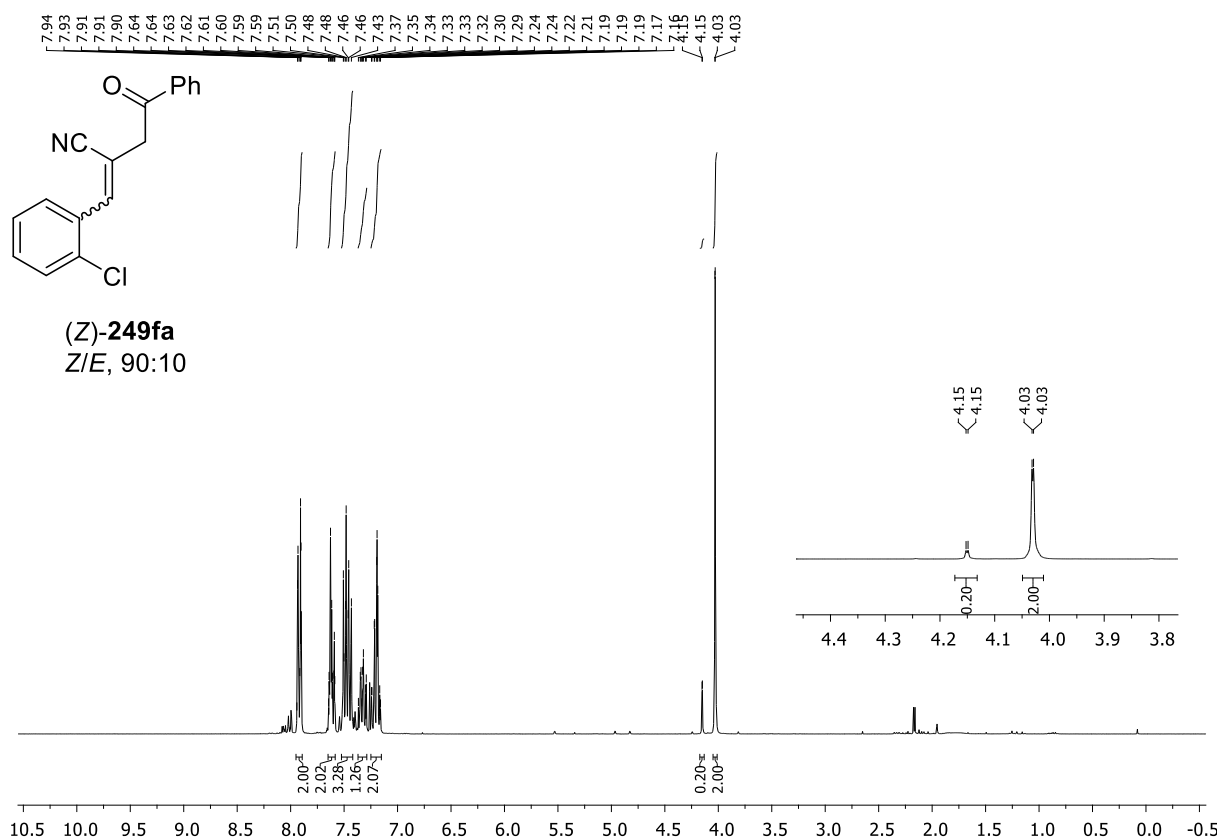


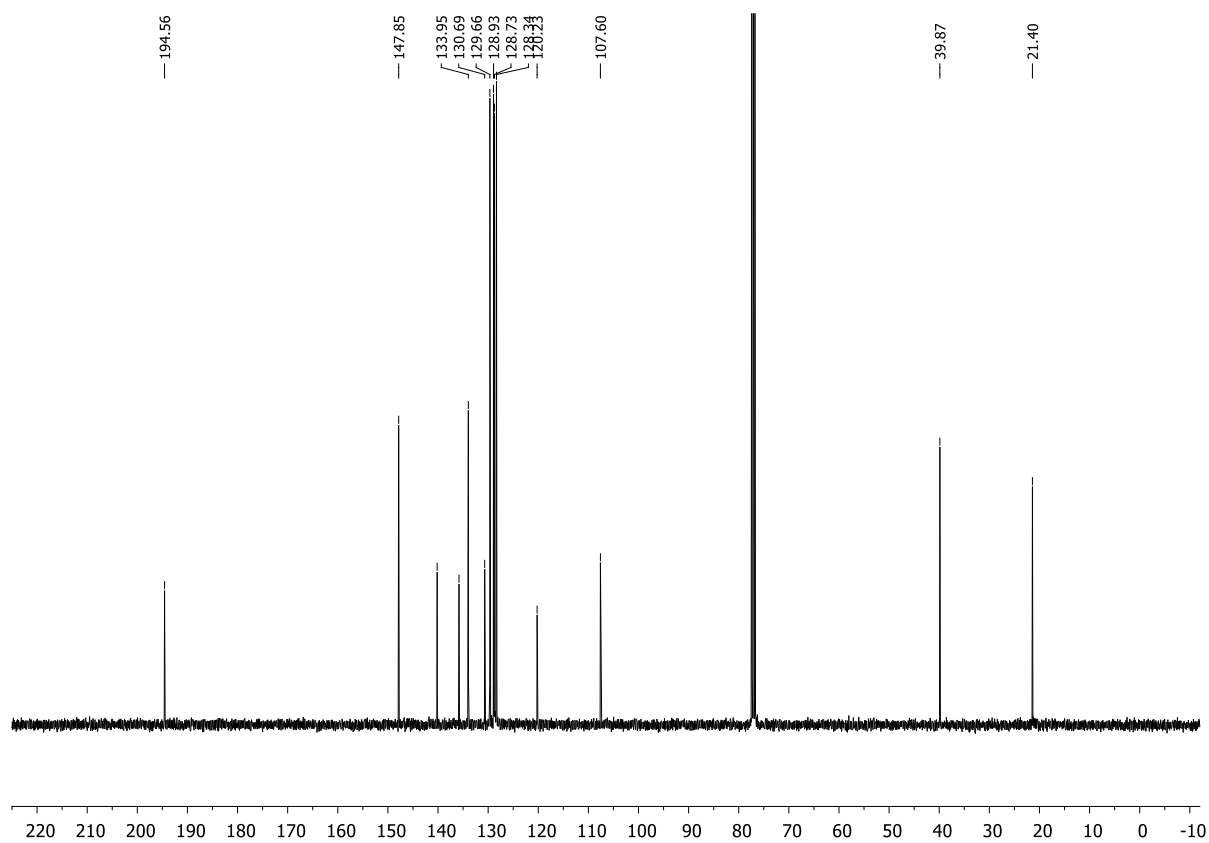
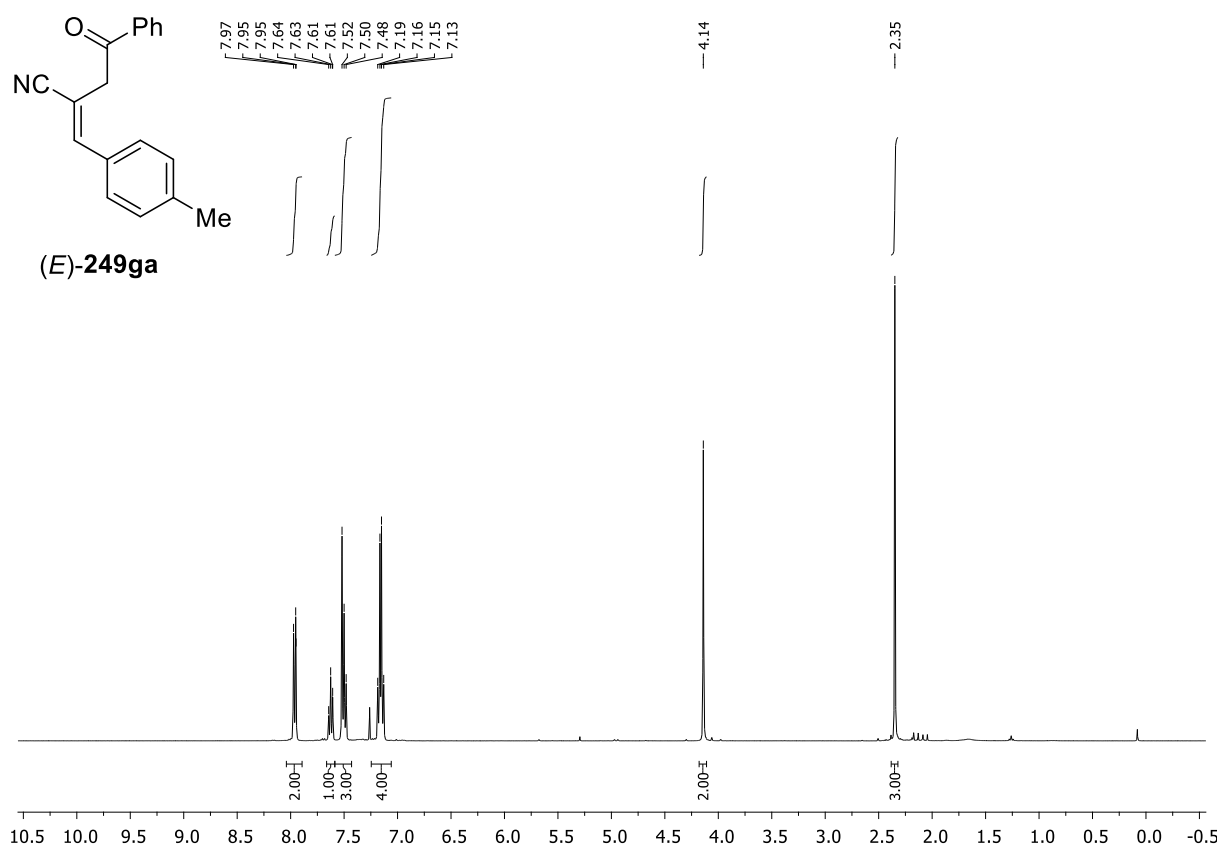




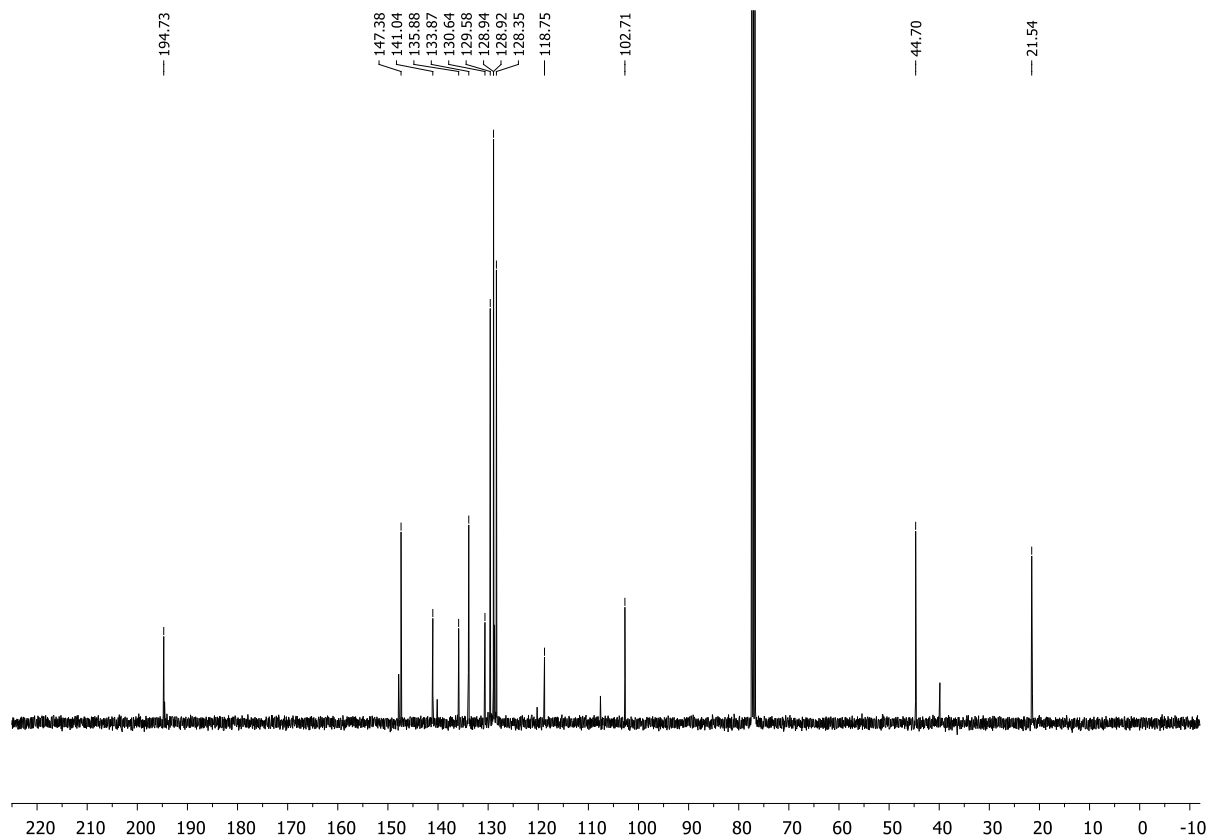
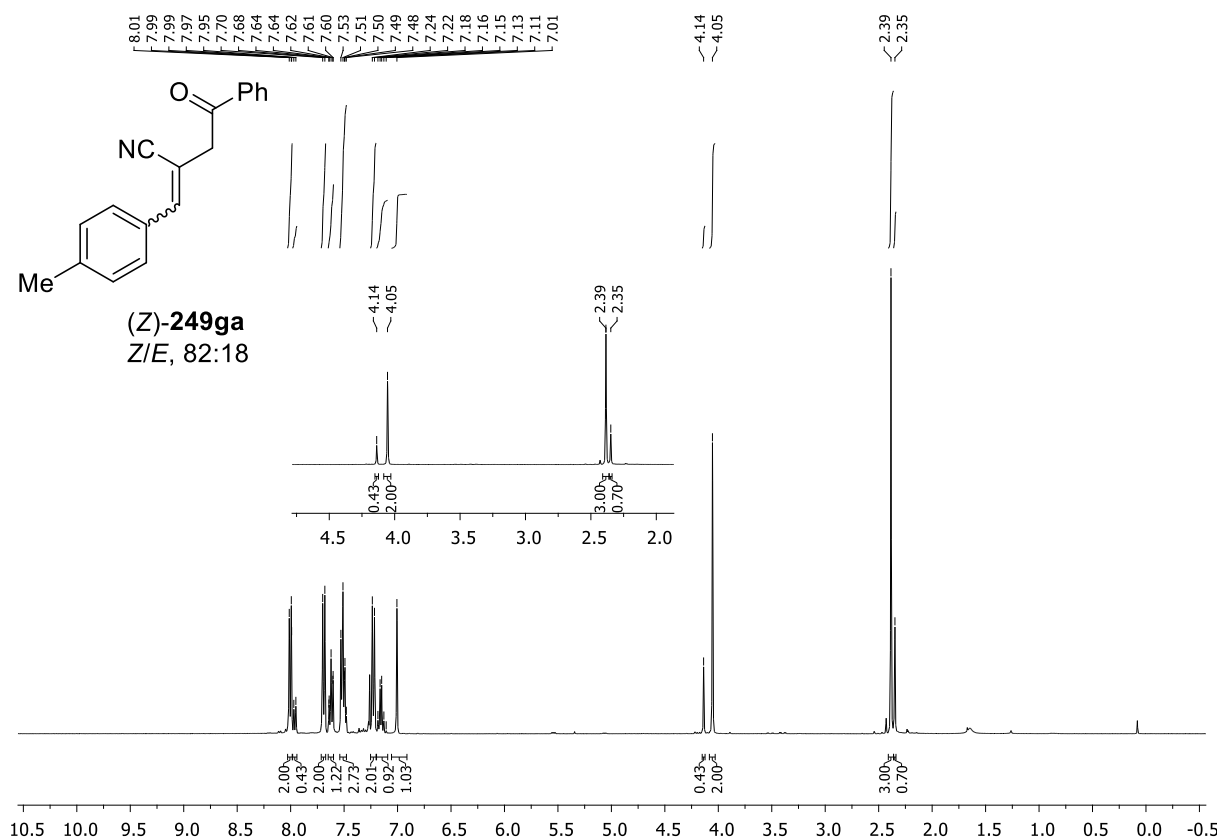






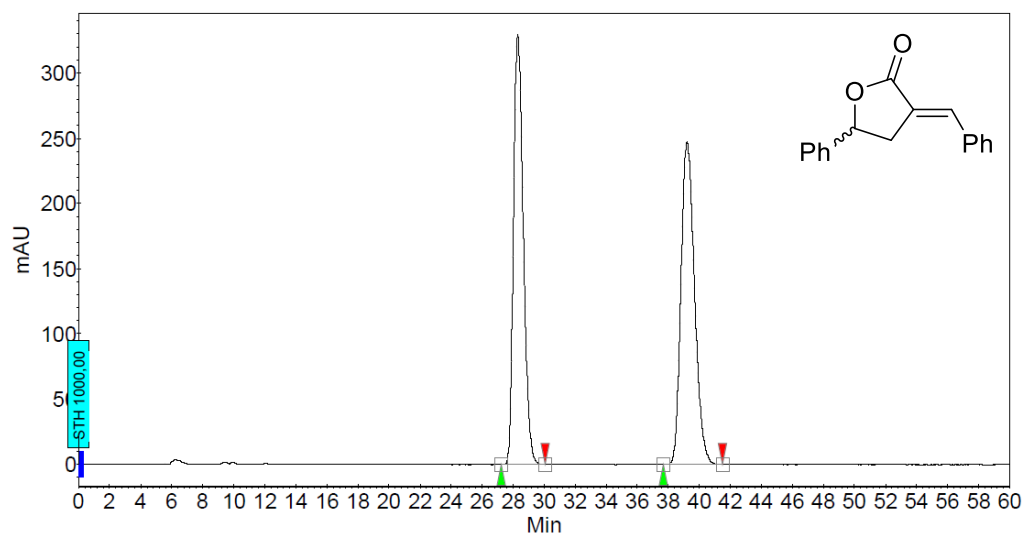






### 3 Chiral HPLC chromatograms

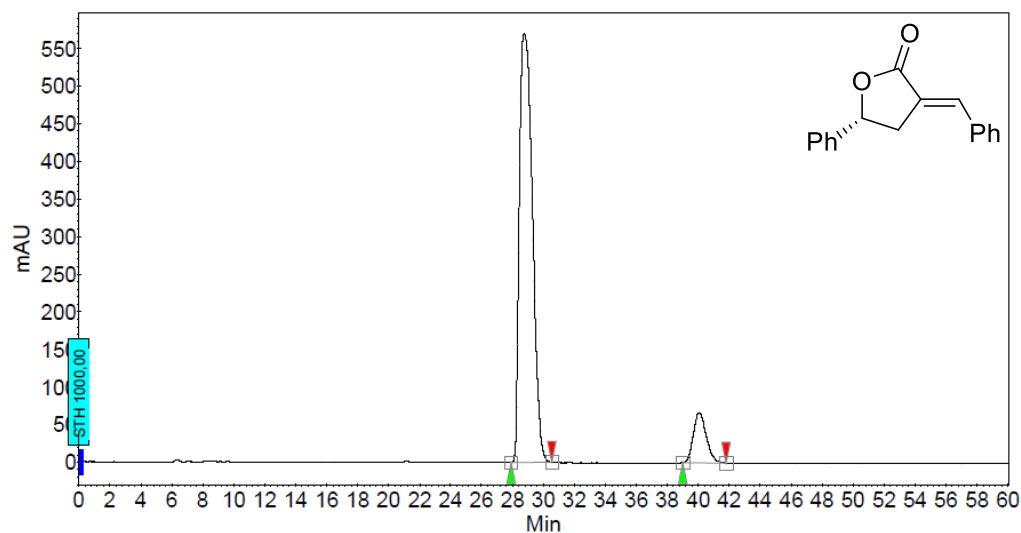
#### (*E*)-3-benzylidene-5-phenyldihydrofuran-2(3*H*)-one ((*E*)-238)



#### Peak Results :

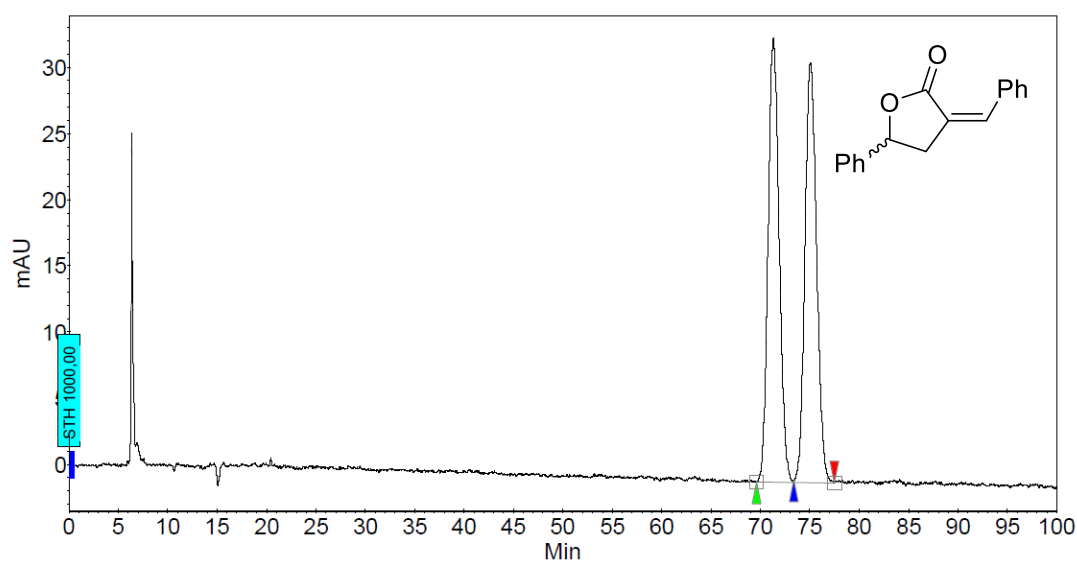
Index	Name	Time [Min]	Quantity [% Area]	Height [mAU]	Area [mAU.Min]	Area % [%]
1	UNKNOWN	28.30	49.08	330.0	241.4	49.082
2	UNKNOWN	39.21	50.92	247.6	250.4	50.918
Total			100.00	577.6	491.8	100.000

#### (*R,E*)-3-benzylidene-5-phenyldihydrofuran-2(3*H*)-one ((*R,E*)-238)

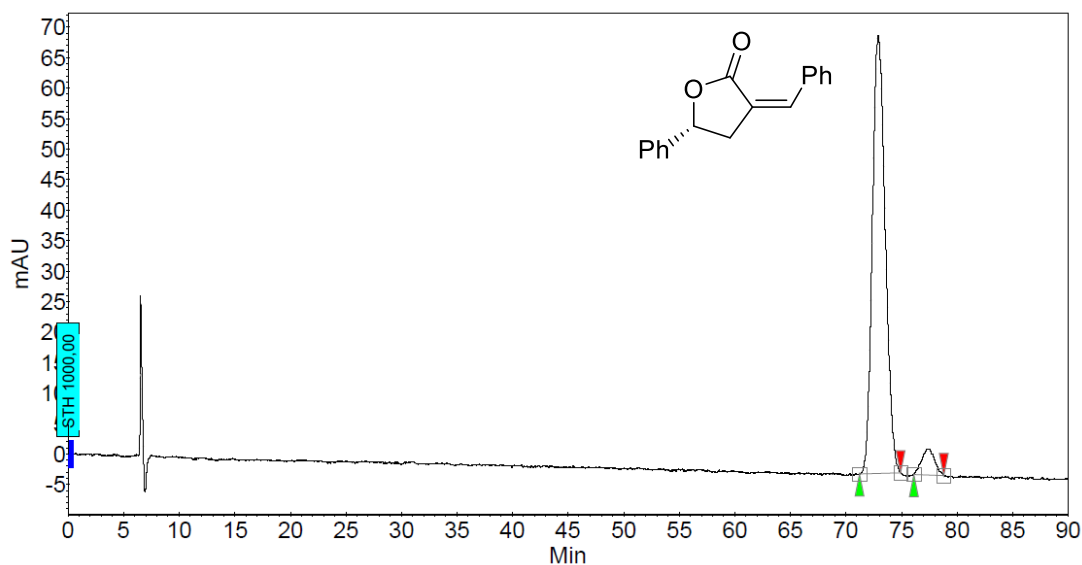


#### Peak Results :

Index	Name	Time [Min]	Quantity [% Area]	Height [mAU]	Area [mAU.Min]	Area % [%]
1	UNKNOWN	28.78	89.53	570.1	556.5	89.528
2	UNKNOWN	40.06	10.47	67.1	65.1	10.472
Total			100.00	637.2	621.6	100.000

**(Z)-3-benzylidene-5-phenyldihydrofuran-2(3H)-one ((Z)-238)****Peak Results :**

Index	Name	Time [Min]	Quantity [% Area]	Height [mAU]	Area [mAU.Min]	Area % [%]
1	UNKNOWN	71.31	50.09	33.6	43.6	50.093
2	UNKNOWN	75.06	49.91	31.7	43.5	49.907
Total			100.00	65.4	87.1	100.000

**(R,Z)-3-benzylidene-5-phenyldihydrofuran-2(3H)-one ((R,Z)-238)****Peak Results :**

Index	Name	Time [Min]	Quantity [% Area]	Height [mAU]	Area [mAU.Min]	Area % [%]
1	UNKNOWN	72.90	94.42	71.8	97.1	94.421
2	UNKNOWN	77.46	5.58	4.3	5.7	5.579
Total			100.00	76.1	102.9	100.000

## 4 X-ray crystallography data

### *(R,Z)*-3-benzylidene-5-phenyldihydrofuran-2(3*H*)-one (*(R,Z)*-238)

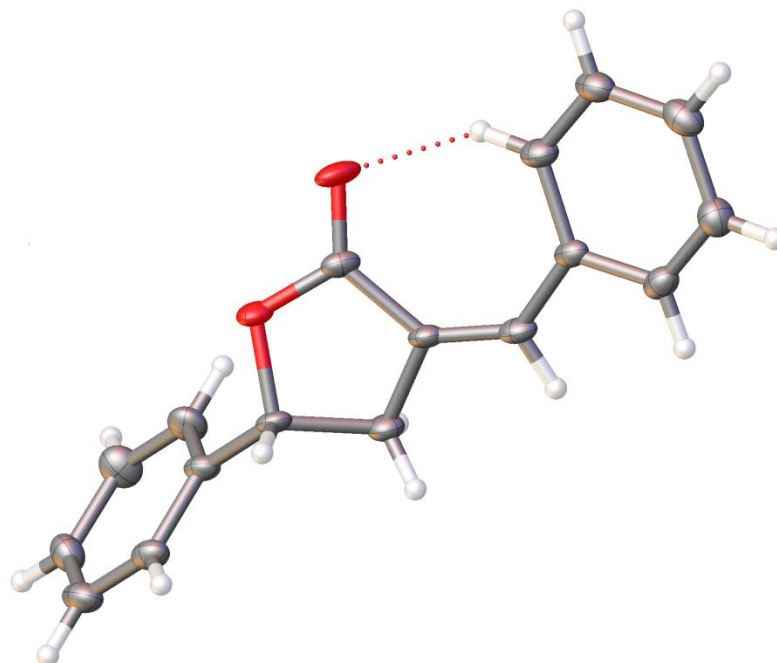


**Table 16.** Crystal data and structure refinement for *(R,Z)*-238.

Empirical formula	C <sub>17</sub> H <sub>14</sub> O <sub>2</sub>
Formula weight	250.28
Temperature /K	123.01(10)
Crystal system	orthorhombic
Space group	P2 <sub>1</sub> 2 <sub>1</sub> 2 <sub>1</sub>
a/Å	5.9605(4)
b/Å	9.7758(9)
c/Å	22.163(2)
$\alpha$ /°	90
$\beta$ /°	90
$\gamma$ /°	90
Volume/Å <sup>3</sup>	1291.39(19)
Z	4
$\rho_{\text{calc}}$ /cm <sup>3</sup>	1.287
$\mu$ /mm <sup>-1</sup>	0.665
F(000)	528.0
Crystal size/mm <sup>3</sup>	0.22×0.09×0.06
Radiation	CuK $\alpha$ ( $\lambda$ = 1.54184)
2 $\theta$ range for data collection/°	3.989 to 74.300

## Appendix

Index ranges	$-7 \leq h \leq 7, -11 \leq k \leq 12, -26 \leq l \leq 27$
Reflections collected	5343
Independent reflections	2556 [ $R_{\text{int}} = 0.0804, R_{\text{sigma}} = 0.0868$ ]
Data/restraints/parameters	2556/0/172
Goodness-of-fit on $F^2$	1.058
Final R indexes [ $I \geq 2\sigma(I)$ ]	$R_1 = 0.0655, wR_2 = 0.1625$
Final R indexes [all data]	$R_1 = 0.0794, wR_2 = 0.1776$
Largest diff. peak/hole / $e \text{ \AA}^{-3}$	0.274/-0.412
Flack parameter	-0.4(3)

**Table 17.** Fractional Atomic Coordinates ( $\times 10^4$ ) and Equivalent Isotropic Displacement Parameters ( $\text{\AA}^2 \times 10^3$ ) for (R,Z)-238.  $U_{eq}$  is defined as 1/3 of the trace of the orthogonalised  $U_{ij}$  tensor.

Atom	x	y	z	$U_{eq}$
O1	5017(4)	7652(3)	3606.4(12)	23.5(6)
O2	2178(5)	6297(3)	3361.3(14)	31.1(7)
C5	4078(6)	6400(4)	3554.6(16)	21.2(8)
C1	7965(6)	8784(4)	4174.1(17)	21.3(7)
C7	4409(6)	3011(4)	3349.5(16)	20.0(8)
C2	7354(6)	7535(4)	3809.0(15)	19.4(7)
C4	5684(6)	5351(4)	3779.4(16)	19.7(7)
C3	7399(6)	6159(4)	4130.3(17)	23.7(8)
C8	2266(7)	3290(4)	3106.8(17)	24.3(8)
C6	5789(6)	3995(4)	3684.7(16)	22.0(8)
C12	5299(7)	1703(4)	3269.6(17)	23.9(8)
C17	9962(6)	9460(4)	4049.7(16)	23.6(8)
C13	6554(6)	9263(4)	4629.1(19)	27.0(8)
C10	2051(7)	1002(4)	2703.1(17)	28.4(9)
C15	9130(7)	11106(4)	4820.7(18)	27.8(9)
C9	1119(7)	2285(4)	2788.2(18)	27.3(8)
C16	10545(7)	10624(5)	4372(2)	29.8(9)
C11	4168(7)	715(5)	2947.7(18)	28.7(9)
C14	7138(8)	10413(5)	4949.6(19)	31.6(10)

**Table 18.** Anisotropic Displacement Parameters ( $\times 10^4$ ) for (R,Z)-238. The anisotropic displacement factor exponent takes the form:  $-2\pi^2 [h^2 a^{*2} U_{11} + \dots + 2hka^* b^* U_{12}]$ .

Atom	$U_{11}$	$U_{22}$	$U_{33}$	$U_{23}$	$U_{13}$	$U_{12}$
O1	15.2(12)	26.2(13)	29.3(14)	-1.1(10)	-9.8(10)	2.0(11)
O2	15.5(13)	36.2(16)	41.4(17)	-8.8(13)	-11.2(11)	8.6(12)
C5	13.9(16)	29.5(19)	20.1(17)	-3.0(14)	-1.2(12)	3.9(15)
C1	12.6(15)	29.2(18)	22.2(17)	5.3(14)	0.2(13)	-0.7(15)
C7	14.3(16)	27.0(18)	18.7(16)	6.4(13)	0.2(12)	0.6(15)
C2	9.7(15)	27.6(17)	20.9(16)	2.4(13)	-1.4(11)	2.1(14)
C4	11.3(15)	26.3(17)	21.6(17)	2.2(13)	-3.0(11)	0.6(14)
C3	16.3(17)	29.2(18)	25.6(18)	2.2(14)	-6.0(13)	0.2(15)
C8	17.7(17)	31.7(19)	23.5(18)	4.3(14)	-3.9(14)	-0.7(16)
C6	14.3(16)	32(2)	19.9(17)	3.7(14)	-3.6(12)	0.8(15)
C12	19.0(17)	28.7(18)	24.1(19)	6.9(14)	2.9(13)	4.1(15)
C17	15.4(16)	32.4(19)	23.1(18)	6.5(14)	3.0(13)	0.9(16)
C13	19.8(18)	32(2)	29(2)	2.4(17)	9.4(14)	-2.9(16)
C10	29(2)	34(2)	21.5(19)	1.5(15)	-0.6(15)	-10.1(18)
C15	30(2)	24.7(18)	29(2)	3.2(15)	-0.2(15)	-6.1(17)

**Table 18.** Anisotropic Displacement Parameters ( $\times 10^4$ ) for (*R,Z*)-**238**. The anisotropic displacement factor exponent takes the form:  $-2\pi^2[h^2a^{*2}U_{11}+\dots+2hka^*b^*U_{12}]$ .

Atom	$U_{11}$	$U_{22}$	$U_{33}$	$U_{23}$	$U_{13}$	$U_{12}$
C9	20.0(17)	35(2)	26.5(19)	6.3(16)	-3.2(14)	-5.7(17)
C16	19.0(18)	37(2)	33(2)	8.5(16)	-2.1(14)	-5.4(18)
C11	31(2)	26.9(19)	28(2)	0.9(15)	0.1(15)	-1.6(18)
C14	32(2)	36(2)	27(2)	-2.9(15)	8.3(16)	-3(2)

**Table 19.** Bond Lengths for (*R,Z*)-**238**.

Atom	Atom	Length/Å	Atom	Atom	Length/Å
O1	C5	1.350(5)	O2	C5	1.215(5)
O1	C2	1.468(4)	C5	C4	1.489(5)
C1	C2	1.510(5)	C8	C9	1.390(6)
C1	C17	1.388(5)	C12	C11	1.377(6)
C1	C13	1.394(5)	C17	C16	1.388(6)
C7	C8	1.413(5)	C13	C14	1.374(6)
C7	C6	1.467(5)	C10	C9	1.384(6)
C7	C12	1.396(6)	C10	C11	1.402(6)
C2	C3	1.522(5)	C15	C16	1.386(6)
C4	C3	1.508(5)	C15	C14	1.397(6)
C4	C6	1.344(6)			

**Table 20.** Bond Angles for (*R,Z*)-**238**.

Atom	Atom	Atom	Angle/°	Atom	Atom	Atom	Angle/°
C5	O1	C2	110.4(3)	C6	C4	C5	131.1(3)
O1	C5	C4	109.2(3)	C6	C4	C3	124.4(3)
O2	C5	O1	119.5(4)	C4	C3	C2	102.1(3)
O2	C5	C4	131.3(4)	C9	C8	C7	120.1(4)
C17	C1	C2	119.0(3)	C4	C6	C7	134.4(4)
C17	C1	C13	120.1(4)	C11	C12	C7	121.5(4)
C13	C1	C2	120.9(3)	C16	C17	C1	120.2(4)
C8	C7	C6	125.0(4)	C14	C13	C1	119.7(4)
C12	C7	C8	118.2(4)	C9	C10	C11	119.4(4)
C12	C7	C6	116.9(3)	C16	C15	C14	119.9(4)
O1	C2	C1	109.3(3)	C10	C9	C8	120.8(4)
O1	C2	C3	103.2(3)	C15	C16	C17	119.7(4)
C1	C2	C3	117.4(3)	C12	C11	C10	120.0(4)
C5	C4	C3	104.4(3)	C13	C14	C15	120.4(4)

**Table 21.** Hydrogen Fractional Atomic Coordinates ( $\times 10^4$ ) and Equivalent Isotropic Displacement Parameters ( $\text{Å}^2 \times 10^3$ ) for (*R,Z*)-**238**.

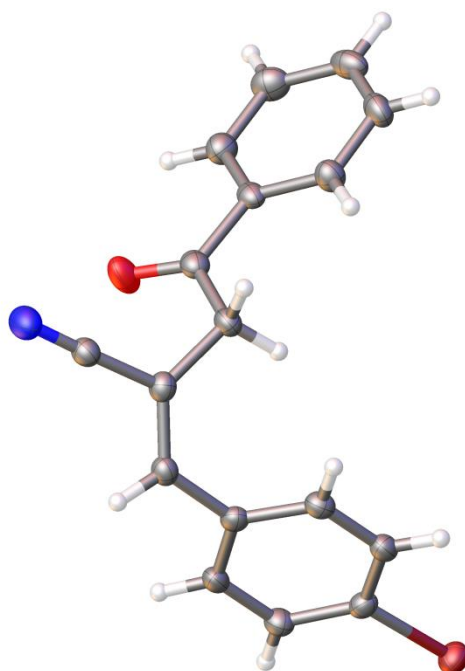
Atom	x	y	z	$U_{eq}$
H2	8333.3	7488.5	3454.39	23
H3A	8871.6	5739.72	4106.5	28
H3B	6970.3	6249.5	4550.62	28
H8	1621.21	4147.74	3160.29	29
H6	7010.25	3588.5	3874.4	26
H12	6687.53	1493.65	3437.57	29
H17	10910.18	9131.6	3749.62	28
H13	5223.1	8806.87	4715.44	32
H10	1279.92	337.89	2485.91	34
H15	9507.56	11889.98	5035.59	33
H9	-292.18	2475.96	2630.17	33
H16	11879.77	11078.09	4288.02	36

## Appendix

---

H11	4808.77	-143.26	2892.48	34
H14	6200.17	10732.07	5254.06	38

---

**(E)-2-(4-bromobenzylidene)-4-oxo-4-phenylbutanenitrile (E)-249da****Table 22.** Crystal data and structure refinement for (E)-249da.

Empirical formula	C <sub>17</sub> H <sub>12</sub> BrNO
Formula weight	326.19
Temperature /K	123.00(10)
Crystal system	monoclinic
Space group	<i>P</i> 2 <sub>1</sub> / <i>n</i>
<i>a</i> /Å	6.06350(10)
<i>b</i> /Å	15.3114(3)
<i>c</i> /Å	14.8777(4)
$\alpha$ /°	90
$\beta$ /°	94.303(2)
$\gamma$ /°	90
Volume/Å <sup>3</sup>	1377.36(5)
<i>Z</i>	4
$\rho_{\text{calc}}$ /cm <sup>3</sup>	1.573
$\mu$ /mm <sup>-1</sup>	4.011
<i>F</i> (000)	656.0
Crystal size/mm <sup>3</sup>	0.36×0.09×0.06
Radiation	CuK $\alpha$ ( $\lambda$ = 1.54184)
2 $\theta$ range for data collection/°	4.149 to 73.419
Index ranges	-7 ≤ <i>h</i> ≤ 7, -18 ≤ <i>k</i> ≤ 19, -17 ≤ <i>l</i> ≤ 18
Reflections collected	18463
Independent reflections	2679 [ <i>R</i> <sub>int</sub> = 0.0926, <i>R</i> <sub>sigma</sub> = 0.0453]



## Appendix

Data/restraints/parameters	2679/0/181
Goodness-of-fit on F <sup>2</sup>	1.052
Final R indexes [ $I \geq 2\sigma(I)$ ]	R <sub>1</sub> = 0.0379, wR <sub>2</sub> = 0.0969
Final R indexes [all data]	R <sub>1</sub> = 0.0466, wR <sub>2</sub> = 0.1024
Largest diff. peak/hole / e Å <sup>-3</sup>	0.592/-0.623

**Table 23.** Fractional Atomic Coordinates ( $\times 10^4$ ) and Equivalent Isotropic Displacement Parameters ( $\text{\AA}^2 \times 10^3$ ) for (*E*)-**249da**.  $U_{eq}$  is defined as 1/3 of the trace of the orthogonalised  $U_{ij}$  tensor.

Atom	x	y	z	$U_{eq}$
Br01	-1087.3(5)	8857.96(16)	5451.6(2)	29.04(14)
O002	8928(3)	5582.6(13)	6854.9(16)	37.0(5)
N003	9772(4)	5815.7(15)	9168.3(19)	35.4(6)
C004	4655(4)	8371.9(14)	7064(2)	25.0(6)
C005	506(4)	7631.1(15)	6771(2)	24.5(6)
C006	5937(4)	7171.8(15)	8093.5(19)	22.7(6)
C007	1057(4)	8379.6(15)	6307.1(19)	23.0(6)
C008	2061(4)	7242.8(15)	7365.5(19)	23.9(6)
C009	7077(4)	5272.1(15)	6853(2)	25.0(6)
C00A	5445(4)	5616.2(14)	7493(2)	24.5(6)
C00B	6446(4)	6320.7(16)	8101.8(19)	22.9(6)
C00C	3122(5)	8761.1(15)	6457(2)	25.4(6)
C00D	4186(4)	7597.1(14)	7503.4(19)	22.6(6)
C00E	6367(4)	4556.6(14)	6210.0(19)	22.8(6)
C00F	7829(5)	4312.4(16)	5582(2)	28.7(6)
C00G	4342(5)	4128.5(16)	6222(2)	27.0(6)
C00H	8298(5)	6047.0(15)	8706(2)	23.9(6)
C00I	5263(5)	3232.1(17)	4974(2)	32.8(7)
C00J	3814(5)	3463.7(17)	5605(2)	32.4(7)
C00K	7279(6)	3659.5(18)	4962(2)	34.3(7)

**Table 24.** Anisotropic Displacement Parameters ( $\times 10^4$ ) for (*E*)-**249da**. The anisotropic displacement factor exponent takes the form:  $-2\pi^2[h^2a^{*2}U_{11} + \dots + 2hka^*b^*U_{12}]$ .

Atom	$U_{11}$	$U_{22}$	$U_{33}$	$U_{23}$	$U_{13}$	$U_{12}$
Br01	25.8(2)	28.69(19)	31.8(2)	4.92(10)	-3.07(15)	2.38(9)
O002	29.1(11)	36.6(10)	46.1(15)	-13.3(9)	8.2(10)	-11.1(8)
N003	36.4(15)	29.4(11)	38.6(16)	0.4(11)	-8.8(13)	-0.6(10)
C004	21.1(13)	19.6(10)	33.9(18)	-6.1(10)	0.3(12)	-1.5(9)
C005	22.0(13)	21.0(10)	30.4(17)	-3.6(10)	1.1(12)	-1.0(9)
C006	21.7(13)	24.1(11)	22.0(16)	-2.7(10)	0.2(11)	-1.5(9)
C007	22.5(13)	22.6(11)	23.8(16)	-1.6(10)	0.5(12)	4.3(9)
C008	26.1(14)	20.3(10)	25.4(16)	-1.1(10)	2.9(12)	-1.3(9)
C009	26.4(14)	20.1(10)	28.0(17)	2.8(10)	-1.8(12)	-0.9(10)
C00A	24.7(14)	20.7(10)	27.6(17)	-1.8(10)	-2.0(12)	-3.2(9)
C00B	21.8(13)	25.6(11)	21.0(16)	0.9(11)	-0.5(12)	-0.3(10)
C00C	26.9(15)	20.7(10)	28.2(18)	0.9(10)	-0.2(13)	-1.2(9)
C00D	22.8(13)	20.1(10)	24.8(16)	-4.3(10)	0.5(12)	2.6(9)
C00E	26.0(14)	17.4(10)	24.0(16)	2.6(10)	-4.5(12)	-0.2(9)
C00F	27.2(15)	27.3(12)	31.5(18)	1.0(11)	2.1(13)	-0.3(10)
C00G	26.9(14)	28.4(11)	25.7(17)	-3.5(11)	2.0(12)	-2.2(10)
C00H	26.0(15)	22.1(11)	23.3(16)	-0.9(10)	-0.5(13)	-2.1(10)
C00I	46.4(18)	24.8(12)	25.6(18)	-5.2(11)	-7.6(15)	3.0(11)
C00J	32.8(16)	27.8(13)	35(2)	-2.1(11)	-7.8(15)	-7.1(10)
C00K	41.6(18)	34.8(13)	26.8(19)	-3.3(12)	3.9(14)	5.3(12)

**Table 25.** Bond Lengths for (*E*)-**249da**.

Atom	Atom	Length/Å	Atom	Atom	Length/Å
Br01	C007	1.897(3)	C009	C00A	1.518(4)
O002	C009	1.219(3)	C009	C00E	1.497(3)
N003	C00H	1.142(4)	C00A	C00B	1.506(3)
C004	C00C	1.381(4)	C00B	C00H	1.447(4)
C004	C00D	1.394(4)	C00E	C00F	1.386(4)
C005	C007	1.391(4)	C00E	C00G	1.393(4)
C005	C008	1.378(4)	C00F	C00K	1.385(4)
C006	C00B	1.339(3)	C00G	C00J	1.392(4)
C006	C00D	1.477(4)	C00I	C00J	1.380(5)
C007	C00C	1.385(4)	C00I	C00K	1.388(5)
C008	C00D	1.399(4)			

**Table 26.** Bond Angles for (*E*)-**249da**.

Atom	Atom	Atom	Angle/°	Atom	Atom	Atom	Angle/°
C00D	C004	C00C	121.5(2)	C007	C00C	C004	118.6(2)
C008	C005	C007	119.7(2)	C006	C00D	C004	119.4(2)
C00D	C006	C00B	126.1(2)	C008	C00D	C004	118.6(2)
C005	C007	Br01	118.21(19)	C008	C00D	C006	122.0(2)
C00C	C007	Br01	120.7(2)	C00F	C00E	C009	117.4(2)
C00C	C007	C005	121.1(2)	C00G	C00E	C009	123.2(3)
C00D	C008	C005	120.3(2)	C00G	C00E	C00F	119.4(2)
C00A	C009	O002	120.5(2)	C00K	C00F	C00E	120.7(3)
C00E	C009	O002	120.5(3)	C00J	C00G	C00E	119.7(3)
C00E	C009	C00A	119.0(2)	C00B	C00H	N003	178.3(3)
C00B	C00A	C009	111.9(2)	C00K	C00I	C00J	119.6(3)
C00A	C00B	C006	127.5(2)	C00I	C00J	C00G	120.7(3)
C00H	C00B	C006	117.1(2)	C00I	C00K	C00F	120.0(3)
C00H	C00B	C00A	115.2(2)				

**Table 27.** Hydrogen Fractional Atomic Coordinates ( $\times 10^4$ ) and Equivalent Isotopic Displacement Parameters ( $\text{Å}^2 \times 10^3$ ) for (*E*)-**249da**.

Atom	x	y	z	$U_{eq}$
H004	6031(4)	8632.7(14)	7182(2)	29.9(7)
H005	-905(4)	7393.9(15)	6680(2)	29.4(7)
H006	6763(4)	7528.6(15)	8497.1(19)	27.2(7)
H008	1695(4)	6742.9(15)	7676.6(19)	28.6(7)
H00a	4158(4)	5848.3(14)	7146(2)	29.4(7)
H00b	4958(4)	5138.6(14)	7858(2)	29.4(7)
H00C	3471(5)	9268.8(15)	6155(2)	30.4(8)
H00F	9192(5)	4589.9(16)	5578(2)	34.4(8)
H00G	3348(5)	4286.2(16)	6641(2)	32.4(7)
H00I	4891(5)	2792.4(17)	4558(2)	39.3(9)
H00J	2471(5)	3172.4(17)	5619(2)	38.9(9)
H00K	8261(6)	3507.4(18)	4537(2)	41.2(9)

## 5 Curriculum Vitae

### Personal data

Name	Thomas Michael Föll
Date of birth	March 13, 1990 in Landshut
Nationality	German
Email	Thomas.Foell@chemie.uni-regensburg.de

### Education

Since 11/2015	Ph.D. thesis in the group of Prof. Dr. O. Reiser at the University of Regensburg, Germany
09/2015	Master of Science in chemistry
01/2015 – 09/2015	Master thesis in the group of Prof. Dr. O. Reiser at the University of Regensburg, Germany
10/2013 – 09/2015	Advanced studies in chemistry, University of Regensburg, Germany
09/2013	Bachelor of Science in chemistry
10/2010 – 09/2013	Studies in chemistry, University of Regensburg, Germany
09/2000 – 06/2009	Abitur (A-levels), Hans-Leinberger-Gymnasium (secondary school), Landshut, Germany

## List of publications

T. Föll, J. Rehbein, O. Reiser, *Org. Lett.* **2018**, *20*, 5794 – 5798.

“Ir(ppy)<sub>3</sub>-Catalyzed, Visible-Light-Mediated Reaction of  $\alpha$ -Chloro Cinnamates with Enol Acetates: An Apparent Halogen Paradox.”

## Conferences

### *26th Lecture Conference on Photochemistry 2018, Garching/Munich (Germany)*

10. – 12.09.2018 (Attendant).

### *7th EuCheMS Chemistry Congress 2018, Liverpool (United Kingdom)*

26. – 30.08.2018 “Generation and trapping of vinyl radicals derived from vinyl chlorides via visible light photoredox catalysis” (Poster).

### *GDCh Wissenschaftsforum 2017, Berlin (Germany)*

10. – 14.09.2017 “Visible light mediated functionalization of  $\alpha$ -chloro cinnamates: Access to highly reactive vinyl radicals” (Poster).

### *26th ISHC Congress 2017, Regensburg (Germany)*

03. – 08.09.2017 “Visible light mediated generation and trapping of vinyl radicals derived from  $\alpha$ -halo chalcones and cinnamates” (Poster).

### *6th EuCheMS Chemistry Congress 2016, Seville (Spain)*

11. – 15.09.2016 “Visible light mediated  $\alpha$ -vinylation of enol acetates: Access to 2-benzylidene-1,4-diketones” (Poster).

## Professional References

Prof. Dr. Oliver Reiser

Institut für Organische Chemie

Universität Regensburg, Universitätsstr. 31

93053 Regensburg, Germany

Phone: 0049 941 943 4631

Email: Oliver.Reiser@chemie.uni-regensburg.de

## **H Acknowledgement**

An erster Stelle möchte ich mich bei Prof. Dr. Oliver Reiser für die Aufnahme in seinen Arbeitskreis und die Überlassung des interessanten und vielseitigen Themas bedanken. Weiterhin danke ich für seine stete Unterstützung bei auftretenden Problemen und Hürden aller Art.

Ein besonderer Dank gebührt Prof. Dr. Julia Rehbein für die Kooperation und den theoretischen Berechnungen, die entscheidend zu der gemeinsamen Publikation beigetragen haben.

Für die finanzielle Unterstützung während meiner Auslandsaufenthalte danke ich dem DFG Research Training Group GRK 1626 und der GDCh.

Für die technische Unterstützung bei allen auftretenden Problemen danke ich vor allem Dr. Peter Kreitmeier. Somit wurden alte oder defekte Geräte stets zügig ersetzt, wodurch ein kontinuierliches Arbeiten ermöglicht wurde. Des Weiteren danke ich Helena Konkel, Roxane Harteis und Brigitte Eichenseher, die den Laboralltag spürbar erleichtert haben.

Bei allen Mitarbeitern der zentralen Analytik danke ich für die Aufnahme von Röntgenstrukturanalysen, der Durchführung unzähliger Massenspektroskopien und NMR-Messungen. Unseren Technikern Helena Konkel und Roxane Harteis danke ich für das zügige Messen chiraler HPLC Proben. Regina Hoheisel (AK König) danke ich für die Messungen der CV-Spektren.

Für die freundliche Integration in die Arbeitsgruppe und das Bereitstellen eines unglaublichen Arbeitsklimas möchte ich mich bei allen damaligen und heutigen Arbeitskollegen bedanken. Ein ganz besonderes Dankeschön gilt dabei Simon Budde, Peter Ehrnsberger, Christian Eichinger, Andreas Hartl, Michael Leitner, Natalija Moor, Lisa Stadler, Lukas Traub, Dr. Matthias Gnahn, Dr. Martin Hofmann, Dr. Benjamin Kastl, Dr. Sabine Kerres, Dr. Verena Leitner, Dr. Thomas Ertl, Dr. Daniel Dobler, Dr. Christian Faderl und Dr. Daniel Rackl.

Allen ehemaligen und aktuellen Laborkollegen gebührt ein Dankeschön. Besonders hervorheben möchte ich dabei die gemeinsame Zeit in 33.1.17 mit Peter Ehrnsberger. Im Labor herrschte stets eine geniale Atmosphäre. Den Boxen danke ich hierbei für die

abwechslungsreiche musikalische Unterhaltung. Zusätzlich möchte ich die gemeinsame Zeit im „Masterandenlabor“ mit Christian Eichinger, Lukas Traub, sowie den Kollegen vom AK König Anna Berger, Simon Düsel, Andreas Graml, Daniel Petzold erwähnen. Es war ein super Jahr mit euch und ich denke es hat uns allen sehr viel Spaß bereitet.

Meinen ehemaligen Bachelorstudenten und Forschungspraktikanten Daniel Schmidhuber, Patrick Hailer, Jessica Stahl, Karsten Donabauer, Nikolai Wurzer und Victoria Scheidler danke ich für ihre engagierte Mitarbeit.

Für ausgiebiges und gewissenhaftes Korrekturlesen bedanke ich mich bei Robert Eckl, Carina Sonnleitner, Lisa Stadler, Simon Budde, Anna Rustler und Dr. Daniel Rackl.

Zuletzt möchte ich mich vom ganzen Herzen bei meiner Familie bedanken, die mich von Anfang an und kontinuierlich unterstützt haben. Ihr seid mir stets zur Seite gestanden.

Liebe Anna, ich bin dir zutiefst für deine stete Unterstützung und deine unerschöpfliche Geduld dankbar. Du hast mir in letzter Zeit so viel Kraft gespendet. Ohne dich hätte ich die Zeit während des Zusammenschreibens nicht so gut überwunden. Vielen Dank!

## **I Declaration**

Herewith I declare that this present thesis is a presentation of my original work prepared single-handed. Wherever contributions from others are involved, all of them are marked clearly, with reference to the literature, license, and acknowledgement of collaborative research.

Regensburg, 30.01.2019



---

Thomas Föll